

**Development and Investigation of Novel Chemoselective Processes in Pd and Cu
Catalysis**

Ciaran P. Seath

July 2017

**Development and Investigation of Novel Chemoselective Processes in Pd and Cu
Catalysis**

Thesis submitted to the University of Strathclyde in fulfilment of the
requirements for the degree of Doctor of Philosophy

By

Ciaran Paul Seath

July 2017

Declaration of Copyright

This thesis is a result of the author's original research. It has been composed by the author and has not been previously submitted for examination which has led to the award of a degree.

The copyright of this thesis belongs to the author under the terms of the United Kingdom Copyright Acts as qualified by University of Strathclyde Regulation 3.50. Due acknowledgement must always be made of the use of any material contained in, or derived from, this thesis.

Signed:

Date: 22nd July 2017

Publication List

1. “*Chemoselective Boronic Ester Synthesis by Controlled Speciation*”: J. W. B. Fyfe, C. P. Seath, A. J. B. Watson, *Angew. Chem. Int. Ed.*, **2014**, *53*, 12077–12080.
2. “*A Modular Synthesis of Functionalized Phenols Enabled by Controlled Boron Speciation*”: J. J. Molloy, R. P. Law, J. W. B. Fyfe, C. P. Seath, D. J. Hirst, A. J. B. Watson, *Org. Biomol. Chem.*, **2015**, *13*, 3093–3102.
3. “*Speciation Control During Suzuki-Miyaura Cross-Coupling of Haloaryl and Haloalkenyl MIDA Boronic Esters*”: J. W. B. Fyfe, E. Valverde, C. P. Seath, J. M. Redmond, N. Anderson, A. J. B. Watson, *Chem. Eur. J.*, **2015**, *24*, 8951–8964.
4. “*Tandem Chemoselective Suzuki-Miyaura Cross-coupling Enabled by Nucleophile Speciation Control*”: C. P. Seath, J. W. B. Fyfe, J. J. Molloy, A. J. B. Watson, *Angew. Chem. Int. Ed.* **2015**, *54*, 9976–9979.
5. “*Synthesis of 2-BMIDA 6,5-Bicyclic Heterocycles by Cu(I)/Pd(0)/Cu(II) Cascade Catalysis of 2-Iodoanilines/phenols*”: C. P. Seath, K. L. Wilson, A. Campbell, J. M. Mowat, A. J. B. Watson, *Chem. Commun.* **2016**, *52*, 8703–8706.
6. “*Chemoselective Sequential Click Ligations Directed by Enhanced Reactivity of an Aromatic Ynamine*”: M. Z. C. Hatit, J. C. Sadler, L. A. McLean, B. C. Whitehurst, C. P. Seath, L. D. Humphreys, R. J. Young, A. J. B. Watson, G. A. Burley, *Org. Lett.* **2016**, *18*, 1694–1697.
7. “*Synthesis of Oxindoles and Benzofuranones via Oxidation of 2-Heterocyclic BMIDAs*” C. P. Seath, J. W. B. Fyfe, J. J. Molloy, A. J. B. Watson, *Synthesis* **2017**, *49*, 891–898 .
8. “*Determining the Origin of Rate-Independent Chemoselectivity in CuAAC Reactions: An Alkyne-Specific Shift in Rate-Determining Step*” C. P. Seath, G. A. Burley, A. J. B. Watson, *Angew. Chem. Int. Ed.* **2017**, *56*, 3314 – 3318.
9. “*Chemoselective Sequential Control of CuAAC Ligations Using Aromatic Ynamine Protecting Groups*” M. Z. C. Hatit, C. P. Seath, A. J. B. Watson, G. A. Burley, *J. Org. Chem.* **2017**, *82*, 5461 – 5468.

Abstract

The development of chemoselective processes is of utmost importance for the future of synthetic organic chemistry, and has been described as ‘the single greatest obstacle to complex molecule synthesis’.^[1] Chemoselectivity is required to exploit the full potential of synthetic developments in organic chemistry, allowing for more efficient procedures and better route design. This thesis will describe the development of chemoselective processes across two cornerstone reactions in organic chemistry.

Chapter one will describe the development of dual nucleophile/electrophile chemoselectivity in the Suzuki-Miyaura reaction. Chemoselectivity in this key cross-coupling reaction has previously only been achieved at either the nucleophile or the electrophile independently. Electrophile chemoselectivity is generally well defined and has been used extensively in both academic and industrial settings. Chemoselectivity of the nucleophilic component has been less well explored, and has only been achieved through three distinct approaches; protecting group chemistries, vicinal/geminal activation, and aryl/benzyl selectivity that is based upon activating Ag additives. Herein, we describe the use of media controlled boron speciation between aryl/vinyl BPins and BMIDAs to realize the first example of dual nucleophile/electrophile chemoselectivity. The method was exemplified through the synthesis of a range of diverse substrates and a BET bromodomain inhibitor.

Chapter two will describe an investigation into the source of rate independent chemoselectivity in the CuAAC reaction. Chemoselectivity in the CuAAC reaction has chiefly been demonstrated through the use of either activated or deactivated azides, whereas alkyne chemoselectivity is less well developed. Recent work from the Watson and Burley groups described the use of aromatic ynamines to afford exquisite chemoselectivity over alkyl alkynes, allowing for sequential functionalization of multifunctional bisalkynes. Herein, we describe the development of a reactivity scale for alkynes in the CuAAC reaction and a kinetic investigation into the origin of selectivity when using ynamine substrates. A chelation-assisted change in the rate-determining step from Cu-acetylide formation to azide ligation/insertion allows for chemoselectivity over more reactive alkynes despite a

slower overall rate. This was harnessed to develop an orthogonal ligation strategy from protected ynamine substrates.

Acknowledgements

First and foremost I would like to thank Dr Allan Watson, El Capitan, for all his guidance over the last 4 years. With relentless encouragement and a healthy amount of sarcasm, Allan has shaped the chemist I am today. The support provided by Allan both academically and emotionally has been a constant source of inspiration. I will miss our chats about chemistry, and life, over coffee or more often, many, many beers.

I would like to thank my examiner, Prof. John Murphy for his help throughout the last three years, and his assistance in preparing me for my viva and what comes after. I would like to thank Dr Glenn Burley for all his help with introducing me to chemical biology, bioorthogonal chemistry, and salt and chilli tofu. I have enjoyed contributing in a small way towards what is destined to be a powerful research platform. The collaboration with your group has pushed me outside of my comfort zone, and broadened my views on the future of chemistry as a whole. Additional thanks go to Marine Hatit, who I worked with on the click chemistry project; your productivity knows no bounds!

I would also like to thank the members of the Watson and Jamieson groups, both past and present for providing a fun atmosphere to work in, I'll never forget the often ridiculous hijinks, banter, and confectionary provided by you all. Particular thanks go to the exceptional members of Team Boron, Jamie Fyfe, John Molloy, and Julien Vantourout. These guys have pushed me to be a better chemist and always been there for a pint, whether to celebrate or commiserate. It has been a pleasure working so closely with you all, I am in no doubt that I could not have accomplished so much without your help.

I would like to thank my thesis-writing partner in crime and long time fellow weekend warrior, Mairi Littleson. Your help and moral support thought the last few months has been invaluable, both in writing this document but also with respect to my first baby steps into synthesis.

Heartfelt thanks go to Frankie Potjewyd who has put up with me for the majority of my time in the group, nothing makes going to work easier and more enjoyable than seeing you there every day.

Finally I would like to thank the Carnegie Trust for the Universities of Scotland for funding my PhD studies. Without the generous funding provided every year I would not have experienced all of the incredible conferences, workshops, and external travel that has made these past three years so great.

Abbreviations

Ac – Acetyl

AMTC – (1-(Trans-2-hydroxycyclohexyl)-4-(*N,N*-dimethylaminomethyl)-1,2,3-triazole

BimPy₂ – Mono(benzimidazolymethyl)-bis(pyridylmethyl)

BINOL – 1,1-Bi-2-naphthol

Bn – Benzyl

Boc – *t*-Butoxycarbonyl

BPin – Boronic acid, pinacolato ester

BSA – Bovine serum albumin

Cat – Catalyst

CataCXium C – *trans*-Bis(acetato)bis[*o*-(di-*o*-tolylphosphino)benzyl]dipalladium(II)

Cbz – Carboxybenzyl

CFL – Compact fluorescent lamp

CuAAC – Cu-catalysed azide-alkyne cycloaddition

DAN – Diaminonaphthalene

DavePhos – 2-Dicyclohexylphosphino-2-(*N,N*-dimethylamino)biphenyl

DCM – Dichloromethane

DMT – 4,4'-Dimethoxytriphenylmethyl

DNA – Deoxyribose nucleic acid

DPAP – 2,2-Dimethoxy-2-phenylacetophenone

Dppe – 1,2-Bis(diphenylphosphino)ethane

Dppp – 1,3-Bis(diphenylphosphino)propane

Dppf – 1,1'-Bis(diphenylphosphino)ferrocene

Dtbbpy – 4,4-Di-*tert*-butylbipyridyl

EDG – Electron donating group

EWG – Electron withdrawing group

Equiv – Equivalents

Fc – Ferrocene

HPLC – High performance liquid chromatography

Im – Imidazole

KIE – Kinetic isotope effect

MIDA - *N*-Methyliminodiacetic acid

NaAsc – Sodium ascorbate
NHC – *N*-Heterocyclic carbene
PEPPSI-IPent – Dichloro[1,3-bis(2,6-di-3-pentylphenyl)imidazol-2-ylidene](3-chloropyridyl)palladium(II)
TBAF – Tetrabutylammonium fluoride
Tf – Triflyl
THPTA – Tris(3-hydroxypropyltriazolylmethyl)amine
RDS – Rate determining step
RNA – Ribonucleic acid
RuPhos – 2-Dicyclohexylphosphino-2,6'-diisopropoxybiphenyl
rt – Room temperature
SM – Suzuki–Miyaura
SPAAC – Strain-promoted azide-alkyne cycloaddition
SPhos – 2-Dicyclohexylphosphino-2',6'-dimethoxybiphenyl
TES – Triethylsilyl
TMP – 2,2,6,6-Tetramethylpiperidine
TIPS – Triisopropylsilyl
THF – Tetrahydrofuran
XantPhos – 4,5-Bis(diphenylphosphino)-9,9-dimethylxanthene
Xphos – 2-Dicyclohexylphosphino-2,4,6-triisopropylbiphenyl

1.0 Chapter 1	1
1.1 Introduction	1
1.1.1 Introduction to the Suzuki-Miyaura Reaction	1
1.1.2 Mechanism of the SM Reaction	2
1.1.2.1 Oxidative Addition	3
1.1.2.2 Transmetalation	3
1.1.3 Advances in the Suzuki Miyaura Reaction	8
1.1.3.1 Increasing the Scope of Electrophiles	8
1.1.3.2 Nature of the Organoboron Reagent	11
1.1.3.2.1 Boronic Acids	11
1.1.3.2.3 Boronic Esters	14
1.1.3.2.4 Organotrifluoroborates	15
1.1.3.2.5 MIDA Boronic Esters	17
1.1.4 Chemoselectivity in the SM reaction	22
1.1.4.1 Electrophile Chemoselectivity	22
1.1.4.2 Chemoselective Transmetalation via Vicinal/Geminal Activation	26
1.1.4.3 Chemoselective Transmetalation via Protected Boron Species	29
1.1.4.4 Use of BMIDA in Chemoselective Transmetalation	29
1.1.4.5 Use of BF ₃ K in Chemoselective Transmetalation	32
1.1.4.6 Use of BDAN in Chemoselective Transmetalation	33
1.1.4.7 Aryl/Benzyl Chemoselectivity	34
1.2 Project Background	36
1.2.1 Boron speciation	36
1.2.2 Speciation in SM coupling	39
1.3 Aims	42
1.4 Results and Discussion	44
1.5 Conclusions	60
1.6 Future Work	62
1.6 Experimental	64
2.0 Chapter 2 - Chemoselectivity in the CuAAC Reaction	100
2.1 Introduction	100
2.1.1 Mechanism of the CuAAC Reaction	102
2.1.2 Chemoselectivity	109
2.1.2.1 Chemoselectivity in the Alkyne Component	109
2.1.2.1.1 Strain-Promoted Azide-Alkyne Cycloadditions	109
2.1.2.1.2 Activation of the Alkyne Component	112
2.1.2.1.3 Protection of the Alkyne Component	113
2.1.2.1.4 Chemoselectivity in the Azide Component	115
2.1.2.1.5 Use of 1-Iodo Alkynes	118
2.1.3 Summary	121
2.2 Previous work - Ynamines as Reactive Substrates in CuAAC	123
2.3 Project Aims	126
2.4 Results and Discussion	128
2.4.1 Determining the Origins of Chemoselectivity	128

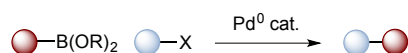
<i>2.4.2 Overturning Protecting Group Strategies in the CuAAC Reaction: Chemoselective CuAAC Reactions of Protected Aromatic Ynamines</i>	<i>141</i>
2.5 Conclusions	148
2.6 Future work	150
2.7 Experimental	154
3.0 References	214

1.0 Chapter 1

1.1 Introduction

1.1.1 Introduction to the Suzuki-Miyaura Reaction

The Suzuki-Miyaura (SM) reaction is one of the most widely used reactions in synthetic chemistry and has become a staple in both academia and industry. This reaction provides a general and effective method for carbon-carbon bond formation through the palladium-catalysed cross-coupling of an organoboron species with an organic halide or pseudo-halide (Scheme 1).



Scheme 1: Suzuki-Miyaura cross-coupling.

The SM reaction was first published in 1979 by Suzuki, Miyaura, and coworkers, it followed on from a range of other cross-coupling reactions developed around the same time that followed a similar general catalytic cycle (Figure 1) but each utilizing a different nucleophile.^[2] Suzuki's contribution to the field of cross-coupling earned him a share of the Nobel Prize in 2010 (with Ei-Ichi Negishi and Richard Heck). An extensive study published in 2011 showed that over 40% of all C-C bond formations in the pharmaceutical industry were carried out using the SM reaction, demonstrating the value and utility of this reaction for synthetic chemists.^[3] The popularity of the SM reaction is due to a set of mild conditions that tolerate of a wide range of functionalities while yielding non-toxic by-products. Although many other methods of Pd-catalysed C-C bond formation are available (for example Kumada, Stille, and Negishi couplings),^[4-7] they often involve handling a highly reactive or toxic organometallic reagent. The boron reagents used in SM coupling are comparatively more benign and they are either widely commercially available or can be readily synthesized using a variety of approaches.^[8] Moreover, the selectivity obtained in the SM and across the broad class of cross-coupling reactions is typically far superior to other methods of substituted aryl synthesis, which mainly rely on Friedel-Crafts-type regioselectivity.^[9]

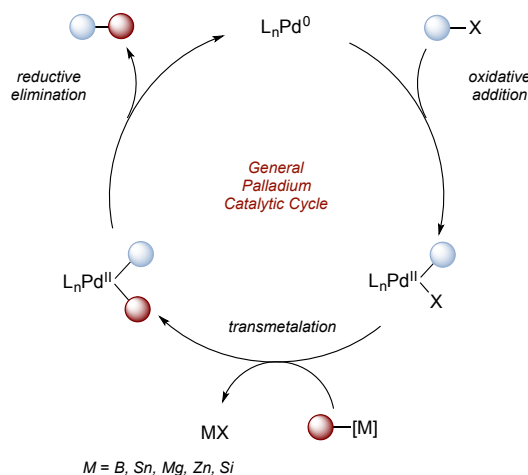


Figure 1: General palladium catalytic cycle.

Over the last few decades, the SM reaction has been the subject of a great deal of research, expanding the boundaries of the reaction beyond the coupling of olefinic boron reagents that Suzuki demonstrated in his groundbreaking paper.^[2] The reaction is now used most commonly in the cross-coupling of unsaturated ring systems, which is of interest to medicinal and materials chemists alike.^[3,10]

1.1.2 Mechanism of the SM Reaction

The catalytic cycle of the SM reaction contains three distinct steps: oxidative addition, transmetalation, and reductive elimination. The cycle is common to many forms of Pd-catalysed cross-coupling and an understanding of each step can explain the various trends seen in Pd catalysis.^[11]

Although the majority of Pd-catalysed cross-coupling reactions all follow the same general mechanistic pathway, each display nuances that differentiate them from each other. The following section will give an overview of the mechanistic aspects associated with SM coupling and describe in detail the current literature relating to the unique transmetalation step.

1.1.2.1 Oxidative Addition

The first step in the catalytic cycle is the oxidative addition of Pd^0 into the carbon-halogen bond to form a Pd^{II} intermediate (Figure 2). This is often the rate-determining step^[8] for the reaction and can be directly influenced by altering the (pseudo)halogen attached to the carbon. A well-defined order of reactivity was set out by Suzuki which follows $\text{I} > \text{OTf} > \text{Br} \gg \text{Cl}$.^[8] Despite not being the most active electrophile, bromides are the most commonly used coupling partners in SM coupling, possibly because they tend to be more commercially available in comparison to iodides and triflates, and are far more reactive than chlorides.^[12] The rate of oxidative addition can also be tuned by changing the substituents in proximity to the halide: electron-withdrawing groups (EWGs) increase the rate while electron-donating groups (EDGs) result in a decrease in rate. The introduction of an EWG to activate the halide is an effective method to allow the use of chlorides in cross-coupling reactions.^[12] Recent developments have allowed the use of unactivated chlorides as coupling partners through the application of novel ligand-catalyst combinations (*vide infra*).

1.1.2.2 Transmetalation

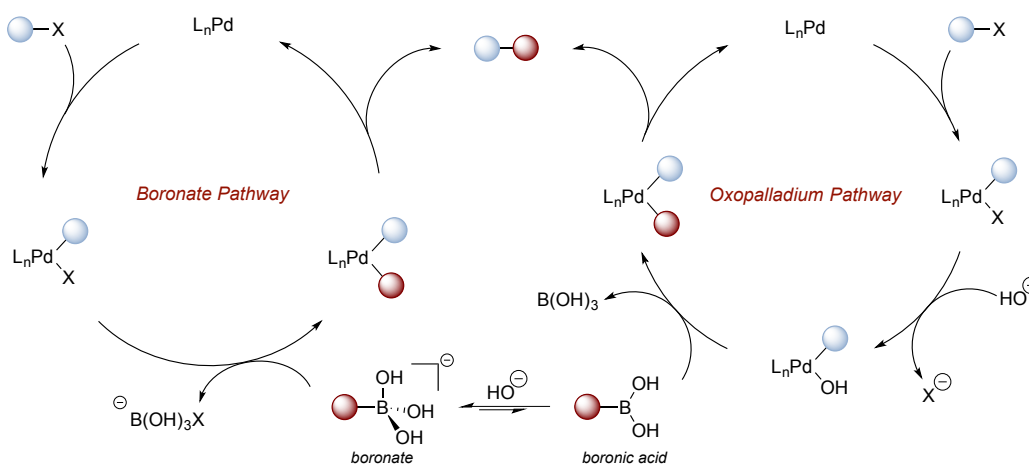


Figure 2: Mechanism of the Suzuki-Miyaura reaction.

While oxidative addition is relatively well understood, the transmetalation step has been the subject of much debate.^[13] Within the literature there are two competing interpretations, the boronate pathway and the oxo-palladium pathway.

The boronate pathway was, for many years, the accepted mechanism of transmetalation (Figure 2) and was proposed by Suzuki, Miyaura, and co-workers in 1979.^[2] In this pathway, the tetrahedral boronate, that is formed from the boronic acid under aqueous basic reaction conditions, undergoes transmetalation with a Pd-halide complex. It was thought that the more nucleophilic boronate was necessary for the transmetalation step (Figure 3).

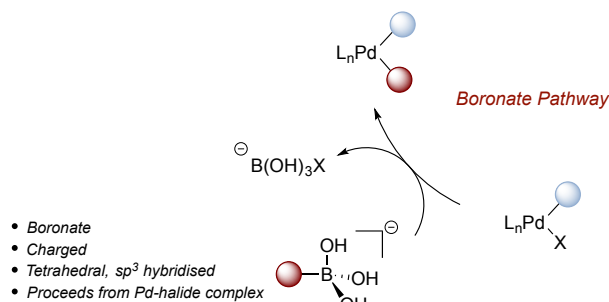


Figure 3: Transmetalation via boronate pathway.

More recently, a body of evidence has been disclosed that strongly supports the oxo-palladium pathway, which proceeds through the neutral boronic acid and an oxo-Pd complex.^[13] The oxo-palladium species is proposed to be formed through anion metathesis between a hydroxide ion and the Pd-halide complex derived from the oxidative addition step (Figure 4).

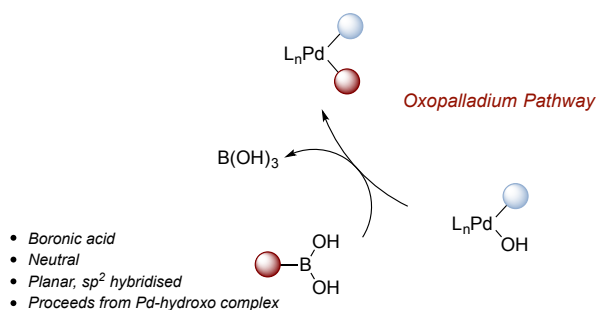
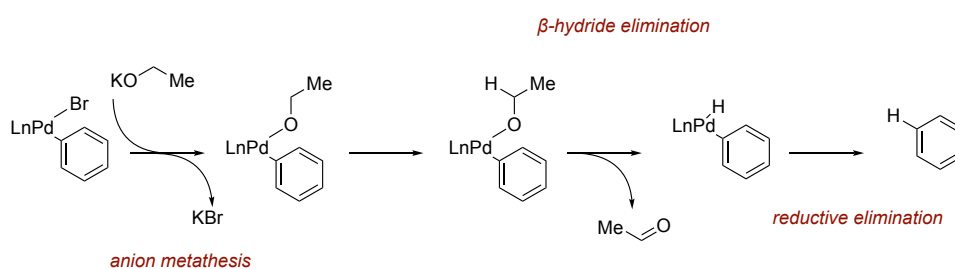


Figure 4: Transmetalation via oxo-palladium pathway.

Suzuki and Miyaura first suggested this pathway in 1985, just 6 years after their original mechanistic proposal.^[14] In an in-depth study on alkene-alkene cross-coupling, the authors noted three key observations:

1. Transmetalation did not occur when Lewis bases such as triethylamine were used, demonstrating the need for hydroxide or alkoxide in the reaction medium.

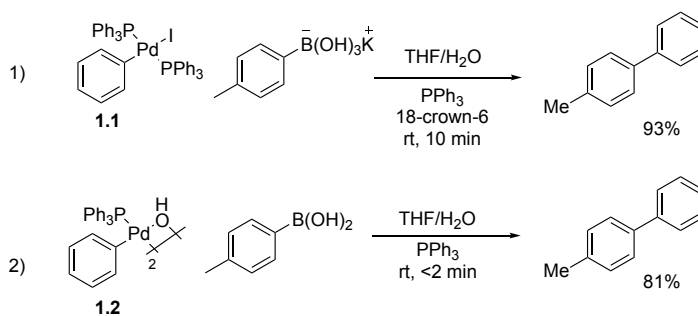
- When a preformed methyl lithium boronate was exposed to the reaction conditions in the absence of base, only 9% cross-coupled product was formed, suggesting that transmetalation does not proceed through an anionic boron species.
- The formation of reduction products were observed in the reaction, which can be attributed to β -hydride elimination of an *in situ* formed Pd-alkoxide species, yielding a Pd-H intermediate that reductively eliminates to afford the corresponding dehalogenated alkene (Scheme 2).



Scheme 2: Mechanism of the formation of reduction products.

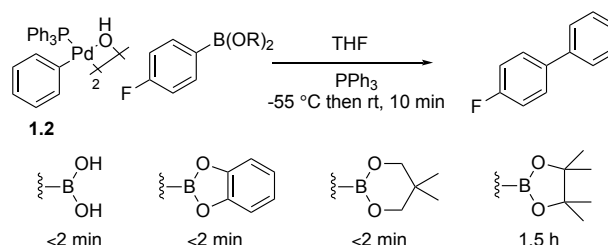
These three observations led to the conclusion that the reaction most likely proceeded through the oxo-palladium pathway. However, neither mechanism could be ruled out completely.^[13,15,16]

Only recently, in three separate studies reported by Amatore and Jutand, Hartwig, and Schmidt has light been shed on the likely course of transmetalation.^[17-19] In Hartwig's study, stoichiometric palladium complexes that resemble both the Pd-halide complex **1.1** and the Pd-oxo complex **1.2** were synthesised. The Pd-halide complex **1.1** was reacted with an aryl trihydroxyboronate to simulate the boronate pathway (Scheme 3, equation 1) and the Pd-oxo complex **1.2** was reacted with neutral tolylboronic acid to simulate the oxo-palladium pathway (Scheme 3, equation 2).



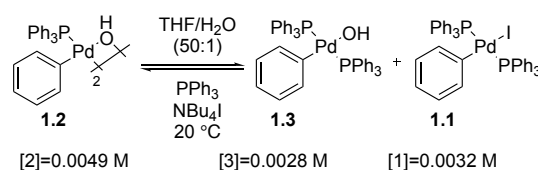
Scheme 3: Measurement of the rates of transmetalation/reductive elimination for model substrates.

The rate of transmetalation for both systems was measured at room temperature; it was shown the neutral boronic acid was coupled at a rate four times higher than its boronate derivative. In addition, it was observed that boronic esters (catechol, neopentyl, pinacol) all reacted at higher rates than the charged trihydroxyboronate, providing further evidence that transmetalation occurs through a neutral species (Scheme 4). The rate data for the pinacol boronic ester (BPin) was most intriguing. In the weakly basic media commonly used in SM coupling the formation of the BPin boronate is highly unfavoured, as is hydrolysis to afford the free boronic acid, indicating a slower, direct transmetalation event that takes place from the BPin rather than the corresponding boronic acid upon hydrolysis. However, it is important to note that this data includes the rates of both transmetalation and subsequent reductive elimination, although transmetalation is most likely rate determining.



Scheme 4: Rates of transmetalation for different boron species.

Transmetalation *via* the boronate was also proposed to proceed through the Pd-oxo species, which can be accessed from the halide complex *via* anion metathesis. This equilibrium was investigated through the use of tetrabutylammonium salts (Scheme 5); ^{31}P NMR was used to measure the resting state equilibria between Pd-halide and -hydroxo complexes.

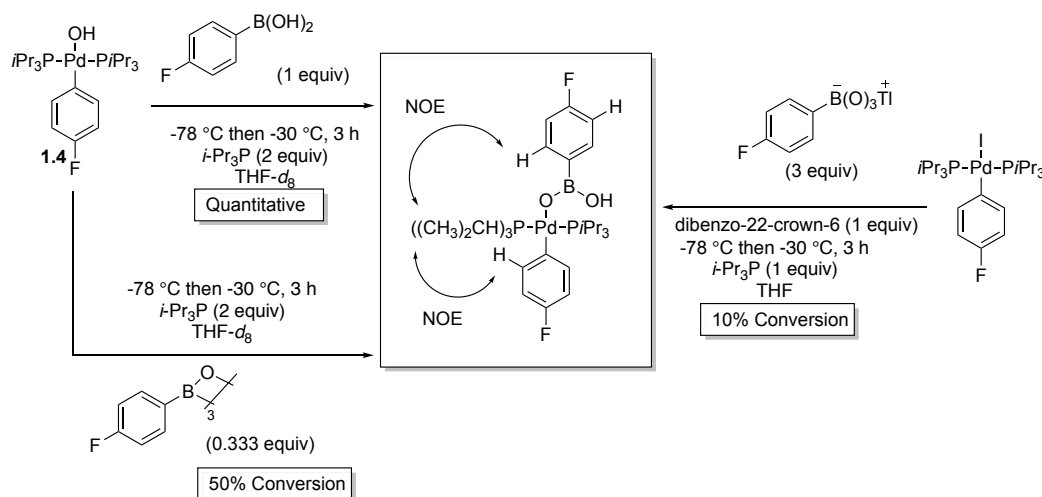


Scheme 5: Resting equilibrium concentrations of Pd complexes in solution.

The authors found that the resting concentration of Pd-halide complex **1.1** is lower than the combined concentrations of the Pd-oxo monomer, **1.3**, and dimer, **1.2**, complexes, although the difference between the two concentrations is less than one order of magnitude. It's worth noting that the concentration of the Pd-oxo species was higher at lower concentrations of water. This was thought to occur because of decreased hydration of free hydroxide ions at lower water concentrations.

In a related study, Amatore and Jutand used electrochemical methods to measure the rates of transmetalation and reductive elimination from isolated Pd-halide complexes.^[18] By measuring the oxidation and reduction currents that are generated in each step of the reaction, the concentration of each reactive species could be accurately determined. This could be extrapolated to provide rates of transmetalation for both Pd-oxo and Pd-halide species. The authors reported a conclusion in agreement with Hartwig, that transmetalation proceeds rapidly through the Pd-oxo complex and sluggishly through the Pd-halide complex, supporting the oxo-palladium pathway. Schmidt, who studied the rates of transmetalation through UV/Vis spectroscopic analysis, also reached the same conclusion.^[19]

While these three important studies all support a reaction mechanism that proceeds through the oxo-palladium pathway, the pre-transmetalation intermediates had never been observed. Denmark and Thomas recently elucidated the mechanistic missing link by using rapid injection low temperature NMR spectroscopy.^[20] The formation and decay of the active intermediates in the transmetalation step was monitored by reacting stoichiometric Pd-oxo complex **1.4** with neutral boronic acids at low temperatures (Scheme 6). Denmark's work represents the first unambiguous evidence for the proposed mechanistic path of this benchmark transformation.



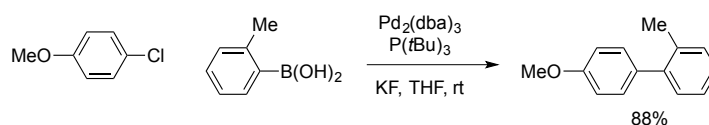
Scheme 6: Observation of B-O-Pd linkage by rapid injection NMR spectroscopy.

The authors also probed the most favourable pathway for transmetalation, showing the Pd-boron catalytically active intermediate is most readily reached from Pd-hydroxo complex **1.4**.

1.1.3 Advances in the Suzuki Miyaura Reaction

1.1.3.1 Increasing the Scope of Electrophiles

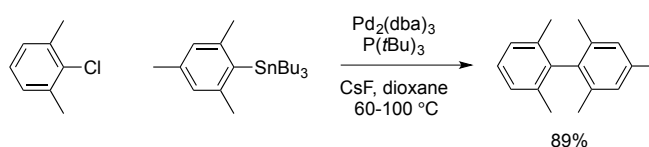
Despite its widespread use since first publication, for many years, the SM reaction was limited to the electrophile scope described in Suzuki's ground-breaking papers; bromides, sulfonates, and iodides.^[8] None of the standard conditions employed in the reaction showed any reactivity with chlorides or other less activated electrophiles (*e.g.*, OTs, OP(O)(OEt)₂). It wasn't until the late 1990's that reports emerged of the cross-coupling of unactivated aryl chlorides through the use of electron-rich phosphines.^[21,22]



Scheme 7: First example of using P(*t*Bu)₃ for the SM coupling of unactivated aryl chlorides.

Fu and co-workers used the bulky trialkyl phosphines P(Cy)₃ and P(*t*Bu)₃ to couple aryl chloride electrophiles effectively at room temperature (Scheme 7).^[21] The heightened reactivity of the Pd-phosphine complex in the oxidative addition step was attributed to the increase in nucleophilicity as a result of the electron-rich alkyl phosphine ligand. The increased steric hindrance also appeared to increase the reactivity of the catalyst as a result of a fast reductive elimination step. This versatile

catalyst system has also been found to facilitate efficient coupling of aryl chlorides in a range of other cross-coupling manifolds including Stille, Heck, and Negishi.^[23] The effectiveness of this catalyst system has been extended beyond aryl chloride electrophiles; Fu has also reported the rapid cross-coupling of hindered biaryls, including the first synthesis of a tetra-*ortho*-substituted biaryl using Stille cross-coupling (Scheme 8).^[23]



Scheme 8: Highly hindered Stille coupling with P(*t*Bu)₃.

Buchwald and co-workers simultaneously described an alternative method to Fu's trialkylphosphines, by using electron-rich dialkyl biaryl phosphines, Buchwald effectively coupled aryl chlorides at room temperature.^[22] The biaryl phosphine ligand employed in this report (DavePhos) became the template for a wide array of electron-rich biaryl phosphines developed within the Buchwald group (Figure 5).^[24]

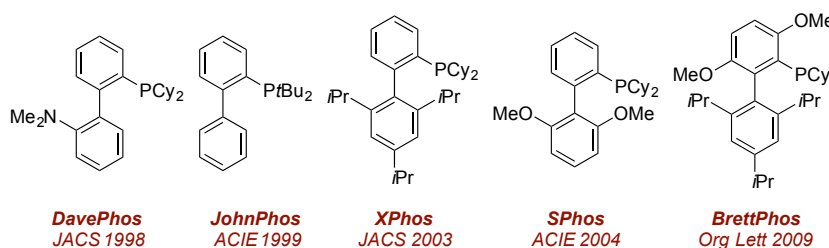


Figure 5: Selection of ligands developed in the Buchwald group.

The modified ligands each have minor changes compared to the template, leading to differing properties.^[25–28] With judicious choice of the correct ligand/catalyst system, almost any cross-coupling can be achieved. Buchwald outlined the importance of each aspect of the ligand systems based on an understanding of the mechanism of the SM reaction (Figure 6).^[29]

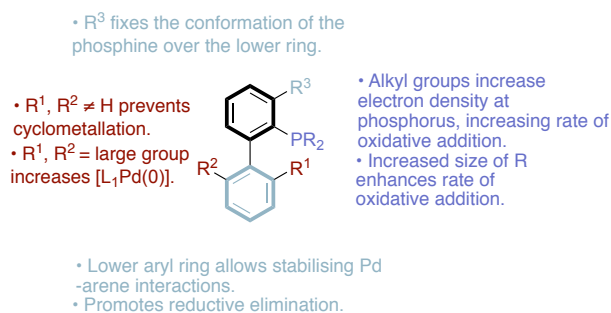


Figure 6: Ligand structure-activity-relationship.

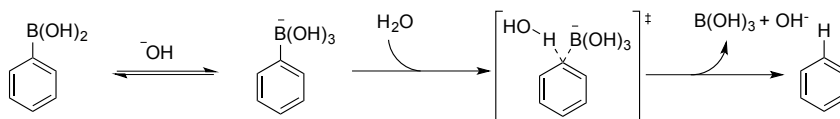
1.1.3.2 Nature of the Organoboron Reagent

While boronic acids remain the most commonly used boron reagents in SM coupling, a number of other reagents are available with differing properties and reactivities.^[34]

1.1.3.2.1 Boronic Acids

Boronic acids were first used in SM coupling in 1981 and are still one of the most commonly used boron reagents.^[35] Their popularity stems from good organic solubility, particularly in the typically polar solvents commonly used in SM chemistry and a wide commercial availability.^[34] Boronic acids are more reactive than their boronic ester counterparts (*vide infra*). While this has extended the utility of boronic acids towards a range of other transformations that are not facile with less reactive boron species (*e.g.*, Hayashi, Chan-Evans-Lam) it also leads to a small set of unwanted side-reactions within SM coupling, namely oxidation, homocoupling, and protodeboronation.^[34]

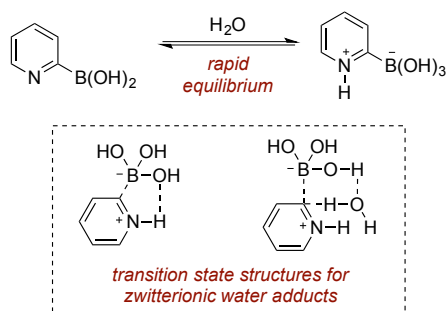
The most common of these is protodeboronation, which occurs under both acidic and basic conditions.^[36,37] Protodeboronated side-products will generally be seen in small quantities under SM conditions but this unwanted reaction is accelerated by high temperatures and variations in the pH of the reaction media.^[38] The mechanism for protodeboronation was first described by Kuivila, and has recently been confirmed and expanded upon by Lloyd-Jones.^[39] The most common source of protodeboronation occurs through a base-mediated pathway; electrophilic aromatic substitution of the boronic acid or its corresponding boronate abstracts a proton from either water, boric acid or another boronic acid to deliver the protodeboronated product (Scheme 10).



Scheme 10: Mechanism of base-promoted protodeboronation.

Protodeboronation is most prominently seen in heterocyclic boronic acids, particularly 2-pyridyl, thiazolium, and pyrazolyl boronic acids. Lloyd-Jones has shown that the degradation of these unstable boronic acids proceeds through a different mechanism to that of standard aryl boron species. The authors propose that

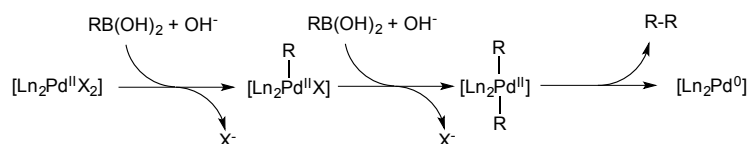
zwitterionic water adducts provide stabilisation of the boric acid leaving group, facilitating rapid protodeboronation at neutral pH (Scheme 11).



Scheme 11: Transition states for water assisted 2-pyridyl protodeboronation.

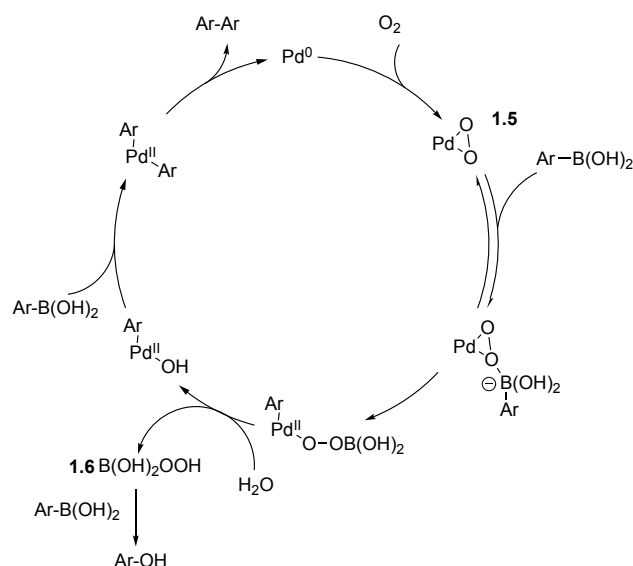
Unusually, this effect can be moderated by either high or low pH through alteration of the proportion of the charged species. Addition of Lewis acids such as CuCl_2 or ZnCl_2 can slow the rate of protodeboronation by up to a factor of 24. This occurs through complexation of the Lewis acids to the pyridine nitrogen, reducing the amount of reactive zwitterion available for fragmentation.

Homocoupling, another prominent side-reaction, can occur *via* two alternative mechanisms, either reductive activation of the Pd^{II} catalyst (Scheme 12)^[34] or through an oxidative mechanism that is typically only seen when the reaction is not run under inert conditions.



Scheme 12: Homocoupling from reductive activation of Pd.

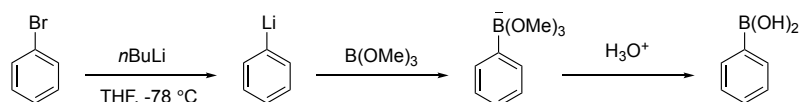
Oxygen present in the reaction mixture reacts with Pd^0 to form Pd^{II} peroxo species **1.5**, which can react with two equivalents of boronic acid to form homocoupled product (Scheme 12). Amatore and Jutand utilised electrochemical methods to illuminate the mechanism of formation of the Pd peroxo species and subsequent oxidative homocoupling.^[40]



Scheme 13: Mechanism of oxidative homocoupling.

This pathway is also responsible for the oxidation of boronic acids to alcohols, through perboric acid **1.6**.

Boronic acids can be synthesised relatively simply through the reaction of an organometallic compound with a boric acid ester, followed by acidic hydrolysis to release the boronic acid (Scheme 13). This method allows facile installation of the boronic acid functionality onto a wide variety of scaffolds.^[41]



Scheme 14: Formation of boronic acids through lithium halogen exchange.

1.1.3.2.2 Organoboranes

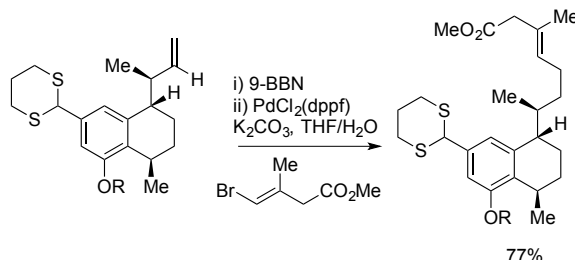
The first boron species to be used in SM were organoboranes with three carbons attached to a planar sp^2 boron (Figure 8). These reagents were widely used in early investigations into SM chemistry, as they are easily prepared *via* hydroboration of alkynes to form alkenyl organoboranes which can undergo subsequent cross-coupling.^[42]



Figure 8: Commonly used organoboranes.

Organoboranes suffer a number of disadvantages compared to boronic acids or esters, such as a lack of selectivity in transmetalation since each of the three substituents on boron can be transferred to Pd. These reagents are also prone to undergo a series of degradation processes such as aerobic oxidation, dehydroboration, and protodeboronation, leading to reduced yields even under the most stringent conditions.^[34] One of the most synthetically useful organoboranes is 9-borabicyclo[3.3.1]nonane (9-BBN), which contains a more rigid structure and thus provides greater selectivity in transmetalation than other organoboranes.

One significant advantage of sp^3 organoboranes over other boron reagents is the higher reactivity in SM cross-coupling, facilitating reluctant C-C bond formations that cannot proceed with other boron species. For these reasons, organoboron species have been used extensively as a class of cross-coupling partners in natural product synthesis. Their prevalence arises from the ease of preparation and they can often be made *in situ* to preclude isolation of the reactive organoborane, for example, a one pot hydroboration/SM reaction was used in the synthesis of dihydroxyserrulatic acid by Hayashi and co-workers (Scheme 15).^[43]



Scheme 15: Hydroboration/SM coupling on dihydroxyserrulatic acid.

1.1.3.2.3 Boronic Esters

Towards the end of the 1990's the use of boronic esters became prominent as more robust methods for their synthesis were developed. The most commonly employed are pinacol esters and catechol esters (Figure 9). Initial reports of boronic esters in SM employed catechol boronic esters, which can be readily prepared through hydroboration of terminal alkynes.^[8] Boronic esters are typically more stable than their boronic acid counterparts because of the σ -donation of carbon; making the oxygen lone pairs more readily able to donate into the adjacent empty p-orbital on boron, therefore reducing the Lewis acidity and reactivity of the boron centre.^[34]

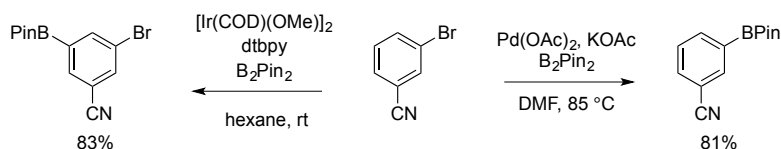
Boronic esters are also stable to chromatography and are soluble in non-polar solvents commonly used in synthetic organic chemistry.



Figure 9: Common boronic esters.

Boronic esters are proposed to react in SM through one of two pathways; partial hydrolysis of the ester under aqueous conditions to liberate the reactive boronic acid or *via* direct transmetalation of the boronic ester.^[34] It is difficult to unequivocally determine which pathway is correct, as water is almost always present under SM conditions.^[13,34]

While many methods for their preparation exist, on a laboratory scale, boronic esters (particularly BPins) are typically synthesised through either the Pd-catalysed Miyaura borylation^[44] or *via* Ir-catalysed C-H borylation^[45,46] (Scheme 16). The invention of these complementary methodologies has opened up the scope of cross-coupling allowing ready access to a wide library of borylated molecules.



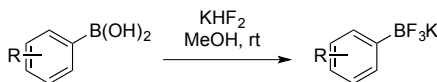
Scheme 16: Borylation of arenes *via* Ir- and Pd-catalysed borylations.

A combination of the ease of synthesis and favourable physical properties of boronic esters, such as solubility and stability, has made them one of the most popular cross-coupling partners in SM chemistry.

1.1.3.2.4 Organotrifluoroborates

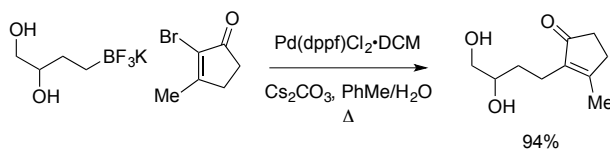
Organotrifluoroborates (BF_3K) were first discovered in the 1960's but the application of this reagent was limited until pioneering work by Molander and Batey in the early 2000's using organotrifluoroborates as an alternative reagent for SM coupling.^[47–49] As bench-stable, crystalline solids, BF_3K salts are appealing reagents in SM chemistry when compared to their boronic acid and ester counterparts.

BF₃K salts can be easily prepared from boronic acids by stirring with aqueous KHF₂ in methanol; the range of available boronic acid compounds gives ready access to vast numbers of BF₃K salts and many are now commercially available (Scheme 17).^[50]



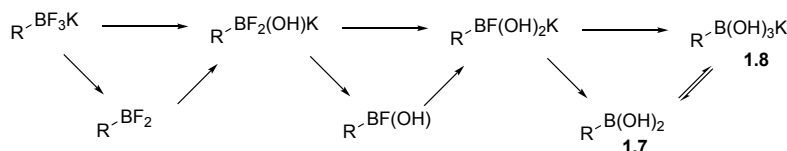
Scheme 17: Synthesis of BF₃Ks from boronic acids.

The Molander group has extensively demonstrated the versatility of these reagents in SM coupling, through the synthesis and application of BF₃Ks across a wide array of substrates.^[51] One particularly appealing feature of BF₃Ks is the capacity to couple sp³ alkyl trifluoroborates with vinyl and aryl bromides in good to excellent yields (Scheme 18).^[52]



Scheme 18: Example of alkyl SM coupling.

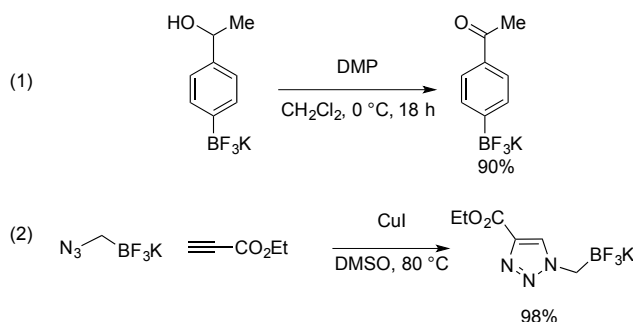
The enhanced reactivity of BF₃K salts towards sp³ nucleophile cross-coupling can be explained in part by their mechanism of action in SM coupling. In biphasic media, BF₃K salts are slowly hydrolysed to give boronic acids, which then undergo rapid transmetalation.³⁶ Slow release of the parent boronic acid ensures a low concentration of the reactive species is maintained throughout the reaction. Hydrolysis of the BF₃K salts proceeds through a complex series of boron species, resulting in an equilibrium between boronic acid **1.7** and boronate **1.8** (Scheme 19).^[53]



Scheme 19: Slow release of boronic acids from BF₃K through hydrolysis cascade.

Another appealing application of BF₃Ks is as a boronic acid protecting group. Due to their increased stability over both boronic acids and esters, BF₃K groups can be taken through multiple steps in a reaction sequence. Molander has shown they will survive exposure to a number of oxidising conditions, such as Swern, Ley, and Dess-Martin oxidations.^[54] OsO₄ and dimethyl dioxirane (DMDO) for the preparation of diols and epoxides were likewise tolerated.^[55] Moreover, the BF₃K salts stayed intact when

subjected to both Wittig/Horner-Wadsworth-Emmons reactions^[56] (Scheme 20, equation 1) and Huisgen type 1,3-dipolar cycloadditions^[57] (Scheme 20, equation 2) to form olefins and triazoles, respectively, leading to various useful compounds with a SM-compatible functional handle present.^[54–58]



Scheme 20: Use of BF₃K as a boronic acid protecting group.

Despite the successes in this area, BF₃Ks are acid- and base-labile and decompose upon exposure to silica and some protic solvents, limiting the use of these reagents to a series of mild transformations.^[34] Many of the manipulations demonstrated by Molander require a KHF₂ work up, suggesting that the BF₃K is not always left intact by the end of the reaction.^[59,60] For small-scale chemistry, these limitations present a disadvantage, as reactions on more highly functionalised molecules often need chromatographic purification. This is perhaps offset by the ease of crystallisation at a larger scale where the use of chromatography is limited.

1.1.3.2.5 MIDA Boronic Esters

MIDA boronic esters (BMIDAs) are another prominent class of boron species. These were first synthesised in the 1980s by Mancilla^[61] but have seen resurgence in the last decade, chiefly through work by the Burke group in Illinois.^[62] BMIDAs are base-labile boronic esters that, like BF₃Ks, are free-flowing solids and are tolerant of a wide range of reaction conditions. Donation of the nitrogen lone pair into the boron empty p-orbital lends the boron sp³ character, which renders the BMIDA unit inert to a range of standard boron chemistries, including transmetalation (Figure 10).

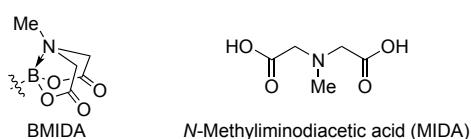
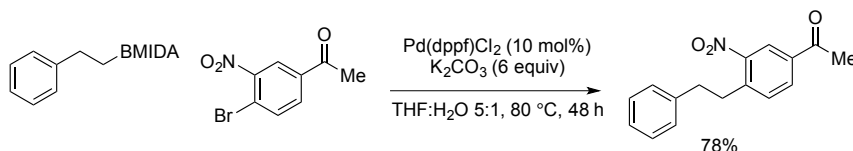


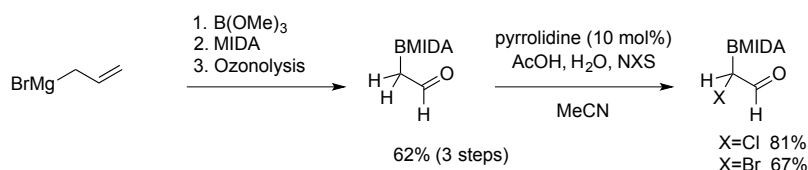
Figure 10: MIDA acid and boronic ester.

In 2014, the Yudin group reported a general method for the SM coupling of sp^3 BMIDAs with aryl bromides.^[65] It was found that excess equivalents of base and a high catalyst loading were necessary for good conversion in this process. A range of alkyl BMIDAs were successfully coupled, providing a complementary approach to Molander's work with BF_3Ks (Scheme 22).^[65]



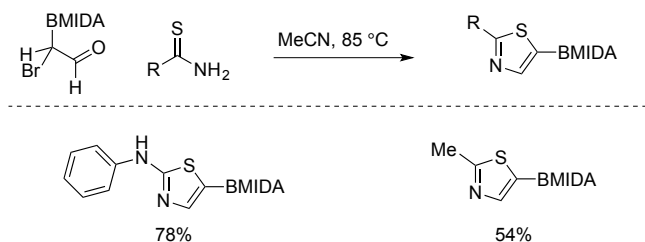
Scheme 22: Intermolecular sp^2 - sp^3 SM cross-coupling.

The Yudin group also used MIDA esters in the preparation of α -boryl aldehydes, which were used as precursors to a wide scope of borylated scaffolds.^[66] The α -boryl aldehyde precursors could be synthesised in three steps by a one-pot procedure from allyl Grignard reagent. Subsequent α -halogenation of the aldehyde in the presence of catalytic pyrrolidine gives the desired halide in good yield (Scheme 23).



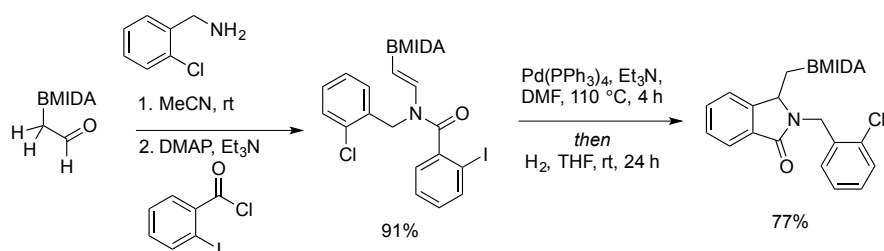
Scheme 23: Synthesis of α -boryl aldehydes.

The halogenated species could then be condensed with thioamides and thioureas to form borylated heterocycles in good to excellent yields (Scheme 24).



Scheme 24: Condensation of α -boryl aldehydes to form thiazoles.

The boryl enamine intermediate could also be trapped with an acyl chloride to give α -boryl enamides in good yields. Sequential intramolecular Heck coupling and hydrogenation on these products were then carried out to provide borylmethyl-isindolones (Scheme 25).

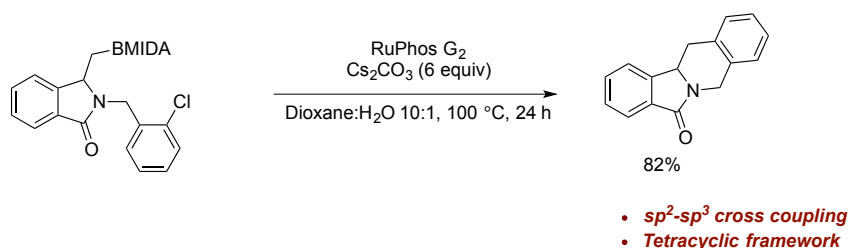


Enamine formation/Trapping

5-exo-trig Heck cyclisation/Hydrogenation

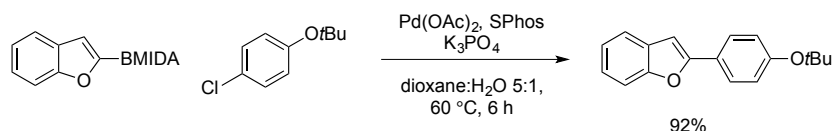
Scheme 25: Synthesis of α -boryl enamides and subsequent Heck cyclisation.

The utility of these borylated heterocycles was then demonstrated through an sp^2 - sp^3 intramolecular SM cross-coupling to provide tetracyclic compounds, which represent the key skeleton of the bioactive natural product lennoxamin (Scheme 26).



Scheme 26: sp^2 - sp^3 Intramolecular SM reaction to form tetracyclic frameworks.

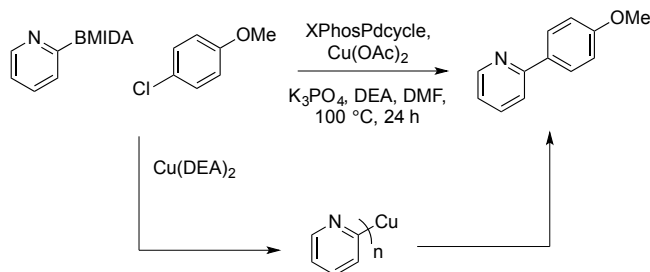
MIDA protection has also been effective in the coupling of unstable boronic acids. 2-Heterocyclic boronic acids are known to readily protodeboronate under ambient conditions, rendering the SM cross-coupling of functionalised heterocycles a difficult task. The employment of protected boronic acids provides one solution to this problem, since 2-heterocyclic BMIDA esters are bench stable solids that can be made on large scale.^[67] In solution the MIDA protecting group is slowly hydrolysed under basic conditions, releasing the free boronic acid in low concentrations throughout the reaction. The reactive boronic acid is then cross-coupled immediately, before degradation can begin (Scheme 27).^[68]



Scheme 27: Slow-release SM coupling of 2-heterocyclic BMIDAs.

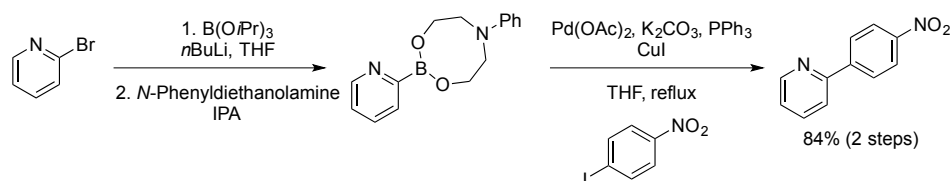
The 2-pyridyl problem is an important example of this issue; while both 3- and 4-pyridyl boronic acids can undergo effective cross-coupling, substitution at the 2-position is not well tolerated due to the very low stability of these residues. The use of copper additives has been shown to dramatically improve the outcome of the SM reaction of 2-pyridyl boronic acids. Burke and co-workers used $Cu(OAc)_2$ and

diethanolamine as additives to facilitate the coupling; the authors suggested that transmetalation occurred through an aryl copper intermediate that is formed *in situ*.^[69] Recent data from Lloyd-Jones has shown this to be a result of Lewis acid-mediated inhibition of protodeboronation (Scheme 28).^[39]



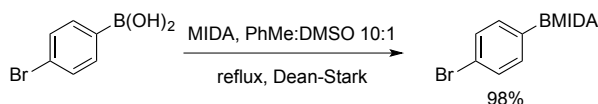
Scheme 28: Cu-mediated SM coupling of 2-pyridyl BMIDAs.

Burke was not the first to employ protected boronic acids to overcome this stability issue. Hodgson cross-coupled 2-pyridyl systems under similar conditions using *N*-phenyl diethanolamine as an alternative mask for the boronic acid (Scheme 29).^[70]



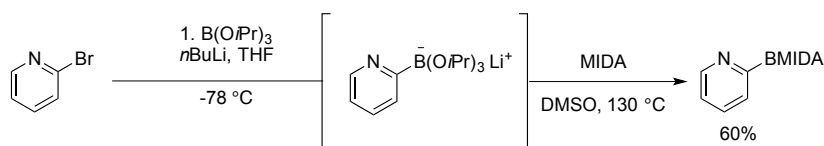
Scheme 29: Early example of a protecting group to enable coupling of 2-pyridyl boronic acids.

BMIDAs can be simply prepared through condensation of *N*-methyliminodiacetic acid with a boronic acid. The BMIDA ester is either directly precipitated out of solution or can be easily recrystallized to yield a white, free flowing, crystalline solid (Scheme 30).^[71]



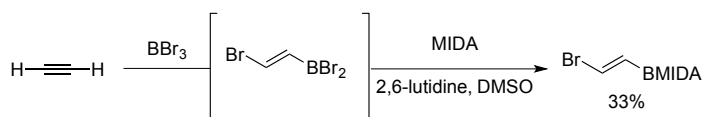
Scheme 30: Synthesis of BMIDA through condensation of MIDA with boronic acid.

If the boronic acid is unavailable or too unstable to be isolated then the BMIDA unit can also be introduced from halogenated species. Borylation of a metalated carbon centre using $B(OiPr)_3$ followed by addition of MIDA acid affords the desired ester in good yield. This method is efficient and atom economical; however, due to the use of highly reactive lithium and magnesium reagents, the application of this method is limited because of its complex operation and functional group intolerance (Scheme 31).^[71]



Scheme 31: Synthesis of 2-pyridyl BMIDA from aryl bromide.

An alternative, non-organometallic method for the formation of BMIDA esters is commenced with bromoborylation of an alkyne with BBr_3 to give an unstable borylalkene intermediate, which can be further trapped with MIDA acid to provide the MIDA ester in modest yield (Scheme 32).^[72]



Scheme 32: Formation of MIDA ester through bromoborylation.

1.1.4 Chemoselectivity in the SM reaction

Chemoselectivity in the SM reaction is mainly achieved through four distinct methods; electrophile chemoselectivity, protecting group strategies, vicinal/geminal activation and aryl/benzyl chemoselectivity (Figure 11).^[73]

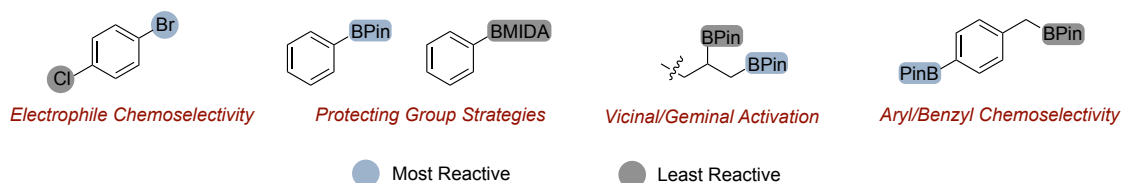


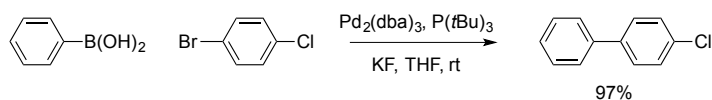
Figure 11: Strategies for chemoselectivity in the SM reaction.

The following section will describe the state of the art in all four areas.

1.1.4.1 Electrophile Chemoselectivity

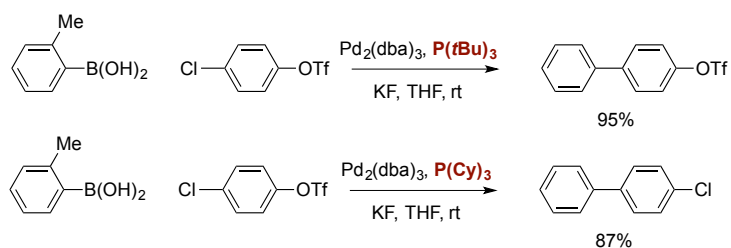
Electrophile chemoselectivity is the most commonly employed method for attaining selectivity in the SM reaction. The selective monofunctionalisation of a more reactive electrophile over a less reactive electrophile has played an important role in the field of cross-coupling. The order of reactivity for halides and pseudo-halides in SM is well established and was set out by Suzuki in his early ground-breaking work on the SM reaction, as $\text{I} > \text{Br}, \text{OTf} \gg \text{Cl}$.^[8] The differences in reactivity are defined by the electronegativity of the leaving group, therefore the C-X bond strength or bond dissociation energy (BDE). As I is least electronegative, it has the lowest BDE and is in turn the most reactive C-X bond.

While this phenomenon has been known for many years the most comprehensive demonstration came in 2000 when Fu exploited this reactivity bias to selectively mono-couple a boronic acid with a dihaloarene (Scheme 33).^[74]



Scheme 33: Chemoselective monocoupling of 1-bromo-4-chlorobenzene.

Of particular note in this report was the ability to reverse the outcome of the SM coupling through alteration of the ligand (Scheme 34).



Scheme 34: Selectivity between Cl and OTf based on ligand selection.

When $P(tBu)_3$ was employed as the ligand, cross-coupling between boronic acid and chloride was observed, while the product of cross-coupling between the boronic acid and triflate was obtained in the presence of $P(Cy)_3$. This unprecedented reactivity can be explained by the difference in reactivity between mono- and bis-ligated palladium complexes, where the mono-ligated complex formed with the bulky $P(tBu)_3$ reacts preferentially with a chloride electrophile instead of a triflate. This phenomenon has been explained in great detail in the work of Schoenebeck and Sigman through both computational and experimental means but is outside the scope of this discussion.^[75,76]

This work by Fu is particularly impressive as selectivity is obtained between two ostensibly equivalent electrophiles (Br vs. OTf) and the concept is pushed further to demonstrate selectivity against the defined reactivity gradient (Cl vs. OTf).

While Fu uses prudent catalyst selection to induce chemoselectivity, it is possible to exploit the natural reactivity of the substrate to gain chemoselective control. This chemoselectivity is of great importance in dihaloheterocycles where two equivalent halides can be differentiated either *via* electronics (where the most electron deficient halide will react first) or by directing group effects (Figure 12).^[77]

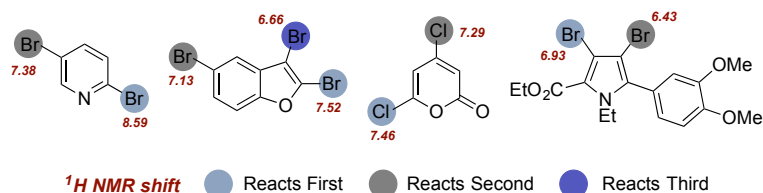
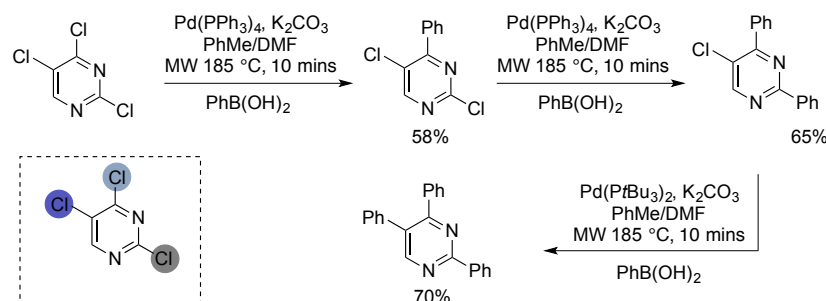


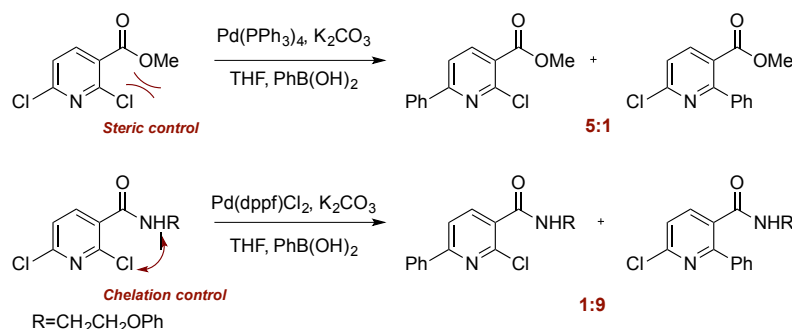
Figure 12: Electronic discrimination within multiple halogenated heterocycles.

A review by Fairlamb^[77] describes the site-selectivity across a wide range of dihaloheterocycles and how the selectivity can be predicted *a priori* through Zhang's method, which correlates the ¹H NMR shifts of the dehalogenated parent heterocycles to the regioselectivity.^[78] For example 2,4,5-trichloropyrimidine will react preferentially at the 4-position, followed by the 2-position, and finally at the 5-position (Scheme 35).^[79]



Scheme 35: Sequential chemoselective coupling of 2,4,5-trichloropyrimidine.

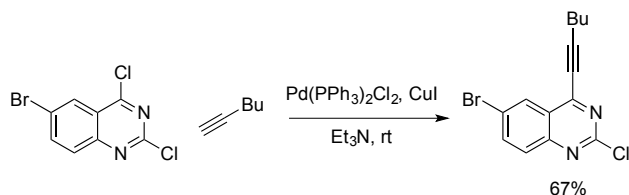
Electronically equivalent halides can be discriminated through the directing effect of neighbouring Lewis bases. For example, the selectivity in 2,6-dibromopyridines can be switched through altering the substituent in the 3-position. When a non-directing ester is used, oxidative addition at the less sterically demanding 6-position is favoured. Switching to a chelating amide alters the site selectivity toward the 2-position (Scheme 36).^[80]



Scheme 36: Selectivity switch through chelation control.

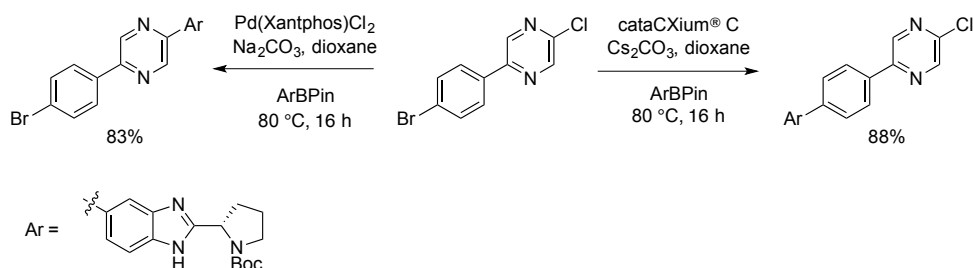
In certain cases the electronic effect arising from heterocyclic halides can overcome the conventional reactivity gradient. The Undheim group showed 2,4-dichloro-6-bromoquinazolines cross-coupled at the more electron deficient chloride in the 4-

position over a typically more reactive bromide across a range of cross-coupling manifolds (Scheme 37).^[81]



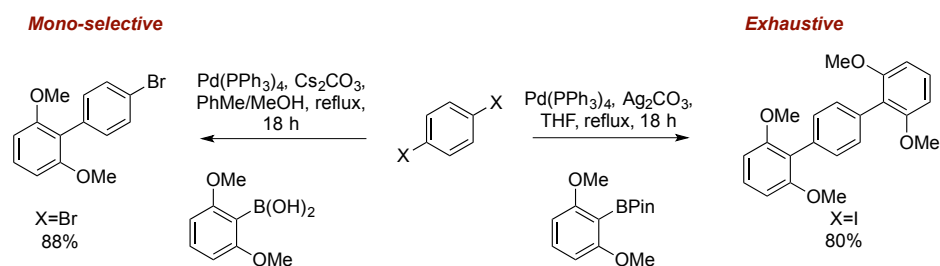
Scheme 37: Site-selective Sonogashira coupling of 2,4-dichloro-6-bromoquinazolines.

A research group at Pfizer have demonstrated chemoselectivity for a chloropyrazine over a bromoarene. Through a systematic ligand screen, the group found that by using a bidentate Xantphos catalyst they could gain selectivity for the ‘less reactive’ chloride. This selectivity could be reversed by moving to a monodentate cataCXium[®] ligand to provide high selectivity for the bromo-coupled product (Scheme 38).^[82]



Scheme 38: Selective SM coupling of chloropyrazine vs aryl bromide.

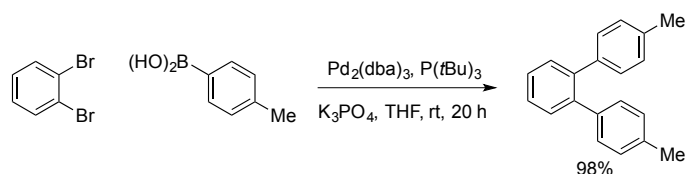
While levels of chemoselectivity between differentiated dihaloarenes are well established, chemoselective control between exhaustive and mono coupling remains a challenge. Sherburn has shown that alteration of the halide electrophile and the boron nucleophile can dramatically influence the outcome of the reaction, providing either exhaustive or mono-coupling (Scheme 39).^[83]



Scheme 39: Mono vs. exhaustive coupling based on substrate control and alteration of the reaction media.

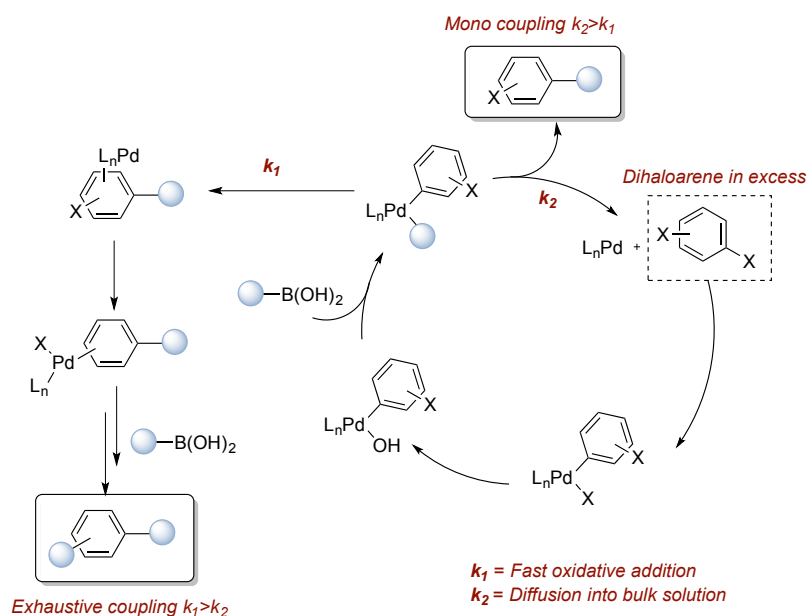
While good selectivities were obtained in this study, the reaction was highly substrate-specific and the chemoselectivity was eroded with even slight changes to the reaction medium. Since Sherburn’s seminal report, the selectivity between mono- and exhaustive cross-coupling has been more comprehensively explored. In 2005,

Hu disclosed a $\text{Pd}_2(\text{dba})_3/\text{P}(t\text{Bu})_3$ catalyst system that effectively furnishes the exhaustive coupling products for a range of dihalobenzenes with exquisite selectivities (Scheme 40).^[84]



Scheme 40: Exhaustive coupling using Pd/P(*t*Bu)₃ catalyst system.

The authors hypothesised that in order to achieve exhaustive coupling with an excess of dihalide, oxidative addition of the regenerated Pd^0 species with the newly formed biaryl halide must occur faster than diffusion of the Pd^0 into the bulk solution (Scheme 41). It is suggested that this selectivity could be applied in controlled Pd-catalysed polymerisation. This theme was continued recently by Larrosa and Goldup who used Pd-NHC complexes (PEPPSI-IPent) to affect exclusive bis-coupling across a wide range of substrates while employing a near universal palette of metal nucleophiles (Mg, Zn, B).^[85] The key advance in this study was the application of the methodology to dichloroarenes, which had been absent in previous studies.

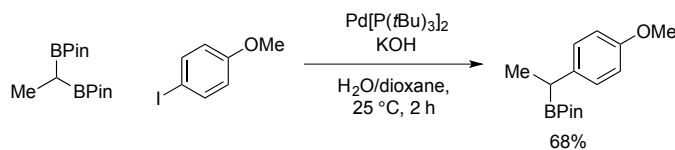


Scheme 41: Rationalisation for exhaustive cross-coupling.

1.1.4.2 Chemoselective Transmetalation *via* Vicinal/Geminal Activation

In 2010, Endo and Shibata reported the first example of geminal activation of sp^3 BPins.^[86] Taking 1,1-diborylethane and iodoanisole the authors showed, under mild

cross-coupling conditions, selective mono-functionalisation of the geminal BPin (Scheme 42).



Scheme 42: Mono-functionalisation of geminal diboron species.

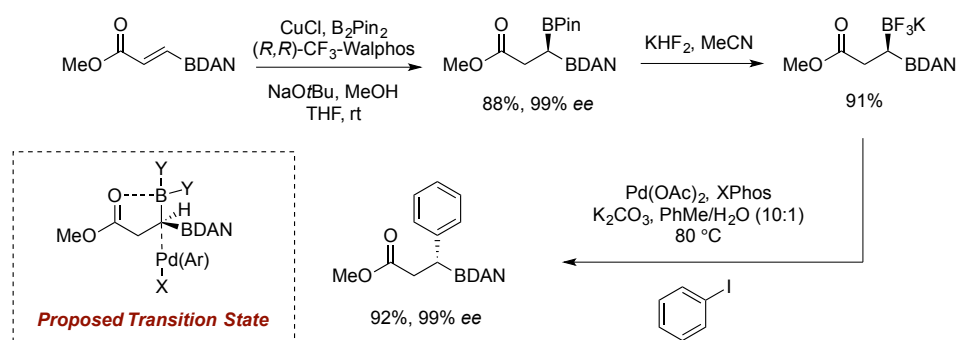
Shibata suggests that the geminal BPin activation arises from an increase in Lewis acidity of one of the boron atoms. The proposed increase in Lewis acidity allows for selective boronate formation of a single BPin boronate, which is proposed to be the active species in transmetalation. This hypothesis is supported experimentally and by NMR. A summary of the key arguments is as follows.

- Formation of a BPin boronate is only achieved under forcing conditions in most systems.
- Formation of a BPin boronate in geminal diboron species was observed by ¹¹B NMR at room temperature with KOH.
- Cross-coupling of geminal diboron species was only observed with strong bases.
- No reaction was observed with 1,1-borylsilylalkanes or with primary borylalkanes.

The compelling evidence presented by Shibata strongly suggests a boronate pathway and was, in effect, contrary to much of the literature published at the time.

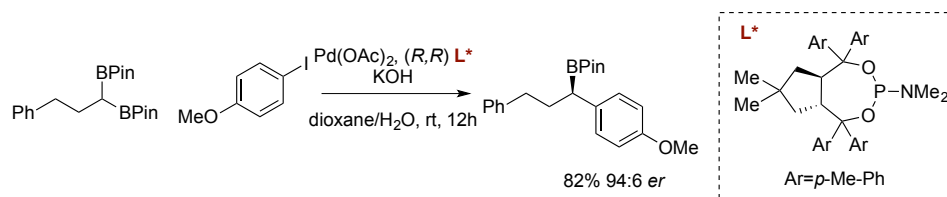
In 2011, Hall reported the synthesis of enantioenriched geminal diboron compounds and their stereospecific cross-coupling.^[87] Using cuproboration chemistry on β -boryl unsaturated esters Hall prepared 1,1-diboron compounds with high enantioselectivity. The chemoselectivity was established in the cross-coupling step by using the protected boronic acid BDAN (*vide infra*), which is inert to transmetalation but is still able to activate a neighbouring boron species (BF₃K in this case) (Scheme 43). To explain the inversion of stereochemistry in this coupling

Hall invokes a model proposed by Suginome and Molander, where backside attack of the palladium complex on the boron bearing carbon is more favourable than a traditional transmetalation step.^[88,89]



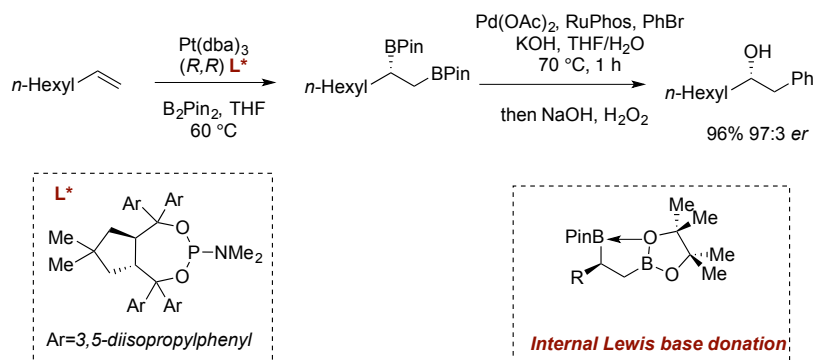
Scheme 43: Stereoinvertive SM cross-coupling of 1,1-diboryl compounds.

More recently, Morken disclosed the enantioselective cross-coupling of geminal BPins.^[90] By using a Taddol-based chiral ligand the enantiotopic geminal BPin can be discriminated with excellent selectivities. While the authors did not comment on the hybridisation of the active boron species, a large excess of KOH was required for selectivity, suggesting that a BPin boronate is present in the reaction (Scheme 44).



Scheme 44: Enantioselective SM coupling of geminal BPins.

Morken has also demonstrated the chemo- and stereoselective cross-coupling of vicinal BPins.^[91] Enantioselective diboration of terminal alkenes using a chiral Pt catalyst yields the enantioenriched vicinal diboron compounds, which could then be cross-coupled under similar conditions to the geminal diboron systems. Morken suggests that rather than external activation with hydroxide the vicinal diboron system self-activates through internal Lewis base donation, allowing for better coordination to a reactive Pd(OH) species (Scheme 45).



Scheme 45: Enantioselective diboration/cross-coupling sequence disclosed by Morken.

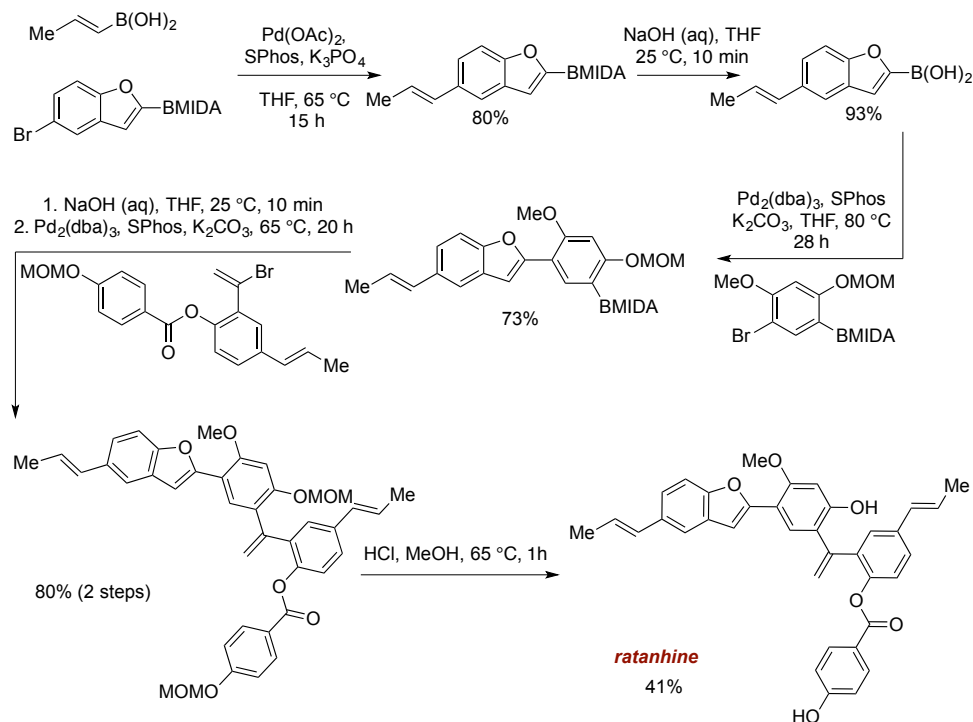
The facile introduction and application of chiral boron species through either vicinal or geminal strategies allow for the rapid construction of enantioenriched frameworks. Discrimination of diboron systems through chemoselective transmetalation opens up many opportunities for the generation of molecular complexity, this burgeoning field will likely continue to produce innovative solutions to the general problem of sp^3 cross-coupling.

1.1.4.3 Chemoselective Transmetalation *via* Protected Boron Species

Over the last 10 years the use of protected boron species has increased dramatically, this can mainly be attributed to the resurgence of BF_3K , BMIDA, and BDAN groups. The use of these protected boronic acids in diboron systems can be regarded as chemoselective transmetalation, as two boron species enter the reaction but only the unprotected boron species is free to react. The following section will describe some recent examples of chemoselective transmetalation using protected boron species and the respective advantages and disadvantages of each protecting group in the context of diboron systems.

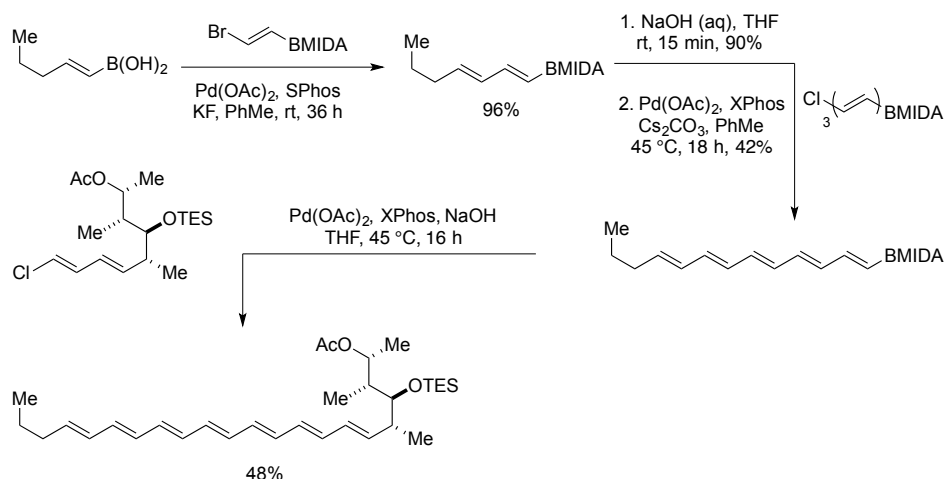
1.1.4.4 Use of BMIDA in Chemoselective Transmetalation

The use of BMIDAs in iterative cross-coupling constitutes some of the first examples of chemoselective transmetalation and indeed, the first application of diboron systems in the context of SM. Using anhydrous SM conditions, the Burke group synthesised the natural product ratanhine from four simple starting materials.^[92] Using a cross-coupling/deprotection strategy the natural product could be synthesised in a modular, iterative fashion in just six steps (Scheme 46).



Scheme 46: Six-step synthesis of ratanhine through iterative cross-coupling using MIDA protected boronic acids.

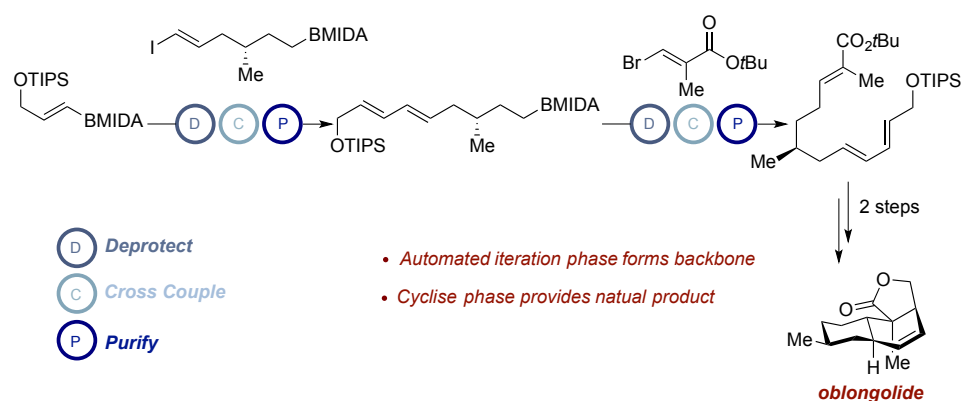
Due to the sensitive nature of the BMIDA functionality towards the aqueous basic conditions required for SM coupling, a number of different ‘dry’ conditions have been developed for their use. Using the mild base KF as an activator for Pd and an electron-rich phosphine ligand, vinyl BMIDAs could be coupled effectively in the absence of water. This technique was exploited in the synthesis of the polyene framework of the natural product amphotericin B (Scheme 47).^[72]



Scheme 47: Synthesis of the polyene framework of amphotericin B through anhydrous iterative SM cross-coupling.

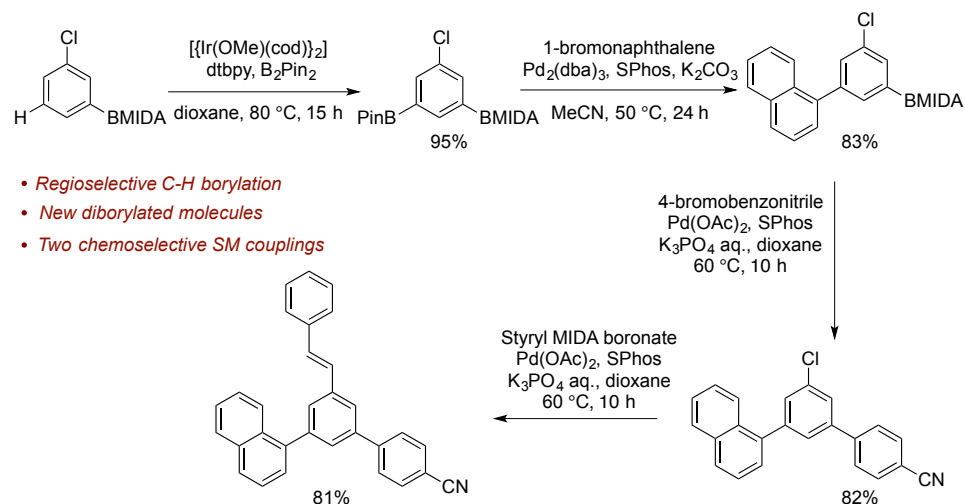
Burke has pushed the limits of this technology through automation; by building a ‘synthesis machine’ that performs SM cross-coupling, chromatographic purification,

and hydrolysis of the MIDA protecting group in an iterative fashion, the synthesis of 14 different classes of small molecule can be achieved.^[93] This advance is built upon the ‘catch and release’ purification step, which is based on the highly polar nature of BMIDA groups. The crude reaction mixture is delivered to a silica column, which is flushed with MeOH in Et₂O to remove any impurities; the BMIDA is then washed through the column with THF. The synthesis machine seamlessly combines chemoselective cross-coupling of haloaryl BMIDAs, ‘catch and release’ purification and deprotection steps to perform multiple iterative cross-couplings in an automated manner. The utility of this technology was demonstrated with the automated synthesis of several natural products (Scheme 48).



Scheme 48: Automated synthesis of the natural product oblongolide via iterative SM cross-coupling.

Further contributions to this area have come from the Li group who synthesised site differentiated diboron compounds using C-H borylation. Li showed that Ir-catalysed C-H borylation could be performed on BMIDA containing molecules, providing an array of aryl diboron compounds.^[94] These could then be chemoselectively coupled to give functionalised aryl BMIDAs, which then in turn could be cross-coupled (Scheme 49).

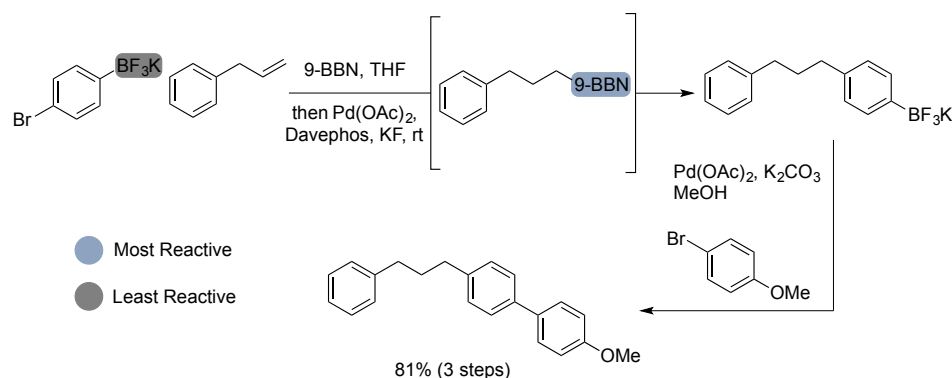


Scheme 49: Synthesis and chemoselective SM coupling of diboron compounds.

1.1.4.5 Use of BF_3K in Chemoselective Transmetalation

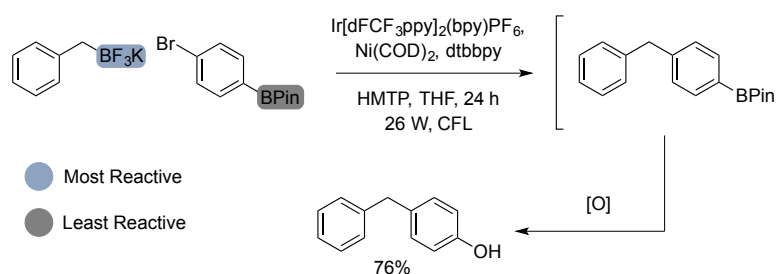
While the physical attributes of BF_3K s have already been discussed, they have also played an important role in diboron systems, facilitating chemoselective transmetalation.

Molander first employed BF_3K s in diboron systems in 2008 when he selectively coupled alkyl organoboranes to haloaryl BF_3K s.^[95] Hydroboration of vinyl bearing BF_3K s with 9-BBN followed by *in situ* cross-coupling with retention of the BF_3K (Scheme 50). It is worth noting that KF is used as base in the coupling reaction, which will help to conserve the integrity of the BF_3K .



Scheme 50: Chemoselective transmetalation of an organoborane over a BF_3K .

Molander was able to reverse this chemoselectivity using photoredox chemistry to selectively cross couple a BF_3K in the presence of a BPin moiety.^[96] A combination of Ni and Ir catalysis is used to selectively activate an sp^3 BF_3K towards cross-coupling forming a new C-C bond with an aryl bromide (Scheme 51).



Scheme 51: Chemoselective transmetalation of a BF_3K over a BPin using photoredox catalysis.

1.1.4.6 Use of BDAN in Chemoselective Transmetalation

BDANs are another class of protected boronic acid, developed by Suginome in 2007 which are derived from the parent boronic acid and diaminonaphthalene.^[97] BDANs possess broadly orthogonal reactivity to BF_3K s and BMIDAs as they are acid labile, but completely tolerant of even strongly basic conditions (Figure 13). Similarly to BMIDAs, they are inert to transmetalation due to donation of the nitrogen lone pairs into the empty p-orbital of boron. As such, they have been exploited in diboron systems to enable chemoselective cross-coupling.

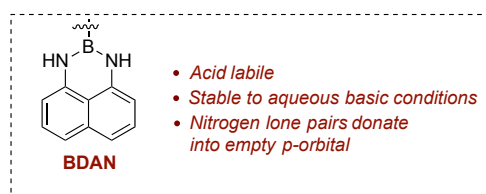
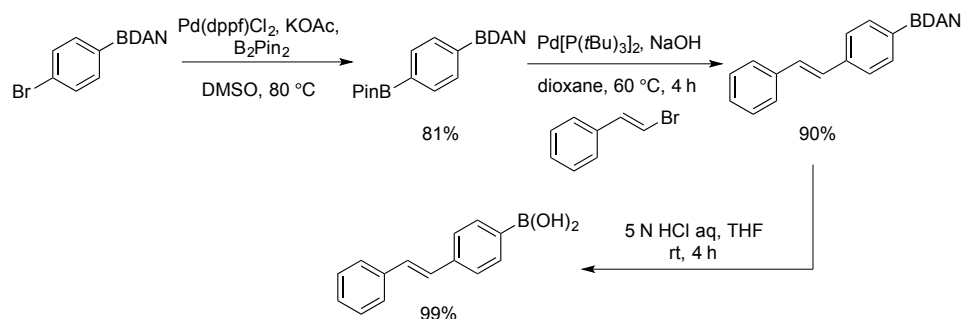


Figure 13: Structure and properties of DAN protected boronic acids.

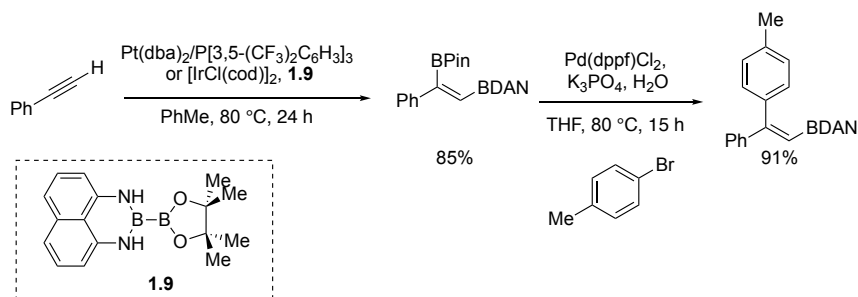
In 2008, Suginome reported the preparation and application of differentially protected diboron systems.^[98] Miyaura borylation of haloaryl BDANs gave access to monoprotected diboronic acid derivatives that could in turn be cross-coupled under standard SM conditions while leaving the BDAN intact. The parent boronic acids could finally be revealed in excellent yields through acidic hydrolysis (Scheme 52).



Scheme 52: Regioselective transmetalation of a BPin over a BDAN .

Intriguingly, Suginome used the large steric demand of the BDAN group to synthesise differentially protected olefinic diboron species with complete

regioselectivity.^[99] Using Ir or Pt catalysis, the unsymmetrical diboron compound **1.9** was added across terminal alkynes to give the BDAN at the least hindered side. The resulting olefinic diboron reagents could be subjected to chemoselective cross-coupling before deprotection of the DAN group (Scheme 53).

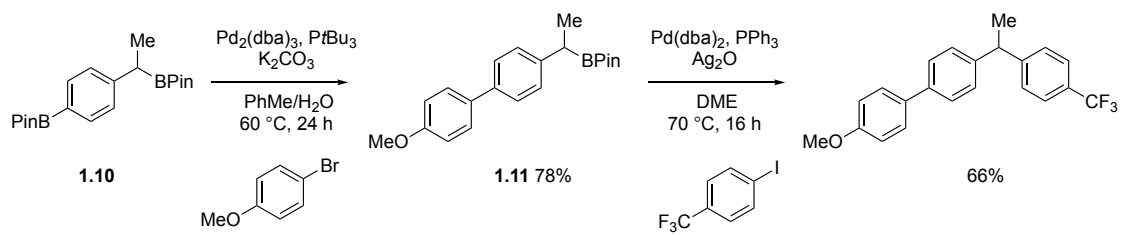


Scheme 53: Chemoselective diboration and subsequent SM cross-coupling.

While the physical properties of BDANs make them perhaps the most logical choice for use in SM coupling, they have been underdeveloped in comparison to BMIDAs and BF₃Ks. This may be in some part a consequence of the relative difficulty of the protection/deprotection steps. It is not challenging to imagine functionalities (including many boronic acids) that are not tolerant of prolonged exposure to concentrated acid. Despite this, BDANs still hold a complimentary place alongside BMIDAs and BF₃Ks.

1.1.4.7 Aryl/Benzyl Chemoselectivity

The Crudden group has shown chemoselectivity between aryl and benzyl BPins. Using di-nucleophile **1.10** the authors demonstrated that in the absence of Ag salt additives aryl BPin couple exclusively in the presence of benzylic BPin nucleophiles. The coupled product **1.11** can then be effectively reacted in a second SM coupling under Ag mediated conditions (Scheme 54).^[100] Previous work from the group has shown that despite being unreactive towards SM under standard conditions, benzylic BPin couple effectively when Ag₂O is used as an additive. While the origin of this reactivity is currently unknown, the phenomenon is relatively general and can also be applied to allylic BPin.^[101]



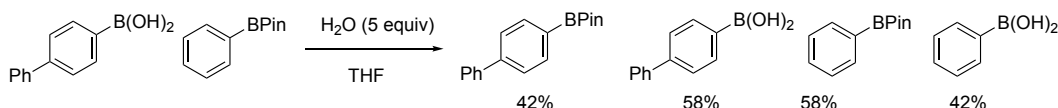
Scheme 54: Sequential SM couplings enabled by aryl/benzyl chemoselectivity.

1.2 Project Background

1.2.1 Boron speciation

In this section the concept of boron speciation will be introduced and examples of this phenomenon in the literature will be discussed, including its application and importance in SM cross-coupling.

Boron speciation refers to the exchange of ligands and a change in oxidation state of boron through a series of equilibria. A simple and representative example of boron speciation is the exchange of pinacol ligands on boronic acids under basic conditions (Scheme 55). When a boronic acid and a BPin are treated with aqueous base, the pinacol ligand will transfer rapidly to give a statistical mixture of products.^[102]



Scheme 55: Boron speciation between B(OH)₂ and BPin.

Brown and Matteson were able to exploit the rates of transesterification of vicinal diols to scavenge pinene-derived chiral auxiliaries, which form very stable boronic esters.^[103,104] Further studies into the stability of boronic esters towards transesterification established an order of stability for various chiral and achiral boronic esters (Figure 14).^[105]

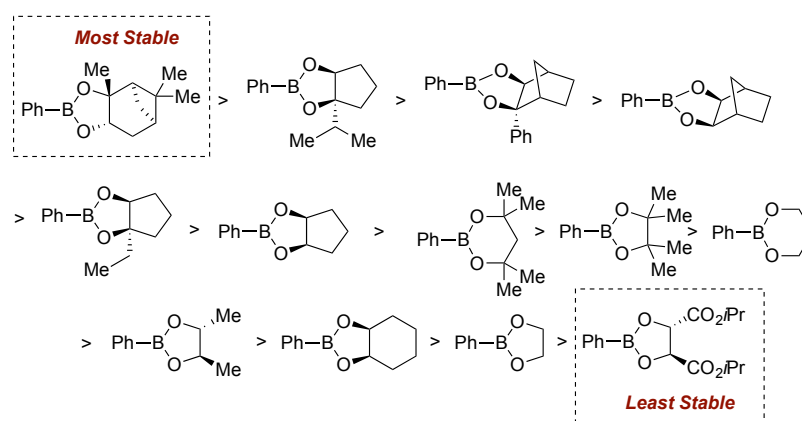
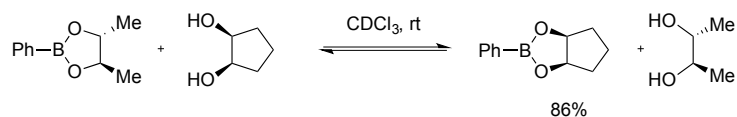


Figure 14: Order of hydrolytic stability for common boronic esters.

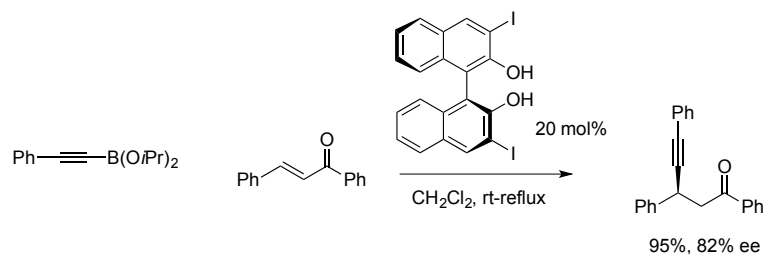
This order was established through the treatment of a boronic ester with a range of vicinal diols and measuring the equilibrium ratios of the two resulting boronic esters (Scheme 56).



Scheme 56: Measurement of relative boronic ester stability through equilibration.

A more detailed study into the effect of reaction media on diol conjugation came from Springsteen and Wang.^[106,107] Through a series of highly intricate experiments the authors proved that the optimum pH range for diol conjugation was between the pK_a of the boronic acid and the diol. While the pK_a of boronic acids can vary considerably (between 4-10), diol conjugation is typically most favoured under basic conditions (pH 8-10). From the data presented, it is difficult to draw any conclusive trend as to what effect the electronics of the boronic acid has on conjugation, despite the prevailing idea that more acidic boronic acids conjugate more rapidly.

While these works laid the foundations for understanding boron speciation and ligand exchange, the importance of their observations in the synthetic sense was not realised until the work of Schauss and Chong. Chong used catalytic chiral diols to induce asymmetry in the conjugate addition of alkynes to α , β -unsaturated ketones (Scheme 57).^[108]

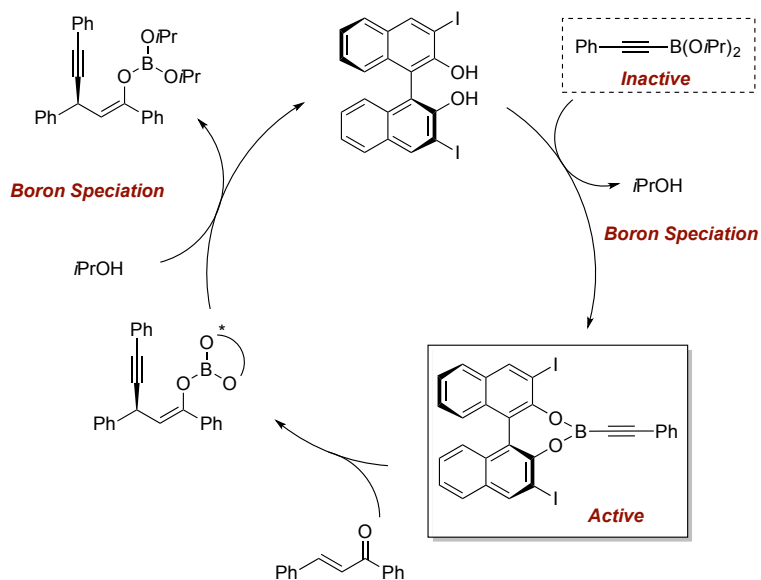


Scheme 57: Asymmetric 1,4-addition of alkynes *via* boron speciation.

While 1,4-addition using stoichiometric quantities of chiral boron species was well documented, the use of catalytic chiral diol presented significant challenges (Scheme 58).

- The chiral diol must be significantly more hydrolytically stable than the achiral ligand to achieve transesterification.
- The chiral, catalytic boron species must be significantly more reactive towards the transformation than the achiral starting material in order to gain stereocontrol.

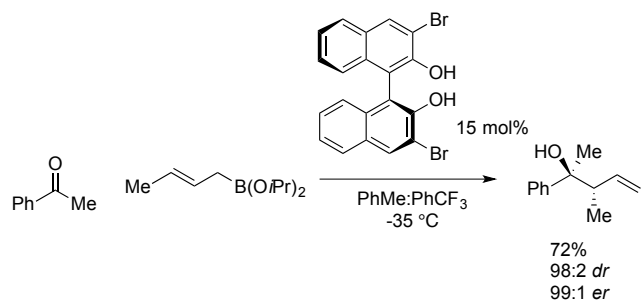
- The chiral ligand must be able to be released at the end of the reaction to complete the catalytic cycle.



Scheme 58: Catalytic cycle for asymmetric 1,4-addition.

Judicious choice of chiral diol was essential for high yields and enantioselectivities. It was found that 1,1-bi-2-naphthol (BINOL) type ligands were effective, while diisopropyl tartrate, another commonly used ligand in asymmetric boron chemistry, only delivered racemic product. Interestingly, most standard achiral diols, such as pinacol and ethylene glycol did not catalyse the reaction, and acyclic alcohols were likewise ineffective.

After this landmark advance in asymmetric boron chemistry, this speciation-driven method was employed in a number of other transformations. One year later, Schaus reported the use of similar BINOL catalysts to effect catalytic asymmetric allylation of ketones (Scheme 59).^[109]



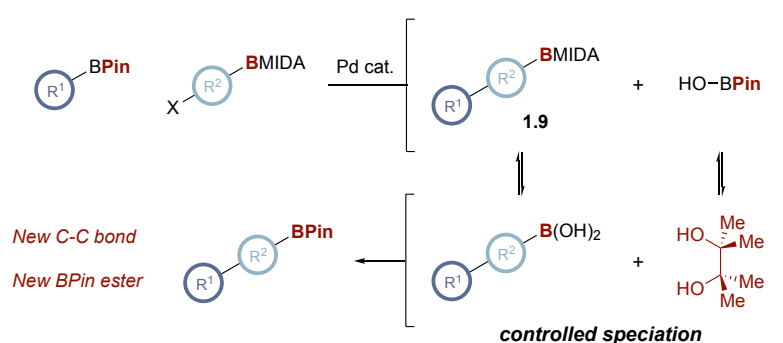
Scheme 59: Asymmetric allylboration via boron speciation.

This elegant work enables the enantioselective formation of two adjacent chiral centres, and provides a facile solution to the allylboration of ketones, which had shown to be difficult substrates. Previous work in the area had required metal catalysis or stoichiometric chiral reagents to achieve high yields and selectivities. This methodology was subsequently expanded upon extending the scopes of both boron conjugate addition and allylation.^[110,111]

Goodman and co-workers have elucidated the mechanisms of these two transformations through computational means. Both Chong's work on 1,4-addition of boryl alkynes and alkenes and Schauss' work on allylboration were shown to be driven by the Lewis acidity of the boron atom. Computational analysis determined that the 'twist' of the BINOL catalyst (147 ° vs. 180 ° for ethylene glycol derivative) reduces the ability of the oxygen lone pairs to donate into the empty p-orbital of boron, increasing its Lewis acidity. This observation can explain why other diol catalysts were ineffective in these reactions.^[112–114]

1.2.2 Speciation in SM coupling

While boron speciation has been used extensively in other areas of chemistry, it has only recently been applied to SM coupling. In 2014, Watson reported the chemoselective synthesis of boronic esters by controlled boron speciation. In this work, the authors demonstrated the formal homologation of aryl and vinyl boronic esters by controlling the solution speciation of pinacol and MIDA esters during the SM reaction (Scheme 60).^[115]

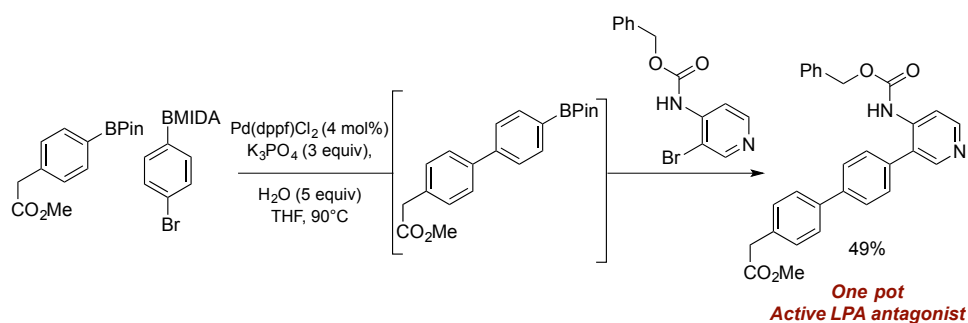


Scheme 60: Chemoselective synthesis of boronic esters *via* controlled speciation.

The cross-coupling of an aryl BPin and a haloaryl BMIDA under aqueous basic conditions afforded biaryl MIDA **1.9**, and the often overlooked by-products of any SM reaction; boric acid and pinacol. The BMIDA group is then slowly hydrolysed to

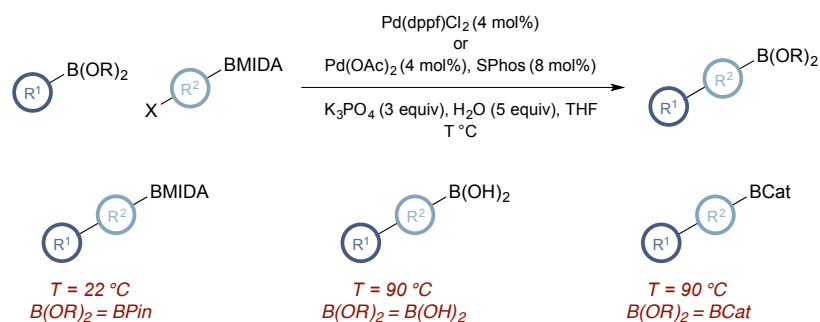
reveal a biaryl boronic acid, which will rapidly conjugate to pinacol at high pH to give the homologated BPin product. The key to successful completion of the reaction was the careful balance of the reaction medium, where an excess of water or base was found to enable premature hydrolysis of the MIDA functionality, leading to oligomeric products. This was modulated through judicious choice of base; by establishing an internal reservoir by exploiting the hygroscopicity of the inorganic base, slow release of water into the organic phase could be effected. K_3PO_4 was found to provide the ideal level of hygroscopicity to mitigate MIDA hydrolysis while delivering a basic biphasic system of sufficient pH to control the boron speciation events.

The delivery of a BPin ester under active SM conditions resulted in an extension of the protocol where a second aryl halide or haloaryl BMIDA was added to the reaction mixture upon formation of the BPin intermediate, leading to a further SM coupling to give a triaryl or doubly homologated product (Scheme 61).



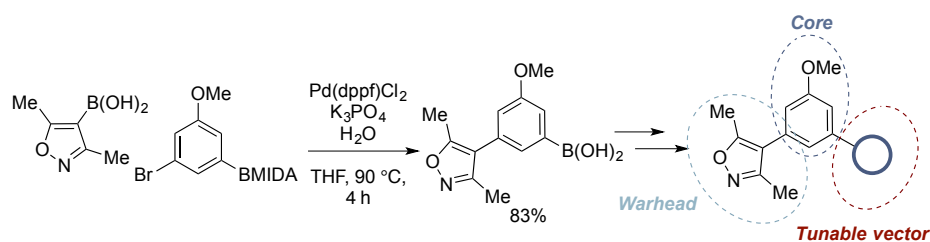
Scheme 61: Sequential SM cross-couplings *via* controlled speciation.

As part of a more detailed study into this speciation phenomenon, the methodology was further extended to include the synthesis of BMIDAs.^[102] After a detailed examination of the reaction parameters, the authors found that if the reaction was carried out at room temperature, the cross-coupled BMIDA product could be obtained. This showed that, at reduced temperatures, the reaction medium was benign enough to retard hydrolysis and subsequent speciation. This study also revealed that the homologation protocol was applicable to the homologation of boronic acids and catechol esters, albeit with the latter being formed in low yields due to instability of the reaction products (Scheme 62).



Scheme 62: Formal homologation of boronic esters *via* boron speciation.

The utility of the boronic acid products and the relative dearth of facile methods for their preparation inspired the optimisation of this boronic acid protocol. Watson described the elegant synthesis of homologated boronic acids as a platform for diversity. By tuning the base/water ratio the products could be synthesised in good yields, including the core of a BET bromodomain inhibitor, which was then derivatised using a range of standard boron transformations (Scheme 63).^[116]

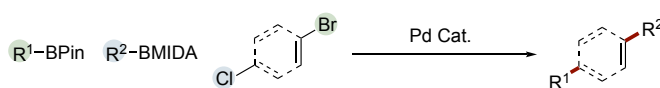


Scheme 63: Homologation of aryl boronic acids *via* controlled speciation as a platform for diversity.

1.3 Aims

Previous work in the Watson group has established that by careful control of the reaction media a chemoselective boronic ester synthesis can be achieved. This study exhibited nucleophile chemoselectivity between a BPin and a BMIDA but also speciation control to enable pinacol transfer from the HO-BPin by-product to a newly formed boronic acid to provide a homologated BPin. As part of this study, the BPin product could be cross-coupled effectively with a second bromide electrophile. This result demonstrated that the Pd catalyst was still active towards a further cross coupling.

With this knowledge, it was proposed that by exploiting electrophile reactivity gradients both cross-couplings could be achieved without any intervention. This methodology would enable the one-pot assembly of complex carbogenic frameworks that are only limited by the availability of the borylated and halogenated starting materials (Scheme 64).



Scheme 64: Proposed tandem chemoselective SM cross-coupling.

Based on previous work, it was clear from the beginning of this study that several difficulties had to be overcome for success.

- While cross-coupling a bromide in the presence of a chloride is facile through the use of a less activated Pd catalyst, the chemoselective cross-coupling of both halides in one-pot is unprecedented.
- The conditions required for two consecutive SM cross couplings must be compatible with the boron speciation required for nucleophile control.
- The yields achieved in the two-step one-pot process were only moderate, with the mass balance consisting of by-products derived from an incomplete second coupling. A more effective method for the second cross-coupling must be developed.

With these challenges in mind a set of clear aims were established for the completion of the project.

1. Develop a one-pot tandem SM coupling.
2. Gain insight into the chemoselectivity of dihalo and diboron systems.
3. Establish a scope to determine the generality of the reaction.
4. Apply the methodology to medicinally relevant scaffolds.

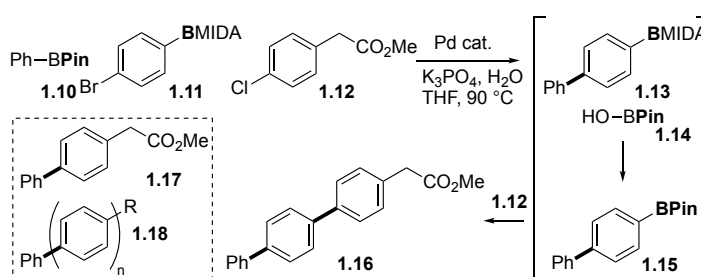
1.4 Results and Discussion

The work in this chapter is based on the following publication:

C. P. Seath, J. W. B. Fyfe, J. J. Molloy, A. J. B. Watson, *Angew. Chem. Int. Ed.* **2015**, *54*, 9976–9979.

The work described herein was performed with Dr J. W. B. Fyfe and Mr J. J. Molloy.

Interrogation of this novel methodology was started with the workhorse reaction of phenylboronic acid, pinacol ester **1.10**, 4-bromophenylboronic acid, MIDA ester **1.11**, and aryl chloride **1.12** (Scheme 65).



Scheme 65: Workhorse reaction for development.

Initial evaluation of the reaction conditions based upon previous work led to no conversion to the desired product, only returning biaryl BPin compound **1.15** (Table 1, entry 1). This was indicative of slow oxidative addition to the chloride electrophile. Moving to a more activated catalyst system Pd(OAc)₂/SPhos led to low conversion to the desired product, with the mass balance consisting of unreacted biaryl BPin and the undesired coupling product **1.17**, which arises from a lack of electrophile chemoselectivity (Table 1, entry 2).

Table 1: Evaluation of base/water relationship.

Entry	Catalyst	K ₃ PO ₄ equiv	H ₂ O equiv	Conversion ^a (%)
1	Pd(dppf)Cl ₂	3	5	0
2	Pd(OAc) ₂ /SPhos	3	5	17
3	Pd(OAc) ₂ /SPhos	3	10	35
4	Pd(OAc) ₂ /SPhos	3	20	53

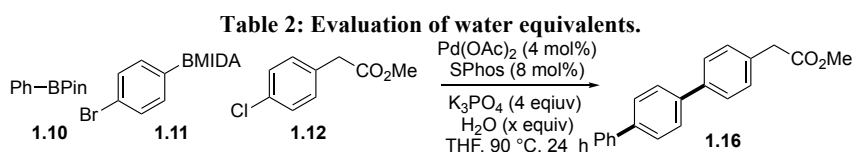
5	Pd(OAc) ₂ /SPhos	4	20	88
6	Pd(OAc) ₂ /SPhos	4	30	41
7	Pd(OAc) ₂ /SPhos	4	40	25
8	Pd(OAc) ₂ /SPhos	5	20	80

^aConversion to **1.16** determined by HPLC against a caffeine internal standard. See Experimental section for further details.

Evaluation of the stoichiometric ratio between water and base led to a significant increase in the productivity of catalysis; demonstrating the need for additional equivalents of both water and base to facilitate a second sequential cross-coupling (Table 1, entries 3-5). Addition of extra water led to higher conversion to **1.16** but significant amounts of oligomer products, **1.18**, arising from premature hydrolysis of BMIDA species (Table 1, entries 6-7). This uncontrolled hydrolysis could be offset by the addition of one equivalent of K₃PO₄ that pleasingly led to good conversion of the desired product.

These data support the suggestion that K₃PO₄ has a desiccant effect in the reaction media, creating a saturated aqueous layer, allowing slow release of water into the organic phase. This slow release of water was vital for control of hydrolysis and subsequent speciation events in the reaction media.

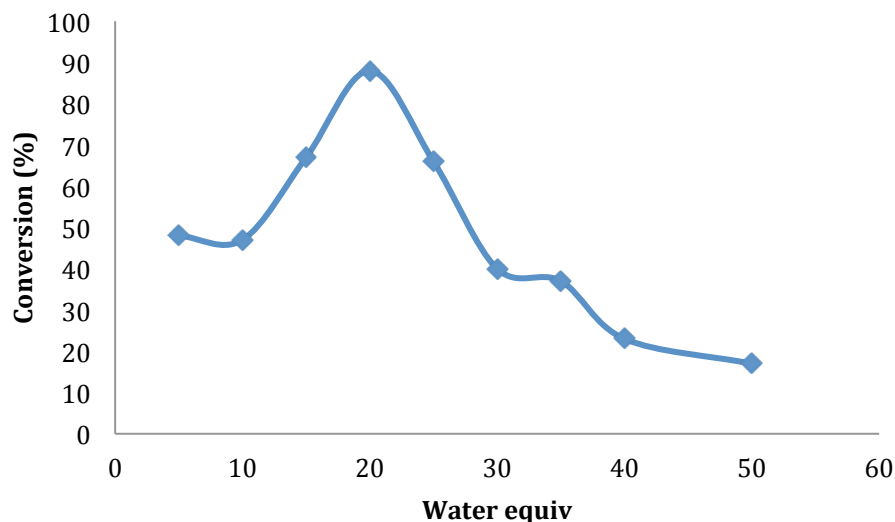
A water study at four equivalents of base showed that addition of extra equivalents of water (Table 2, Graph 1) led to a decrease in conversion to **1.16** and a commensurate increase in oligomer products.



Entry	Water equiv	Conversion ^a (%)
1	5	48
2	10	47
3	15	67
4	20	88
5	25	66
6	30	40
7	35	37

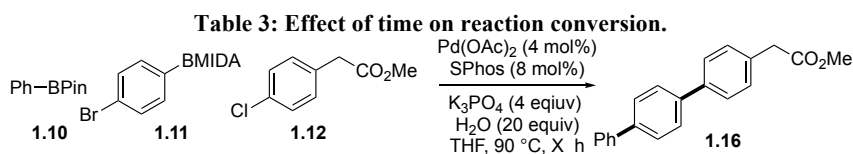
8	40	23
9	50	17

^aConversion to **1.16** determined by HPLC against a caffeine internal standard. See Experimental section for further details.



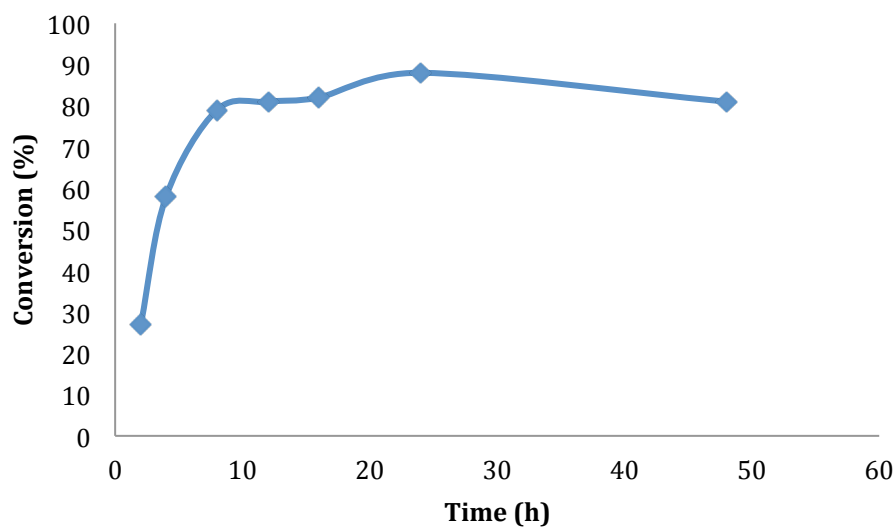
Graph 1: Relationship between water equivalents and conversion. Determined by HPLC.

A time study showed that while the reaction progressed to almost 80% in 8-10 h, full conversion was not reached until 24 h; this was consistent with previous work in the group that had showed that full speciation of the MIDA functionality to the corresponding BPin required extended reaction times.^[115] Prolonged heating after this time led to a slight decrease in conversion to **1.16**, arising from hydrolysis of the ester functionality (Table 3, Graph 2).



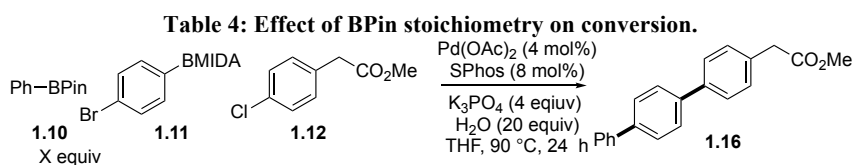
Entry	Time (h)	Conversion ^a (%)
1	2	27
2	4	58
3	8	79
4	12	81
5	16	82
6	24	88
7	48	81

^aDetermined by HPLC



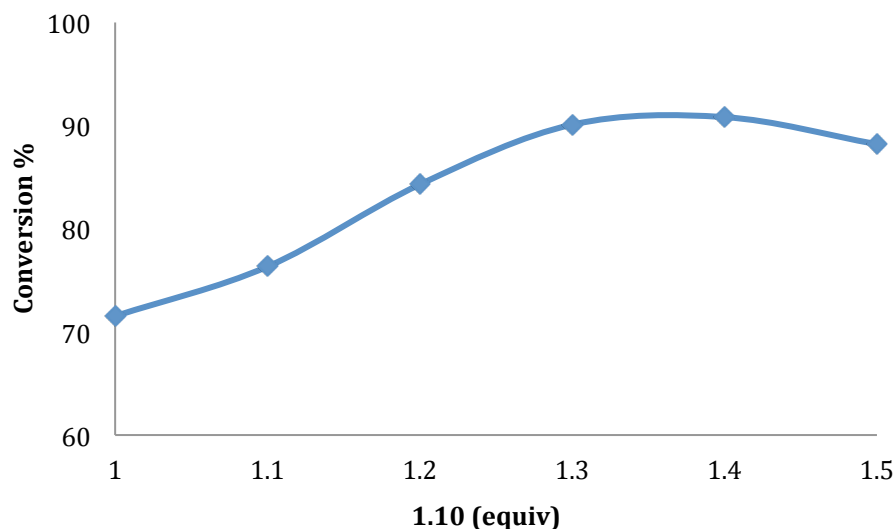
Graph 2: Effect of time on reaction conversion. Determined by HPLC.

Following this, a brief evaluation of the stoichiometry showed that 1.3 equivalents of the BPin were optimal for full conversion (Table 4, Graph 3).



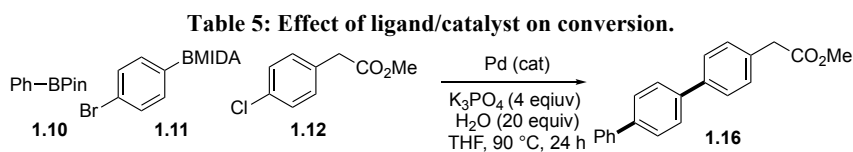
Entry	BPin equiv	Conversion ^a (%)
1	1	71
2	1.1	76
3	1.2	84
4	1.3	90
5	1.4	90
6	1.5	88

^aConversion to 1.16 determined by HPLC against a caffeine internal standard. See Experimental section for further details.



Graph 3: Effect of BPin stoichiometry on conversion to 1.16. Determined by HPLC against a caffeine internal standard.

A survey of different catalyst systems showed no further improvement although other Buchwald ligands did provide reasonable conversion (Table 5). Unsurprisingly, use of less electron-rich catalysts provided no conversion; as they cannot oxidatively add into aryl chlorides.



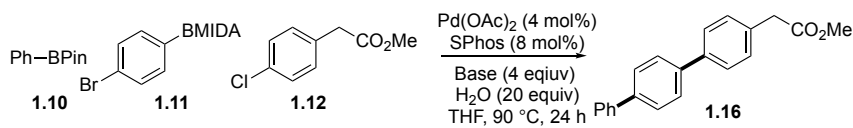
Entry	Catalyst/Ligand	Conversion ^a (%)
1	Pd(OAc) ₂ /SPhos	88
2	Pd(OAc) ₂ /CyJohnPhos	69
3	Pd(OAc) ₂ /XPhos	34
4	Pd(OAc) ₂ /DavePhos	76
5	Pd(PPh ₃) ₄	0
6	Pd(dppf)Cl ₂	0
7	Pd ₂ (dba) ₃	0
8	Pd ₂ (dba) ₃ /SPhos	0

^aConversion to 1.16 determined by HPLC against a caffeine internal standard. See Experimental section for further details.

Exploration of different bases only showed decreased conversions; this was not unexpected, based on previous work. Extensive studies on the role of the base in MIDA hydrolysis and boron speciation have shown that K₃PO₄ is unique in its

ability to create a saturated biphasic medium, allowing for controlled hydrolysis of the MIDA functionality (Table 6).

Table 6: Effect of base on conversion.

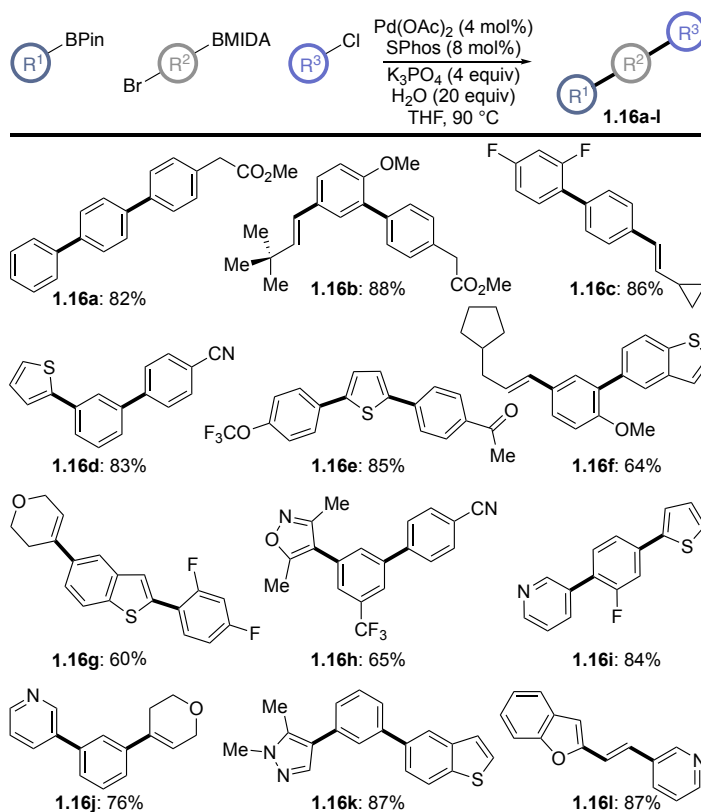


Entry	Base	Conversion ^a (%)
1	K ₃ PO ₄	88
2	KOH	6
3	K ₂ CO ₃	41
4	Cs ₂ CO ₃	65
5	K ₂ HPO ₄	0
6	Na ₂ CO ₃	0

^aConversion to **1.16** determined by HPLC against a caffeine internal standard. See Experimental section for further details.

Significantly, the optimum reaction conditions were effective with only slight excesses of the aryl BPin and aryl chloride, demonstrating that the yields and chemoselectivity are not statistically biased through the use of large excesses of a single component or through electronic tailoring of the nucleophile. The reaction rates of the optimised system are harmonized so that aryl BPin reacts only with bromoaryl BMIDA **1.11** to deliver biaryl BMIDA **1.13**. The corresponding MIDA can then undergo hydrolysis and boron speciation to give biaryl BPin **1.15** at a rate that avoids oligomerization. Meanwhile, the reaction media and catalyst are still able to facilitate another effective cross coupling.

With optimal conditions in hand the scope of the methodology was explored (Scheme 63).



Scheme 66: Substrate scope for chemoselective tandem SM cross-coupling using conjunctive haloaryl BMIDA components. Isolated yields. Substrates 1.16b,d, and j were purified by JJM.

A broad range of coupling partners were tolerated in the process including heteroaromatics, alkenyl species, and a range of standard functional groups – ketones, esters, nitriles, ethers, and fluorinated species. The substrates attempted typically worked very well or very poorly, with those that worked well shown in Scheme 66. The success of any substrate was often determined by either (i) the chemoselectivity in the first step of the process, (*i.e.*, whether the BPin couples to the bromoaryl BMIDA or the aryl chloride) or (ii) the efficiency of the second cross coupling (*i.e.*, how much of the intermediate biaryl BPin couples to the remaining aryl chloride). The mass balance of unsuccessful substrates consisted of biaryl resulting from (i) or biaryl BPin resulting from (ii). For case (i), this could be influenced by the solubility of the halide-bearing coupling partners. Aryl BMIDAs are typically highly insoluble, and in extreme cases their insolubility will invert the selectivity of oxidative addition leaving the BPin to couple with the more soluble aryl chloride. In addition, when particularly activated chlorides are used (*e.g.*, pyrazine, pyrimidine) the chemoselectivity of the first coupling can invert, once again producing biaryl compounds exclusively.

For case (ii), when particularly electron-rich chlorides are used, or Lewis basic moieties that are able to deactivate the palladium catalyst the reaction can falter before completion of the second cross coupling. Some unsuccessful substrates are shown in figure 15.

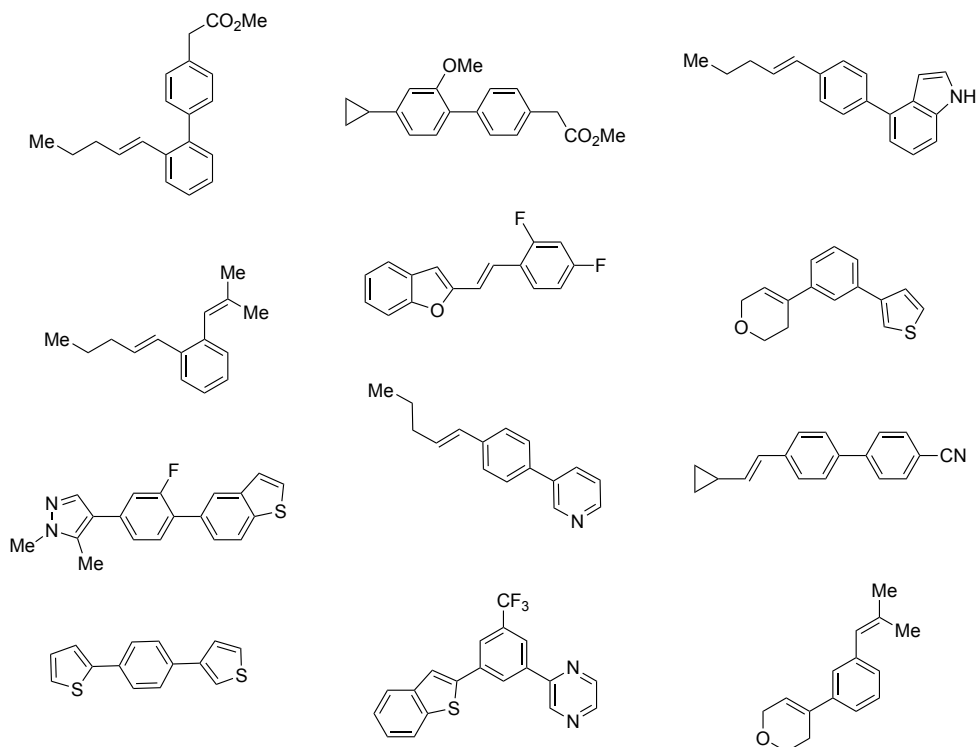
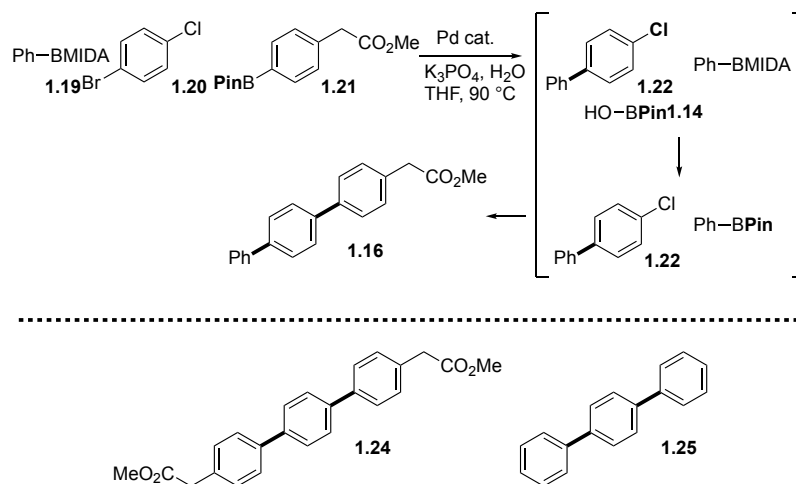


Figure 15: Unsuccessful substrates.

Due to the lack of diversity in commercial haloaryl BMIDAs, it was determined to be advantageous for the procedure to be transferable to a system utilising dihalide starting materials. These common building blocks would react with two differentiated boronic acid nucleophiles, all of which are more commercially available than the corresponding haloaryl BMIDAs.

We began our investigation by exposing dihalide **1.20** to phenyl BMIDA **1.19** and BPin **1.21** under the previously optimised conditions. To our dismay, conversion to the desired triaryl product was only 67% with the mass balance of the reaction consisting of unselective coupling products **1.24** and **1.25** (Scheme 64).

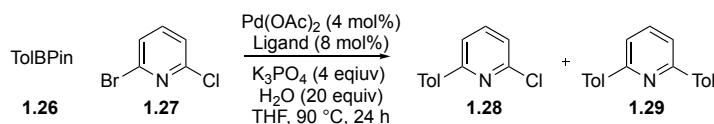


Scheme 67: Development of iterative cross coupling using dihaloarenes.

These by-products arise as a result of unselective oxidative addition and a preference for exhaustive coupling as seen in the work of Hu and Larossa.⁶⁰⁻⁶¹ It can be assumed that the rate of MIDA hydrolysis can be controlled through alterations to the temperature and reaction medium. With this in mind, achieving selectivity in the first cross-coupling will likely determine the reaction outcome.

At this point a switch in the optimization substrate was made to a dihalopyridine; this was chosen because pyridine cores were not tolerated in the previous process and are highly activated towards oxidative addition. We hypothesized that by optimising on a ‘difficult’ substrate the scope would be more general. Optimization began with the screening of several ligands on 2,6-dihalopyridine **1.27** at three temperatures to access selectivity. In general, selectivity was better at lower temperatures, with less electron-rich ligands (Table 7).

Table 7: Mono vs exhaustive selectivity with alteration of catalyst and temperature.



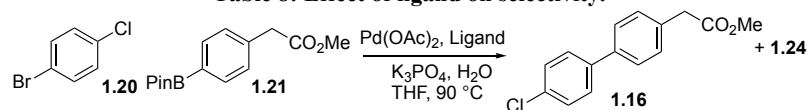
Entry	Temp ($^\circ\text{C}$)	Ligand	Ratio ^a (1.28/1.29)	Full conversion ^a (Y/N)
1	23	SPhos	88/12	N
2	23	DavePhos	100/0	N
3	23	PPh_3	100/0	N
4	70	SPhos	44/56	Y
5	70	DavePhos	65/35	Y

6	70	PPh ₃	70/30	Y
7	90	SPhos	36/63	Y
8	90	DavePhos	54/45	Y
9	90	PPh ₃	80/20	Y
10	90	RuPhos	36/64	Y
12	90	dppf	79/21	Y
13	90	dppp	85/15	N

^aConversion of 1.27 starting material. Determined by HPLC against a caffeine internal standard. See Experimental section for further details.

This short study showed Pd(OAc)₂ with either DavePhos or PPh₃ at room temperature to give complete selectivity for the bromide electrophile, with SPhos giving mixtures of mono-, **1.28**, and bis-coupled, **1.29**, products even at room temperature. The best conditions from this study were then used on a less activated system to probe the reproducibility; on the less activated aryl system **1.20**, both DavePhos and PPh₃ ligand combinations did not produce any of the bis-coupled product **1.24**, and SPhos was once again inferior (Table 8).

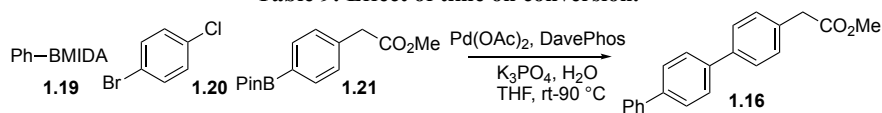
Table 8: Effect of ligand on selectivity.



Entry	Ligand	Ratio ^a (1.16/1.24)
1	PPh ₃	100:0
2	DavePhos	100:0
3	SPhos	88:12

^aConversion to **1.16** determined by HPLC against a caffeine internal standard. See Experimental section for further details.

At this point we proceeded with a catalyst system of Pd(OAc)₂ and DavePhos as PPh₃ was not able to effectually couple unactivated aryl chlorides. A time/temperature study was then executed to gain maximum selectivity. We postulated that by performing the reaction at room temperature until the first coupling is complete (T1), then increasing the temperature to hydrolyse the BMIDA (T2), high levels of selectivity could be achieved in a minimal amount of time (Table 9).

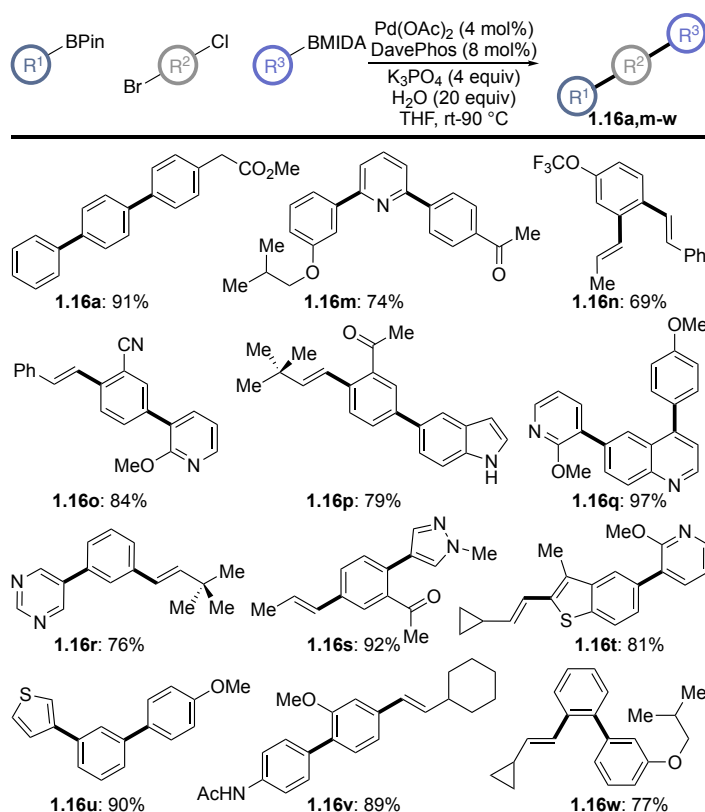
Table 9: Effect of time on conversion.

Entry	T1 (h) (rt)	T2 (h) (90 °C)	Conversion ^a (%)
1	2	24	86
2	4	24	86
3	6	24	92
4	8	24	96
5	16	24	88
6	8	2	6
7	8	16	91 (isolated)
8	8	20	93

^aConversion to **1.16** determined by HPLC against a caffeine internal standard. See Experimental section for further details. T1 refers to the time the reaction was run at the lower temperature. T2 refers to the time the reaction was run at increased temperature.

The study showed that six to eight hours at room temperature was required for optimal conversion and following this, a further 16 hours was required for boron speciation and cross coupling of the second boron nucleophile. Isolation of product **1.16** under the optimum conditions gave a 91% yield.

With a fully optimised system, the scope of the reaction was explored. Once again the reaction proved to be tolerant of a wide range of functionality in all three components. Heterocyclic and vinylic groups could both be smoothly incorporated in good to excellent yields (Scheme 68).



Scheme 68: Substrate scope for chemoselective SM cross coupling using conjunctive dihalide components. Isolated yields.

During the synthesis of the substrates for this scoping exercise it was noted that almost all the reactions gave desired product, but for a high yield to be obtained the initial room temperature coupling must proceed completely and selectively. This could be hampered by slow cross-coupling due to steric concerns or an electronic bias for the chloride. While substrates in this process were generally effective, a number of unsuccessful cases were noted (Figure 16). Typically, low levels of electrophile selectivity caused complex mixtures of products that could not be separated. Additionally, some Lewis basic functionalities led to a decrease in the productivity of the catalyst.

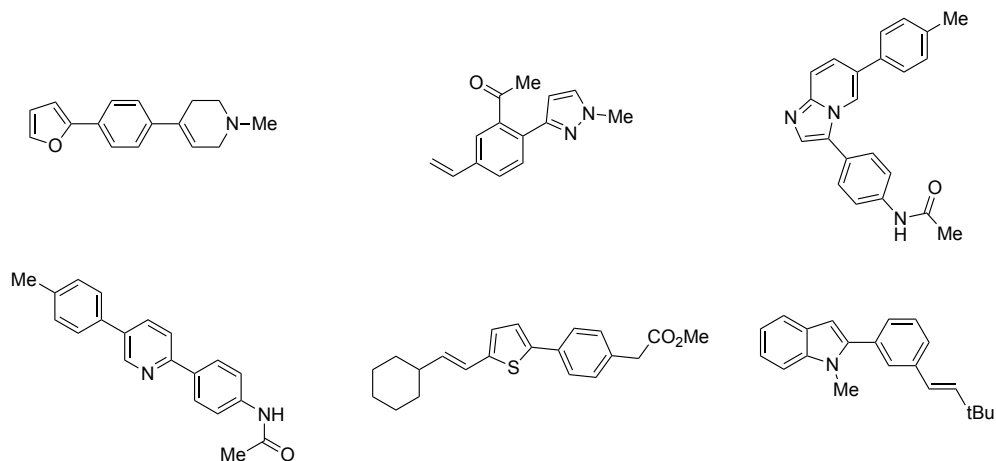


Figure 16: Unsuccessful substrates.

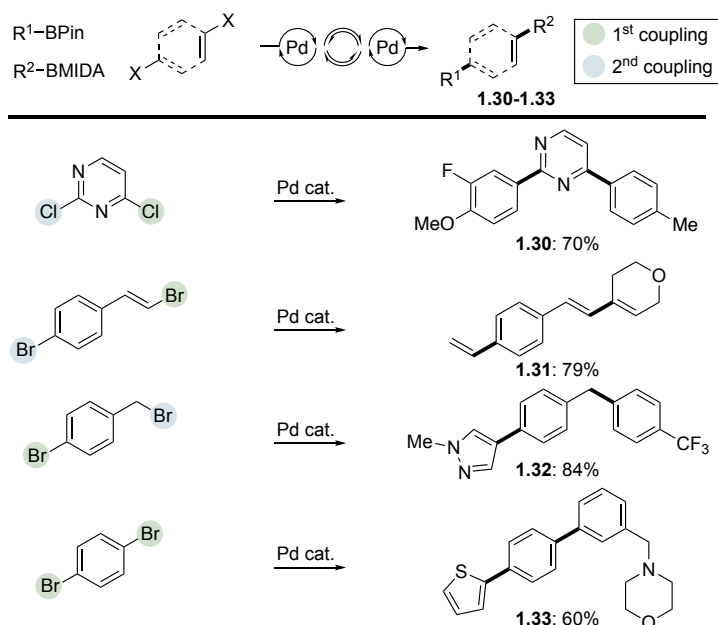
After exploiting the standard reactivity gradient for electrophile control, we sought to use specific and subtle differences in dibromo- and dichloro-electrophiles to further exemplify our tandem process. While electrophile selectivity has been demonstrated in a great many dihalide systems, we chose four different scaffolds based on four different fundamental principles for achieving chemoselectivity.

- Selectivity based upon electronic bias.
- Selectivity for vinyl halides over aryl halides.
- Selectivity for sp^2 halides over sp^3 halides.
- Selectivity for mono-coupling over exhaustive coupling.

2,4-Dichloropyrimidine was used to exploit electronic bias, first reacting at the 4-position followed by the 2-position. The high reactivity of this substrate required the use of a much less active catalyst than the Buchwald ligand systems previously employed in this work. Pd(dppf)Cl₂ proved to be effective for attaining selectivity at room temperature. However in order to facilitate the second cross coupling the reaction was heated to 90 °C for 48 hours. Despite the extended reaction time, the tandem cross-coupled product **1.30** was obtained in good yield (Scheme 66).

Vinyl halides are more reactive toward oxidative addition; this is likely due to a favourable agostic interaction between the π -system of the olefin and the Pd⁰ complex.^[117] In order to access this chemoselectivity a simple styrenyl dibromide was used. Once again, optimal chemoselectivity was attained using the less activated

Pd(dppf)Cl₂ catalyst and extended reaction times were required for good conversion to the styrenyl product **1.31** (Scheme 66).



Scheme 69: Chemoselective tandem Suzuki–Miyaura cross-coupling using dibromo and dichloro electrophiles. Isolated yields. Reactions performed by JWBF.

The preference for oxidative addition of Pd into an sp² halide over a sp³ halide is also likely derived from agostic interactions between the Pd catalyst and the aryl ring.

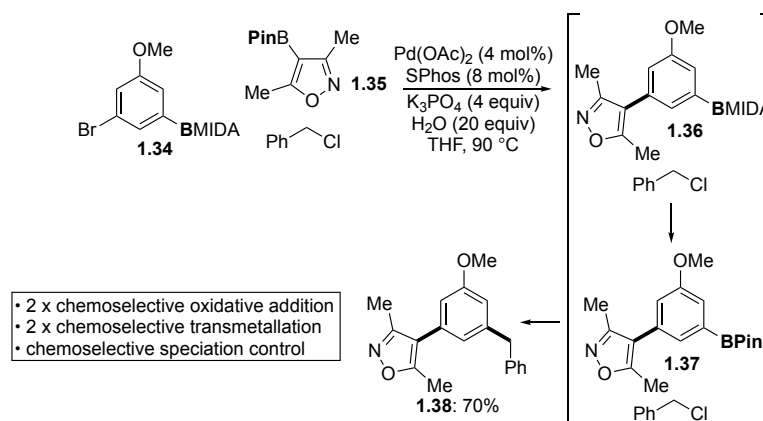
While this phenomenon is less pronounced in an aryl system than an alkenyl system, the effect still renders the aryl halide more reactive toward oxidative addition than an unactivated sp³ halide. To exploit this reactivity, we chose 4-bromobenzyl bromide as the model system, the benzyl halide can be considered as pseudo-aromatic as it has no β-hydrogens, and as such is more stable to SM coupling than other sp³ halides that can undergo β-hydride elimination after the oxidative addition step. This scaffold was effectively employed in the tandem cross-coupling using Pd(dppf)Cl₂ to give **1.32** in good yield (Scheme 66).

The difference in bond strength (bond dissociation energy, BDE) between a Csp²(aryl)-Br bond and a Csp³(benzyl)-Br bond was also considered, however, the experimental bond strengths for both bonds (Csp²(aryl)-Br – 84 kcal/mol vs. Csp³(benzyl)-Br – 63 kcal/mol) reported by Blanksby and Ellson^[118] do not correlate with chemoselectivity. Indeed, by this metric, benzyl chlorides (Csp³(benzyl)-Cl – 74 kcal/mol) would couple preferentially over aryl bromides and at a similar rate to aryl iodides (Csp²(aryl)-I – 67 kcal/mol).

Further analysis of this data shows that while selectivity between aryl bromides and chlorides should be relatively straightforward, with a $\Delta\Delta H_{298} = 13$ kcal/mol, the small difference between aryl and vinyl bromides $\Delta\Delta H_{298} = 3.2$ kcal/mol should make chemoselectivity in this system more challenging. In practice, the relative chemoselectivity across the scope of this study did not purely reflect the BDE of the substrates. For this reason, we propose a more favourable catalyst pre-coordination to the π -system provides levels of selectivity that are outwith the experimentally derived BDEs.

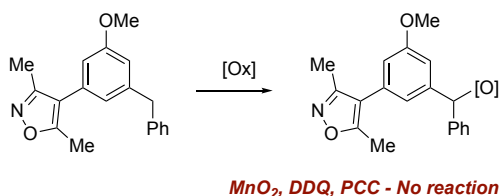
The last dihalide system employed was 1,4-dibromobenzene, which has been shown to undergo either selective mono-coupling or exhaustive coupling depending on the reaction conditions.⁵⁹ We envisioned that through selective mono-coupling of the BPin to the dihalide and subsequent hydrolysis of the BMIDA, we could achieve two chemoselective SM couplings without the use of any electrophile bias. This challenging tandem process was carried out without the need for any change in the reaction medium or catalyst system to provide **1.33** in moderate yield (Scheme 66).

After exploring the tandem process across a range of multinucleophile/multielectrophile systems, we sought to demonstrate the synthetic applicability of this method in the synthesis of the BET bromodomain inhibitor **1.39**.^[119] Employing the optimised method to conjunctive bromoaryl BMIDA **1.34**, commercial dimethylisoxazole BPin **1.35**, and benzyl chloride gave the core scaffold, **1.38**, of the bioactive molecule in 70% yield in one synthetic operation (Scheme 70).



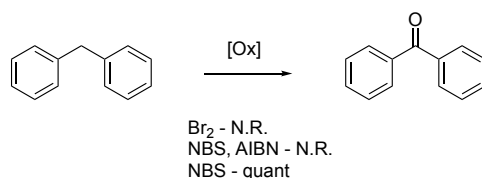
Scheme 70: One-pot synthesis of BET bromodomain scaffold. Isolated yields.

This process demonstrates chemoselective sp^2 - sp^2 SM coupling, boron speciation, and a subsequent sp^2 - sp^3 SM cross-coupling to considerably shorten the route to this important class of tool compounds. From the basic carbon scaffold, oxidation of the benzylic position was proposed to access the target compound. A range of oxidation methods was employed from the literature, with no success (Scheme 71).^[120–122]



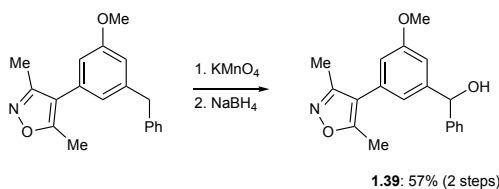
Scheme 71: Attempted oxidation of bromodomain scaffold.

However, using diphenylmethane as a surrogate, oxidation of the benzylic position was realized through the use of NBS, which delivered benzophenone in quantitative yield (Scheme 72).^[123]



Scheme 72: Oxidation of diphenylmethane. Isolated yields.

This reaction presumably proceeds through the intermediacy of a geminal dibromide that upon hydrolysis gives the ketone. Upon application of this method to the desired BET inhibitor, none of the desired product was detected. A $[M+Br]$ peak indicated bromination of the molecule, but not at the desired benzylic position. Fortunately, application of more strongly oxidizing conditions ($KMnO_4$) led to good conversion to the desired ketone product (Scheme 73). Reduction of the ketone using $NaBH_4$ gave the desired benzyl alcohol **1.39** in 57% over two redox steps. This novel path to this molecule represents a significantly shorter route than the published synthesis of six steps by the Conway group.^[119]



Scheme 73: $KMnO_4$ oxidation followed by reduction to provide bromodomain inhibitor. Isolated yield.

1.5 Conclusions

In conclusion, a tandem chemoselective SM cross-coupling procedure has been developed.^[124] In this protocol we demonstrated, for the first time, simultaneous nucleophile and electrophile control by exploiting boron speciation. Careful control of the reaction media is key to balancing the rates of MIDA hydrolysis with SM cross-coupling. This procedure was applied to the synthesis of the BET bromodomain inhibitor **1.39**.

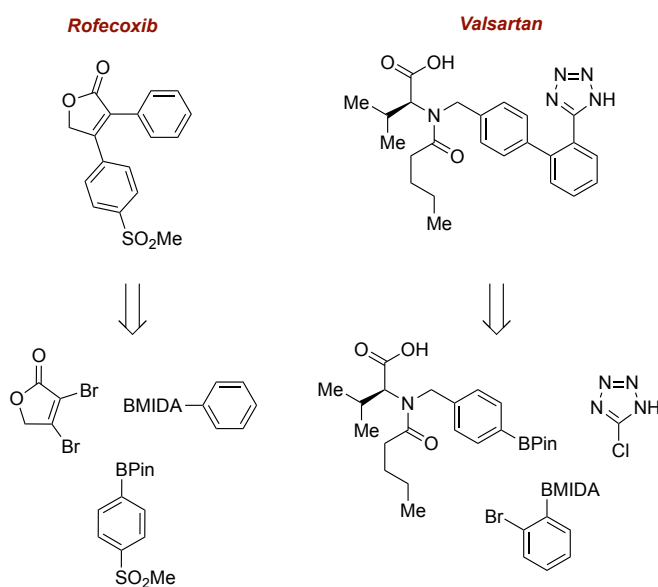
Throughout the reaction development, the rate of MIDA hydrolysis was shown to be the most important factor for establishing nucleophile selectivity. The stoichiometry of base and water were vital to temper the hydrolysis step. Use of strong base led to rapid hydrolysis and subsequent oligomerization; less hygroscopic bases also resulted in premature hydrolysis. The amount of water present in the reaction also had a profound effect on chemoselectivity, while hydrolysis of the MIDA functionality only requires five equivalents of water; the efficiency of the second cross-coupling is severely impaired. An additional 15 equivalents were needed to ensure completion of the second SM reaction. This is likely due to the availability of hydroxide, which is required for the formation of the catalytic oxo-palladium species.

Another key conclusion from this study was the ligand-controlled electrophile chemoselectivity. Achieving selectivity between chloride and bromide electrophiles in mono-boron systems is relatively facile; use of a catalyst that is not active enough to react with chloride electrophile can ensure complete chemoselectivity. In multi-boron systems where both electrophiles are required to react, achieving selectivity is more difficult. During this study it was shown that very minor variations in the electronics of the ligand employed can dramatically affect selectivity. Use of Buchwald ligands was important for facilitating both effective cross-coupling and high levels of selectivity. The versatility of the set of ligands developed by the Buchwald group allows for effective and rapid optimisation of chemoselective processes.

Another aspect of interest that was uncovered during the course of this work was the differences in reactivity in dibromo- and dichloro- electrophiles. While examples of chemoselective cross-coupling using these dihalides are known, they are uncommon, and the levels of chemoselectivity in these systems have never been leveraged towards multi nucleophile systems. We found that even subtle differences in reactivity between halides could be utilised for chemoselective catalysis.

1.6 Future Work

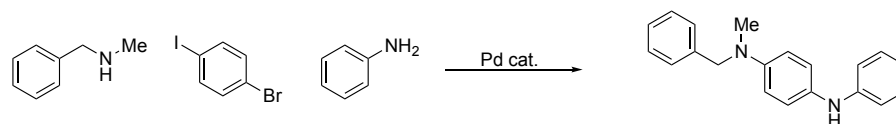
While the utility of this process towards the synthesis of bioactive compounds was demonstrated with a BET bromodomain inhibitor, the methodology could feasibly be utilised in high throughput array chemistry to develop structure activity relationships around COX-2 (Rofecoxib), or AT1 inhibitors (Valsartan) (Scheme 71).^[125,126]



Scheme 74: Tandem SM bond disconnections for block buster drugs.

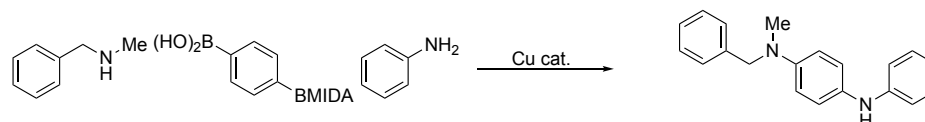
Many bioactive scaffolds contain biaryls and many can be disconnected back to two discrete cross-coupling steps. With the high throughput purification techniques available to industrial synthetic chemists, array-like synthesis of complex frameworks through chemoselective cross-couplings could feasibly be used to prepare a series of analogues efficiently.

In this methodology we exploited the chemoselectivity between two boron nucleophiles; a natural extension to this would be to employ heteroatom nucleophiles in Buchwald-Hartwig amination and etherification protocols, this would broaden the scope of products and building blocks that could be used in tandem cross-coupling reactions. Buchwald has previously exploited differences in amine nucleophilicity to perform sequential cross-couplings in the synthesis of heterocycles. Extending this work to include more diverse amines, alcohols and halide electrophile partners would provide a useful method for sequential functionalization (Scheme 73).



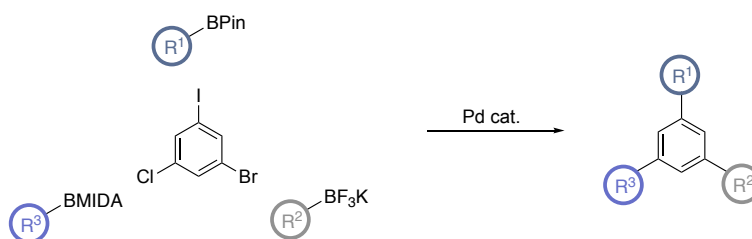
Scheme 75: Sequential one-pot Buchwald-Hartwig coupling.

In addition, this same method could be exploited in the Chan-Lam reaction. Control of the boron nucleophile could be achieved through the speciation protocols described within the group, and amine selectivity can be naturally derived from natural nucleophilicities, *e.g.*, primary amines react faster than anilines (Scheme 74).



Scheme 76: Sequential one-pot Chan-Evans-Lam coupling.

Using three discrete nucleophiles and three different electrophiles could also increase the limits of chemoselectivity; iodides and triflates could be employed as electrophiles as they are already established as competent coupling partners. The additional nucleophile could come in the form of a BF_3K , which could undergo controlled hydrolysis followed by cross coupling in a similar manner to a BMIDA (Scheme 75).



Scheme 77: Chemoselective four component SM coupling

Additionally, in this study only one sp^3 coupling partner was utilised, the development of a process that includes both sp^2 and sp^3 nucleophiles and electrophiles would greatly broaden the scope of the reaction and in turn, greatly increase its utility in industrial settings.

1.6 Experimental

1. General

All reagents and solvents were obtained from commercial suppliers and were used without further purification unless otherwise stated. Purification was carried out according to standard laboratory methods.⁹¹

1.1 Purification of Solvents

Dry solvents for reactions were either obtained from a PureSolv SPS-400-5 solvent purification system (THF). These solvents were transferred to and stored in a septum-sealed oven-dried flask over previously activated 4 Å molecular sieves and purged with and stored under nitrogen. CH₂Cl₂, Et₂O, EtOAc, MeCN, and petroleum ether 40-60° for purification purposes were used as obtained from suppliers without further purification.

1.2 Drying of Inorganic Bases

Inorganic bases were dried in a Heraeus Vacutherm oven at 60 °C under vacuum for a minimum of 24 hours before use.

1.3 Experimental Details

Reactions were carried out using conventional glassware (preparation of intermediates) or in capped 5 mL microwave vials. Glassware was oven-dried (150 °C) and purged with N₂ before use. Purging refers to a vacuum/nitrogen-refilling procedure. Room temperature was generally 18 °C. Reactions were carried out at elevated temperatures using a temperature-regulated hotplate/stirrer.

1.4 Purification of Products

Thin layer chromatography was carried out using Merck silica plates coated with fluorescent indicator UV254. These were analyzed under 254 nm UV light or

developed using potassium permanganate solution. Normal phase flash chromatography was carried out using ZEOprep 60 HYD 40-63 μm silica gel. Reverse phase flash chromatography was carried out using IST Isolute C18 cartridges.

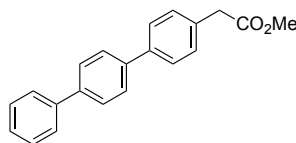
1.5 Analysis of Products

Fourier Transformed Infra-Red (FTIR) spectra were obtained on a Shimadzu IRAffinity-1 machine. ^{19}F NMR spectra were obtained on a Bruker AV 400 spectrometer at 376 MHz. ^{11}B NMR spectra were obtained on a Bruker AV 400 spectrometer at 128 MHz. ^1H and ^{13}C NMR spectra were obtained on either a Bruker AV 400 at 400 MHz and 125 MHz, respectively, or Bruker DRX 500 at 500 MHz and 126 MHz, respectively. Chemical shifts are reported in ppm and coupling constants are reported in Hz with CDCl_3 referenced at 7.26 ppm (^1H) and 77.0 ppm (^{13}C) and DMSO-d_6 referenced at 2.50 ppm (^1H) and 39.5 ppm (^{13}C). High-resolution mass spectra were obtained through analysis at the EPSRC UK National Mass Spectrometry Facility at Swansea University. Reverse phase HPLC data was obtained on an Agilent 1200 series HPLC using a Machery-Nagel Nucleodur C18 column. Analysis was performed using a gradient method, eluting with 5–80% $\text{MeCN}/\text{H}_2\text{O}$ over 16 minutes at a flow rate of 2 mL/min. Samples for HPLC analysis were prepared through the addition of 2 mL of caffeine standard to the completed reaction mixture, the resulting solution was then stirred before the removal of a 200 μL aliquot. The aliquot was diluted to 1 mL with MeCN , a 200 μL aliquot of the diluted solution was then filtered and further diluted with 800 μL MeCN and 500 μL H_2O for HPLC analysis against established conversion factors.

2. General Experimental Procedures

General Procedure 1A: Optimized reaction (Scheme 66)

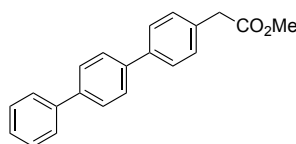
For example synthesis of methyl 2-([1,1':4',1''-terphenyl]-4-yl)acetate, **1.16a**



To an oven dried 5 mL microwave vessel was added 4-bromophenylboronic acid, MIDA ester (78 mg, 0.25 mmol, 1 equiv), phenylboronic acid pinacol ester (66 mg, 0.325 mmol, 1.3 equiv), Pd(OAc)₂ (2.2 mg, 0.01 mmol, 4 mol%), SPhos (8.2 mg, 0.02 mmol, 8 mol%), methyl 2-(4-chlorophenyl)acetate (69 mg, 57 μL, 0.375 mmol, 1.5 equiv), and K₃PO₄ (212 mg, 1 mmol, 4 equiv). The vessel was then capped and purged with N₂ before addition of THF (1 mL, 0.25 M) and H₂O (90 μL, 5 mmol, 20 equiv). The reaction mixture was then heated to 90 °C in a sand bath for 24 h. The vessel was allowed to cool to room temperature, vented, and decapped. The solution was then concentrated under reduced pressure before being diluted with EtOAc (10 mL) and washed with water (10 mL) and brine (10 mL). The organics were then concentrated to give a crude yellow oil, which was purified by reverse phase flash chromatography (20–70% MeCN in H₂O). The fractions containing product were concentrated under reduced pressure, diluted with EtOAc (2 × 100 mL) and washed with water (50 mL) before being dried through a hydrophobic frit. The dry organic solution was then concentrated to give the desired product as an off-white solid. (62 mg, 82%).

General Procedure 1B: Optimized reaction (Scheme 68)

For example synthesis of methyl 2-([1,1':4',1''-terphenyl]-4-yl)acetate, **1.16a**

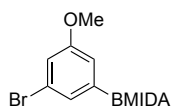


To a 5 mL microwave vessel was added 1-bromo-4-chlorobenzene (47.5 mg, 0.25 mmol, 1 equiv), (4-(2-methoxy-2-oxoethyl)phenyl)boronic acid pinacol ester (76 mg, 0.275 mmol, 1.1 equiv), Pd(OAc)₂ (2.24 mg, 0.01 mmol, 0.04 equiv), DavePhos (7.8 mg, 0.02 mmol, 0.08 equiv), phenylboronic acid MIDA ester (75 mg, 0.325 mmol, 1.3 equiv), and K₃PO₄ (212 mg, 1 mmol, 4 equiv). The vessel was then capped and purged with N₂ before addition of THF (1 mL, 0.25 M) and H₂O (90 μL, 5 mmol, 20

equiv). The reaction mixture was stirred at room temperature for 8 h before being heated to 90 °C in a sand bath for 16 h. Upon completion of the reaction, the vessel was allowed to cool to room temperature, vented, and decapped. The reaction mixture was then concentrated under reduced pressure before being diluted with EtOAc (10 mL) and washed with water (10 mL). The organics were dried and concentrated at reduced pressure before purification by silica chromatography (0–10% EtOAc/petroleum ether) to afford the desired product as a white solid (69 mg, 91%).

General Procedure 1C: Synthesis of MIDA esters from boronic acids

For example, for the preparation of (3-bromo-5-methoxyphenyl)boronic acid MIDA ester, **S1**



A mixture of (3-bromo-5-methoxyphenyl)boronic acid (1.0 g, 4.34 mmol, 1 equiv), *N*-methyliminodiacetic acid (671 mg, 4.56 mmol, 1.05 equiv) in DMF (50 mL) was heated to 90 °C for 18 h under air. The reaction mixture was allowed to cool to room temperature and concentrated under vacuum to give an off-white slurry. EtOAc (100 mL) was added and the resulting precipitate was collected by filtration. The precipitate was washed with H₂O (2 × 50 mL) and Et₂O (2 × 50 mL) before being dried under vacuum to give the desired product as a white crystalline solid (1.4 g, 94%).

General Procedure 1D: General procedure for optimization process Tables 1-6

To an oven dried 5 mL microwave vessel was added 4-bromophenylboronic acid, MIDA ester (78 mg, 0.25 mmol, 1 equiv), phenylboronic acid pinacol ester (66 mg, 0.325 mmol, 1.3 equiv), PdCl₂dppf•CH₂Cl₂ (8.2 mg, 0.01 mmol, 4 mol%), methyl 2-(4-chlorophenyl)acetate (69 mg, 57 μL, 0.375 mmol, 1.5 equiv), and K₃PO₄ (159 mg, 1 mmol, 3 equiv). The vessel was then capped and purged with N₂ before addition of THF (1 mL, 0.25 M) and H₂O (22.5 μL, 5 mmol, 5 equiv). The reaction mixture was then heated to 90 °C in a sand bath for 24 h. The reaction mixture was allowed to cool to room temperature before analysis by HPLC against a known internal standard.

General Procedure 1E: General procedure for optimization process Tables 7-9

To an oven dried 5 mL microwave vessel was added 2-bromo-6-chloropyridine (48 mg, 0.25 mmol, 1 equiv), Pd(OAc)₂ (2.2 mg, 0.01 mmol, 4 mol%), SPhos (8.2 mg, 0.02 mmol, 8 mol%), 4-methylphenylboronic acid, pinacol ester (60 mg, 0.275 mmol, 1.1 equiv), H₂O (90 μL, 5 mmol, 20 equiv), and K₃PO₄ (212 mg, 1 mmol, 4 equiv). The vessel was then capped and purged with N₂ before addition of THF (1 mL, 0.25 M) and H₂O (22.5 μL, 5 mmol, 5 equiv). The reaction mixture was then heated to 90 °C in a sand bath for 24 h. The reaction mixture was allowed to cool to room temperature before analysis by HPLC against a known internal standard.

3. Reaction optimization data

Results from Table 1

Reactions were carried out according to General Procedure 1D using 4-bromophenylboronic acid MIDA ester (70.6 mg, 0.226 mmol, 1 equiv), phenylboronic acid pinacol ester (60 mg, 0.294 mmol, 1.3 equiv), Pd(OAc)₂ (2 mg, 0.009 mmol, 4 mol%), SPhos (7.4 mg, 0.018 mmol, 8 mol%), methyl 2-(4-chlorophenyl)acetate (62 mg, 0.339 mmol, 1.5 equiv), H₂O (X μL, X mmol, X equiv), and K₃PO₄ (X mg, X mmol, X equiv) for 24 h.

Entry	Catalyst	K ₃ PO ₄ equiv	H ₂ O equiv	Conversion ^a (%)
1	Pd(dppf)Cl ₂ (7.4 mg)	3 (144 mg)	5 (20 μL)	0
2	Pd(OAc) ₂ /SPhos (2 mg/7.4 mg)	3 (144 mg)	5 (20 μL)	17
3	Pd(OAc) ₂ /SPhos (2 mg/7.4 mg)	3 (144 mg)	10 (41 μL)	35
4	Pd(OAc) ₂ /SPhos (2 mg/7.4 mg)	3 (144 mg)	20 (81 μL)	53
5	Pd(OAc) ₂ /SPhos (2 mg/7.4 mg)	4 (192 mg)	20 (81 μL)	88
6	Pd(OAc) ₂ /SPhos (2 mg/7.4 mg)	4 (192 mg)	30 (122 μL)	41
7	Pd(OAc) ₂ /SPhos (2 mg/7.4 mg)	4 (192 mg)	40 (163 μL)	25

		mg/7.4 mg)		
8	Pd(OAc) ₂ /SPhos (2	5 (240 mg)	20 (81 μL)	80
		mg/7.4 mg)		

^aConversion to 1.16 determined by HPLC against a caffeine internal standard. See Experimental section for further details.

Results from Table 2

Reactions were carried out according to General Procedure 1D using 4-bromophenylboronic acid MIDA ester (70.6 mg, 0.226 mmol, 1 equiv), phenylboronic acid pinacol ester (60 mg, 0.294 mmol, 1.3 equiv), Pd(OAc)₂ (2 mg, 0.009 mmol, 4 mol%), SPhos (7.4 mg, 0.018 mmol, 8 mol%), methyl 2-(4-chlorophenyl)acetate (62 mg, 0.339 mmol, 1.5 equiv), K₃PO₄ (192 mg, 0.905 mmol, 4 equiv), and H₂O (X equiv).

Entry	H ₂ O equiv	Conversion ^a (%)
1	5 (20 μL)	48
2	10 (41 μL)	47
3	15 (61 μL)	67
4	20 (81 μL)	88
5	25 (101 μL)	66
6	30 (122 μL)	40
7	35 (143 μL)	37
8	40 (163 μL)	23
9	50 (204 μL)	17

^aConversion to 1.16 determined by HPLC against a caffeine internal standard. See Experimental section for further details.

Results from Table 3

3.1 Time study

Reactions were carried out according to General Procedure 1D using 4-bromophenylboronic acid MIDA ester (70.6 mg, 0.226 mmol, 1 equiv), phenylboronic acid pinacol ester (60 mg, 0.294 mmol, 1.3 equiv), Pd(OAc)₂ (2 mg, 0.009 mmol, 4 mol%), SPhos (7.4 mg, 0.018 mmol, 8 mol%), methyl 2-(4-chlorophenyl)acetate (62 mg, 0.339 mmol, 1.5 equiv), H₂O (81 μL, 4.5 mmol, 20 equiv), and K₃PO₄ (192 mg, 0.905 mmol, 4 equiv) for X h.

Entry	Time (h)	Conversion ^a (%)
1	2	27
2	4	58
3	8	79
4	12	81
5	16	82
6	24	88
7	48	81

^aConversion to 1.16 determined by HPLC against a caffeine internal standard. See Experimental section for further details.

Results from Table 4

Reactions were carried out according to General Procedure 1D using 4-bromophenylboronic acid MIDA ester (70.6 mg, 0.226 mmol, 1 equiv), phenylboronic acid pinacol ester (**X** mg), Pd(OAc)₂ (2 mg, 0.009 mmol, 4 mol%), SPhos (7.4 mg, 0.018 mmol, 8 mol%), methyl 2-(4-chlorophenyl)acetate (62 mg, 0.339 mmol, 1.5 equiv), H₂O (81 μL, 4.5 mmol, 20 equiv), and K₃PO₄ (192 mg, 0.905 mmol, 4 equiv) for 24 h.

Entry	BPin equiv (mass)	Conversion ^a (%)
1	1 (46 mg)	71
2	1.1 (50 mg)	76
3	1.2 (55 mg)	84
4	1.3 (60 mg)	90
5	1.4 (65 mg)	90
6	1.5 (69 mg)	88

^aConversion to 1.16 determined by HPLC against a caffeine internal standard. See Experimental section for further details.

Results from Table 5

3.2 Catalyst Screen

Reactions were carried out according to General Procedure 1D using 4-bromophenylboronic acid MIDA ester (70.6 mg, 0.226 mmol, 1 equiv), phenylboronic acid pinacol ester (60 mg, 0.294 mmol, 1.3 equiv), Pd catalyst (**X** mg, 0.009 mmol, 4 mol%), ligand (**X** mg, 0.018 mmol, 8 mol%), methyl 2-(4-

chlorophenyl)acetate (62 mg, 0.339 mmol, 1.5 equiv), H₂O (81 μ L, 4.5 mmol, 20 equiv), and K₃PO₄ (192 mg, 0.905 mmol, 4 equiv).

Entry	Catalyst/Ligand (mass)	Conversion ^a (%)
1	Pd(OAc) ₂ /SPhos (2 mg/7.4 mg)	88
2	Pd(OAc) ₂ /CyJohnPhos (2 mg/6.3 mg)	69
3	Pd(OAc) ₂ /XPhos (2 mg/8.6 mg)	34
4	Pd(OAc) ₂ /DavePhos (2 mg/7.1 mg)	76
5	Pd(PPh ₃) ₄ (10.5 mg)	0
6	Pd(dppf)Cl ₂ (7.4 mg)	0
7	Pd ₂ (dba) ₃ (8.3 mg)	0
8	Pd ₂ (dba) ₃ /SPhos (8.3 mg/7.4 mg)	0

^aConversion to 1.16 determined by HPLC against a caffeine internal standard. See Experimental section for further details.

Results from Table 6

3.4 Base Study

Reactions were carried out according to General Procedure 1D using 4-bromophenylboronic acid, MIDA ester (78 mg, 0.25 mmol, 1 equiv), phenylboronic acid, pinacol ester (66 mg, 0.325 mmol, 1.3 equiv), Pd(OAc)₂ (2.2 mg, 0.01 mmol, 4 mol%), SPhos (8.2 mg, 0.02 mmol, 8 mol%), methyl 2-(4-chlorophenyl)acetate (62 mg, 0.375 mmol, 1.5 equiv), H₂O (81 μ L, 4.5 mmol, 20 equiv), and Base (X mg, 1 mmol, 4 equiv).

Entry	Base (mass)	Conversion ^a (%)
1	K ₃ PO ₄ (212 mg)	88
2	KOH (56 mg)	6
3	K ₂ CO ₃ (138 mg)	41
4	Cs ₂ CO ₃ (325 mg)	65
5	K ₂ HPO ₄ (174 mg)	0
6	Na ₂ CO ₃ (105 mg)	0

^aConversion to 1.16 determined by HPLC against a caffeine internal standard. See Experimental section for further details.

Results from Table 7

Reactions were carried out according to General Procedure 1E using 2-bromo-6-chloropyridine (48 mg, 0.25 mmol, 1 equiv), Pd(OAc)₂ (2.2 mg, 0.01 mmol, 4 mol%), ligand (**X** mg, 0.02 mmol, 8 mol%), 4-methylphenylboronic acid, pinacol ester (60 mg, 0.275 mmol, 1.1 equiv), H₂O (90 μL, 5 mmol, 20 equiv), and K₃PO₄ (212 mg, 1 mmol, 4 equiv). The ratio of mono (**1.16**) to bis (**1.24**) coupled product was recorded by HPLC analysis.

Entry	Temp (°C)	Ligand (mass)	Ratio ^a (1.28/1.29)	Full conversion (Y/N)
1	23	SPhos (8.2 mg)	88/12	N
2	23	DavePhos (7.8 mg)	100/0	N
3	23	PPh ₃ (5.2 mg)	100/0	N
4	70	SPhos (8.2 mg)	44/56	Y
5	70	DavePhos (7.8 mg)	65/35	Y
6	70	PPh ₃ (5.2 mg)	70/30	Y
7	90	SPhos (8.2 mg)	36/63	Y
8	90	DavePhos (7.8 mg)	54/45	Y
9	90	PPh ₃ (5.2 mg)	80/20	Y
10	90	RuPhos (9.3 mg)	36/64	Y
12	90	dppf (11.1 mg)	79/21	Y
13	90	dppp (8.2 mg)	85/15	N

^aConversion to **1.16** determined by HPLC against a caffeine internal standard. See Experimental section for further details.

Results from Table 8

Reactions were carried out according to General Procedure 1E using 1-bromo-4-chlorobenzene (48 mg, 0.25 mmol, 1 equiv), Pd(OAc)₂ (2.2 mg, 0.01 mmol, 4 mol%), ligand (**X** mg, 0.02 mmol, 8 mol%), (4-(2-methoxy-2-oxoethyl)phenyl)boronic acid, pinacol ester (76 mg, 0.275 mmol, 1.1 equiv), H₂O

(90 μ L, 5 mmol, 20 equiv), and K_3PO_4 (212 mg, 1 mmol, 4 equiv). The ratio of mono (**16**) to bis (**24**) coupled product was recorded by HPLC analysis.

Entry	Ligand	Ratio ^a (1.16/1.24)
1	PPh ₃	100:0
2	DavePhos	100:0
3	SPhos	88:12

^aConversion to 1.16 determined by HPLC against a caffeine internal standard. See Experimental section for further details.

Results from Table 9

Reactions were carried out according to General Procedure 1E using 1-bromo-4-chlorobenzene (48 mg, 0.25 mmol, 1 equiv), phenylboronic acid, MIDA ester (75 mg, 0.325 mmol, 1.3 equiv), Pd(OAc)₂ (2.2 mg, 0.01 mmol, 4 mol%), SPhos (8.2 mg, 0.02 mmol, 8 mol%), (4-(2-methoxy-2-oxoethyl)phenyl)boronic acid, pinacol ester (76 mg, 0.275 mmol, 1.1 equiv), H₂O (90 μ L, 5 mmol, 20 equiv), and K_3PO_4 (212 mg, 1 mmol, 4 equiv). Stirring the reaction at room temperature for T1 (X h) before heating the reaction to 90 °C for T2 (X h), before HPLC analysis against a known standard.

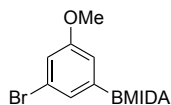
Entry	T1 (h) (rt)	T2 (h) (90 °C)	Conversion ^a (%)
1	2	24	86
2	4	24	86
3	6	24	92
4	8	24	96
5	16	24	88
6	8	2	6
7	8	16	91 (isolated)
8	8	20	93

^aConversion to 1.16 determined by HPLC against a caffeine internal standard. See Experimental section for further details.

4. Compound Characterization Data

4.1 Intermediates

(3-Bromo-5-methoxyphenyl)boronic acid MIDA ester, **S1.1**



Prepared according to General Procedure 1C using (3-bromo-5-methoxyphenyl)boronic acid (1.0 g, 4.34 mmol, 1 equiv), *N*-methyliminodiacetic acid (671 mg, 4.56 mmol, 1.05 equiv), and DMF (50 mL) to afford the desired product as a white solid (1.4 g, 94%).

ν_{\max} (solid): 3070, 2963, 2935, 1748, 1668, 1569, 1461, 1405, 1269 cm^{-1} .

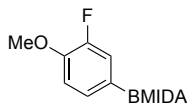
$^1\text{H NMR}$ (DMSO- d_6 , 400 MHz): δ 7.21–7.06 (m, 2H), 6.95 (d, $J = 1.4$ Hz, 1H), 4.33 (d, $J = 17.2$ Hz, 2H), 4.14 (d, $J = 17.2$ Hz, 2H), 3.77 (s, 3H), 2.56 (s, 3H).

$^{13}\text{C NMR}$ (DMSO- d_6 , 101 MHz): δ 169.2, 162.3, 159.8, 127.0, 122.1, 117.3, 117.0, 62.0, 55.4, 47.7.

$^{11}\text{B NMR}$ (DMSO- d_6 , 128 MHz): δ 11.03.

HRMS: exact mass calculated for $[\text{M}+\text{Na}]^+$ ($\text{C}_{12}\text{H}_{13}\text{BBrNNaO}_5$) requires m/z 365.9942, found m/z 365.9943.

(3-Fluoro-4-methoxyphenyl)boronic acid MIDA ester, **S1.2**



Prepared according to General Procedure 1C using (3-fluoro-4-methoxyphenyl)boronic acid (500 mg, 2.9 mmol, 1 equiv), *N*-methyliminodiacetic acid (448 mg, 3.05 mmol, 1.05 equiv), and DMF (20 mL) to afford the desired product as a white solid (800 mg, 98%).

ν_{\max} (solid): 3010, 2966, 1745, 1614, 1514, 1448, 1413, 1338, 1273 cm^{-1} .

$^1\text{H NMR}$ (DMSO- d_6 , 400 MHz): δ 7.26–7.07 (m, 3H), 4.31 (d, $J = 17.2$ Hz, 2H), 4.10 (d, $J = 17.1$ Hz, 2H), 3.84 (s, 3H), 2.52 (s, 3H).

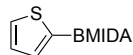
$^{13}\text{C NMR}$ (DMSO- d_6 , 101 MHz): δ 169.2, 151.3 (d, $^1J_{\text{C-F}} = 244.2$ Hz), 147.6 (d, $^2J_{\text{C-F}} = 10.6$ Hz), 128.9 (d, $^3J_{\text{C-F}} = 3.0$ Hz), 119.2 (d, $^2J_{\text{C-F}} = 15.5$ Hz), 113.3, 61.8, 55.7, 47.5. Carbon bearing boron not observed.

$^{11}\text{B NMR}$ (DMSO- d_6 , 128 MHz): δ 11.12.

$^{19}\text{F NMR}$ (DMSO- d_6 , 376 MHz): δ -136.83.

HRMS: exact mass calculated for $[M+NH_4]^+$ ($C_{12}H_{17}BFN_2O_5$) requires m/z 299.1209, found m/z 299.1210.

Thiophen-2-ylboronic acid MIDA ester, **S1.3**



Prepared according to General Procedure 1C using thiophen-2-ylboronic acid (1 g, 7.8 mmol, 1 equiv), *N*-methyliminodiacetic acid (1.2 g, 8.2 mmol, 1.05 equiv), and DMF (30 mL) to afford the desired product as a white solid (1.1 g, 58%).

ν_{\max} (solid): 2999, 2958, 1747, 1737, 1514, 1454, 1402, 1334, 1298 cm^{-1} .

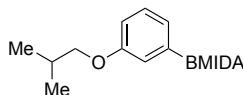
1H NMR (DMSO- d_6 , 400 MHz): δ 7.71 (dd, $J = 4.7, 0.9$ Hz, 1H), 7.24 (dd, $J = 3.3, 0.9$ Hz, 1H), 7.19 (dd, $J = 4.7, 3.4$ Hz, 1H), 4.35 (d, $J = 17.2$ Hz, 2H), 4.12 (d, $J = 17.2$ Hz, 2H), 2.58 (s, 3H).

^{13}C NMR (DMSO- d_6 , 101 MHz): δ 168.9, 132.9, 129.6, 128.3, 61.4, 47.4. Carbon bearing boron not observed.

^{11}B NMR (DMSO- d_6 , 128 MHz): δ 11.27.

HRMS: exact mass calculated for $[M+NH_4]^+$ ($C_9H_{14}BSN_2O_4$) requires m/z 257.0762, found m/z 257.0763.

(3-Isobutoxyphenyl)boronic acid, MIDA ester, **S1.4**



Prepared according to General Procedure 1C using (3-isobutoxyphenyl)boronic acid (600 mg, 3.1 mmol, 1 equiv), *N*-methyliminodiacetic acid (477 mg, 3.24 mmol, 1.05 equiv), and DMF (30 mL) to afford the desired product as a white solid (900 mg, 95%).

ν_{\max} (solid): 3004, 2956, 2872, 1768, 1748, 1577, 1457, 1424, 1286, 1253 cm^{-1} .

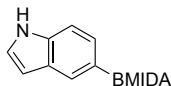
1H NMR (DMSO- d_6 , 400 MHz): δ 7.26 (t, $J = 7.7$ Hz, 1H), 6.99–6.92 (m, 2H), 6.91 (dd, $J = 8.1, 2.6$ Hz, 1H), 4.31 (d, $J = 17.2$ Hz, 2H), 4.10 (d, $J = 17.2$ Hz, 2H), 3.73 (d, $J = 6.5$ Hz, 2H), 2.51 (s, 3H), 2.00 (m, 1H), 0.98 (d, $J = 6.7$ Hz, 6H).

^{13}C NMR (DMSO- d_6 , 101 MHz): δ 169.4, 158.3, 128.8, 124.4, 118.2, 114.7, 73.4, 61.8, 47.5, 27.8, 19.1. Carbon bearing boron not observed.

^{11}B NMR (DMSO- d_6 , 128 MHz): δ 11.06.

HRMS: exact mass calculated for $[M+H]^+$ ($C_{15}H_{20}BNO_5$) requires m/z 305.1507, found m/z 305.1513.

(1*H*-Indol-5-yl)boronic acid, MIDA ester, **S1.5**



Prepared according to General Procedure 1C using (1*H*-indol-5-yl)boronic acid (2 g, 12.4 mmol, 1 equiv), *N*-methyliminodiacetic acid (1.9 g, 13.02 mmol, 1.05 equiv), and DMF (50 mL) to afford the desired product as a white solid (3.3 g, 98%).

ν_{\max} (solid): 3401, 3008, 2962, 1766, 1744, 1578, 1455, 1340, 1245, 1236 cm^{-1} .

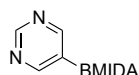
1H NMR ($CDCl_3$, 400 MHz): δ 11.02 (s, 1H), 7.62 (s, 1H), 7.37 (d, $J = 8.2$ Hz, 1H), 7.3 (t, $J = 2.7$ Hz, 1H), 7.14 (d, $J = 8.2$ Hz, 1H), 6.41 (s, 1H), 4.30 (d, $J = 17.2$ Hz, 2H), 4.08 (d, $J = 17.2$ Hz, 2H), 2.45 (s, 3H).

^{13}C NMR ($CDCl_3$, 101 MHz): δ 169.5, 136.5, 127.5, 124.9, 124.5, 110.8, 101.1, 61.6, 47.5. Carbon bearing boron not observed.

^{11}B NMR ($CDCl_3$, 128 MHz): δ 12.52.

HRMS: exact mass calculated for $[M+H]^+$ ($C_{13}H_{13}BN_2O_4$) requires m/z 273.1041, found m/z 273.1045.

Pyrimidin-5-ylboronic acid, MIDA ester, **S1.6**



Prepared according to General Procedure 1C using pyrimidin-5-ylboronic acid (1 g, 8.13 mmol, 1 equiv), *N*-methyliminodiacetic acid (1.26 g, 8.54 mmol, 1.05 equiv), and DMF (80 mL) to afford the desired product as a white solid (1.8 g, 94%).

ν_{\max} (solid): 3030, 2939, 1748, 1763, 1582, 1424, 1413, 1286, 1254 cm^{-1} .

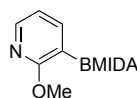
1H NMR ($DMSO-d_6$, 400 MHz): δ 9.19 (s, 1H), 8.81 (d, $J = 4.7$ Hz, 2H), 4.42 (d, $J = 17.2$ Hz, 2H), 4.22 (d, $J = 17.1$ Hz, 2H), 2.68 (s, 3H).

^{13}C NMR ($DMSO-d_6$, 101 MHz): δ 171.5, 169.0, 160.9, 158.9, 62.1, 47.8.

^{11}B NMR ($DMSO-d_6$, 128 MHz): δ 10.58.

HRMS: exact mass calculated for $[M+H]^+$ ($C_9H_{10}BN_3O_4$) requires m/z 236.037, found m/z 236.0839.

(2-Methoxypyridin-3-yl)boronic acid, MIDA ester, **S1.7**



Prepared according to General Procedure 1C using (2-methoxypyridin-3-yl)boronic acid (600 mg, 3.9 mmol, 1 equiv), *N*-methyliminodiacetic acid (605 mg, 4.1 mmol, 1.05 equiv), and DMF (40 mL) to afford the desired product as a white solid (1 g, 97%).

ν_{\max} (solid): 3029, 2960, 1770, 1755, 1578, 1460, 1392, 1340 cm^{-1} .

$^1\text{H NMR}$ (DMSO- d_6 , 400 MHz): δ 8.17 (dd, $J = 5.0, 2.0$ Hz, 1H), 7.80 (dd, $J = 7.0, 2.0$ Hz, 1H), 6.98 (dd, $J = 7.0, 5.0$ Hz, 1H), 4.38 (d, $J = 17.1$ Hz, 2H), 4.06 (d, $J = 17.1$ Hz, 2H), 3.81 (s, 3H), 2.61 (s, 3H).

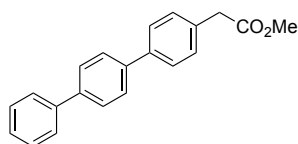
$^{13}\text{C NMR}$ (DMSO- d_6 , 101 MHz): δ 169.1, 165.4, 147.7, 143.7, 116.9, 63.1, 52.8, 47.1. Carbon bearing boron not observed.

$^{11}\text{B NMR}$ (DMSO- d_6 , 128 MHz): δ 11.27.

HRMS: exact mass calculated for $[\text{M}+\text{NH}_4]^+$ ($\text{C}_{11}\text{H}_{13}\text{BN}_2\text{O}_5$) requires m/z 265.0990, found m/z 265.0985.

4.2 Products from Scheme 66

Methyl 2-([1,1':4',1''-terphenyl]-4-yl)acetate, **1.16a**



Prepared according to General Procedure 1A using 4-bromophenylboronic acid, MIDA ester (78 mg, 0.25 mmol, 1 equiv), phenylboronic acid pinacol ester (66 mg, 0.325 mmol, 1.3 equiv), $\text{Pd}(\text{OAc})_2$ (2.2 mg, 0.01 mmol, 4 mol%), SPhos (8.2 mg, 0.02 mmol, 8 mol%), methyl 2-(4-chlorophenyl)acetate (69 mg, 57 μL , 0.375 mmol, 1.5 equiv), K_3PO_4 (212 mg, 1 mmol, 4 equiv), THF (1 mL, 0.25 M), and H_2O (90 μL , 5 mmol, 20 equiv). After 24 h the reaction mixture was subjected to the purification outlined in the General Procedure (C18 silica gel, 20–70% MeCN in H_2O) to afford the desired product as a white solid (62 mg, 82%).

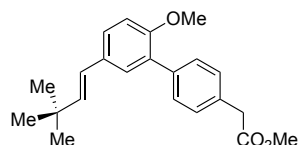
ν_{\max} (solid): 3032, 2954, 1732, 1506, 1486 cm^{-1} .

$^1\text{H NMR}$ (CDCl_3 , 500 MHz): δ 7.67–7.70 (m, 4H), 7.64–7.67 (m, 2H), 7.61–7.63 (m, 2H), 7.45–7.49 (m, 2H), 7.35–7.41 (m, 3H), 3.74 (s, 3H), 3.70 (s, 2H).

^{13}C NMR (CDCl_3 , 126 MHz): δ 172.0, 140.7, 140.2, 139.7, 139.6, 133.1, 129.7, 128.8, 127.5, 127.4, 127.4, 127.2, 127.0, 52.1, 40.9.

HRMS: exact mass calculated for $[\text{M}+\text{H}^+]$ ($\text{C}_{21}\text{H}_{19}\text{O}_2$) requires m/z 303.1380, found m/z 303.1382.

Methyl (*E*)-2-(5'-(3,3-dimethylbut-1-en-1-yl)-2'-methoxy-[1,1'-biphenyl]-4-yl)acetate, **1.16b**



Prepared according to General Procedure 1A using 2-(5-bromo-2-methoxyphenyl)-6-methyl-1,3,6,2-dioxazaborocane-4,8-dione (85.5 mg, 0.25 mmol, 1 equiv), (*E*)-2-(3,3-dimethylbut-1-en-1-yl)-4,4,5,5-tetramethyl-1,3,2-dioxaborolane (68.3 mg, 0.325 mmol, 1.3 equiv), methyl 2-(4-chlorophenyl)acetate (69 mg, 0.375 mmol, 1.5 equiv), $\text{Pd}(\text{OAc})_2$ (2.2 mg, 0.01 mmol, 4 mol%), SPhos (8.4 mg, 0.02 mmol, 8 mol%), K_3PO_4 (212 mg, 0.1 mmol, 4 equiv), THF (1 mL, 0.25 M), and H_2O (90 μL , 5 mmol, 20 equiv). After 24 h the reaction mixture was subjected to the purification outlined in the General Procedure (C18 silica gel, 10–40% MeCN in H_2O) to afford the title compound as a yellow oil (74 mg, 88%).

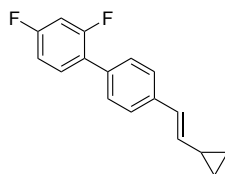
ν_{max} (film): 2953, 2926, 2854, 1735, 1602, 1517, 1492, 1460 cm^{-1} .

^1H NMR (CDCl_3 , 400 MHz): δ 7.55–7.50 (m, 2H), 7.38–7.34 (m, 3H), 7.31 (dd, J = 8.5, 2.3 Hz, 1H), 6.94 (d, J = 8.4 Hz, 1H), 6.31 (d, J = 16.1 Hz, 1H), 6.18 (d, J = 16.2 Hz, 1H), 3.82 (s, 3H), 3.74 (s, 3H), 3.69 (s, 2H), 1.14, (s, 9H).

^{13}C NMR (CDCl_3 , 101 MHz): δ 172.1, 155.6, 140.3, 137.5, 132.6, 131.0, 130.3, 129.7, 128.9, 128.4, 126.3, 123.7, 111.3, 55.7, 52.1, 41.0, 33.3, 29.7.

HRMS: exact mass calculated for $[\text{M}+\text{H}]^+$ ($\text{C}_{22}\text{H}_{27}\text{O}_3$) requires m/z 339.1955, found m/z 339.1958.

(*E*)-4'-(2-Cyclopropylvinyl)-2,4-difluoro-1,1'-biphenyl, **1.16c**



Prepared according to General Procedure 1A using 4-bromophenylboronic acid MIDA ester (78 mg, 0.25 mmol, 1 equiv), (*E*)-2-(2-cyclopropylvinyl)-4,4,5,5-tetramethyl-1,3,2-dioxaborolane (63 mg, 0.325 mmol, 1.3 equiv), 1-chloro-2,4-difluorobenzene (55.5 mg, 0.375 mmol, 1.5 equiv), Pd(OAc)₂ (2.2 mg, 0.01 mmol, 4 mol%), SPhos (8.4 mg, 0.02 mmol, 8 mol%), K₃PO₄ (212 mg, 0.1 mmol, 4 equiv), THF (1 mL, 0.25 M) and H₂O (90 μL, 5 mmol, 20 equiv). After 24 h the reaction mixture was subjected to the purification outlined in the General Procedure (C18 silica gel, 10–40% MeCN in H₂O) to afford the title compound as a yellow solid (55 mg, 86%).

ν_{\max} (film): 3076, 3014, 2924, 2852, 1645, 1614, 1597, 1523, 1490, 1402 cm⁻¹.

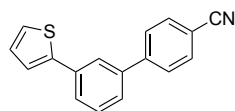
¹H NMR (CDCl₃, 400 MHz): δ 7.49–7.36 (m, 5H), 7.02–6.88 (m, 2H), 6.53 (d, *J* = 15.7 Hz, 1H), 5.82 (dd, *J* = 15.7, 9.0 Hz, 1H), 1.69–1.56 (m, 1H), 0.93–0.83 (m, 2H), 0.60–0.53 (m, 2H).

¹³C NMR (CDCl₃, 101 MHz): δ 161.7 (dd, ¹*J*_{C-F} = 238.3 Hz, ³*J*_{C-F} = 11.2 Hz), 159.2 (dd, ¹*J*_{C-F} = 240.2 Hz, ³*J*_{C-F} = 11.4 Hz), 136.8, 135.2, 132.5, 130.7 (dd, ³*J*_{C-F} = 9.3, ³*J*_{C-F} = 5.1 Hz), 128.5 (d, *J*_{C-F} = 3.3 Hz), 126.3, 125.2, 124.6 (dd, ²*J*_{C-F} = 13.7 Hz, *J*_{C-F} = 3.8 Hz), 111.0 (dd, ²*J*_{C-F} = 21.5, *J*_{C-F} = 4.0 Hz), 103.9 (t, ²*J*_{C-F} = 26.0 Hz), 14.2, 6.9.

¹⁹F NMR (CDCl₃, 376 MHz): δ -111.82 (d, *J* = 7.4 Hz, 1F), -113.35 (d, *J* = 7.4 Hz, 1F).

HRMS: exact mass calculated for [M+H]⁺ (C₁₇H₁₅F₂) requires *m/z* 257.1136, found *m/z* 257.1138.

3'-(Thiophen-2-yl)-[1,1'-biphenyl]-4-carbonitrile, **1.16d**



Prepared according to General Procedure 1A using 3-bromophenylboronic acid MIDA ester (78 mg, 0.25 mmol, 1 equiv), 4,4,5,5-tetramethyl-2-(thiophen-2-yl)-1,3,2-dioxaborolane (68 mg, 0.325 mmol, 1.3 equiv), 4-chlorobenzonitrile (51.4 mg, 0.375 mmol, 1.5 equiv), Pd(OAc)₂ (2.2 mg, 0.01 mmol, 4 mol%), SPhos (8.2 mg, 0.02 mmol, 8 mol%), K₃PO₄ (212 mg, 0.1 mmol, 4 equiv), THF (1 mL, 0.25 M), and H₂O (90 μL, 5 mmol, 20 equiv). After 24 h the reaction mixture was subjected to the

purification outlined in the General Procedure (C18 silica gel, 20–60% MeCN in H₂O) to afford the desired compound as a colorless oil (54 mg, 83%).

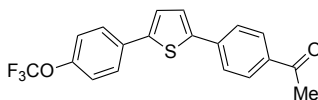
ν_{\max} (film): 3099, 2918, 2850, 2223, 1600, 1475 cm⁻¹.

¹H NMR (CDCl₃, 400 MHz): δ 7.84–7.80 (m, 1H), 7.82–7.71 (m, 4H), 7.72–7.66 (m, 1H), 7.54–7.50 (m, 2H), 7.41 (dd, J = 3.6, 1.2 Hz, 1H), 7.36 (dd, J = 5.1, 1.2 Hz, 1H), 7.14 (dd, J = 5.1, 3.6 Hz, 1H).

¹³C NMR (CDCl₃, 101 MHz): δ 144.8, 143.2, 139.5, 134.9, 132.2, 129.2, 127.7, 127.3, 125.8, 125.7, 124.9, 124.3, 123.2, 118.4, 110.7.

HRMS: exact mass calculated for [M+NH₄]⁺ (C₁₇H₁₅N₂S) requires m/z 279.0954, found m/z 279.0950.

1-(4-(5-(4-(Trifluoromethoxy)phenyl)thiophen-2-yl)phenyl)ethan-1-one, **1.16e**



Prepared according to General Procedure 1A using 2-(5-bromothiophen-2-yl)-6-methyl-1,3,6,2-dioxaborocane-4,8-dione (79.4 mg, 0.25 mmol, 1 equiv), 4,4,5,5-tetramethyl-2-(4-(trifluoromethoxy)phenyl)-1,3,2-dioxaborolane (93.7 mg, 0.325 mmol, 1.3 equiv), 1-(4-chlorophenyl)ethan-1-one (42.8 mg, 0.375 mmol, 1.5 equiv), Pd(OAc)₂ (2.2 mg, 0.01 mmol, 4 mol%), SPhos (8.4 mg, 0.02 mmol, 8 mol%), K₃PO₄ (212 mg, 0.1 mmol, 4 equiv), THF (1 mL, 0.25 M), and H₂O (90 μ L, 5 mmol, 20 equiv). After 24 h the reaction mixture was subjected to the purification outlined in the General Procedure (C18 silica gel, 10–40% MeCN in H₂O) to afford the title compound as a bright yellow solid (77 mg, 85%).

ν_{\max} (film): 3072, 2926, 2854, 1676, 1598, 1541, 1514, 1496, 1452 cm⁻¹.

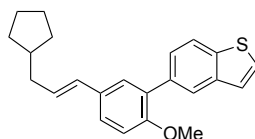
¹H NMR (CDCl₃, 400 MHz): δ 8.03–7.99 (m, 2H), 7.76–7.71 (m, 2H), 7.70–7.65 (m, 2H), 7.43 (d, J = 3.8 Hz, 1H), 7.32 (d, J = 3.9 Hz, 1H), 7.32–7.23 (m, 2H), 2.65 (s, 3H).

¹³C NMR (CDCl₃, 101 MHz): δ 196.8, 148.2, 143.1, 142.1, 137.9, 135.4, 132.2, 128.7, 126.5, 125.2, 124.9, 124.4, 121.0, 120.0 (q, ¹J_{C-F} = 257.8 Hz), 26.1.

¹⁹F NMR (CDCl₃, 376 MHz): δ -57.81.

HRMS: exact mass calculated for [M+H]⁺ (C₁₉H₁₄F₃O₂S₁) requires m/z 363.0661, found m/z 363.0662.

(*E*)-5-(5-(3-Cyclopentylprop-1-en-1-yl)-2-methoxyphenyl)benzo[*b*]thiophene, **1.16f**



Prepared according to General Procedure 1A using 2-(5-bromo-2-methoxyphenyl)-6-methyl-1,3,6,2-dioxazaborocane-4,8-dione (85.5 mg, 0.25 mmol, 1 equiv), (*E*)-2-(3-cyclopentylprop-1-en-1-yl)-4,4,5,5-tetramethyl-1,3,2-dioxaborolane (76.7 mg, 0.325 mmol, 1.3 equiv), 5-chlorothiophene (42.4 mg, 0.375 mmol, 1.5 equiv), Pd(OAc)₂ (2.2 mg, 0.01 mmol, 4 mol%), SPhos (8.4 mg, 0.02 mmol, 8 mol%), K₃PO₄ (212 mg, 0.1 mmol, 4 equiv), THF (1 mL, 0.25 M), and H₂O (90 μL, 5 mmol, 20 equiv). After 24 h the reaction mixture was subjected to the purification outlined in the General Procedure (C18 silica gel, 10–40% MeCN in H₂O) to afford the title compound as a yellow oil (58 mg, 64%).

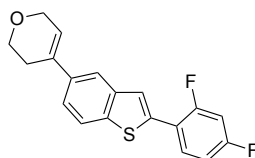
ν_{max} (film): 2997, 2945, 2856, 2362, 1600, 1500, 1458, 1438 cm⁻¹.

¹H NMR (CDCl₃, 400 MHz): δ 8.04 (s, 1H), 7.85 (d, *J* = 8.3 Hz, 1H), 7.55 (dd, *J* = 8.2, 1.5 Hz, 1H), 7.45 (d, *J* = 5.4 Hz, 1H), 7.39 (d, *J* = 2.2 Hz, 1H), 7.36 (d, *J* = 5.4 Hz, 1H), 7.31 (dd, *J* = 8.5, 2.2 Hz, 1H), 6.95 (d, *J* = 8.5 Hz, 1H), 6.38 (d, *J* = 15.8 Hz, 1H), 6.15 (dt, *J* = 7.1, 7.1, 15.7, 1H), 3.83 (s, 3H), 2.22 (t, *J* = 6.7 Hz, 2H), 2.02–1.87 (m, 1H), 1.83–1.74 (m, 2H), 1.68–1.59 (m, 2H), 1.57–1.52 (m, 2H), 1.25–1.16 (m, 2H).

¹³C NMR (CDCl₃, 101 MHz): δ 155.1, 139.2, 137.9, 134.3, 130.5, 130.0, 128.8, 128.4, 128.1, 125.9, 125.7, 125.7, 123.1, 122.6, 122.3, 110.8, 55.2, 39.6, 38.9, 31.8, 24.6.

HRMS: exact mass calculated for [M+H]⁺ (C₂₃H₂₅O₁S₁) requires *m/z* 349.1621, found *m/z* 349.1622.

4-(2-(2,4-Difluorophenyl)benzo[*b*]thiophen-5-yl)-3,6-dihydro-2*H*-pyran, **1.16g**



Prepared according to General Procedure 1A using (5-bromobenzo[*b*]thiophen-2-yl)boronic acid MIDA ester (92 mg, 0.25 mmol, 1 equiv), (3,6-dihydro-2*H*-pyran-4-yl)boronic acid pinacol ester (68.3 mg, 0.325 mmol, 1.3 equiv), 1-chloro-2,4-difluorobenzene (55 mg, 0.375 mmol, 1.5 equiv), Pd(OAc)₂ (2.2 mg, 0.01 mmol, 4 mol%), SPhos (8.4 mg, 0.02 mmol, 8 mol%), K₃PO₄ (212 mg, 0.1 mmol, 4 equiv), THF (1 mL, 0.25 M), and H₂O (90 μL, 5 mmol, 20 equiv). After 24 h the reaction mixture was subjected to the purification outlined in the General Procedure (C18 silica gel, 20–70% MeCN in H₂O) to afford the title compound as a white solid (49 mg, 60%).

ν_{\max} (film): 3070, 3057, 2924, 2852, 1708, 1614, 1591, 1525, 1492 cm⁻¹.

¹H NMR (CDCl₃, 400 MHz): δ 7.80 (d, *J* = 8.4 Hz, 2H), 7.71–7.62 (m, 2H), 7.44 (dd, *J* = 8.5, 1.6 Hz, 1H), 7.01–6.92 (m, 2H), 6.21 (s, 1H), 4.38 (dd, *J* = 5.3, 2.6 Hz, 2H), 3.99 (t, *J* = 5.4 Hz, 2H), 2.62 (d, *J* = 1.7 Hz, 2H).

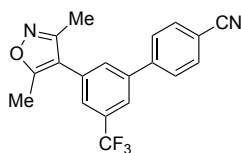
¹³C NMR (CDCl₃, 101 MHz): δ 162.5 (dd, ¹*J*_{C-F} = 251.2 Hz, ³*J*_{C-F} = 12.2 Hz), 159.7 (dd, ¹*J*_{C-F} = 254.0 Hz, ³*J*_{C-F} = 11.9 Hz), 140.6, 138.2 (d, ⁴*J*_{C-F} = 2.3 Hz), 137.3, 136.9 (d, ⁴*J*_{C-F} = 3.4 Hz), 134.1, 130.4 (dd, ³*J*_{C-F} = 9.5 Hz, ⁴*J*_{C-F} = 4.8 Hz), 123.2 (d, ³*J*_{C-F} = 8.3 Hz), 122.6, 122.0, 121.9, 119.8, 118.7 (dd, ³*J*_{C-F} = 12.5 Hz, ⁴*J*_{C-F} = 4.0 Hz), 112.0 (d, ²*J*_{C-F} = 21.5 Hz), 104.8 (t, ²*J*_{C-F} = 25.9 Hz), 65.9, 64.5, 27.5.

¹⁹F NMR (CDCl₃, 376 MHz): δ -108.82 (d, *J* = 8.5 Hz, 1F), -109.74 (d, *J* = 8.4 Hz, 1F).

HRMS: exact mass calculated for [M+H]⁺ (C₁₉H₁₄F₂OSH) requires *m/z* 329.0806, found *m/z* 329.0806.

3'-(3,5-Dimethylisoxazol-4-yl)-5'-(trifluoromethyl)-[1,1'-biphenyl]-4-carbonitrile,

1.16h



Prepared according to General Procedure 1A using 2-(3-bromo-5-(trifluoromethyl)phenyl)-6-methyl-1,3,6,2-dioxaborocane-4,8-dione (94.5 mg, 0.25 mmol, 1 equiv), 3,5-dimethyl-4-(4,4,5,5-tetramethyl-1,3,2-dioxaborolan-2-yl)isoxazole (72.4 mg, 0.325 mmol, 1.3 equiv), 4-benzonitrile (51.4 mg, 0.375 mmol, 1.5 equiv), Pd(OAc)₂ (2.2 mg, 0.01 mmol, 4 mol%), SPhos (8.4 mg, 0.02 mmol, 8

mol%), K₃PO₄ (212 mg, 0.1 mmol, 4 equiv), THF (1 mL, 0.25 M), and H₂O (90 μL, 5 mmol, 20 equiv). After 24 h the reaction mixture was subjected to the purification outlined in the General Procedure (C18 silica gel, 10–40% MeCN in H₂O) to afford the title compound as a white solid (55.3 mg, 65%).

ν_{\max} (film): 2991, 2926, 2852, 2227, 1633, 1606, 1467, 1354 cm⁻¹.

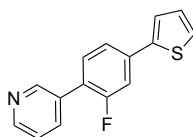
¹H NMR (CDCl₃, 400 MHz): δ 7.86–7.80 (m, 3H), 7.76–7.72 (m, 2H), 7.65 (s, 1H), 7.59 (s, 1H), 2.49 (s, 3H), 2.34 (s, 3H).

¹³C NMR (CDCl₃, 101 MHz): δ 165.6, 157.7, 143.1, 140.4, 132.4, 132.1, 131.9 (d, ²J_{C-F} = 32.5 Hz), 130.5, 127.4, 125.2 (d, ³J_{C-F} = 4.7 Hz), 123.1 (d, ¹J_{C-F} = 272.7 Hz), 122.7 (d, ³J_{C-F} = 4.1 Hz), 117.9, 114.8, 111.8, 11.2, 10.3.

¹⁹F NMR (CDCl₃, 376 MHz): δ -62.71 (s, 3F).

HRMS: exact mass calculated for [M+H]⁺ (C₁₉H₁₄F₃N₂O₁) requires *m/z* 343.1053, found *m/z* 343.1055.

3-(2-Fluoro-4-(thiophen-2-yl)phenyl)pyridine, **1.16i**



Prepared according to General Procedure 1A using 2-(4-bromo-2-fluorophenyl)-6-methyl-1,3,6,2-dioxazaborocane-4,8-dione (83 mg, 0.25 mmol, 1 equiv), 4,4,5,5-tetramethyl-2-(thiophen-2-yl)-1,3,2-dioxaborolane (68.3 mg, 0.325 mmol, 1.3 equiv), 3-chloropyridine (42.4 mg, 0.375 mmol, 1.5 equiv), Pd(OAc)₂ (2.2 mg, 0.01 mmol, 4 mol%), SPhos (8.4 mg, 0.02 mmol, 8 mol%), K₃PO₄ (212 mg, 0.1 mmol, 4 equiv), THF (1 mL, 0.25 M), and H₂O (90 μL, 5 mmol, 20 equiv). After 24 h the reaction mixture was subjected to the purification outlined in the General Procedure (C18 silica gel, 10–40% MeCN in H₂O) to afford the title compound as an off white solid (53 mg, 84%).

ν_{\max} (film): 3045, 3030, 2924, 2852, 1616, 1552, 1537, 1471, 1400 cm⁻¹.

¹H NMR (CDCl₃, 400 MHz): δ 8.85 (s, 1H), 8.64 (dd, *J* = 4.8, 1.7 Hz, 1H), 7.95–7.87 (m, 1H), 7.52 (dd, *J* = 8.0, 1.7 Hz, 1H), 7.50–7.43 (m, 2H), 7.43–7.38 (m, 2H), 7.36 (dd, *J* = 5.1, 1.1 Hz, 1H), 7.13 (dd, *J* = 5.1, 3.6 Hz, 1H).

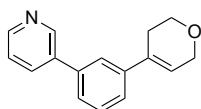
¹³C NMR (CDCl₃, 101 MHz): δ 159.6 (d, ¹J_{C-F} = 248.6 Hz), 149.0 (d, ⁴J_{C-F} = 3.4 Hz), 148.3, 141.8, 136.0 (d, ³J_{C-F} = 8.5 Hz), 135.6 (d, ³J_{C-F} = 3.6 Hz), 130.7, 130.3

(d, $^3J_{\text{C-F}} = 3.8$ Hz), 127.8, 125.4, 123.8 (d, $^2J_{\text{C-F}} = 14.3$ Hz), 123.6, 122.8, 121.6 (d, $^4J_{\text{C-F}} = 2.9$ Hz), 113.0 (d, $^2J_{\text{C-F}} = 24.3$ Hz).

^{19}F NMR (CDCl_3 , 376 MHz): δ -117.45 (s, 1F).

HRMS: exact mass calculated for $[\text{M}+\text{H}]^+$ ($\text{C}_{15}\text{H}_{11}\text{F}_1\text{N}_1\text{S}_1$) requires m/z 256.0592, found m/z 256.0591.

3-(3-(3,6-Dihydro-2H-pyran-4-yl)phenyl)pyridine, **1.16j**



Prepared according to General Procedure 1A using 3-bromophenylboronic acid MIDA ester (78 mg, 0.25 mmol, 1 equiv), 2-(3,6-dihydro-2H-pyran-4-yl)-4,4,5,5-tetramethyl-1,3,2-dioxaborolane (68 mg, 0.325 mmol, 1.3 equiv), 3-chloropyridine (42.4 mg, 0.375 mmol, 1.5 equiv), $\text{Pd}(\text{OAc})_2$ (2.2 mg, 0.01 mmol, 4 mol%), SPhos (8.4 mg, 0.02 mmol, 8 mol%), K_3PO_4 (212 mg, 0.1 mmol, 4 equiv), THF (1 mL, 0.25 M), and H_2O (90 μL , 5 mmol, 20 equiv). After 24 h the reaction mixture was subjected to the purification outlined in the General Procedure (C18 silica gel, 10–40% MeCN in H_2O) to afford the title compound as a brown oil (45 mg, 76%).

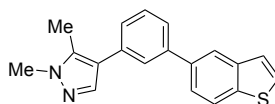
ν_{max} (film): 3030, 2922, 2850, 2358, 1718, 1600, 1577, 1469, 1429 cm^{-1} .

^1H NMR (CDCl_3 , 400 MHz): δ 8.87 (d, $J = 2.5$ Hz, 1H), 8.62 (dd, $J = 4.8, 1.6$ Hz, 1H), 7.90 (ddd, $J = 7.9, 2.4, 1.6$ Hz, 1H), 7.60 (q, $J = 1.4$ Hz, 1H), 7.51–7.45 (m, 3H), 7.39 (ddd, $J = 7.9, 4.9, 0.9$ Hz, 1H), 6.23 (m 1H), 4.37 (q, $J = 2.8$ Hz, 2H), 3.99 (t, $J = 5.5$ Hz, 2H), 2.63–2.57 (m, 2H).

^{13}C NMR (CDCl_3 , 101 MHz): δ 148.0, 147.8, 140.8, 137.6, 136.3, 133.9, 133.4, 128.7, 125.6, 124.0, 123.2, 123.0, 122.8, 65.4, 63.9, 26.8.

HRMS: exact mass calculated for $[\text{M}+\text{H}]^+$ ($\text{C}_{16}\text{H}_{16}\text{N}_1\text{O}_1$) requires m/z 238.1226, found m/z 238.1229.

4-(3-(Benzo[*b*]thiophen-5-yl)phenyl)-1,5-dimethyl-1H-pyrazole, **1.16k**



Prepared according to General Procedure 1A using 3-bromophenylboronic acid MIDA ester (78 mg, 0.25 mmol, 1 equiv), 1,5-dimethyl-4-(4,4,5,5-tetramethyl-1,3,2-dioxaborolan-2-yl)-1H-pyrazole (72.1 mg, 0.325 mmol, 1.3 equiv), 4-

chlorobenzothiophene (63 mg, 0.375 mmol, 1.5 equiv), Pd(OAc)₂ (2.2 mg, 0.01 mmol, 4 mol%), SPhos (8.4 mg, 0.02 mmol, 8 mol%), K₃PO₄ (212 mg, 0.1 mmol, 4 equiv), THF (1 mL, 0.25 M), and H₂O (90 μL, 5 mmol, 20 equiv). After 24 h the reaction mixture was subjected to the purification outlined in the General Procedure (C18 silica gel, 10–40% MeCN in H₂O) to afford the title compound as a yellow oil (66 mg, 87%).

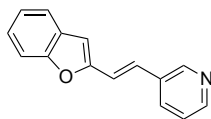
ν_{\max} (film): 2924, 2852, 1732, 1604, 1558, 1487, 1454, 1396 cm⁻¹.

¹H NMR (CDCl₃, 400 MHz): δ 8.17–8.11 (m, 1H), 7.92 (d, *J* = 8.3 Hz, 1H), 7.70–7.63 (m, 3H), 7.62–7.55 (m, 1H), 7.58–7.45 (m, 2H), 7.42–7.36 (m, 2H), 3.90 (s, 3H), 2.46 (s, 3H).

¹³C NMR (CDCl₃, 101 MHz): δ 141.1, 140.0, 138.3, 137.1, 136.8, 134.7, 134.1, 128.6, 126.3, 126.3, 126.1, 124.8, 123.5, 123.3, 123.1, 120.4, 120.2, 36.0, 10.0.

HRMS: exact mass calculated for [M+H]⁺ (C₁₉H₁₇N₂S₁) requires *m/z* 305.1107, found *m/z* 305.1108.

(*E*)-3-(2-(Benzofuran-3-yl)vinyl)pyridine, **1.161**



Prepared according to General Procedure 1A using (*E*)-2-(2-bromovinyl)-6-methyl-1,3,6,2-dioxazaborocane-4,8-dione (65 mg, 0.25 mmol, 1 equiv), 2-(benzofuran-3-yl)-4,4,5,5-tetramethyl-1,3,2-dioxaborolane (79.3 mg, 0.325 mmol, 1.3 equiv), 3-chloropyridine (42.4 mg, 0.375 mmol, 1.5 equiv), Pd(OAc)₂ (2.2 mg, 0.01 mmol, 4 mol%), SPhos (8.4 mg, 0.02 mmol, 8 mol%), K₃PO₄ (212 mg, 0.1 mmol, 4 equiv), THF (1 mL, 0.25 M), and H₂O (90 μL, 5 mmol, 20 equiv). After 24 h the reaction mixture was subjected to the purification outlined in the General Procedure (C18 silica gel, 10–40% MeCN in H₂O) to afford the title compound as a pale yellow solid (48 mg, 87%).

ν_{\max} (film): 3076, 3014, 1645, 1614, 1597, 1523, 1408, 1267 cm⁻¹.

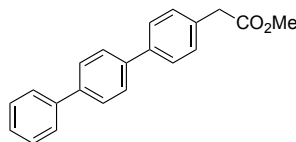
¹H NMR (CDCl₃, 400 MHz): δ 8.76 (d, *J* = 2.5 Hz, 1H), 8.51 (dd, *J* = 4.8, 1.6 Hz, 1H), 7.82 (dt, *J* = 8.0, 1.9 Hz, 1H), 7.56 (d, *J* = 7.7 Hz, 1H), 7.49 (dd, *J* = 8.2, 1.0 Hz, 1H), 7.34–7.20 (m, 4H), 7.06 (d, *J* = 16.3 Hz, 1H), 6.73 (s, 1H).

¹³C NMR (CDCl₃, 101 MHz): δ 155.0, 154.3, 148.9, 148.7, 132.8, 132.3, 128.9, 126.3, 125.1, 123.6, 123.1, 121.1, 118.4, 111.0, 106.3.

HRMS: exact mass calculated for $[M+H]^+$ ($C_{15}H_{12}N_1O_1$) requires m/z 222.0914, found m/z 222.0913.

4.3 Products from Scheme 68

Methyl 2-([1,1':4',1''-terphenyl]-4-yl)acetate, **1.16a**



Prepared according to General Procedure 1B using 1-bromo-4-chlorobenzene (47.5 mg, 0.25 mmol, 1 equiv), (4-(2-methoxy-2-oxoethyl)phenyl)boronic acid pinacol ester (76 mg, 0.275 mmol, 1.1 equiv), $Pd(OAc)_2$ (2.2 mg, 0.001 mmol, 4 mol%), DavePhos (7.8 mg, 0.02 mmol, 8 mol%), phenylboronic acid MIDA ester (75 mg, 0.325 mmol, 1.3 equiv), K_3PO_4 (212 mg, 1 mmol, 4 equiv), THF (1 mL, 0.25 M), and H_2O (90 μ L, 5 mmol, 20 equiv). After 24 h the reaction mixture was subjected to the purification outlined in the General Procedure (silica gel, 0–10% EtOAc/Petroleum ether) to afford the title compound as a white solid (69 mg, 91%).

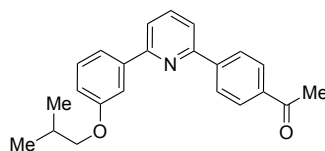
ν_{max} (solid): 3032, 2954, 1732, 1506, 1486 cm^{-1} .

1H NMR ($CDCl_3$, 500 MHz): δ 7.67–7.70 (m, 4H), 7.64–7.67 (m, 2H), 7.61–7.63 (m, 2H), 7.45–7.49 (m, 2H), 7.35–7.41 (m, 3H), 3.74 (s, 3H), 3.70 (s, 2H).

^{13}C NMR ($CDCl_3$, 126 MHz): δ 172.0, 140.7, 140.2, 139.7, 139.6, 133.1, 129.7, 128.8, 127.5, 127.4, 127.4, 127.2, 127.0, 52.1, 40.9.

HRMS: exact mass calculated for $[M+H]^+$ ($C_{21}H_{19}O_2$) requires m/z 303.1380, found m/z $[M+H]^+$ 303.1382.

1-(3-(6-(4-Isobutoxyphenyl)pyridin-2-yl)phenyl)ethan-1-one, **1.16m**



Prepared according to General Procedure 1B using 2-bromo-6-chloropyridine (47.5 mg, 0.25 mmol, 1 equiv), (3-acetylphenyl)boronic acid pinacol ester (68 mg, 0.275 mmol, 1.1 equiv), (3-isobutoxyphenyl)boronic acid MIDA ester (99 mg, 0.325 mmol, 1.3 equiv), $Pd(OAc)_2$ (2.2 mg, 0.001 mmol, 4 mol%), DavePhos (7.8 mg, 0.02 mmol, 8 mol%), K_3PO_4 (212 mg, 1 mmol, 4 equiv), THF (1 mL, 0.25 M), and H_2O (90 μ L, 5 mmol, 20 equiv). After 24 h the reaction mixture was subjected to the

purification outlined in the General Procedure (silica gel, 0–20% EtOAc/Petroleum ether) to afford the title compound as an off white solid (64 mg, 74%).

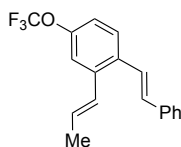
ν_{\max} (solid): 3060, 2954, 2917, 1683, 1608, 1584, 1459, 1267 cm^{-1} .

$^1\text{H NMR}$ (CDCl_3 , 400 MHz): δ 8.30–8.24 (m, 2H), 8.13–8.08 (m, 2H), 7.89–7.83 (m, 1H), 7.79–7.74 (m, 3H), 7.72–7.69 (m, 1H), 7.43 (t, $J = 7.9$ Hz, 1H), 7.01 (ddd, $J = 8.2, 2.6, 0.8$ Hz, 1H), 3.87 (d, $J = 6.5$ Hz, 2H), 2.68 (s, 3H), 2.23–2.12 (m, 1H), 1.10 (d, $J = 6.7$ Hz, 6H).

$^{13}\text{C NMR}$ (CDCl_3 , 101 MHz): δ 197.4, 159.3, 156.6, 154.9, 143.2, 140.1, 137.1, 136.7, 129.2, 128.3, 126.6, 119.2, 118.7, 114.8, 112.9, 74.1, 27.9, 26.2, 18.8.

HRMS: exact mass calculated for $[\text{M}+\text{H}]^+$ ($\text{C}_{23}\text{H}_{23}\text{NO}_2$) requires m/z 346.1802, found m/z 346.1801.

(*E*)-5-(3-(3,3-Dimethylbut-1-en-1-yl)phenyl)pyrimidine, **1.16n**



Prepared according to General Procedure 1B using 1-bromo-2-chloro-4-(trifluoromethoxy)benzene (69 mg, 0.25 mmol, 1 equiv), (*E*)-styrylboronic acid pinacol ester (63.3 mg, 0.275 mmol, 1.1 equiv), (*E*)-prop-1-en-1-ylboronic acid MIDA ester (4:1 *E:Z*, 64 mg, 0.325 mmol, 1.3 equiv), $\text{Pd}(\text{OAc})_2$ (2.2 mg, 0.001 mmol, 4 mol%), DavePhos (7.8 mg, 0.02 mmol, 8 mol%), K_3PO_4 (212 mg, 1 mmol, 4 equiv), THF (1 mL, 0.25 M), and H_2O (90 μL , 5 mmol, 20 equiv). After 24 h the reaction mixture was subjected to the purification outlined in the General Procedure (silica gel, 0–3% EtOAc/Petroleum ether) to afford the title compound as a pale yellow oil (53mg, 69%). Product isolated as a 4:1 mixture of propenyl stereoisomers (*E:Z*).

ν_{\max} (film): 3029, 2960, 2928, 1580 1462, 1221, 1254, 1161 cm^{-1} .

Major stereoisomer (*E*)

$^1\text{H NMR}$ (CDCl_3 , 400 MHz): δ 7.59–7.51 (m, 3H), 7.44–7.29 (m, 4H), 7.27 (s, 1H), 7.10 (d, $J = 6.8$ Hz, 1H), 6.97 (d, $J = 16.1$ Hz, 1H), 6.72 (dd, $J = 15.6, 1.7$ Hz, 1H), 6.23–6.08 (m, 1H), 1.97 (dd, $J = 6.7, 1.8$ Hz, 3H).

$^{13}\text{C NMR}$ (CDCl_3 , 101 MHz): δ 148.2, 137.8, 136.8, 133.3, 131.0, 129.7, 128.3, 127.4, 127.3, 127.2, 126.2, 125.0, 120.1 (d, $^1J_{\text{C-F}} = 270.7$ Hz), 118.8, 118.3, 18.3.

Observable signals for minor stereoisomer (*Z*)

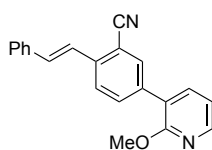
¹H NMR (CDCl₃, 400 MHz): δ 7.68 (d, *J* = 8.6 Hz, 1H), 7.03 (d, *J* = 15.5 Hz, 1H), 6.57 (d, *J* = 11.5 Hz, 1H), 5.99 (dq, *J* = 14.0, 7.0 Hz, 1H), 1.75 (dd, *J* = 7.0, 1.8 Hz, 1H).

¹³C NMR (CDCl₃, 101 MHz): δ 137.2, 131.4, 130.1, 129.1, 128.9, 126.9, 126.2 (s, *J* = 3.9 Hz), 125.2, 121.3, 119.0, 118.8, 13.9.

¹⁹F NMR (CDCl₃, 376 MHz): δ -57.68 (s, 3F).

HRMS: exact mass calculated for [M+H]⁺ (C₁₈H₁₅F₃O) requires *m/z* 305.1148, found *m/z* 305.1145.

(*E*)-5-(2-Methoxypyridin-3-yl)-2-styrylbenzonitrile, 1.16o



Prepared according to General Procedure 1B using 2-bromo-5-chlorobenzonitrile (54 mg, 0.25 mmol, 1 equiv), (*E*)-styrylboronic acid pinacol ester (63.3 mg, 0.275 mmol, 1.1 equiv), (3-methoxypyridin-2-yl)boronic acid MIDA ester (86 mg, 0.325 mmol, 1.3 equiv), Pd(OAc)₂ (2.2 mg, 0.001 mmol, 4 mol%), DavePhos (7.8 mg, 0.02 mmol, 8 mol%), K₃PO₄ (212 mg, 1 mmol, 4 equiv), THF (1 mL, 0.25 M), and H₂O (90 μL, 5 mmol, 20 equiv). After 24 h the reaction mixture was subjected to the purification outlined in the General Procedure (silica gel, 0–8% EtOAc/Petroleum ether) to afford the title compound as an off white solid (66 mg, 84%).

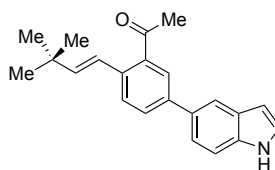
ν_{max} (solid): 3017, 2999, 2922, 2843, 2222, 1632, 1580, 1452 cm⁻¹.

¹H NMR (CDCl₃, 400 MHz): δ 8.24 (dd, *J* = 5.0, 1.9 Hz, 1H), 7.91 (d, *J* = 1.6 Hz, 1H), 7.88 (d, *J* = 8.4 Hz, 1H), 7.82–7.79 (m, 1H), 7.66 (dd, *J* = 7.3, 1.9 Hz, 1H), 7.64–7.61 (m, 2H), 7.55–7.32 (m, 5H), 7.04 (dd, *J* = 7.3, 5.0 Hz, 1H), 4.03 (s, 3H).

¹³C NMR (CDCl₃, 101 MHz): δ 160.2, 146.3, 138.9, 137.8, 135.8, 135.7, 133.1, 133.0, 128.4, 126.7, 124.6, 123.2, 121.5, 117.5, 116.8, 110.8, 53.2.

HRMS: exact mass calculated for [M+H]⁺ (C₂₁H₁₆N₂O) requires *m/z* 313.1335, found *m/z* 313.1337.

(*E*)-1-(2-(3,3-Dimethylbut-1-en-1-yl)-5-(1*H*-indol-5-yl)phenyl)ethan-1-one, **1.16p**



Prepared according to General Procedure 1B using 1-(2-bromo-5-chlorophenyl)ethan-1-one (58 mg, 0.25 mmol, 1 equiv), (*E*)-(3,3-dimethylbut-1-en-1-yl)boronic acid, pinacol ester (58 mg, 0.275 mmol, 1.1 equiv), (1*H*-indol-5-yl)boronic acid, MIDA ester (88 mg, 0.325 mmol, 1.3 equiv), Pd(OAc)₂ (2.2 mg, 0.001 mmol, 4 mol%), DavePhos (7.8 mg, 0.02 mmol, 8 mol%), K₃PO₄ (212 mg, 1 mmol, 4 equiv), THF (1 mL, 0.25 M), and H₂O (90 μL, 5 mmol, 20 equiv). After 24 h the reaction mixture was subjected to the purification outlined in the General Procedure (silica gel, 0–9% EtOAc/Petroleum ether) to afford the title compound as a brown solid (63 mg, 84%).

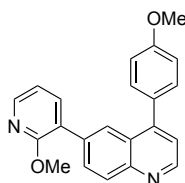
ν_{max} (solid): 3339, 2954, 2859, 1664, 1599, 1398 cm⁻¹.

¹H NMR (CDCl₃, 400 MHz): δ 8.28 (s, 1H), 7.87 (d, *J* = 9.8 Hz, 2H), 7.72 (d, *J* = 8.1 Hz, 1H), 7.59 (d, *J* = 8.1 Hz, 1H), 7.52–7.41 (m, 2H), 7.27 (s, 1H), 6.84 (d, *J* = 16.0 Hz, 1H), 6.63 (s, 1H), 6.18 (d, *J* = 16.0 Hz, 1H), 2.64 (s, 3H), 1.17 (s, 9H).

¹³C NMR (CDCl₃, 101 MHz): δ 203.2, 144.8, 140.9, 138.1, 135.7, 135.5, 132.1, 130.0, 128.5, 127.9, 127.3, 125.1, 123.2, 121.5, 119.1, 111.4, 103.1, 33.8, 30.3, 29.5.

HRMS: exact mass calculated for [M+H]⁺ (C₂₂H₂₃NO) requires *m/z* 318.1852, found *m/z* 318.1852.

4-(4-Methoxyphenyl)-6-(2-methoxypyridin-3-yl)quinolone, **1.16q**



Prepared according to General Procedure 1B using 4-bromo-6-chloroquinoline (61 mg, 0.25 mmol, 1 equiv), (4-methoxyphenyl)boronic acid pinacol ester (65 mg, 0.275 mmol, 1.1 equiv), (2-methoxypyridin-3-yl)boronic acid MIDA ester (86 mg, 0.325 mmol, 1.3 equiv), Pd(OAc)₂ (2.2 mg, 0.001 mmol, 4 mol%), DavePhos (7.8 mg, 0.02 mmol, 8 mol%), K₃PO₄ (212 mg, 1 mmol, 4 equiv), THF (1 mL, 0.25 M), and H₂O (90 μL, 5 mmol, 20 equiv). After 24 h the reaction mixture was subjected to

the purification outlined in the General Procedure (silica gel, 0–25% EtOAc/Petroleum ether) to afford the title compound as a pale yellow solid (84 mg, 97%).

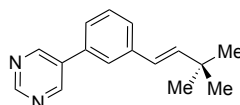
ν_{\max} (solid): 3036, 2984, 2924, 2837, 1610, 1578, 1496, 1405 cm^{-1} .

$^1\text{H NMR}$ (CDCl_3 , 400 MHz): δ 8.95 (d, $J = 4.2$ Hz, 1H), 8.36 (dd, $J = 5.0, 1.8$ Hz, 1H), 8.23 (d, $J = 8.8$ Hz, 1H), 7.97 (dd, $J = 8.7, 1.9$ Hz, 1H), 7.71 (d, $J = 1.8$ Hz, 1H), 7.64 (dd, $J = 7.2, 1.8$ Hz, 1H), 7.54 (d, $J = 8.7$ Hz, 2H), 7.35 (d, $J = 4.4$ Hz, 1H), 7.09 (dd, $J = 7.2, 5.1$ Hz, 1H), 6.99 (d, $J = 8.7$ Hz, 2H), 3.93 (s, 3H), 3.86 (s, 3H).

$^{13}\text{C NMR}$ (CDCl_3 , 101 MHz): δ 160.7, 159.0, 149.0, 147.0, 143.3, 139.3, 138.5, 132.5, 130.3, 129.7, 128.5, 128.0, 126.7, 122.2, 122.0, 120.4, 116.3, 113.9, 54.9, 53.1.

HRMS: exact mass calculated for $[\text{M}+\text{H}]^+$ ($\text{C}_{22}\text{H}_{18}\text{N}_2\text{O}_2$) requires m/z 343.1441, found m/z 343.1440.

(*E*)-5-(3-(3,3-Dimethylbut-1-en-1-yl)phenyl)pyrimidine, **1.16r**



Prepared according to General Procedure 1B using 1-bromo-3-chlorobenzene (47.5 mg, 0.25 mmol, 1 equiv), (*E*)-(3,3-dimethylbut-1-en-1-yl)boronic acid pinacol ester (58 mg, 0.275 mmol, 1.1 equiv), pyrimidin-5-ylboronic acid MIDA ester (76 mg, 0.325 mmol, 1.3 equiv), $\text{Pd}(\text{OAc})_2$ (2.2 mg, 0.001 mmol, 4 mol%), DavePhos (7.8 mg, 0.02 mmol, 8 mol%), K_3PO_4 (212 mg, 1 mmol, 4 equiv), THF (1 mL, 0.25 M), and H_2O (90 μL , 5 mmol, 20 equiv). After 24 h the reaction mixture was subjected to the purification outlined in the General Procedure (silica gel, 0–20% EtOAc/Petroleum ether) to afford the title compound as a yellow solid (45 mg, 76%).

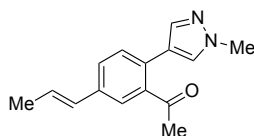
ν_{\max} (solid): 3032, 2950, 2863, 1560, 1463, 1416 cm^{-1} .

$^1\text{H NMR}$ (CDCl_3 , 400 MHz): δ 9.23 (s, 1H), 8.98 (s, 2H), 7.56 (s, 1H), 7.51–7.39 (m, 3H), 6.39 (d, $J = 1.7$ Hz, 2H), 1.17 (s, 9H).

$^{13}\text{C NMR}$ (CDCl_3 , 101 MHz): δ 156.9, 154.4, 142.9, 138.9, 134.0, 134.0, 129.1, 126.1, 124.8, 124.2, 123.4, 33.0, 29.0.

HRMS: exact mass calculated for $[\text{M}+\text{H}]^+$ ($\text{C}_{16}\text{H}_{18}\text{N}_2$) requires m/z 239.1543, found m/z 239.1543.

(*E*)-1-(2-(1-Methyl-1*H*-pyrazol-4-yl)-5-(prop-1-en-1-yl)phenyl)ethan-1-one, **1.16s**



Prepared according to General Procedure 1B using 1-(2-bromo-5-chlorophenyl)ethan-1-one (58 mg, 0.25 mmol, 1 equiv), (1-methyl-1*H*-pyrazol-4-yl)boronic acid, pinacol ester (57 mg, 0.275 mmol, 1.1 equiv), prop-1-en-1-ylboronic acid MIDA ester (4:1 *E:Z*, 64 mg, 0.325 mmol, 1.3 equiv), Pd(OAc)₂ (2.2 mg, 0.001 mmol, 4 mol%), DavePhos (7.8 mg, 0.02 mmol, 8 mol%), K₃PO₄ (212 mg, 1 mmol, 4 equiv), THF (1 mL, 0.25 M), and H₂O (90 μL, 5 mmol, 20 equiv). After 24 h the reaction mixture was subjected to the purification outlined in the General Procedure (silica gel, 40–80% EtOAc/Petroleum ether) to afford the title compound as a yellow oil. Product isolated as a 4:1 mixture of propenyl stereoisomers (*E:Z*) (56 mg, 92%).

ν_{\max} (film): 2975, 2934, 1684, 1603, 1565, 1411, 1357, 1180 cm⁻¹.

Major stereoisomer (*E*)

¹H NMR (CDCl₃, 400 MHz): δ 7.65 (s, 1H), 7.52 (s, 1H), 7.44–7.41 (m, 2H), 7.32 (d, *J* = 7.8 Hz, 1H), 6.43 (dd, *J* = 15.8, 1.3 Hz, 1H), 6.33 (dq, *J* = 15.7, 6.4 Hz, 1H), 4.01 (s, 3H), 2.36 (s, 3H), 1.93 (dd, *J* = 6.3, 1.2 Hz, 3H).

¹³C NMR (CDCl₃, 101 MHz): δ 204.4, 139.8, 137.4, 136.6, 129.9, 129.7, 129.2, 127.3, 127.1, 126.9, 124.2, 120.6, 38.3, 30.1, 18.0.

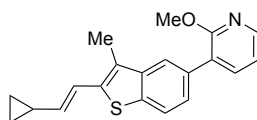
Observable signals for minor stereoisomer (*Z*)

¹H NMR (CDCl₃, 400 MHz): δ 7.67 (s, 1H), 7.54 (s, *J* = 3.5 Hz, 1H), 7.36 (dd, *J* = 7.6, 0.8 Hz, 1H), 6.46 (dd, *J* = 11.6, 1.8 Hz, 1H), 5.90 (dq, *J* = 11.6, 7.2 Hz, 1H), 4.01 (s, 3H), 2.37 (s, 3H), 1.95 (d, *J* = 1.8 Hz, 3H).

¹³C NMR (CDCl₃, 101 MHz): δ 137.5, 136.2, 130.5, 129.5, 128.0, 127.8, 127.2.

HRMS: exact mass calculated for [M+H]⁺ (C₁₅H₁₆N₂O) requires *m/z* 241.1335, found *m/z* 241.1337.

(*E*)-3-(2-(2-Cyclopropylvinyl)-3-methylbenzo[*b*]thiophen-5-yl)-2-methoxypyridine, **1.16t**



Prepared according to General Procedure 1B using 2-bromo-5-chloro-3-methylbenzo[b]thiophene (65 mg, 0.25 mmol, 1 equiv), (*E*)-cyclopropylvinylboronic acid pinacol ester (54 mg, 0.275 mmol, 1.1 equiv), (3-methoxypyridin-2-yl)boronic acid MIDA ester (86 mg, 0.325 mmol, 1.3 equiv), Pd(OAc)₂ (2.2 mg, 0.001 mmol, 4 mol%), DavePhos (7.8 mg, 0.02 mmol, 8 mol%), K₃PO₄ (212 mg, 1 mmol, 4 equiv), THF (1 mL, 0.25 M), and H₂O (90 μL, 5 mmol, 20 equiv). After 24 h the reaction mixture was subjected to the purification outlined in the General Procedure (silica gel, 0–20% EtOAc/Petroleum ether) to afford the title compound as a yellow oil (66 mg, 89%).

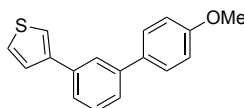
ν_{\max} (film): 2947, 2924, 2855, 1662, 1578, 1463, 1396 cm⁻¹.

¹H NMR (CDCl₃, 400 MHz): δ 8.20 (dd, *J* = 5.0, 1.9 Hz, 1H), 7.78–7.74 (m, 2H), 7.69 (dd, *J* = 7.3, 1.9 Hz, 1H), 7.48 (dd, *J* = 8.2, 1.7 Hz, 1H), 7.02 (dd, *J* = 7.3, 5.0 Hz, 1H), 6.83 (d, *J* = 15.4 Hz, 1H), 5.69 (dd, *J* = 15.4, 9.0 Hz, 1H), 4.01 (s, 3H), 2.41 (s, 3H), 1.63 (m, 1H), 0.92–0.88 (m, 2H), 0.64–0.56 (m, 2H).

¹³C NMR (CDCl₃, 101 MHz): δ 160.5, 145.1, 141.0, 138.3, 136.8, 136.8, 136.5, 132.3, 126.5, 125.1, 124.6, 121.5, 121.2, 119.2, 116.6, 53.1, 14.4, 11.2, 7.2.

HRMS: exact mass calculated for [M+H]⁺ (C₂₀H₁₉NOS) requires *m/z* 322.1264, found *m/z* 322.1260.

3-(4'-Methoxy-[1,1'-biphenyl]-3-yl)thiophene, **1.16u**



Prepared according to General Procedure 1B using 1-bromo-3-chlorobenzene (47.5 mg, 0.25 mmol, 1 equiv), (4-methoxyphenyl)boronic acid pinacol ester (64 mg, 0.275 mmol, 1.1 equiv), thiophen-3-ylboronic acid MIDA ester (78 mg, 0.325 mmol, 1.3 equiv), Pd(OAc)₂ (2.2 mg, 0.001 mmol, 4 mol%), DavePhos (7.8 mg, 0.02 mmol, 8 mol%), K₃PO₄ (212 mg, 1 mmol, 4 equiv), THF (1 mL, 0.25 M), and H₂O (90 μL, 5 mmol, 20 equiv). After 24 h the reaction mixture was subjected to the purification outlined in the General Procedure (silica gel, 0–8% EtOAc/Petroleum ether) to afford the title compound as a white solid (60 mg, 90%).

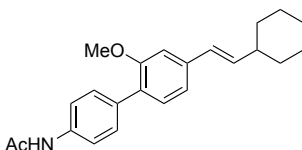
ν_{\max} (solid): 3096, 3004, 2954, 2837, 1603, 1513, 1441 cm⁻¹.

¹H NMR (CDCl₃, 400 MHz): δ 7.78 (t, *J* = 1.6 Hz, 1H), 7.60–7.57 (m, 2H), 7.57–7.40 (m, 6H), 7.01 (d, *J* = 8.7 Hz, 2H), 3.88 (s, 3H).

¹³C NMR (CDCl₃, 101 MHz): δ 159.3, 142.4, 141.5, 136.3, 133.7, 129.2, 128.2, 126.5, 126.2, 125.6, 125.0, 124.9, 120.5, 114.3, 55.4.

HRMS: exact mass calculated for [M+H]⁺ (C₁₇H₁₄SO) requires *m/z* 266.0760, found *m/z* 266.0759.

(*E*)-*N*-(4'-(2-Cyclohexylvinyl)-2'-methoxy-[1,1'-biphenyl]-4-yl)acetamide, **1.16v**



Prepared according to General Procedure 1B using 1-bromo-4-chloro-2-methoxybenzene (55 mg, 0.25 mmol, 1 equiv), (4-acetamidophenyl)boronic acid pinacol ester (72 mg, 0.275 mmol, 1.1 equiv), (*E*)-(2-cyclohexylvinyl)boronic acid MIDA ester (86 mg, 0.325 mmol, 1.3 equiv), Pd(OAc)₂ (2.2 mg, 0.001 mmol, 4 mol%), DavePhos (7.8 mg, 0.02 mmol, 8 mol%), K₃PO₄ (212 mg, 1 mmol, 4 equiv), THF (1 mL, 0.25 M), and H₂O (90 μL, 5 mmol, 20 equiv). After 24 h the reaction mixture was subjected to the purification outlined in the General Procedure (silica gel, 0–50% EtOAc/Petroleum ether) to afford the title compound as a light brown solid (78 mg, 89%).

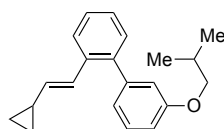
ν_{max} (solid): 3304, 3043, 2921, 2850, 1660, 1601, 1539, 1370, 1223 cm⁻¹.

¹H NMR (CDCl₃, 400 MHz): δ 7.62–7.53 (m, 4H), 7.50 (d, *J* = 8.0 Hz, 1H), 7.40 (d, *J* = 11.0 Hz, 1H), 7.13 (dd, *J* = 7.9, 1.5 Hz, 1H), 7.05 (d, *J* = 1.6 Hz, 1H), 6.72 (d, *J* = 15.8 Hz, 1H), 6.23 (dd, *J* = 16.1, 7.0 Hz, 1H), 3.92 (s, 3H), 2.22 (s, 3H), 1.90–1.64 (m, 6H), 1.40–1.29 (m, 3H), 1.25–1.18 (m, 2H).

¹³C NMR (CDCl₃, 101 MHz): δ 167.9, 156.1, 139.6, 137.1, 136.7, 136.6, 126.9, 126.0, 125.6, 120.9, 119.7, 118.7, 108.9, 55.1, 41.1, 32.6, 25.7, 25.6, 24.4.

HRMS: exact mass calculated for [M+H]⁺ (C₂₃H₂₇NO₂) requires *m/z* 350.2215, found *m/z* 350.2216.

(*E*)-2-(2-Cyclopropylvinyl)-3'-isobutoxy-1,1'-biphenyl, **1.16w**



Prepared according to General Procedure 1B using 1-bromo-2-chlorobenzene (47.5 mg, 0.25 mmol, 1 equiv), (*E*)-(2-cyclopropylvinyl)boronic acid pinacol ester (53 mg, 0.275 mmol, 1.1 equiv), (3-isobutoxyphenyl)boronic acid MIDA ester (99 mg, 0.325 mmol, 1.3 equiv), Pd(OAc)₂ (2.2 mg, 0.001 mmol, 4 mol%), DavePhos (7.8 mg, 0.02 mmol, 8 mol%), K₃PO₄ (212 mg, 1 mmol, 4 equiv), THF (1 mL, 0.25 M), and H₂O (90 μL, 5 mmol, 20 equiv). After 24 h the reaction mixture was subjected to the purification outlined in the General Procedure (silica gel, 0–6% EtOAc/Petroleum ether) to afford the title compound as a yellow oil (56 mg, 77%).

ν_{max} (film): 2958, 2928, 2872, 1597, 1578, 1470 cm⁻¹.

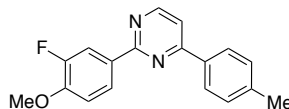
¹H NMR (CDCl₃, 400 MHz): δ 7.58–7.51 (m, 1H), 7.38–7.24 (m, 4H), 6.99–6.90 (m, 3H), 6.51 (d, *J* = 15.7 Hz, 1H), 5.68 (dd, *J* = 15.7, 8.9 Hz, 1H), 3.79 (d, *J* = 6.6 Hz, 2H), 2.21–2.08 (m, 1H), 1.55–1.43 (m, 1H), 1.07 (d, *J* = 6.7 Hz, 6H), 0.83–0.74 (m, 2H), 0.53–0.44 (m, 2H).

¹³C NMR (CDCl₃, 101 MHz): δ 158.4, 142.1, 139.4, 135.2, 135.1, 129.5, 128.4, 126.9, 125.9, 125.7, 124.8, 121.6, 115.4, 112.9, 74.0, 27.8, 18.8, 14.1, 6.7.

HRMS: exact mass calculated for [M+H]⁺ (C₂₁H₂₄O) requires *m/z* 293.1900, found *m/z* 293.1904.

4.4 Products from Scheme 69

2-(3-Fluoro-4-methoxyphenyl)-4-(*p*-tolyl)pyrimidine, **1.30**



Prepared according to General Procedure 1B using 2,4-dichloropyrimidine (37 mg, 0.25 mmol, 1 equiv), 4-tolylboronic acid pinacol ester (60 mg, 0.275 mmol, 1.1 equiv), ((3-fluoro-4-methoxyphenyl)boronic acid MIDA ester (91 mg, 0.325 mmol, 1.3 equiv), PdCl₂dppf•CH₂Cl₂ (8.2 mg, 0.001 mmol, 4 mol%), K₃PO₄ (212 mg, 1 mmol, 4 equiv), THF (1 mL, 0.25 M), and H₂O (90 μL, 5 mmol, 20 equiv). After 8 h stirring at room temperature the reaction was heated to 90 °C for a further 48 h. The reaction mixture was then subjected to the purification outlined in the General

Procedure (silica gel, 10-20% Et₂O/Petroleum ether) to afford the title compound as a white solid (51 mg, 70%).

ν_{max} (solid): 2956, 2922, 2850, 1621, 1565, 1547, 1513 cm⁻¹.

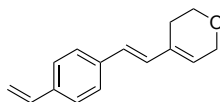
¹H NMR (CDCl₃, 400 MHz): δ 8.79 (d, J = 5.3 Hz, 1H), 8.42–8.32 (m, 2H), 8.14 (d, J = 8.2 Hz, 2H), 7.56 (d, J = 5.3 Hz, 1H), 7.37 (d, J = 8.0 Hz, 2H), 7.10 (t, J = 8.7 Hz, 1H), 4.00 (s, 3H), 2.48 (s, 3H).

¹³C NMR (CDCl₃, 101 MHz): δ 163.8, 163.3 (d, J = 2.8 Hz), 157.6, 152.4 (d, $^1J_{\text{C-F}}$ = 244.8 Hz), 149.9 (d, $^2J_{\text{C-F}}$ = 11.0 Hz), 141.5, 134.0, 131.3 (d, $^3J_{\text{C-F}}$ = 6.3 Hz), 129.7, 127.1, 124.6 (d, J = 2.9 Hz), 116.0 (d, $^2J_{\text{C-F}}$ = 19.8 Hz), 113.9, 112.8, 56.2, 21.5.

¹⁹F NMR (CDCl₃, 376 MHz): δ -135.42 (s, 1F).

HRMS: exact mass calculated for [M+H]⁺ (C₁₈H₁₅FN₂O) requires m/z 295.1241, found m/z 295.1239.

(*E*)-4-(4-Vinylstyryl)-3,6-dihydro-2*H*-pyran, **1.31**



Prepared according to General Procedure 1B using (*E*)-1-bromo-4-(2-bromovinyl)benzene (65 mg, 0.25 mmol, 1 equiv), (3,6-dihydro-2*H*-pyran-4-yl)boronic acid pinacol ester (58 mg, 0.275 mmol, 1.1 equiv), vinylboronic acid MIDA ester (68 mg, 0.325 mmol, 1.5 equiv), PdCl₂dppf•CH₂Cl₂ (8.2 mg, 0.001 mmol, 4 mol%), K₃PO₄ (212 mg, 1 mmol, 4 equiv), THF (1 mL, 0.25 M), and H₂O (90 μ L, 5 mmol, 20 equiv). After 24 h stirring at room temperature the reaction was heated to 90 °C for a further 24 h. The reaction mixture was then subjected to the purification outlined in the General Procedure (silica gel, 10% Et₂O/Petroleum ether) to afford the title compound as an off-white solid (42 mg, 79%).

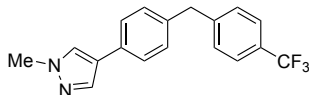
ν_{max} (solid): 2956, 2922, 2854, 1716, 1696, 1604, 1511, 1385 cm⁻¹.

¹H NMR (CDCl₃, 400 MHz): δ 7.40 (s, 4H), 6.81 (d, J = 16.2 Hz, 1H), 6.73 (dd, J = 17.6, 10.9 Hz, 1H), 6.51 (d, J = 16.1 Hz, 1H), 5.88 (s, 1H), 5.77 (d, J = 17.6 Hz, 1H), 5.26 (d, J = 10.9 Hz, 1H), 4.32 (d, J = 2.2 Hz, 2H), 3.92 (t, J = 5.5 Hz, 2H), 2.42 (s, 2H).

¹³C NMR (CDCl₃, 101 MHz): δ 136.9, 136.6, 136.5, 133.5, 130.4, 127.4, 126.5, 126.5, 125.8, 113.6, 65.8, 64.2, 25.0.

HRMS: exact mass calculated for $[M+H]^+$ ($C_{15}H_{16}O$) requires m/z 213.1274, found m/z 213.1269.

1-Methyl-4-(4-(4-(trifluoromethyl)benzyl)phenyl)-1*H*-pyrazole, **1.32**



Prepared according to General Procedure 1B using 1-bromo-4-(bromomethyl)benzene (62 mg, 0.25 mmol, 1 equiv), (1-methyl-1*H*-pyrazol-4-yl)boronic acid, pinacol ester (52 mg, 0.275 mmol, 1.1 equiv), (4-(trifluoromethyl)phenyl)boronic acid MIDA ester (98 mg, 0.325 mmol, 1.3 equiv), $PdCl_2dppf \cdot CH_2Cl_2$ (8.2 mg, 0.001 mmol, 4 mol%), K_3PO_4 (212 mg, 1 mmol, 4 equiv), THF (1 mL, 0.25 M), and H_2O (90 μ L, 5 mmol, 20 equiv). After 24 h stirring at room temperature the reaction was heated to 90 °C for a further 24 h. The reaction mixture was then subjected to the purification outlined in the General Procedure (silica gel, 10-40% EtOAc/Petroleum ether) to afford the title compound as a yellow solid (66 mg, 84%).

ν_{max} (solid): 3079, 3030, 2926, 2852, 1617, 1608, 1502, 1400, 1331 cm^{-1} .

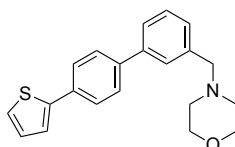
1H NMR ($CDCl_3$, 400 MHz): δ 7.68 (s, 4H), 7.53 (d, $J = 8.2$ Hz, 2H), 7.36 (s, 1H), 7.31 (d, $J = 8.2$ Hz, 2H), 7.14 (s, 1H), 3.87 (s, 2H), 3.86 (s, 3H).

^{13}C NMR ($CDCl_3$, 101 MHz): δ 144.9, 141.9, 139.5, 138.0, 129.5, 129.3, 127.8, 127.7, 126.1 (q, $^3J_{C-F} = 3.9$ Hz), 122.1 (d, $^1J_{C-F} = 272.0$ Hz), 120.9, 39.3, 30.7. Carbon bearing CF_3 not observed.

^{19}F NMR ($CDCl_3$, 376 MHz): δ -62.40 (s, 3F).

HRMS: exact mass calculated for $[M+H]^+$ ($C_{18}H_{15}F_3N_2$) requires m/z 317.1260, found m/z 317.1260.

4-((4'-(Thiophen-2-yl)-[1,1'-biphenyl]-3-yl)methyl)morpholine, **1.33**



Prepared according to General Procedure 1B using 1,4-dibromobenzene (59 mg, 0.25 mmol, 1 equiv), (3-(morpholinomethyl)phenyl)boronic acid, pinacol ester (83 mg, 0.275 mmol, 1.1 equiv), thiophen-2-ylboronic acid MIDA ester (66 mg, 0.325 mmol,

1.1 equiv), PdCl₂dppf•CH₂Cl₂ (8.2 mg, 0.001 mmol, 4 mol%), K₃PO₄ (212 mg, 1 mmol, 4 equiv), THF (1 mL, 0.25 M), and H₂O (90 μL, 5 mmol, 20 equiv). After 16 h stirring at room temperature the reaction was heated to 90 °C for a further 8 h. The reaction mixture was subjected to the purification outlined in the General Procedure (silica gel, 10-40% EtOAc/Petroleum ether) to afford the title compound as an off white solid (50 mg, 60%).

ν_{\max} (solid): 3068, 2921, 2861, 2809, 2768, 1601, 1483, 1455, 1353, 1115 cm⁻¹.

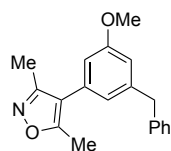
¹H NMR (CDCl₃, 400 MHz): δ 7.72–7.61 (m, 4H), 7.60 (s, 1H), 7.54–7.50 (m, 1H), 7.43–7.38 (m, 1H), 7.36 (dd, *J* = 3.6, 1.1 Hz, 1H), 7.35–7.31 (m, 1H), 7.30 (dd, *J* = 5.1, 1.1 Hz, 1H), 7.11 (dd, *J* = 5.1, 3.6 Hz, 1H), 3.74 (t, *J* = 4.6 Hz, 4H), 3.59 (s, 2H), 2.51 (s, 4H).

¹³C NMR (CDCl₃, 101 MHz): δ 144.2, 140.7, 140.2, 133.6, 129.0, 128.5, 128.2, 127.9, 127.7, 126.4, 126.0, 125.0, 123.3, 67.1, 63.6, 53.8.

HRMS: exact mass calculated for [M+H]⁺ (C₂₁H₂₁NOS) requires *m/z* 336.1417, found *m/z* 336.1418.

4.4 Products from Scheme 70 and 73

4-(3-Benzyl-5-methoxyphenyl)-3,5-dimethylisoxazole, **1.38**



Prepared according to General Procedure 1A using (3-bromo-5-methoxyphenyl)boronic acid MIDA ester (85 mg, 0.25 mmol, 1 equiv), (3,5-dimethylisoxazol-4-yl)boronic acid pinacol ester (61 mg, 0.275 mmol, 1.1 equiv), benzyl chloride (41 mg, 0.325 mmol, 1.3 equiv), Pd(OAc)₂ (2.2 mg, 0.01 mmol, 4 mol%), SPhos (8.2 mg, 0.02 mmol, 8 mol%), K₃PO₄ (212 mg, 1 mmol, 4 equiv), THF (1 mL, 0.25 M), and H₂O (90 μL, 5 mmol, 20 equiv). After 24 h, the reaction mixture was subjected to the purification outlined in the General Procedure (silica gel, 0-10% EtOAc/Petroleum ether) to afford the title compound as a colourless oil (51 mg, 70%).

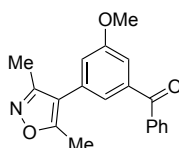
ν_{\max} (film): 3007, 2966, 2671, 1591, 1456, 1415, 1278 cm⁻¹.

¹H NMR (CDCl₃, 400 MHz): δ 7.37–7.30 (m, 2H), 7.25 (m, 3H), 6.78–6.74 (m, 1H), 6.69–6.65 (m, 1H), 6.66–6.63 (m, 1H), 4.02 (s, 2H), 3.82 (s, 3H), 2.40 (s, 3H), 2.26 (s, 3H).

¹³C NMR (CDCl₃, 101 MHz): δ 165.2, 160.0, 158.6, 143.3, 140.5, 131.7, 128.9, 128.6, 126.3, 122.1, 116.6, 113.5, 112.6, 55.3, 41.9, 11.6, 10.8.

HRMS: exact mass calculated for [M+H]⁺ (C₁₉H₂₀NO₂) requires *m/z* 294.1489, found *m/z* 294.1487.

(3-(3,5-Dimethylisoxazol-4-yl)-5-methoxyphenyl)(phenyl)methanone, **1.39a**



To a solution of 4-(3-benzyl-5-methoxyphenyl)-3,5-dimethylisoxazole **1.38** (90 mg, 0.3 mmol, 1 equiv) and tetrabutylammonium bromide (148 mg, 0.46 mmol, 1.5 equiv) in CH₂Cl₂ (1.5 mL) was added KMnO₄ (291 mg, 1.84 mmol, 6 equiv) portionwise. The reaction mixture was stirred at reflux for 24 h. The reaction mixture was then warmed to room temperature and MeOH (50 mL) was added dropwise. The resulting black precipitate was filtered and washed with CH₂Cl₂ (50 mL). The resulting solution was concentrated at reduced pressure to afford a deep purple solid. To this, a further 50 mL of MeOH was added until the solution became colourless. The mixture was filtered again to remove the black solid precipitate and the filtrate was concentrated at reduced pressure to give the crude product as a brown oil. The crude product was then purified by flash chromatography (silica gel, 0-15% EtOAc/Petroleum ether) to afford the title compound as a cloudy oil (58 mg, 62%).

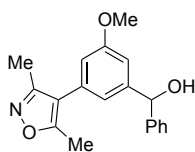
***v*_{max}** (film): 3066, 2933, 2850, 1658, 1633, 1587, 1446, 1409 cm⁻¹.

¹H NMR (CDCl₃, 400 MHz): δ 7.86 (d, *J* = 7.0 Hz, 2H), 7.64 (t, *J* = 7.4 Hz, 1H), 7.52 (t, *J* = 7.6 Hz, 2H), 7.37 (dd, *J* = 2.5, 1.4 Hz, 1H), 7.24 (t, *J* = 1.4 Hz, 1H), 7.04 (dd, *J* = 2.5, 1.5 Hz, 1H), 3.92 (s, 3H), 2.44 (s, 3H), 2.31 (s, 3H).

¹³C NMR (CDCl₃, 101 MHz): δ 195.6, 165.2, 159.4, 158.0, 139.0, 136.8, 132.3, 131.4, 129.5, 127.9, 122.9, 119.1, 115.3, 112.7, 55.2, 11.2, 10.4.

HRMS: exact mass calculated for [M+H]⁺ (C₁₉H₁₇NO₃) requires *m/z* 308.1281, found *m/z* 308.1279.

(3-(3,5-Dimethylisoxazol-4-yl)-5-methoxyphenyl)(phenyl)methanol, **1.39b**



A solution of (3-(3,5-dimethylisoxazol-4-yl)-5-methoxyphenyl)(phenyl)methanone **1.39a** (50 mg, 0.18 mmol, 1 equiv) in CH₂Cl₂:MeOH (10:1, 0.9 mL) was cooled to 0 °C. NaBH₄ (14 mg, 0.36 mmol, 2 equiv) was then added portion wise. The reaction mixture was stirred at 0 °C for 30 min before being warmed to room temperature and stirred for a further 30 min. The mixture was quenched with H₂O (5 mL) and was diluted with CH₂Cl₂ (5 mL). The organics were separated and dried through a hydrophobic frit before being concentrated at reduced pressure to give the crude product as a brown oil. The crude product was then purified by flash chromatography (silica gel, 30% EtOAc/Petroleum ether) to afford the title compound as an opaque oil (46 mg, 92%).

ν_{max} (film): 3345, 2956, 2924, 1590, 1496, 1464, 1407 cm⁻¹.

¹H NMR (CDCl₃, 400 MHz): δ 7.44–7.34 (m, 4H), 7.33–7.27 (m, 1H), 7.01–6.97 (m, 1H), 6.83–6.85 (m, 1H), 6.69 (dd, $J = 2.4, 1.5$ Hz, 1H), 5.86 (s, 1H), 3.83 (s, 3H), 2.37 (s, 3H), 2.22 (s, 3H).

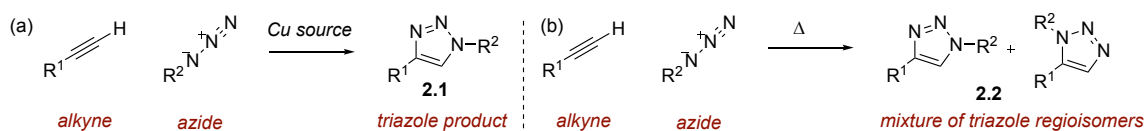
¹³C NMR (CDCl₃, 101 MHz): δ 164.8, 159.5, 158.1, 145.6, 143.2, 131.2, 128.1, 127.3, 126.0, 119.2, 116.0, 113.5, 110.4, 75.5, 54.9, 11.1, 10.3.

HRMS: exact mass calculated for [M+H]⁺ (C₁₉H₁₉NO₃) requires m/z 310.1438, found m/z 310.1440.

2.0 Chapter 2 - Chemoselectivity in the CuAAC Reaction

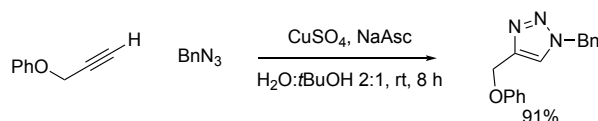
2.1 Introduction

The copper-catalysed azide alkyne (3+2) cycloaddition (CuAAC) is the reaction between a terminal alkyne and an organic azide to form a 1,2,3-triazole product, **2.1** (Scheme 78a). Huigsen reported the first example of this type of reaction under thermal promotion in the 1960's: terminal alkynes and azide substrates were heated together to obtain mixtures of 1,2,3-triazole regioisomers, **2.2** (Scheme 78b).^[127,128] However, the full potential of this reaction was not realised until the Cu-mediated version was discovered in 2002 by the groups of Finn, Sharpless and Fokin,^{[129],[130]} and Meldal.^[131]



Scheme 78: General scheme of the CuAAC reaction.

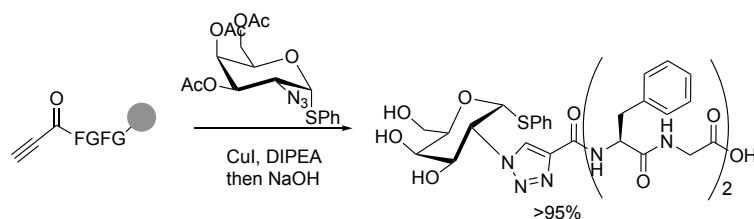
The two seminal reports of the CuAAC reaction provided very different methods for its use, and both reports have significantly affected the way this reaction is used to date. The report from Sharpless and Fokin^[129] described the use of what many consider to be 'classic' CuAAC conditions: a $CuSO_4$ precatalyst with NaAsc as a reductant in a solvent mixture of *t*BuOH/ H_2O (Scheme 79). The group carried out a substrate scope to explore the reactions compatibility with standard functionality and proposed a basic mechanism, *vide infra*.



Scheme 79: Seminal report of CuAAC from the group of Sharpless and Fokin.

The Meldal report^[131] described a more applied approach to the development of the CuAAC reaction. Using polymer-supported alkynes, the group reacted a range of azides using a CuI catalyst with *N,N*-diisopropylethylamine (DIPEA) as a base. Apart from the use of polymer-supported reagents, the key difference in this report is the scope of the reaction. Meldal uses this powerful reaction to ligate a diverse range of amino acids and small peptides to a number of highly functionalised azides, including saccharides, and molecules containing polar amines and acid moieties, in

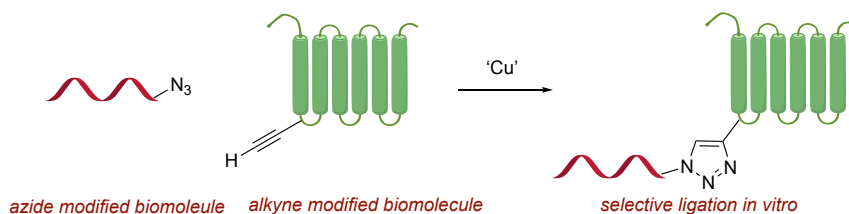
addition to a range of more standard functional groups (Scheme 80). This report in particular set the scene for many of the future applications of the CuAAC.



Scheme 80: Polymer-supported sugar-peptide ligation from Meldal's seminal contribution.

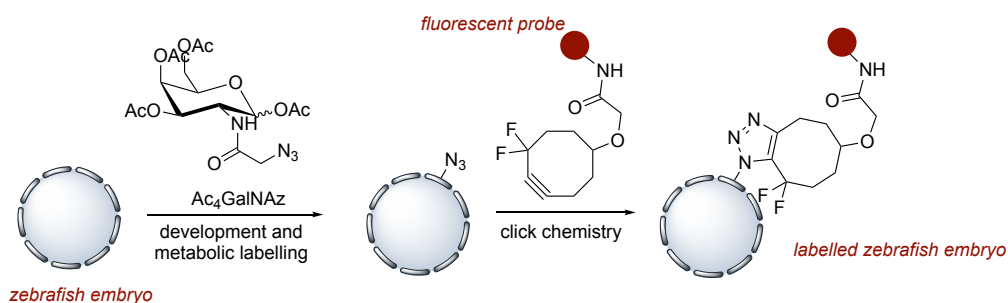
Since then, the CuAAC has become the method of choice for the connection of discrete molecules. CuAAC has seen uptake throughout a range of broadly different areas of chemistry and biology, perhaps due to the benign conditions employed and operationally facile nature of the transformation.^[132–134]

Chemical biology in particular has been profoundly impacted, with advances in bioconjugation, DNA modification, and in the synthesis of multifunctional biomaterials, among others, being aided by the CuAAC reaction. Chemical biology has embraced this chemistry principally because it is termed a ‘bio-orthogonal’ reaction (Scheme 81).^[135] This means CuAAC chemistry can be performed under conditions that are tolerant of sensitive biomolecules; such as proteins, DNA, and even living cells.^[136]



Scheme 81: Ligation of biomolecules using CuAAC.

This technology has even allowed selective modification *in vivo*. For example, in 2008, Bertozzi used the strain promoted azide alkyne cycloaddition (SPAAC), a copper free, yet closely related reaction (*vide infra*) to attach fluorescent probes (**2.3**) to azide-modified glycans in live developing zebrafish (Scheme 82).^[137] This allowed the authors to interrogate the distribution of the labelled glycans throughout the early lifetime of the zebrafish. The concept of using simple, benign chemistry to look closely at biological systems was revolutionary, and has been a keystone in the development of the burgeoning field of chemical biology.^[138]



Scheme 82: Use of SPAAC chemistry to label glycans in developing zebrafish.

2.1.1 Mechanism of the CuAAC Reaction

Due to its great importance to academics and industrialists within chemical biology, a fundamental understanding of how this reaction proceeds is vital. While the applications that have stemmed from this chemistry have been transformative in chemical biology, the wide range of substrates and conditions employed with this reaction has made probing the mechanism a significant challenge.^[139]

While the fundamental reactivity of the two reactive species, a Cu-acetylide **2.4** (formed *in situ* from the Cu catalyst and alkyne) and an organoazide **2.5**, are highly complementary, with both possessing nucleophilic and electrophilic sites, the exact mechanism of the cycloaddition is not straightforward (Figure 17a). Much of the subtlety in the catalytic cycle lies around the precise role of the Cu catalyst, and the nature of the azide ligation step.

Over the last 10 years, the mechanism has slowly been elucidated. The original mechanistic proposal by Sharpless, Finn, and Fokin in their seminal paper described the reaction over four mechanistic steps.^[129] It was proposed that the reaction proceeded through Cu-acetylide formation **2.6**, followed by azide coordination/ligation, rearrangement **2.7**, and protonation of the Cu-triazole **2.8** to give the desired product **2.9** (Figure 17b).

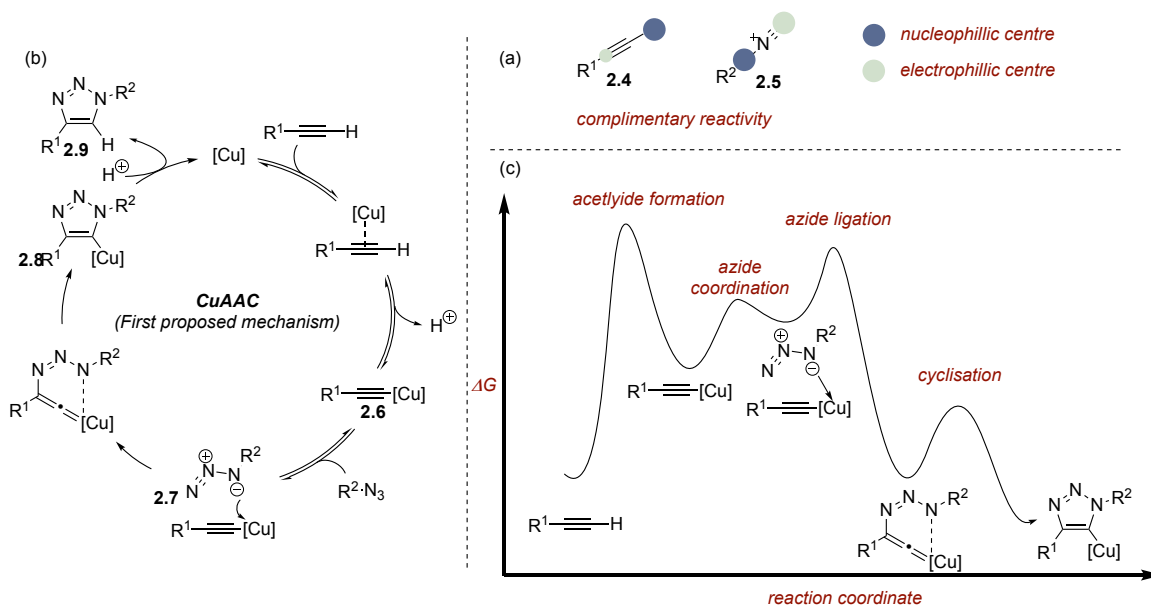


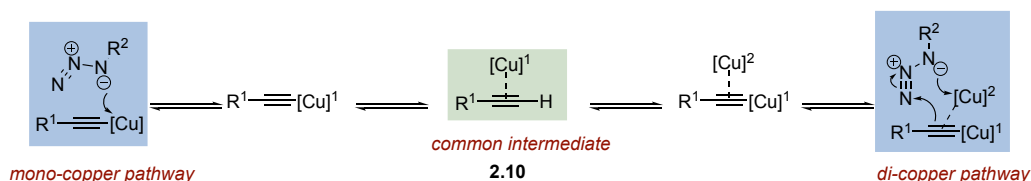
Figure 17: a) Complimentary reactivity of azide and Cu-acetylide b) Mechanism of the CuAAC initially proposed by Sharpless c) Representative energy diagram for the CuAAC mechanism.

In an early mechanistic study from the groups of Noodleman, Fokin, and Sharpless, density functional theory (DFT) calculations were carried out to verify the feasibility of the group's proposed catalytic cycle.^[140] Initial studies determined that π -coordination of the Cu species to the alkyne dramatically reduced the pK_a of the acetylenic proton. This activation reduces the pK_a of propyne from 25 to approximately 15, which makes formation of the Cu-acetylide feasible in the aqueous systems that are commonly employed in CuAAC. The group then ruled out a direct, concerted cycloaddition from the π -coordinated alkyne, as the projected energy barrier was too high to explain the experimental results (*ca.* 27.8 kcal/mol for the Cu-coordinated alkyne *vs.* 26 kcal/mol for the uncatalysed process). Moving to look at the step-wise process that had been previously suggested, the energy barrier required for a reaction proceeding through a Cu(III) metallacycle was significantly lower (Figure 17c). Formation of the 6-membered transition state was calculated to have an energy barrier of 14.9 kcal/mol, which is significantly lower than the uncatalysed process, explaining the rate enhancement of 7-8 orders of magnitude observed with Cu-catalysis.

In addition to this computational report, Finn and Fokin released a kinetic evaluation of the CuAAC reaction.^[141] Monitoring the reaction between benzyl azide and phenylacetylene by HPLC quench kinetics allowed the calculation of rate orders for the reaction components. Under catalytic conditions, the reaction was found to be

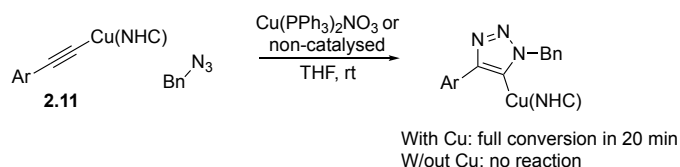
first order in acetylene, zero order in azide, and second order in copper. When a large excess of azide was used a slight negative dependency was observed, consistent with an unproductive azide-Cu interaction. Under conditions employing stoichiometric copper, the reaction was found to be first order in both alkyne and azide, and zero order in copper.

Fokin and co-workers later expanded on this work, proposing an alternative mechanistic pathway.^[142] This detailed study intended to verify the role of the π -coordinated copper species **2.10** in the azide ligation/coordination step. While π -coordination has been shown to accelerate the rate of Cu-acetylide formation, it was unknown whether this copper species is catalytically active in azide ligation. Two possible mechanistic pathways were postulated, the first involved π -coordination to accelerate acetylide formation, at which point the π -ligated Cu leaves to allow azide ligation: a mono-copper catalytic cycle. In the second mechanism, the acetylene bound copper atom plays a role in the azide ligation step, indicating a di-copper mechanism (Scheme 83).



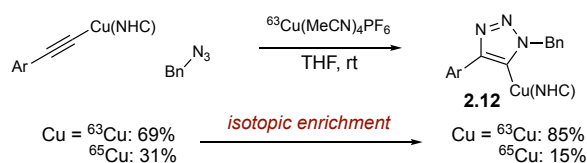
Scheme 83: CuAAC is proposed to go through either a mono or di-copper pathway.

The group first probed these two possible mechanisms through the application of a stable, pre-formed Cu-acetylide **2.11** to both catalysed and non-catalysed conditions. While the catalysed conditions gave full conversion to product after 10 minutes, the reactions without an additional Cu-catalyst were unreactive, suggesting a role for a second Cu atom, other than purely facilitating acetylide formation (Scheme 84).



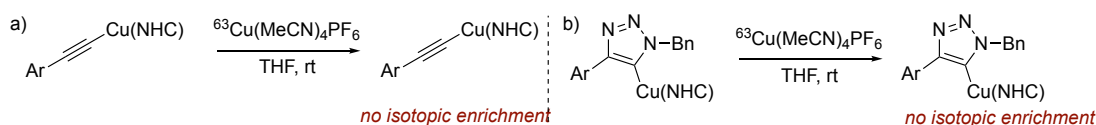
Scheme 84: Reaction of preformed Cu-acetylide with and without exogenous catalyst.

Following this, three simple experiments were carried out to further explore the role of an external copper source. Using an isotopically enriched ⁶³Cu catalyst under the standard reaction conditions, the group observed 50% isotopic enrichment upon isolation of the corresponding Cu triazole **2.12** (Scheme 85).



Scheme 85: Isotopic enrichment is observed through triazole formation.

Two further control experiments were carried out to determine if either the copper acetylide or copper triazole species would readily facilitate isotopic exchange.



Scheme 86: Control experiments to probe mechanism.

As enrichment was shown to not to occur at either the Cu-acetylide step (Scheme 86a) or from the Cu-triazole species (Scheme 86b) the authors conclude, by process of elimination, that the isotopic enrichment must arise from an intermediate mechanistic event. These data indicate that at some point during the azide ligation/insertion step, both copper atoms must become equivalent.



Scheme 87: Ligand exchange between equivalent Cu atoms.

In addition, the enrichment observed would require the migration of the NHC ligand on copper, which the authors suggest arises from two copper atoms bound to the same carbon atom which undergo a rapid exchange of the NHC ligand before a significantly slower cyclisation event to form the second C-N bond (Scheme 87). The combination of these experiments has led to the proposal of a more detailed mechanism of the CuAAC reaction, shown in Figure 18 below, the key addition to the mechanism from this study was moving to a di-copper azide ligation step **2.13**, which had not been suggested previously.

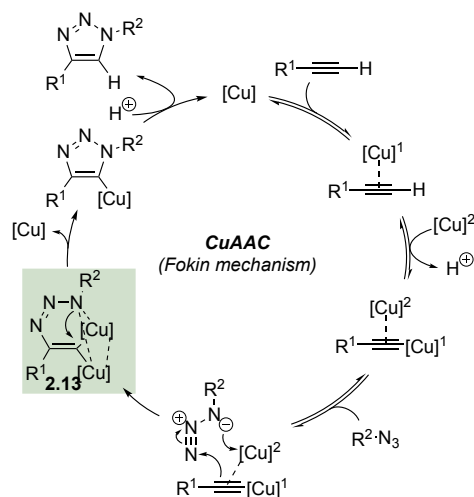


Figure 18: Fokin mechanism of the CuAAC. Azide ligation step shown in green .

Bertrand later extended this work through use of custom cyclic alkyl amino-carbene (CAAC) ligands.^[143] The Bertrand group has demonstrated the ability of these ligands to stabilise highly reactive metallic intermediates.^[144] Using this technology, they were able to isolate bis-copper complex **2.14** and obtain a crystal structure of this previously elusive reactive intermediate. The authors found that the counterion was crucial for isolation, with only trifluoromethanesulfonate allowing reliable preparation of the desired dinuclear complex **2.14**. Kinetic analysis of both mono- (**2.15**) and di-copper species after exposure to BnN_3 showed a significant rate enhancement (by two orders of magnitude) for di-copper species **2.14**. In addition, use of mono- (**2.16**) and di- (**2.17**) nuclear Cu-triazole species as catalysts in the reaction also exhibited the same trend. With this data, the authors were able to propose that while the bis-ligated complex proceeds through the kinetically favoured pathway, the mono-ligated copper species is also catalytically active (Figure 19).

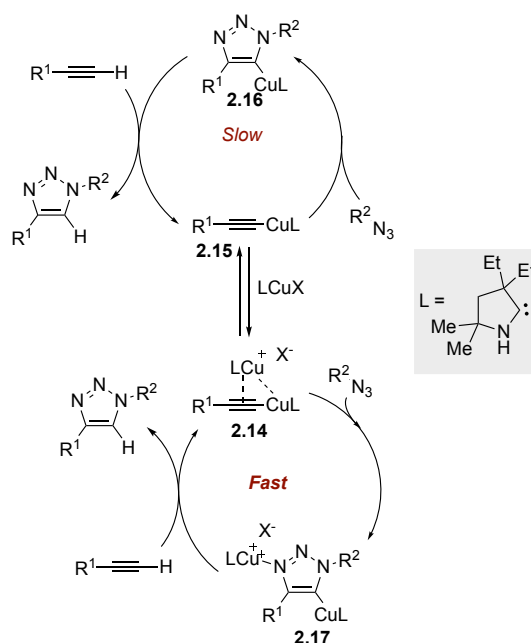


Figure 19: CAAC ligands reveal a rate difference between mono- and di-copper pathways.

More recently Tilley and co-workers have provided experimental support for an alternative di-nuclear Cu species. Using a custom chelating ligand, the group were able to synthesise a di-Cu $\mu - \eta^1:\eta^1$ alkyne complex **2.18**. This symmetrical di-Cu structure bears two Cu(I) atoms bound to the terminal carbon of the alkyne; these Cu atoms are stabilised by neighbouring pyridine and 1,8-naphthyridine ligands **2.19**. 2D-NMR and X-ray crystallography were used to unambiguously confirm the structure of the complex (Figure 20).

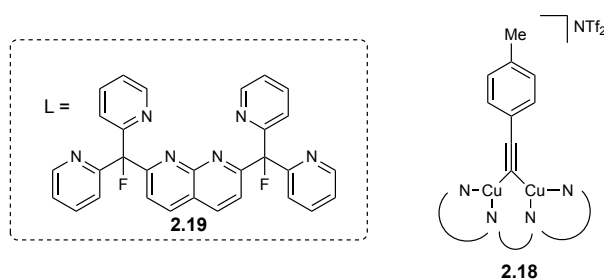
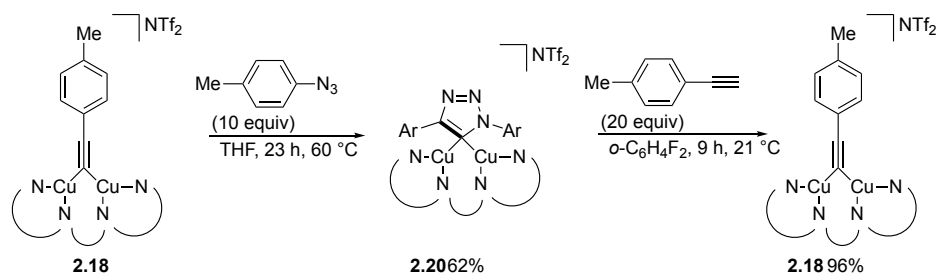


Figure 20: Di-nuclear Cu species isolated by the Tilley group.

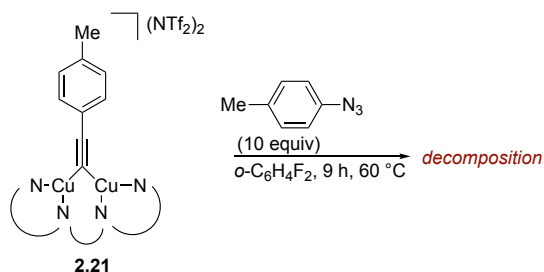
Di-Cu complex **2.18** was then reacted with 4-tolyl azide in THF to provide a bridging di-Cu triazolide complex **2.20**. This complex was also stable enough to be crystallised. Reaction of the bridging triazolide complex with an alkyne led to almost quantitative yield of complex **2.18**, which is presumably formed through protodemetalation of the triazolide, in analogy to the final step of the CuAAC reaction (Scheme 88).



Scheme 88: Reaction of di-nuclear complex with azides and alkynes.

While both key steps of the CuAAC reaction were shown to be competent using stoichiometric Cu-complexes, **2.18** was also investigated as a catalyst. Heating *p*-tolyl azide with *p*-tolyl acetylene with 10 mol% of **2.18** provided the desired triazole product in 90% yield.

Additionally, **2.18** was oxidised using ([AcFc]NTf₂) to a mixed valence di-Cu(I,II) (**2.21**) complex in order to investigate the viability of a di-Cu intermediate of this type as a reactive intermediate in the CuAAC reaction. Exposure of the mixed valence complex to either alkynes or azides led to decomposition of the di-Cu species and only low levels of the desired products (Scheme 89). This suggests that if a di-Cu $\mu - \eta^1:\eta^1$ alkyne is catalytically active in the CuAAC reaction then both Cu atoms are likely in the +1 oxidation state.



Scheme 89: Decomposition of mixed valence di-Cu complex after exposure to azide.

This study may have greater implications for the mechanism of the CuAAC, particularly in determining the valence of Cu in any di-Cu species that have been previously proposed. However, the conditions used for the synthesis of these complexes are unlike any of the conditions used in the CuAAC reaction on a practical level. In addition, the single mechanistic steps proceeding from this bridging di-Cu complex are unusually sluggish in comparison to other stoichiometrically prepared intermediates, requiring high temperatures and extended reaction times. While this does not rule out the existence of complexes of this type in

the CuAAC reaction, it would suggest that these copper complexes are less kinetically competent than their π -ligated counterparts.

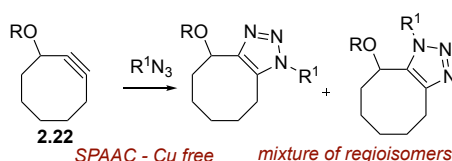
2.1.2 Chemoselectivity

The power of CuAAC is greatly enhanced through the accumulation of additional azide or alkyne partners on a single molecular scaffold. The success of this strategy is well documented and has relied on the exploitation of known reactivity profiles of the individual components. The following section will detail the approaches currently employed in the literature.

2.1.2.1 Chemoselectivity in the Alkyne Component

2.1.2.1.1 Strain-Promoted Azide-Alkyne Cycloadditions

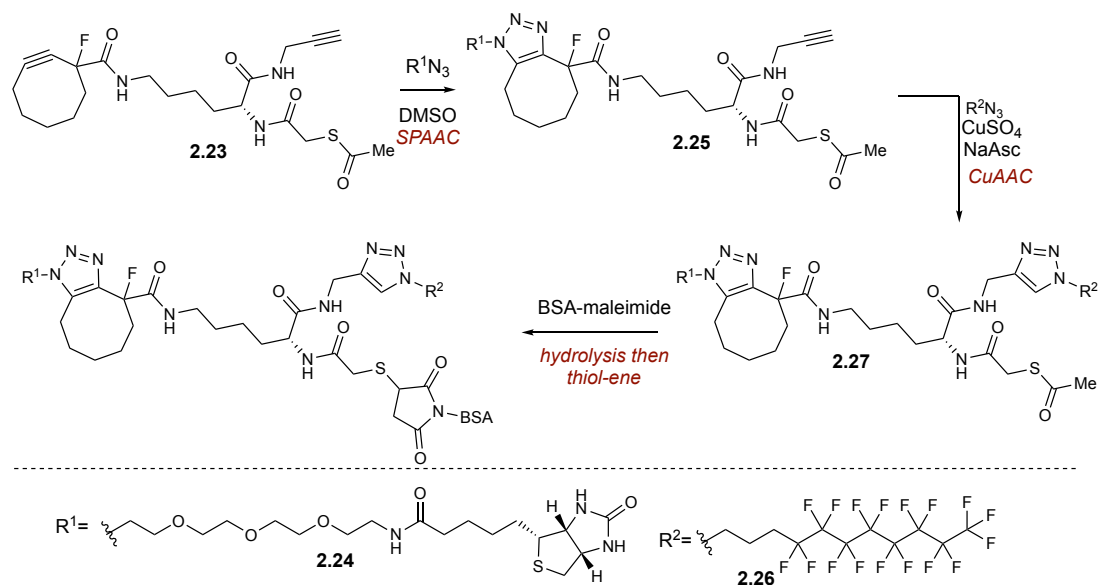
Selectivity in the alkyne component of the CuAAC reaction has been achieved through a number of methods. The most prevalent technique to date has involved the use of highly strained cyclic alkynes **2.22**. This method, invented in 2004 by the Bertozzi group (termed SPAAC, or Strain Promoted Azide Alkyne Cycloaddition) utilises Cu-free conditions to promote the rapid union of a wide variety of azide and cyclic alkyne partners (Scheme 90).^[145] The broad utility of this reaction stems from its comparably mild, Cu-free conditions, which are ideally suited towards use in sensitive environments such as cells.^[130,138] However, SPAAC coupling produces a mixture of triazole regioisomers when used with unsymmetrical alkynes and the mechanistic behaviour of these systems remains largely unknown. Despite this, SPAAC can be used to leverage chemoselectivity over terminal alkynes, which can then be reacted further upon addition of a Cu catalyst to the system.



Scheme 90: Strain promoted azide-alkyne cycloaddition.

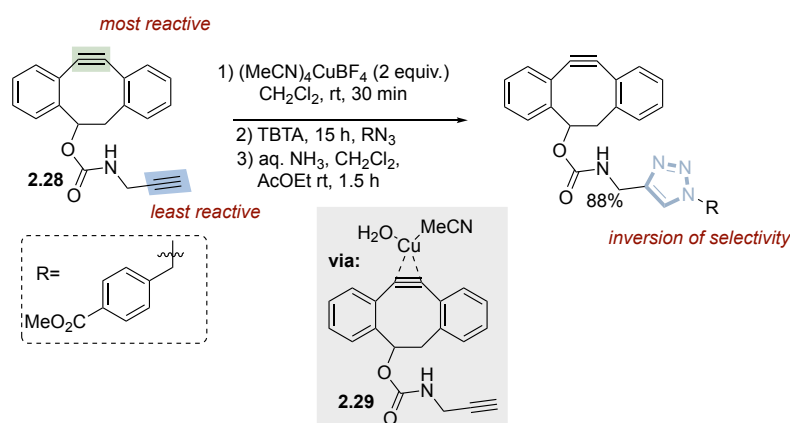
Beal and co-workers used bifunctional bis-alkyne **2.23** to perform sequential SPAAC/CuAAC coupling to selectively functionalise a dipeptide fragment.^[146] Treatment of **2.23** with biotin bearing azide **2.24** gave complete conversion to SPAAC product **2.25**. Further reaction with fluoros azide **2.26**, under standard CuAAC conditions, gave bis-triazole **2.27** in reasonable yield across both steps. The peptide conjugate was then reacted with Bovine Serum Albumin (BSA) through a

thiol-ene reaction (Scheme 91). This work demonstrated the feasibility of CuAAC/SPAAC sequential ligation strategies for the diversification of proteins.



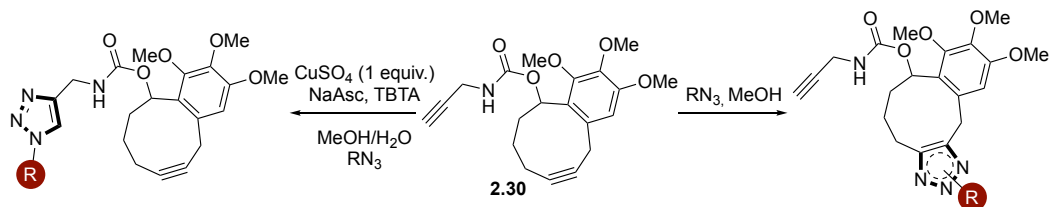
Scheme 91: SPAAC/CuAAC sequential ligation for the dual functionalization of BSA.

This parallel reactivity has been employed throughout a number of applications; however, the most significant advance came from the group of Hosoya in 2014.^[147] The authors were able to exploit the enhanced reactivity of a strained cyclic alkyne by transient protection through stoichiometric complexation of copper. When this was applied to bifunctional bis-alkyne **2.28**, the group were able to overturn the traditional SPAAC/CuAAC reactivity gradient and perform CuAAC on the pendant terminal alkyne in the presence of the highly reactive strained alkyne. The complex formed from the cyclooctyne and $\text{Cu}(\text{MeCN})_4\text{BF}_4$ (**2.29**) was stable enough to crystallise. The resulting crystal structure showed a tricoordinate cycloalkyne-Cu(I) species that was ligated to water and MeCN (Scheme 92). The reactive cyclic alkyne could be regenerated from the Cu complex by treatment with aqueous ammonia.



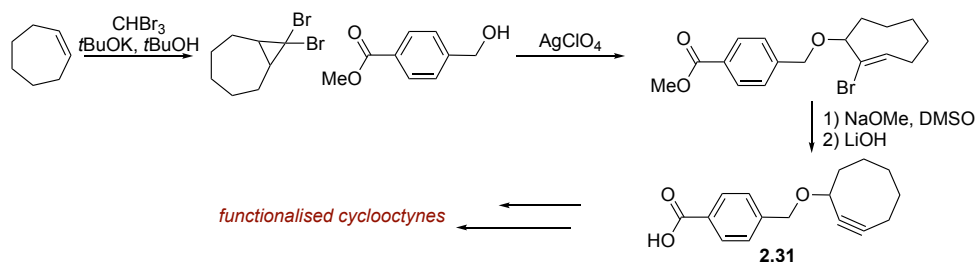
Scheme 92: SPAAC/CuAAC diyne can display orthogonal reactivity.

This seminal work was extended by Dudley who demonstrated that stoichiometric levels of CuSO_4 allows for *in situ* complexation of strained cyclic alkyne **2.30** while facilitating a CuAAC on a pendant terminal alkyne, once again inverting the standard selectivity profile (Scheme 93).^[148]



Scheme 93: Orthogonal control in CuAAC/SPAAC using stoichiometric copper.

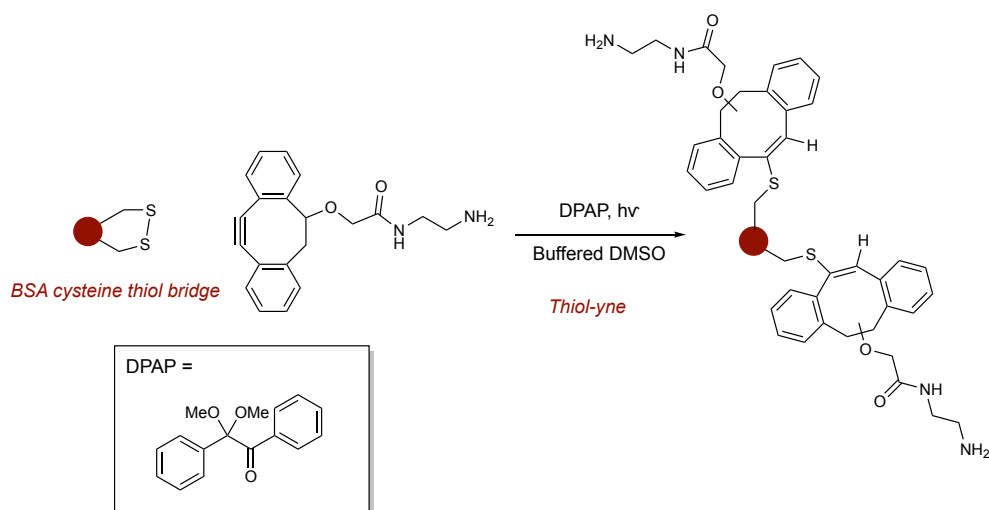
However, despite its widespread utility, SPAAC has a number of significant drawbacks. Firstly, the cyclooctyne starting materials often require a lengthy synthesis, with little opportunity for diversification. For example, the Bertozzi group synthesised the first SPAAC alkyne partner **2.31** in four steps from cycloheptene, which represents a significant investment in time and resource compared to the commercial terminal alkynes commonly used in CuAAC (Scheme 94).^[145]



Scheme 94: Synthesis of functionalised cyclooctyne.

In addition, while CuAAC delivers a single regioisomer, SPAAC typically gives an equimolar mixture of regioisomers, making purification and characterisation challenging.^[149] When used in biological systems, due to differences in structure, these regioisomers do not always provide the same biological effect.

Finally, the strained nature of SPAAC precursors renders them promiscuous towards a number of other reactive nucleophiles. In particular, background ‘thiol-yne’ reactions with cysteine residues (as disulfide bridges) can reduce the efficiency of SPAAC processes (Scheme 95).^[138,150]

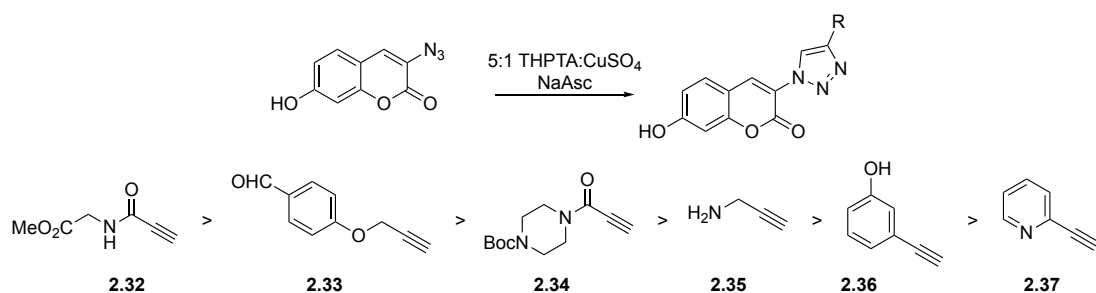


Scheme 95: Light initiated thiol-yne coupling with cyclooctyne.

While SPAAC remains the most common method for achieving selectivity, a small number of other reactive alkynes have been reported in the literature.

2.1.2.1.2 Activation of the Alkyne Component

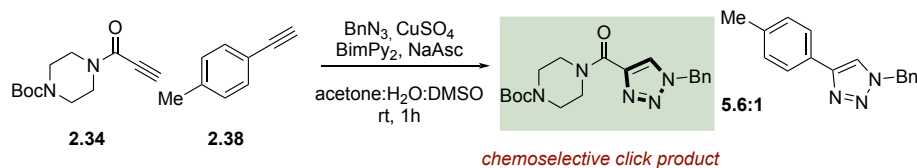
As part of a wider interest in bioconjugation, Finn and co-workers explored a wide range of alkynes for use in the CuAAC reaction.^[151] By measuring the relative performance of these alkynes under standard bio-orthogonal conditions, the authors were able to establish a reactivity scale to inform the use of CuAAC chemistry for bio-conjugation, based on the relative rate of reaction (Scheme 96). The authors found glycine-derived propiolamide **2.32** to be the fastest, followed closely by aryl propargyl alkyne **2.33** and Boc-protected piperazine propiolamide **2.34**. Propargyl amine **2.35** was next fastest, and aromatic alkynes **2.36** and **2.37** were significantly slower.



Scheme 96: Alkyne reactivity scale for bioconjugation.

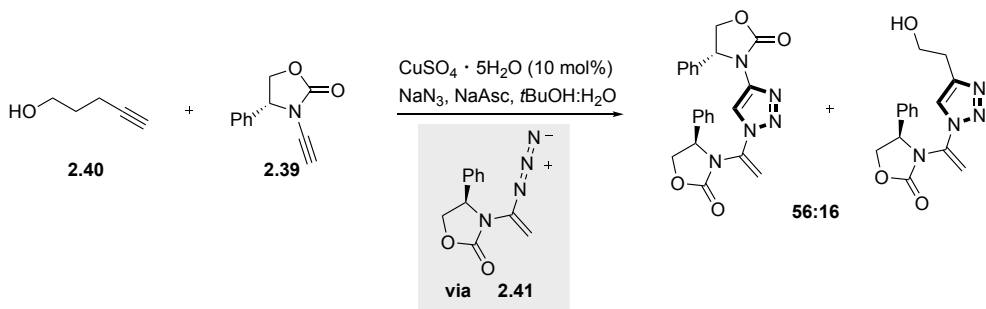
While the aim of the study was to determine which alkynes were optimal for application in more complex systems, chemoselectivity between alkynes was also disclosed. Reacting one of the fastest alkynes, propiolamide **2.34**, and tolyl acetylene **2.38** which was shown to be comparably slow, in a 1:1 ratio with benzyl azide

provided reasonable levels of chemoselectivity (5.6:1) in favour of the propiolamide triazole product (Scheme 97).



Scheme 97: Chemoselective CuAAC using reactive propiolamide.

The Hsung group, who have a long-standing interest in the chemistry of ynamides, have reported another example of alkyne chemoselectivity.^[152] The authors have demonstrated the selective engagement of oxazolidinone ynamide **2.39** over terminal alkyne **2.40** in CuAAC reaction with hydroazinated ynamide intermediate **2.41**. The intermediate **2.41**, was formed through reaction of NaN_3 with the ynamide starting material under Cu-catalysed conditions (Scheme 98).



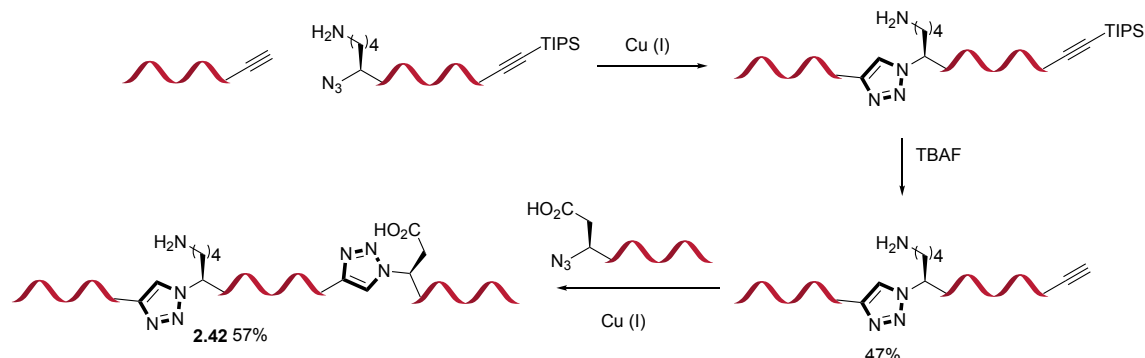
Scheme 98: Chemoselective CuAAC with oxazolidinone ynamide.

2.1.2.1.3 Protection of the Alkyne Component

Due to the scarcity of methods for achieving selectivity purely based on alkyne reactivity, selective functionalisation has primarily been realised through the use of protecting groups. Protection of one alkyne, usually through the use of silyl species, allows for completely chemoselective CuAAC reactions on the unprotected alkyne. This method has been widely reported for the sequential functionalisation of biomolecules.

Aucagne and Delmas used this method for the selective union of peptide fragments.^[153] The group used CuAAC as an alternative to native chemical ligation of long peptide fragments. In an impressive display, the authors demonstrated the union of three peptide chains, each with >30 residues, to form a chain 98 residues long in reasonable yields. The diversity of functionality and high number of Lewis basic sites required the use of stoichiometric Cu(I) to facilitate the reaction.

Deprotection of the TIPS protecting group with TBAF was followed by a second CuAAC reaction to provide the 98' mer **2.42** (Scheme 99). This was the first use of the CuAAC as a viable alternative to classical ligation procedures.



Scheme 99: Sequential CuAAC enabled by protecting groups.

Building upon this pioneering work, Carell used a similar sequential ligation method for the functionalisation of oligonucleotides.^[154] In this report, the authors use differentially protected alkynes to perform three successive ligations onto a DNA strand. Three custom nucleobase building blocks were effectively incorporated into DNA strands using phosphoramidite chemistry (Figure 21). These nucleobases, based on thymidine **2.43** and cytidine **2.44**, were modified at the 5-position with an alkyne-bearing chain. The pendant alkynes were unprotected, TMS protected, or TIPS protected; this established a reactivity gradient for sequential functionalisation.

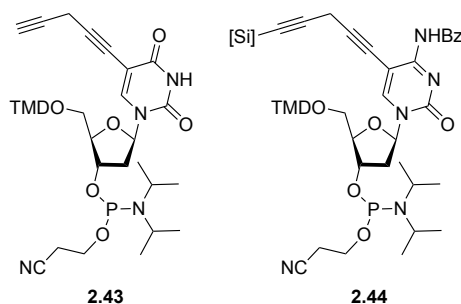
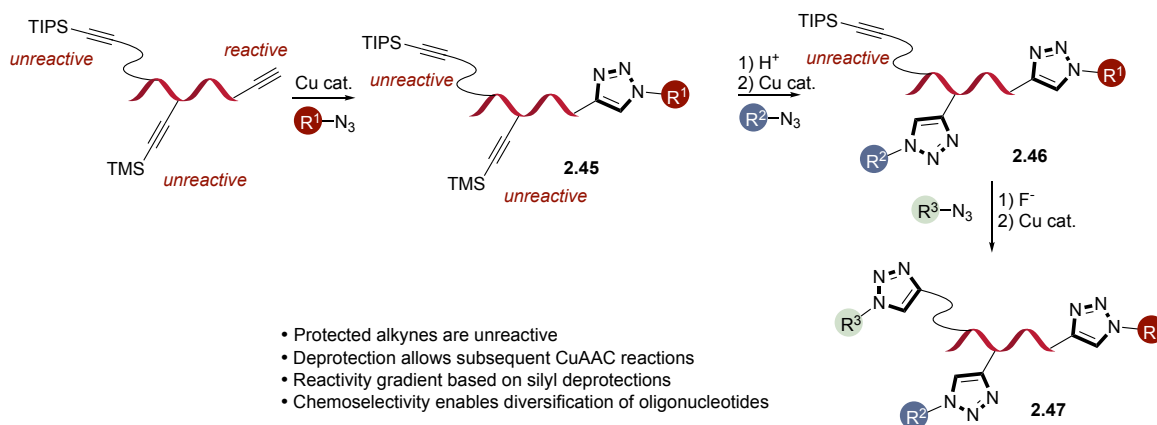


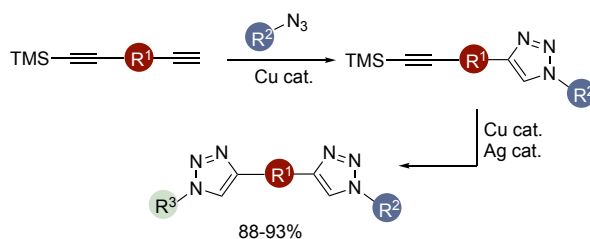
Figure 21: Custom phosphoramidite used in sequential DNA functionalization.

Exposure of the oligonucleotide to CuBr, TBTA, and a wide scope of azides led to high conversion to the corresponding triazole products. The mono-functionalised DNA strand **2.45** was then washed with 1% acetic acid solution, cleaving the TMS protecting group, and revealing another reactive alkyne. A second CuAAC reaction under the same conditions yielded the doubly modified oligonucleotide **2.46**. Deprotection of the TIPS group on the final modified nucleobase using TBAF provided a further free alkyne for modification. A final CuAAC reaction led to the triply modified oligonucleotide **2.47** in 50% yield (Scheme 100).



Scheme 100: Triple modification of oligonucleotides using sequential CuAAC.

Leigh and co workers later extended this theme, performing sequential CuAAC ligations to synthesise short peptide sequences.^[155] In this report, the authors use TMS-protected alkynes to achieve selectivity, which can be deprotected and subsequently reacted in a single operation using catalytic amounts of CuSO₄ and AgPF₆ in an alcohol/water mixture (Scheme 101).



Scheme 101: Sequential CuAAC/deprotection-CuAAC of peptide fragments.

2.1.2.1.4 Chemoselectivity in the Azide Component

Two primary methods have been disclosed for achieving selectivity in the azide component of the CuAAC reaction: through either activation of the azide *via* a neighbouring chelating group or by deactivating the azide through steric hindrance. The better exemplified of these two approaches is the use of chelating azides. Zhu has shown that a number of azides with an appropriately disposed chelating group will accelerate the CuAAC reaction (Figure 22).^[156] Pyridine (**2.48**, **2.49**), quinoline (**2.50**) and even a triazole (**2.51**) were shown to be competent chelating groups.

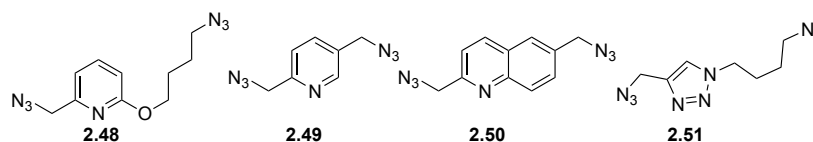
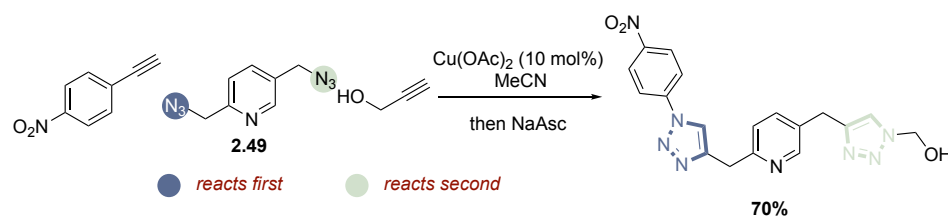


Figure 22: Chelating azides used for selective functionalization.

This approach has allowed for chemoselective CuAAC reactions versus standard, non-chelating azides, **2.50** (Scheme 102). In addition, bifunctional diazides such as

2.49 can be used for sequential CuAAC reactions to provide access to highly functionalised frameworks with excellent levels of selectivity.

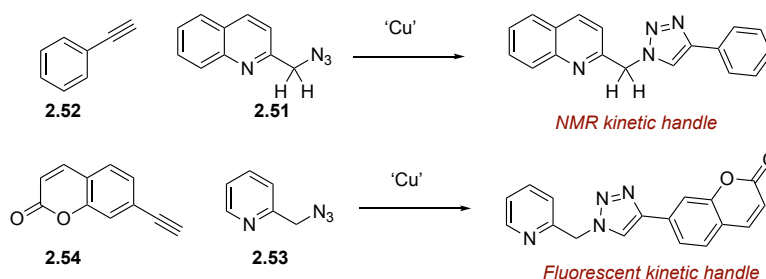


Scheme 102: Sequential CuAAC facilitated by chelating azide.

The authors have shown that the use of a Cu(II) precatalyst is essential for high levels of selectivity and optimal rate enhancement when using these activated azides.^[157] In their initial report, the authors suggest that the Cu(OAc)₂ precatalyst is reduced by either alkyne-alkyne homocoupling or, if the reaction is performed in MeOH, by oxidation of the alcoholic solvent. UV/Vis absorption spectroscopy measurements throughout the reaction time course show that after an initial induction period where Cu(II) persists, the absorbance signal abruptly disappears, suggesting the rapid reduction to Cu(I). EPR measurements of the reaction mixture before and after the addition of the azide showed that the chelation is required for reduction of Cu(II). While a strong EPR signal is observed for Cu(II) species, Cu(I) is EPR silent; the authors show that in the absence of azide, Cu(II) is not reduced. However, upon addition of the chelating azide the characteristic Cu(II) signal disappears with completion of the reaction, providing further evidence for an *in situ* azide-assisted reduction of Cu(II) to Cu(I) *via* alkyne-alkyne homocoupling.

A further mechanistic investigation into this chelate effect revealed the nature of the active catalytic species and provided further evidence for an *in situ* reduction via two separate mechanisms.^[158] Kinetic evaluation of the reaction was performed through both fluorescence spectroscopy and NMR analysis in both MeCN and MeOH using quinoline bearing azide **2.51** with phenylacetylene **2.52**, and picolinyl azide **2.53** with alkynyl coumarin **2.54** (Scheme 103). Initial experiments showed a significant induction period that was attributed to the formation of the active catalyst complex. Pre-mixing the catalyst with the chelating azide in MeOH effectively eliminated the induction period, lending support to this hypothesis. In MeCN, very little difference in the induction period was observed, indicating a divergent mechanism for catalyst activation. In addition, a significant deuterium kinetic isotope effect (KIE) was observed using CD₃OD, whereas no effect was observed using CH₃OD, suggesting

that cleavage of the C-H bond plays a mechanistically significant role, such as the reduction of Cu(II).



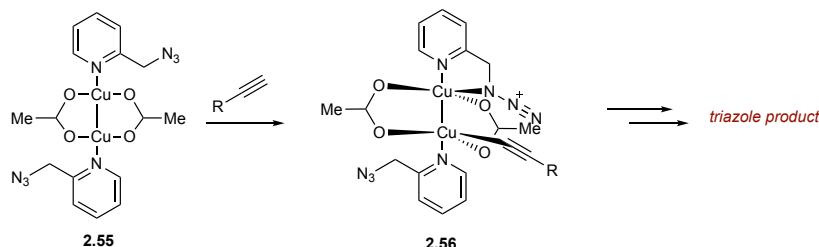
Scheme 103: Model systems used for NMR and fluorescent kinetic studies.

Measurement of the reaction orders of all of the components revealed similar results to the work of Fokin and Finn.^[141] The reaction had a second order dependence on Cu(OAc)₂, suggesting a dinuclear Cu species is the active catalyst. In MeOH, the reaction was first order in alkyne and showed a slight positive dependence (0.4) on azide. In MeCN, azide is zero order and there is a second order dependency on alkyne. These data signify that both alkyne and Cu are involved in the rate-determining step (RDS), which in this case is Cu-acetylide formation. Further evidence for a Cu-acetylide RDS came from deuterium KIE experiments; deuteration of the acetylenic C-H bond gave a primary KIE of 2.3 and significantly extended the induction period in MeCN.

The authors propose a mechanistic model to explain the kinetic variation between MeCN and MeOH. The slight positive dependence on azide when the reaction is performed in MeOH is attributed to the role of the pyridine (**2.53**) as a base, aiding the oxidation of MeOH and subsequent reduction of Cu, a step that is shown to be kinetically significant. This positive dependence is not observed in MeCN, as Cu(I) is produced through alkyne homocoupling. The 2nd order dependence on alkyne in MeCN is proposed to arise from its role in both acetylide formation and reduction of Cu, and also as a proton source for protonation of the Cu-triazole species. In MeOH, the protonation of the Cu-triazole will occur from the solvent, rather than the alkyne. Additionally the alkyne species does not play a role in the reduction of Cu, which accounts for its first order dependency.

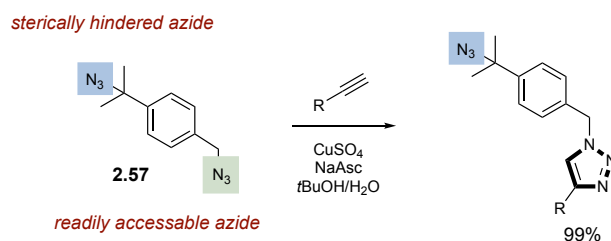
Guided by the kinetic investigation and a crystal structure obtained from a mixture of the Cu(OAc)₂ catalyst and chelating azide **2.53**, the authors proposed dinuclear complex **2.55** as the active catalytic species.^[158] Their model contains an acetate-

bridged dimer with each copper bearing a pyridyl azide ligand (Scheme 104). This dimer then undergoes Cu-acetylide formation to give **2.56**, followed by intramolecular azide insertion to form the Cu-triazole product. Protonation of the resulting Cu species provides the product.



Scheme 104: Mechanistic model featuring a dinuclear copper complex.

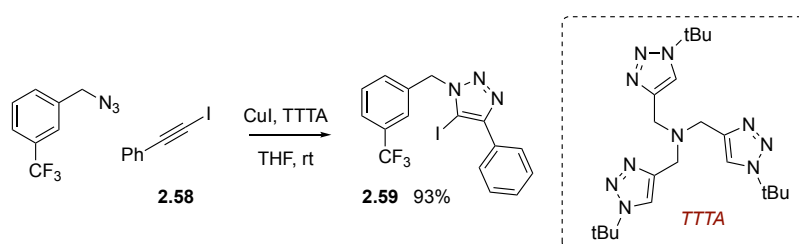
In contrast to the work of Zhu with chelating azides, Koert has shown that sterically hindered azides react sluggishly, providing chemoselectivity when used with less hindered primary azides.^[159] Bifunctional bis-azide **2.57** was shown to provide complete selectivity for the less sterically encumbered primary benzyl azide. While the authors make no comment about the mechanistic aspects of this reactivity, it can be assumed that pre-coordination of the less hindered azide is energetically more favourable, resulting in high levels of chemoselectivity (Scheme 105). The authors go on to demonstrate the application of this methodology by making a thin film in a layer-by-layer (LbL) approach.



Scheme 105: Chemoselectivity based on steric hindrance.

2.1.2.1.5 Use of 1-Iodo Alkynes

In 2009, Fokin and Sharpless demonstrated that 1-iodoalkynes **2.58** undergo a rapid Cu-catalysed cycloaddition with organic azides to give iodotriazoles **2.59** with complete regioselectivity (Scheme 106).^[160]



Scheme 106: CuAAC reaction with 1-iodoalkynes.

Using CuI and a tris-triazole ligand (TTTA, Scheme 106), the CuAAC reaction between the iodoalkyne **2.58** and azide is complete in 1 h at room temperature, which is significantly faster than the corresponding terminal alkyne and is competitive with other ‘fast’ CuAAC substrates. The authors propose two different mechanistic pathways that could account for both the regioselectivity and the rate of the reaction (Figure 23).

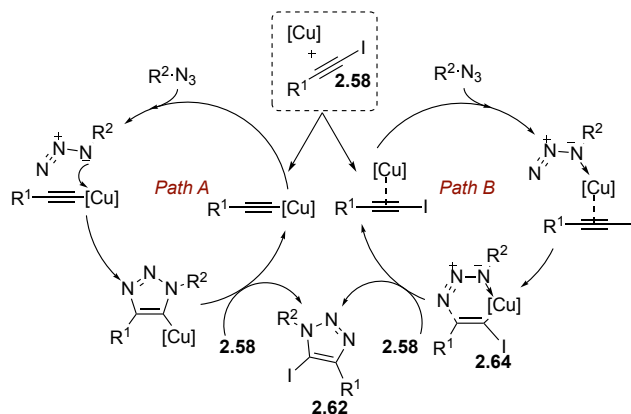


Figure 23: Postulated mechanistic pathways for iodoalkyne cycloaddition.

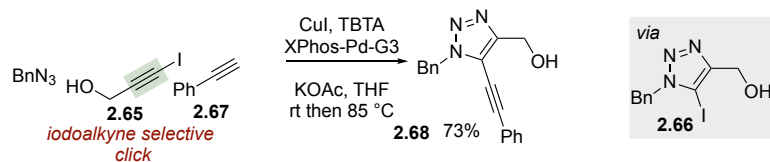
The first proposed mechanism starts with addition of Cu(I) into the C-I bond to form an acetylide **2.60**, azide coordination followed by cyclisation provides a Cu-triazole **2.61**. Copper exchange through σ -bond metathesis with another molecule of iodoalkyne yields an iodotriazole **2.62** and completes the catalytic cycle.

The alternative mechanistic hypothesis does not proceed through a Cu-acetylide species; instead, π -coordination of the Cu-catalyst to the iodoalkyne **2.63** facilitates azide ligation. Cyclisation to form the triazole product then proceeds through 6-membered transition state **2.64**.

Fokin and co-workers favour the second mechanism, as when the reaction is performed in protic solvents, the iodotriazole remains the exclusive product. If the iodotriazole is formed through a recombination event from a cuprate intermediate, such as in mechanism A, then in the presence of a proton source some protiotriazole should be formed. In mechanism B, the iodine-carbon bond is never broken, leaving the iodotriazole as the sole product.

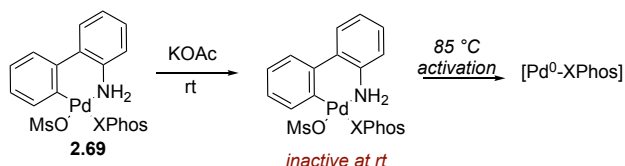
In 2016, a chemoselective iodotriazole CuAAC reaction was used in a novel cascade reaction.^[161] Lautens used tandem Cu- and Pd-catalysis to perform a chemoselective

CuAAC reaction on an iodoalkyne **2.65** over a terminal alkyne to form an iodotriazole product **2.66** (Scheme 107). This intermediate then undergoes Sonogashira coupling with the unreacted terminal alkyne **2.67** to construct a fully substituted alkynyl triazole **2.68**.



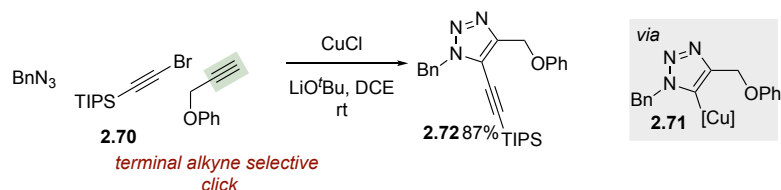
Scheme 107: Use of iodoalkyne for chemoselective CuAAC.

Careful control of the reaction mixture was required to preclude the formation of a number of unwanted by-products that arise in the presence of both Cu and Pd catalysts. The authors observed significant quantities of alkyne dimerisation as well as the undesired triazole product. The group found that when weak bases are employed, Buchwald precatalysts **2.69** do not activate via reductive elimination at room temperature (Scheme 108). This allowed for temperature-dependent selectivity; the CuAAC reaction could be performed at room temperature, effectively Pd free, before the reaction mixture is heated, inducing reductive elimination and activation of the Pd-catalyst, which can subsequently undergo Sonogashira coupling to afford the final product.



Scheme 108: Buchwald precatalyst allows temperature-dependent activation.

The group of Xu later reversed the selectivity in this tandem process. Using CuCl and moving to less activated bromoalkyne **2.70**, an initial CuAAC reaction on the terminal alkyne provided Cu-triazole compound **2.71** which was able to engage the unreacted bromoalkyne to provide the alkynyl triazole product **2.72** in good yield (Scheme 109).^[162]



Scheme 109: Bromoalkyne provides alkyne chemoselectivity in CuAAC/Ullmann tandem coupling.

This study, in concert with the work of Lautens, demonstrated the synthetic power of chemoselectivity in the CuAAC reaction, effectively building highly functionalised heterocyclic products in excellent yields.

2.1.3 Summary

The CuAAC reaction has become a highly important tool for the linkage of discrete biomolecules. The mild and selective conditions employed allow for a wide substrate scope including sensitive proteins, nucleotides, and saccharide moieties. The utility of this reaction is greatly enhanced through the use of polyfunctionalised systems to selectively ligate a diverse array of biomolecules and activity modifying groups to a target of interest.

To achieve this, a number of chemoselective approaches have been developed to facilitate sequential chemoselective ligations. These can be broadly separated into alkyne selectivity and azide selectivity. Alkyne selectivity has been dominated by the use of strained cyclic alkynes and protecting group strategies, both of which offer perfect selectivity but low atom economy and step efficiency. Activation of one alkyne over another has received far less attention due to the lower levels of selectivity that are commonly observed, although these techniques have enabled the discovery of novel methods in small molecule chemistry.

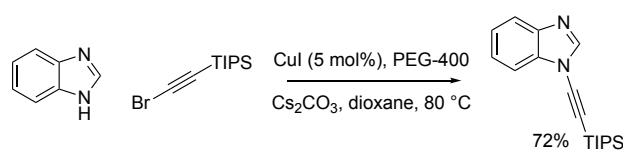
Chemoselectivity in the azide component has been limited to two approaches; through chelation control and by exploiting steric hindrance, of which, use of a neighbouring chelating group is by far the most prominent. This method has allowed for complete chemoselectivity versus a range of standard azide substrates. Use of sterically demanding azides provides a method for deactivation, and also provides excellent levels of selectivity.

In addition, a wealth of excellent mechanistic work has shed light on the elusive mechanism of the reaction. In particular, by examining the mechanistic origins behind the selectivity of chelating azides, Zhu was able to examine the key mechanistic steps in great detail, proposing a novel dinuclear copper complex and reaction pathway that may have bearing on the CuAAC reaction in the general sense.

The development and investigation of chemoselective protocols not only delivers new synthetic methods but also provides a different lens with which to investigate fundamental reactivity that is often overlooked.

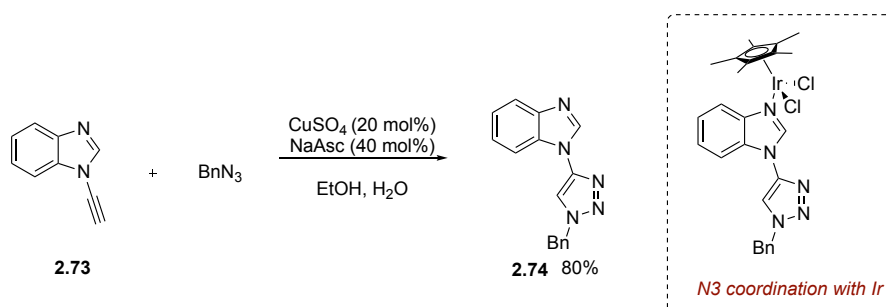
2.2 Previous work - Ynamines as Reactive Substrates in CuAAC

While many groups have explored the diverse chemistry of ynamides,^[163] significantly less research has been devoted towards the use of aromatic ynamines. In 2010, the Burley group developed a robust, Cu(I)-catalysed method for the synthesis of imidazole based ynamines using microwave irradiation.^[164] The group found that catalytic polyethylene glycol 400 (PEG 400) was highly beneficial, acting as both a phase transfer reagent and as a Cu-stabilising ligand (Scheme 110).



Scheme 110: Synthesis of benzimidazole ynamine.

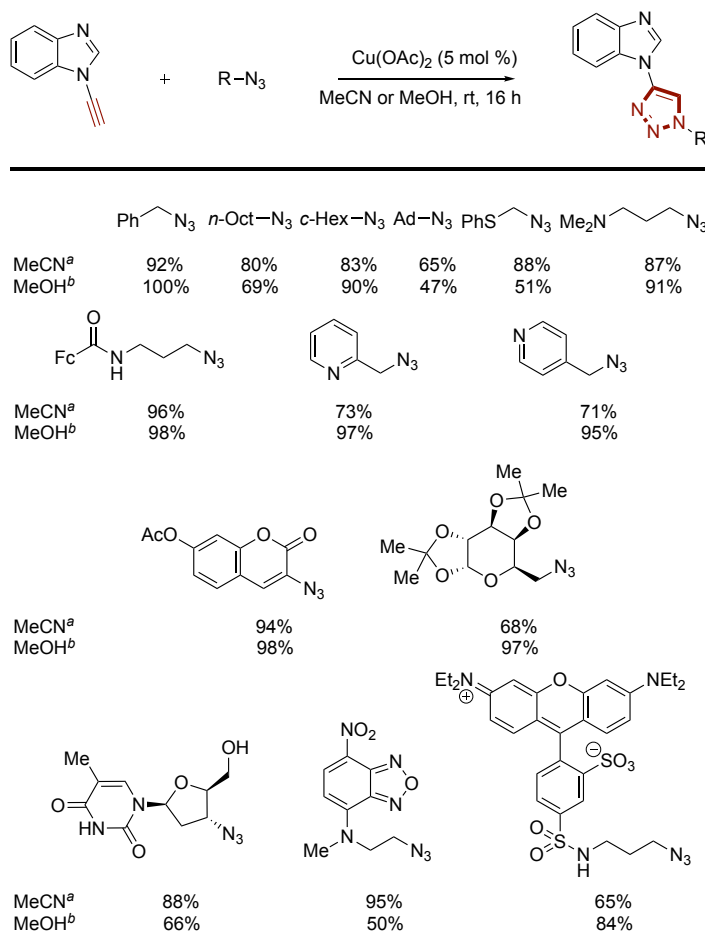
Two years later, the group demonstrated the proficiency of the ynamine substrates towards CuAAC.^[165] Upon exposure to standard CuAAC conditions (Scheme 110), benzimidazole ynamine **2.73** underwent complete reaction to form triazole product **2.74** in just five minutes. The group went on to investigate the reactivity of the CuAAC products towards Ir, noting that coordination at N3 of the imidazole ring was favoured over chelation to the triazole.



Scheme 111: CuAAC to form ynamine triazole and its complexation with Ir.

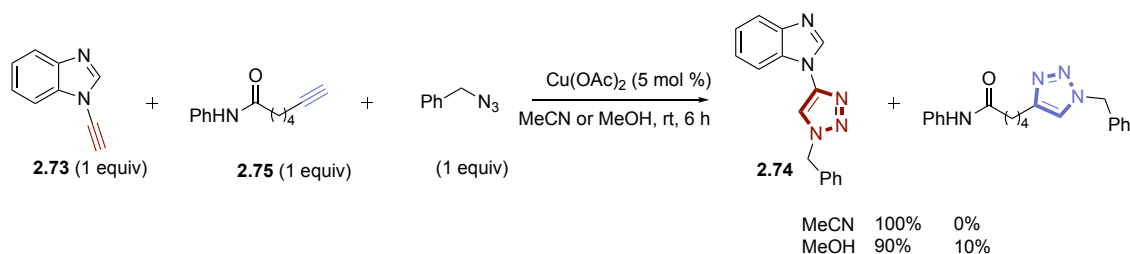
This unusually rapid reactivity in the CuAAC was further investigated in 2016, where benzimidazole ynamine **2.73** was shown to be a robust partner in the CuAAC reaction.^[166] Optimisation of the reaction conditions showed that the reaction was highly tolerant of a wide range of Cu salts, although Cu(OAc)₂ was most effective, and could be performed with catalyst loadings as low as 1 mol%. In addition, the reaction was shown to be efficient in a range of media; however, MeCN and MeOH were found to be optimal.

The scope of the reaction was excellent, with a broad array of biologically relevant molecules such as dyes, nucleobases, and saccharides all reacting smoothly (Scheme 112).



Scheme 112: Substrate scope.

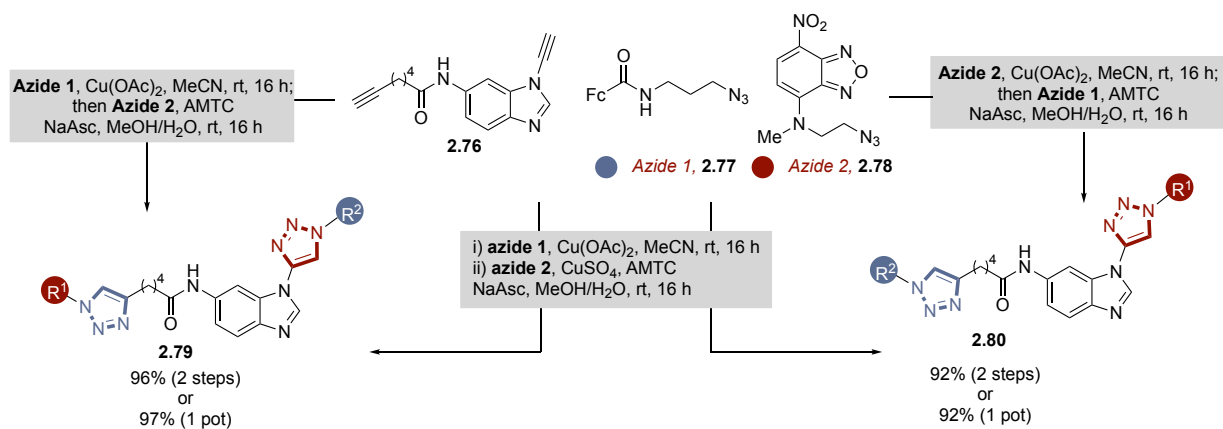
Intermolecular competition experiments employing equimolar amounts of both benzimidazole ynamine **2.73** and aliphatic alkyne **2.75** showed complete chemoselectivity for the ynamine triazole product **2.74**. This selectivity was conserved with both benzyl and cyclohexyl azides (Scheme 113).



Scheme 113: Chemoselective CuAAC using benzimidazole ynamine.

Selectivity was then addressed in intramolecular competition experiments using diyne **2.76**. Two azides of biological significance (ferrocene azide **2.77** and green dye **2.78**) were reacted with the bifunctional scaffold, once again demonstrating

complete chemoselectivity for the ynamine triazole products. Upon the completion of the first reaction, application of more standard CuAAC conditions led to excellent yields of the bis-triazole products **2.79** and **2.80** (Scheme 114).



Scheme 114: Chemoselective sequential and one-pot CuAAC ligations of diyne 2.76.

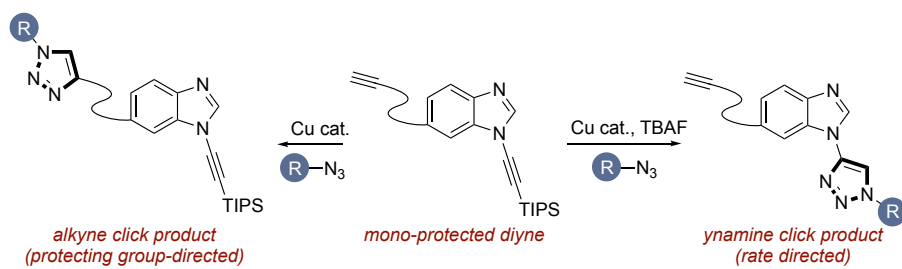
2.3 Project Aims

Previous work in the Watson and Burley groups has established that aromatic ynamines are highly reactive substrates for CuAAC reactions. This distinct substrate class undergo rapid CuAAC reactions with a broad scope of azide partners. In addition, this class displayed high levels of chemoselectivity versus aliphatic alkynes. This chemoselectivity has allowed for the sequential dual functionalization of bis-alkynes, providing a platform for bio-orthogonal ligation.

We aimed to probe the limits of this unprecedented alkyne chemoselectivity, and establish a guide for use of this reagent in bioconjugation. A number of reactive alkynes are available in the literature for use in biologically relevant systems, establishment of a general reactivity scale will allow the generation of novel chemoselective processes that do not rely on protecting group strategies, streamlining synthetic routes towards labelled biomolecules.

After determining how aromatic ynamines behave in comparison to other reactive alkynes, we proposed that through kinetic and spectroscopic studies we could determine the origin of this unusual chemoselectivity. Classic approaches towards alkyne selectivity have relied on exploitation of a difference in overall rate, which is principally determined by the rate of Cu-acetylide formation (as the typical RDS). Through investigation of the mechanism of the ynamine CuAAC we aimed to further understand how chemoselectivity is established and shed light on the mechanism of the CuAAC in a more general sense.

In addition to determining the source of selectivity, we aimed to utilise the levels of chemoselectivity offered by aromatic ynamine substrates to develop a novel orthogonal platform for sequential CuAAC. Orthogonal control has previously only been achieved through SPAAC/CuAAC diyne systems using stoichiometric Cu masking groups. We hypothesised that traditional protecting group strategies could be overturned through exploitation of a rapid deprotection/CuAAC sequence. This strategy would require a silyl protected ynamine substrate to be deprotected and undergo Cu-acetylide formation before a second, competing alkyne can react (Scheme 115).



Scheme 115: Proposed method for orthogonal reactivity.

2.4 Results and Discussion

The work in this chapter is based on the following publications:

C. P. Seath, G. A. Burley, A. J. B. Watson, *Angew. Chem. Int. Ed.* **2017**, *56*, 3314 – 3318 and M. Z. C. Hatit, C. P. Seath, A. J. B. Watson, G. A. Burley *J. Org. Chem.* **2017**, *82*, 5461 – 5468.

The work described herein was performed with Ms M. Z. C. Hatit

2.4.1 Determining the Origins of Chemoselectivity

While benzimidazole ynamine **2.73** had previously been shown to provide perfect chemoselectivity versus aliphatic alkynes, it was unknown whether this impressive reactivity would translate when used in competition with more reactive alkynes. In order to investigate this, a representative palette of alkynes from the literature was chosen to probe the chemoselectivity of **2.73**. The group of alkynes consisted of pentyne **2.81**, tolyl acetylene **2.38**, propargyl alkyne **2.82**, oxazolidinone ynamide **2.83**, and tertiary propiolamide **2.34**, in addition to dimethyl benzimidazole ynamine **2.84**, which was chosen for its more characteristic ¹H NMR signals. This small set of alkynes covers all of the major classes of alkyne used in CuAAC, including other alkynes that have demonstrated chemoselective reactivity (Figure 24).

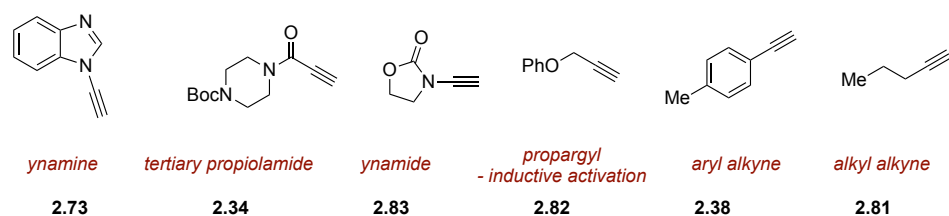
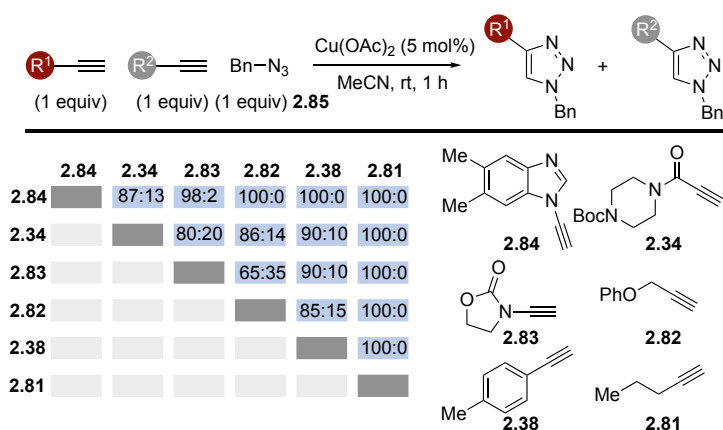


Figure 24: Alkynes screened for chemoselectivity.

In order to establish a reactivity scale bearing these six alkyne classes, a series of 1:1 competition experiments was carried out (Scheme 116). Based on previous literature, ynamine and ynamide should be chemoselective versus the alkyl alkyne and propiolamide should be selective versus both aryl alkyne and alkyl alkyne. Using the conditions previously optimised by the Watson and Burley groups (Cu(OAc)₂ in MeCN), with BnN₃ **2.85** as a representative azide partner, a reactivity scale was quickly established.



Scheme 116: Competition CuAAC reactions of systems containing two alkynes. Ratios are products arising from horizontal number:vertical number. Determined by ^1H NMR spectroscopy.

Ynamine **2.84** was the most reactive alkyne chemotype, outcompeting all other alkyne classes. Exclusive formation of the ynamine triazole product was observed in reactions with alkynes **2.38**, **2.81**, and **2.82** and was favoured over propiolamide triazole product by more than 8:1. Tertiary propiolamide **2.34** provided 8:1 selectivity over alkynes **2.83**, **2.82**, and **2.38** and complete selectivity against alkyl alkyne **2.81**. Ynamide **2.83** was only moderately selective against propargyl alkyne **2.82** but provided good selectivity against aryl alkyne **2.38**, and complete selectivity when in competition with alkyl alkyne **2.81**. Propargyl alkyne **2.81** gave 8:1 selectivity versus aryl alkyne **2.38** and complete selectivity against alkyl alkyne **2.81**, which was completely unreactive under the reaction conditions.

These data allowed the creation of a reactivity scale for chemoselective CuAAC which is as follows: ynamine > propiolamide > ynamide > propargyl > Aryl > alkyl (Figure 25). We propose that this guide will inform the selection of alkyne partners for chemoselective sequential CuAAC reactions on multi-functional systems.

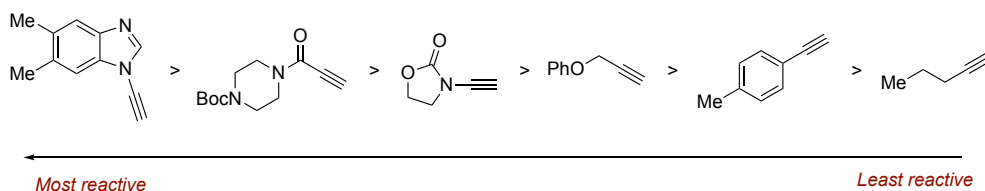
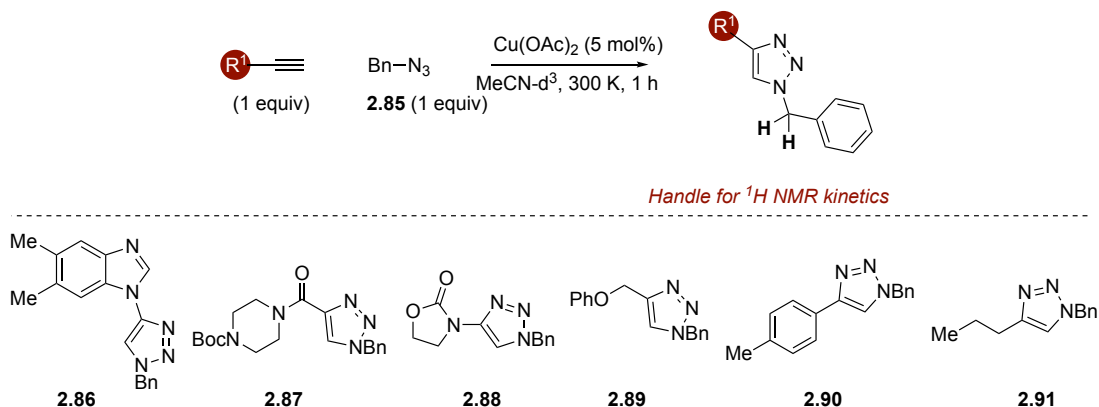


Figure 25: Reactivity scale established through competition experiments.

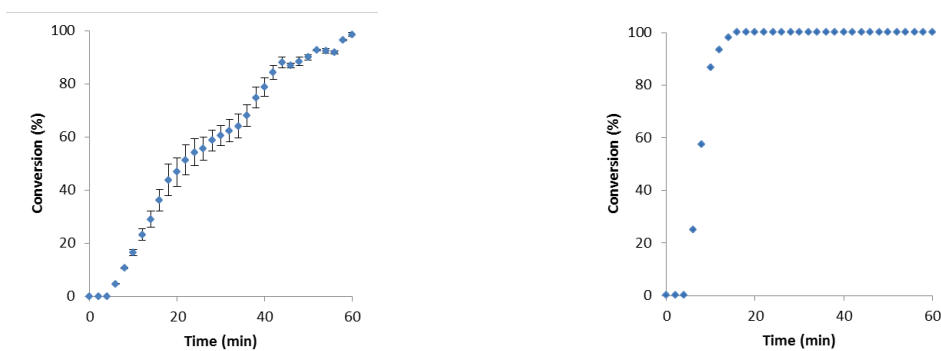
In order to further investigate the origins of this observed chemoselectivity, the kinetic profiles of the reactions were monitored by ^1H NMR over a 1 h time course. The benzyl protons from both the azide starting material and the product provided a

useful handle for analysis; conversion was measured against an internal standard at two minute intervals (Scheme 117).

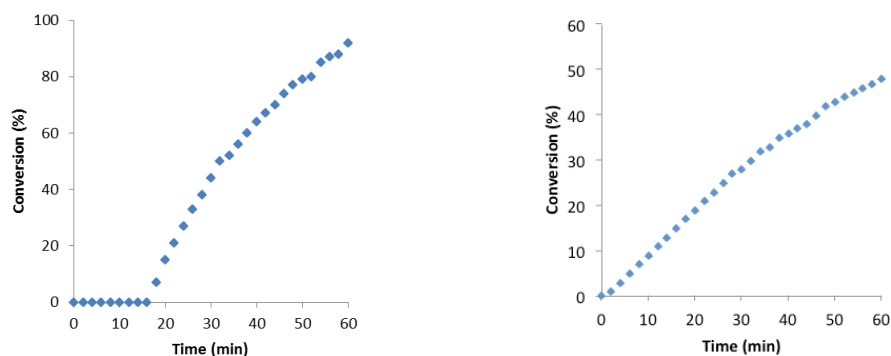


Scheme 117: Representative reaction used for kinetic experiments, and their products.

Initial observations of the kinetic profiles was immediately surprising, based on the data from the competition experiments we expected to see an increase in rate that was consonant with the chemoselectivity profiles. However, the initial rate measurements did not follow the expected trend. Based on extracted k_{obs} , propiolamide **2.34** was fastest with an initial rate of $2.4 \times 10^{-4} \text{ M}^{-1} \text{ s}^{-1}$. Ynamine **2.84** was the next fastest ($5.5 \times 10^{-5} \text{ M}^{-1} \text{ s}^{-1}$) followed closely by ynamide **2.83** ($5.1 \times 10^{-5} \text{ M}^{-1} \text{ s}^{-1}$) (Graph 4).

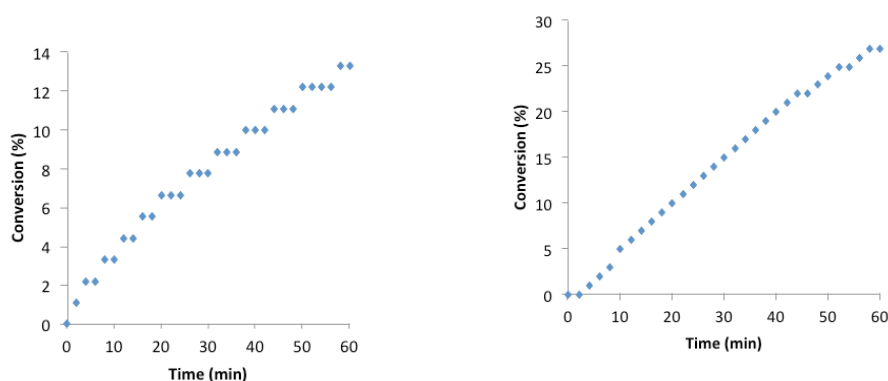


Graph 4: Kinetic profiles for alkynes **2.84** (left) and **2.34** (right). Error bars from $N=3$ data shown for **2.84**. Conversion refers to formation of desired triazole product.



Graph 5: Kinetic profiles from alkynes 2.83 (left) and 2.82 (right). Conversion refers to formation of desired triazole product.

The reaction of propargyl alkyne, aryl alkyne and alkyl alkyne all required the presence of NaAsc to induce initiation of the reaction within the time course. In the presence of NaAsc, propargyl alkyne displayed an initial rate of $4.1 \times 10^{-5} \text{ M}^{-1} \text{ s}^{-1}$, aryl alkyne reacted at $0.3 \times 10^{-5} \text{ M}^{-1} \text{ s}^{-1}$ and alkyl alkyne at $1 \times 10^{-5} \text{ M}^{-1} \text{ s}^{-1}$ (Graphs 4-6).



Graph 6: Kinetic profiles for alkynes 2.38 (left) and 2.81 (right). Conversion refers to formation of desired triazole product.

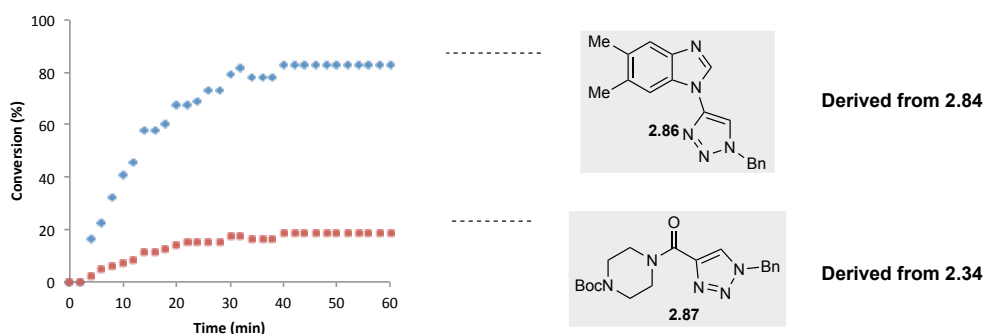
Under the reaction conditions, all six alkynes displayed induction periods. For alkynes **2.84**, **2.34** and **2.83** this was relatively short at ca. < 5 min for **2.84** and **2.34**, and 16 min for ynamide **2.83**. However, for the remaining three alkyne chemotypes the induction periods were significantly extended, with no reaction even after > 1 h. This can be attributed to the requirement for oxidative homocoupling to produce the active Cu(I) catalyst, which is clearly much faster for alkynes **2.84**, **2.34** and **2.83**.

This kinetic data is consistent with only some of the data derived from the competition experiments. Propiolamide, which has the highest rate of reaction, is also chemoselective versus all alkynes except ynamine **2.84**. Ynamide **2.83** is chemoselective versus aryl and alkyl alkynes and only moderately selective in

competition with propargyl system **2.82**. This is consistent with the rate data extracted from the kinetic profiles, as there is a significant difference in rate between **2.83** and **2.38/2.81** but the small difference between propargyl alkyne **2.82** and ynamide **2.83** only allows for moderate selectivity to be observed. Propargyl alkyne **2.82** is chemoselective in competition with aryl and alkyl alkynes (**2.81**, **2.38**), which is consistent with the rate data extracted.

Aryl alkyne **2.38** displays a slower rate of reaction than alkyl alkyne **2.81** in isolation but is chemoselective in competition. This difference is due to the addition of NaAsc as a promoter; while aryl alkyne reacts slowly under the standard reaction conditions alkyl alkyne **2.81** is completely unreactive without the addition of NaAsc.

The key differences come when the rate of ynamine **2.84** is considered. In competition, ynamine outcompetes propiolamide by 8:1, however in isolation the rate of reaction is less than half than **2.34** (Graph 7).

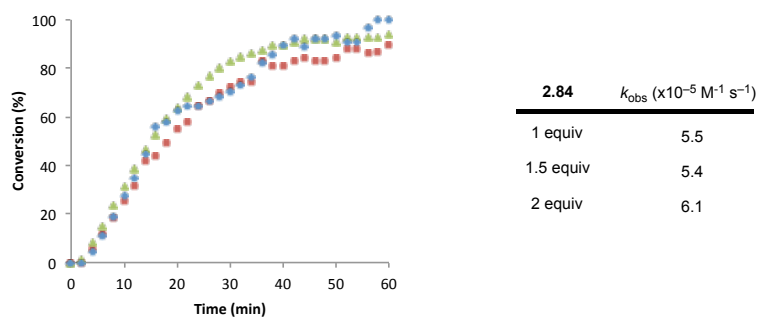


Graph 7: Reaction profile for competition reaction of 2.84/2.34 with BnN₃. Product 2.86 corresponding to 2.84 shown as blue diamonds, product 2.87 corresponding to 2.34 as red squares. Conversion refers to formation of desired triazole product.

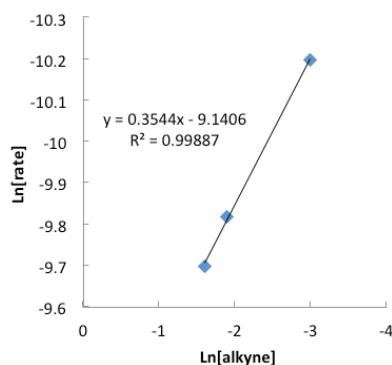
In addition, the rate of ynamide **2.83** is similar to ynamine **2.84**, but displays a longer initiation time. In competition, initiation time cannot be considered, as upon generation of Cu(I) by the ynamine in ca. 5 min, this would presumably accelerate the reaction of both alkynes.

These data suggest that selectivity is not purely contingent on the overall rate of the reaction, indicating a different origin for the observed chemoselectivity profiles of ynamine **2.84**.

In order to further explore the mechanism of the ynamine CuAAC reaction, the dependence on both azide and alkyne were probed to determine the rate-determining step in the reaction. Data reported previously by both Finn and Fokin, and Zhu showed that under their conditions Cu-acetylide formation is the RDS. In those cases the reaction had a positive dependency on the alkynyl component but a zero order dependency (or a slight negative dependency) on the azide component^[141,158].

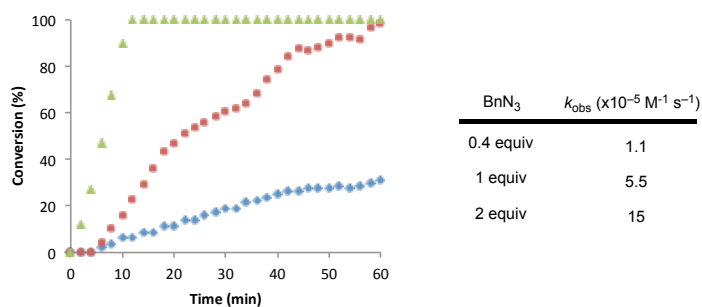


Graph 8: Variation of [2.84] in reaction with $\text{Cu}(\text{OAc})_2$ and BnN_3 . Conversion refers to formation of desired triazole product.

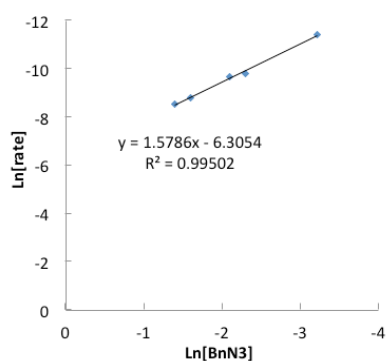


Graph 9: Calculation of order in [2.84].

Further kinetic experiments showed that the reaction rate was largely independent of [2.84] but showed a significant dependency on $[\text{BnN}_3]$ with kinetic order of 1.6 (Graphs 8-11).



Graph 10: Variation of [BnN₃] in reaction with 2.84 and Cu(OAc)₂. Conversion refers to formation of desired triazole product.

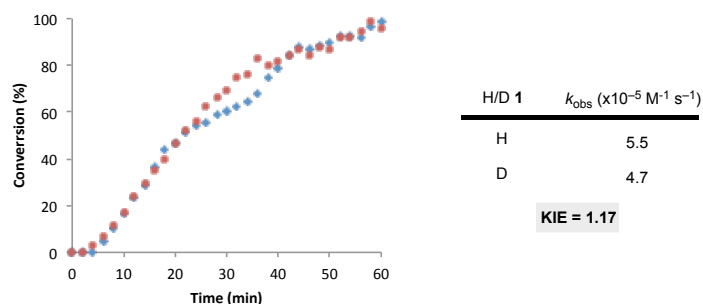


Graph 11: Calculation of order in [BnN₃].

These data suggest that the RDS of the CuAAC reaction with alkyne **2.84** is azide ligation/insertion rather than Cu-acetylide formation.

To further probe the RDS, a series of deuterium kinetic isotope effect experiments were carried out. Deuteration of ynamine, propiolamide and ynamide was performed simply by stirring the alkynes with K₂CO₃ and D₂O to provide the enriched products with high levels of ²D incorporation.

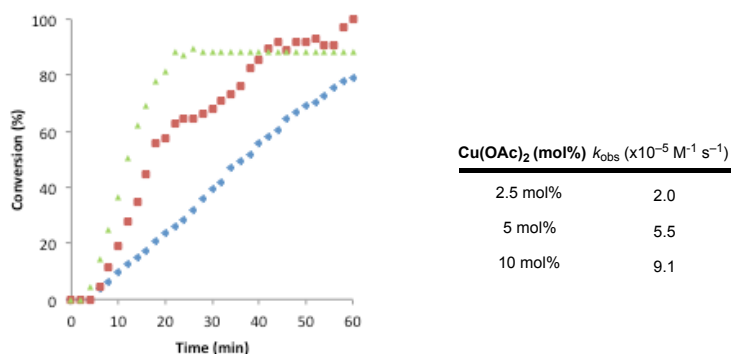
In similar experiments using an aryl alkyne, Zhu observed a significant primary KIE of 2.3, in addition to a significant increase in initiation time. In contrast to this, Ynamine did not display a primary KIE (1.17), which supports a switch in RDS, away from Cu-acetylide formation (Graph 12).



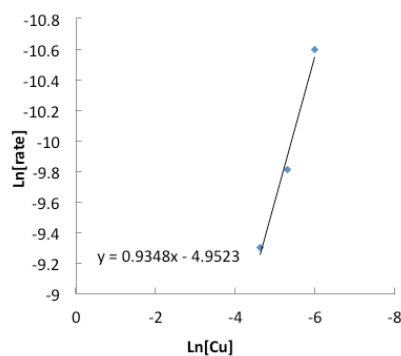
Graph 12: KIE experiment for 2.84. Deuterated 2.84 shown as red squares, standard 2.84 shown as blue diamonds. Conversion refers to formation of desired triazole product.

Both ynamide and propiolamide both displayed a primary KIE of 1.57 and 2.66 respectively, consistent with previous reports.

The effect of $[\text{Cu}(\text{OAc})_2]$ was interrogated next. While under catalytic conditions Fokin and Finn had reported a second order dependence on $[\text{Cu}]$, this was not observed using ynamine **2.84**. Instead, a first order dependence was observed, suggesting a mechanism based upon a mono copper intermediate (Graphs 13-14).



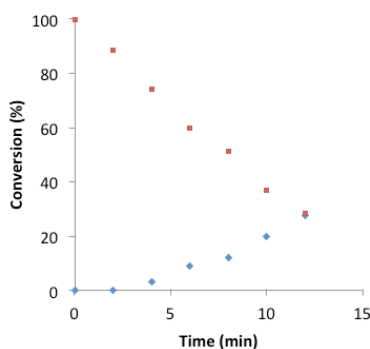
Graph 13: Variation of $[\text{Cu}(\text{OAc})_2]$ in reaction with **2.84 and **2.85**. Conversion refers to formation of desired triazole product.**



Graph 14: Calculation of order in $[\text{Cu}(\text{OAc})_2]$.

These experiments can assist in the explanation of the discrepancy between the overall rate and the chemoselectivity. If Cu-acetylide formation were the product-determining step then acceleration of this step would have a positive impact on the selectivity. In addition, based upon the work of Bertrand, if a mono-copper pathway is operative then the azide ligation step would be comparatively slow, which could account for the slower overall rate in comparison to Cu-acetylide formation.

Further examination of the kinetic profile of ynamine **2.84** allowed for the extraction of the rate of Cu-acetylide formation. This was measured *via* the disappearance of the acetylenic proton of the ynamine, which arises from formation of the acetylide and subsequent deuteration by D₂O. Upon analysis of this data, it was immediately obvious that the Cu-acetylide formation is significantly faster than the overall reaction ($1 \times 10^{-4} \text{ M}^{-1} \text{ s}^{-1}$ for Cu-acetylide formation vs. $5.5 \times 10^{-5} \text{ M}^{-1} \text{ s}^{-1}$ for the overall reaction, Graph 15).



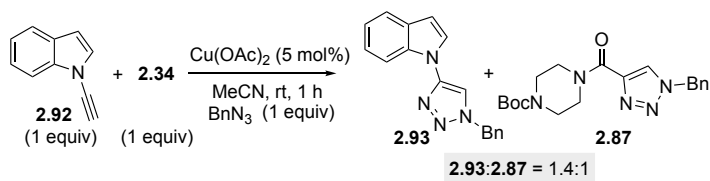
Graph 15: Comparison of the rate of formation of Cu-acetylide versus product. Conversion refers to consumption of ynamine acetylenic proton (red squares) and formation of the desired triazole product (blue diamonds).

This data suggests that the Cu-acetylide formation is both rapid and reversible, as the decrease in concentration of the acetylenic proton is greater than the amount of copper present in the reaction. In addition, while the rate of Cu-acetylide formation is rapid, it is still lower than the rate of reaction for propiolamide **2.34**. This discrepancy can be accounted through various means. The rate measured for the Cu-acetylide formation is, in reality, the combination of Cu-acetylide formation and deuteration of the alkyne, minus the rate of protonation of the alkyne from residual water present. While protonation/deuteration of the acetylide is likely a rapid process, this equilibrium does not allow for the measurement of the true rate of acetylide formation. This equilibrium is also supported by evidence generated by a co-worker in the group that has shown that water has an inhibitory effect on the reaction rate. This is presumably because the equilibrium concentration of acetylide is higher at lower concentrations of water. Finally, it is conceivable that chemoselectivity is not influenced purely by the rate of the product-determining step, but another mechanistic effect, such as a beneficial complexation between ynamine **2.84** with Cu, *vide infra*.

At this juncture, it was clear that the RDS of the ynamine CuAAC reaction is the azide ligation/migratory insertion step, and that a rapid Cu-acetylide step formation provides high levels of chemoselectivity. However, it was still unclear why ynamine **2.84** provided such remarkable selectivity compared to the structurally similar ynamide **2.83**.

We hypothesised that the pK_a of the ynamine could be modulated through a Lewis acid-Lewis base interaction with the $\text{Cu}(\text{OAc})_2$. A number of control experiments were designed to interrogate this theory.

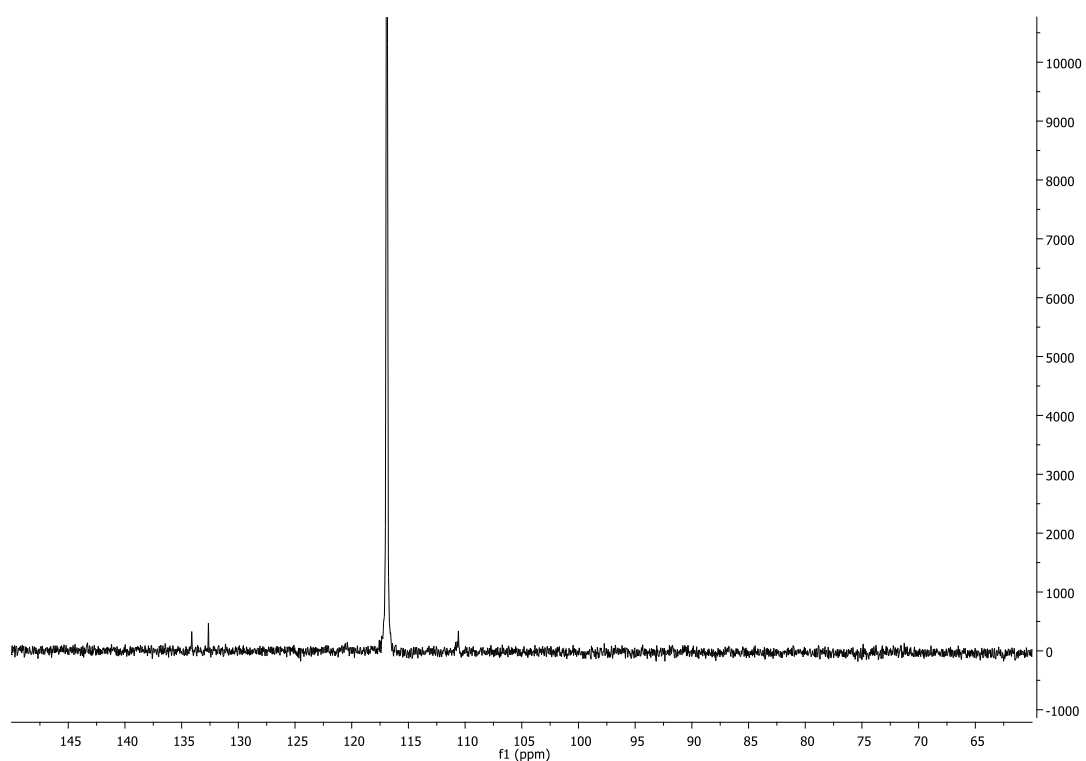
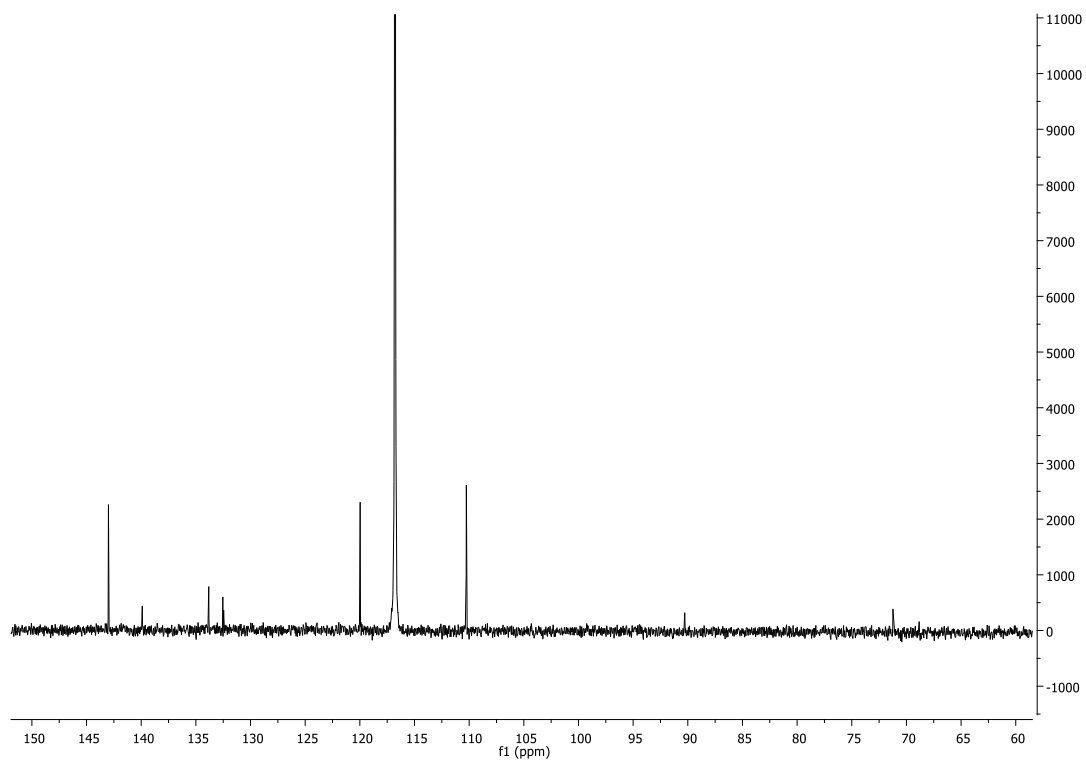
Firstly, indole ynamine **2.92** was prepared to access the role of the N3 of the benzimidazole. Kinetic analysis of the indole ynamine CuAAC revealed an identical rate as the benzimidazole variant. However, in competition with propiolamide **2.34** chemoselectivity was negligible with only a 1.4:1 preference for indole ynamine product **2.93**. This experiment demonstrated the importance of the N3 of the benzimidazole for chemoselectivity (Scheme 118).



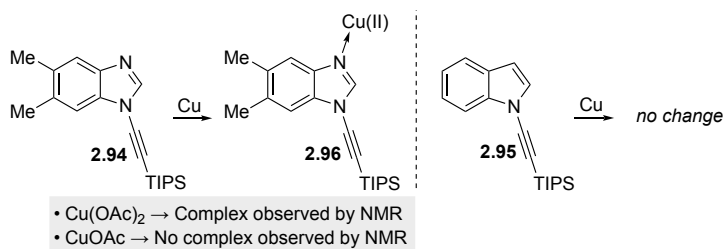
Scheme 118: Competition reaction between 2.92 and 2.34.

NMR analysis was used to aid in the determination the role of the benzimidazole N3. Samples of TIPS protected benzimidazole (**2.94**) and indole ynamines (**2.95**) were treated with both $\text{Cu}(\text{OAc})_2$ and CuOAc in $\text{MeCN-}d^3$ to look for any evidence of an interaction at N3. TIPS protecting groups on the alkynes were used to prevent the formation of a Cu-acetylide species. ^{13}C NMR analysis of the resulting solutions revealed that the combination of benzimidazole ynamine and $\text{Cu}(\text{OAc})_2$ was singularly effective at generating a complex, as evidenced by the disappearance of a number of the aromatic signals, and movement of others. The other three solutions all showed a clean ^{13}C spectrum, consistent with the starting materials. This simple experiment demonstrated that the N3 promoted a strong interaction with copper, and that N1 did not. In addition, only the $\text{Cu}(\text{II})$ precatalyst formed a complex (**2.96**) with the benzimidazole. While this is not unexpected, as $\text{Cu}(\text{II})$ is Lewis acidic, if this

interaction is catalytically relevant then some of the pre-catalyst must be present throughout the reaction (Scheme 119, Spectra 1).

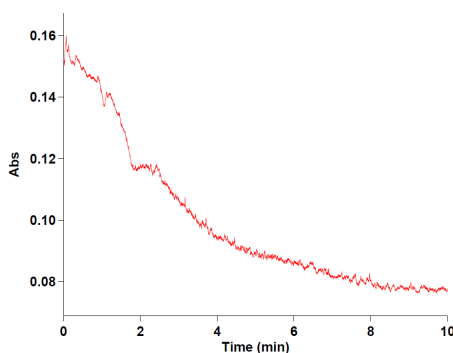


Spectra 1: ¹³C spectra of 2.94(Above). ¹³C Spectra of 2.94 upon addition of Cu(OAc)₂.



Scheme 119: Reaction of protected ynamines with Cu salts.

In order to probe whether Cu(II) persists throughout the reaction course UV/Vis spectroscopic analysis was used. Measurement of the absorption at 690 nm over the first ten minutes of the reaction gave a qualitative look at the concentration of Cu(II) left in the reaction mixture. A rapid decrease in the concentration over the initial 2-4 minutes corresponds to the initiation time observed by ¹H NMR. At this point the absorption levelled out at half the original value, demonstrating that Cu(II) is present throughout the course of the reaction (Graph 16).



Graph 16: Absorption spectra of the reaction of 2.84 with BnN₃ with Cu(OAc)₂ in MeCN over 10 minutes at 690 nm. Curve shows a decrease in absorption over time as Cu(II) is reduced.

In addition to the spectroscopic evidence presented above, HRMS experiments were undertaken to support an interaction between Cu(II) and the benzimidazole N3. TIPS protected benzimidazole **2.94** and indole ynamines **2.95** and were stirred with Cu(OAc)₂ and analysed by HRMS. While only starting materials were observed in the reaction with indole ynamine, dimeric Cu-benzimidazole species **2.97** was detected in the reaction of TIPS benzimidazole ynamine with Cu(OAc)₂ (Figure 26).

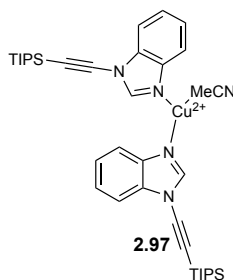
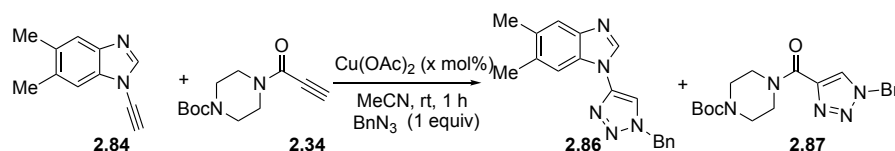


Figure 26: Dimeric copper complex observed by HRMS.

This dimeric complex with an MeCN ligand supports the presence of a favourable complexation between N3 and Cu(II) in the reaction mixture. A Lewis acid interaction of this type could lower the pK_a of the ynamine acetylenic proton through an inductive electron-withdrawing effect and therefore accelerate Cu-acetylide formation. Additionally, a Cu-chelation at N3 could increase chemoselectivity purely based on proximity. A strong interaction at N3 could sequester the Cu-catalyst, allowing movement of the catalyst within the immediate vicinity (solvent cage effects) and therefore providing chemoselectivity. However, while this scenario remains a possibility, chemoselectivity in this case would decrease upon an increase in [Cu(OAc)₂] which was not observed (Table 10).

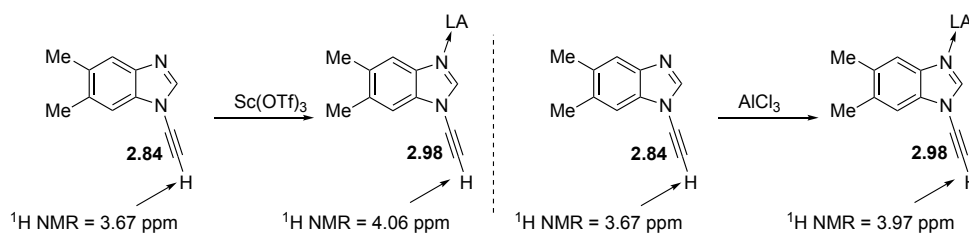
Table 10: Comparison of chemoselectivity with increasing [Cu(OAc)₂].



Entry	Cu(OAc) ₂ (mol%)	2.86/2.87
1	5	87:13
2	10	91:9
3	25	91:9
4	50	95:5
5	75	91:5
6	100	88:12

^aDetermined by ¹H NMR

To assess the effect of Lewis acids on the pK_a of benzimidazole ynamine **2.84**, we looked for changes in the ¹H NMR shift of the acetylenic proton upon exposure to a range of Lewis acids. While not a perfect measure of pK_a, a downfield shift in an acidic proton can be indicative of an increase in acidity.^[167] A downfield shift such as this is more commonly used to measure the protonation of an amine *via* pH NMR titration but in this case provided qualitative support for our hypothesis. Treatment of **2.84** with either Sc(OTf)₃ or AlCl₃ yielded a significant downfield shift of the acetylenic proton. Sc(OTf)₃ had the most pronounced effect with a shift of 0.39 ppm, while AlCl₃ provided a downfield shift of 0.3 ppm (Scheme 120). TiCl₄ was also tested but degraded the ynamine starting material upon exposure.



Scheme 120: Effect of Lewis acids of the acetylinic proton of benzimidazole ynamine 2.84.

While copper Lewis acids could not be tested due to rapid acetylide formation, the above data suggests that catalytic amounts of a copper Lewis acid could accelerate Cu-acetylide formation by lowering the pK_a of the acetylene proton.

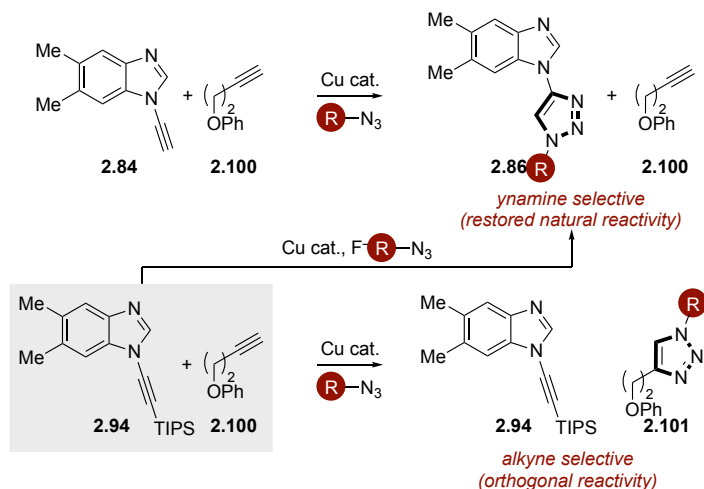
The pK_a of the benzimidazole ynamine was measured by NMR titration with phosphazene bases. Use of BEMP and BTTP allowed for a pK_a of 27.9 (MeCN) to be calculated for **2.84** and a pK_a of 28.8 (MeCN) for indole ynamine **2.92**. This small difference in pK_a between **2.84** and **2.92** demonstrates the importance of the inductive contribution of the N3 nitrogen of the benzimidazole. By extension, a Lewis acid interaction at the N3 position would increase the inductive electron withdrawing effect, decreasing the pK_a further.

2.4.2 Overturning Protecting Group Strategies in the CuAAC Reaction: Chemoselective CuAAC Reactions of Protected Aromatic Ynamines

Based on previous work in the Watson and Burley groups describing sequential ligation strategies and the unprecedented levels of alkyne chemoselectivity, we aimed to develop a truly orthogonal sequential CuAAC platform. As previously discussed, alkyne chemoselectivity has remained uni-directional, with use of protecting groups being the most common method employed. While this allows for reliable selectivity, the order of reaction has to be determined at inception with little opportunity for late stage diversification. Based on this, we sought to harness the selectivity afforded from aromatic ynamines to overturn conventional protecting group strategies.

We aimed to take protected ynamines and perform orthogonal CuAAC reactions with aliphatic alkynes. Based upon previous work in the literature, using conventional CuAAC conditions, unprotected alkynes react with complete selectivity in the presence of protected alkynes. More challenging is a selective CuAAC

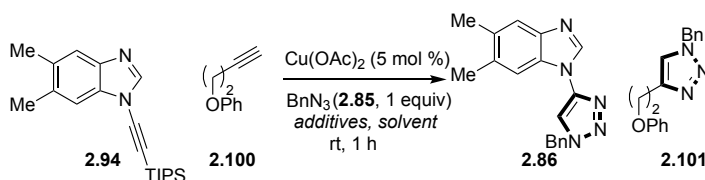
reaction of the protected alkyne before engagement of the unprotected alkyne. A combination of these two reactions would provide a bidirectional strategy for the control of sequential CuAAC reactions based upon control of the reaction conditions (Scheme 121).



Scheme 121: Design plan for orthogonal CuAAC reaction.

We began our investigation through the reaction of TIPS protected ynamine **2.94**, representative aliphatic alkyne **2.100** and BnN_3 **2.101**. As expected, exposure to standard CuAAC conditions provided complete selectivity for unprotected alkyne triazole product **2.101** in quantitative yield and without any degradation of **2.94** (Table 11).

Table 11: Optimisation of orthogonal CuAAC protocol.



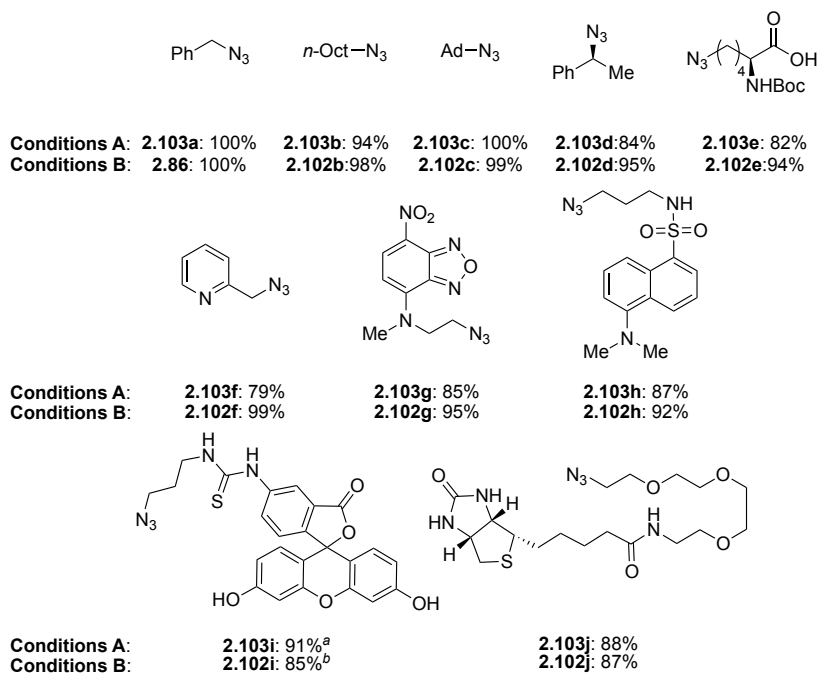
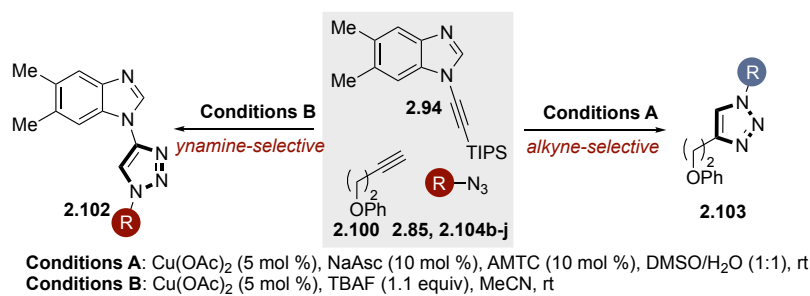
Entry	reaction conditions	2.86/2.101 %
1	NaAsc, AMTC, DMSO/H ₂ O (1:1)	0:100
2	NaAsc, AMTC, TBAF, DMSO/H ₂ O (1:1)	20:80
3	NaAsc, AMTC, TBAF, MeOH/H ₂ O (1:1)	47:53
4	NaAsc, AMTC, PS-F, DMSO/H ₂ O (1:1)	15:85
5	NaAsc, THPTA, TBAF, DMSO/H ₂ O (1:1)	43:57
6	NaAsc, THPTA, PS-F, DMSO/H ₂ O (1:1)	63:37
7	PS-F, DMSO	35:65
8	TBAF, DMSO	47:53

9	TBAF, MeOH	16:84
10	TBAF, MeCN	100:0

^aDetermined by HPLC against a caffeine internal standard. See Experimental section for further details. Performed by MZCH.

We then aimed to restore chemoselectivity for ynamine triazole product **2.86** through addition of TBAF or polymer-supported fluoride (PS-F) a source of F⁻. Direct addition of either fluoride source to systems containing NaAsc as a reductant and Cu(I) stabilising ligands such as (1-(trans-2-hydroxycyclohexyl)-4-(*N,N*-dimethylaminomethyl)-1,2,3-triazole (AMTC) or tris(3-hydroxypropyltriazolylmethyl)amine (THPTA) in a range of solvent systems led to mixtures of products (entries 2-6). Removal of these additives and a short solvent study revealed MeCN as the optimum solvent, providing complete selectivity for the ynamine CuAAC product.

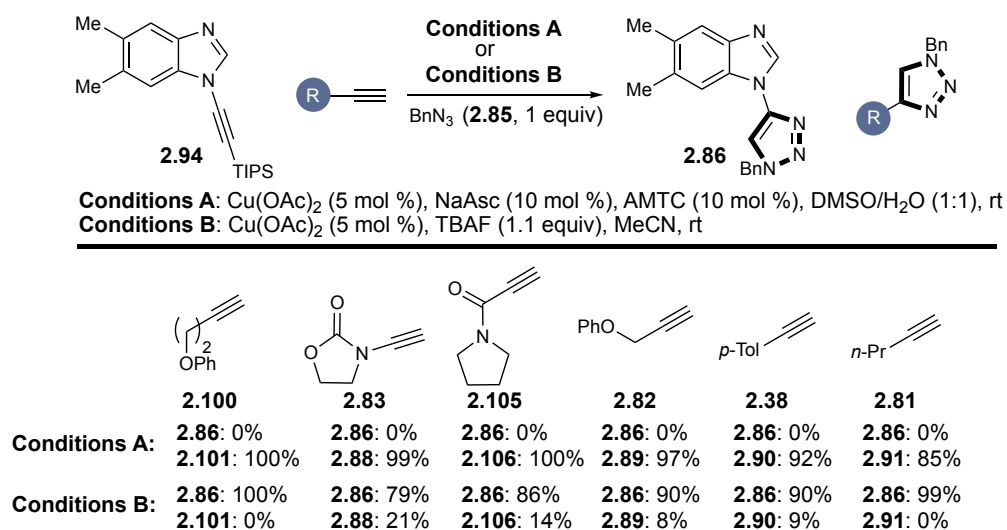
Use of a Cu(II) pre-catalyst without NaAsc was key for chemoselective control. Based on previous work, **2.84** (produced via deprotection of **2.94**) will reduce Cu(II) to Cu(I) via homocoupling of the alkyne (Glaser coupling), however, aliphatic alkyne **2.100** undergoes Glaser coupling extremely slowly. This provides a window for the deprotection step to proceed before any Cu(I) is present in the reaction mixture. Removal of any Cu(I) stabilising ligands also improved selectivity; this can be attributed to the positive effect of Cu(II) salts in the reaction mixture. We have shown that Cu(II) may act as a Lewis acid, accelerating the product-determining Cu-acetylide formation step of the ynamine CuAAC reaction.



Scheme 122: Selective orthogonal CuAAC reactions of 2.94 or 2.100 with a variety of azides using conditions A or B. Isolated yields. Performed by MZCH.

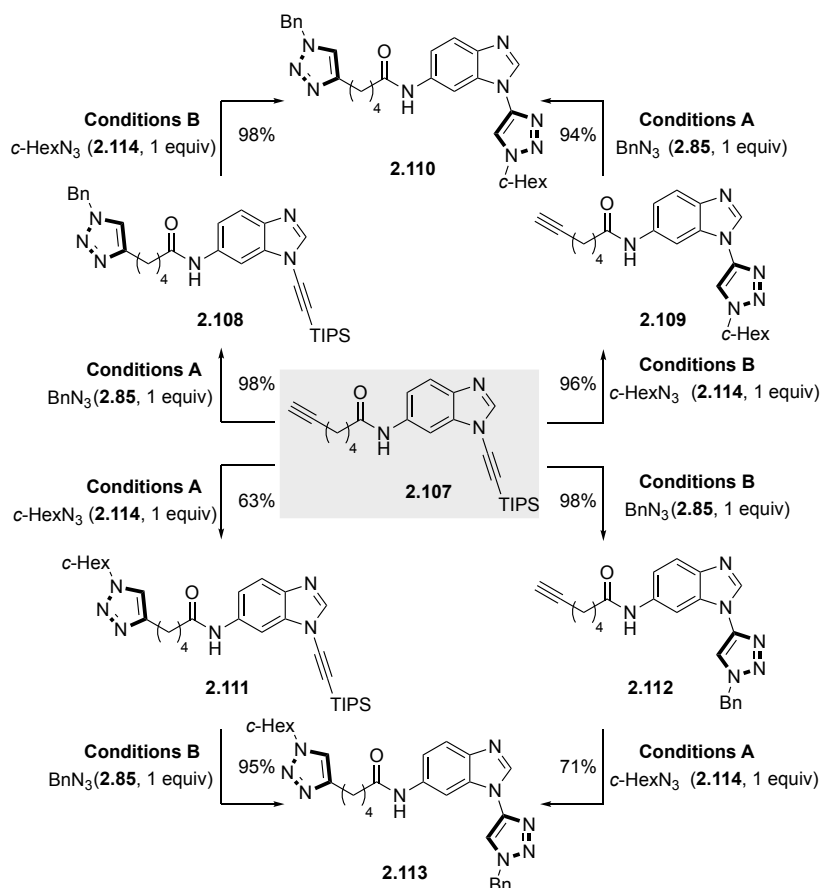
The scope of the optimum conditions for both aliphatic alkyne and ynamine CuAAC products was then probed (Scheme 122). Reaction with a set of diverse and highly functionalised azide partners delivered high yields and selectivities for both alkyne and ynamine products. The conversions and selectivities were retained regardless of the steric or electronic demand of the azides. In addition, a number of azides with direct relevance to chemical biology were tolerated; such as the dyes and fluorophores **2.104g-i** and biotinylated azide **2.104j**. Following this, we investigated the scope of the reaction with respect to the competing alkyne component. We took five alkynes representing different electronic classes to provide a representative slice of the literature, ynamide **2.83**, propiolamide **2.105**, propargyl alkyne **2.82**, aryl alkyne **2.38**, and alkyl alkyne **2.81**. Pleasingly, all alkynes were tolerated in the alkyne selective protocol and all provided good selectivity under the ynamine selective conditions. When using more activated alkynes some of the undesired product was formed under the reaction conditions; this was consistent with previous

work and in most cases the selectivity remained >9:1 in favour of the ynamine CuAAC product (Scheme 123).



Scheme 123: Competition reactions of **2.94** with a range of alkynes using conditions A or B. Isolated yields.

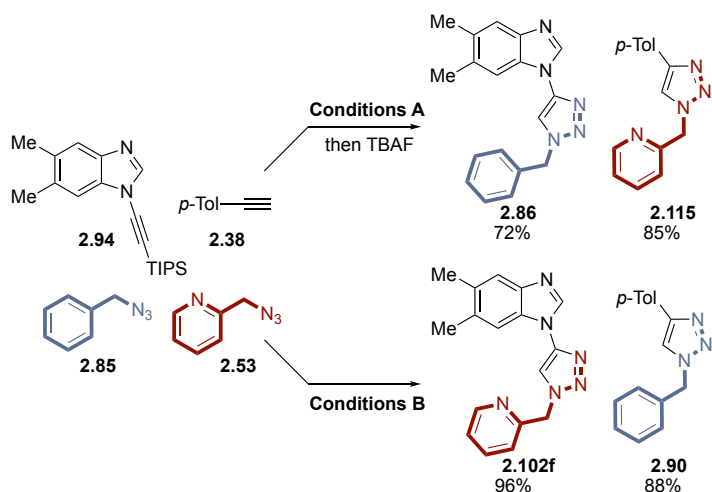
This orthogonal reactivity was next explored in an intramolecular sense through the use of mono-protected diyne **2.107**. Exposure of **2.107** to conditions A led to complete conversion of the unprotected alkyne triazole product **2.108**, this compound could then be reacted under conditions B to give bis-triazole **2.110** in good yield over two steps. The order of reaction could be reversed, with selective CuAAC on the protected ynamine using conditions B giving **2.112** before subsequent reaction of aliphatic alkyne to give the regioisomeric product **2.113** while still maintaining high yields across both steps. In addition, the selectivity was shown not to be dependent on the azide component as the opposite regioisomers could be effectively synthesised by switching the order of addition of the two azide coupling partners (Scheme 124).



Scheme 124: Orthogonal CuAAC reactions of diyne scaffold 2.107. Performed by MZCH.

This intramolecular experiment demonstrates the excellent levels of selectivity that can be achieved across this orthogonal reaction template and establishes a viable platform for sequential ligation of multifunctional molecules.

Finally, we investigated whether the alkyne selectivity developed throughout this study could be married with Zhu's azide chemoselective protocol^[156] to deliver two selective CuAAC reactions in one pot. We anticipated that use of chelating azide **2.53** would provide high levels of azide selectivity over benzyl azide **2.85**.



Scheme 125: Dual orthogonal CuAAC reaction by exploiting alkyne and azide chemoselectivities.

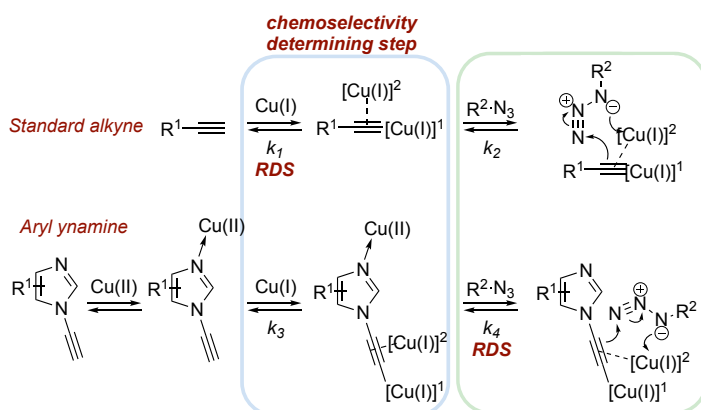
The dual-CuAAC reaction was first performed under conditions A, coupling the more active picolinyl azide **2.53** with the unprotected tolyl acetylene **2.38** to selectively form triazole **2.115**. Addition of TBAF to release the free ynamine **2.84** delivered the second triazole product **2.86** in good yield and high selectivity.

Alternatively, using conditions B the ynamine undergoes a rapid deprotection followed by a selective CuAAC reaction with chelating azide **2.54** to provide triazole **2.102f**. This is followed by the union of the remaining alkyne **2.38** and azide **2.85** components to give the second triazole product **2.90**.

2.5 Conclusions

We have demonstrated that aromatic ynamine **2.84** undergoes chemoselective CuAAC reactions versus a range of other alkynes including the highly reactive propiolamide **2.34**. A series of competition experiments has allowed for the generation of an alkyne reactivity scale that can be used for sequential CuAAC reactions. Investigation into the source of the selectivity led to the discovery that selectivity is not based purely on the rate of the reaction. In fact, ynamine was shown to be chemoselective versus alkynes with a faster overall rate.

A kinetic investigation into this phenomenon showed that the RDS of the ynamine CuAAC reaction is azide ligation/insertion rather than the more commonly reported Cu-acetylide formation. Further mechanistic studies ascertained that a Lewis acid/Lewis Base interaction between the Cu(II) pre-catalyst may lower the pK_a of the acetylinic proton and subsequently increase the rate of Cu-acetylide formation, the product-determining step in the reaction (Scheme 126).



Scheme 126: Summary of chemoselectivity-determining and rate-determining events for standard alkynes and aryl ynamines.

We propose that the comparatively slow azide ligation step arises from the inherent electronics of the ynamine. The highly electron-rich alkyne will render the Cu atom bound to the π -system comparatively less electrophilic than an electron poor alkyne e.g. (Scheme 127, **2.84**) resulting in a lower rate of azide ligation/insertion.



Scheme 127: Rationale for comparatively slow azide ligation event of aryl ynamine **2.84**.

In a broader sense, this study has demonstrated that selectivity in catalysis is not based on rate alone and that other factors may be involved. In addition, taken together with previous mechanistic reports, we show that the RDS of the CuAAC reaction is not set and may change based on conditions and alkyne class.

Following on from this, we have developed a conditional strategy for orthogonal control in the CuAAC reaction. Use of a silyl protecting group on a highly active ynamine allows a rapid deprotection-CuAAC reaction to be performed before a competing alkyne can react. This strategy is contingent on the reaction conditions; deprotection of the ynamine must be rapid and the competing CuAAC must be sufficiently slow for high levels of selectivity. This can be influenced by solvent and additive selection.

The orthogonal method proved to be robust, tolerating a number of azides and alkynes commonly used in bioconjugation. In addition, the conditions were amenable to an intramolecular sequential ligation strategy; dual functionalization of a bifunctional diyne was shown to work effectively, with initial CuAAC occurring at either alkyne depending on the conditions used. Finally, the method could be combined with azide chemoselectivity to perform two chemoselective CuAAC reactions in one pot with no intervention.

This application of the alkyne chemoselectivity previously developed within the group can provide a more flexible method for sequential functionalization in both chemical biology and materials chemistry.

2.6 Future work

After these original communications, there are two clear avenues of research that should be undertaken to better understand the reactivity of ynamines in CuAAC.

Firstly, the reactivity of ynamines in general should be investigated. The kinetics of the benzimidazole ynamine have been investigated; however a broad range of aromatic ynamines have been synthesised and should be assessed for their competency in the CuAAC reaction, both alone, and in competition (Figure 27). In addition, kinetic analysis should be performed through another medium to confirm the results generated by NMR. Preliminary results within the group have shown FTIR to be a competent method for kinetic analysis of this reaction.

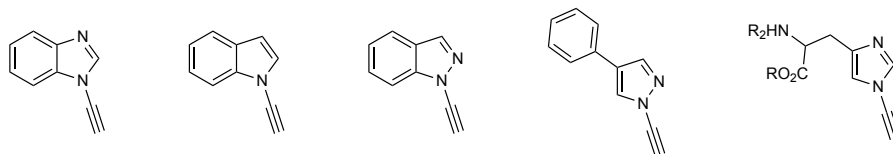


Figure 27: Range of ynamines that could be investigated.

This can be extended to ynamides, which have been underused as substrates for CuAAC but may possess mechanistic similarities. Ynamides are generally more accessible and their electronics can be more readily tuned, making them attractive substrates for investigation (Figure 28).

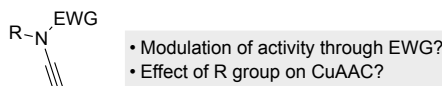


Figure 28: Ynamides present interesting opportunities for mechanistic investigation.

In addition, stoichiometric Cu-acetylide and dicopper species of ynamine should be synthesised and assessed for reactivity. CAAC ligated copper species could provide more evidence for why the azide ligation step is comparatively slow. This could be due to the electronics of the alkyne, but based on the first order dependence on $[\text{Cu}(\text{OAc})_2]$, this could also be attributed to a mono-copper pathway. Synthesis of the stoichiometric organocopper compounds could aid in unravelling this problem (Figure 29).

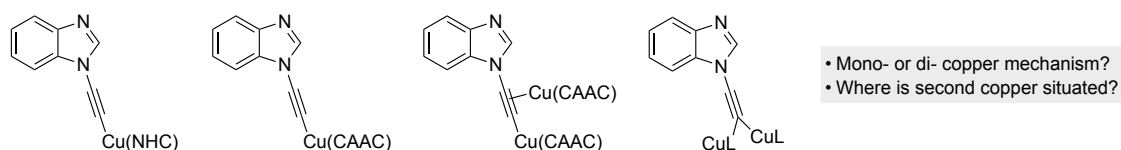


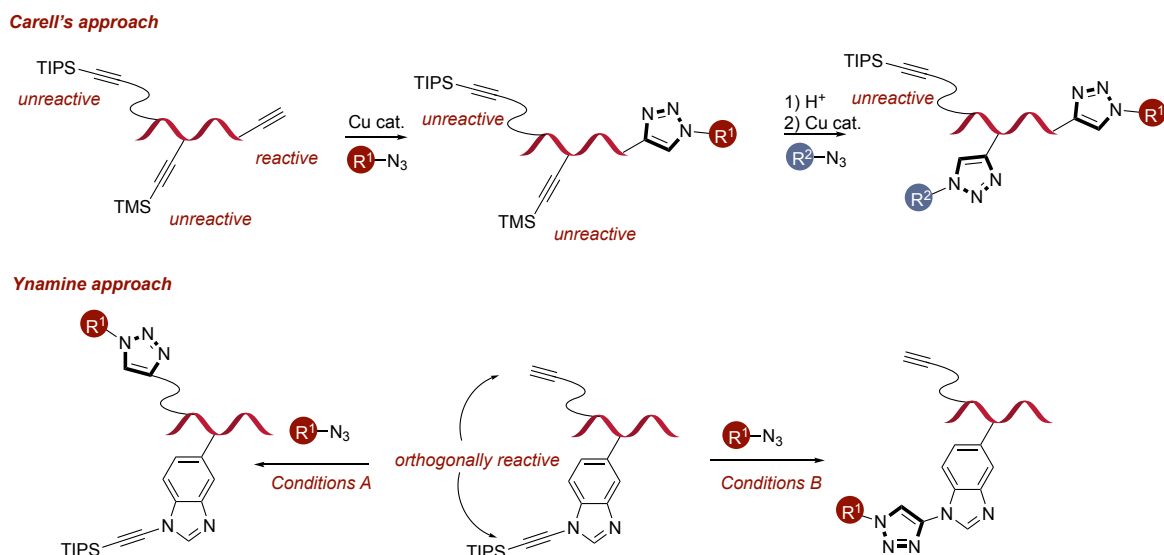
Figure 29: Synthesis of proposed complexes may provide further insight into the mechanism of ynamine CuAAC.

In order to aid chemical biologists in the development of multi-alkyne systems for sequential functionalisation, a body of data based on more classical ligand based systems should be assembled. Use of Cu(I) stabilising ligands is important for avoiding degradation in biological systems; it would be of great utility to develop a general chemoselectivity scale using these more active conditions, in a similar fashion to Finn. Incorporation of other rapid CuAAC substrates would be advantageous, such as SPAAC cyclic alkynes.

The second, more academic, source of future enquiry lies in better understanding the RDS of the CuAAC reaction. Alteration of the electronic properties of a wide-ranging set of alkynes, and analysis of their mechanism could help to unpick the factors that influence chemoselectivity and reactivity in a broader sense. While many mechanistic studies have looked at tailored catalyst systems in order to understand the role of copper in the reaction, the effect of altering the alkyne substrate remains undeveloped.

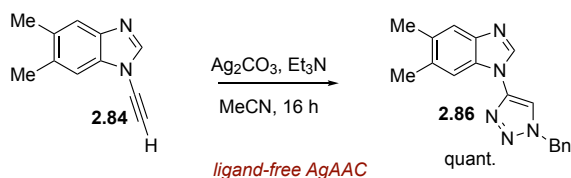
Application of the orthogonal approach described here towards the sequential functionalization of biomolecules would be a logical extension to the initial communication. In addition, this method could be applied towards the synthesis of multifunctional surfaces that can have applications in biomedical science.

When compared with the work of Carell, who demonstrated sequential ligation of labelled oligonucleotides, *vide supra*, the application of ynamines and protected ynamines could provide a significant advance in step economy and allow for a diversity-oriented functionalization (Scheme 128).



Scheme 128: Comparison of previous (Carell) and our approach towards sequential functionalization.

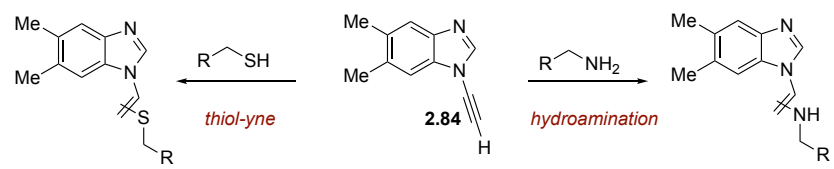
During this study it was shown that ynamine **2.84** is able to undergo a cycloaddition with BnN_3 that is catalysed by Ag_2CO_3 . While Ag-catalysed (3+2) cycloadditions (AgAAC) have been reported in the literature,^[168] the mild, ligandless conditions that are amenable with **2.84** would represent a significant advance. In terms of chemoselectivity, this would provide complete selectivity over standard alkynes based on catalyst selection (Scheme 129).



Scheme 129: First reported ligand-free, room temperature AgAAC reaction using **2.84.**

The high levels of reactivity displayed by aromatic ynamine **2.84** should also be further investigated using other metals. By performing high-throughput optimisation using a wide array of transition metal salts (e.g. Fe, Au), we hope to discover novel reactivity.

In addition to CuAAC and AgAAC, the ability of ynamines to react with other biomolecules commonly used for ligation (e.g. thiols or amines) would be a useful advance (Scheme 130). In particular, a conditional basis for selectivity between different ligation partners would provide users with a highly selective and flexible tool for bioconjugation.



Scheme 130: Amine and thiol ligation of 2.84.

2.7 Experimental

2.7.1 General

All reagents and solvents were obtained from commercial suppliers and were used without further purification unless otherwise stated. Purification was carried out according to standard laboratory methods.^[169] Compounds **2.34**^[151], **2.83**^[170], **2.94**,^[164] **2.100**,^[171] **2.104b**,^[172] **2.104d**,^[173] **2.104e**,^[174] **2.104g**,^[175] **2.104h**,^[176] **2.104i**,^[177] **2.104j**,^[178] **2.105**,^[179] **2.82**,^[180] **2.107**,^[166] and AMTC^[181] were prepared according to literature procedures.

2.7.2 Purification of Solvents

Dry solvents for reactions were either obtained from a PureSolv SPS-400-5 solvent purification system (THF) or *via* distillation over a suitable drying agent following the prescribed methods (1,4-dioxane, MeCN). These solvents were transferred to and stored in a septum-sealed oven-dried flask over previously activated 4 Å molecular sieves and purged with and stored under nitrogen. CH₂Cl₂, Et₂O, EtOAc, MeCN, and petroleum ether 40-60° for purification purposes were used as obtained from suppliers without further purification.

2.7.3 Experimental Details

Reactions were carried out using conventional glassware (preparation of intermediates) or in 5 mL or 20 mL microwave vials. The glassware was oven-dried (140 °C) and purged with N₂ before use. Purging refers to a vacuum/nitrogen-refilling procedure. Room temperature was generally 18 °C. Reactions were carried out at elevated temperatures using a temperature-regulated hotplate/stirrer.

2.7.4 Purification of Products

Thin layer chromatography was carried out using Merck silica plates coated with fluorescent indicator UV254. These were analyzed under 254 nm UV light or developed using potassium permanganate solution. Normal phase flash chromatography was carried out using ZEOprep 60 HYD 40-63 µm silica gel.

2.7.5 Analysis of Products

Fourier Transformed Infra-Red (FTIR) spectra were obtained on a Shimadzu IRAffinity-1 machine. ^{19}F NMR spectra were obtained on a Bruker AV 400 spectrometer at 376 MHz. ^1H and ^{13}C NMR spectra were obtained on a Bruker AV 400 at 400 MHz and 125 MHz, respectively. Chemical shifts are reported in ppm and coupling constants are reported in Hz with CDCl_3 referenced at 7.26 (^1H) and 77.0 ppm (^{13}C), MeCN-d_3 referenced at 2.05 (^1H) and 118.3 (^{13}C), DMSO-d_6 referenced at 2.50 ppm (^1H) and 39.52 ppm (^{13}C), and MeOD referenced at 3.31 ppm (^1H) and 49.0 ppm (^{13}C). High-resolution mass spectra were obtained through analysis at the EPSRC UK National Mass Spectrometry Facility at Swansea University or recorded on a Bruker maXis Impact TOF mass spectrometer, equipped with an ESI interface, over a mass range of 50–1000 Da, with a scan time of 1 s.

Reverse phase HPLC data was obtained on an Agilent 1200 series HPLC using a Machery-Nagel Nucleodur C18 column. Analysis was performed using a gradient method, eluting with 5–80% $\text{MeCN}/\text{H}_2\text{O}$ over 50 min at a flow rate of 1 mL/min. Samples for HPLC analysis were prepared through the removal of 30 μL of the reaction mixture in which 100 μL of EDTA solution (10 mg/mL) was added. The product was extracted with 100 μL of DCM. The organics were concentrated, and the product was dissolved in MeOH (1 mL). To 110 μL of this solution was added 5 μL of 2-bromopyrimidine solution (10 mg/mL in MeOH) for HPLC analysis. Note: Due to the high heteroatom count in specific products, ^{13}C NMR analysis was not possible due to issues with relaxation.

2.7.6 General Procedures

General Procedure 2A – Competition experiments

To a 10 mL microwave vial charged with alkyne **A** (0.1 mmol, 1 equiv), alkyne **B** (0.1 mmol, 1 equiv) and (azidomethyl)benzene (12.5 μL , 0.1 mmol, 1 equiv) was added MeCN (0.6 mL, 0.15 M) followed by $\text{Cu}(\text{OAc})_2$ (0.9 mg, 0.005 mmol, 5 mol%). The reaction was stirred at room temperature for 4 h before the addition of EDTA solution (20 mg/mL) and EtOAc (10 mL). The organics were separated and the aqueous layer extracted with a further 10 mL EtOAc. The combined organics were then dried and concentrated to provide a mixture of the crude products. The

crude residue was analyzed by NMR, with the product ratio taken from the ratio between the benzyl protons.

General Procedure 2B – Deuteration of alkynes

All novel deuterated alkynes were prepared according to the procedure of Bew *et al.*^[182]

A flame dried 10 mL round bottomed flask was charged with an alkyne (0.3 mmol, 1 equiv) and K₂CO₃ (4.5 mmol, 1.5 equiv) in MeCN (3 mL, 0.1 M). This was allowed to stir under an atmosphere of N₂ for 30 min. To this, D₂O (500 μL, 80 equiv) was added and left to stir for 1 h. The resulting crude reaction mixture was diluted with DCM (10 mL). The organic layer was separated and dried with MgSO₄, filtered, and solvent removed under reduced pressure to provide the deuterated product.

General procedure 2C

Kinetic NMR measurements were performed on either a Bruker AV 400 at 400 MHz or a Bruker DRX 500 at 500 MHz. Data sets were collected using a using a multi_zgvd pulse program with a fixed delay of 120 seconds over 60 min at 300 K. Each reaction was performed in MeCN-D₃. Cu(OAc)₂ was added as an 0.25 mM solution in D₂O, directly before the acquisition of the data set. Stock solutions of BnN₃ (63 μL/mL) and dinitrobenzene (42 mg/mL) in MeCN-D₃ were prepared. To a 1.5 mL vial was added alkyne (0.05 mmol, 1 equiv), BnN₃ solution (100 μL, 0.05 mmol, 1 equiv) and dinitrobenzene solution (100 μL, 0.025 mmol, 0.5 equiv). The mixture was diluted with MeCN (300 μL) before being transferred to an NMR tube. Cu(OAc)₂ solution (8 μL, 0.0025 mmol, 5 mol%) was added directly before acquisition. Conversion was measured as a comparison to the internal standard. Conversions were checked by isolation of the desired product. The rate of the reaction was obtained from the slope of the linear portion immediately after the induction period.

General procedure 2D

Kinetic NMR measurements were performed on either a Bruker AV 400 at 400 MHz or a Bruker DRX 500 at 500 MHz. Data sets were collected using a using a multi_zgvd pulse program with a fixed delay of 120 seconds over 60 min at 300 K. Each reaction was performed in MeCN-D₃. Cu(OAc)₂ was added as an 0.25 mM

solution in D₂O, directly before the acquisition of the data set. Stock solutions of BnN₃ (63 μL/mL) and dinitrobenzene (42 mg/mL) in MeCN-D₃ were prepared. To a 1.5 mL vial was added alkyne (0.05 mmol, 1 equiv), BnN₃ solution (100 μL, 0.05 mmol, 1 equiv) and dinitrobenzene solution (100 μL, 0.025 mmol, 0.5 equiv). The mixture was diluted with MeCN (300 μL) before being transferred to an NMR tube. NaAsc solution in water (10 μL, 100 mg/mL), was added to the tube followed by Cu(OAc)₂ solution (8 μL, 0.0025 mmol, 5 mol%) which was added directly before acquisition. Conversion was measured as a comparison to the internal standard. Conversions were checked by isolation of the desired product. The rate of the reaction was obtained from the slope of the linear portion immediately after the induction period.

General Procedure 2E –Formation of 2.86, 2.103b–j (Scheme 122).

To a solution of 5,6-dimethyl-1-((triisopropylsilyl)ethynyl)-1*H*-benzo[*d*]imidazole (45 mg, 0.14 mmol, 1 equiv), (but-3-yn-1-yloxy)benzene (20 mg, 0.14 mmol, 1 equiv), and azide 6a–j (0.14 mmol, 1 equiv) at rt in MeCN (1 mL) was added TBAF (49 μL, 0.15 mmol, 1.1 equiv) followed by Cu(OAc)₂ (1 mg, 0.007 mmol, 0.05 equiv). The reaction was stirred for 16 h, after which EtOAc (10 mL) was added. The mixture was washed with EDTA (10 mg/mL, 10 mL) and brine (2 × 10 mL), dried over Na₂SO₄, and concentrated under vacuum. The resulting residue was purified by flash chromatography (silica gel) to provide the desired compound.

General Procedure 2F –Formation of 2.103a–j (Scheme 122).

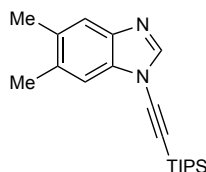
To a solution of 5,6-dimethyl-1-((triisopropylsilyl)ethynyl)-1*H*-benzo[*d*]imidazole (45 mg, 0.14 mmol, 1 equiv), (but-3-yn-1-yloxy)benzene (20 mg, 0.14 mmol, 1 equiv), and azide 5a–j (0.14 mmol, 1 equiv) at rt in DMSO/H₂O (1/1, 1 mL) was added AMTC (3 mg, 0.014 mmol, 0.1 equiv) followed by Cu(OAc)₂ (1 mg, 0.007 mmol, 0.05 equiv) and NaAsc (3 mg, 0.014 mmol, 0.1 equiv). The reaction was stirred for 16 h, after which EtOAc (10 mL) was added. The mixture was washed with EDTA (10 mg/mL, 10 mL) and brine (2 × 10 mL), dried over Na₂SO₄, and concentrated under vacuum. The resulting residue was purified by flash chromatography (silica gel) to provide the desired compound.

General Procedure 2G – Formation of 2.101, 2.88, 2.106, 2.89, 2.90, and 2.91 (Scheme 123).

To a solution of 5,6-dimethyl-1-((triisopropylsilyl)ethynyl)-1*H*-benzo[*d*]-imidazole (132 mg, 0.41 mmol, 1 equiv), alkyne (0.41 mmol, 1 equiv), and benzyl azide (53 μ L, 0.41 mmol, 1 equiv) at rt in DMSO/H₂O (1/1, 1 mL) was added AMTC (9 mg, 0.041 mmol, 0.1 equiv) followed by Cu(OAc)₂ (3 mg, 0.02 mmol, 0.05 equiv) and NaAsc (9 mg, 0.041 mmol, 0.1 equiv). The reaction was stirred for 16 h, after which EtOAc was added. The mixture was washed with EDTA (10 mg/mL, 10 mL) and brine (2 \times 10 mL), dried over Na₂SO₄, and concentrated under vacuum. The resulting residue was purified by flash chromatography (silica gel) to provide the desired compound.

2.7.7 Synthesis of Starting Materials.

5,6-Dimethyl-1-((triisopropylsilyl)ethynyl)-1*H*-benzo[*d*]imidazole, 2.94^[164]



An oven dried 20 mL microwave vial was charged with 5,6-dimethyl-1*H*-benzo[*d*]imidazole (511 mg, 3.5 mmol, 1 equiv), (bromoethynyl)triisopropylsilane (2.01 g, 7.7 mmol, 2.2 equiv), CuI (33 mg, 0.175 mmol, 5 mol%), Cs₂CO₃ (1365 mg, 4.2 mmol, 1.2 equiv) and PEG-400 (140 mg, 0.35 mmol, 10 mol%). The vial was capped and purged before the addition of 1,4-dioxane (11 mL, 0.3 M). The reaction mixture was then heated to 160 °C for 1 h. Upon completion of the reaction, the vial was vented and cooled to room temperature before being filtered through Celite and concentrated under reduced pressure. The crude oil was purified by flash chromatography (silica gel, 0-5% Et₂O/petroleum ether) to provide the desired compound as a clear oil (900 mg, 79%).

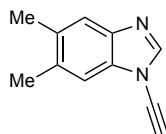
ν_{max} (neat): 2939, 2863, 2177, 1498, 1465 cm⁻¹.

¹H NMR (CDCl₃, 400 MHz): δ 3.71 (dd, *J* = 6.2, 4.3 Hz, 2H), 3.57 (dd, *J* = 6.3, 4.3 Hz, 2H), 3.45 (dd, *J* = 6.2, 4.2 Hz, 2H), 3.39 (dd, *J* = 6.3, 4.3 Hz, 2H), 1.44 (s, 9H).

¹³C NMR (CDCl₃, 126 MHz): δ 143.0, 140.2, 134.2, 133.0, 120.8, 111.1, 90.6, 72.4, 20.6, 20.2, 18.6, 11.2.

Data consistent with previously reported spectra.^[164]

1-Ethynyl-5,6-dimethyl-1*H*-benzo[*d*]imidazole, 2.84



To a solution of 5,6-dimethyl-1-((triisopropylsilyl)ethynyl)-1*H*-benzo[*d*]imidazole (1.3 g, 4 mmol, 1 equiv) in THF (25 mL, 0.15 M) at 0 °C was added TBAF (1M in THF, 6 mL, 6 mmol, 1.5 equiv). The reaction was stirred at 0 °C for 30 min then warmed to room temperature before the addition of EtOAc (10 mL) and H₂O (10 mL). The organics were separated and washed with H₂O (10 mL) and brine (10 mL) before being dried and concentrated under reduced pressure. The crude mixture was purified by flash chromatography (silica gel, 0-20% Et₂O/petroleum ether) to provide the desired compound as a white solid (800 mg, 88 %).

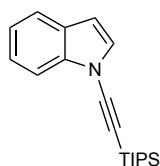
ν_{\max} (neat): 3196, 3099, 2917, 2149, 1493, 1450 cm⁻¹.

¹H NMR (CDCl₃, 400 MHz): δ 7.95 (s, 1H), 7.54 (s, 1H), 7.31 (s, 1H), 3.25 (s, 1H), 2.37 (s, 3H), 2.35 (s, 3H).

¹³C NMR (CDCl₃, 101 MHz): δ 142.3, 139.8, 133.8, 132.6, 132.3, 120.3, 110.5, 70.2, 61.2, 19.9, 19.7.

HRMS: exact mass calculated for [M+H]⁺ (C₁₁H₁₁N₂) requires *m/z* 171.0917, found *m/z* 171.0914.

1-((Triisopropylsilyl)ethynyl)-1*H*-indole, 2.95



An oven dried 20 mL microwave vial was charged with indole (468 mg, 4 mmol, 1 equiv), (bromoethynyl)triisopropylsilane (2.1 g, 8 mmol, 2 equiv), CuI (38 mg, 0.2 mmol, 5 mol%), Cs₂CO₃ (1560 mg, 4.8 mmol, 1.2 equiv) and PEG-400 (160 mg, 0.4 mmol, 10 mol%). The vial was capped and purged before the addition of 1,4 dioxane (11.5 mL, 0.35 M). The reaction mixture was then heated to 160 °C for 16 h. Upon completion of the reaction the vial was cooled to room temperature, vented, decapped, filtered through Celite, and concentrated under reduced pressure. The

crude oil was purified by flash chromatography (silica gel, 0-1% Et₂O/petroleum ether) to provide the desired compound as a clear oil (1030 mg, 86%).

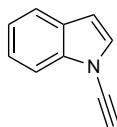
ν_{\max} (neat): 2939, 2861, 2179, 1522, 1457, 1325 cm⁻¹.

¹H NMR (CDCl₃, 400 MHz): δ 3.71 (dd, J = 6.2, 4.3 Hz, 2H), 3.57 (dd, J = 6.3, 4.3 Hz, 2H), 3.45 (dd, J = 6.2, 4.2 Hz, 2H), 3.39 (dd, J = 6.3, 4.3 Hz, 2H), 1.44 (s, 9H).

¹³C NMR (CDCl₃, 126 MHz): δ 138.4, 129.1, 127.8, 123.7, 122.1, 121.3, 111.53, 105.3, 94.8, 68.9, 18.9, 11.5.

HRMS: exact mass calculated for [M+H]⁺ (C₁₉H₂₇NSi) requires m/z 298.1991, found m/z 298.1994.

1-Ethynyl-1H-indole, 2.92



To a solution of 1-((triisopropylsilyl)ethynyl)-1H-indole (520 mg, 1.75 mmol, 1 equiv) in THF (17.5 mL, 0.1 M) at 0 °C was added TBAF (1M in THF, 2.65 mL, 2.65 mmol, 1.5 equiv). The reaction was stirred at 0 °C for 30 min then warmed to room temperature before the addition of EtOAc (10 mL) and H₂O (10 mL). The organics were separated and washed with H₂O (10 mL) and brine (10 mL) before being dried and concentrated under reduced pressure. The crude mixture was purified by flash chromatography (silica gel, 0-5% Et₂O/petroleum ether) to provide the desired compound as a brown oil (130 mg, 53 %).

ν_{\max} (neat): 3264, 3110, 2147, 1521, 1455, 1316, 1212 cm⁻¹.

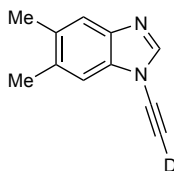
¹H NMR (CDCl₃, 400 MHz): δ 7.68 (t, J = 8.1 Hz, 1H), 7.44 – 7.39 (m, 1H), 7.34 – 7.30 (m, 1H), 7.29 (d, J = 3.4 Hz, 1H), 6.65 – 6.60 (m, 1H), 3.21 (s, 1H).

¹³C NMR (CDCl₃, 101 MHz): δ 138.3, 128.9, 127.8, 123.8, 122.2, 121.3, 111.4, 105.7, 74.5, 58.9.

HRMS: exact mass calculated for [M-H] (C₁₀H₆N) requires m/z 140.0500, found m/z 140.0493.

Deuterated products

1-(Ethynyl-*d*)-5,6-dimethyl-1H-benzo[*d*]imidazole, 2.84b



Prepared according to General Procedure 2B using 1-ethynyl-5,6-dimethyl-1H-benzo[d]imidazole (51 mg, 0.3 mmol, 1 equiv) and K₂CO₃ (62 mg, 0.45 mmol, 1.5 equiv) to provide the desired product as an off-white solid (45 mg, 87%, 95%D).

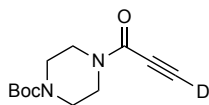
ν_{max} (neat): 3099, 2917, 2541, 2002, 1745, 1493 cm⁻¹.

¹H NMR (CDCl₃, 400 MHz): δ 7.97 (s, 1H), 7.56 (s, 1H), 7.34 (s, 1H), 2.40 (s, 3H), 2.37 (s, 3H).

¹³C NMR (CDCl₃, 101 MHz): δ 143.0, 140.4, 134.5, 133.2, 132.9, 121.0, 111.1, 70.4 (t, J_{C-D} = 7.7 Hz), 61.7 (t, J_{C-D} = 40.4 Hz), 20.6, 20.3.

HRMS: exact mass calculated for [M]⁺ (C₁₁H₉DN₂) requires m/z 171.0907, found m/z 171.0909.

***tert*-Butyl 4-(propioloyl-*d*)piperazine-1-carboxylate, 2.34b**



Prepared according to General Procedure 2B using *tert*-butyl 4-propioloylpiperazine-1-carboxylate (71 mg, 0.3 mmol, 1 equiv) and K₂CO₃ (62 mg, 0.45 mmol, 1.5 equiv) to provide the desired product as an off white solid (52 mg, 73%, 91%D).

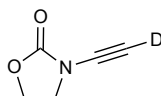
ν_{max} (neat): 3194, 2969, 2922, 2541, 2102, 1943, 1680, 1625, 1439 cm⁻¹.

¹H NMR (CDCl₃, 400 MHz): δ 3.71 (dd, J = 6.2, 4.3 Hz, 2H), 3.57 (dd, J = 6.3, 4.3 Hz, 2H), 3.45 (dd, J = 6.2, 4.2 Hz, 2H), 3.39 (dd, J = 6.3, 4.3 Hz, 2H), 1.44 (s, 9H).

¹³C NMR (CDCl₃, 101 MHz): δ 153.9, 151.4, 80.0, 79.2, 74.2 (t, J_{C-D} = 7 Hz), 46.2, 40.8, 27.8.

HRMS: exact mass calculated for [M]⁺ (C₁₂H₁₇DN₂O₃) requires m/z 239.1380, found m/z 239.1388.

3-(Ethynyl-*d*)oxazolidin-2-one, 2.83b



Prepared according to General Procedure 2B using 3-ethynylloxazolidin-2-one (33 mg, 0.3 mmol, 1 equiv) and K_2CO_3 (62 mg, 0.45 mmol, 1.5 equiv) to provide the desired product as a yellow gum (20 mg, 60%, 85%D).

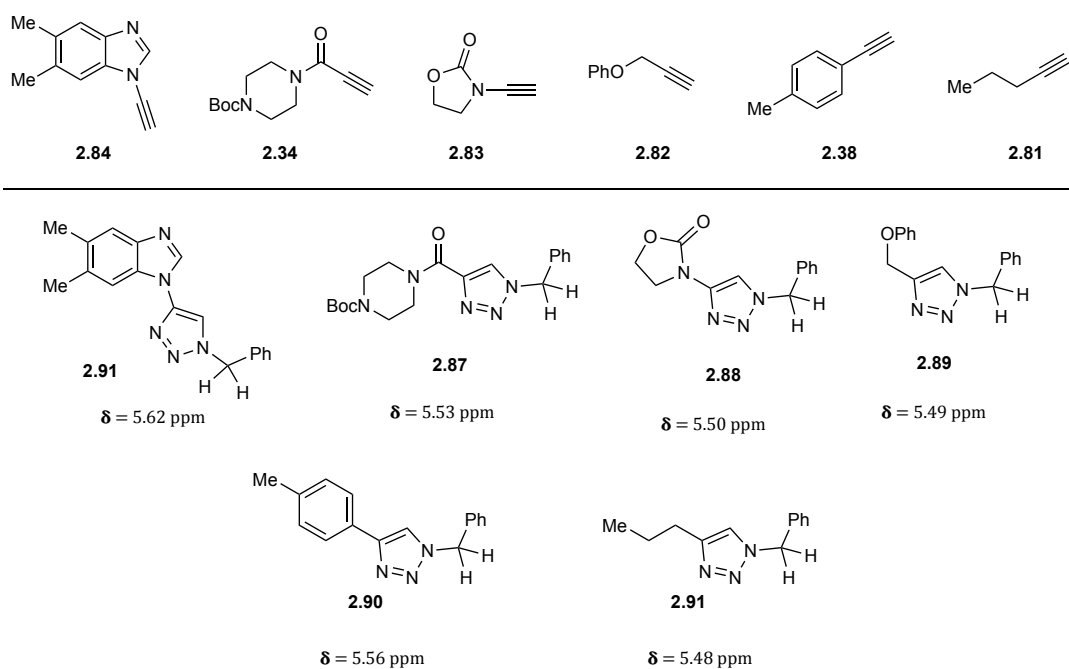
ν_{\max} (neat): 3237, 2919, 2562, 2149, 2008, 1759, 1476, 1409 cm^{-1} .

1H NMR ($CDCl_3$, 400 MHz): δ 4.43 (dd, $J = 8.7, 7.3$ Hz, 2H), 3.91 (dd, $J = 8.7, 7.3$ Hz, 2H).

^{13}C NMR ($CDCl_3$, 126 MHz): δ 156.3, 72.3 (t, $J = 8.5$ Hz), 63.3, 59.5 (t, $J = 40.2$ Hz), 46.5.

HRMS: exact mass calculated for $[M]^+$ ($C_5H_4NO_2$) requires m/z 122.0383, found m/z 122.0387.

2.7.8 Competition Experiments from Scheme 116



2.84 vs. 2.34

Reaction was carried out according to General Procedure 2B using 1-ethynyl-5,6-dimethyl-1H-benzo[d]imidazole (17 mg, 0.1 mmol, 1 equiv) and *tert*-butyl 4-propiolylpiperazine-1-carboxylate (24 mg, 0.1 mmol, 1 equiv) to provide a 87:13 ratio of products by 1H NMR.

2.84 vs. 2.83

Reaction was carried out according to General Procedure 2B using 1-ethynyl-5,6-dimethyl-1*H*-benzo[*d*]imidazole (17 mg, 0.1 mmol, 1 equiv) and 3-ethynyloxazolidin-2-one (11 mg, 0.1 mmol, 1 equiv) to provide a 98:2 ratio of products by ¹H NMR.

2.84 vs. 2.82

Reaction was carried out according to General Procedure 2B using 1-ethynyl-5,6-dimethyl-1*H*-benzo[*d*]imidazole (17 mg, 0.1 mmol, 1 equiv) and (prop-2-yn-1-yloxy)benzene (13 mg, 0.1 mmol, 1 equiv) to provide a 100:0 ratio of products by ¹H NMR.

2.84 vs. 2.38

Reaction was carried out according to General Procedure 2B using 1-ethynyl-5,6-dimethyl-1*H*-benzo[*d*]imidazole (17 mg, 0.1 mmol, 1 equiv) and 1-ethynyl-4-methylbenzene (12.5 μ L, 0.1 mmol, 1 equiv) to provide a 100:0 ratio of products by ¹H NMR.

2.84 vs. 2.81

Reaction was carried out according to General Procedure 2B using 1-ethynyl-5,6-dimethyl-1*H*-benzo[*d*]imidazole (17 mg, 0.1 mmol, 1 equiv) and pent-1-yne (10 μ L, 0.1 mmol, 1 equiv) to provide a 100:0 ratio of products by ¹H NMR.

2.34 vs. 2.83

Reaction was carried out according to General Procedure 2B using *tert*-butyl 4-propioloylpiperazine-1-carboxylate (24 mg, 0.1 mmol, 1 equiv) and 3-ethynyloxazolidin-2-one (11 mg, 0.1 mmol, 1 equiv) to provide a 80:20 ratio of products by ¹H NMR.

2.34 vs. 2.82

Reaction was carried out according to General Procedure 2B using *tert*-butyl 4-propioloylpiperazine-1-carboxylate (24 mg, 0.1 mmol, 1 equiv) and (prop-2-yn-1-yloxy)benzene (13 mg, 0.1 mmol, 1 equiv) to provide a 86:14 ratio of products by ¹H NMR.

2.34 vs. 2.38

Reaction was carried out according to General Procedure 2B using *tert*-butyl 4-propioloylpiperazine-1-carboxylate (24 mg, 0.1 mmol, 1 equiv) and 1-ethynyl-4-methylbenzene (12.5 μ L, 0.1 mmol, 1 equiv) to provide a 90:10 ratio of products by ^1H NMR.

2.34 vs. 2.81

Reaction was carried out according to General Procedure 2B using *tert*-butyl 4-propioloylpiperazine-1-carboxylate (24 mg, 0.1 mmol, 1 equiv) and pent-1-yne (12.5 μ L, 0.1 mmol, 1 equiv) to provide a 100:0 ratio of products by ^1H NMR.

2.83 vs. 2.82

Reaction was carried out according to General Procedure 2B using 3-ethynyloxazolidin-2-one (11 mg, 0.1 mmol, 1 equiv) and (prop-2-yn-1-yloxy)benzene (13 mg, 0.1 mmol, 1 equiv) to provide a 65:35 ratio of products by ^1H NMR.

2.83 vs. 2.38

Reaction was carried out according to General Procedure 2B using 3-ethynyloxazolidin-2-one (11 mg, 0.1 mmol, 1 equiv) and 1-ethynyl-4-methylbenzene (12.5 μ L, 0.1 mmol, 1 equiv) to provide a 90:10 mixture of products by ^1H NMR.

2.83 vs. 2.81

Reaction was carried out according to General Procedure 2B using 3-ethynyloxazolidin-2-one (11 mg, 0.1 mmol, 1 equiv) and pent-1-yne (12.5 μ L, 0.1 mmol, 1 equiv) to provide a 100:0 ratio of products by ^1H NMR.

2.82 vs. 2.38

Reaction was carried out according to General Procedure 2B using (prop-2-yn-1-yloxy)benzene (13 mg, 0.1 mmol, 1 equiv) and 1-ethynyl-4-methylbenzene (12.5 μ L, 0.1 mmol, 1 equiv) to provide a 85:15 mixture of products by ^1H NMR.

2.82 vs. 2.81

Reaction was carried out according to General Procedure 2B using (prop-2-yn-1-yloxy)benzene (13 mg, 0.1 mmol, 1 equiv) and pent-1-yne (12.5 μ L, 0.1 mmol, 1 equiv) to provide a 100:0 ratio of products by ^1H NMR.

2.38 vs. 2.81

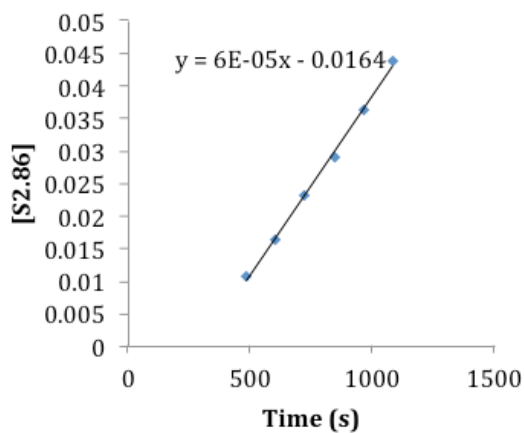
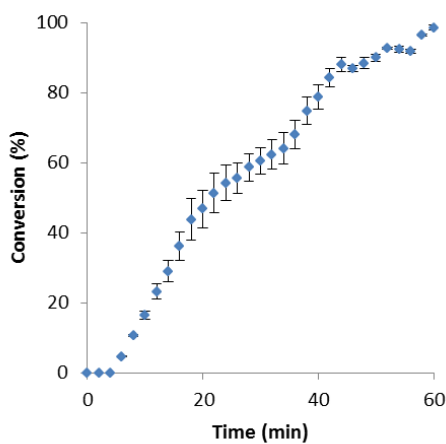
Reaction was carried out according to General Procedure 2B using 1-ethynyl-4-methylbenzene (12.5 μ L, 0.1 mmol, 1 equiv) and pent-1-yne (12.5 μ L, 0.1 mmol, 1 equiv) to provide a 100:0 ratio of products by ^1H NMR.

2.7.9 Kinetic data

Determination of rates for alkynes 2.84, 2.34, 2.83, 2.82, 2.38, and 2.81.

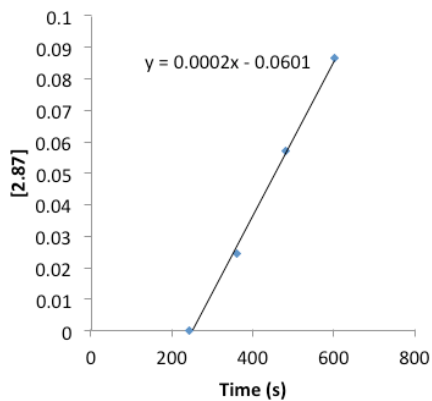
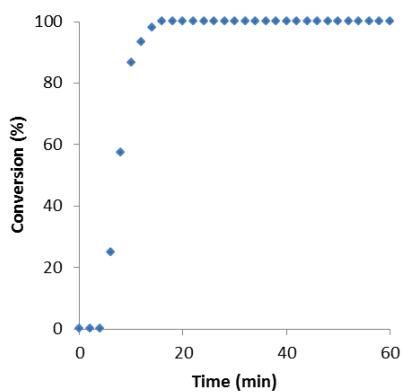
Rate of 2.86

Data was obtained according to General Procedure 2C using 1-ethynyl-5,6-dimethyl-1*H*-benzo[*d*]imidazole (8.5 mg, 0.05 mmol, 1 equiv). Data was acquired by taking an average over two runs.



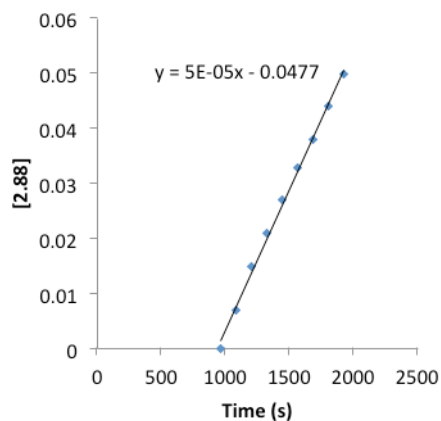
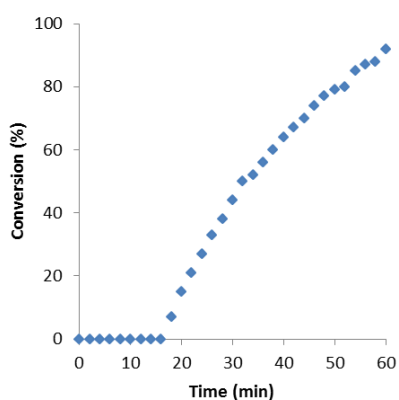
Rate of 2.34

Data was obtained according to General Procedure 2C using *tert*-butyl 4-propionylpiperazine-1-carboxylate (11.9 mg, 0.05 mmol, 1 equiv).



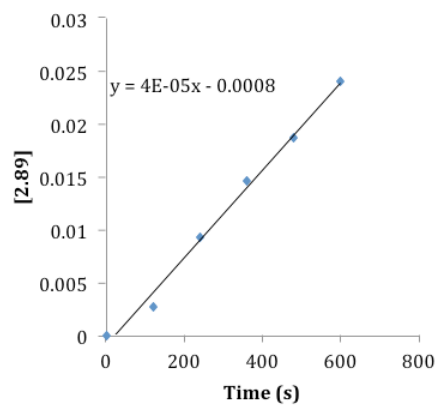
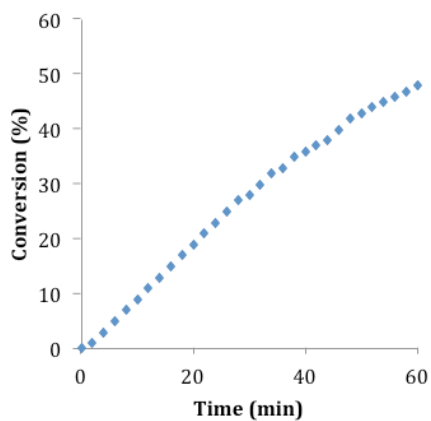
Rate of 2.83

Data was obtained according to General Procedure 2C using 3-ethynyloxazolidin-2-one (5.6 mg, 0.05 mmol, 1 equiv).



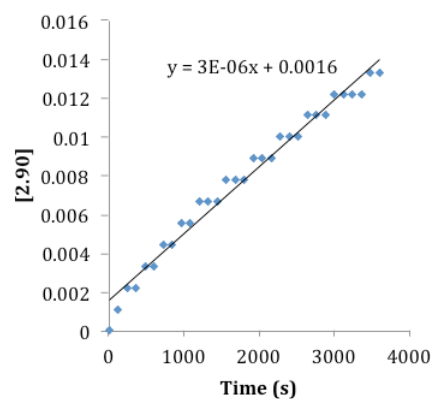
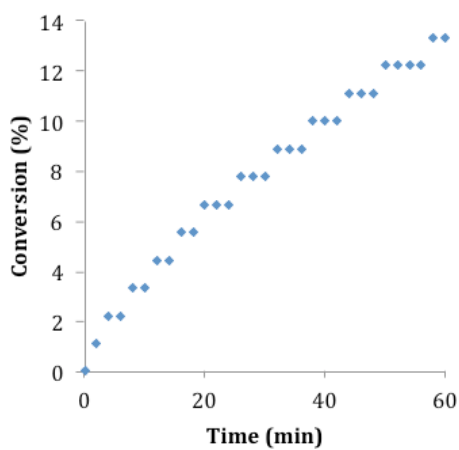
Rate of 2.82

Data was obtained according to General Procedure 2D using (prop-2-yn-1-yloxy)benzene (6.6 mg, 0.05 mmol, 1 equiv).



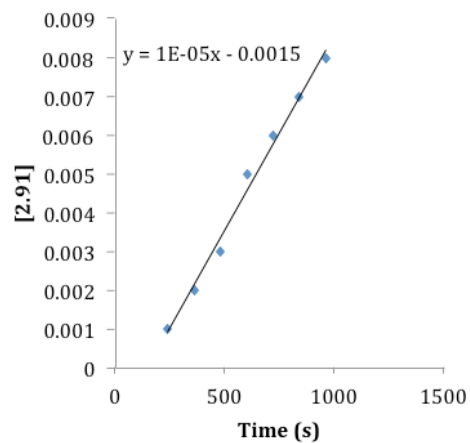
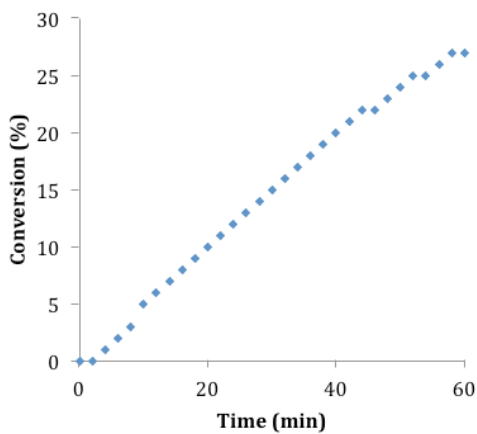
Rate of 2.38

Data was obtained according to General Procedure 2D using 1-ethynyl-4-methylbenzene (5.8 mg, 0.05 mmol, 1 equiv).



Rate of 2.81

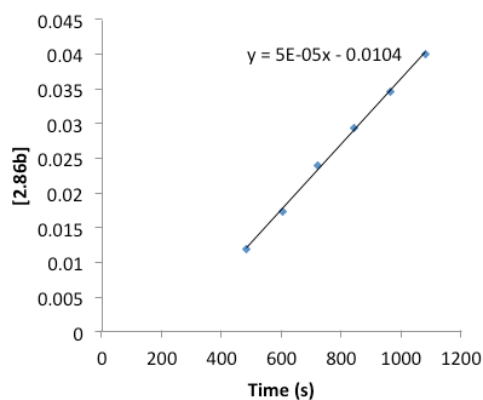
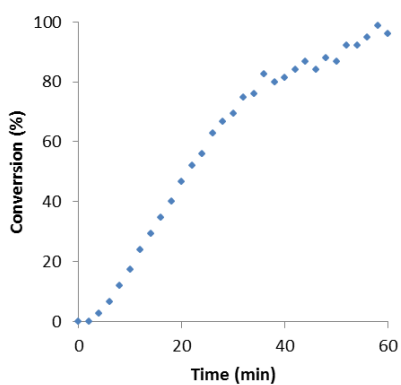
Data was obtained according to General Procedure 2D using 1-pentyne (3.4 mg, 0.05 mmol, 1 equiv).



Deuterium KIE

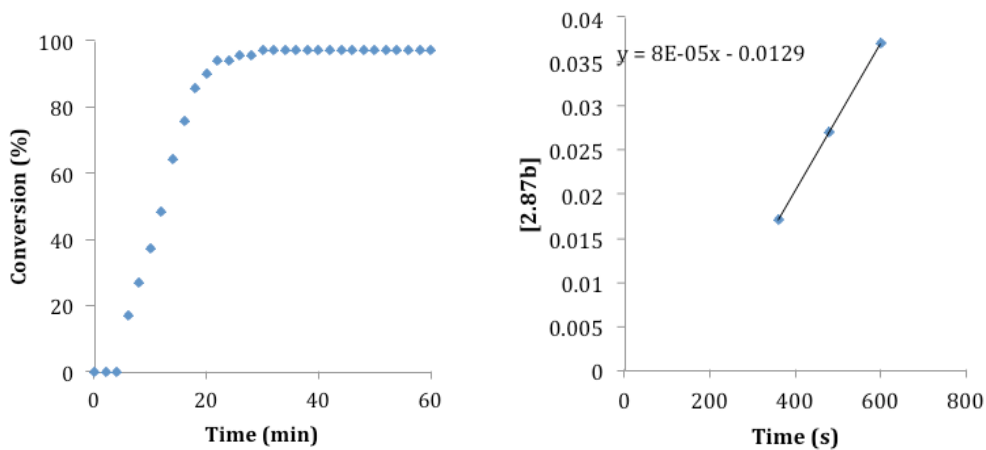
Rate of 1-(ethynyl-*d*)-5,6-dimethyl-1*H*-benzo[*d*]imidazole, 2.84b

Data was obtained according to General Procedure 2C using 1-(ethynyl-*d*)-5,6-dimethyl-1*H*-benzo[*d*]imidazole (8.5 mg, 0.05 mmol, 1 equiv).



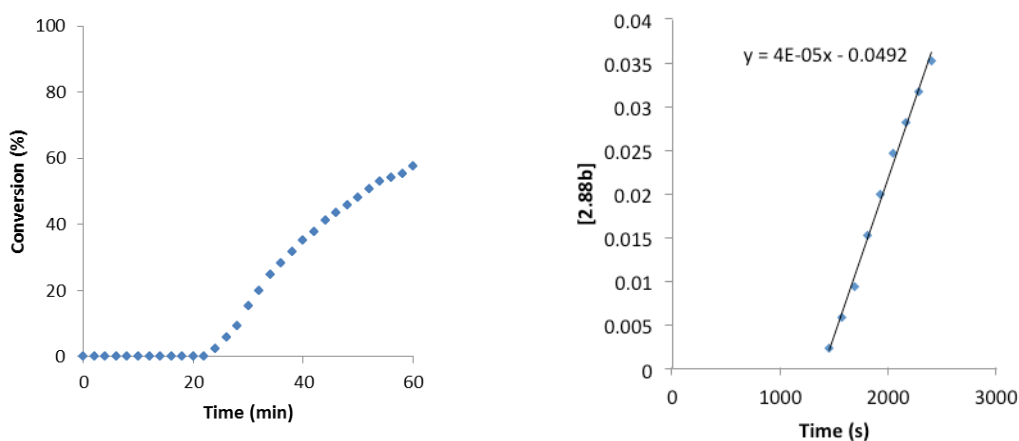
Rate of *tert*-butyl-4-(propioloyl-*d*)piperazine-1-carboxylate, 2.34b

Data was obtained according to General Procedure 2C using *tert*-butyl-4-(propioloyl-*d*)piperazine-1-carboxylate (11.9 mg, 0.05 mmol, 1 equiv).



Rate of 3-(ethynyl-*d*)oxazolidin-2-one, 2.83b

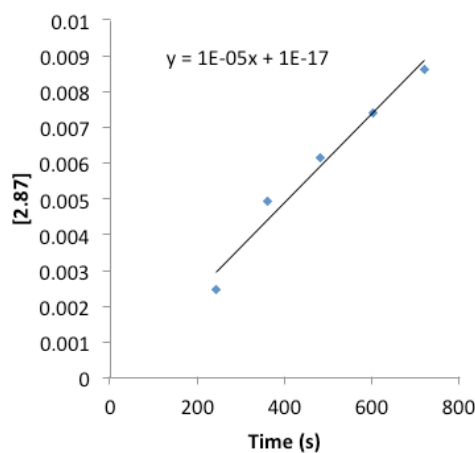
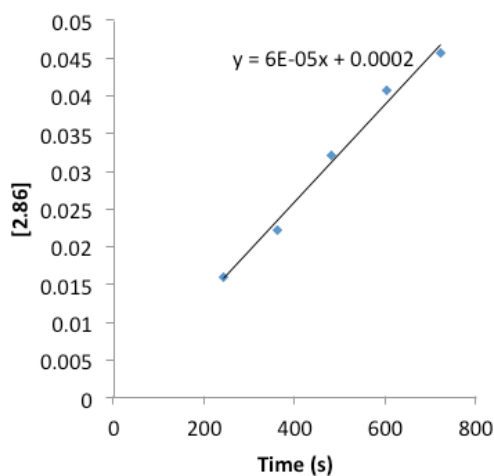
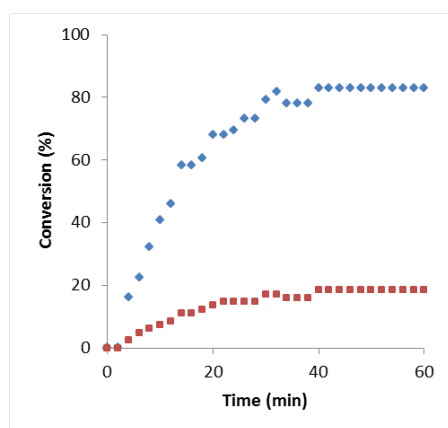
Data was obtained according to General Procedure 2C using 3-(ethynyl-*d*)oxazolidin-2-one (5.6 mg, 0.05 mmol, 1 equiv).



NMR competition experiments

Competition reaction of 2.84 vs. 2.34

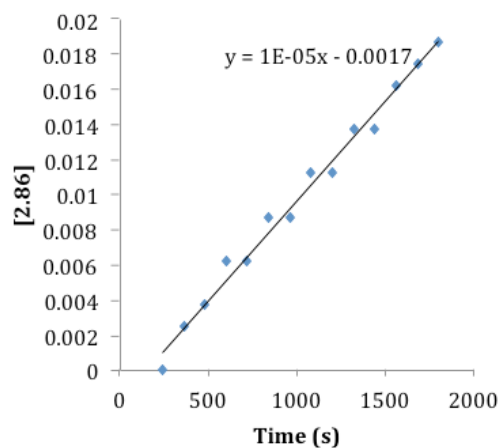
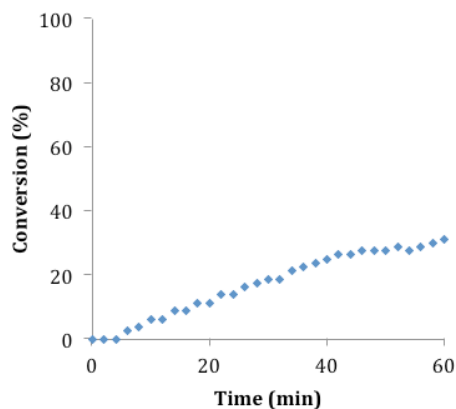
Data was obtained according to General Procedure 2C using 1-ethynyl-5,6-dimethyl-1*H*-benzo[*d*]imidazole (8.5 mg, 0.05 mmol, 1 equiv) and *tert*-butyl-4-(propioloyl)piperazine-1-carboxylate (11.9 mg, 0.05 mmol, 1 equiv). Blue diamonds show formation of product **2.86**. Red squares show formation of product **2.87**.



Dependence on benzyl azide concentration

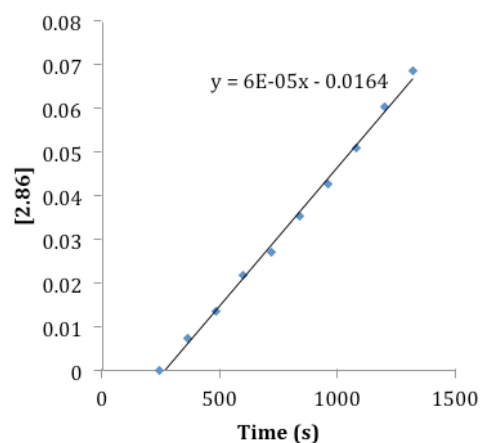
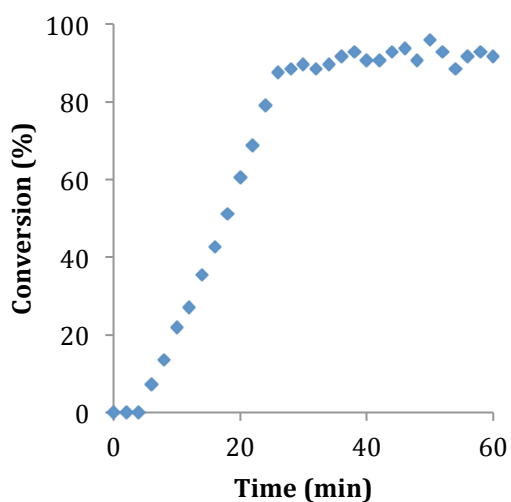
0.4 eq azide

Data was obtained according to General Procedure 2C using 1-ethynyl-5,6-dimethyl-1*H*-benzo[*d*]imidazole (8.5 mg, 0.05 mmol, 1 equiv) and benzyl azide (2.66 mg, 0.02 mmol, 0.4 equiv).



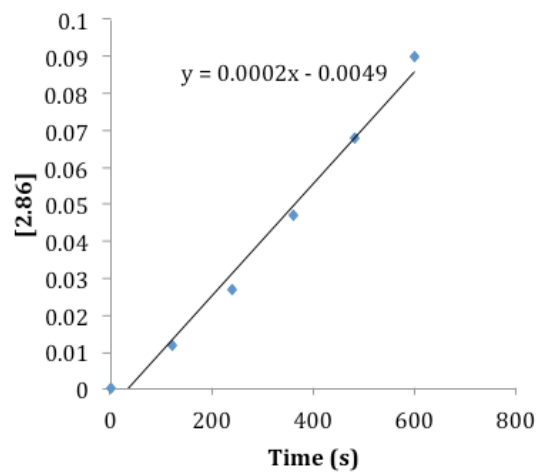
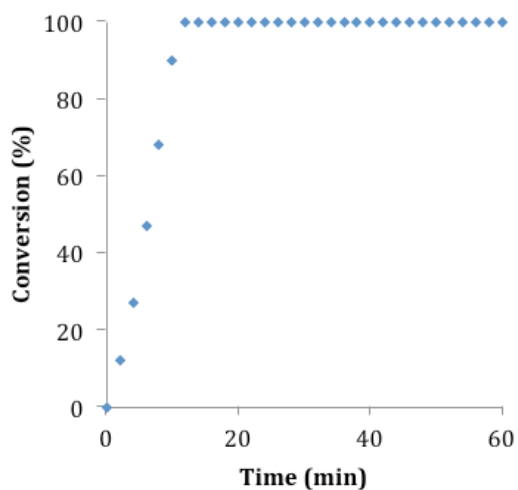
1.25 eq azide

Data was obtained according to General Procedure 2C using 1-ethynyl-5,6-dimethyl-1*H*-benzo[*d*]imidazole (8.5 mg, 0.05 mmol, 1 equiv) and benzyl azide (8.3 mg, 0.063 mmol, 1.25 equiv).



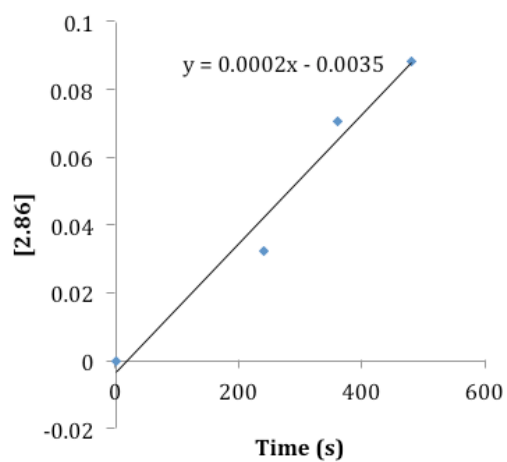
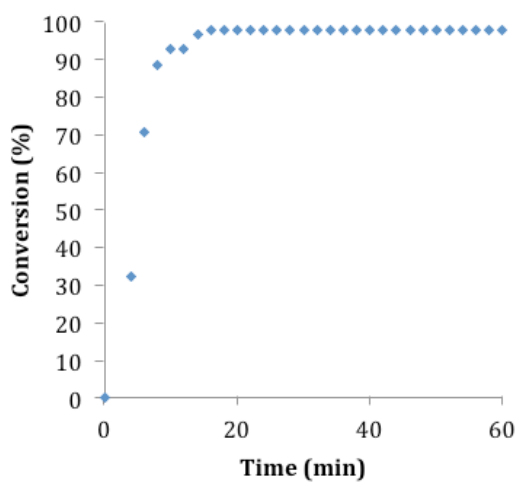
2 eq azide

Data was obtained according to General Procedure 2C using 1-ethynyl-5,6-dimethyl-1*H*-benzo[*d*]imidazole (8.5 mg, 0.05 mmol, 1 equiv) and benzyl azide (13.3 mg, 0.1 mmol, 2 equiv).

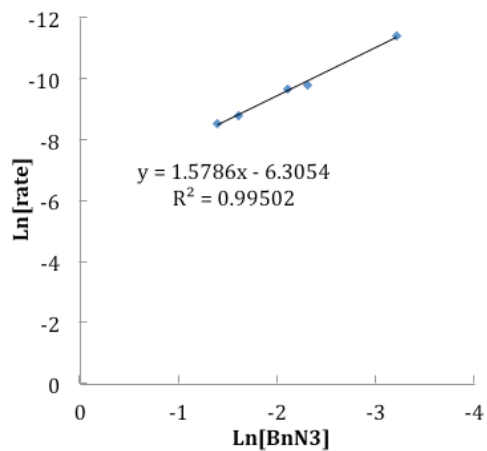


2.2 eq azide

Data was obtained according to General Procedure 2C using 1-ethynyl-5,6-dimethyl-1*H*-benzo[*d*]imidazole (8.5 mg, 0.05 mmol, 1 equiv) and benzyl azide (14.6 mg, 0.11 mmol, 2.2 equiv).



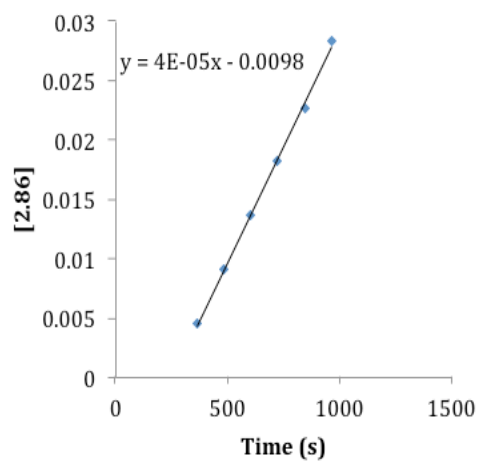
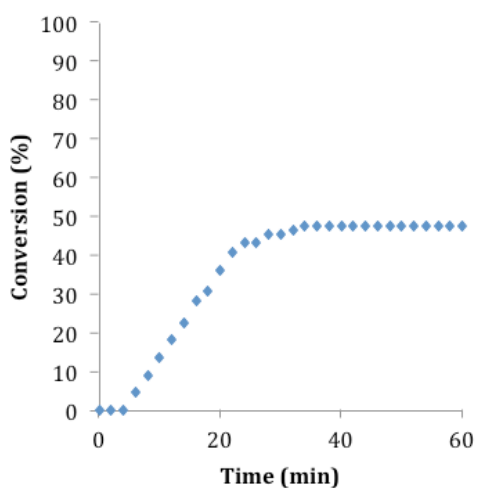
Calculation of order in [benzyl azide]



Dependence on ynamine (2.84) concentration

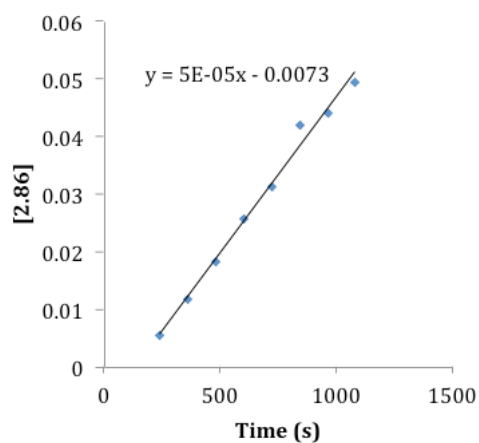
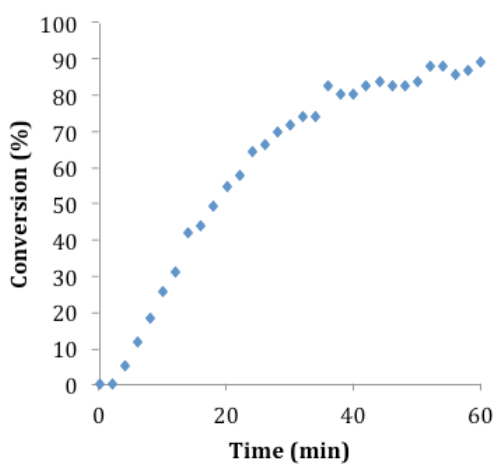
0.5 equiv

Data was obtained according to General Procedure 2C using 1-ethynyl-5,6-dimethyl-1*H*-benzo[*d*]imidazole (4.25 mg, 0.025 mmol, 0.5 equiv) and benzyl azide (6.7 mg, 0.05 mmol, 1 equiv).



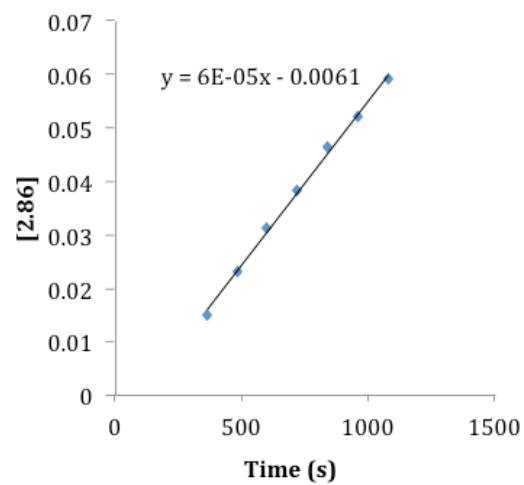
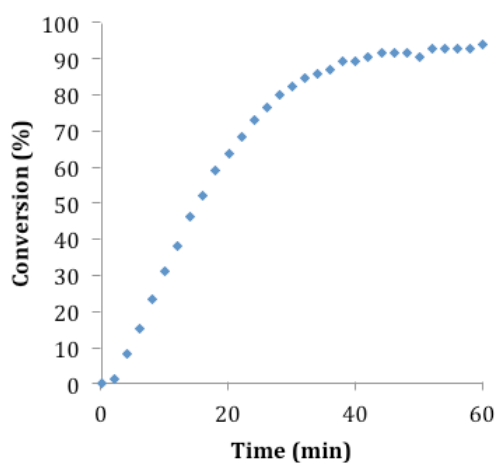
1.5 equiv

Data was obtained according to General Procedure 2C using 1-ethynyl-5,6-dimethyl-1*H*-benzo[*d*]imidazole (12.75 mg, 0.075 mmol, 1.5 equiv) and benzyl azide (6.7 mg, 0.05 mmol, 1 equiv).



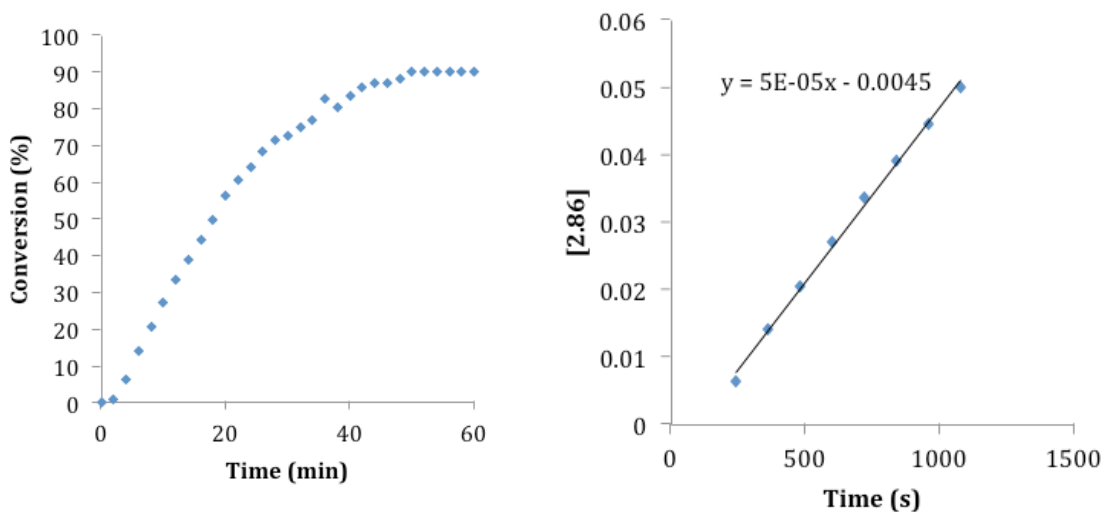
2 equiv

Data was obtained according to General Procedure 2C using 1-ethynyl-5,6-dimethyl-1*H*-benzo[*d*]imidazole (17 mg, 0.1 mmol, 2 equiv) and benzyl azide (6.7 mg, 0.05 mmol, 1 equiv).

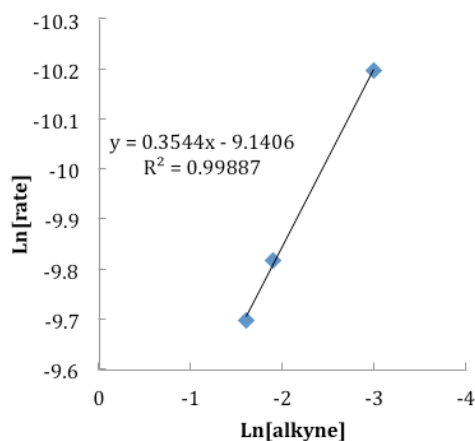


2.5 equiv

Data was obtained according to General Procedure 2C using 1-ethynyl-5,6-dimethyl-1*H*-benzo[*d*]imidazole (21.25 mg, 0.015 mmol, 2.5 equiv) and benzyl azide (6.7 mg, 0.05 mmol, 1 equiv).



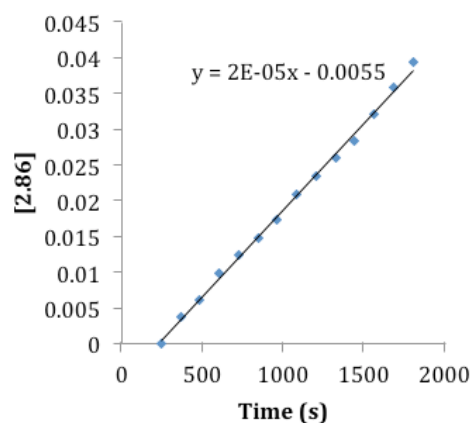
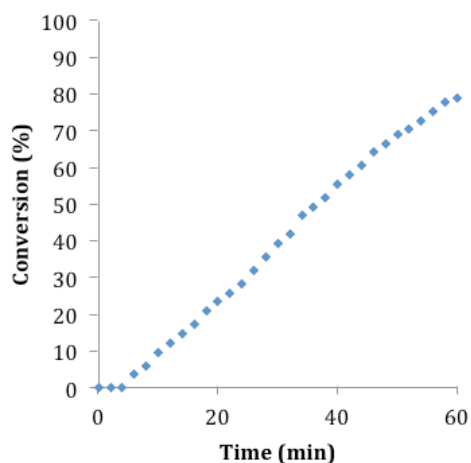
Calculation of order in [2.84]



Dependence on Cu(OAc)₂ concentration

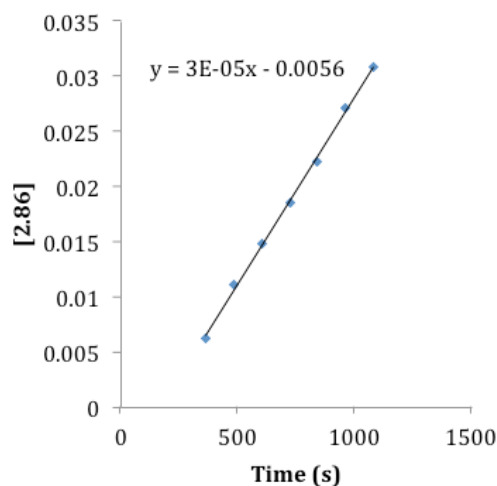
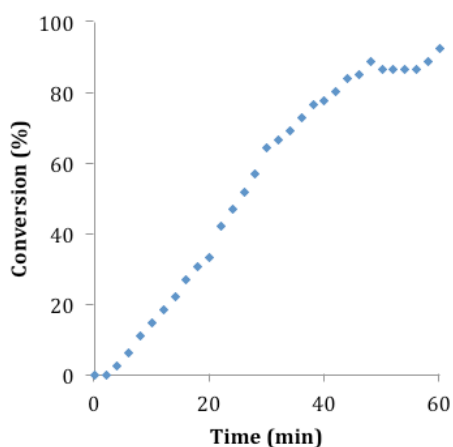
2.5 mol% Cu

Data was obtained according to General Procedure 2C using 1-ethynyl-5,6-dimethyl-1*H*-benzo[*d*]imidazole (8.5 mg, 0.05 mmol, 1 equiv), benzyl azide (6.7 mg, 0.05 mmol, 1 equiv) and Cu(OAc)₂ (4 μ L, 0.25 mM solution, 0.00125 mmol, 2.5 mol%).



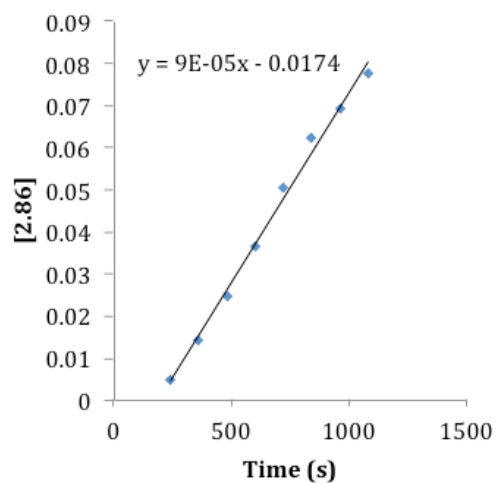
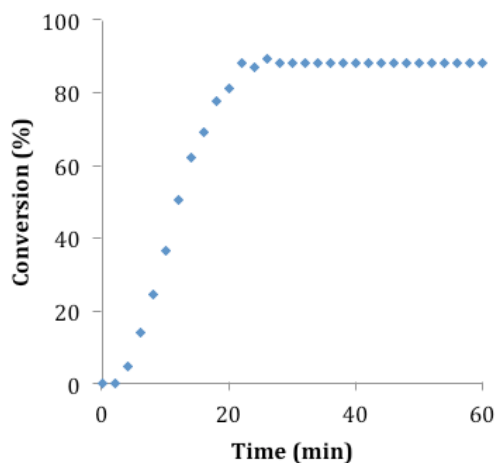
7.5 mol% Cu

Data was obtained according to General Procedure 2C using 1-ethynyl-5,6-dimethyl-1*H*-benzo[*d*]imidazole (8.5 mg, 0.05 mmol, 1 equiv), benzyl azide (6.7 mg, 0.05 mmol, 1 equiv) and Cu(OAc)₂ (12 μL, 0.25 mM solution, 0.00375 mmol, 7.5 mol%).



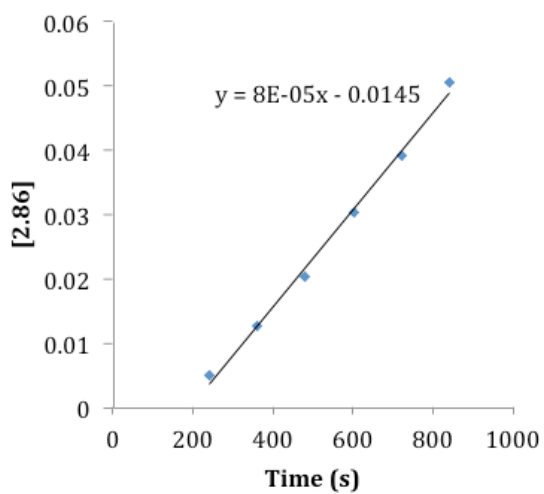
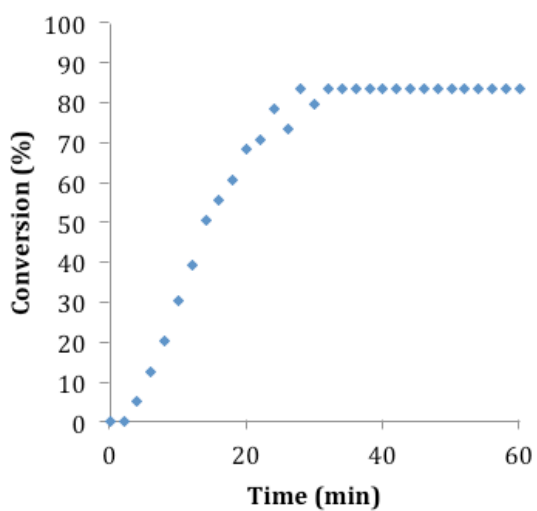
10 mol% Cu

Data was obtained according to General Procedure 2C using 1-ethynyl-5,6-dimethyl-1*H*-benzo[*d*]imidazole (8.5 mg, 0.05 mmol, 1 equiv), benzyl azide (6.7 mg, 0.05 mmol, 1 equiv) and Cu(OAc)₂ (16 μL, 0.25 mM solution, 0.005 mmol, 10 mol%).

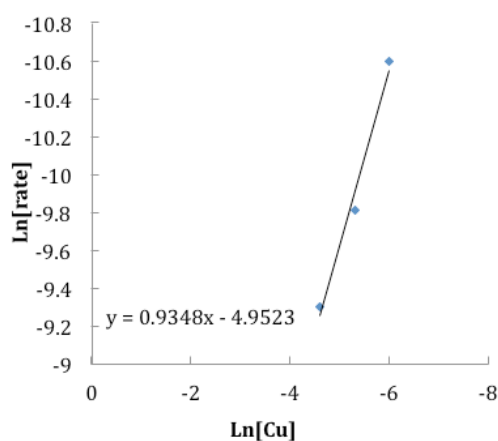


20 mol% Cu

Data was obtained according to General Procedure 2C using 1-ethynyl-5,6-dimethyl-1*H*-benzo[*d*]imidazole (8.5 mg, 0.05 mmol, 1 equiv), benzyl azide (6.7 mg, 0.05 mmol, 1 equiv) and Cu(OAc)₂ (32 μ L, 0.25 mM solution, 0.01 mmol, 20 mol%).

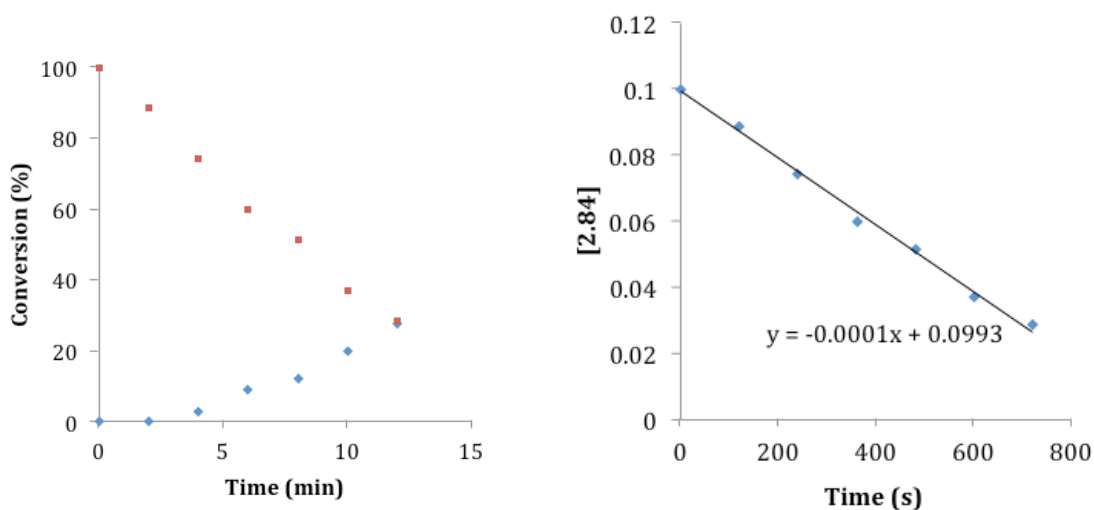


Calculation of order in Cu(OAc)₂



Rate of Cu acetylide formation of 2.84

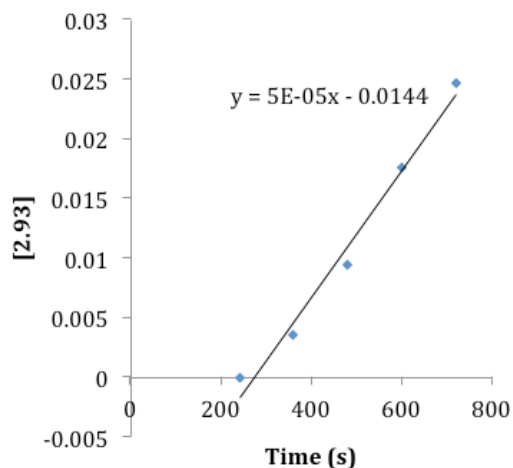
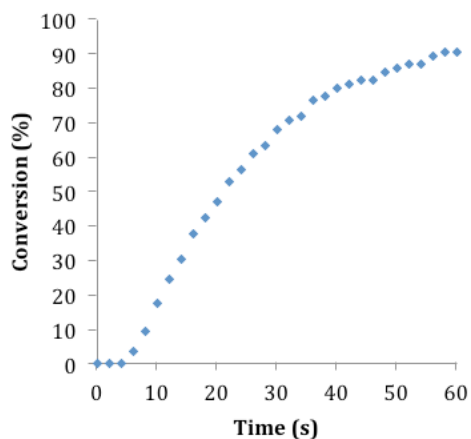
Data was obtained according to General Procedure 2C using 1-ethynyl-5,6-dimethyl-1*H*-benzo[*d*]imidazole (8.5 mg, 0.05 mmol, 1 equiv) and benzyl azide (6.7 mg, 0.05 mmol, 1 equiv). Both the disappearance of the acetylinic C-H and the appearance of the product benzyl peaks were monitored.



Red squares indicate the decrease in concentration of the alkyne methine proton.
Blue diamonds show the increase in click product.

Kinetics of indole ynamine 2.92

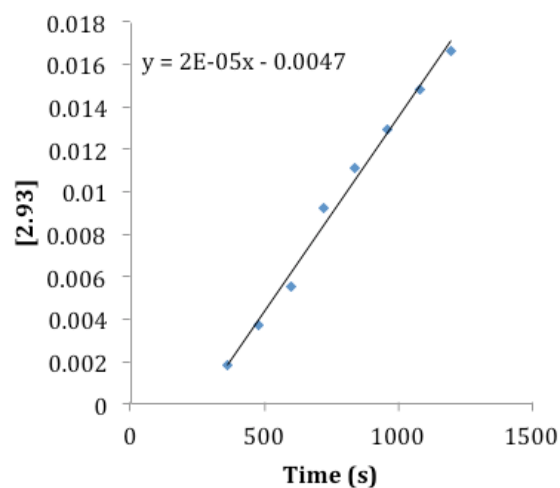
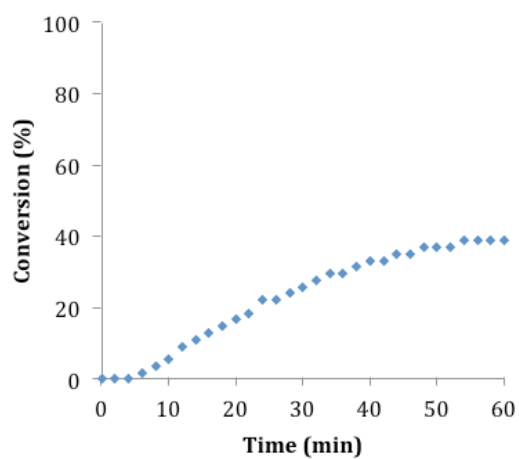
Data was obtained according to General Procedure 2C using 1-ethynyl-1*H*-indole (7.1 mg, 0.05 mmol, 1 equiv) and benzyl azide (6.7 mg, 0.05 mmol, 1 equiv).



Dependence on concentration of benzyl azide

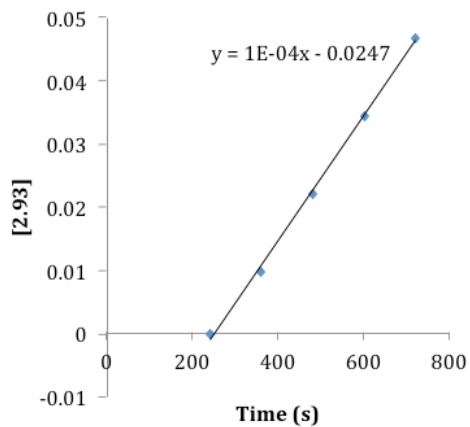
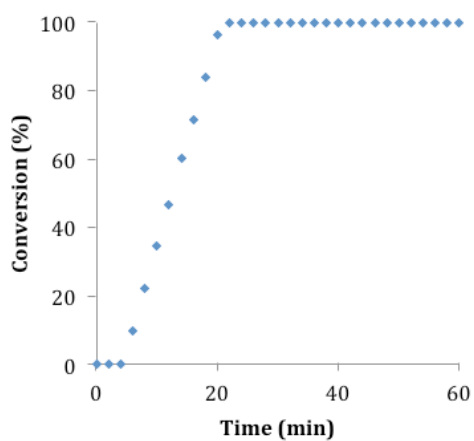
0.5 eq azide

Data was obtained according to General Procedure 2C using 1-ethynyl-1*H*-indole (7.1 mg, 0.05 mmol, 1 equiv) and benzyl azide (3.35 mg, 0.025 mmol, 0.5 equiv).

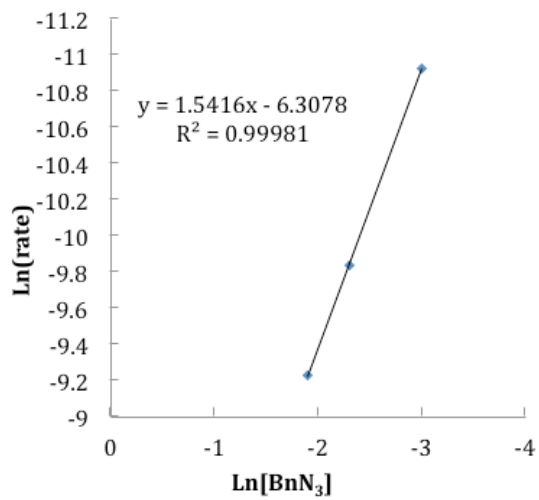


1.5 eq azide

Data was obtained according to General Procedure 2C using 1-ethynyl-1*H*-indole (7.1 mg, 0.05 mmol, 1 equiv) and benzyl azide (10.05 mg, 0.075 mmol, 1.5 equiv).

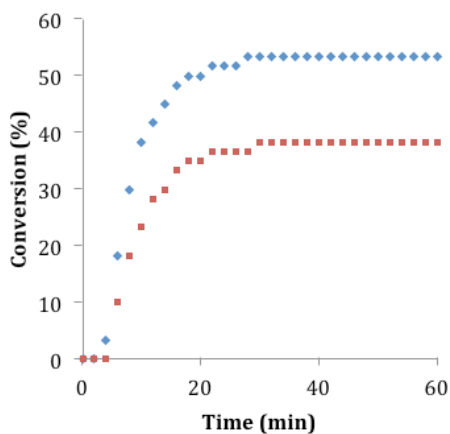


Calculation of order in benzyl azide



NMR competition experiment between 2.92 and 2.34

Data was obtained according to General Procedure 2C using 1-ethynyl-1*H*-indole (7.1 mg, 0.05 mmol, 1 equiv), *tert*-butyl-4-(propioloyl)piperazine-1-carboxylate (11.9 mg, 0.05 mmol, 1 equiv) and benzyl azide (6.7 mg, 0.05 mmol, 1 equiv). Blue diamonds show formation of product **2.93**. Red squares show formation of product **2.87**.



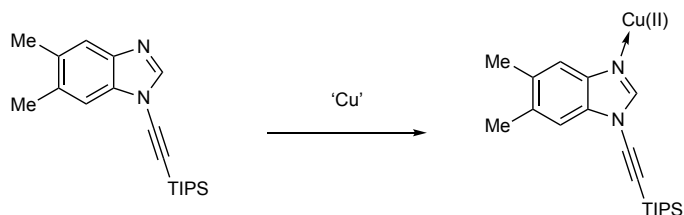
2.7.6 Mechanistic and control experiments

Treatment of TIPS protected ynamines with Cu salts

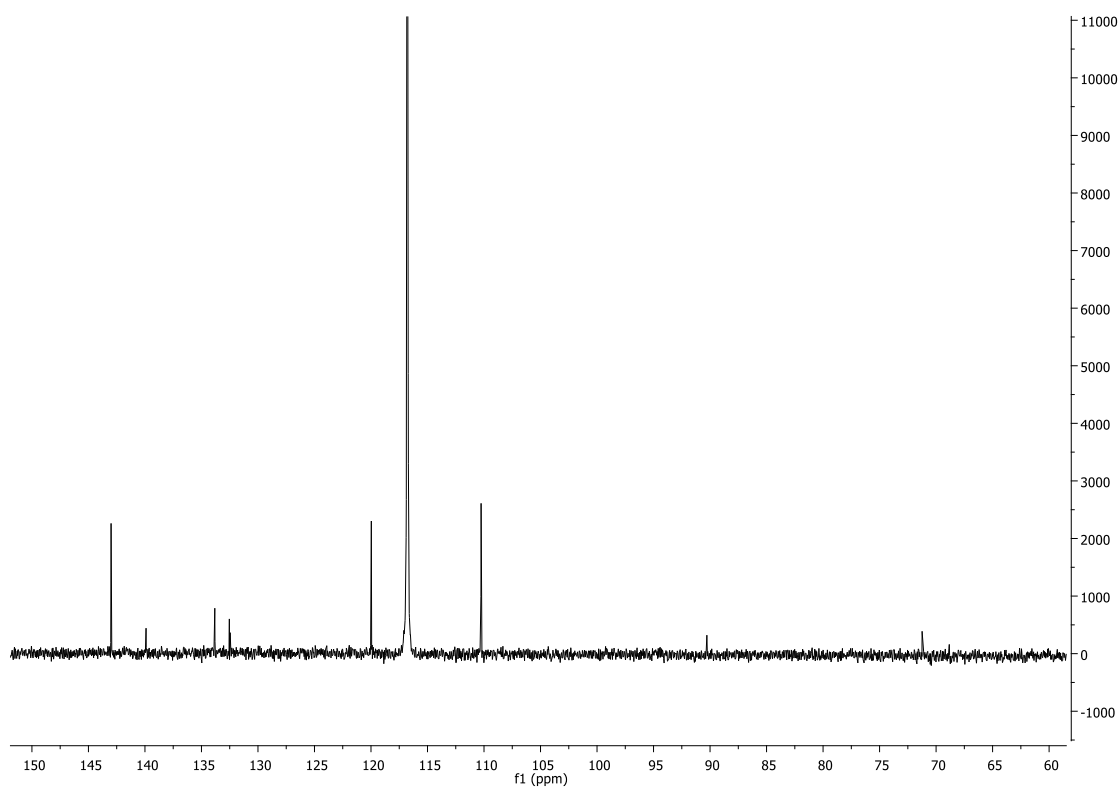
Procedure

To a solution of 5,6-dimethyl-1-((triisopropylsilyl)ethynyl)-1*H*-benzo[*d*]imidazole (16.3 mg, 0.05 mmol, 1 equiv) in MeCN (0.5 mL) was added Cu(OAc)₂ (16 μL, 0.25 mM solution, 0.005 mmol, 10 mol%). The resulting mixture was analyzed by ¹³C NMR.

Reaction of 5,6-dimethyl-1-((triisopropylsilyl)ethynyl)-1*H*-benzo[*d*]imidazole with Cu salts

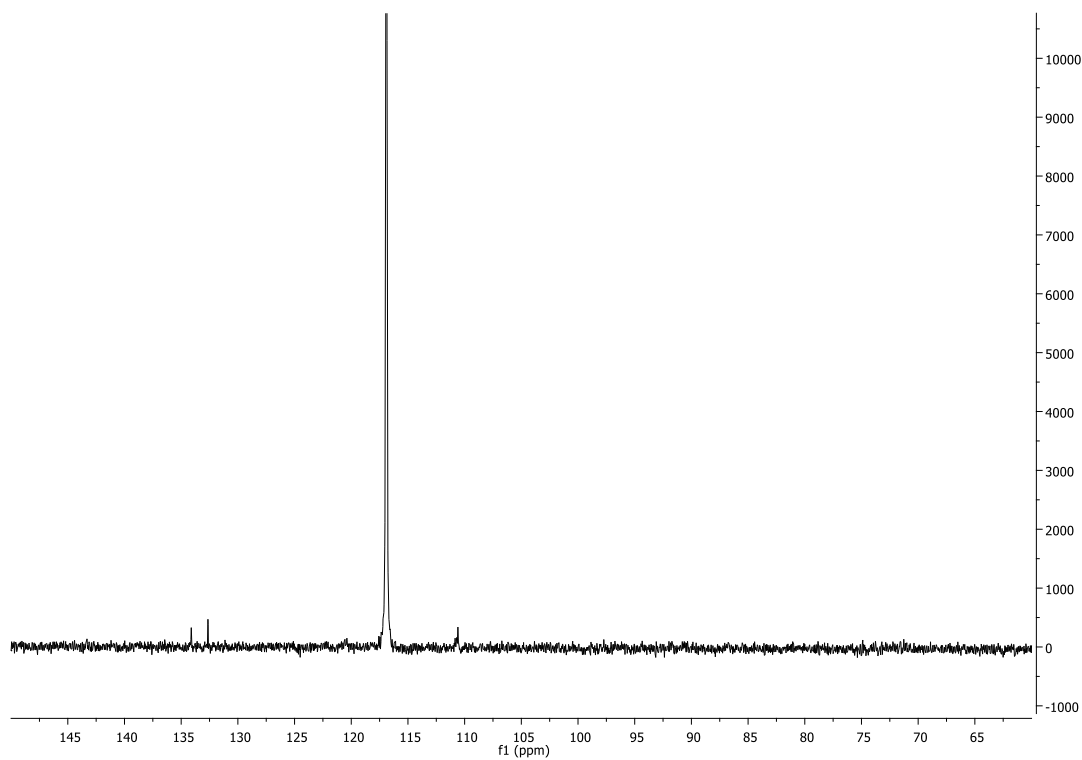


¹³C NMR of 5,6-dimethyl-1-((triisopropylsilyl)ethynyl)-1*H*-benzo[*d*]imidazole

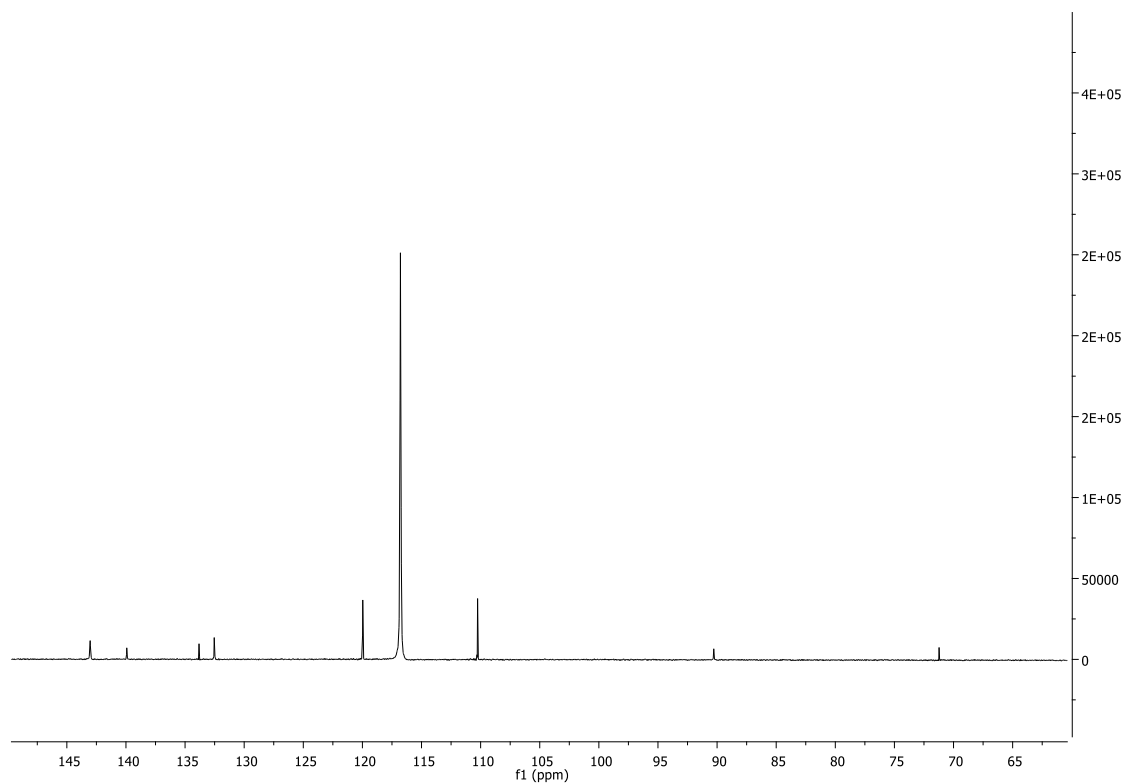


^{13}C NMR of 5,6-dimethyl-1-((triisopropylsilyl)ethynyl)-1*H*-benzo[*d*]imidazole + $\text{Cu}(\text{OAc})_2$

To a solution of 5,6-dimethyl-1-((triisopropylsilyl)ethynyl)-1*H*-benzo[*d*]imidazole (16.3 mg, 0.05 mmol, 1 equiv) in MeCN (0.5 mL) was added $\text{Cu}(\text{OAc})_2$ (16 μL , 0.25 mM solution, 0.005 mmol, 10 mol%). The resulting mixture was analyzed by ^{13}C NMR.

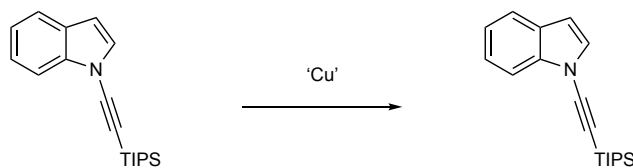


^{13}C NMR of 5,6-dimethyl-1-((triisopropylsilyl)ethynyl)-1*H*-benzo[*d*]imidazole + CuOAc

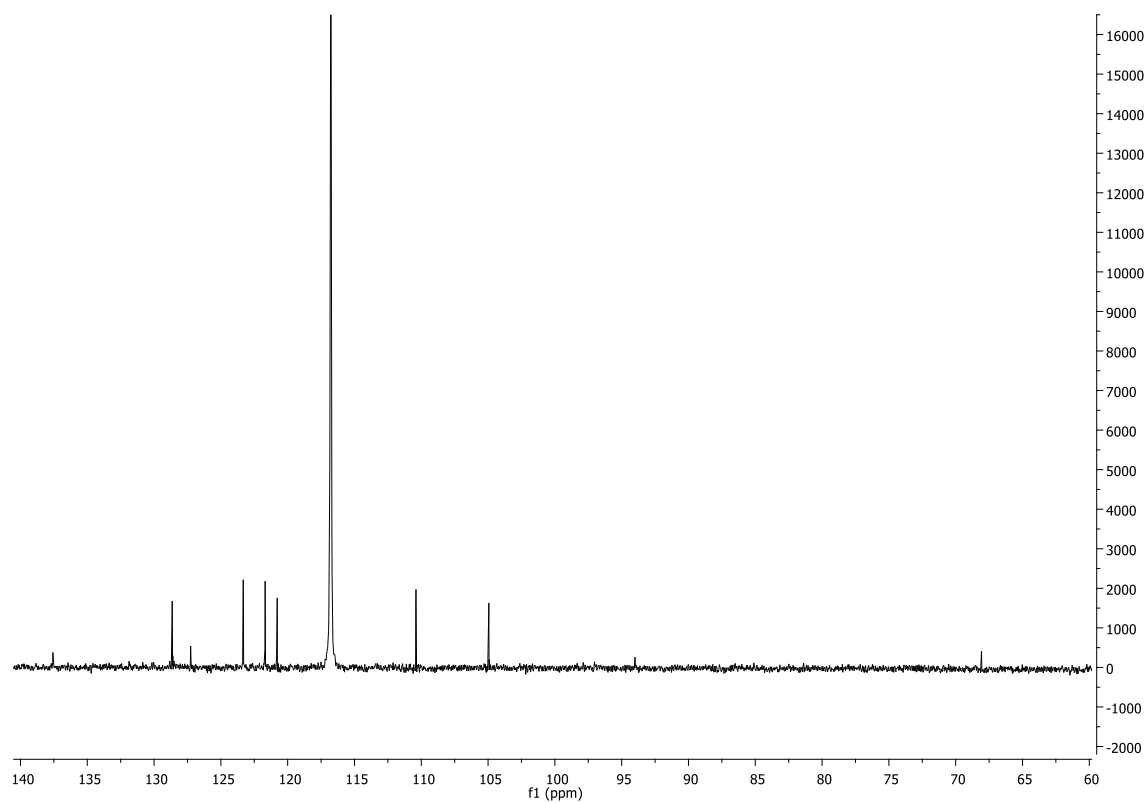


To a solution of 5,6-dimethyl-1-((triisopropylsilyl)ethynyl)-1*H*-benzo[*d*]imidazole (16.3 mg, 0.05 mmol, 1 equiv) in MeCN (0.5 mL) was added CuOAc (0.61 mg, 0.005 mmol, 10 mol%). The resulting mixture was analyzed by ^{13}C NMR.

Reactions of 1-((triisopropylsilyl)ethynyl)-1*H*-indole with Cu salts

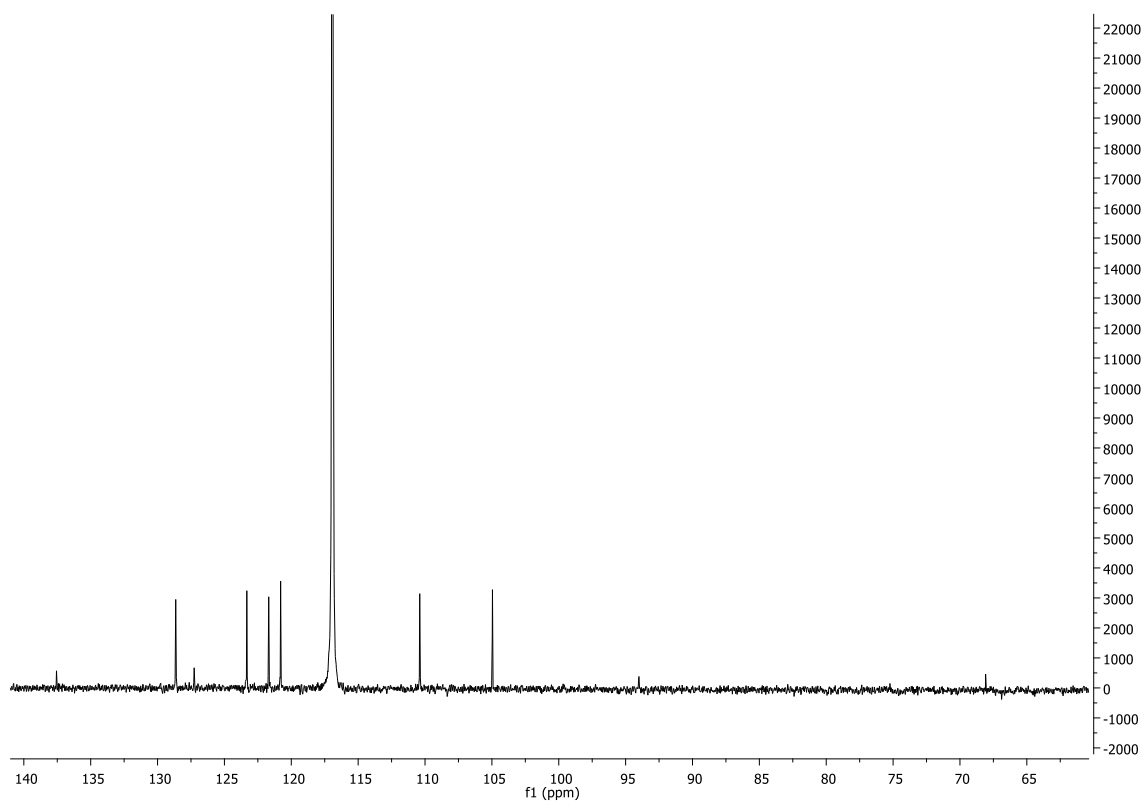


¹³C NMR of 1-((triisopropylsilyl)ethynyl)-1*H*-indole.



¹³C NMR of 1-((triisopropylsilyl)ethynyl)-1*H*-indole + Cu(OAc)₂

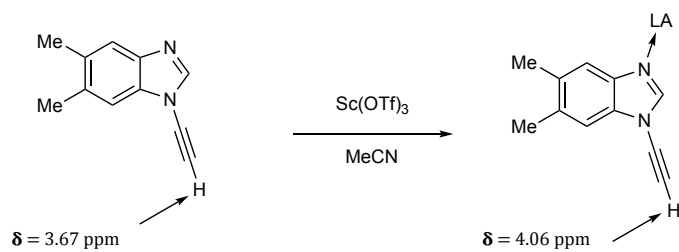
To a solution of 1-((triisopropylsilyl)ethynyl)-1*H*-indole (14.9 mg, 0.05 mmol, 1 equiv) in MeCN (0.5 mL) was added Cu(OAc)₂ (16 μL, 0.25 mM solution, 0.005 mmol, 10 mol%). The resulting mixture was analyzed by ¹³C NMR.



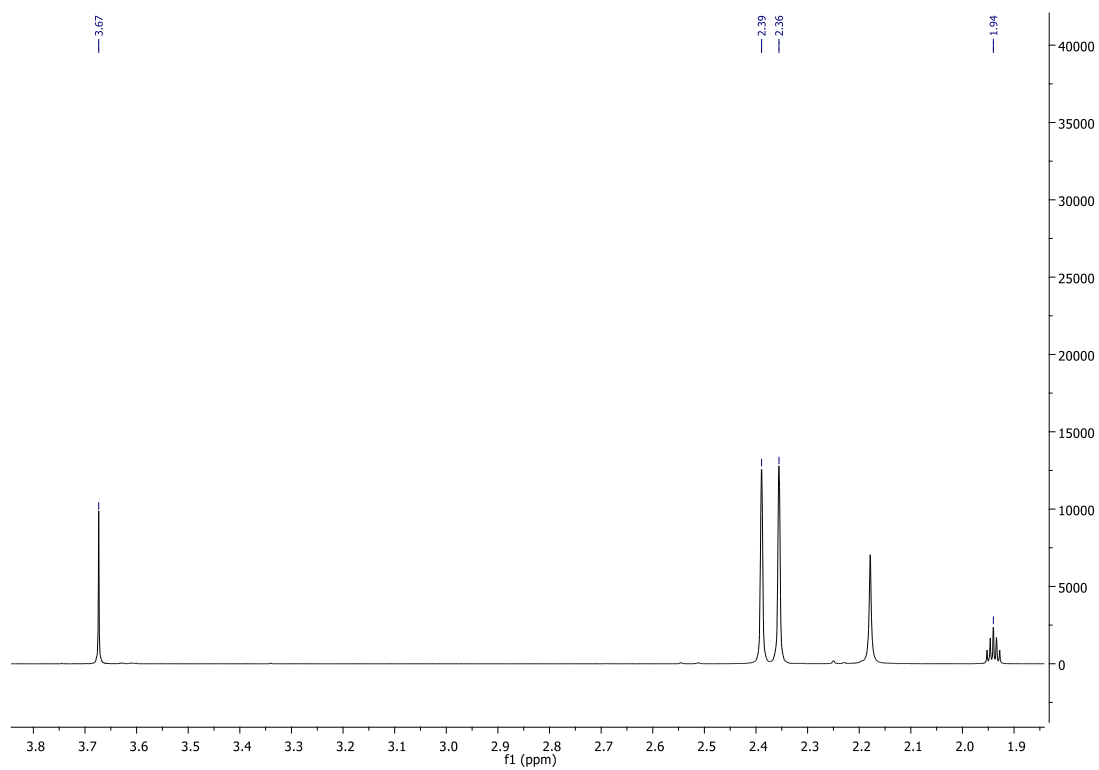
Treatment of 1-ethynyl-5,6-dimethyl-1*H*-benzo[*d*]imidazole with Lewis acids

Sc(OTf)₃

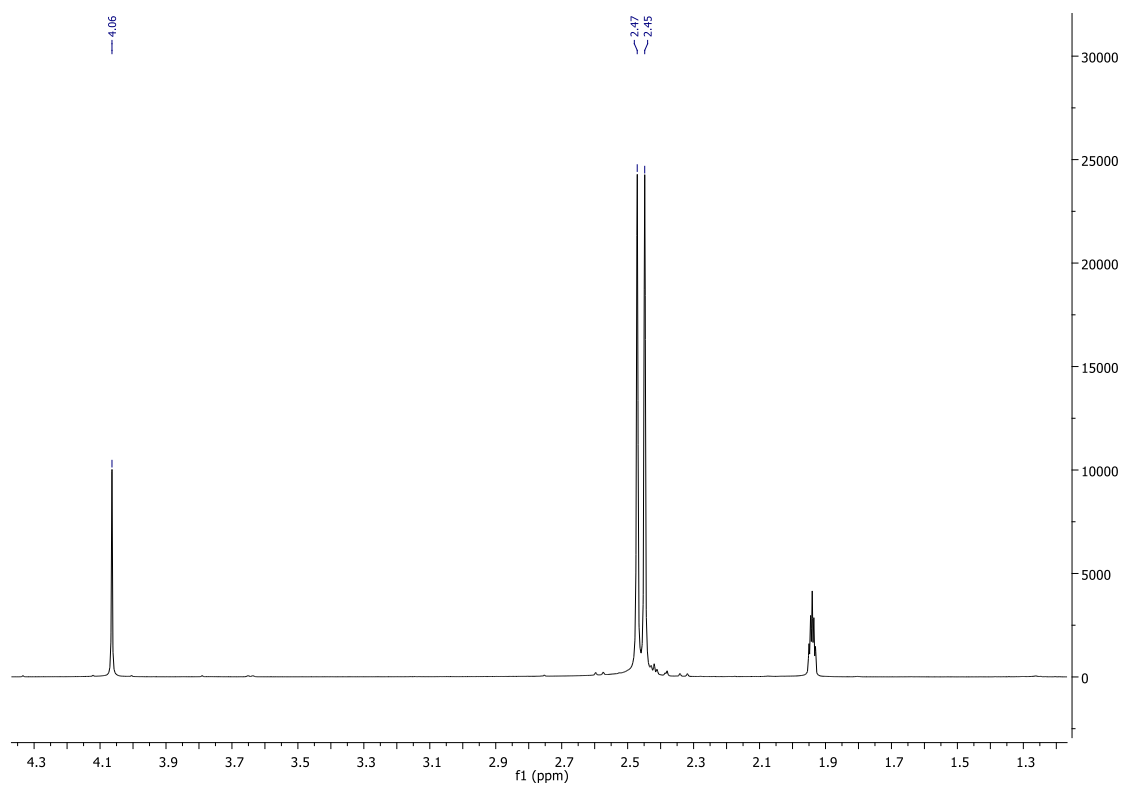
To a solution of 1-ethynyl-5,6-dimethyl-1*H*-benzo[*d*]imidazole (8.5 mg, 0.05 mmol, 1 equiv) in MeCN (0.5 mL) was added Sc(OTf)₃ (24.6 mg, 0.05 mmol, 1 equiv). The resulting mixture was analyzed by ¹H NMR.



^1H NMR before

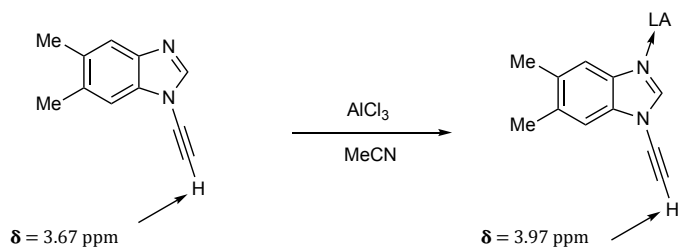


^1H NMR after

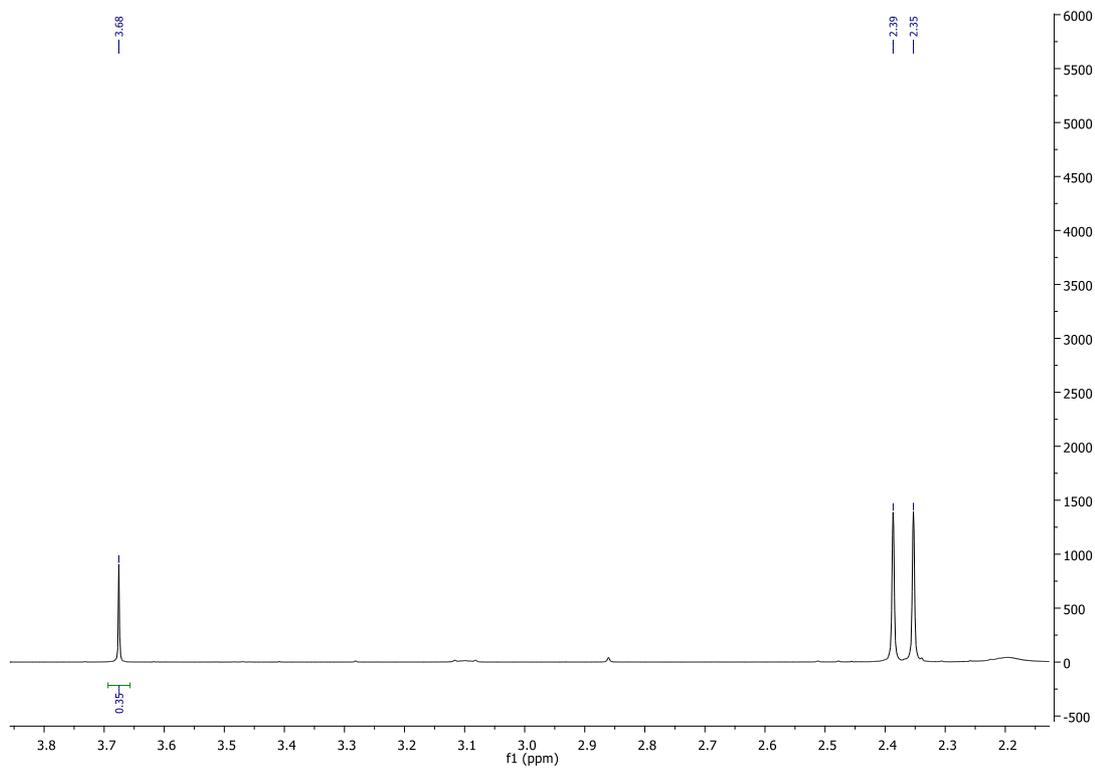


AlCl₃

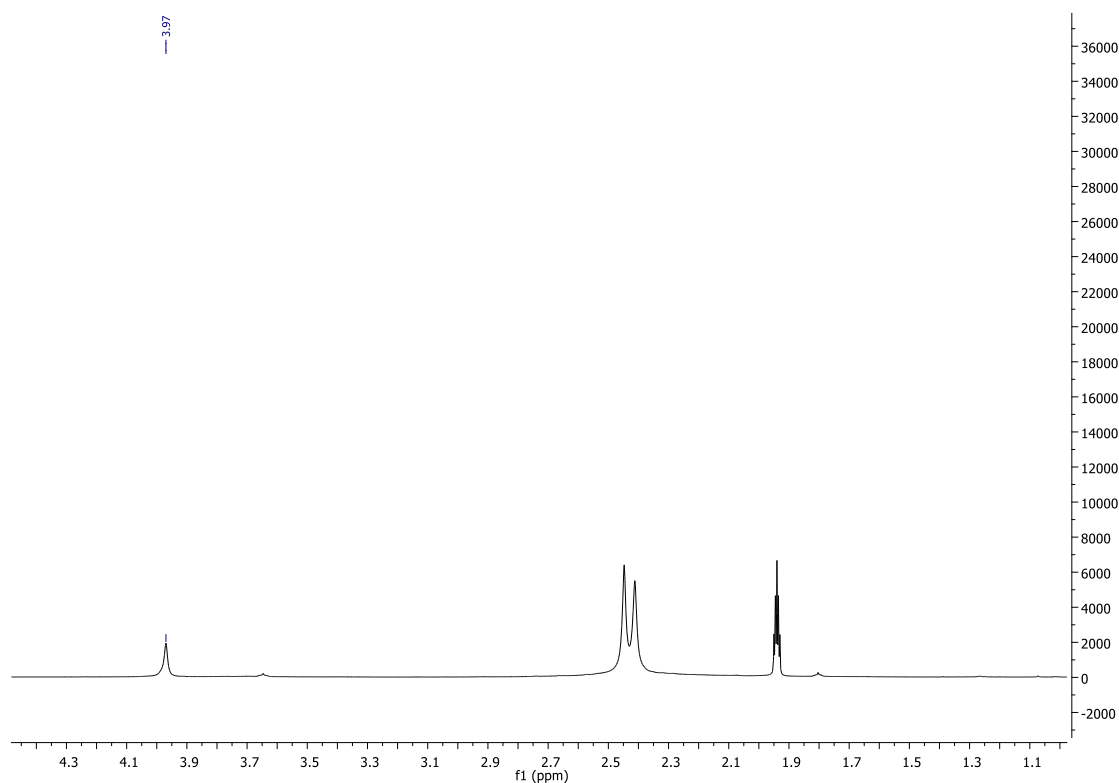
To a solution of 1-ethynyl-5,6-dimethyl-1*H*-benzo[*d*]imidazole (8.5 mg, 0.05 mmol, 1 equiv) in MeCN (0.5 mL) was added AlCl₃ (6.65 mg, 0.05 mmol, 1 equiv). The resulting mixture was analyzed by ¹H NMR.



¹H NMR before



¹H NMR after



Determination of ynamine pK_a by treatment with amine bases

Procedure

To a solution of ynamine (8.5 mg, 0.05 mmol, 1 equiv) in MeCN (0.5 mL) was added amine base (0.05 mmol, 1 equiv) and the reaction was stirred at room temperature for 1 h. The resulting mixture was analysed by ¹H NMR. The extent of deprotonation of the alkyne methine was measured with a range of bases of various pK_a .

pK_a of 2.84

Base	DBU	BEMP	BTPP
pK_a (MeCN) ^[183]	24.3	27.6	28.4
pK_a (H ₂ O)	11.5	-	-
% deprotonation	0%	34%	100%

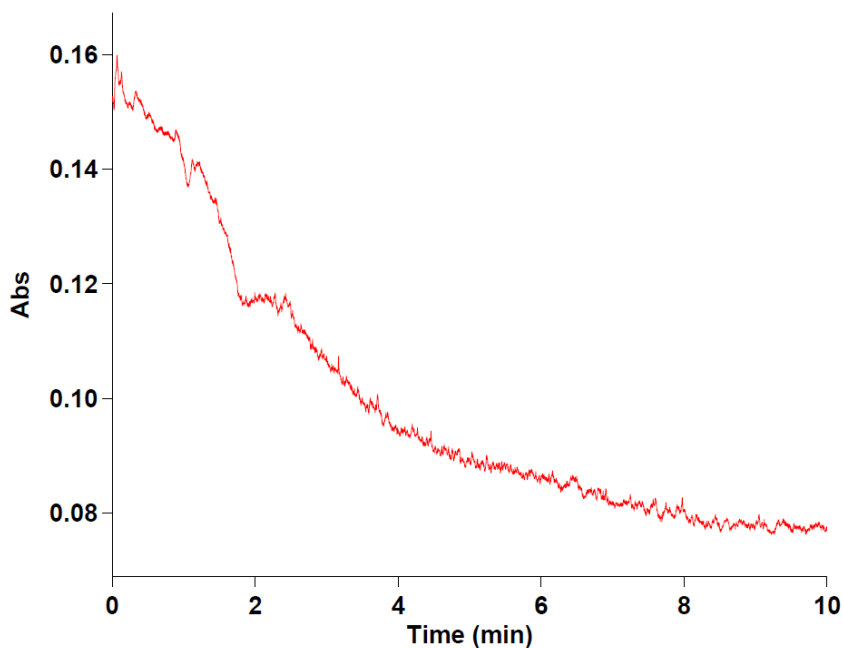
pK_a of 2.92

Base	BEMP	BTPP
pK_a (MeCN) ^[183]	27.6	28.4
% deprotonation	18%	48%

UV/vis measurement of Cu(OAc)₂ persistence

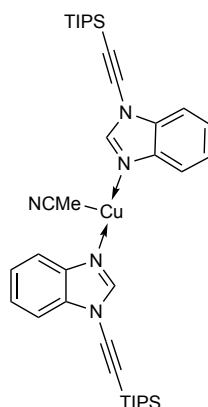
Procedure

To a cuvette containing 1-ethynyl-5,6-dimethyl-1*H*-benzo[*d*]imidazole (17 mg, 0.1 mmol, 1 equiv) and benzyl azide (13.3 mmol, 0.1 mmol, 1 equiv) in MeCN (4 mL) was added Cu(OAc)₂ (16 μL, 0.25 mM solution, 0.005 mmol, 5 mol%) the absorbance at 690 nm was monitored over 10 min.



HRMS determination of chelated intermediates

A mixture of 1-((triisopropylsilyl)ethynyl)-1*H*-benzo[*d*]imidazole (15 mg, 0.05 mmol, 1 equiv) and Cu(OAc)₂ (8 μL, 0.25 mM solution, 0.0025 mmol, 5 mol%) in MeCN (0.5 mL) was analysed by HRMS (XEVO-G2XSQ – 10 min run, formic acid modifier).

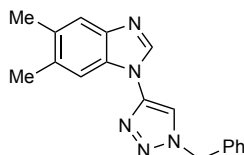


The above copper complex was observed in the reaction media.

HRMS: exact mass calculated for $[M+H]^+$ ($C_{38}H_{55}CuN_5Si_2$) requires m/z 701.3370, found m/z 701.4120.

2.7.7 Compound Characterization

1-(1-Benzyl-1*H*-1,2,3-triazol-4-yl)-5,6-dimethyl-1*H*-benzo[*d*]imidazole, 2.86



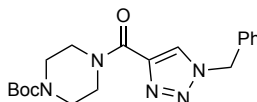
ν_{\max} (neat): 3237, 2919, 2562, 2149, 2008, 1759, 1476, 1409 cm^{-1} .

$^1\text{H NMR}$ (CDCl_3 , 400 MHz): δ 8.20 (s, 1H), 7.67 (s, 1H), 7.58 (s, 1H), 7.45 – 7.38 (m, 3H), 7.38 – 7.31 (m, 2H), 5.62 (s, 2H), 2.37 (s, 6H).

$^{13}\text{C NMR}$ (CDCl_3 , 101 MHz): δ 142.6, 141.8, 139.8, 133.4, 133.0, 131.7, 130.5, 128.9, 128.7, 127.7, 120.1, 112.9, 110.7, 54.6, 20.1, 19.7.

HRMS: exact mass calculated for $[M+H]^+$ ($C_{18}H_{17}N_5$) requires m/z 304.1557, found m/z 304.1557.

tert-Butyl 4-(1-benzyl-1*H*-1,2,3-triazole-4-carbonyl)piperazine-1-carboxylate, 2.87^[151]

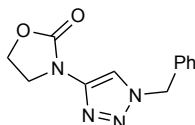


$^1\text{H NMR}$ (CDCl_3 , 400 MHz): δ 7.99 (s, 1H), 7.39 – 7.34 (m, 3H), 7.32 – 7.27 (m, 2H), 5.53 (s, 2H), 4.33 – 4.22 (m, 2H), 3.75 – 3.67 (m, 2H), 3.56 – 3.44 (m, 4H), 1.47 (s, 9H).

$^{13}\text{C NMR}$ (CDCl_3 , 101 MHz): δ 159.4, 154.1, 143.9, 133.2, 128.8, 128.6, 127.9, 79.7, 53.9, 46.0, 42.1, 27.9.

Data consistent with previously reported spectra.^[151]

3-(1-Benzyl-1*H*-1,2,3-triazol-4-yl)oxazolidin-2-one, 2.88^[152]

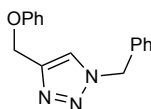


$^1\text{H NMR}$ (CDCl_3 , 400 MHz): δ 7.84 (s, 1H), 7.40 – 7.34 (m, 3H), 7.31 – 7.26 (m, 2H), 5.50 (s, 2H), 4.56 (dd, $J = 8.9, 7.3$ Hz, 2H), 4.25 (dd, $J = 8.9, 7.3$ Hz, 2H).

$^{13}\text{C NMR}$ (CDCl_3 , 101 MHz): δ 154.9, 144.0, 134.4, 129.2, 128.9, 128.2, 111.9, 63.4, 54.9, 43.7.

Data consistent with previously reported spectra.^[152]

1-Benzyl-4-(phoxymethyl)-1*H*-1,2,3-triazole, 2.89^[184]

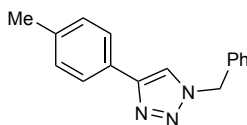


$^1\text{H NMR}$ (CDCl_3 , 400 MHz): δ 7.49 (s, 1H), 7.37 – 7.30 (m, 2H), 7.26 – 7.20 (m, 5H), 6.97 – 6.88 (m, 3H), 5.49 (s, 2H), 5.15 (s, 2H).

$^{13}\text{C NMR}$ (CDCl_3 , 101 MHz): δ 157.7, 144.1, 134.0, 129.0, 128.7, 128.3, 127.6, 122.1, 120.8, 114.3, 61.5, 53.7.

Data consistent with previously reported spectra.^[184]

1-Benzyl-4-(*p*-tolyl)-1*H*-1,2,3-triazole, 2.90^[185]

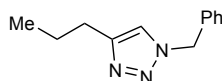


$^1\text{H NMR}$ (CDCl_3 , 500 MHz): δ 7.68 (d, $J = 8.1$ Hz, 2H), 7.63 (s, 1H), 7.40 – 7.33 (m, 3H), 7.31 – 7.28 (m, 2H), 7.19 (d, $J = 7.9$ Hz, 2H), 5.54 (s, 2H), 2.35 (s, 3H).

$^{13}\text{C NMR}$ (CDCl_3 , 101 MHz): δ 147.8, 137.5, 134.3, 129.0, 128.6, 128.2, 127.6, 127.2, 125.1, 118.8, 53.7, 20.8.

Data consistent with previously reported spectra.^[185]

1-Benzyl-4-propyl-1*H*-1,2,3-triazole, 2.91^[186]

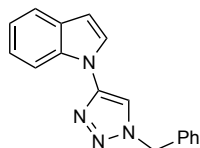


$^1\text{H NMR}$ (CDCl_3 , 400 MHz): δ 7.24 – 7.17 (m, 4H), 7.13 (m, 2H), 5.36 (s, 2H), 2.54 (t, $J = 7.6$ Hz, 2H), 1.60 – 1.48 (m, 2H), 0.82 (t, $J = 7.4$ Hz, 3H).

$^{13}\text{C NMR}$ (CDCl_3 , 101 MHz): δ 148.0, 134.6, 128.4, 127.9, 127.3, 120.4, 53.2, 27.1, 22.0, 13.2.

Data consistent with previously reported spectra.^[186]

1-(1-Benzyl-1*H*-1,2,3-triazol-4-yl)-1*H*-indole, 2.93



ν_{\max} (neat): 3125, 3053, 2350, 1569, 1454 cm^{-1} .

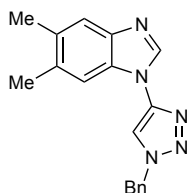
$^1\text{H NMR}$ (CDCl_3 , 400 MHz): δ 7.72 (dd, $J = 8.2, 0.7$ Hz, 1H), 7.68 (d, $J = 7.8$ Hz, 1H), 7.61 – 7.57 (m, 2H), 7.47 – 7.39 (m, 3H), 7.39 – 7.33 (m, 2H), 7.32 – 7.26 (m, 1H), 7.25 – 7.18 (m, 1H), 6.70 (d, $J = 3.4$ Hz, 1H), 5.61 (s, 2H).

$^{13}\text{C NMR}$ (CDCl_3 , 101 MHz): δ 145.32, 134.6, 133.8, 128.9, 128.8, 128.5, 127.6, 125.9, 122.5, 120.7, 120.5, 112.2, 110.7, 104.3, 54.4.

HRMS: exact mass calculated for $[\text{M}+\text{H}]^+$ ($\text{C}_{17}\text{H}_{15}\text{N}_4$) requires m/z 275.1291, found m/z 275.1296.

2.7.8 Products from Scheme 122

1-(1-Benzyl-1*H*-1,2,3-triazol-4-yl)-5,6-dimethyl-1*H*-benzo[*d*]-imidazole (2.86).



Prepared using General Procedure 2E. White solid (31 mg, 66%). Purification on silica gel using hexane/EtOAc 3/7.

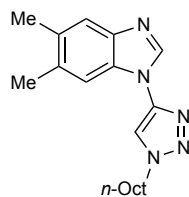
ν_{\max} (neat): 3086, 2922, 2854, 1724, 1584, 1495, 1459, 1407, 1284, 1213, 1053, 867, 718 cm^{-1} .

$^1\text{H NMR}$ (CDCl_3 , 400 MHz): δ 8.20 (br. s, 1H), 7.67 (s, 1H), 7.58 (br. s, 1H), 7.39–7.45 (m, 4H), 7.37–7.34 (m, 2H), 5.62 (s, 2H), 2.37 (s, 6H).

$^{13}\text{C NMR}$ (CDCl_3 , 100 MHz): δ 143.2, 142.4, 140.4, 134.0, 133.6, 132.2, 131.1, 129.5, 129.3, 128.3, 120.7, 113.5, 111.3, 55.2, 20.7, 20.3.

HRMS: exact mass calculated for $[\text{M}+\text{H}]^+$ ($\text{C}_{18}\text{H}_{18}\text{N}_5$) requires m/z 304.1557, found m/z 304.1551.

5,6-Dimethyl-1-(1-octyl-1*H*-1,2,3-triazol-4-yl)-1*H*-benzo[*d*]-imidazole (2.102b).



Prepared using General Procedure 2E. White solid (88 mg, 98%). Purification on silica gel using hexane/EtOAc 3/7.

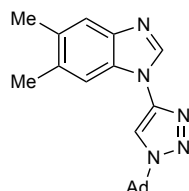
ν_{\max} (neat): 3135, 2924, 2857, 1740, 1597, 1500, 1470, 1383, 1292, 1206, 1156, 1091, 1053, 1033, 949, 869, 785 cm^{-1} .

$^1\text{H NMR}$ (CDCl_3 , 500 MHz): δ 8.62 (br. s, 1H), 7.77–7.68 (m, 3H), 4.45 (t, $J = 7.1$ Hz, 2H), 2.40 (s, 3H), 2.38 (s, 3H), 2.00 (app. quint, $J = 6.6$ Hz, 2H), 1.40–1.26 (m, 10H), 0.87 (t, $J = 7.2$ Hz, 3H).

$^{13}\text{C NMR}$ (CDCl_3 , 100 MHz): δ 133.9, 132.0, 113.8, 51.5, 31.8, 30.4, 29.8, 29.2, 29.1, 26.6, 22.7, 20.7, 20.4, 14.2.

HRMS: exact mass calculated for $[\text{M}+\text{H}]^+$ ($\text{C}_{19}\text{H}_{28}\text{N}_5$) requires m/z 326.2339, found m/z 326.2323.

1-(1-((3s,5s,7s)-Adamantan-1-yl)-1H-1,2,3-triazol-4-yl)-5,6-di-methyl-1H-benzo[d]imidazole (**2.102c**).



Prepared using General Procedure 2E. White solid (95 mg, 99%). Purification on silica gel using hexane/EtOAc 3/7.

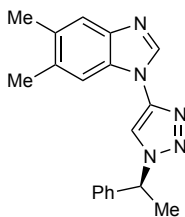
ν_{\max} (neat): 3080, 2917, 2852, 1725, 1586, 1495, 1467, 1448, 1281, 1216, 1149, 1019, 948, 861, 844 cm^{-1} .

$^1\text{H NMR}$ (CDCl_3 , 400 MHz): δ 8.22 (br. s, 1H), 7.82 (s, 1H), 7.60 (s, 1H), 7.47 (s, 1H), 2.39 (s, 3H), 2.38 (s, 3H), 2.33 (br. s, 9H), 1.83 (br. s, 6H).

$^{13}\text{C NMR}$ (CDCl_3 , 100 MHz): δ 142.4, 142.1, 140.7, 133.5, 132.1, 131.4, 120.7, 111.4, 110.6, 61.0, 43.1, 35.9, 29.8, 29.6, 20.7, 20.4.

HRMS: exact mass calculated for $[\text{M}+\text{H}]^+$ ($\text{C}_{21}\text{H}_{26}\text{N}_5$) requires m/z 348.2183, found m/z 348.2179.

(*S*)-5,6-Dimethyl-1-(1-(1-phenylethyl)-1*H*-1,2,3-triazol-4-yl)-1*H*-benzo[*d*]imidazole (2.102d).



Prepared using General Procedure 2E. White solid (46 mg, 95%). Purification on silica gel using hexane/EtOAc 3/7.

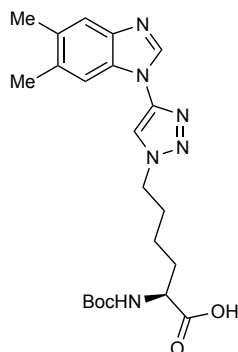
ν_{\max} (neat): 3110, 2926, 2857, 1724, 1590, 1498, 1459, 1383, 1286, 1212, 1143, 910, 731 cm^{-1} .

$^1\text{H NMR}$ (CDCl_3 , 400 MHz): δ 8.20 (br. s, 1H), 7.63 (s, 1H), 7.59 (br. s, 1H), 7.45–7.35 (m, 6H), 5.88 (q, $J = 7.0$ Hz, 1H), 2.37 (s, 6H), 2.09 (d, $J = 7.1$ Hz, 3H).

$^{13}\text{C NMR}$ (CDCl_3 , 100 MHz): δ 139.3, 133.6, 132.3, 129.4, 126.7, 120.7, 112.6, 111.5, 61.5, 29.8, 21.3, 20.7, 20.4. Four signals not observed/coincident.

HRMS: exact mass calculated for $[\text{M}+\text{H}]^+$ ($\text{C}_{19}\text{H}_{20}\text{N}_5$) requires m/z 318.1713, found m/z 318.1704.

(*S*)-2-((*tert*-Butoxycarbonyl)amino)-6-(4-(5,6-dimethyl-1*H*-benzo[*d*]imidazol-1-yl)-1*H*-1,2,3-triazol-1-yl)hexanoic acid (2.102e).



Prepared using General Procedure 2E. Yellow solid (56 mg, 94%). Purification on silica gel using DCM/MeOH 9/1 + 0.01% AcOH.

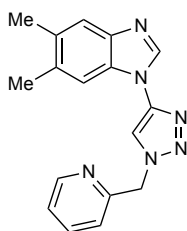
ν_{\max} (neat): 3382, 3127, 2974, 2867, 2485, 2233, 2071, 1686, 1591, 1422, 1392, 1368, 1247, 1165, 1119, 1052, 974 cm^{-1} .

$^1\text{H NMR}$ (MeOD, 400 MHz): δ 9.80 (br. s, 1H), 8.79 (s, 1H), 7.91 (s, 1H), 7.71 (s, 1H), 4.60 (br. s, 2H), 4.08 (br. s, 1H), 2.48 (s, 6H), 2.08 (br. s, 2H), 1.89 (br. s, 1H), 1.74 (br. s, 1H), 1.51 (br. s, 2H), 1.41 (s, 9H).

^{13}C NMR (MeOD, 100 MHz): δ 175.9, 158.1, 141.0, 139.2, 138.9, 119.9, 116.0, 114.8, 80.4, 54.6, 52.4, 32.2, 30.6, 28.7, 23.9, 20.7, 20.5. Two signals not observed/coincident.

HRMS: exact mass calculated for $[\text{M}+\text{H}]^+$ ($\text{C}_{22}\text{H}_{31}\text{N}_6\text{O}_4$) requires m/z 443.2401, found m/z 443.2389.

5,6-Dimethyl-1-(1-(pyridin-2-ylmethyl)-1*H*-1,2,3-triazol-4-yl)-1*H*-benzo[*d*]imidazole (**2.102f**).



Prepared using General Procedure 2E. Yellow oil (83 mg, 99%). Purification on silica gel using hexane/EtOAc 3/7.

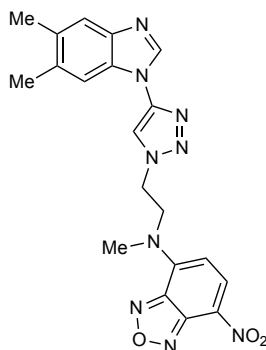
ν_{max} (neat): 3105, 2960, 2917, 2852, 1586, 1502, 1465, 1435 cm^{-1} .

^1H NMR (CDCl_3 , 500 MHz): δ 8.61 (d, $J = 4.5$ Hz, 1H), 8.24 (s, 1H), 8.03 (s, 1H), 7.72 (dt, $J = 7.7, 1.7$ Hz, 1H), 7.57 (s, 1H), 7.45 (s, 1H), 7.33 (d, $J = 7.7$ Hz, 1H), 7.29 (m, 1H), 5.72 (s, 2H), 2.36 (s, 6H).

^{13}C NMR (CDCl_3 , 100 MHz): δ 153.6, 150.1, 143.0, 142.3, 140.4, 137.6, 133.6, 133.5, 133.4, 132.3, 132.2, 132.1, 131.0, 123.8, 122.8, 120.6, 114.3, 111.3.

HRMS: exact mass calculated for $[\text{M}+\text{H}]^+$ ($\text{C}_{17}\text{H}_{17}\text{N}_6$) requires m/z 305.1509, found m/z 305.1508.

N-(2-(4-(5,6-Dimethyl-1*H*-benzo[*d*]imidazol-1-yl)-1*H*-1,2,3-triazol-1-yl)ethyl)-*N*-methyl-7-nitrobenzo[*c*][1,2,5]oxadiazol-4-amine (**2.102g**).



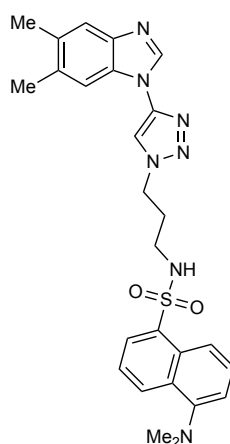
Prepared using General Procedure 2E. Red solid (119 mg, 95%). Purification on silica gel using hexane/EtOAc 1/9.

ν_{\max} (neat): 3599, 3108, 3082, 2917, 2852, 1613, 1597, 1550, 1424, 1288, 1216, 1149, 1087, 1002, 918, 732 cm^{-1} .

$^1\text{H NMR}$ (CDCl_3 , 400 MHz): δ 8.48 (m, 2H), 7.63 (s, 1H), 7.49 (br. s, 1H), 6.38 (d, $J = 9.3$ Hz, 1H), 4.98 (t, $J = 4.5$ Hz, 2H), 3.45–3.42 (m, 2H), 2.39 (d, $J = 4.7$ Hz, 6H), 2.03 (s, 3H). One signal not observed/coincident.

HRMS: exact mass calculated for $[\text{M}+\text{H}]^+$ ($\text{C}_{20}\text{H}_{20}\text{N}_9\text{O}_3$) requires m/z 434.1684, found m/z 434.1613.

N-(3-(4-(5,6-Dimethyl-1*H*-benzo[*d*]imidazol-1-yl)-1*H*-1,2,3-triazol-1-yl)propyl)-5-(dimethylamino)naphthalene-1-sulfonamide (**2.102g**).



Prepared using General Procedure 2E. Yellow solid (43 mg, 92%). Purification on silica gel using DCM/MeOH 9/1.

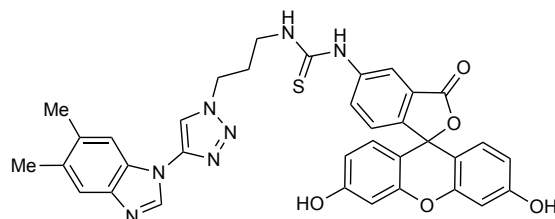
ν_{\max} (neat): 3127, 2924, 2857, 2794, 1750, 1597, 1457, 1396, 1325, 1312, 1234, 1146, 1092, 1042, 951, 789 cm^{-1} .

$^1\text{H NMR}$ (CDCl_3 , 500 MHz): δ 8.52 (d, $J = 8.6$ Hz, 1H), 8.27 (d, $J = 8.6$ Hz, 1H), 8.24 (s, 1H), 8.21 (d, $J = 8.6$ Hz, 1H), 7.80 (s, 1H), 7.61 (s, 1H), 7.55 (t, $J = 7.6$ Hz, 1H), 7.50–7.46 (m, 2H), 7.16 (d, $J = 7.6$ Hz, 1H), 5.38 (t, $J = 6.5$ Hz, 1H), 4.54 (t, $J = 5.5$ Hz, 2H), 2.94 (q, $J = 6.2$ Hz, 2H), 2.86 (s, 6H), 2.39 (s, 6H), 2.15 (m, 2H).

$^{13}\text{C NMR}$ (CDCl_3 , 100 MHz): δ 152.4, 142.6, 142.4, 140.5, 134.2, 133.8, 132.4, 131.0, 130.1, 129.9, 129.6, 128.9, 123.4, 120.7, 118.3, 115.5, 114.7, 111.4, 47.7, 45.5, 39.9, 30.2, 20.7, 20.4.

HRMS: exact mass calculated for $[\text{M}+\text{H}]^+$ ($\text{C}_{26}\text{H}_{30}\text{N}_7\text{O}_2\text{S}$) requires m/z 504.2176, found m/z 504.2153.

1-(3',6'-Dihydroxy-3-oxo-3*H*-spiro[isobenzofuran-1,9'-xanthen]-5-yl)-3-(3-(4-(5,6-dimethyl-1*H*-benzo[*d*]imidazol-1-yl)-1*H*-1,2,3-triazol-1-yl)propyl)thiourea (**2.102h**).



Prepared using General Procedure 2E. Red solid (66 mg, 85%). Purification on silica gel using DCM/MeOH 9/1).

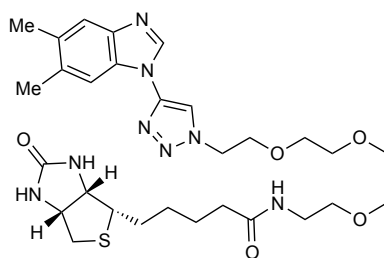
ν_{\max} (neat): 2924, 2113, 1716, 1593, 1541, 1457, 1381, 1303, 1245, 1210, 854 cm^{-1} .

$^1\text{H NMR}$ (DMSO- d_6 , 400 MHz): δ 9.32 (br. s, 1H), 9.00 (s, 1H), 8.45 (s, 1H), 7.86 (d, $J = 8.0$ Hz, 1H), 7.82 (s, 1H), 7.65–7.62 (m, 2H), 7.16 (d, $J = 8.3$ Hz, 1H), 6.72–6.68 (m, 2H), 6.60–6.56 (m, 3H), 4.66 (t, $J = 6.9$ Hz, 2H), 3.51 (s, 2H), 3.16 (s, 2H), 2.40 (s, 3H), 2.38 (s, 3H).

HRMS: exact mass calculated for $[\text{M}-\text{H}]^-$ ($\text{C}_{35}\text{H}_{28}\text{N}_7\text{O}_5\text{S}$) requires m/z 658.1878, found m/z 642.1632 $[\text{M}-\text{OH}]^-$.

$^{13}\text{C NMR}$ could not be obtained due to relaxation issues.

N-(2-(2-(2-(2-(4-(5,6-Dimethyl-1*H*-benzo[*d*]imidazol-1-yl)-1*H*-1,2,3-triazol-1-yl)ethoxy)ethoxy)ethoxy)ethyl)-5-((3*aS*,4*S*,6*aR*)-2-oxohexahydro-1*H*-thieno[3,4-*d*]imidazol-4-yl)pentanamide (**2.102i**).



Prepared using General Procedure 2E. White solid (24 mg, 87%). Purification on silica gel using DCM/MeOH 9/1.

ν_{\max} (neat): 3375, 3124, 2922, 2867, 2470, 2068, 1690, 1645, 1591, 1454, 1098, 1055 cm^{-1} .

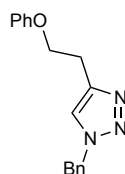
$^1\text{H NMR}$ (MeOD, 400 MHz): δ 8.52 (s, 2H), 7.63 (br. s, 1H), 7.55 (br. s, 1H), 4.71 (t, $J = 5.2$ Hz, 2H), 4.45 (dd, $J = 7.8, 4.9$ Hz, 1H), 4.25 (dd, $J = 7.9, 4.5$ Hz, 1H), 3.99 (t, $J = 4.9$ Hz, 2H), 3.69–3.66 (m, 2H), 3.64–3.62 (m, 2H), 3.58–3.55 (m, 2H), 3.49–3.47 (m, 2H), 3.38 (t, $J = 5.4$ Hz, 2H), 3.24 (t, $J = 5.4$ Hz, 2H), 3.17–3.12 (m,

1H), 2.88 (dd, $J = 12.8, 5.0$ Hz, 1H), 2.68 (d, $J = 12.7$ Hz, 1H), 2.41 (s, 3H), 2.40 (s, 3H), 2.17–2.13 (m, 2H), 1.73–1.50 (m, 4H), 1.42–1.34 (m, 2H).

^{13}C NMR (MeOD, 100 MHz): δ 176.0, 166.1, 135.2, 133.9, 120.6, 118.2, 112.9, 71.5, 71.4, 71.1, 70.5, 63.3, 61.6, 57.0, 52.3, 41.0, 40.2, 36.7, 29.7, 29.4, 26.8, 20.7, 20.3.

HRMS: exact mass calculated for $[\text{M}+\text{H}]^+$ ($\text{C}_{28}\text{H}_{43}\text{N}_8\text{O}_5\text{S}$) requires m/z 615.3072, found m/z 615.3149.

1-Benzyl-4-(2-phenoxyethyl)-1*H*-1,2,3-triazole (**2.103a**).



Prepared using General Procedure 2F. White solid (81 mg, quant). Purification on silica gel using hexane/EtOAc 3/7.

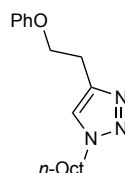
ν_{max} (neat): 3120, 3071, 3038, 2958, 2935, 1604, 1590, 1496, 1459, 1251, 1219, 1176, 1059, 1042, 890, 828, 789, 752, 720 cm^{-1} .

^1H NMR (CDCl_3 , 400 MHz): δ 7.40–7.34 (m, 4H), 7.29–7.26 (m, 2H), 7.25–7.24 (m, 2H), 6.94 (tt, $J = 7.4, 1.1$ Hz), 6.89–6.85 (m, 2H), 5.50 (s, 2H), 4.23 (t, $J = 6.5$ Hz, 2H), 3.19 (t, $J = 6.5$ Hz, 2H).

^{13}C NMR (CDCl_3 , 100 MHz): δ 158.8, 135.0, 129.6, 129.2, 128.8, 128.1, 122.0, 121.1, 114.7, 66.8, 54.2, 26.4.

HRMS: exact mass calculated for $[\text{M}+\text{Na}]^+$ ($\text{C}_{17}\text{H}_{17}\text{N}_3\text{ONa}$) requires m/z 302.1264, found m/z 302.1256.

1-Octyl-4-(2-phenoxyethyl)-1*H*-1,2,3-triazole (**2.103b**).



Prepared using General Procedure 2F. White solid (78 mg, 94%). Purification on silica gel using hexane/EtOAc 3/7.

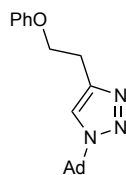
ν_{max} (neat): 3142, 2956, 2922, 2852, 1604, 1591, 1500, 1487, 1388, 1247, 1217, 1176, 1057, 1035, 886, 817, 756, 694 cm^{-1} .

¹H NMR (CDCl₃, 400 MHz): δ 7.41 (s, 1H), 7.29–7.25 (m, 2H), 6.96–6.89 (m, 3H), 4.30 (t, *J* = 7.2 Hz, 2H), 4.24 (t, *J* = 6.5 Hz, 2H), 3.21 (t, *J* = 6.5 Hz, 2H), 1.87 (app. quint, *J* = 7.1 Hz, 2H), 1.30–1.25 (m, 10H), 0.87 (t, *J* = 6.6 Hz, 3H).

¹³C NMR (CDCl₃, 100 MHz): δ 158.7, 144.6, 129.6, 121.7, 121.0, 114.6, 66.8, 50.3, 31.8, 30.4, 29.1, 29.0, 26.6, 26.3, 22.7, 14.1.

HRMS: exact mass calculated for [M+Na]⁺ (C₁₈H₂₇N₃ONa) requires *m/z* 324.2046, found *m/z* 324.2035.

1-((3s,5s,7s)-Adamantan-1-yl)-4-(2-phenoxyethyl)-1*H*-1,2,3-triazole (**2.103c**).



Prepared using General Procedure 2F. White solid (81 mg, quant). Purification on silica gel using hexane/EtOAc 3/7.

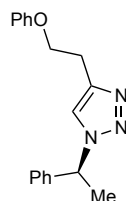
v_{max} (neat): 2909, 2857, 1599, 1590, 1556, 1500, 1476, 1457, 1420, 1348, 1292, 1243, 1035, 1016, 780, 759, 694 cm⁻¹.

¹H NMR (CDCl₃, 400 MHz): δ 7.49 (s, 1H), 7.30–7.28 (m, 2H), 7.00–6.90 (m, 3H), 4.25 (t, *J* = 6.6 Hz, 2H), 3.22 (t, *J* = 6.6 Hz, 2H), 2.25–2.23 (m, 9H), 1.82–1.75 (m, 6H).

¹³C NMR (CDCl₃, 100 MHz): δ 158.9, 143.7, 129.6, 121.0, 118.2, 114.7, 67.1, 59.4, 43.1, 36.1, 29.6, 26.5.

HRMS: exact mass calculated for [M+Na]⁺ (C₂₀H₂₅N₃ONa) requires *m/z* 346.1890, found *m/z* 346.1881.

(*S*)-4-(2-Phenoxyethyl)-1-(1-phenylethyl)-1*H*-1,2,3-triazole (**2.103d**).



Prepared using General Procedure 2F. White solid (67 mg, 84%). Purification on silica gel using hexane/EtOAc 3/7).

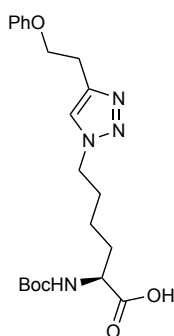
v_{max} (neat): 3170, 3066, 3030, 3045, 2941, 2924, 2870, 1604, 1588, 1498, 1463, 1387, 1366, 1305, 1251, 1038, 811, 756, 733, 705, 694 cm⁻¹.

¹H NMR (CDCl₃, 400 MHz): δ 7.38–7.32 (m, 8H), 6.94 (tt, *J* = 7.4, 1.1 Hz, 1H), 6.88–6.85 (m, 2H), 5.78 (q, *J* = 7.2 Hz, 1H), 4.23 (t, *J* = 6.5 Hz, 2H), 3.19 (t, *J* = 6.5 Hz, 2H), 1.97 (d, *J* = 7.1 Hz, 3H).

¹³C NMR (CDCl₃, 100 MHz): δ 158.7, 144.6, 140.2, 129.6, 129.1, 128.5, 126.6, 121.0, 120.8, 114.7, 66.8, 60.2, 25.4, 21.4.

HRMS: exact mass calculated for [M+Na]⁺ (C₁₈H₁₉N₃O₃Na) requires *m/z* 316.1420, found *m/z* 316.1410.

(*S*)-2-((*tert*-Butoxycarbonyl)amino)-6-(4-(2-phenoxyethyl)-1*H*-1,2,3-triazol-1-yl)hexanoic acid (**2.103e**).



Prepared using General Procedure 2F. White solid (46 mg, 82%). Purification on silica gel using DCM/MeOH 9/1, 0.1% AcOH.

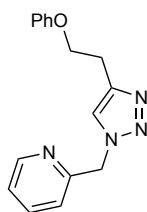
ν_{\max} (neat): 3398, 2952, 2922, 2868, 2482, 2242, 2071, 1688, 1600, 1368, 1167, 1119, 974 cm⁻¹.

¹H NMR (MeOD, 500 MHz): δ 7.83 (br. s, 1H), 7.24 (t, *J* = 7.8 Hz, 2H), 6.92–6.89 (m, 3H), 4.37 (t, *J* = 7.1 Hz, 2H), 4.22 (t, *J* = 6.5 Hz, 2H), 4.08–4.05 (m, 1H), 3.15 (t, *J* = 6.4 Hz, 2H), 1.94–1.89 (m, 2H), 1.87–1.80 (m, 2H), 1.70–1.55 (m, 2H), 1.42 (s, 9H).

¹³C NMR (MeOD, 100 MHz): δ 176.0, 158.1, 130.5, 121.9, 115.6, 80.5, 67.7, 54.6, 52.2, 51.1, 32.3, 32.2, 29.4, 28.7, 26.9, 23.9.

HRMS: exact mass calculated for [M+Na]⁺ (C₂₁H₃₀N₄O₅Na) requires *m/z* 441.2108, found *m/z* 441.2102.

2-((4-(2-Phenoxyethyl)-1*H*-1,2,3-triazol-1-yl)methyl)pyridine (**2.103f**).



Prepared using General Procedure 2F. White solid (60 mg, 79%). Purification on silica gel using hexane/EtOAc 3/7.

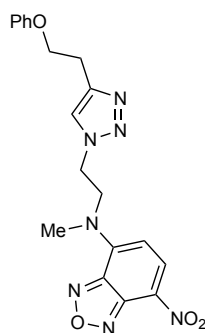
ν_{\max} (neat): 3142, 2932, 1601, 1590, 1496, 1474, 1441, 1295, 1241, 1052, 1022, 1035, 998, 752, 692 cm^{-1} .

$^1\text{H NMR}$ (CDCl_3 , 400 MHz): δ 8.60 (s, 1H), 7.67 (tt, $J = 7.8, 1.8$ Hz, 1H), 7.60 (s, 1H), 7.29–7.24 (m, 4H), 7.15 (d, $J = 7.7$ Hz, 1H), 6.93 (tt, $J = 7.3, 1.2$ Hz, 1H), 6.88 (m, 1H), 5.63 (s, 2H), 4.25 (t, $J = 6.5$ Hz, 2H), 3.22 (t, $J = 6.5$ Hz, 2H).

$^{13}\text{C NMR}$ (CDCl_3 , 100 MHz): δ 158.8, 137.5, 129.6, 123.5, 121.1, 114.7, 66.8, 55.7, 26.4. Three signals not observed/ coincident.

HRMS: exact mass calculated for $[\text{M}+\text{Na}]^+$ ($\text{C}_{16}\text{H}_{16}\text{N}_4\text{ONa}$) requires m/z 303.1216, found m/z 303.1214.

N-Methyl-7-nitro-*N*-(2-(4-(2-phenoxyethyl)-1*H*-1,2,3-triazol-1-yl)-ethyl)benzo[*c*][1,2,5]oxadiazol-4-amine (**2.103g**).



Prepared using General Procedure 2F. Yellow solid (118 mg, 85%). Purification on silica gel using hexane/EtOAc 1/9.

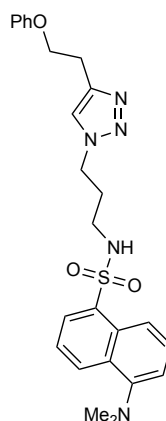
ν_{\max} (neat): 3142, 1617, 1556, 1483, 1429, 1303, 1281, 1095, 1035, 1000, 801, 756, 682 cm^{-1} .

$^1\text{H NMR}$ (CDCl_3 , 500 MHz): δ 8.37 (d, $J = 9.0$ Hz, 1H), 7.86 (br. s, 1H), 7.24 (t, $J = 7.7$ Hz, 2H), 6.92 (t, $J = 7.3$ Hz, 1H), 6.84 (d, $J = 8.0$ Hz, 2H), 6.20 (d, $J = 8.9$ Hz, 1H), 4.68 (m, 2H), 4.01 (t, $J = 6.0$ Hz, 2H), 3.03 (t, $J = 6.0$ Hz, 2H), 1.34–1.29 (m, 5H).

HRMS: exact mass calculated for $[M+Na]^+$ ($C_{19}H_{19}N_7O_4Na$) requires m/z 432.1391, found m/z 432.1376.

^{13}C NMR could not be obtained due to relaxation issues.

5-(Dimethylamino)-*N*-(3-(4-(2-phenoxyethyl)-1*H*-1,2,3-triazol-1-yl)propyl)naphthalene-1-sulfonamide (**2.103h**).



Prepared using General Procedure 2F. Yellow solid (38 mg, 87%). Purification on silica gel using DCM/MeOH 9/1.

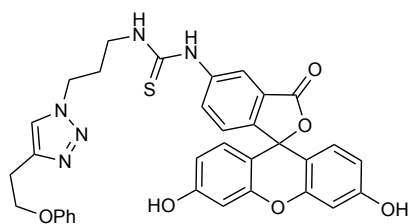
ν_{max} (neat): 3293, 3142, 2935, 2870, 2790, 1603, 1590, 1577, 1500, 1457, 1409, 1396, 1314, 1236, 1145, 1038, 947, 910, 791, 757, 731, 694 cm^{-1} .

1H NMR ($CDCl_3$, 400 MHz): δ 8.53 (dt, $J = 8.5, 0.9$ Hz, 1H), 8.27 (dt, $J = 8.5, 0.9$ Hz, 1H), 8.18 (dd, $J = 7.3, 1.2$ Hz, 1H), 7.55 (dd, $J = 8.6, 7.6$ Hz, 1H), 7.47 (dd, $J = 8.5, 7.2$ Hz, 1H), 7.33 (s, 1H), 7.28–7.24 (m, 2H), 7.16 (d, $J = 7.6$ Hz, 1H), 6.95–6.88 (m, 3H), 5.41 (t, $J = 6.5$ Hz, 1H), 4.32 (t, $J = 6.6$ Hz, 2H), 4.20 (t, $J = 6.3$ Hz, 2H), 3.15 (t, $J = 6.3$ Hz, 2H), 2.87 (s, 6H), 2.01 (m, 4H).

^{13}C NMR ($CDCl_3$, 100 MHz): δ 158.7, 152.2, 134.5, 130.8, 130.0, 129.8, 129.6, 128.7, 123.3, 121.0, 118.6, 115.4, 114.7, 66.7, 46.9, 45.5, 40.1, 32.0, 30.4, 29.8, 26.2, 14.3.

HRMS: exact mass calculated for $[M+Na]^+$ ($C_{25}H_{29}N_5O_3SNa$) requires m/z 502.1883, found m/z 502.1862.

1-(3',6'-Dihydroxy-3-oxo-3*H*-spiro[isobenzofuran-1,9'-xanthen]-5-yl)-3-(3-(4-(2-phenoxyethyl)-1*H*-1,2,3-triazol-1-yl)propyl)thiourea (**2.103i**).



Prepared using General Procedure 2F. Red solid (68 mg, 91%). Purification on silica gel using DCM/MeOH 9/1.

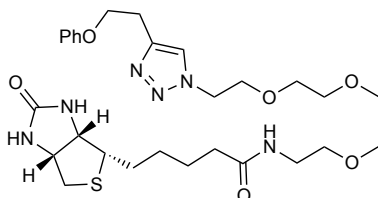
ν_{\max} (neat): 2928, 1638, 1591, 1541, 1457, 1381, 1295, 1238, 1210, 1176, 1120, 852 cm^{-1} .

$^1\text{H NMR}$ (DMSO- d_6 , 500 MHz): δ 8.72 (br. s, 1H), 8.38 (s, 1H), 8.06 (s, 1H), 7.83 (d, $J = 7.7$ Hz, 1H), 7.27 (t, $J = 7.1$ Hz, 2H), 7.17 (d, $J = 7.1$ Hz, 1H), 6.95 (m, 2H), 6.71 (s, 3H), 6.57–5.59 (m, 3H), 4.45 (t, $J = 6.4$ Hz, 2H), 4.22 (t, $J = 6.6$ Hz, 4H), 3.51 (m, 2H), 3.09 (t, $J = 6.4$ Hz, 2H).

HRMS: exact mass calculated for $[\text{M}-\text{H}]^-$ ($\text{C}_{34}\text{H}_{28}\text{N}_5\text{O}_6\text{S}$) requires m/z 634.1766, found m/z 618.2001 $[\text{M}-\text{OH}]$.

$^{13}\text{C NMR}$ could not be obtained due to relaxation issues.

5-((3*aS*,4*S*,6*aR*)-2-Oxohexahydro-1*H*-thieno[3,4-*d*]imidazol-4-yl)-*N*-(2-(2-(2-(2-(4-(2-phenoxyethyl)-1*H*-1,2,3-triazol-1-yl)ethoxy)-ethoxy)ethoxy)ethyl)pentanamide (**2.103j**).



Prepared using General Procedure 2F. White solid (32 mg, 88%). Purification on silica gel using DCM/MeOH 9/1.

ν_{\max} (neat): 3274, 3071, 2917, 2861, 1695, 1679, 1643, 1545, 1474, 1238, 1104, 1035, 756 cm^{-1} .

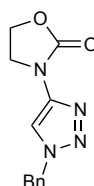
$^1\text{H NMR}$ (CD_3OD , 400 MHz): δ 7.96 (br. s, 1H), 7.25 (t, $J = 7.7$ Hz, 2H), 6.92 (d, $J = 7.2$ Hz, 3H), 4.56 (t, $J = 4.6$ Hz, 2H), 4.47 (dd, $J = 7.6, 5.6$ Hz, 1H), 4.28 (dd, $J = 7.9, 4.3$ Hz, 1H), 4.24 (t, $J = 5.1$ Hz, 2H), 3.88 (t, $J = 4.7$ Hz, 2H), 3.63–3.54 (m, 8H), 3.50 (t, $J = 5.1$ Hz, 2H), 3.37–3.33 (m, 2H), 3.20–3.17 (m, 3H), 2.90 (dd, $J = 12.5, 4.8$ Hz, 1H), 2.70 (d, $J = 12.7$ Hz, 1H), 2.19 (t, $J = 7.4$ Hz, 2H), 1.75–1.54 (m, 4H), 1.41 (app. quint, $J = 7.5$ Hz, 2H).

^{13}C NMR (MeOD, 100 MHz): δ 176.1, 166.1, 160.2, 130.5, 121.9, 115.7, 71.6, 71.5, 71.4, 71.2, 10.6, 70.4, 67.8, 63.4, 61.6, 57.0, 51.5, 41.1, 40.3, 36.7, 29.7, 29.5, 27.0, 26.8. One signal not observed/coincident.

HRMS: exact mass calculated for $[\text{M}+\text{H}]^+$ ($\text{C}_{28}\text{H}_{43}\text{N}_6\text{O}_6\text{S}$) requires m/z 591.2959, found m/z 591.2811.

2.7.9 Products from Scheme 123

3-(1-Benzyl-1*H*-1,2,3-triazol-4-yl)oxazolidin-2-one (**2.88**).^[152]

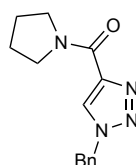


Prepared using General Procedure 2G. White solid (99 mg, 99%). Purification on silica gel using hexane/EtOAc 7/3.

^1H NMR (CDCl_3 , 400 MHz): δ 7.82 (s, 1H), 7.36–7.33 (m, 3H), 7.28–7.26 (m, 2H), 5.48 (s, 2H), 4.56–4.52 (m, 2H), 4.25–4.21 (m, 2H).

^{13}C NMR (CDCl_3 , 100 MHz): δ 154.9, 144.1, 134.4, 129.2, 129.0, 128.2, 111.9, 63.4, 54.9, 43.7.

(1-Benzyl-1*H*-1,2,3-triazol-4-yl) (pyrrolidin-1-yl)methanone (**2.106**).



Prepared using General Procedure 2G. White solid (105 mg, quant). Purification on silica gel using hexane/EtOAc 7/3.

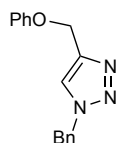
ν_{max} (neat): 3298, 3099, 2939, 5466, 2861, 2190, 1600, 1543, 1498, 1424, 1342, 1279, 1229, 1048 cm^{-1} .

^1H NMR (CDCl_3 , 400 MHz): δ 8.02 (s, 1H), 7.36–7.34 (m, 3H), 7.28–7.26 (m, 2H), 5.52 (s, 2H), 4.09 (t, $J = 6.7$ Hz, 2H), 3.62 (t, $J = 6.9$ Hz, 2H), 1.97 (app. quint, $J = 7.1$ Hz, 2H), 1.88 (app. quint, $J = 7.1$ Hz, 2H).

^{13}C NMR (CDCl_3 , 100 MHz): δ 159.5, 145.5, 134.1, 129.3, 129.0, 128.3, 127.6, 54.3, 48.7, 47.0, 26.6, 23.8.

HRMS: exact mass calculated for $[M+Na]^+$ ($C_{14}H_{16}N_4ONa$) requires m/z 279.1216, found m/z 279.1206.

1-Benzyl-4-(phenoxyethyl)-1*H*-1,2,3-triazole (**2.89**).^[187]

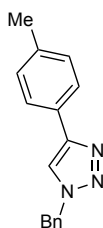


Prepared using General Procedure 2G. White solid (106 mg, 97%). Purification on silica gel using hexane/EtOAc 9/1.

¹H NMR ($CDCl_3$, 400 MHz): δ 7.52 (s, 1H), 7.37–7.35 (m, 3H), 7.29–7.25 (m, 4H), 6.97–6.95 (m, 3H), 5.52 (s, 2H), 5.18 (s, 2H).

¹³C NMR ($CDCl_3$, 100 MHz): δ 157.7, 144.2, 134.0, 129.0, 128.7, 128.3, 127.6, 122.1, 120.8, 114.3, 61.6, 53.7.

1-Benzyl-4-(*p*-tolyl)-1*H*-1,2,3-triazole (**2.90**).^[188]

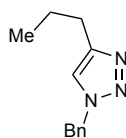


Prepared using General Procedure 2G. White solid (94 mg, 92%). Purification on silica gel using hexane/EtOAc 9/1.

¹H NMR ($CDCl_3$, 400 MHz): δ 7.70 (s, 1H), 7.68 (s, 1H), 7.62 (s, 1H), 7.39–7.36 (m, 3H), 7.32–7.31 (m, 1H), 7.30–7.29 (m, 1H), 7.21 (s, 1H), 7.19 (s, 1H), 5.56 (s, 2H), 2.36 (s, 3H).

¹³C NMR ($CDCl_3$, 100 MHz): δ 148.4, 138.1, 134.9, 129.6, 129.3, 128.9, 128.2, 127.9, 125.7, 119.3, 54.3, 21.4.

1-Benzyl-4-propyl-1*H*-1,2,3-triazole (**2.91**).^[189]



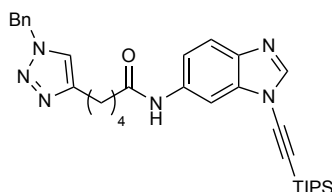
Prepared using General Procedure 2G. White solid (70 mg, 85%). Purification on silica gel using hexane.

¹H NMR (CDCl₃, 400 MHz): δ 7.36–7.31 (m, 3H), 7.24–7.21 (m, 2H), 7.18 (s, 1H), 5.47 (s, 2H), 2.64 (t, *J* = 7.4 Hz, 2H), 1.64 (sextet, *J* = 7.4 Hz, 2H), 0.9 (t, *J* = 7.4 Hz, 3H).

¹³C NMR (CDCl₃, 100 MHz): δ 148.8, 135.1, 129.1, 128.6, 128.0, 120.7, 54.0, 27.8, 22.7, 13.8.

2.7.10 Products from Scheme 124

5-(1-Benzyl-1*H*-1,2,3-triazol-4-yl)-*N*-(1-((triisopropylsilyl)ethynyl)-1*H*-benzo[*d*]imidazol-6-yl)pentanamide (**2.108**).



To a solution of *N*-(1-((triisopropylsilyl)ethynyl)-1*H*-benzo[*d*]imidazol-6-yl)hept-6-ynamide (50 mg, 0.119 mmol, 1 equiv) in MeOH/H₂O (1/1, 2 mL) was added benzyl azide (15 μL, 0.119 mmol, 1 equiv), AMTC (3 mg, 0.012 mmol, 0.1 equiv), Cu(OAc)₂ (1 mg, 0.006 mmol, 0.05 equiv), and NaAsc (3 mg, 0.012 mmol, 0.1 equiv). The reaction was stirred at rt for 16 h, after which DCM (10 mL) was added. The mixture was washed with aq. EDTA (10 mg/mL, 10 mL), brine (2 × 10 mL), dried over Na₂SO₄, and concentrated under reduced pressure. The resulting residue was purified by flash chromatography (silica gel, hexane/ EtOAc 3/7) to provide the desired product as a white solid (62 mg, 98%).

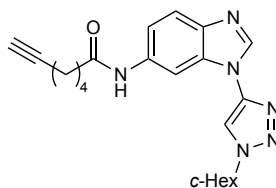
v_{max} (neat): 3251, 2937, 2859, 2184, 1664, 1602, 1548, 1498, 1441, 1216, 909, 883, 730 cm⁻¹.

¹H NMR (CDCl₃, 400 MHz): δ 8.75 (s, 1H), 8.24 (s, 1H), 8.05 (br. s, 1H), 7.64 (br. s, 1H), 7.35–7.30 (m, 4H), 7.23–7.21 (m, 3H), 5.45 (s, 2H), 2.71 (t, *J* = 6.9 Hz, 2H), 2.43 (t, *J* = 6.9 Hz, 2H), 1.79–1.70 (m, 4H), 1.14 (s, 21H).

¹³C NMR (CDCl₃, 100 MHz): δ 171.8, 136.3, 134.8, 129.2, 128.8, 128.1, 120.6, 117.0, 102.6, 73.5, 54.2, 37.1, 29.8, 28.6, 25.1, 25.0, 18.7, 11.3. Five signals not observed/ coincident.

HRMS: exact mass calculated for [M+Na]⁺ (C₃₂H₄₂N₆OSiNa) requires *m/z* 577.3082, found *m/z* 577.3122.

N-(1-(1-Cyclohexyl-1*H*-1,2,3-triazol-4-yl)-1*H*-benzo[*d*]imidazol-6-yl)hept-6-ynamide (**2.109**).



To a solution of *N*-(1-((triisopropylsilyl)- ethynyl)-1*H*-benzo[*d*]imidazol-6-yl)hept-6-ynamide (50 mg, 0.12 mmol, 1 equiv) in MeCN (1 mL) was added cyclohexylazide (15 mg, 0.12 mmol, 1 equiv), TBAF (43 μ L, 0.13 mmol, 1.1 equiv), and Cu(OAc)₂ (1 mg, 0.006 mmol, 0.05 equiv). The reaction was stirred at rt for 16 h, after which DCM (10 mL) was added. The mixture was washed with aq. EDTA (10 mg/mL, 10 mL), brine (2 \times 10 mL), dried over Na₂SO₄, and concentrated under reduced pressure. The resulting residue was purified by flash chromatography (silica gel, 7/3 EtOAc/ hexane) to provide the desired product as a white solid (45 mg, 96%).

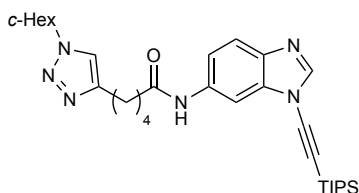
ν_{\max} (neat): 3289, 3259, 3123, 3080, 2930, 2855, 1673, 1604, 1587, 1550, 1487, 1442, 1299, 1240, 911, 803, 730 cm^{-1} .

¹H NMR (CDCl₃, 400 MHz): δ 8.40 (br. s, 1H), 8.34 (s, 1H), 8.08 (br. s, 1H), 7.85 (s, 1H), 7.68 (br. s, 1H), 7.07 (d, $J = 5.9$ Hz, 1H), 4.48 (tt, $J = 11.8, 3.6$ Hz, 1H), 2.41 (t, $J = 7.4$ Hz, 2H), 2.27 (d, $J = 12.4$ Hz, 2H), 2.21 (dt, $J = 7.2, 2.1$ Hz, 2H), 1.96 (m, 3H), 1.89–1.82 (m, 4H), 1.59 (app. quint, $J = 7.8$ Hz, 2H), 1.52–1.41 (m, 2H), 1.32 (dt, $J = 12.8, 2.7$ Hz, 2H).

¹³C NMR (CDCl₃, 100 MHz): δ 171.5, 141.7, 135.1, 120.7, 116.1, 112.4, 102.7, 84.1, 68.9, 61.4, 37.2, 33.5, 28.0, 25.2, 25.1, 24.8, 18.3. Three signals not observed/coincident.

HRMS: exact mass calculated for [M+Na]⁺ (C₂₂H₂₆N₆ONa) requires m/z 413.2060, found m/z 413.2049.

5-(1-Cyclohexyl-1*H*-1,2,3-triazol-4-yl)-*N*-(1-((triisopropylsilyl)-ethynyl)-1*H*-benzo[*d*]imidazol-6-yl)pentanamide (**2.111**).



To a solution of *N*-(1-((triisopropylsilyl)ethynyl)-1*H*-benzo[*d*]imidazol-6-yl)-

hept-6-ynamide (50 mg, 0.119 mmol, 1 equiv) in MeOH/H₂O (1/1, 2 mL) was added cyclohexylazide (15 mg, 0.12 mmol, 1 equiv), AMTC (3 mg, 0.012 mmol, 0.1 equiv), Cu(OAc)₂ (1 mg, 0.006 mmol, 0.05 equiv), and NaAsc (3 mg, 0.012 mmol, 0.1 equiv). The reaction was stirred at rt for 24 h, after which DCM (10 mL) was added. The mixture was washed with aq. EDTA (10 mg/mL, 10 mL), brine (2 × 10 mL), dried over Na₂SO₄, and concentrated under reduced pressure. The resulting residue was purified by flash chromatography (silica gel, hexane/EtOAc 3/7) to provide the desired product as a white solid (42 mg, 63%).

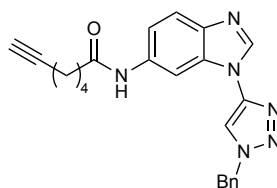
ν_{\max} (neat): 3296, 3132, 3075, 2935, 2859, 2184, 1686, 1664, 1602, 1547, 1500, 1483, 1441, 1376, 1284, 1216, 1071, 998, 885, 680 cm⁻¹.

¹H NMR (CDCl₃, 400 MHz): δ 8.51 (br. s, 1H), 8.20 (d, J = 1.6 Hz, 1H), 8.01 (s, 1H), 7.66 (d, J = 8.7 Hz, 1H), 7.32 (dd, J = 8.6, 1.7 Hz, 1H), 7.29 (s, 1H), 4.38 (tt, J = 11.8, 3.8 Hz, 1H), 2.75 (t, J = 6.9 Hz, 2H), 2.45 (t, J = 6.7 Hz, 2H), 2.18–2.15 (m, 2H), 1.92–1.87 (m, 2H), 1.83–1.65 (m, 6H), 1.48–1.37 (m, 2H), 1.27–1.21 (m, 2H), 1.16–1.14 (m, 21H).

¹³C NMR (CDCl₃, 100 MHz): δ 171.8, 147.2, 143.8, 138.2, 136.2, 135.0, 120.8, 118.7, 117.0, 102.6, 90.1, 73.4, 60.1, 37.2, 33.7, 28.6, 25.3, 25.3, 25.1, 25.0, 18.8, 11.3. Nine signals not observed/coincident.

HRMS: exact mass calculated for [M+Na]⁺ (C₃₁H₄₆N₆OSiNa) requires m/z 569.3395, found m/z 569.3382.

N-(1-(1-Benzyl-1*H*-1,2,3-triazol-4-yl)-1*H*-benzo[*d*]imidazol-6-yl)-hept-6-ynamide (**2.112**).



To a solution of *N*-(1-((triisopropylsilyl)-ethynyl)-1*H*-benzo[*d*]imidazol-6-yl)hept-6-ynamide (50 mg, 0.12 mmol, 1 equiv) in MeCN (1 mL) was added benzyl azide (15 μ L, 0.119 mmol, 1 equiv), TBAF (43 μ L, 0.13 mmol, 1.1 equiv), and Cu(OAc)₂ (1 mg, 0.006 mmol, 0.05 equiv). The reaction was stirred at rt for 2 h, after which DCM (10 mL) was added. The mixture was washed with aq. EDTA (10 mg/mL, 10 mL), brine (2 × 10 mL), dried over Na₂SO₄, and concentrated under reduced pressure. The

resulting residue was purified by flash chromatography (silica gel, 9/1 EtOAc/hexane) to provide the desired product as a white solid (47 mg, 98%).

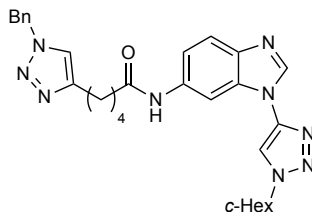
ν_{\max} (neat): 2954, 2961, 2865, 1599, 1589, 1439, 1396, 1080, 1065, 1041, 866, 775 cm^{-1} .

$^1\text{H NMR}$ (CDCl_3 , 400 MHz): δ 8.37 (br. s, 1H), 8.25 (br. s, 1H), 8.01 (br. s, 1H), 7.88 (s, 1H), 7.68 (d, $J = 8.7$ Hz, 1H), 7.39–7.34 (m, 5H), 7.20 (dd, $J = 8.6, 1.7$ Hz, 1H), 5.61 (s, 2H), 3.12–3.08 (m, 2H), 2.42 (t, $J = 7.3$ Hz, 2H), 2.22 (td, $J = 7.2, 2.7$ Hz, 2H), 1.95 (t, $J = 2.5$ Hz, 1H), 1.88–1.80 (m, 2H).

$^{13}\text{C NMR}$ (CDCl_3 , 100 MHz): δ 171.3, 135.2, 134.1, 129.4, 129.2, 128.3, 120.6, 116.2, 114.2, 102.5, 84.2, 68.8, 55.2, 37.1, 28.0, 24.7, 19.7, 18.3. Six signals not observed/coincident.

HRMS: exact mass calculated for $[\text{M}+\text{Na}]^+$ ($\text{C}_{23}\text{H}_{22}\text{N}_6\text{ONa}$) requires m/z 421.1747, found m/z 421.1732.

5-(1-Benzyl-1*H*-1,2,3-triazol-4-yl)-*N*-(1-(1-cyclohexyl-1*H*-1,2,3-triazol-4-yl)-1*H*-benzo[*d*]imidazol-6-yl)pentanamide (**2.110**).



Method A: To a solution of 5-(1-benzyl-1*H*-1,2,3-triazol-4-yl)-*N*-(1-((triisopropylsilyl)ethynyl)-1*H*-benzo[*d*]imidazol-6-yl)pentanamide (64 mg, 0.12 mmol, 1 equiv) in MeCN (1 mL) was added cyclohexylazide (15 mg, 0.12 mmol, 1 equiv), TBAF (43 μL , 0.13 mmol, 1.1 equiv) and $\text{Cu}(\text{OAc})_2$ (1 mg, 0.006 mmol, 0.05 equiv). The reaction was stirred at rt for 16 h, after which DCM (10 mL) was added. The mixture was washed with aq. EDTA (10 mg/mL, 10 mL), brine (2×10 mL), dried over Na_2SO_4 and concentrated under reduced pressure. The resulting residue was purified by flash chromatography (silica gel, 9/1 EtOAc/hexane) to provide the desired product as a white solid (61 mg, 98%).

Method B: To a solution of 5-(1-benzyl-1*H*-1,2,3-triazol-4-yl)-*N*-(1-((triisopropylsilyl)- ethynyl)-1*H*-benzo[*d*]imidazol-6-yl)pentanamide (20 mg, 0.051 mmol, 1 equiv) in MeOH/ H_2O (1/1, 2 mL) was added benzyl azide (7 μL , 0.051 mmol, 1 equiv), AMTC (1 mg, 0.0051 mmol, 0.1 equiv), $\text{Cu}(\text{OAc})_2$ (0.5 mg, 0.0026

mmol, 0.05 equiv), and NaAsc (1 mg, 0.0026 mmol, 0.1 equiv). The reaction was stirred at rt for 16 h, after which DCM (10 mL) was added. The mixture was washed with aq. EDTA (10 mg/mL, 10 mL) and brine (2 × 10 mL), dried over Na₂SO₄, and concentrated under reduced pressure. The resulting residue was purified by flash chromatography (silica gel, 9/1 EtOAc/ hexane) to provide the desired product as a white solid (25 mg, 94%).

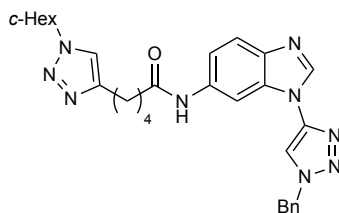
ν_{\max} (neat): 3257, 3125, 3062, 2922, 2852, 2093, 1671, 1584, 1547, 1496, 1485, 1446, 1299, 1216, 1050, 816, 799, 729 cm⁻¹.

¹H NMR (CDCl₃, 400 MHz): δ 8.23 (s, 1H), 8.40 (br. s, 1H), 8.38 (s, 1H), 7.92 (s, 1H), 7.68 (d, J = 7.5 Hz, 1H), 7.33–7.30 (m, 4H), 7.23–7.20 (m, 3H), 5.45 (s, 2H), 4.47 (tt, J = 11.8, 3.8 Hz, 1H), 2.69 (t, J = 6.5 Hz, 2H), 2.43 (t, J = 6.7 Hz, 2H), 2.25 (dd, J = 12.7, 2.4 Hz, 2H), 1.95–1.89 (m, 2H), 1.84 (dd, J = 12.1, 3.6 Hz, 2H), 1.79–1.70 (m, 6H), 1.47 (tt, J = 12.9, 3.5 Hz, 2H).

¹³C NMR (CDCl₃, 100 MHz): δ 172.0, 135.5, 134.9, 129.2, 128.8, 128.1, 121.1, 120.6, 116.3, 112.3, 102.4, 61.3, 54.1, 37.1, 33.4, 28.6, 25.3, 26.2, 25.1, 25.0. Five signals not observed/coincident.

HRMS: exact mass calculated for [M+Na]⁺ (C₂₉H₃₃N₉ONa) requires m/z 546.2700, found m/z 546.2660.

N-(1-(1-Benzyl-1*H*-1,2,3-triazol-4-yl)-1*H*-benzo[*d*]imidazol-6-yl)-5-(1-cyclohexyl-1*H*-1,2,3-triazol-4-yl)pentanamide (**2.113**).



Method A: To a solution of 5-(1-cyclohexyl-1*H*-1,2,3-triazol-4-yl)-*N*-(1-((triisopropylsilyl)ethynyl)-1*H*-benzo[*d*]imidazol-6-yl)pentanamide (30 mg, 0.06 mmol, 1 equiv) in MeCN (1 mL) was added benzyl azide (7 μ L, 0.06 mmol, 1 equiv), TBAF (20 μ L, 0.07 mmol, 1.1 equiv), and Cu(OAc)₂ (0.5 mg, 0.003 mmol, 0.05 equiv). The reaction was stirred at rt for 2 h, after which DCM (10 mL) was added. The mixture was washed with aq. EDTA (10 mg/mL, 10 mL) and brine (2 × 10 mL), dried over Na₂SO₄, and concentrated under reduced pressure. The resulting residue was purified by flash chromatography (silica gel, 9/1 EtOAc/hexane) to

provide the desired product as a white solid (30 mg, 95%). Method B: To a solution of *N*-(1-(1-benzyl-1*H*-1,2,3-triazol-4-yl)-1*H*-benzo[*d*]imidazol-6-yl)hept-6-ynamide (30 mg, 0.08 mmol, 1 equiv) in MeOH/H₂O (1/1, 2 mL) was added cyclohexylazide (10 mg, 0.08 mmol, 1 equiv), AMTC (1.6 mg, 0.008 mmol, 0.1 equiv), Cu(OAc)₂ (0.8 mg, 0.004 mmol, 0.05 equiv), and NaAsc (3 mg, 0.008 mmol, 0.1 equiv). The reaction was stirred at rt for 24 h, after which DCM (10 mL) was added. The mixture was washed with aq. EDTA (10 mg/mL, 10 mL) and brine (2 × 10 mL), dried over Na₂SO₄, and concentrated under reduced pressure. The resulting residue was purified by flash chromatography (silica gel, 9/1 EtOAc/hexane) to provide the desired product as a yellow solid (30 mg, 71%).

ν_{\max} (neat): 3300, 2954, 2928, 2855, 1736, 1677, 1628, 1600, 1587, 1548, 1496, 1441, 1455, 1379, 1364, 1301, 1234, 864, 821, 725 cm⁻¹.

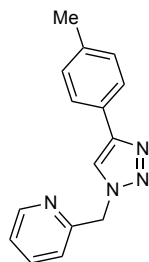
¹H NMR (CDCl₃, 400 MHz): δ 8.67 (br. s, 1H), 8.10 (br. s, 1H), 7.88 (br. s, 1H), 7.41–7.38 (m, 6H), 7.23 (m, 2H), 5.65 (s, 2H), 3.24 (m, 2H), 2.48 (t, *J* = 5.8 Hz, 2H), 2.29–2.26 (m, 1H), 2.20–2.18 (m, 2H), 1.90–1.75 (m, 6H), 1.69–1.60 (m, 4H), 1.45–1.42 (m, 2H).

¹³C NMR (CDCl₃, 100 MHz): δ 129.4, 129.2, 128.3, 124.6, 31.6, 30.3, 29.8, 29.6, 28.0, 25.3, 24.8, 24.5, 20.0, 13.9. Fifteen signals not observed/coincident.

HRMS: exact mass calculated for [M+Na]⁺ (C₂₉H₃₃N₉ONa) requires *m/z* 546.2700, found *m/z* 546.2689.

2.7.11 Products from Scheme 125

2-((4-(*p*-Tolyl)-1*H*-1,2,3-triazol-1-yl)methyl)pyridine (**2.115**).^[190]



To a solution of 5,6-dimethyl-1-((triisopropylsilyl)ethynyl)-1*H*-benzo[*d*]-imidazole (49 mg, 0.15 mmol, 1 equiv) and 1-ethynyl-4-methylbenzene (19 μ L, 0.15 mmol, 1 equiv) in MeCN (0.75 mL) was added 2-(azidomethyl)pyridine (20 mg, 0.15 mmol, 1 equiv), (azidomethyl)benzene (19 μ L, 0.15 mmol, 1 equiv), and Cu(OAc)₂ (1.4 mg, 0.0075 mmol, 0.05 equiv). The reaction was stirred at rt for 5 h before being filtered through Celite and concentrated under reduced pressure. The crude mixture was

dissolved in MeCN (0.75 mL) before adding Cu(OAc)₂ (1.4 mg, 0.0075 mmol, 0.05 equiv) and TBAF (1 M in THF, 22.5 μ L, 0.225 mmol, 1.5 equiv). The reaction was stirred at rt for a further 16 h, after which EtOAc (10 mL) was added. The mixture was washed with aq. EDTA (10 mg/mL, 10 mL) and brine (2 \times 10 mL), dried over Na₂SO₄, and concentrated under reduced pressure. The resulting residue was purified by flash chromatography (silica gel, Et₂O/MeOH/NEt₃ 20/1/1) to provide the desired product as a white solid (32 mg, 85%).

¹H NMR (CDCl₃, 500 MHz): δ 8.61 (br. s, 1H), 7.89 (s, 1H), 7.72 (s, 1H), 7.71 (s, 1H), 7.68 (td, *J* = 7.6, 1.4 Hz, 1H), 7.26 (t, *J* = 5.4 Hz, 1H), 7.22 (t, *J* = 5.6 Hz, 3H), 5.69 (s, 2H), 2.36 (s, 3H).

¹³C NMR (CDCl₃, 100 MHz): δ 154.7, 149.8, 148.5, 138.1, 137.5, 129.6, 127.8, 125.7, 123.6, 122.6, 120.0, 55.8, 21.4.

3.0 References

- [1] R. A. Shenvi, D. P. O'Malley, P. S. Baran, *Acc. Chem. Res.* **2009**, *42*, 530–541.
- [2] N. Miyaura, K. Yamada, A. Suzuki, *Tetrahedron Lett.* **1979**, *36*, 3437–3440.
- [3] S. D. Roughley, A. M. Jordan, *J. Med. Chem.* **2011**, *54*, 3451–3479.
- [4] D. Milstein, J. K. Stille, *J. Am. Chem. Soc.* **1979**, *101*, 4992–4998.
- [5] A. O. King, N. Okukado, E. Negishi, *J. Chem. Soc. Chem. Commun.* **1977**, 683.
- [6] K. Tamao, K. Sumitani, M. Kumada, *J. Am. Chem. Soc.* **1972**, *94*, 4374–4376.
- [7] R. J. P. Corriu, J. P. Masse, *Chem. Commun.* **1972**, 144.
- [8] N. Miyaura, A. Suzuki, *Chem. Rev.* **1995**, *95*, 2457–2483.
- [9] G. Bringmann, R. Walter, R. Weirich, *Angew. Chem. Int. Ed.* **1990**, *29*, 977–991.
- [10] Y. J. Chang, T. J. Chow, *Tetrahedron* **2009**, *65*, 9626–9632.
- [11] C. C. C. Johansson Seechurn, M. O. Kitching, T. J. Colacot, V. Snieckus, *Angew. Chem. Int. Ed.* **2012**, *51*, 5062–5085.
- [12] V. V. Grushin, H. Alper, *Chem. Rev.* **1994**, *94*, 1047–1062.
- [13] A. J. J. Lennox, G. C. Lloyd-Jones, *Angew. Chem. Int. Ed.* **2013**, *52*, 7362–7370.
- [14] N. Miyaura, K. Yamada, H. Suginome, A. Suzuki, *J. Am. Chem. Soc.* **1985**, *107*, 972–980.
- [15] K. Matos, J. A. Soderquist, *J. Org. Chem.* **1998**, *63*, 461–470.
- [16] A. A. C. Braga, N. H. Morgon, G. Ujaque, F. Maseras, *J. Am. Chem. Soc.* **2005**, *127*, 9298–9307.
- [17] B. Carrow, J. Hartwig, *J. Am. Chem. Soc.* **2011**, *133*, 2116–2119.
- [18] C. Amatore, A. Jutand, G. Le Duc, *Chem. Eur. J.* **2011**, *17*, 2492–503.
- [19] A. F. Schmidt, A. A. Kurokhtina, E. V. Larina, *Russ. J. Gen. Chem.* **2011**, *81*, 1573–1574.
- [20] A. A. Thomas, S. E. Denmark, *Science* **2016**, *352*, 329–332.

- [21] A. F. Littke, G. C. Fu, *Angew. Chem. Int. Ed.* **1998**, *37*, 3387–3388.
- [22] D. W. Old, J. P. Wolfe, S. L. Buchwald, *J. Am. Chem. Soc.* **1998**, *120*, 9722–9723.
- [23] A. F. Littke, G. C. Fu, *Angew. Chem. Int. Ed.* **2002**, *41*, 4176–4211.
- [24] R. Martin, S. L. Buchwald, *Acc. Chem. Res.* **2008**, *41*, 1461–73.
- [25] J. P. Wolfe, S. L. Buchwald, *Angew. Chem. Int. Ed.* **1999**, *38*, 2413–2416.
- [26] H. N. Nguyen, X. Huang, S. L. Buchwald, *J. Am. Chem. Soc.* **2003**, *125*, 11818–11819.
- [27] S. D. Walker, T. E. Barder, J. R. Martinelli, S. L. Buchwald, *Angew. Chem. Int. Ed.* **2004**, *43*, 1871–1876.
- [28] B. Bhayana, B. P. Fors, S. L. Buchwald, *Org. Lett.* **2009**, *11*, 3954–3957.
- [29] D. S. Surry, S. L. Buchwald, *Chem. Sci.* **2011**, *2*, 27–50.
- [30] T. Kinzel, Y. Zhang, S. L. Buchwald, *J. Am. Chem. Soc.* **2010**, *132*, 14073–14075.
- [31] M. A. Düfert, K. L. Billingsley, S. L. Buchwald, *J. Am. Chem. Soc.* **2013**, *135*, 12877–12885.
- [32] A. C. Sather, H. G. Lee, J. R. Colombe, A. Zhang, S. L. Buchwald, *Nature* **2015**, *524*, 208–211.
- [33] W. Shu, S. L. Buchwald, *Chem. Sci.* **2011**, *2*, 2321.
- [34] A. J. J. Lennox, G. C. Lloyd-Jones, *Chem. Soc. Rev.* **2014**, *43*, 412–443.
- [35] N. Miyaura, T. Yanagi, A. Suzuki, *Synth. Commun.* **1981**, *11*, 513–519.
- [36] H. G. Kuivila, K. V. Nahabedian, *J. Am. Chem. Soc.* **1961**, *83*, 2159–2163.
- [37] H. G. Kuivila, J. F. Reuwer, J. A. Mangravite, *Can. J. Chem.* **1963**, *41*, 3081–3090.
- [38] H. G. Kuivila, K. V. Nahabedian, *J. Am. Chem. Soc.* **1961**, *83*, 2159–2163.
- [39] P. A. Cox, A. G. Leach, A. D. Campbell, G. C. Lloyd-Jones, *J. Am. Chem. Soc.* **2016**, *138*, 9145–9157.
- [40] C. Adamo, C. Amatore, I. Ciofini, A. Jutand, H. Lakmini, *J. Am. Chem. Soc.* **2006**, *128*, 6829–6836.

- [41] W. Li, D. P. Nelson, M. S. Jensen, R. S. Hoerrner, D. Cai, R. D. Larsen, P. J. Reider, *J. Org. Chem.* **2002**, *67*, 5394–5397.
- [42] N. Miyaura, A. Suzuki, *J. Chem. Soc. Chem. Commun.* **1979**, 866–867.
- [43] M. Uemura, H. Nishimura, T. Minami, Y. Hayashi, *J. Am. Chem. Soc.* **1991**, *113*, 5402–5410.
- [44] T. Ishiyama, M. Murata, N. Miyaura, *J. Org. Chem.* **1995**, 7508–7510.
- [45] T. Ishiyama, J. Takagi, K. Ishida, N. Miyaura, N. R. Anastasi, J. F. Hartwig, *J. Am. Chem. Soc.* **2002**, *124*, 390–391.
- [46] M. R. I. Cho, J.-Y. Tse, M. K. Holmes, D. Maleczka, R. E. Jr Smith, *Science* **2002**, *295*, 305–308.
- [47] R. Chambers, H. Clark, C. Willis, *J. Am. Chem. Soc.* **1960**, *82*, 5298–5301.
- [48] G. A. Molander, T. Ito, *Org. Lett.* **2001**, *3*, 393–396.
- [49] R. A. Batey, T. D. Quach, *Tetrahedron Lett.* **2001**, *42*, 9099–9103.
- [50] E. Vedejs, R. W. Chapman, S. C. Fields, S. Lin, M. R. Schrimpf, *J. Org. Chem.* **1995**, *60*, 3020–3027.
- [51] G. A. Molander, N. Ellis, *Acc. Chem. Res.* **2007**, *40*, 275–286.
- [52] G. A. Molander, J. Ham, D. G. Seapy, *Tetrahedron* **2007**, *63*, 768–775.
- [53] A. J. J. Lennox, G. C. Lloyd-Jones, *J. Am. Chem. Soc.* **2012**, *134*, 7431–41.
- [54] G. A. Molander, D. E. Petrillo, *J. Am. Chem. Soc.* **2006**, *128*, 9634–9635.
- [55] G. A. Molander, D. J. Cooper, *J. Org. Chem.* **2007**, *72*, 3558–3560.
- [56] G. A. Molander, R. Figueroa, *J. Org. Chem.* **2006**, *71*, 6135–6140.
- [57] G. A. Molander, J. Ham, *Org. Lett.* **2006**, *8*, 2767–2770.
- [58] G. A. Molander, W. Febo-Ayala, L. Jean-Gérard, *Org. Lett.* **2009**, *11*, 3830–3833.
- [59] G. A. Molander, D. J. Cooper, *J. Org. Chem.* **2008**, *73*, 3885–3891.
- [60] G. A. Molander, N. M. Ellis, *J. Org. Chem.* **2006**, *71*, 7491–7493.
- [61] T. Mancilla, R. Contreras, B. Wrackmeyer, *J. Organomet. Chem.* **1986**, *307*, 1–6.
- [62] J. Li, A. S. Grillo, M. D. Burke, *Acc. Chem. Res.* **2015**, *48*, 2297–2307.

- [63] B. E. Uno, E. P. Gillis, M. D. Burke, *Tetrahedron*. **2009**, *65*, 3130–3138.
- [64] E. Gillis, M. Burke, *Aldrichimica Acta* **2009**, *42*, 17–27.
- [65] J. D. St Denis, C. C. G. Scully, C. F. Lee, A. K. Yudin, *Org. Lett.* **2014**, *16*, 1338–41.
- [66] J. D. St Denis, A. Zajdlik, J. Tan, P. Trinchera, C. F. Lee, Z. He, S. Adachi, A. K. Yudin, *J. Am. Chem. Soc.* **2014**, DOI 10.1021/ja510963k.
- [67] S. G. Ballmer, E. P. Gillis, M. D. Burke, *Org. Synth.* **2009**, *86*, 344.
- [68] D. M. Knapp, E. P. Gillis, M. D. Burke, *J. Am. Chem. Soc.* **2009**, *131*, 6961–6963.
- [69] G. R. Dick, E. M. Woerly, M. D. Burke, *Angew. Chem. Int. Ed.* **2012**, *51*, 2667–2672.
- [70] P. B. Hodgson, F. H. Salingue, *Tetrahedron Lett.* **2004**, *45*, 685–687.
- [71] G. R. Dick, D. M. Knapp, E. P. Gillis, M. D. Burke, *Org. Lett.* **2010**, *12*, 2314–2317.
- [72] S. J. Lee, K. C. Gray, J. S. Paek, M. D. Burke, *J. Am. Chem. Soc.* **2008**, *130*, 466–468.
- [73] J. W. B. Fyfe, A. J. B. Watson, *Synlett* **2015**, *26*, 1139–1144.
- [74] A. F. Littke, C. Dai, G. C. Fu, *J. Am. Chem. Soc.* **2000**, *122*, 4020–4028.
- [75] F. Proutiere, M. Aufiero, F. Schoenebeck, *J. Am. Chem. Soc.* **2012**, *134*, 606–612.
- [76] Z. L. Niemeyer, A. Milo, D. P. Hickey, M. S. Sigman, *Nat. Chem.* **2016**, *8*, 610–617.
- [77] I. J. S. Fairlamb, *Chem. Soc. Rev.* **2007**, *36*, 1036.
- [78] S. T. Handy, Y. Zhang, *Chem. Commun.* **2006**, 299–301.
- [79] S. C. Ceide, A. G. Montalban, *Tetrahedron Lett.* **2006**, *47*, 4415–4418.
- [80] W. Yang, Y. Wang, J. R. Corte, *Org. Lett.* **2003**, *5*, 3131–3134.
- [81] I. Mangalagiu, T. Benneche, K. Undheim, Z. Jászay, E. Fogassy, K. R. Pedersen, M. N. Homsí, F. K. H. Kuske, M. Haugg, N. Trabesinger-Rüf, et al., *Acta Chem. Scand.* **1996**, *50*, 914–917.

- [82] C. P. Ashcroft, S. J. Fussell, K. Wilford, *Tetrahedron Lett.* **2013**, *54*, 4529–4532.
- [83] D. J. Sinclair, M. S. Sherburn, **2005**, 3987–3990.
- [84] C. G. Dong, Q. S. Hu, *J. Am. Chem. Soc.* **2005**, *127*, 10006–10007.
- [85] B. J. Groombridge, S. M. Goldup, I. Larrosa, *Chem. Commun.* **2015**, *51*, 3832–3834.
- [86] K. Endo, T. Ohkubo, M. Hirokami, T. Shibata, *J. Am. Chem. Soc.* **2010**, *132*, 11033–11035.
- [87] J. C. H. Lee, R. McDonald, D. G. Hall, *Nat. Chem.* **2011**, *3*, 894–899.
- [88] D. L. Sandrock, L. Jean-Gérard, C. Y. Chen, S. D. Dreher, G. A. Molander, *J. Am. Chem. Soc.* **2010**, *132*, 17108–17110.
- [89] T. Ohmura, T. Awano, M. Suginome, *J. Am. Chem. Soc.* **2010**, *132*, 13191–13193.
- [90] C. Sun, B. Potter, J. P. Morken, *J. Am. Chem. Soc.* **2014**, *136*, 6534–6537.
- [91] S. N. Mlynarski, C. H. Schuster, J. P. Morken, *Nature* **2014**, *505*, 386–390.
- [92] E. P. Gillis, M. D. Burke, *J. Am. Chem. Soc.* **2007**, *129*, 6716–6717.
- [93] J. Li, S. G. Ballmer, E. P. Gillis, S. Fujii, M. J. Schmidt, A. M. E. Palazzolo, J. W. Lehmann, G. F. Morehouse, M. D. Burke, *Science* **2015**, *347*, 1221–1226.
- [94] L. Xu, S. Ding, P. Li, *Angew. Chem. Int. Ed.* **2014**, *53*, 1822–1826.
- [95] G. A. Molander, D. L. Sandrock, *J. Am. Chem. Soc.* **2008**, *130*, 15792–15793.
- [96] Y. Yamashita, J. C. Tellis, G. A. Molander, *Proc. Natl. Acad. Sci.* **2015**, *112*, 12026–12029.
- [97] H. Noguchi, K. Hojo, M. Suginome, *J. Am. Chem. Soc.* **2007**, *129*, 758–759.
- [98] H. Noguchi, T. Shioda, C.-M. Chou, M. Suginome, *Org. Lett.* **2008**, *10*, 377–380.
- [99] N. Iwadate, M. Suginome, *J. Am. Chem. Soc.* **2010**, *132*, 2548–2549.
- [100] C. M. Crudden, C. Ziebenhaus, J. P. G. Rygus, K. Ghozati, P. J. Unsworth, M. Nambo, S. Voth, M. Hutchinson, V. S. Laberge, Y. Maekawa, et al., *Nat. Commun.* **2016**, *7*, 11065.
- [101] B. W. Glasspoole, K. Ghozati, J. W. Moir, C. M. Crudden, *Chem. Commun.* **2012**, *48*, 1230–1232.

- [102] J. W. B. Fyfe, E. Valverde, C. P. Seath, A. R. Kennedy, J. M. Redmond, N. A. Anderson, A. J. B. Watson, *Chem. Eur. J.* **2015**, *21*, 8951–8964.
- [103] H. C. Brown, M. V. Rangaishenvi, *J. Organomet. Chem.* **1988**, *358*, 15–30.
- [104] D. S. Matteson, *Tetrahedron* **1989**, *45*, 1859–1885.
- [105] C. D. Roy, H. C. Brown, *Monatsh. Chem.* **2007**, *138*, 879–887.
- [106] J. Yan, G. Springsteen, S. Deeter, B. Wang, *Tetrahedron* **2004**, *60*, 11205–11209.
- [107] G. Springsteen, B. Wang, *Tetrahedron* **2002**, *58*, 5291–5300.
- [108] T. R. Wu, J. M. Chong, *J. Am. Chem. Soc.* **2005**, *127*, 3244–3245.
- [109] S. Lou, P. N. Moquist, S. E. Schaus, *Synth. Met.* **2006**, *128*, 12660.
- [110] T. R. Wu, J. M. Chong, *J. Am. Chem. Soc.* **2007**, *129*, 4908–4909.
- [111] S. Lou, P. N. Moquist, S. E. Schaus, *J. Am. Chem. Soc.* **2007**, *129*, 15398–15404.
- [112] S. C. Pellegrinet, J. M. Goodman, *J. Am. Chem. Soc.* **2006**, *128*, 3116–3117.
- [113] R. S. Paton, J. M. Goodman, S. C. Pellegrinet, *Org. Lett.* **2009**, *11*, 37–40.
- [114] R. S. Paton, J. M. Goodman, S. C. Pellegrinet, *J. Org. Chem.* **2008**, *73*, 5078–5089.
- [115] J. W. B. Fyfe, C. P. Seath, A. J. B. Watson, *Angew. Chem. Int. Ed.* **2014**, *53*, 12077–12080.
- [116] C. W. Muir, J. C. Vantourout, A. Isidro-Llobet, S. J. F. Macdonald, A. J. B. Watson, *Org. Lett.* **2015**, *17*, 6030–6033.
- [117] M. R. Yadav, M. Nagaoka, M. Kashihara, R. L. Zhong, T. Miyazaki, S. Sakaki, Y. Nakao, *J. Am. Chem. Soc.* **2017**, *139*, 9423–9426.
- [118] S. J. Blanksby, G. B. Ellison, *Acc. Chem. Res.* **2003**, *36*, 255–263.
- [119] D. S. Hewings, O. Fedorov, P. Filippakopoulos, S. Martin, S. Picaud, A. Tumber, C. Wells, M. M. Olcina, K. Freeman, A. Gill, et al., *J. Med. Chem.* **2013**, *56*, 3217–3227.
- [120] M. Bouquet, A. Guy, M. Lemaire, J. P. Guetté, *Synth. Commun.* **1985**, *15*, 1153–1157.
- [121] H. Yi, Q. Liu, J. Liu, Z. Zeng, Y. Yang, A. Lei, *ChemSusChem* **2012**, *5*, 2143–2146.

- [122] W. Y. Lee, C. H. Park, *J. Org. Chem.* **1993**, *58*, 7149–7157.
- [123] C. He, X. Zhang, R. Huang, J. Pan, J. Li, X. Ling, Y. Xiong, X. Zhu, *Tetrahedron Lett.* **2014**, *55*, 4458–4462.
- [124] C. P. Seath, J. W. B. Fyfe, J. J. Molloy, A. J. B. Watson, *Angew. Chem. Int. Ed.* **2015**, *54*, 9976–9979.
- [125] C. Bombardier, L. Laine, A. Reicin, D. Shapiro, R. Burgos-Vargas, B. Davis, R. Day, M. B. Ferraz, C. J. Hawkey, M. C. Hochberg, et al., *N. Engl. J. Med.* **2000**, *343*, 1520–1528.
- [126] The NAVIGATOR Study Group, *N. Engl. J. Med.* **2010**, *362*, 1477–1490.
- [127] R. Huisgen, G. Szeimies, L. Möbius, *Chem. Ber.* **1967**, *100*, 2494–2507.
- [128] R. Huisgen, *Pure Appl. Chem.* **1989**, *61*, 613–628.
- [129] V. V. Rostovtsev, L. G. Green, V. V. Fokin, K. B. Sharpless, *Angew. Chem. Int. Ed.* **2002**, *41*, 2596–2599.
- [130] H. C. Kolb, M. G. Finn, K. B. Sharpless, *Angew. Chem. Int. Ed. Engl.* **2001**, *40*, 2004–2021.
- [131] C. W. Tornøe, C. Christensen, M. Meldal, *J. Org. Chem.* **2002**, *67*, 3057–3064.
- [132] J. E. Hein, V. V. Fokin, *Chem. Soc. Rev.* **2010**, *39*, 1302–1315.
- [133] J. E. Moses, A. D. Moorhouse, *Chem. Soc. Rev.* **2007**, *36*, 1249–1262.
- [134] M. Meldal, C. W. Tomøe, *Chem. Rev.* **2008**, *108*, 2952–3015.
- [135] E. M. Sletten, C. R. Bertozzi, *Angew. Chem. Int. Ed.* **2009**, *48*, 6974–6998.
- [136] C. D. Spicer, B. G. Davis, *Nat. Commun.* **2014**, *5*, 4740.
- [137] S. T. Laughlin, J. M. Baskin, S. L. Amacher, C. R. Bertozzi, *Science* **2008**, *320*, 664–667.
- [138] P. V. Chang, J. A. Prescher, E. M. Sletten, J. M. Baskin, I. A. Miller, N. J. Agard, A. Lo, C. R. Bertozzi, *Proc. Natl. Acad. Sci. U. S. A.* **2010**, *107*, 1821–1826.
- [139] R. Berg, B. F. Straub, *Beilstein J. Org. Chem.* **2013**, *9*, 2715–2750.
- [140] F. Himo, T. Lovell, R. Hilgraf, V. V. Rostovtsev, L. Noodleman, K. B. Sharpless, V. V. Fokin, *J. Am. Chem. Soc.* **2005**, *127*, 210–216.

- [141] V. O. Rodionov, V. V. Fokin, M. G. Finn, *Angew. Chem. Int. Ed.* **2005**, *44*, 2210–2215.
- [142] B. T. Worrell, J. A. Malik, V. V. Fokin, *Science* **2013**, *340*, 457–460.
- [143] L. Jin, D. R. Tolentino, M. Melaimi, G. Bertrand, *Sci. Adv.* **2015**, *1*, 1–5.
- [144] M. Soleilhavoup, G. Bertrand, *Acc. Chem. Res.* **2015**, *48*, 256–266.
- [145] N. J. Agard, J. A. Prescher, C. R. Bertozzi, *J. Am. Chem. Soc.* **2004**, *126*, 15046–15047.
- [146] D. M. Beal, V. E. Albrow, G. Burslem, L. Hitchen, C. Fernandes, C. Laphorn, L. R. Roberts, M. D. Selby, L. H. Jones, *Org. Biomol. Chem.* **2012**, *10*, 548.
- [147] S. Yoshida, Y. Hatakeyama, K. Johmoto, H. Uekusa, T. Hosoya, *J. Am. Chem. Soc.* **2014**, *136*, 13590–13593.
- [148] R. R. Ramsubhag, G. B. Dudley, *Org. Biomol. Chem.* **2016**, 1–4.
- [149] J. Tummatorn, P. Batsomboon, R. J. Clark, I. V Alabugin, G. B. Dudley, *J. Org. Chem.* **2012**, *77*, 2093–2097.
- [150] M. Lo Conte, S. Staderini, A. Marra, M. Sanchez-Navarro, B. G. Davis, A. Dondoni, *Chem. Commun.* **2011**, *47*, 11086.
- [151] A. a Kislukhin, V. P. Hong, K. E. Breitenkamp, M. G. Finn, *Bioconjug. Chem.* **2013**, *24*, 684–689.
- [152] X. Zhang, R. P. Hsung, L. You, *Org. Biomol. Chem.* **2006**, *4*, 2679–2682.
- [153] I. E. Valverde, F. Lecaille, G. Lalmanach, V. Aucagne, A. F. Delmas, *Angew. Chem. Int. Ed.* **2012**, *51*, 718–722.
- [154] P. M. E. Gramlich, S. Warncke, J. Gierlich, T. Carell, *Angew. Chem. Int. Ed.* **2008**, *47*, 3442–3444.
- [155] V. Aucagne, D. a. Leigh, *Org. Lett.* **2006**, *8*, 4505–4507.
- [156] Z. Yuan, G. C. Kuang, R. J. Clark, L. Zhu, *Org. Lett.* **2012**, *14*, 2590–2593.
- [157] W. S. Brotherton, H. a Michaels, J. T. Simmons, R. J. Clark, N. S. Dalal, L. Zhu, *Org. Lett.* **2009**, *11*, 4954–4957.
- [158] G.-C. Kuang, P. M. Guha, W. S. Brotherton, J. T. Simmons, L. A. Stankee, B. T. Nguyen, R. J. Clark, L. Zhu, *J. Am. Chem. Soc.* **2011**, *133*, 13984–14001.
- [159] N. Münster, P. Nikodemiak, U. Koert, *Org. Lett.* **2016**, *18*, 4296–4299.

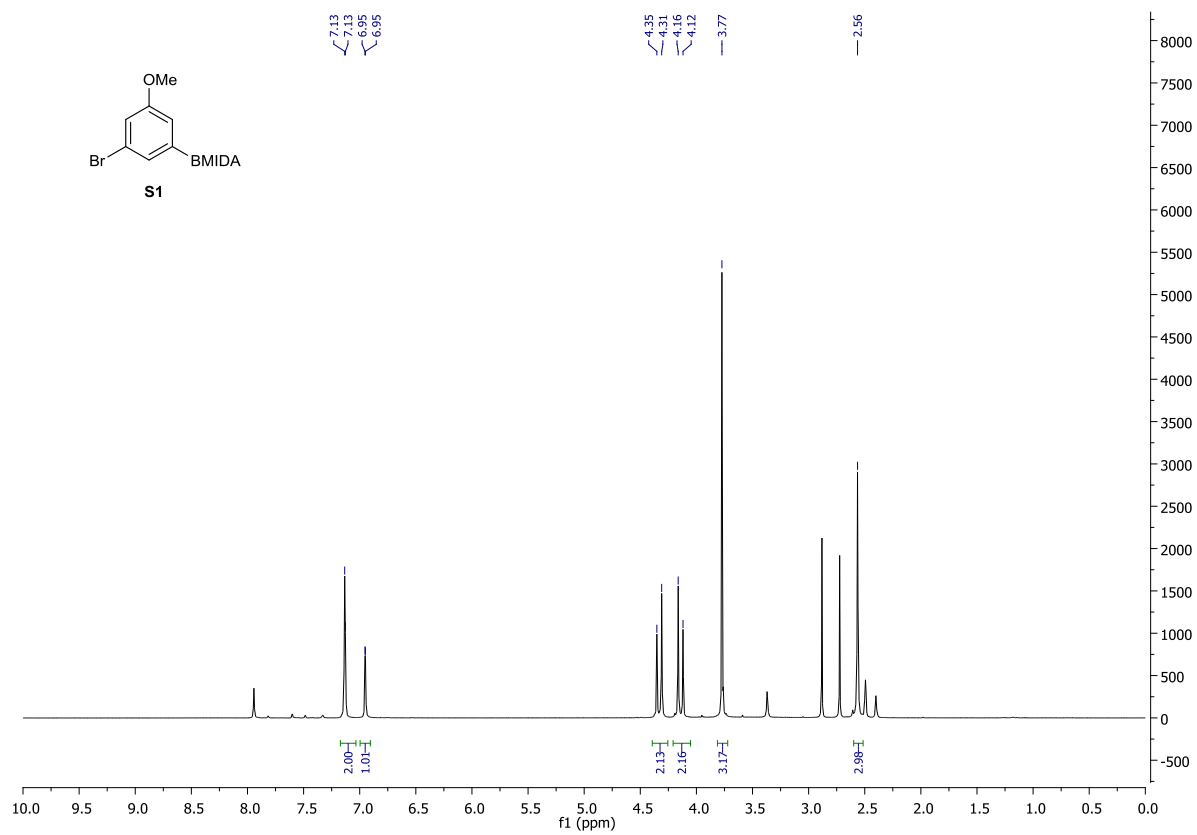
- [160] J. E. Hein, J. C. Tripp, L. B. Krasnova, K. B. Sharpless, V. V. Fokin, *Angew. Chem. Int. Ed.* **2009**, *48*, 8018–8021.
- [161] K. Yamamoto, T. Bruun, J. Y. Kim, L. Zhang, M. Lautens, *Org. Lett.* **2016**, *18*, 2644–2647.
- [162] W. Wang, F. Wei, Y. Ma, C. H. Tung, Z. Xu, *Org. Lett.* **2016**, *18*, 4158–4161.
- [163] G. Evano, A. Coste, K. Jouvin, *Angew. Chem. Int. Ed.* **2010**, *49*, 2840–2859.
- [164] G. A. Burley, D. L. Davies, G. A. Griffith, M. Lee, K. Singh, *J. Org. Chem.* **2010**, *75*, 980–983.
- [165] G. A. Burley, Y. Boutadla, D. L. Davies, K. Singh, *Organometallics* **2012**, *31*, 1112–1117.
- [166] M. Z. C. Hatit, J. C. Sadler, L. a. McLean, B. C. Whitehurst, C. P. Seath, L. D. Humphreys, R. J. Young, A. J. B. Watson, G. A. Burley, *Org. Lett.* **2016**, *18*, 1694–1697.
- [167] J. B. Metternich, D. G. Artiukhin, M. C. Holland, M. Von Bremen-Kü, J. Neugebauer, R. Gilmour, **2017**, DOI 10.1021/acs.joc.7b01281.
- [168] G. Fang, X. Bi, *Chem. Soc. Rev.* **2015**, *44*, 8124–8173.
- [169] W. L. Armarego, D. D. Perrin, *Purification of Laboratory Chemicals*, Butterworth-Heinemann, **1996**.
- [170] B. S. L. Collins, M. G. Suero, M. J. Gaunt, *Angew. Chem. Int. Ed.* **2013**, *52*, 5799–5802.
- [171] G. Bélanger, M. Dupuis, R. Larouche-Gauthier, *J. Org. Chem.* **2012**, *77*, 3215–3221.
- [172] L. Sahoo, A. Singhamahapatra, D. Loganathan, *Org. Biomol. Chem.* **2014**, *12*, 2615–2625.
- [173] P. Khedar, K. Pericherla, A. Kumar, *Synlett* **2014**, *25*, 515–518.
- [174] J. Schmitz, T. Li, U. Bartz, M. Gütschow, *ACS Med. Chem. Lett.* **2016**, *7*, 211–216.
- [175] S. K. Mamidyala, M. a. Cooper, *Chem. Commun.* **2013**, *49*, 8407.
- [176] K. Sivakumar, F. Xie, B. M. Cash, S. Long, H. N. Barnhill, Q. Wang, *Org. Lett.* **2004**, *6*, 4603–4606.
- [177] S. Wolfram, H. Würfel, S. H. Habenicht, C. Lembke, P. Richter, E. Birckner, R. Beckert, G. Pohnert, *Beilstein J. Org. Chem.* **2014**, *10*, 2470–2479.

- [178] B. Huang, J. F. Kukowska-Latallo, S. Tang, H. Zong, K. B. Johnson, A. Desai, C. L. Gordon, P. R. Leroueil, J. R. Baker, *Bioorganic Med. Chem. Lett.* **2012**, *22*, 3152–3156.
- [179] J. S. Oakdale, R. K. Sit, V. V. Fokin, *Chem. Eur. J.* **2014**, *20*, 11101–11110.
- [180] Y.-L. Chen, P. Sharma, R.-S. Liu, *Chem. Commun.* **2016**, *52*, 3187–3190.
- [181] P. W. Szafranski, P. Kasza, M. T. Cegła, *Tetrahedron Lett.* **2015**, *56*, 6244–6247.
- [182] S. P. Bew, G. D. Hiatt-Gipson, J. A. Lovell, C. Poullain, *Org. Lett.* **2012**, *14*, 456–459.
- [183] www.sigmaaldrich.com
- [184] B. R. Buckley, S. E. Dann, H. Heaney, *Chem. Eur. J.* **2010**, *16*, 6278–6284.
- [185] X. Cheng, Y. Yang, C. Kuang, Q. Yang, *Synthesis* **2011**, 2907–2912.
- [186] F. Jalilian, B. Yadollahi, S. Tangestaninejad, H. A. Rudbari, *RSC Adv.* **2016**, *6*, 13609–13613.
- [187] R. H. Tale, V. B. Gopula, G. K. Toradmal, *Tetrahedron Lett.* **2015**, *56*, 5864–5869.
- [188] Z. Zheng, L. Shi, *Tetrahedron Lett.* **2016**, *57*, 5132–5134.
- [189] A. Taher, D. Nandi, R. U. Islam, M. Choudhary, K. Mallick, *RSC Adv.* **2015**, *5*, 47275–47283.
- [190] A. Bolje, D. Urankar, J. Košmrlj, *European J. Org. Chem.* **2014**, *2014*, 8167–8181.

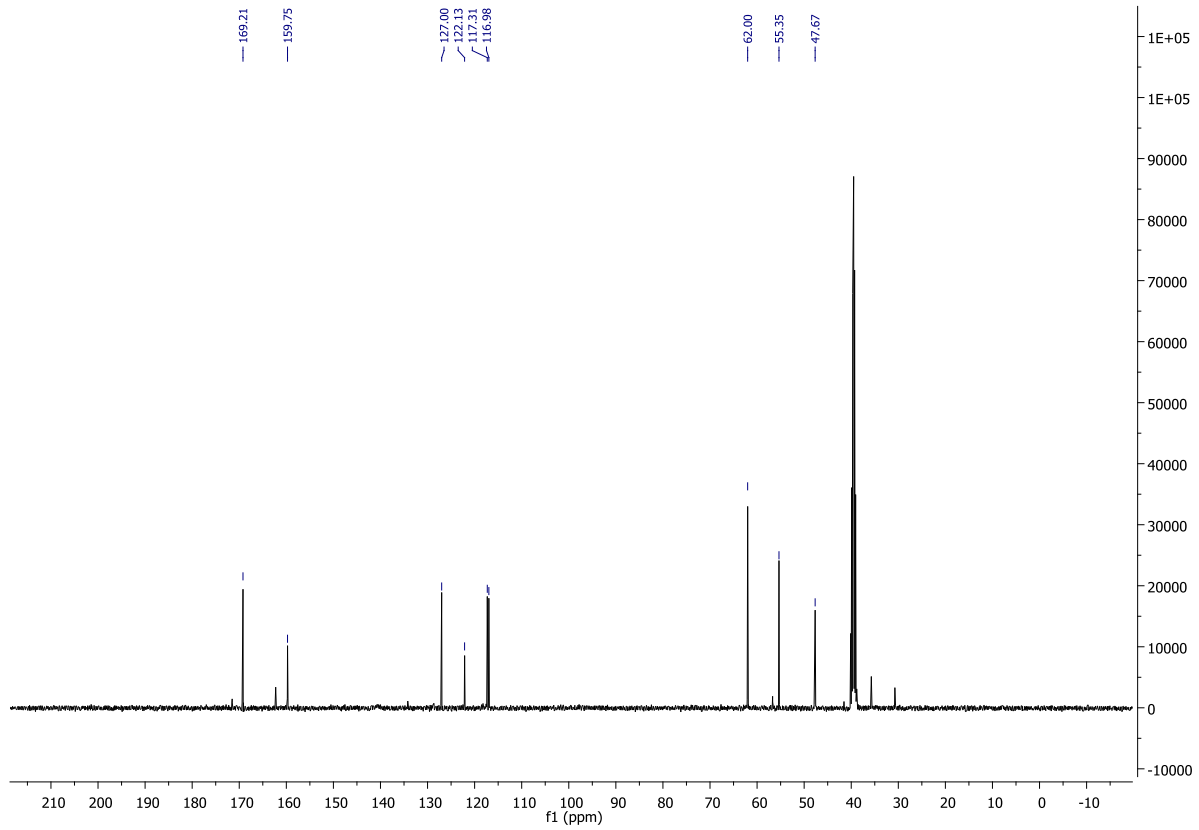
Appendix

Chapter 1

^1H NMR of S1



¹³C NMR of S1

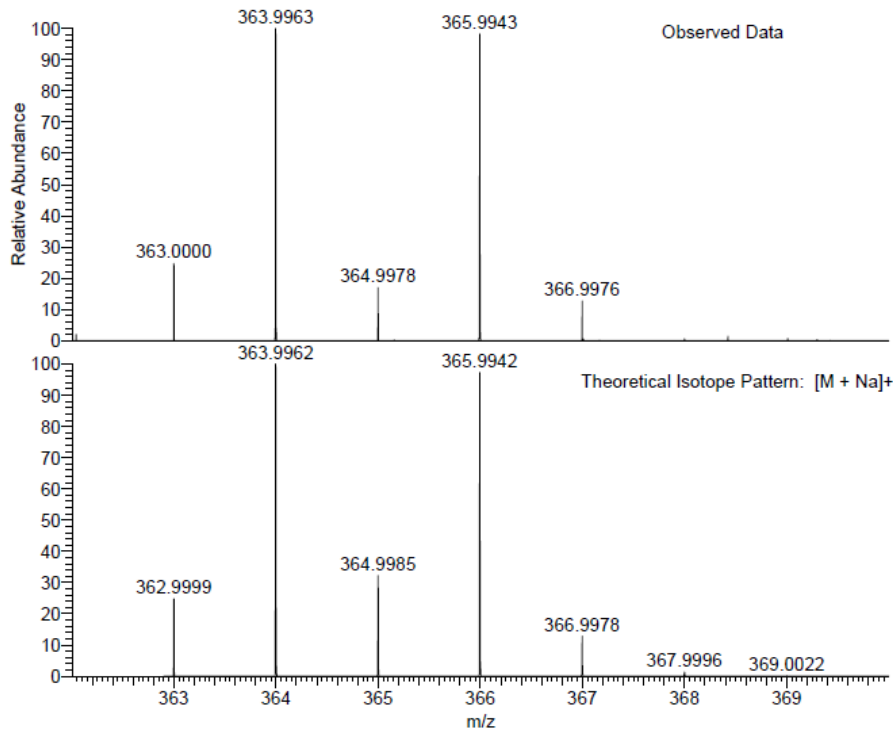


HRMS of S1

cs265 MW=341?
C₁₂H₁₃BBrNO₅
(MeCN)/MeCN

EPSRC National Facility Swansea
LTQ Orbitrap XL

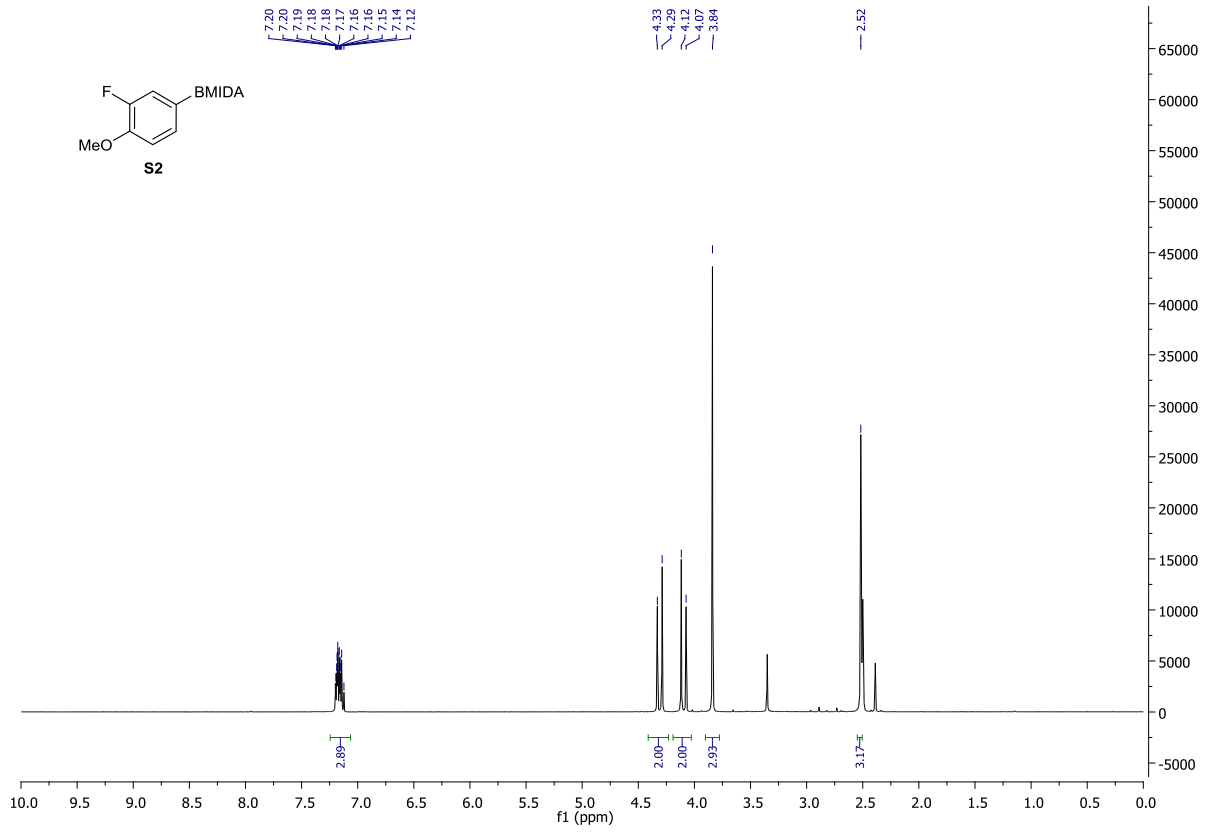
Ciaran Seath
01/05/2015 12:25:08



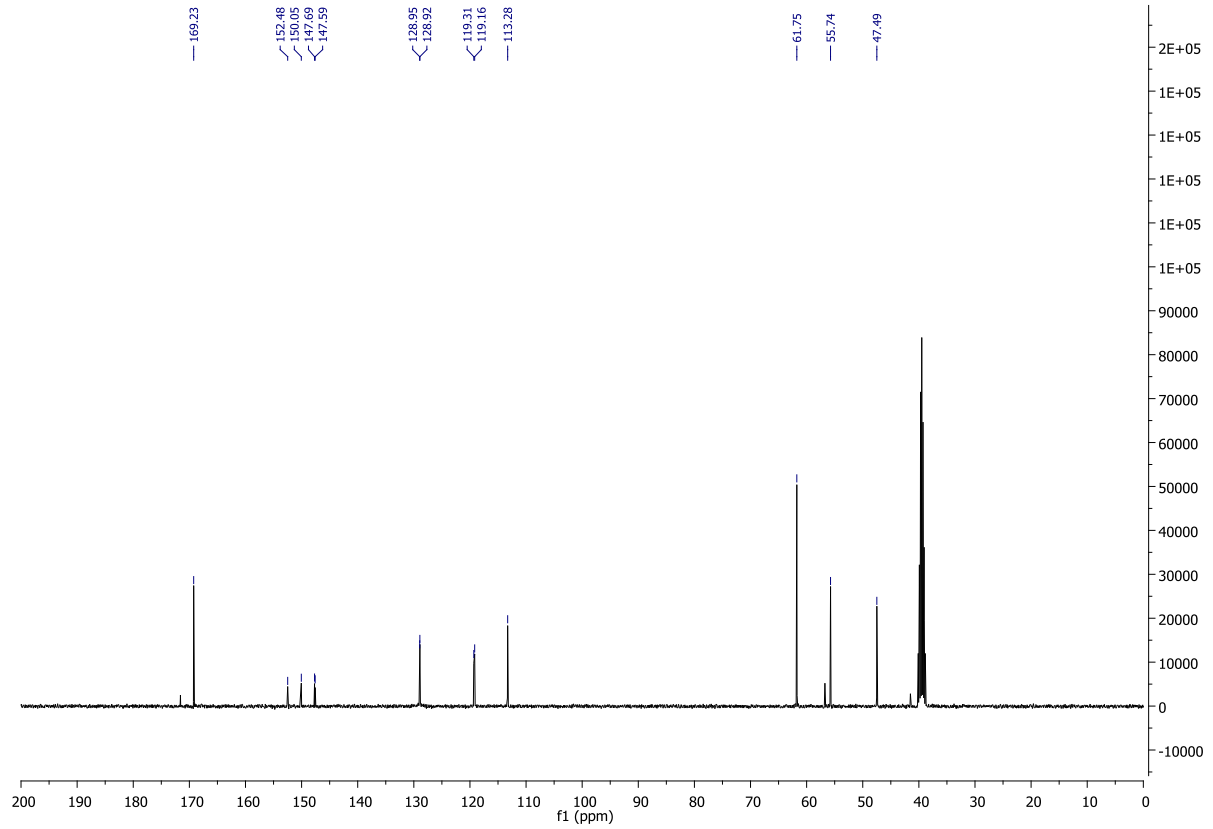
NL:
3.03E5
STRWAT490-OR-HNESP#26-
46 RT: 0.66-1.04 AV: 15 T:
FTMS + p NSI Full ms
[140.00-1935.00]

NL:
8.24E3
C₁₂H₁₃BBrNO₅Na:
C₁₂H₁₃Br₁N₁O₅Na₁
p (gss, s /p:40) Chrg 1
R: 100000 Res .Pwr . @FWHM

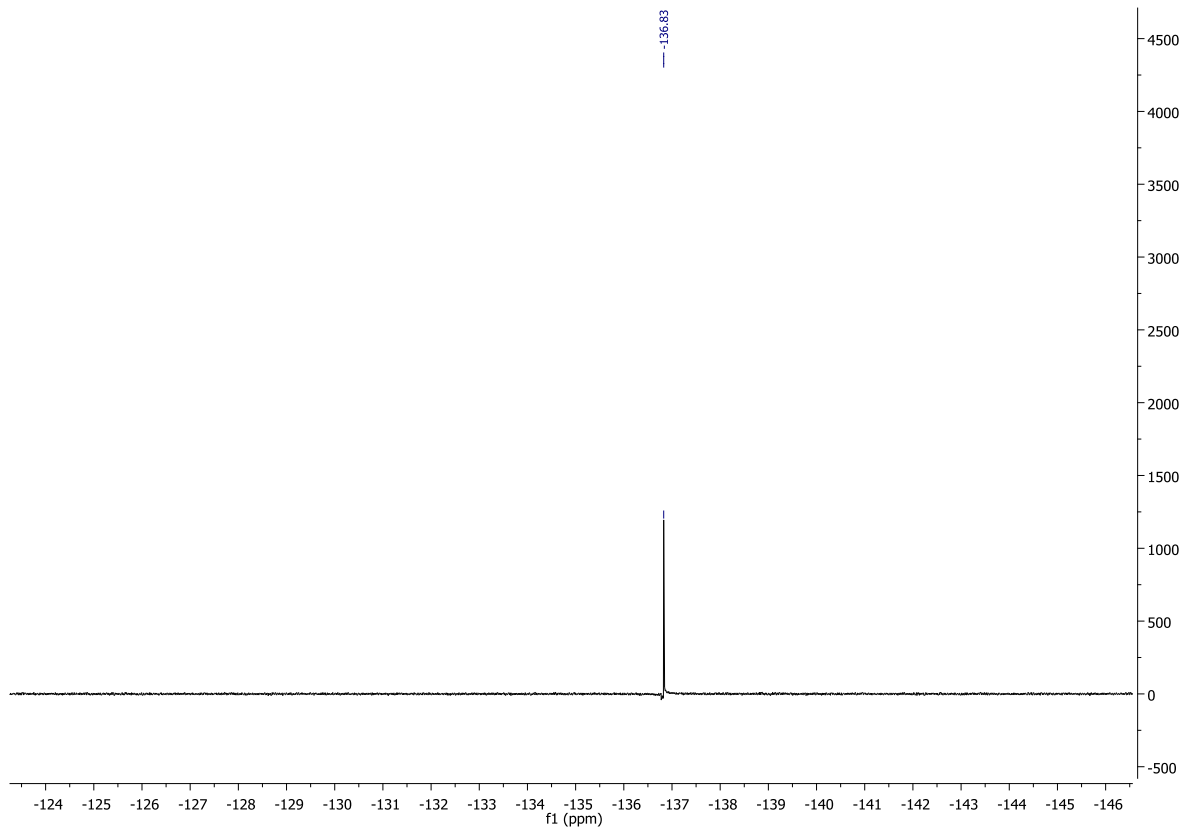
¹H NMR of S2



¹³C NMR of S2



¹⁹F NMR of S2

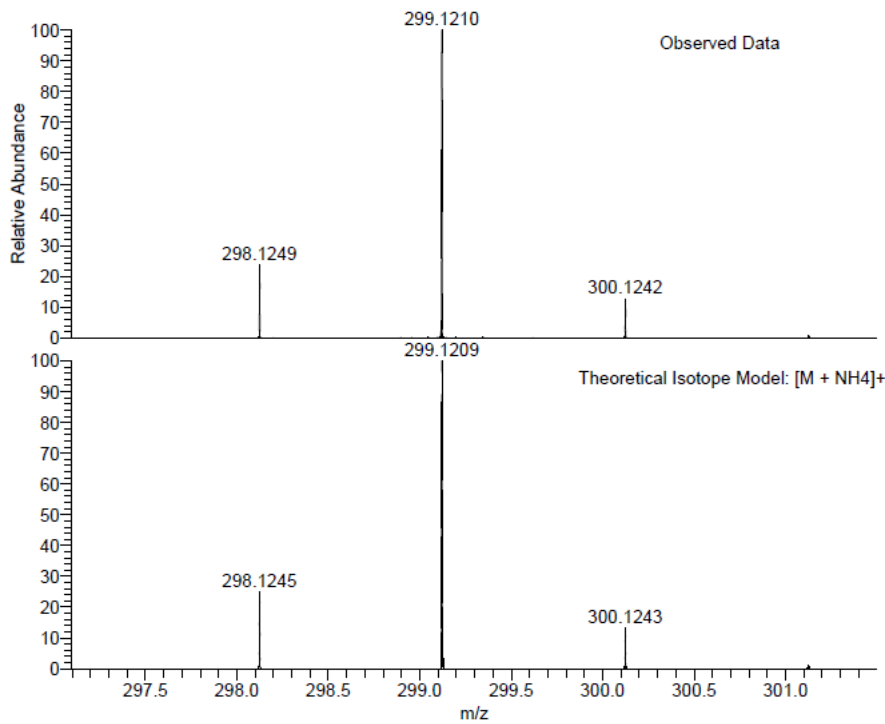


HRMS of S2

JF360 MW=281?
C₁₂H₁₃BFNO₅
MeCN/MeOH + NH₄OAc

EPSRC National Facility Swansea
LTQ Orbitrap XL

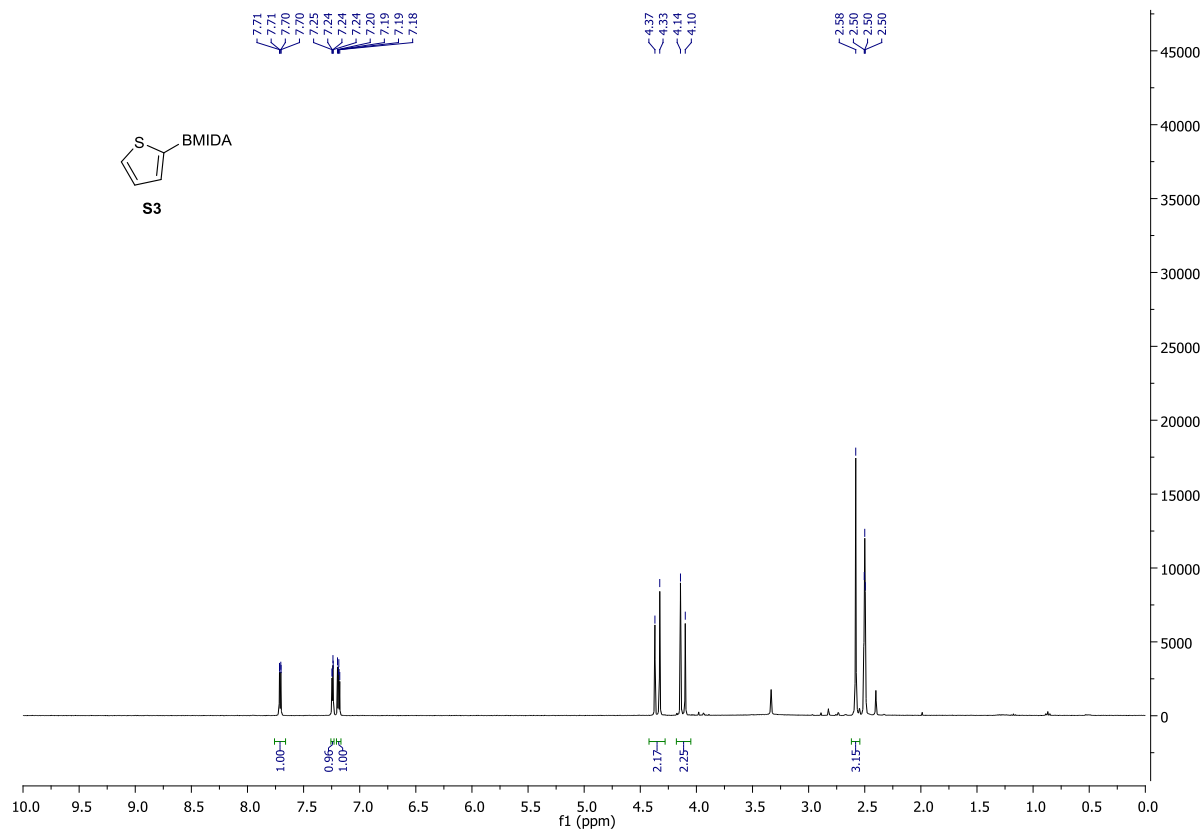
James Fyfe
16/04/2015 07:12:18



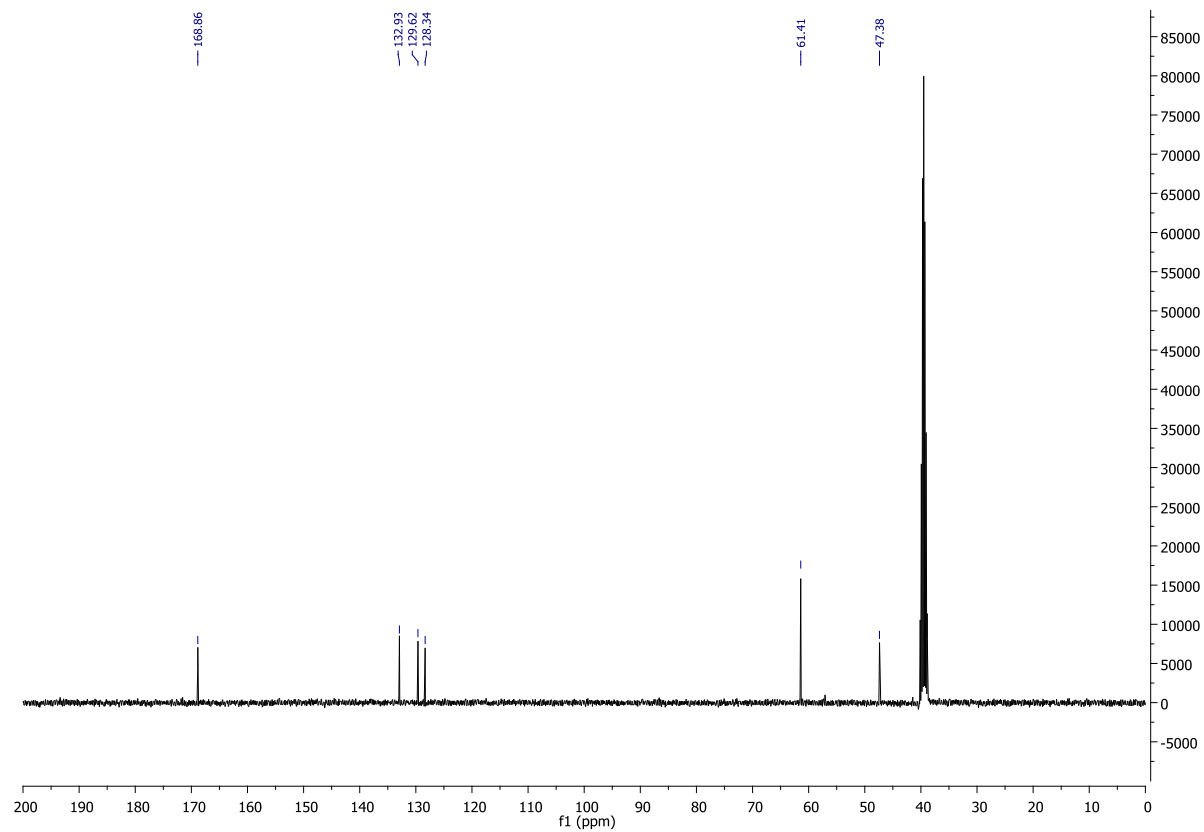
NL:
3.90E7
STRWAT470-OA-HNESP#31-
44 RT: 0.67-1.03 AV: 14 T:
FTMS + p NSI Full ms
[140.00-1935.00]

NL:
1.62E4
C₁₂H₁₃BFNO₅NH₄
C₁₂H₁₇B₁F₁N₂O₅
p (gss, s /p:40) Chrg 1
R: 100000 Res .Pwr . @FWHM

¹H NMR of S3



¹³C NMR of S3

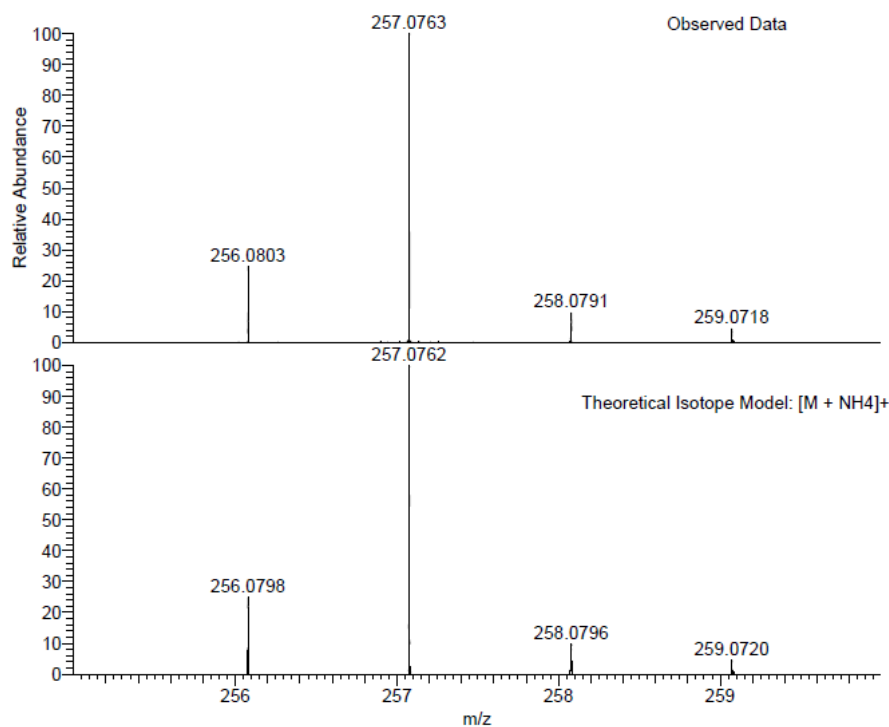


HRMS of S3

JF358 MW=239?
C₉H₁₀BNO₄S
MeCN/MeOH + NH₄OAc

EPSRC National Facility Swansea
LTQ Orbitrap XL

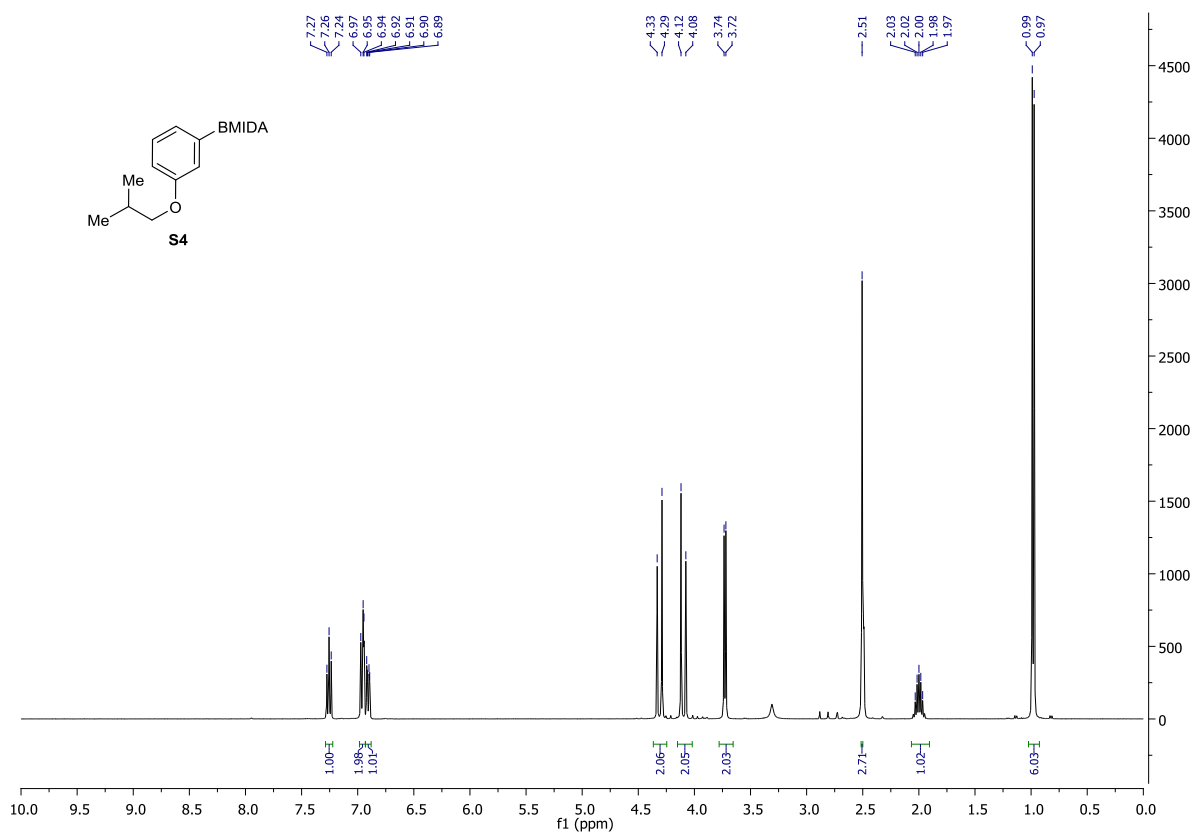
James Fyfe
16/04/2015 07:15:09



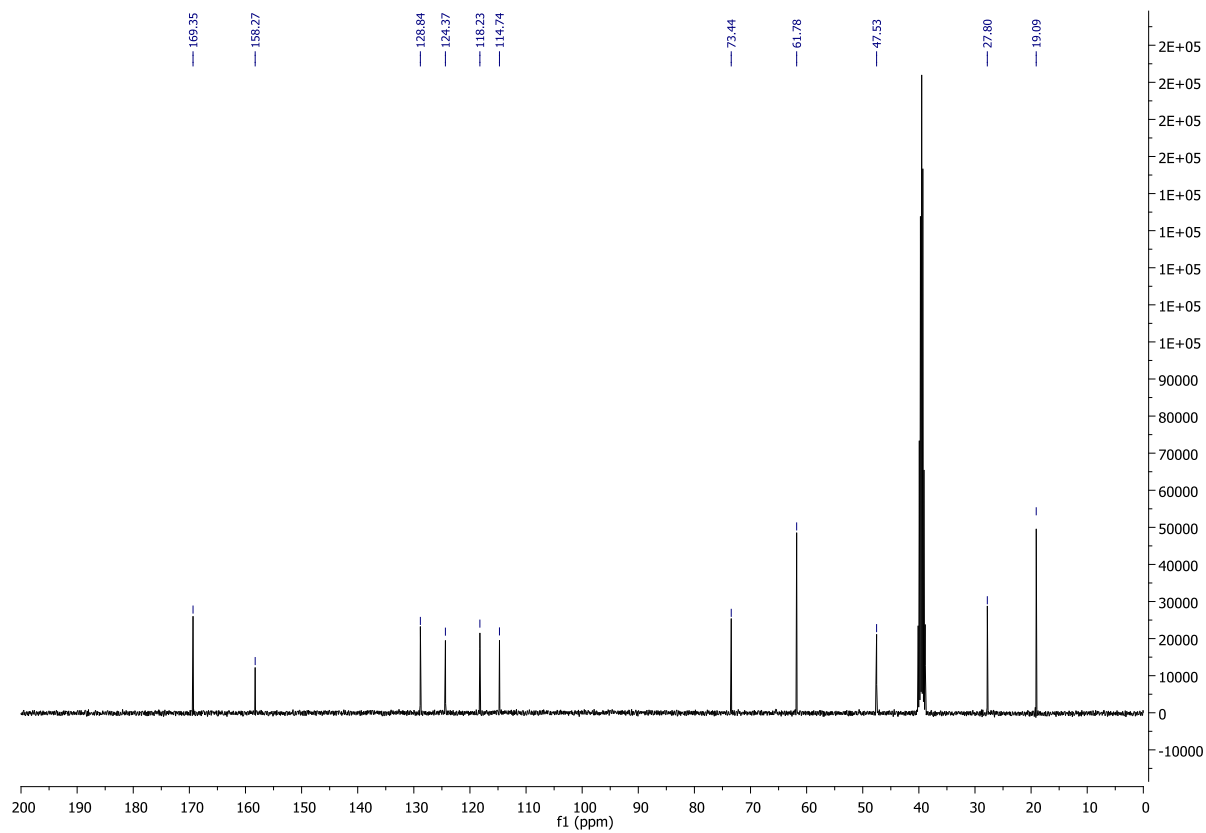
NL:
5.76E7
STRWAT471-OA-HNESP#31-
43 RT: 0.69-1.02 AV: 13 T:
FTMS + p NSI Full ms
[140.00-1935.00]

NL:
1.59E4
C₉H₁₀BNO₄SNH₄:
C₉H₁₄B₁N₂O₄S₁
p (gss, s/p:40) Chrg 1
R: 100000 Res .Pwr .@FWHM

¹H NMR of S4



¹³C NMR of S4

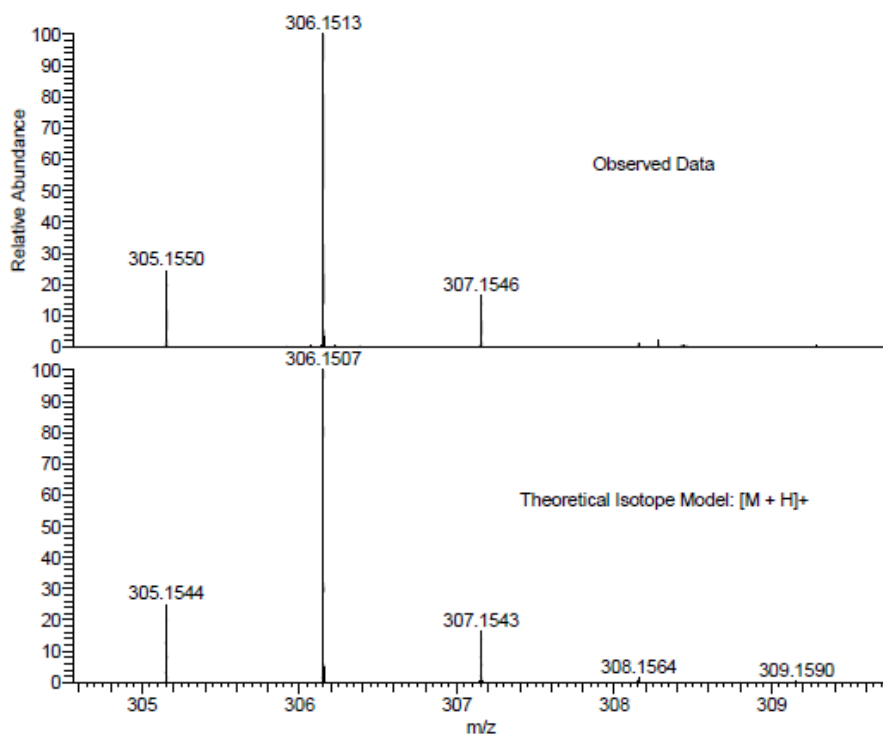


HRMS of S4

CS164-A1 MW=305?
C15H20BNO5
(MeCN)/MeOH + NH4OAc

EPSRC National Facility Swansea
LTQ Orbitrap XL

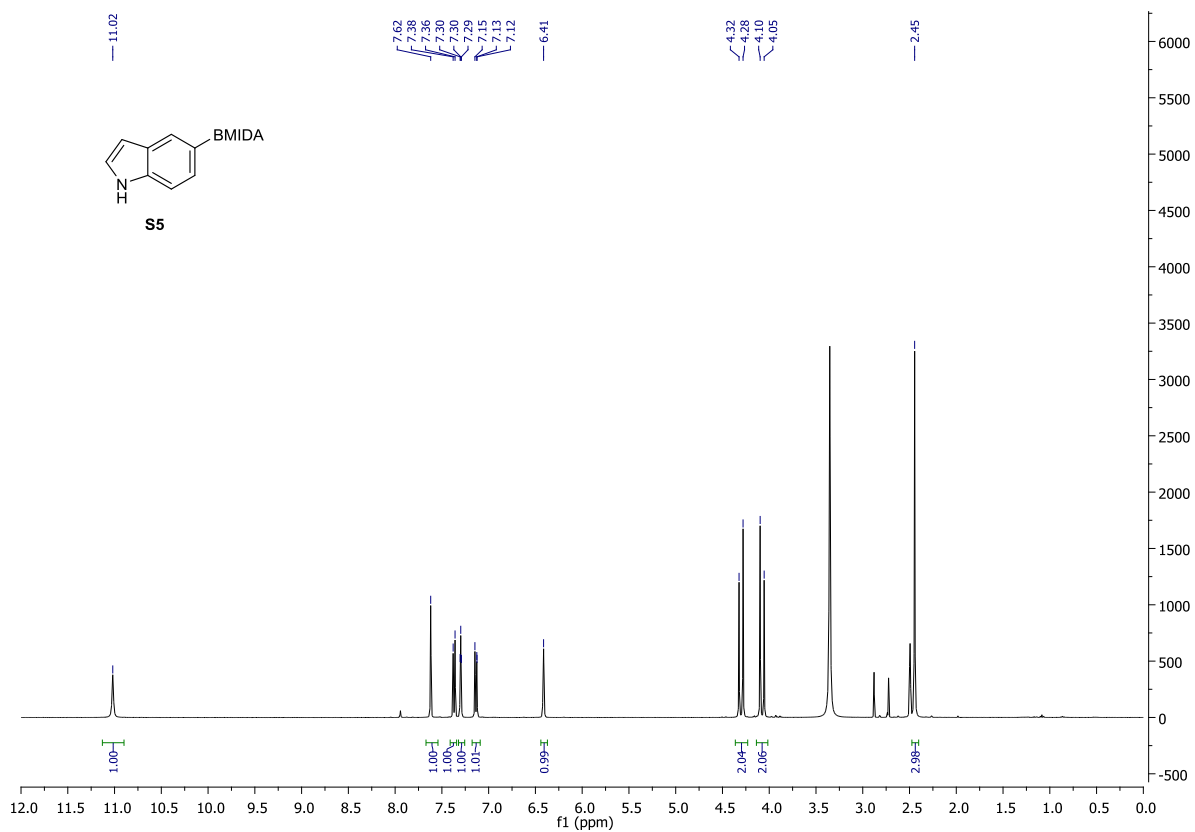
Ciaran Seath
03/02/2015 02:18:10 PM



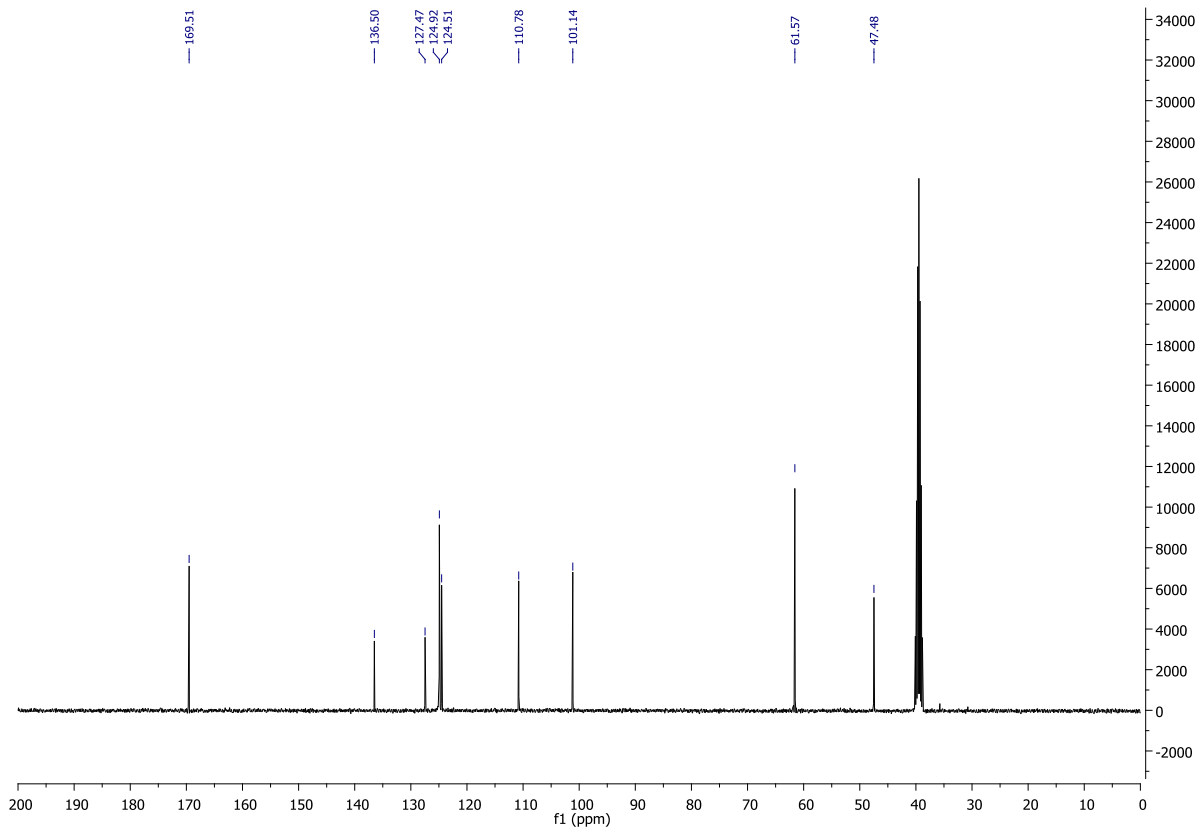
NL:
1.62E6
STRWAT405-OA-HNESP#28-
44 RT: 0.66-1.04 AV: 15 T:
FTMS + p NSI Full ms
[140.00-1935.00]

NL:
1.57E4
C15 H20 BNO5 H:
C15 H21 B1 N1 O5
p (gss, s /p:40) Chrg 1
R: 100000 Res .Pwr .@FWHM

¹H NMR of S5



¹³C NMR of S5

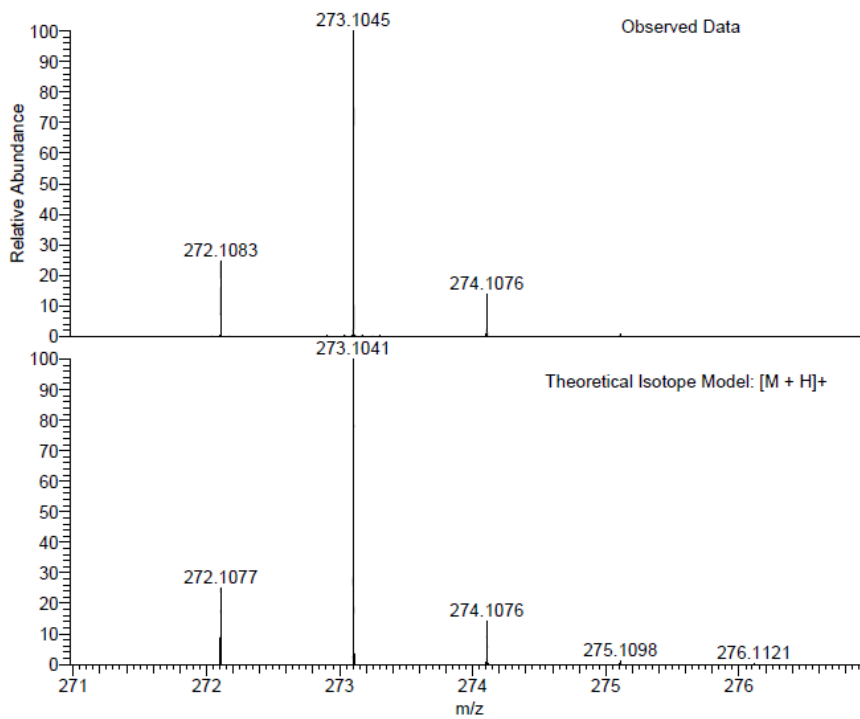


HRMS of S5

JF300-A1 MW=272?
C₁₃H₁₃N₂O₄
MeCN/MeOH + NH₄OAc

EPSRC National Facility Swansea
LTQ Orbitrap XL

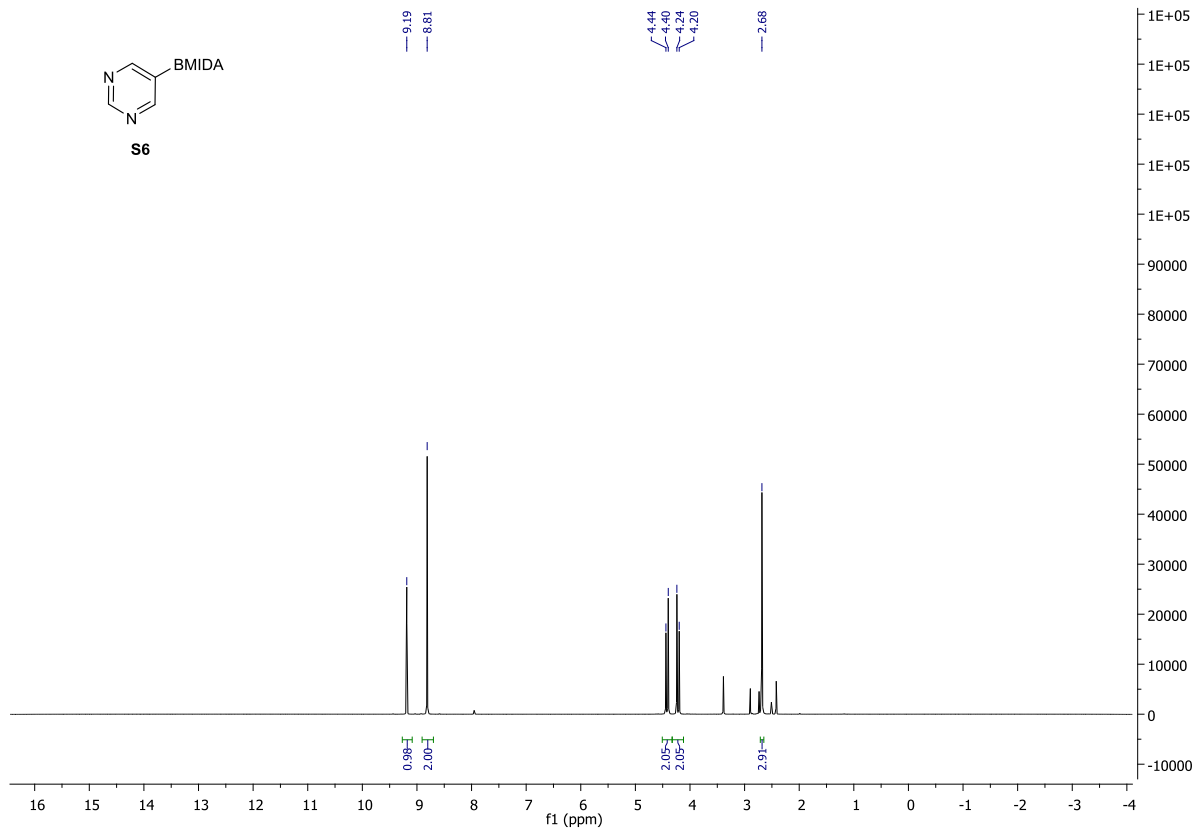
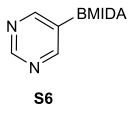
Ciaran Seath
16/04/2015 07:09:29



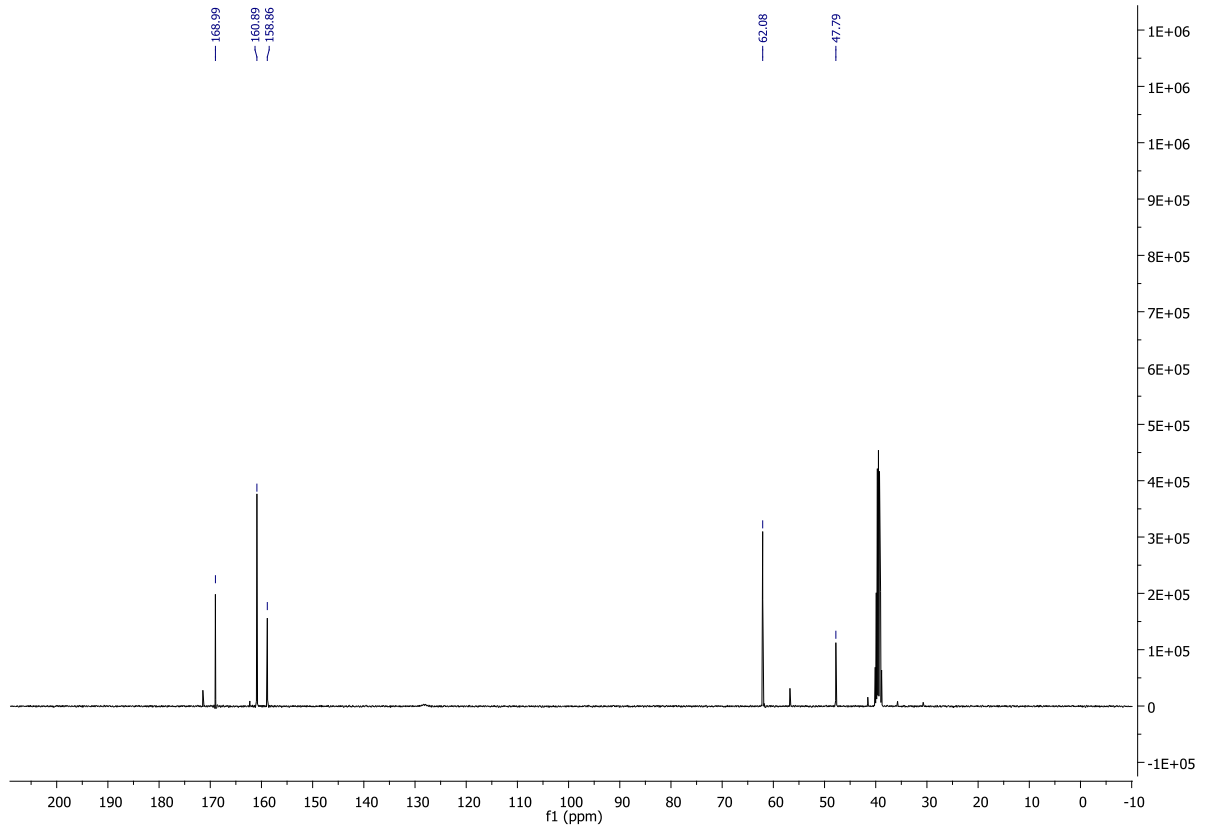
NL:
1.28E7
STRWAT469-OA-HNESP#31-
43 RT: 0.69-1.02 AV: 13 T:
FTMS + p NSI Full ms
[140.00-1935.00]

NL:
1.61E4
C₁₃H₁₃N₂O₄H:
C₁₃H₁₄B₁N₂O₄
p (gss, s /p:40) Chrg 1
R: 100000 Res .Pwr. @FWHM

¹H NMR of S6



¹³C NMR of S6

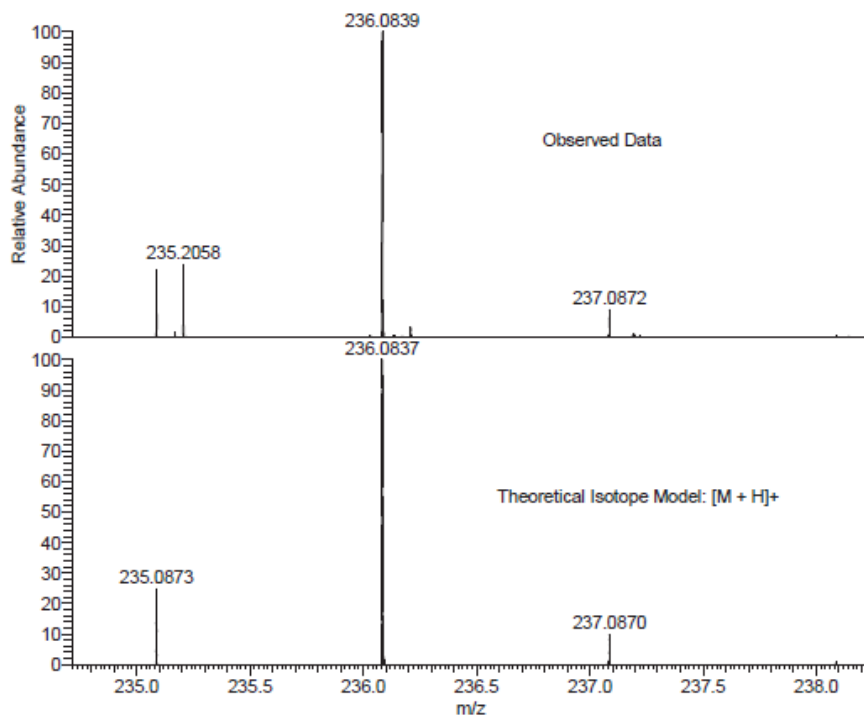


HRMS of S6

CS182-A1 MW=235?
C9H10BN3O4
(MeCN)/MeOH + NH4OAc

EPSRC National Facility Swansea
LTQ Orbitrap XL

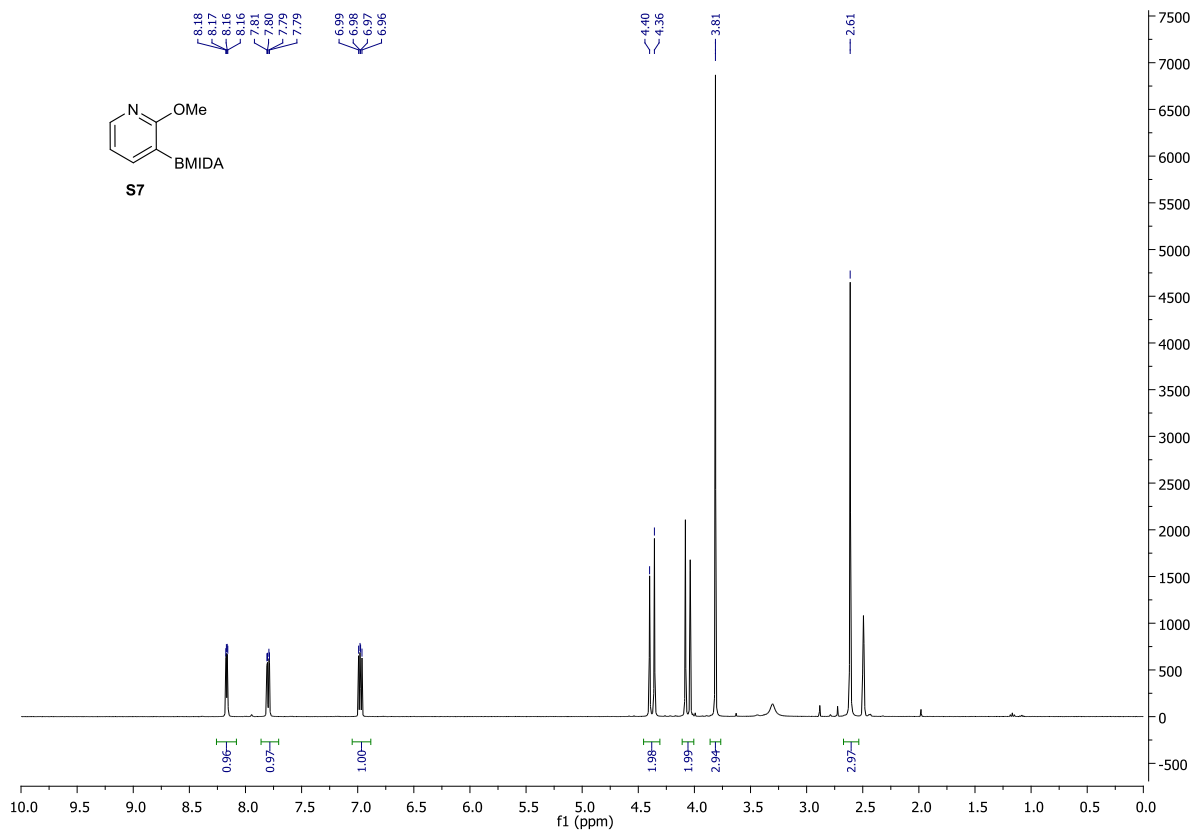
Ciaran Seath
03/02/2015 02:15:23 PM



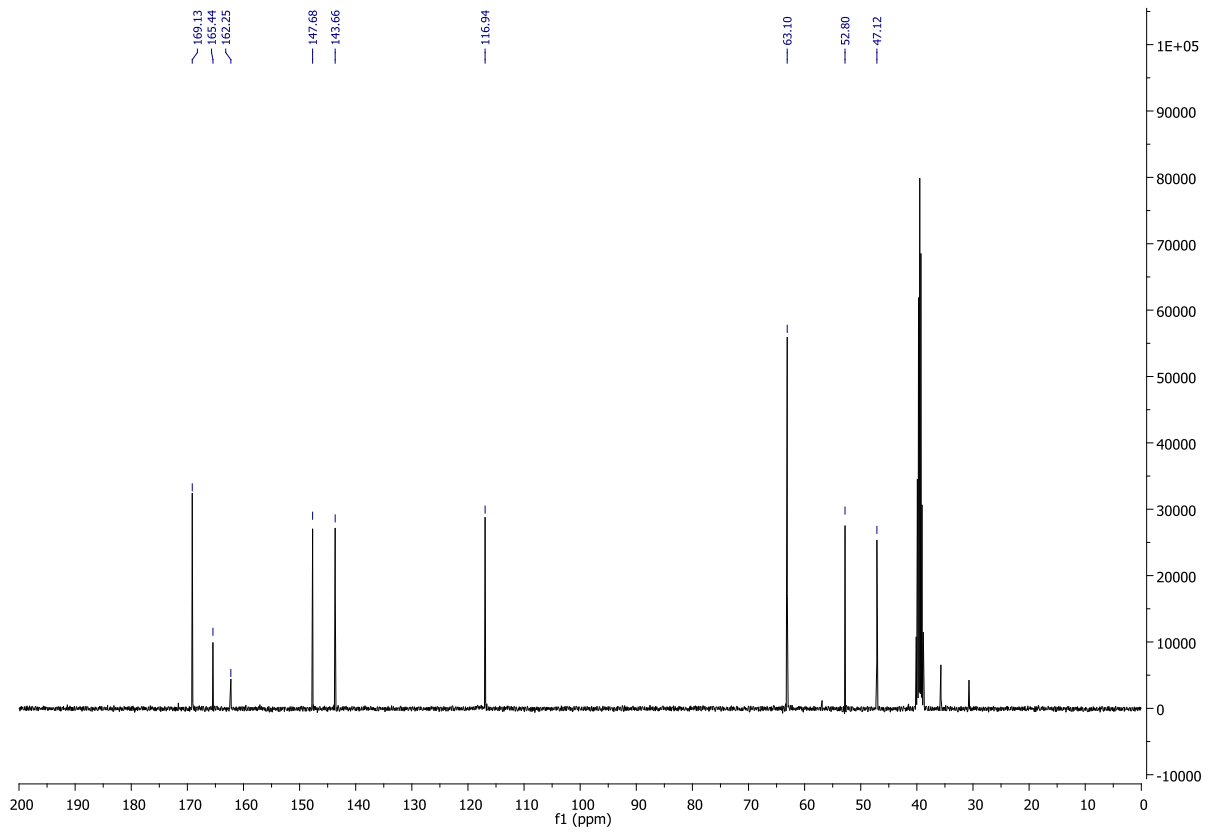
NL:
3.03E5
STRWAT404-OA-HNESP#27-
42 RT: 0.65-1.03 AV: 14 T:
FTMS + p NSI Full ms
[140.00-1935.00]

NL:
1.67E4
C₉H₁₀BN₃O₄H:
C₉H₁₁B₁N₃O₄
p (gss, s/p:40) Chrg 1
R: 100000 Res .Pwr .@FWHM

¹H NMR of S7



¹³C NMR of S7

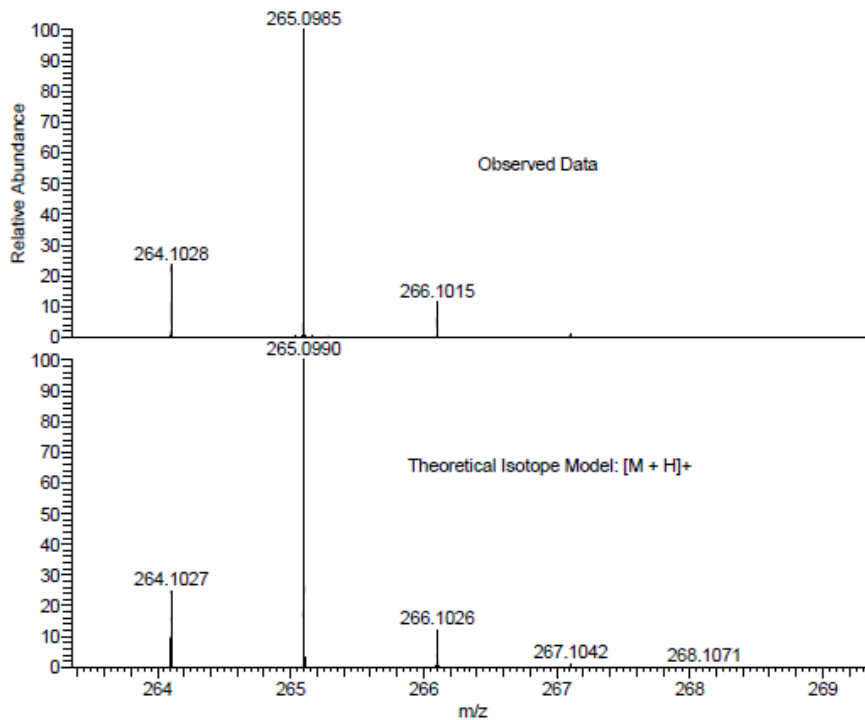


HRMS of S7

CS163-A1 MW=264?
C11H13BN2O5
(MeCN)/MeOH + NH4OAc

EPSRC National Facility Swansea
LTQ Orbitrap XL

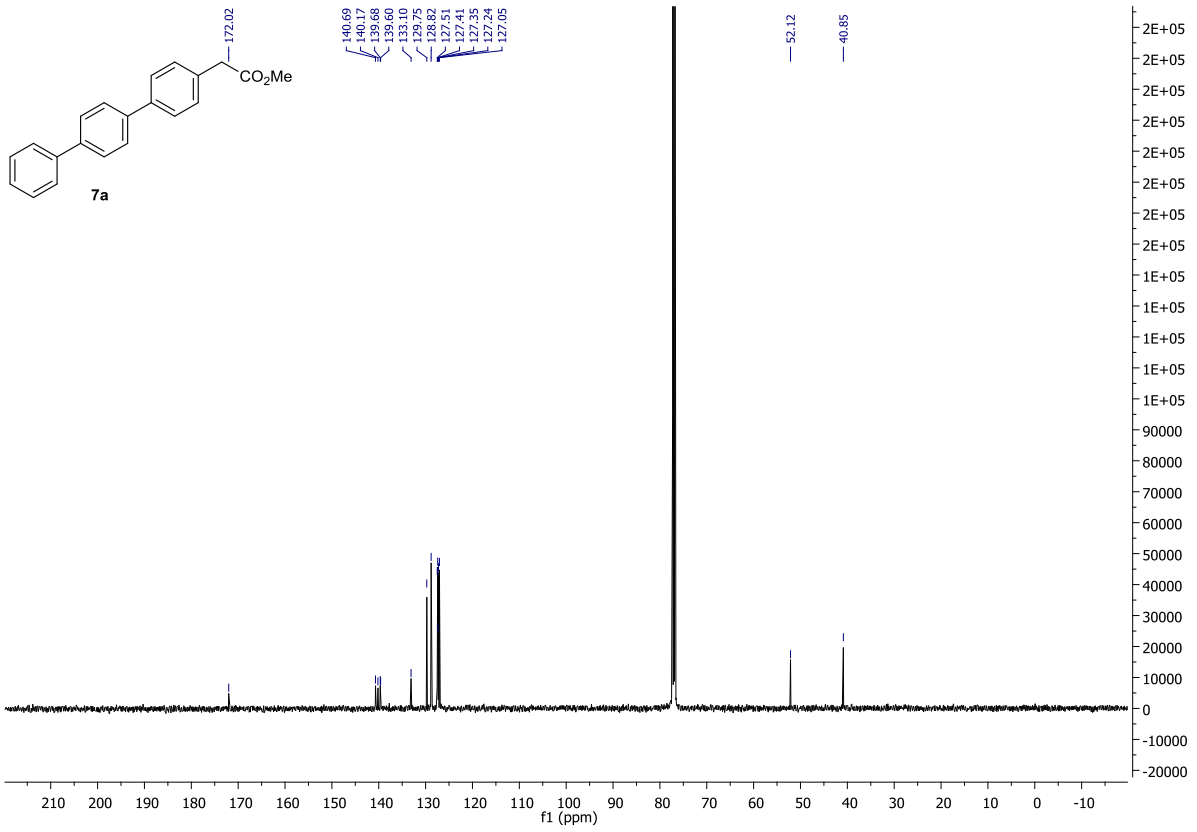
Ciaran Seath
03/02/2015 02:46:24 PM



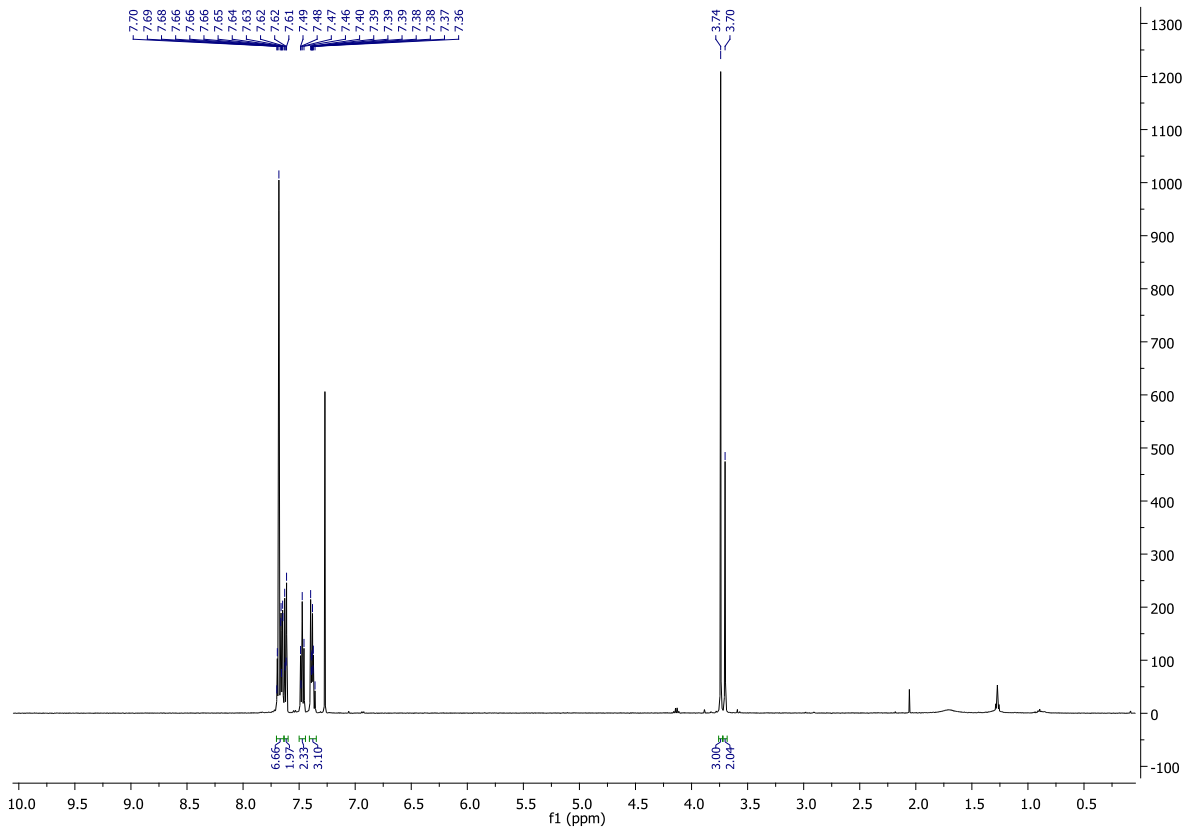
NL:
3.74E7
STRWAT415-OA-HNESP#7-23
RT: 0.11-0.54 AV: 17 T:
FTMS + p NSI Full ms
[140.00-1935.00]

NL:
1.64E4
C11H13BN2O5H:
C11H14B1N2O5
p (gss, s/p:40) Chrg 1
R: 100000 Res .Pwr . @FWHM

¹H NMR of 7a



¹³C NMR of 7a

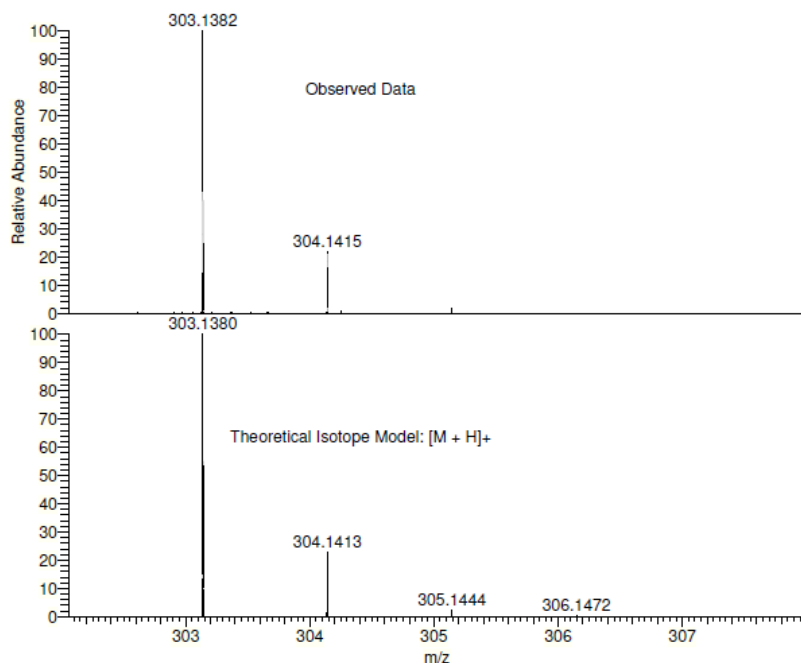


HRMS of 7a

CS31-A1 MW=302?
C₂₁H₁₈O₂
(MeOH)/MeOH + NH₄OAc

EPSRC National Facility Swansea
LTO Orbitrap XL

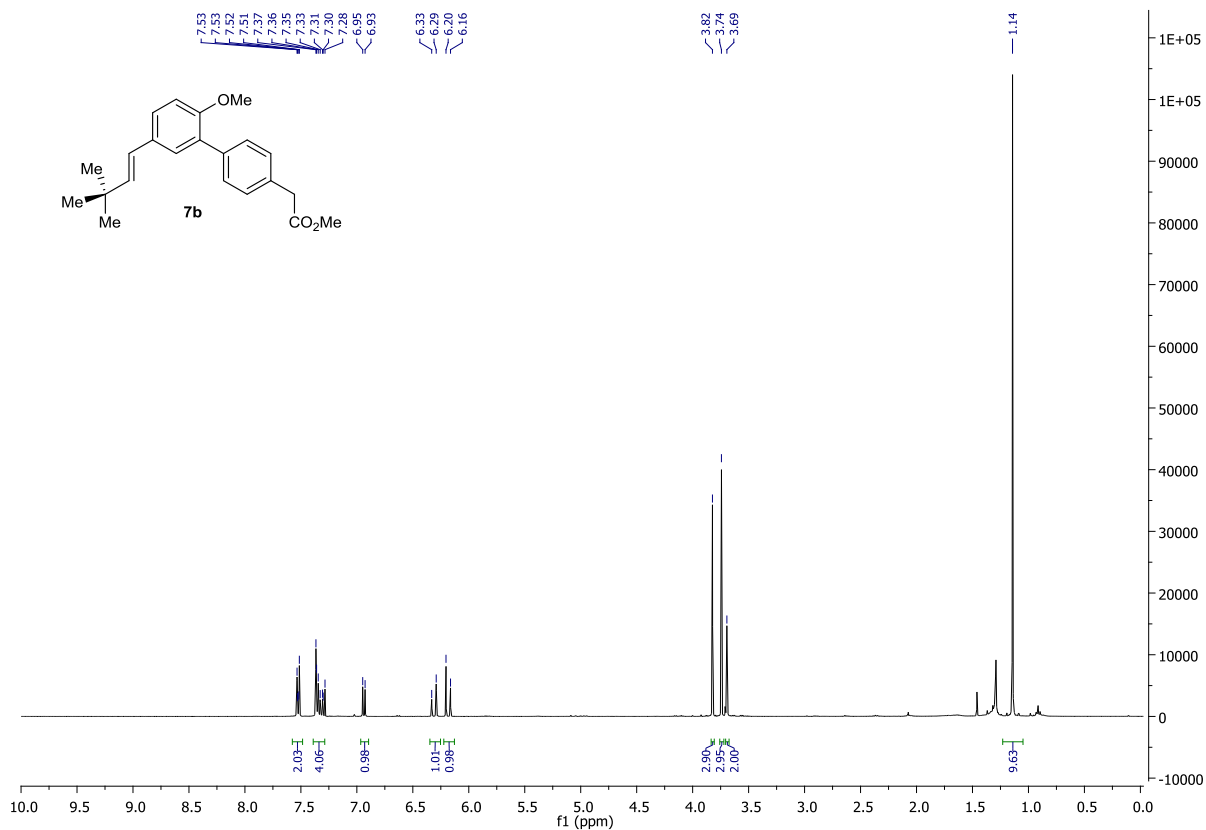
James Fyfe
03/02/2014 11:36:23



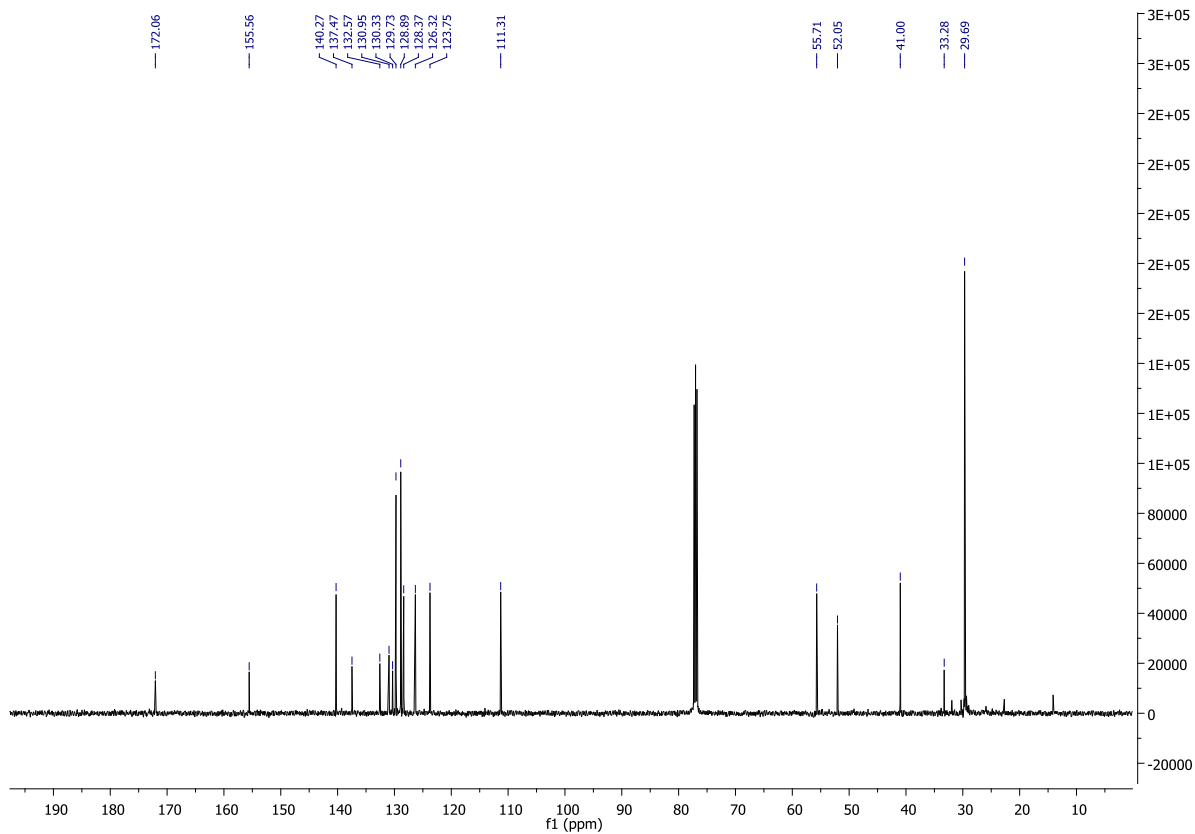
NL:
1.10E7
STRWAT166-OA-HNESP#30-
47 RT: 0.69-1.14 AV: 17 T:
FTMS + p NSI Full ms
[120.00-2000.00]

NL:
1.86E4
C₂₁H₁₈O₂ H:
C₂₁H₁₉O₂
p (gss, s /p:40) Chrg 1
R: 100000 Res .Pwr .@FWHM

¹H NMR of 7b



¹³C NMR of 7b

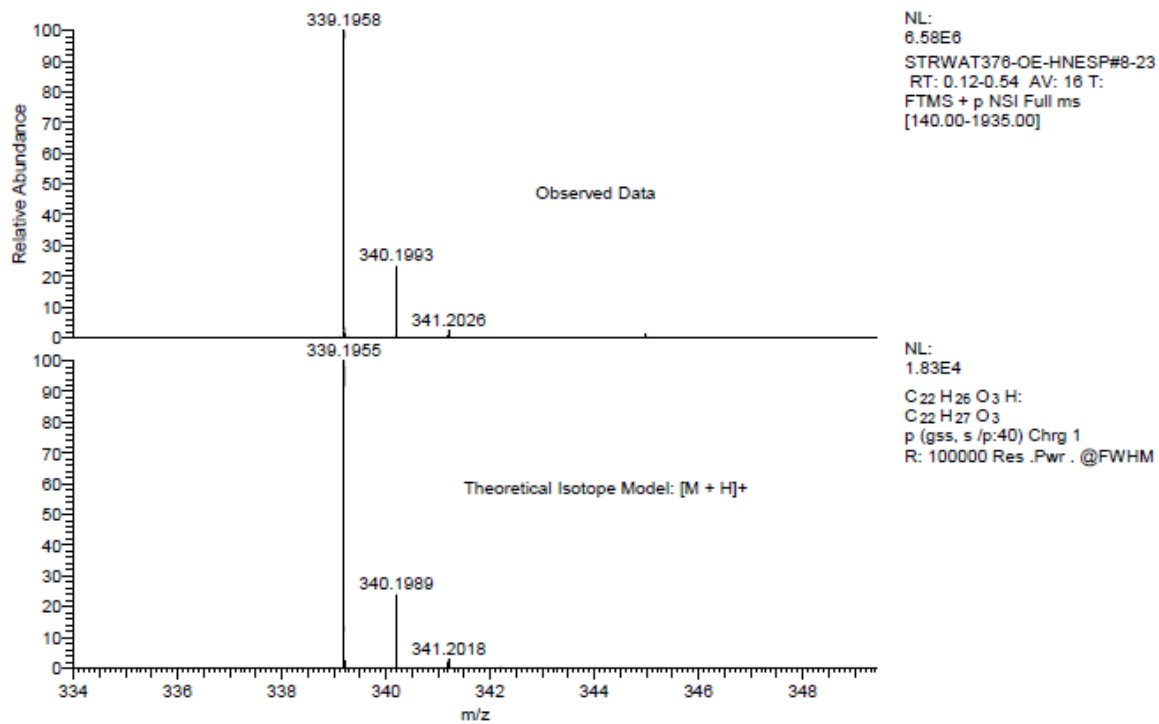


HRMS of 7b

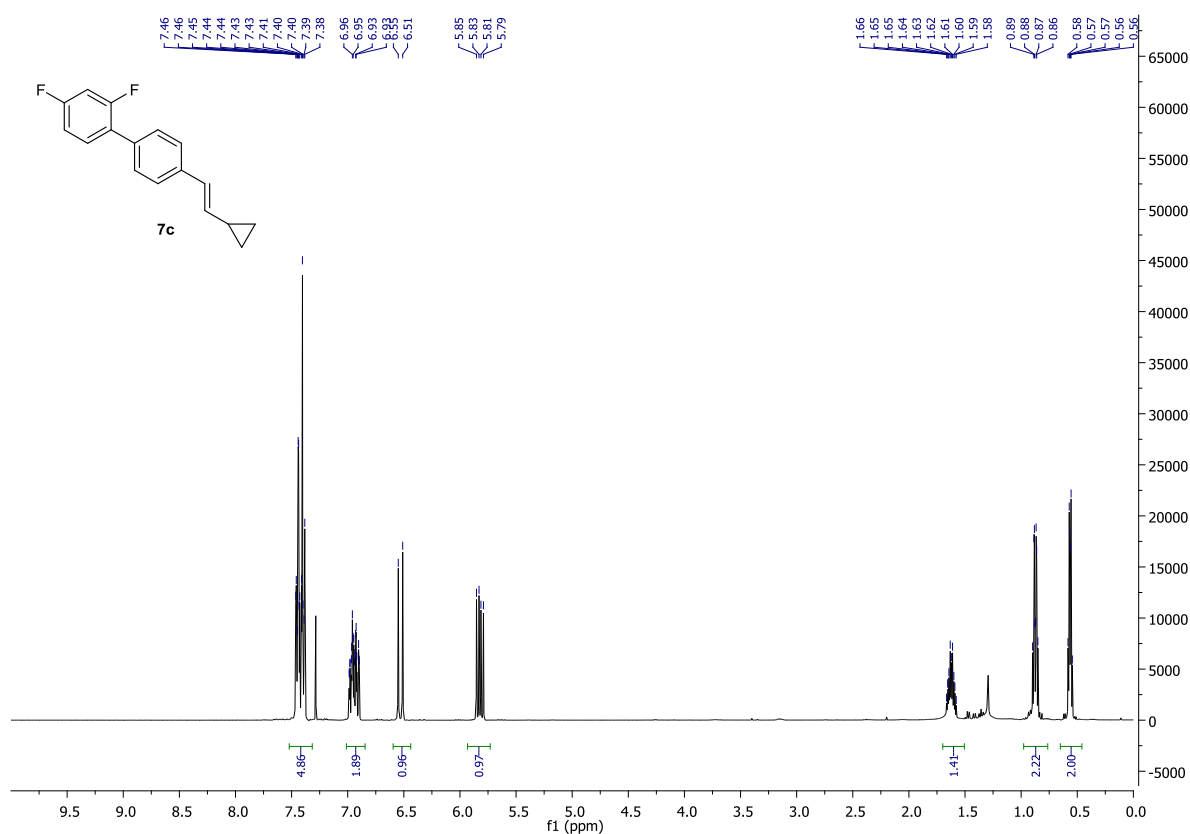
cs103 MW=338?
(MeOH)/MeOH + NH4OAc
C22H26O3

EPSRC National Facility Swansea
LTQ Orbitrap XL

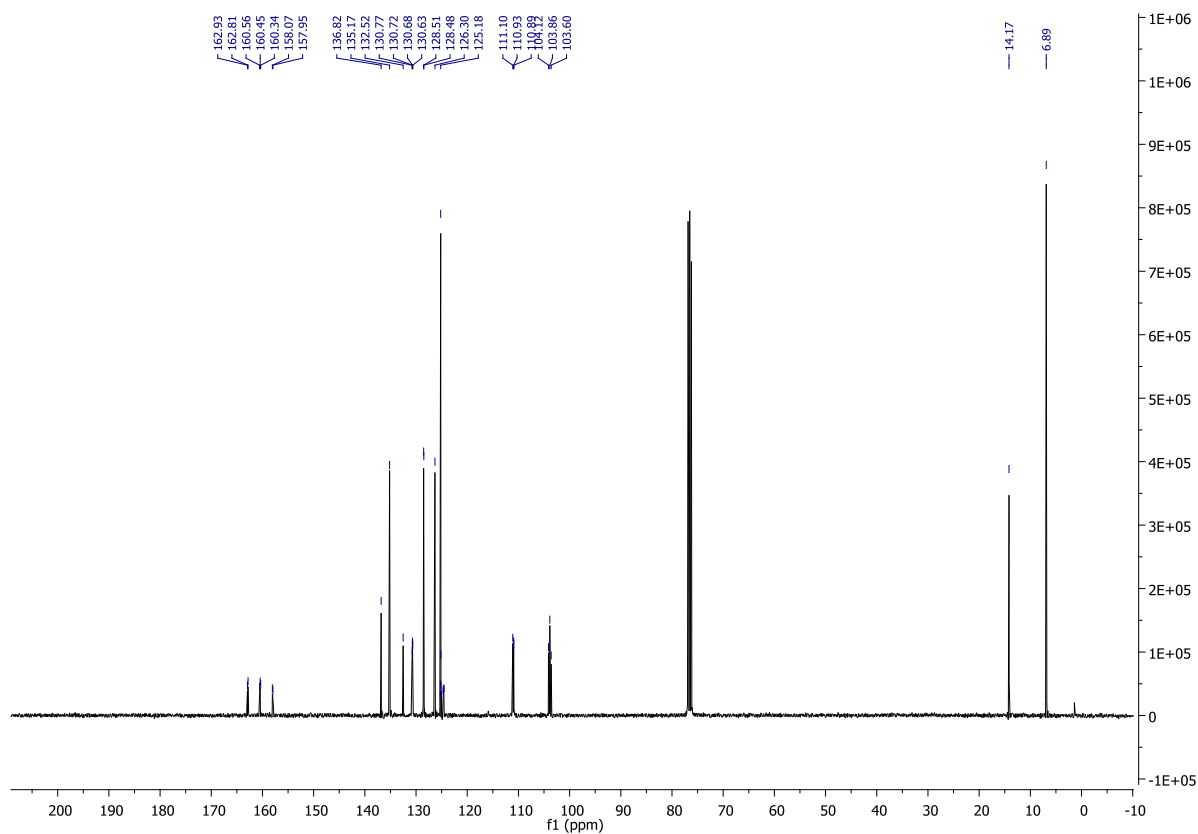
Ciaran Seath
11/11/2014 11:37:02



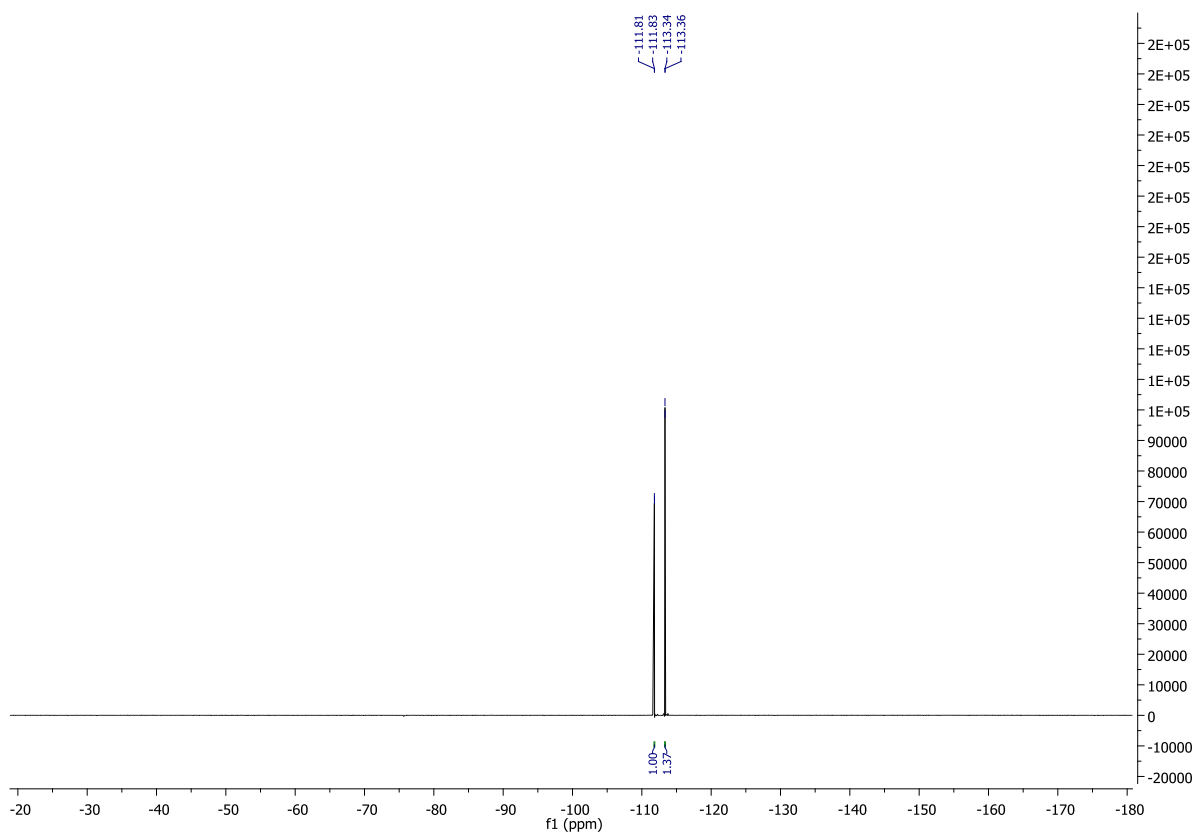
¹H NMR of 7c



¹³C NMR of 7c



¹⁹F NMR of 7c



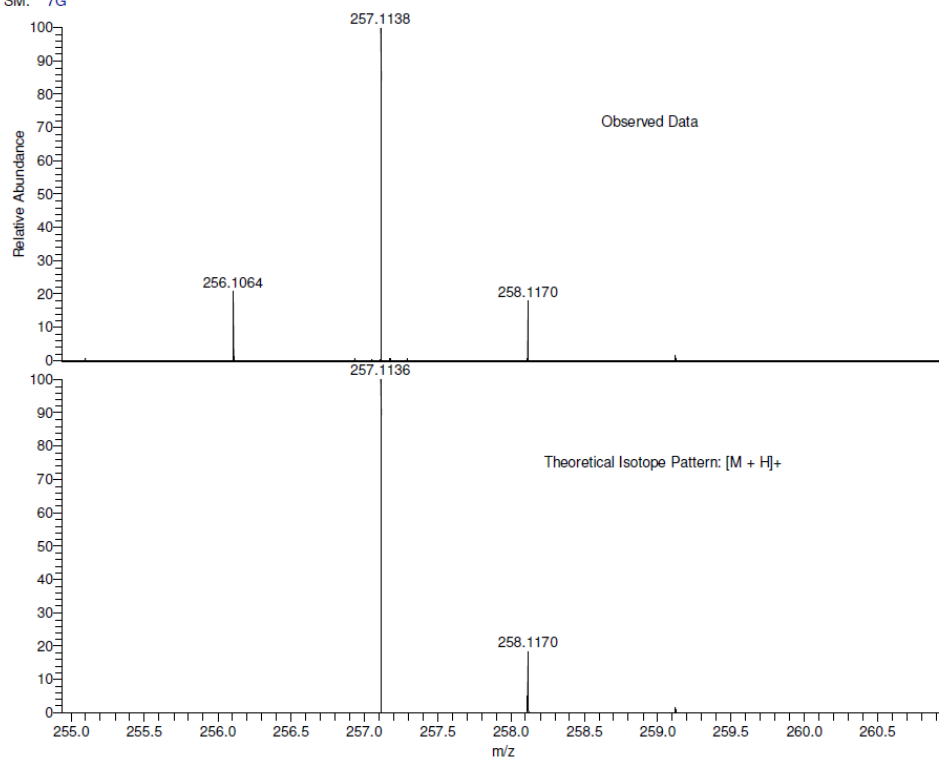
HRMS of 7c

CS92 MW=256?
ASAP(SOLID)

EPSRC National Centre Swansea
LTQ Orbitrap XL

Ciaran
05/11/2014 15:25:20

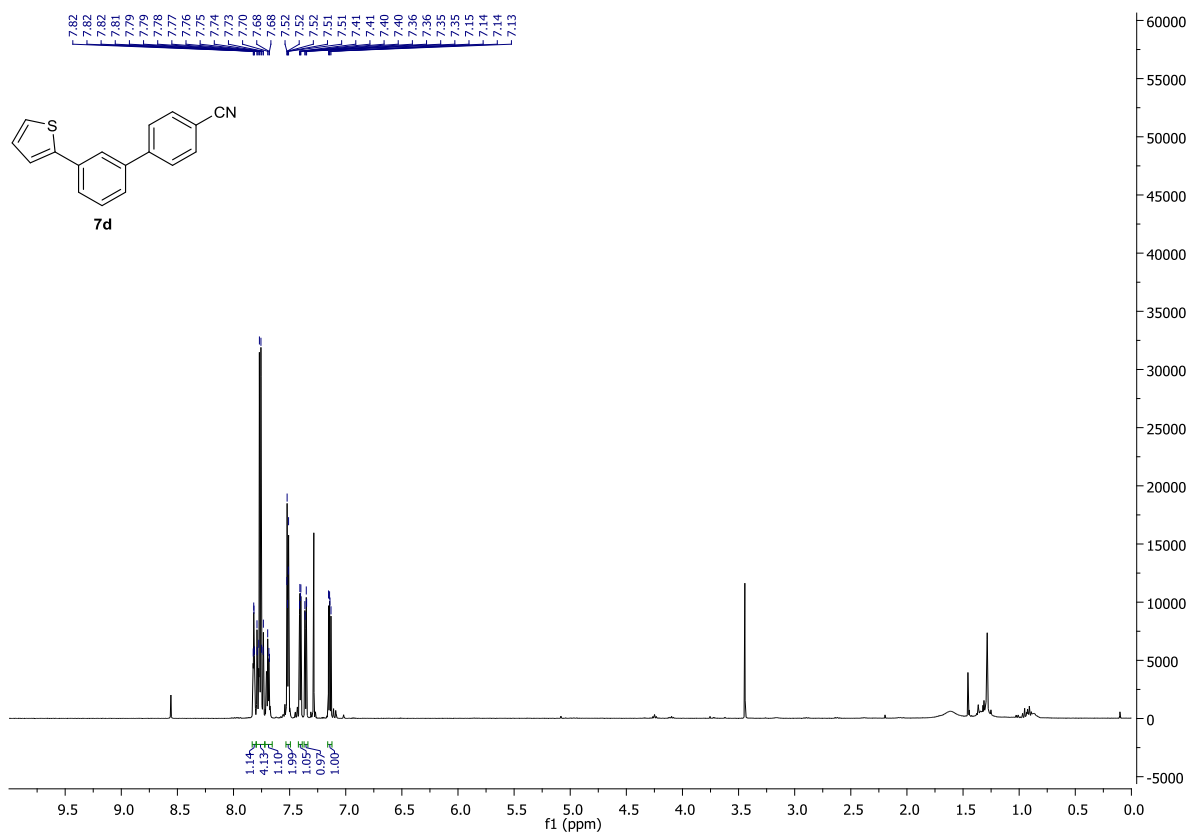
SM: 7G



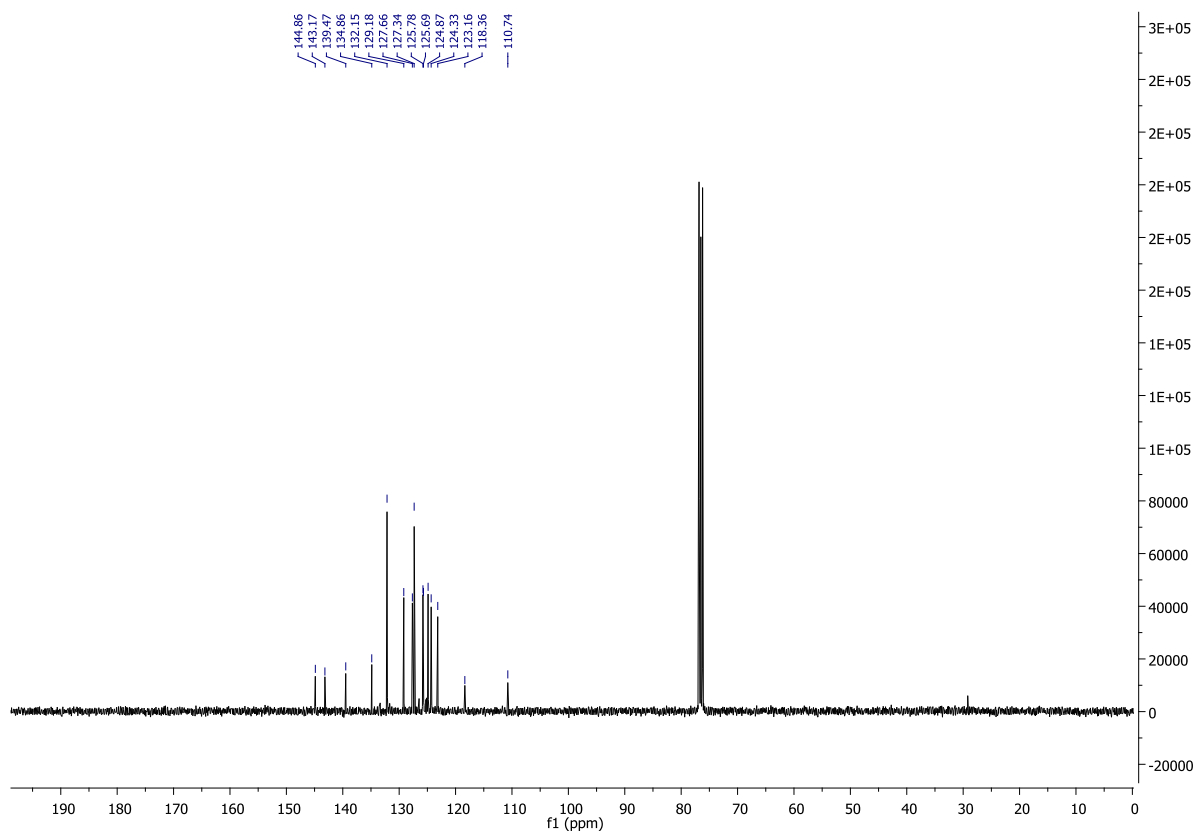
NL:
2.62E7
STRWAT360-PG-HASP#4-6
RT: 0.19-0.30 AV: 3 T: FTMS
+ p APCI corona Full ms
[100.00-800.00]

NL:
1.95E4
C: 17 H: 14 F: 2
C: 17 H: 15 F: 2
p (gss, s/p:40) Chrg 1
R: 100000 Res .Pwr . @FWHM

¹H NMR of 7d



¹³C NMR of 7d

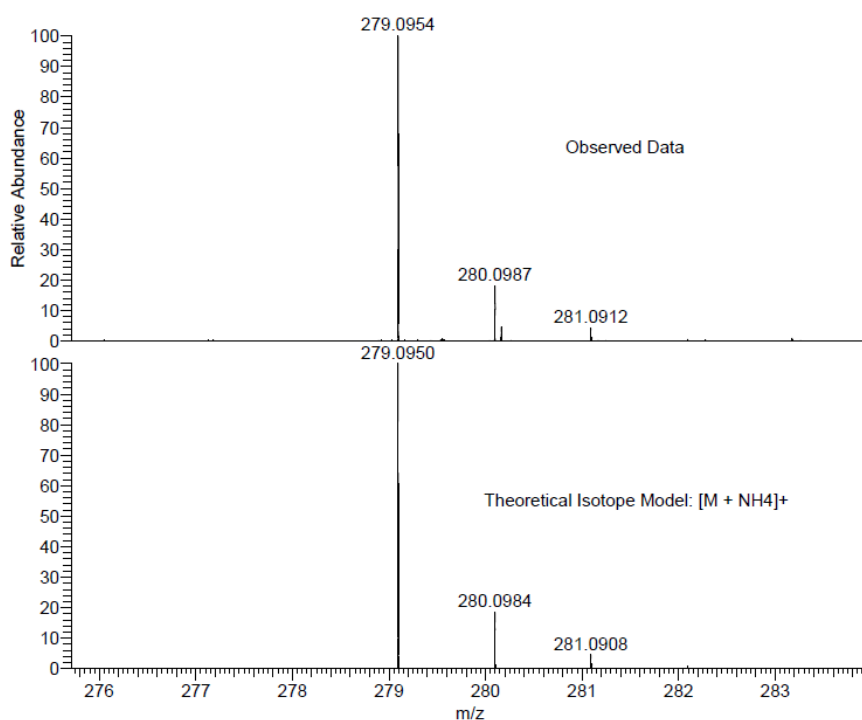


HRMS of 7d

CS60-A1 MW=261?
C₁₇H₁₁NS
(DCM)/MeOH + NH₄OAc

EPSRC National Facility Swansea
LTQ Orbitrap XL

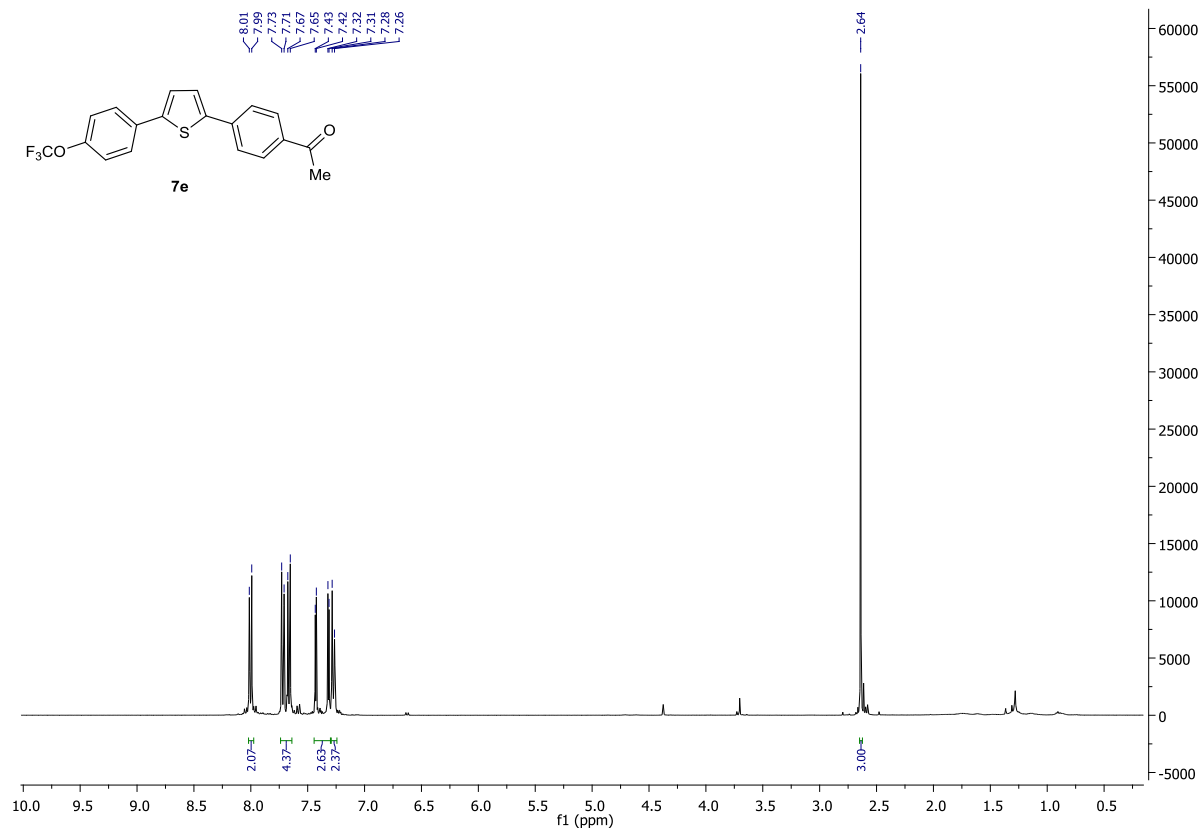
Ciaran Seath
08/09/2014 11:14:36



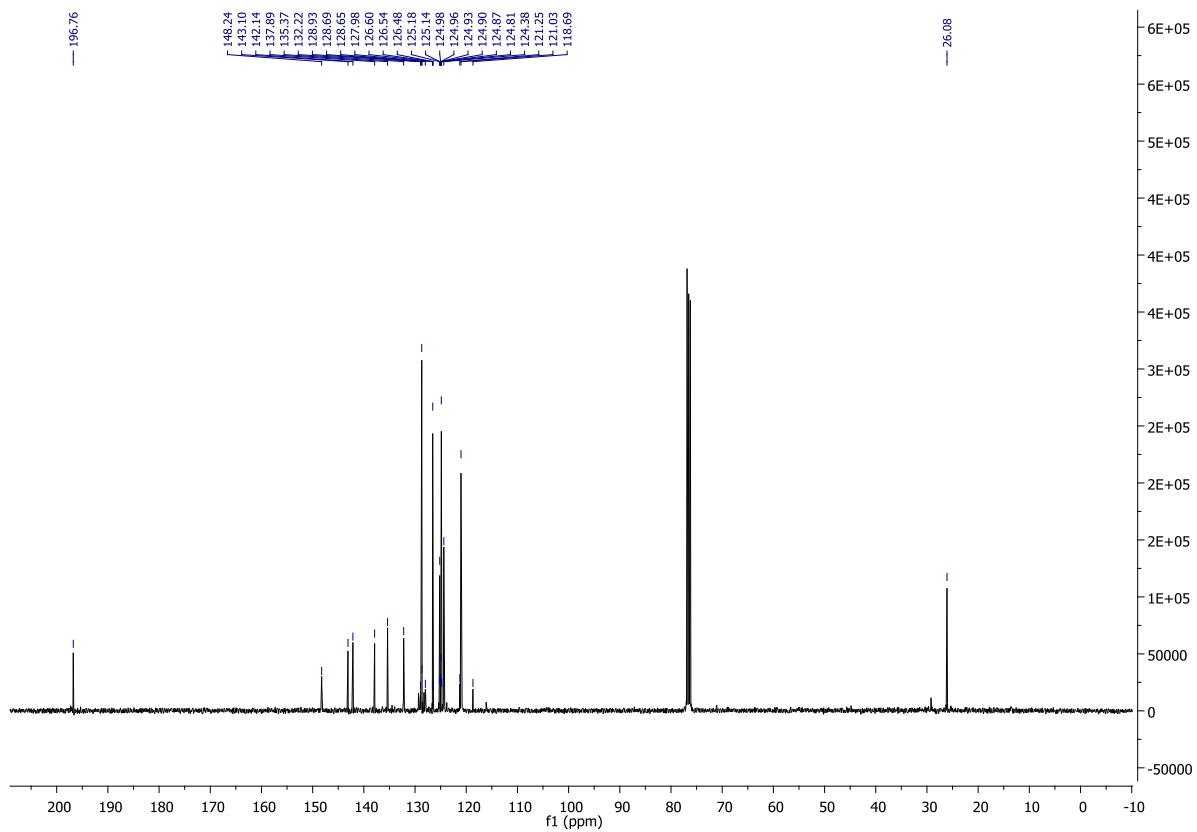
NL:
3.68E6
STRWAT323-OE-HNESP-
2#29-46 RT: 0.66-1.05 AV: 16
T: FTMS + p NSI Full ms
[140.00-1935.00]

NL:
1.84E4
C₁₇H₁₁NSNH₄⁺
C₁₇H₁₅N₂S₁
p (gss, s/p:40) Chrg 1
R: 100000 Res .Pwr . @FWHM

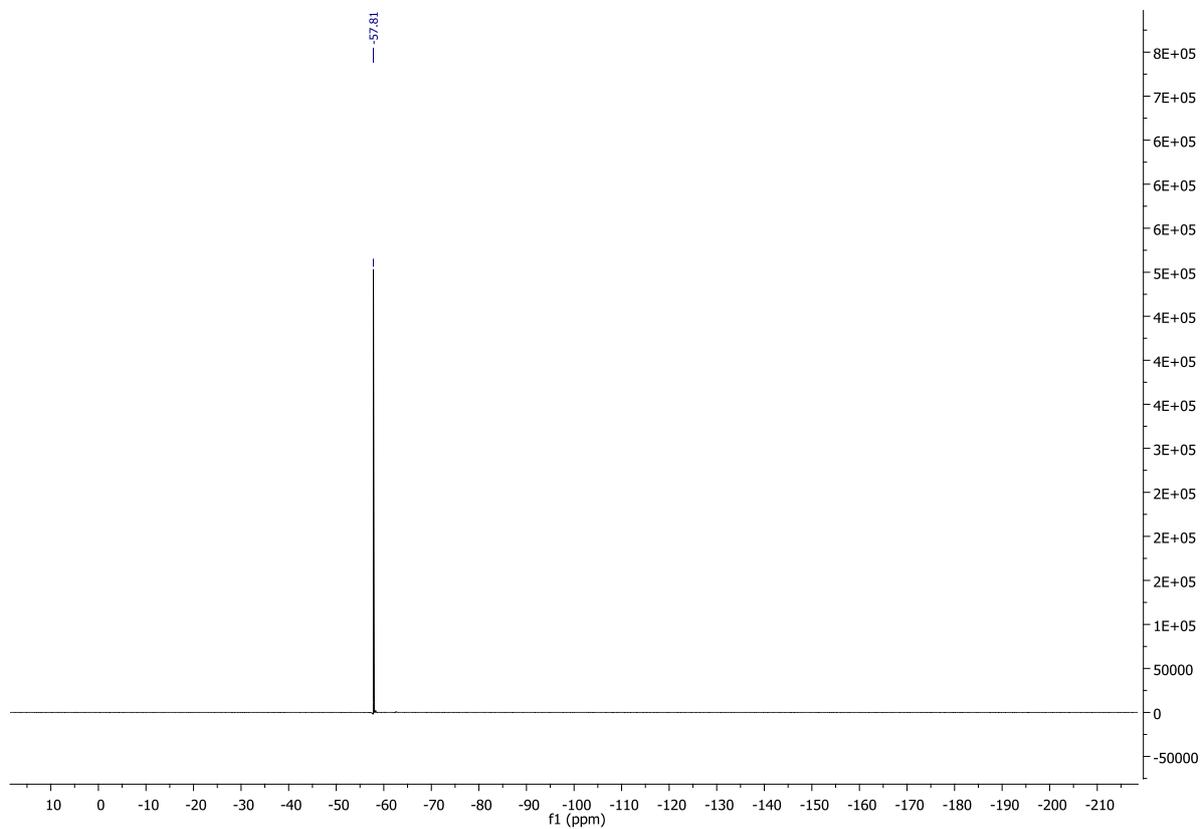
¹H NMR of 7e



¹³C NMR of 7e



¹⁹F NMR of 7e

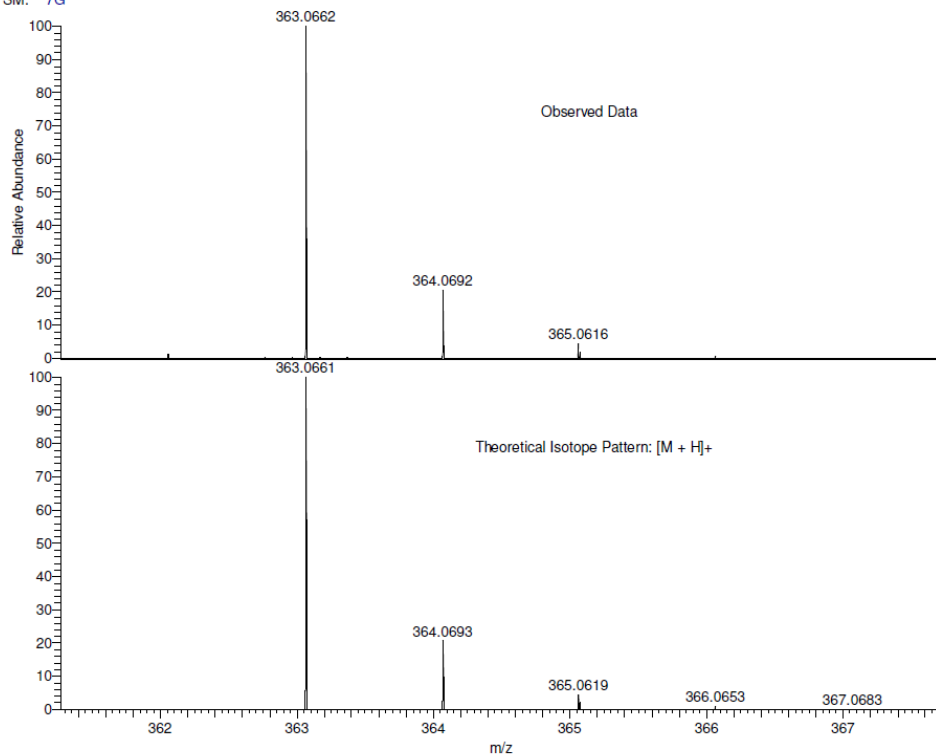


HRMS of 7e

cs116 MW=362?
ASAP(SOLID)
SM: 7G

EPSRC National Centre Swansea
LTO Orbitrap XL

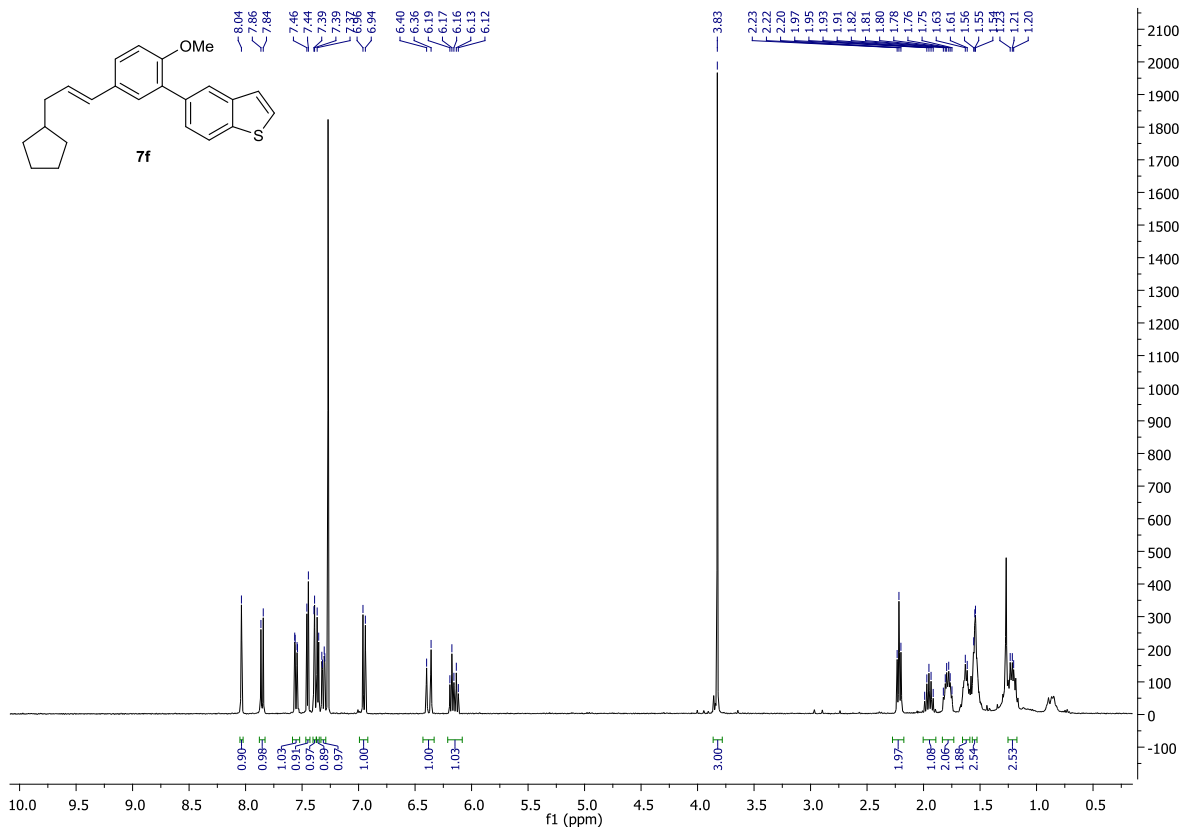
Ciaran
11/11/2014 12:51:22



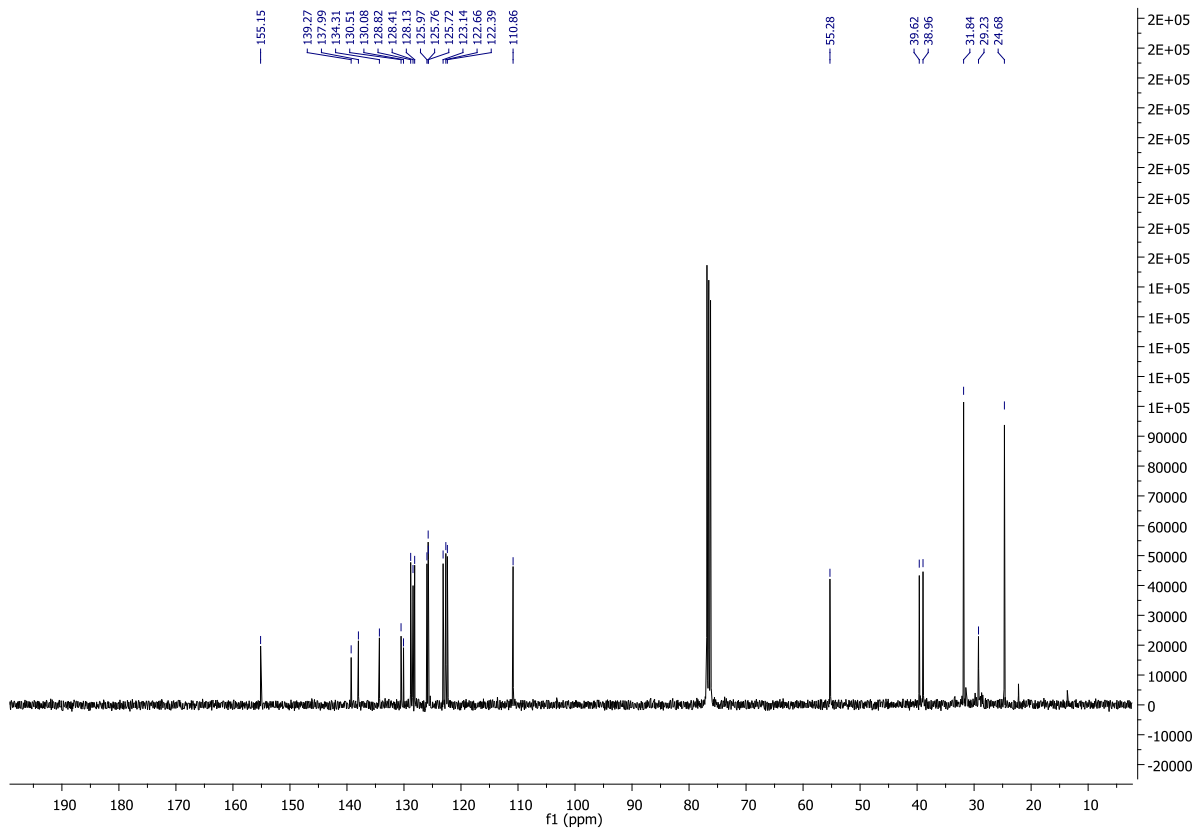
NL:
1.97E7
STRWAT375-PG-HASP#13-19
RT: 0.71-1.06 AV: 7 T: FTMS
+ p APCI corona Full ms
[100.00-800.00]

NL:
1.80E4
C₁₉H₁₃F₃O₂SH:
C₁₉H₁₄F₃O₂S₁
p (gss, s/p:40) Chrg 1
R: 100000 Res .Pwr . @FWHM

¹H NMR of 7f



¹³C NMR of 7f

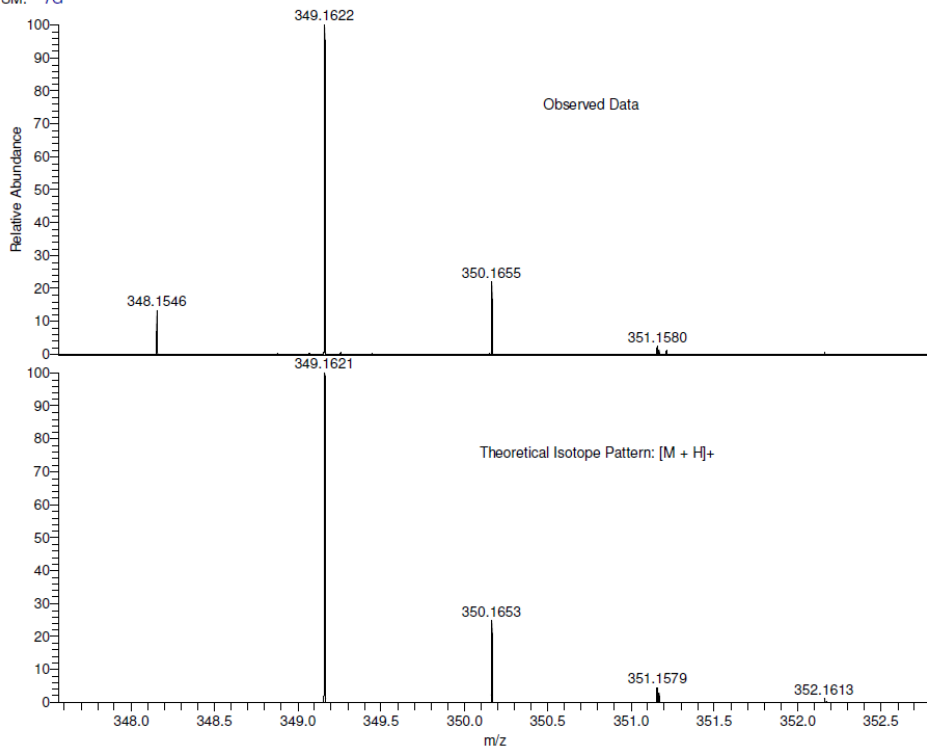


HRMS of 7f

cs124 MW=348?
ASAP(SOLID)
SM: 7G

EPSRC National Centre Swansea
LTQ Orbitrap XL

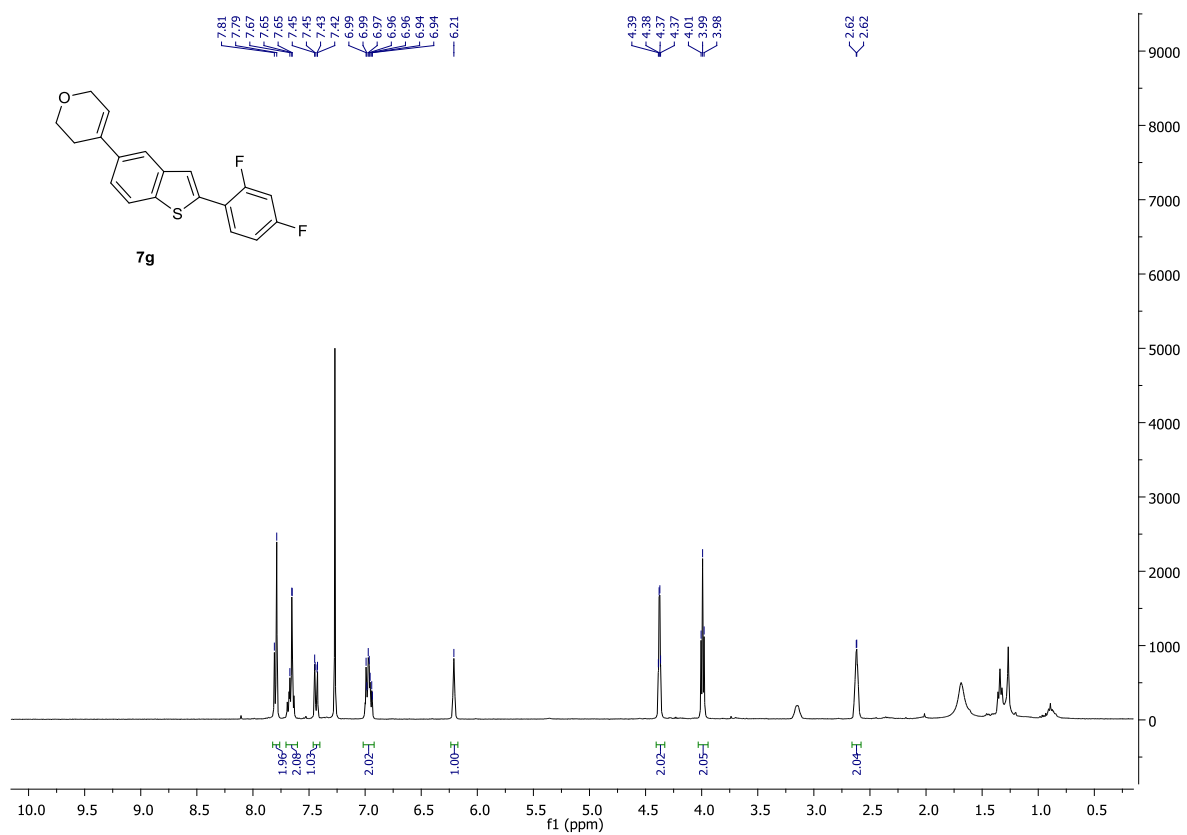
Ciaran
11/11/2014 12:46:35



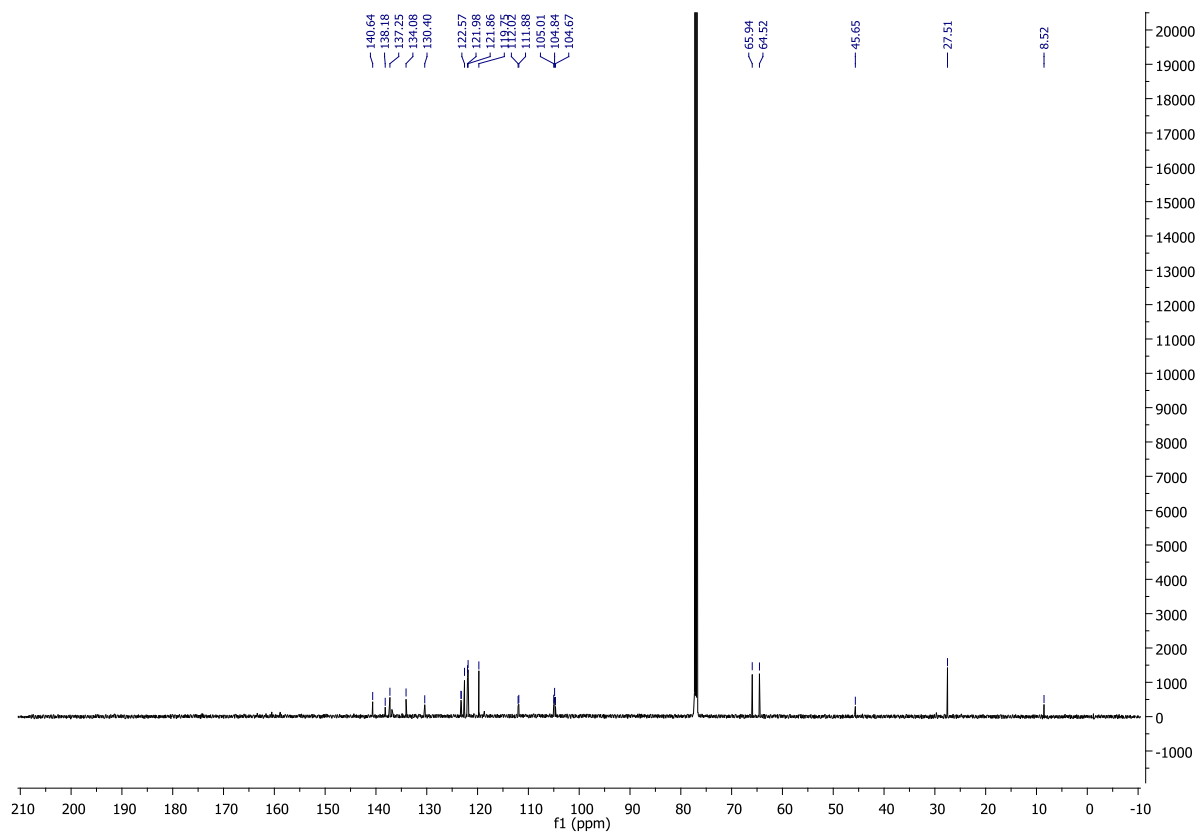
NL:
7.35E6
STRWAT374-PG-HASP#13-16
RT: 0.71-0.88 AV: 4 T: FTMS
+ p APCI corona Full ms
[100.00-800.00]

NL:
1.73E4
C₂₃H₂₄OSH:
C₂₃H₂₅O₁S₁
p (gss, s/p:40) Chrg 1
R: 100000 Res. Pwr. @FWHM

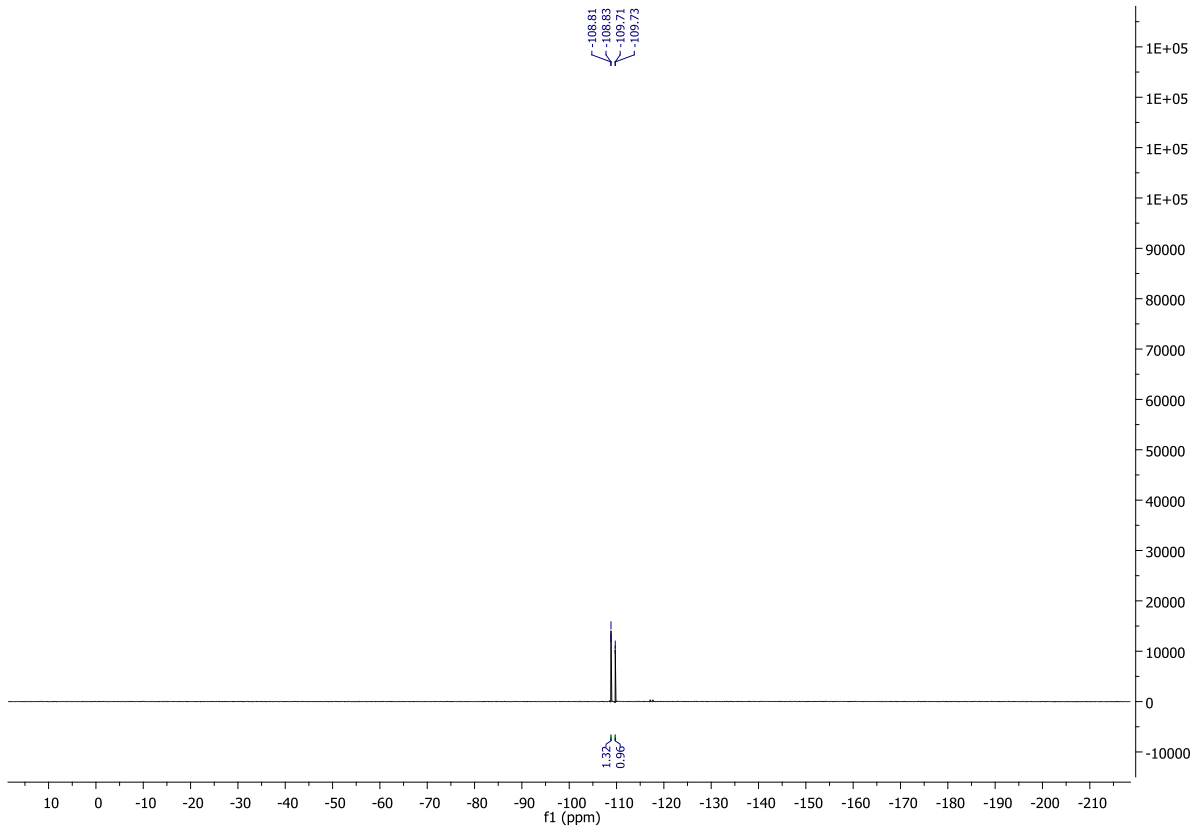
¹H NMR of 7g



¹³C NMR of 7g



¹⁹F NMR of 7g

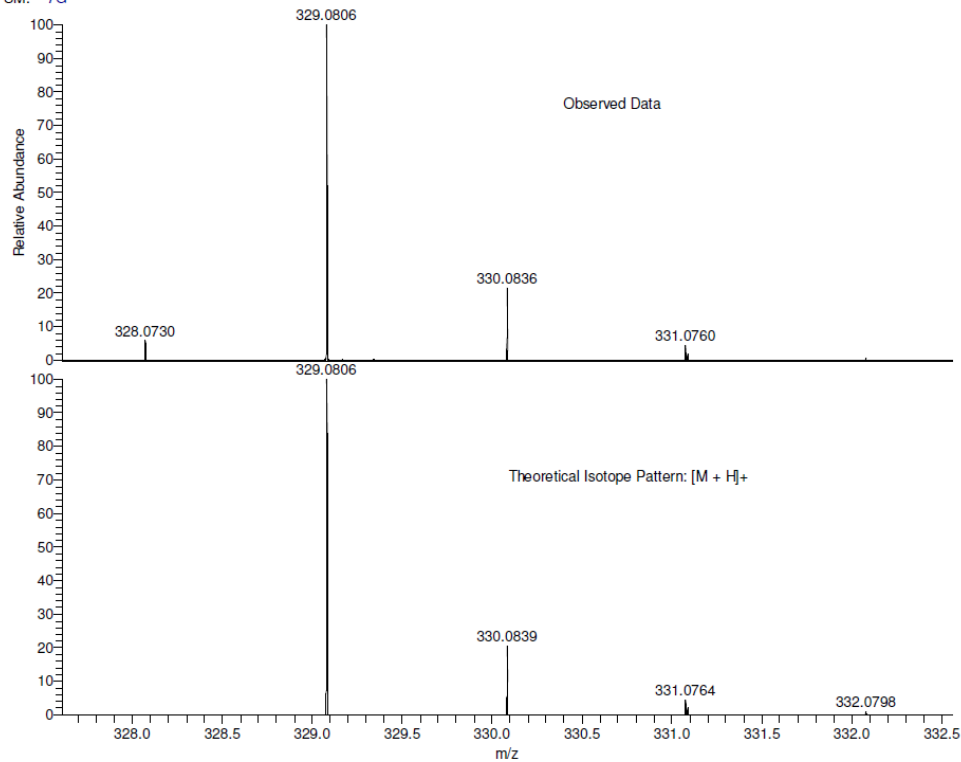


HRMS of 7g

CS104 MW=328?
ASAP(SOLID)
SM: 7G

EPSRC National Centre Swansea
LTQ Orbitrap XL

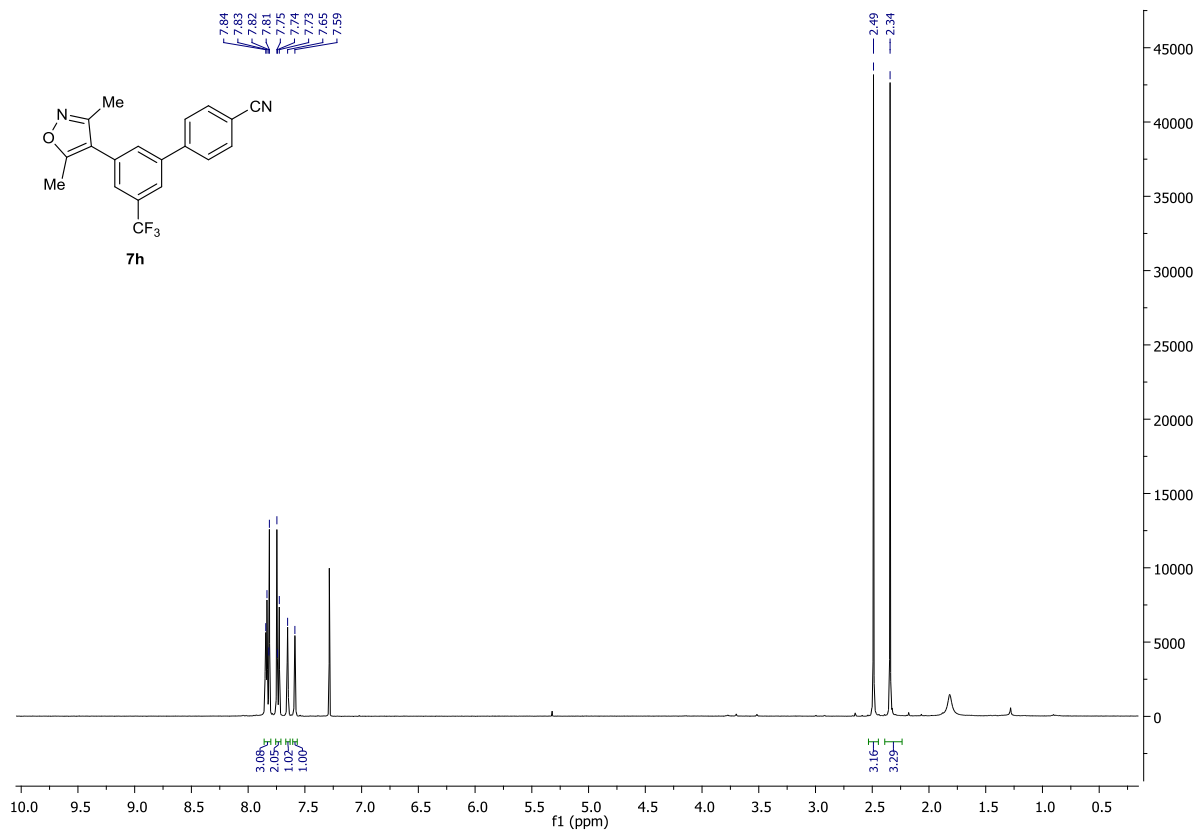
Ciaran
11/11/2014 12:55:40



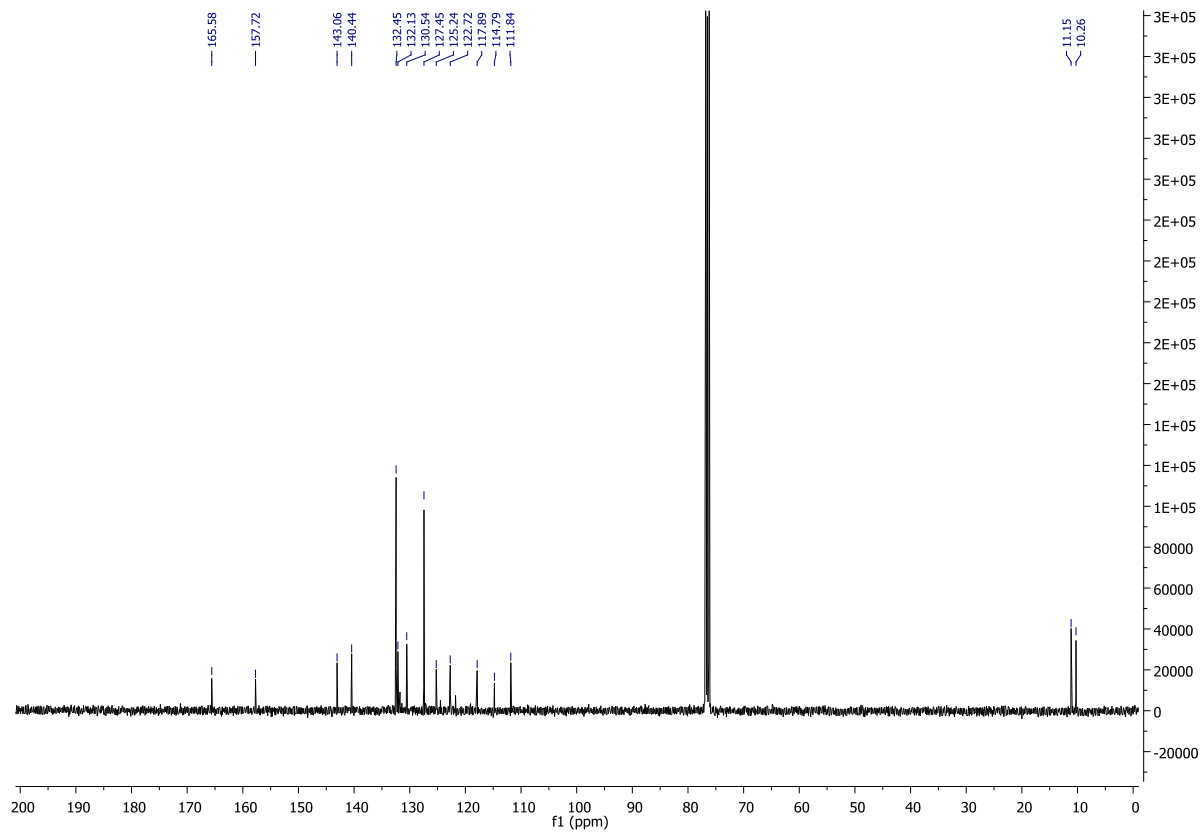
NL:
9.30E7
STRWAT377-PG-HASP#5-8
RT: 0.26-0.43 AV: 4 T: FTMS
+ p APCI corona Full ms
[100.00-800.00]

NL:
1.81E4
C₁₉H₁₄F₂O₂S
C₁₉H₁₅F₂O₁S₁
p (gss, s/p:40) Chrg 1
R: 100000 Res .Pwr . @FWHM

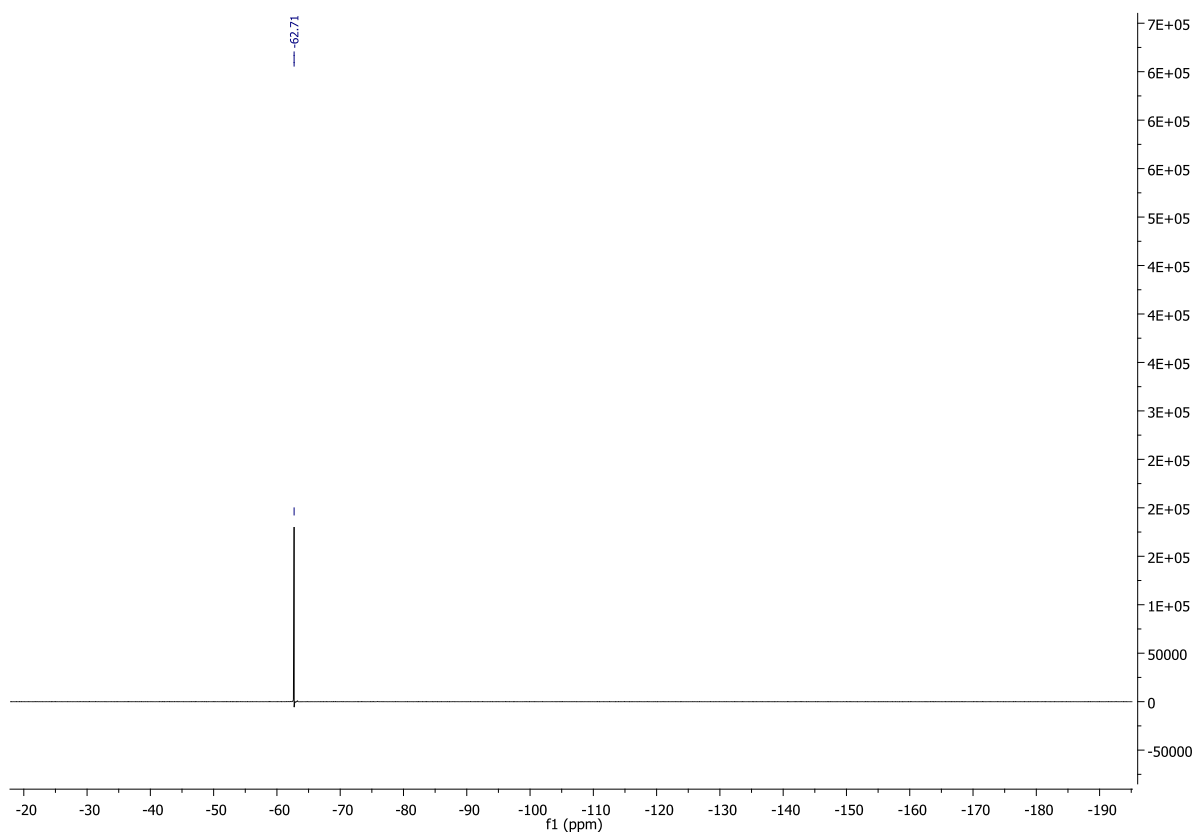
¹H NMR of 7h



¹³C NMR of 7h



¹⁹F NMR of 7h



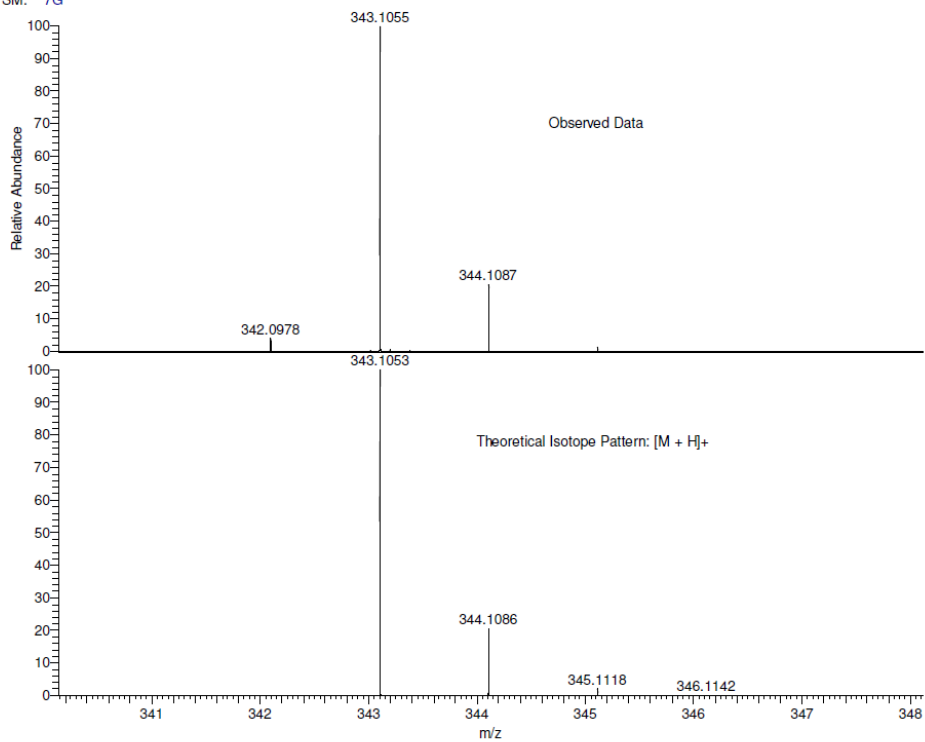
HRMS of 7h

CS102 MW-342?
ASAP(SOLID)

EPSRC National Centre Swansea
LTQ Orbitrap XL

Ciaran
05/11/2014 15:17:58

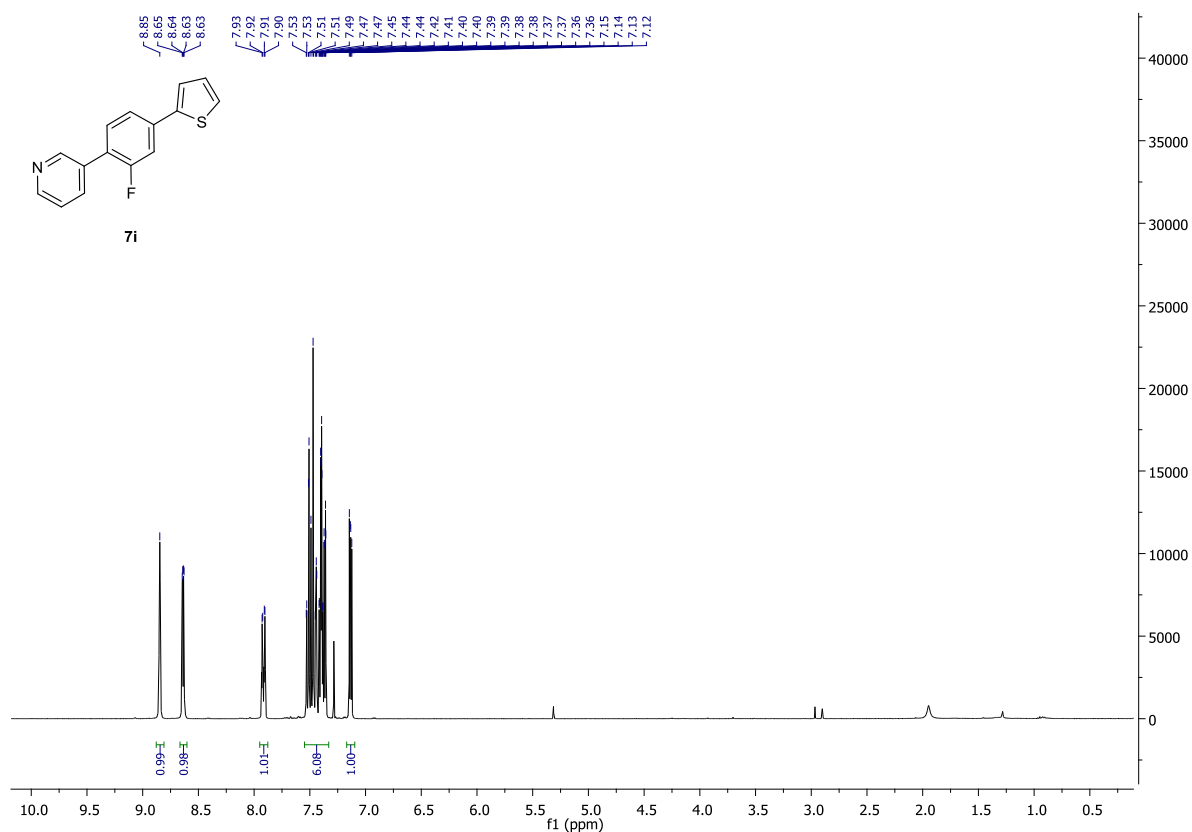
SM: 7G



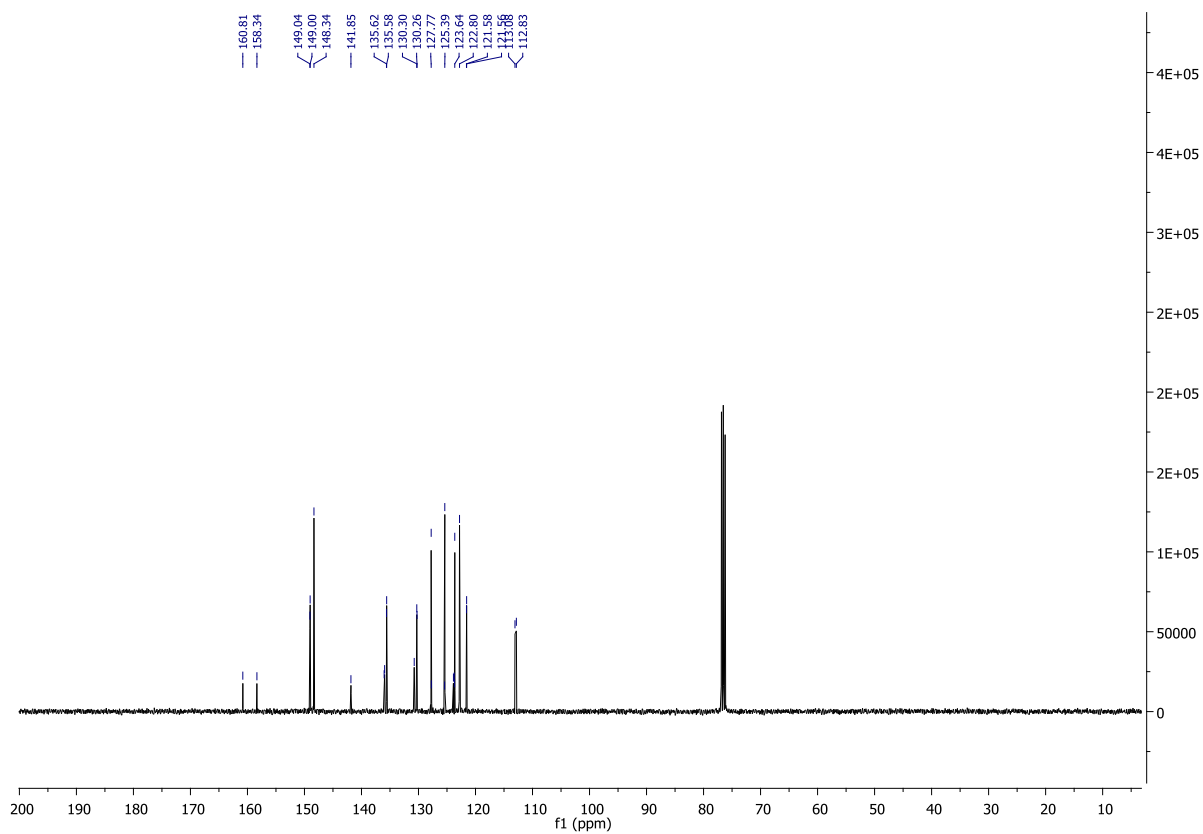
NL:
6.37E6
STRWAT358-PG-HASP#7-13
RT: 0.37-0.72 AV: 7 T: FTMS
+ p APCI corona Full ms
[100.00-800.00]

NL:
1.89E4
C₁₉H₁₃F₃N₂O₁
C₁₉H₁₄F₃N₂O₁
p (gss, s/p:40) Chrg 1
R: 100000 Res .Pwr . @FWHM

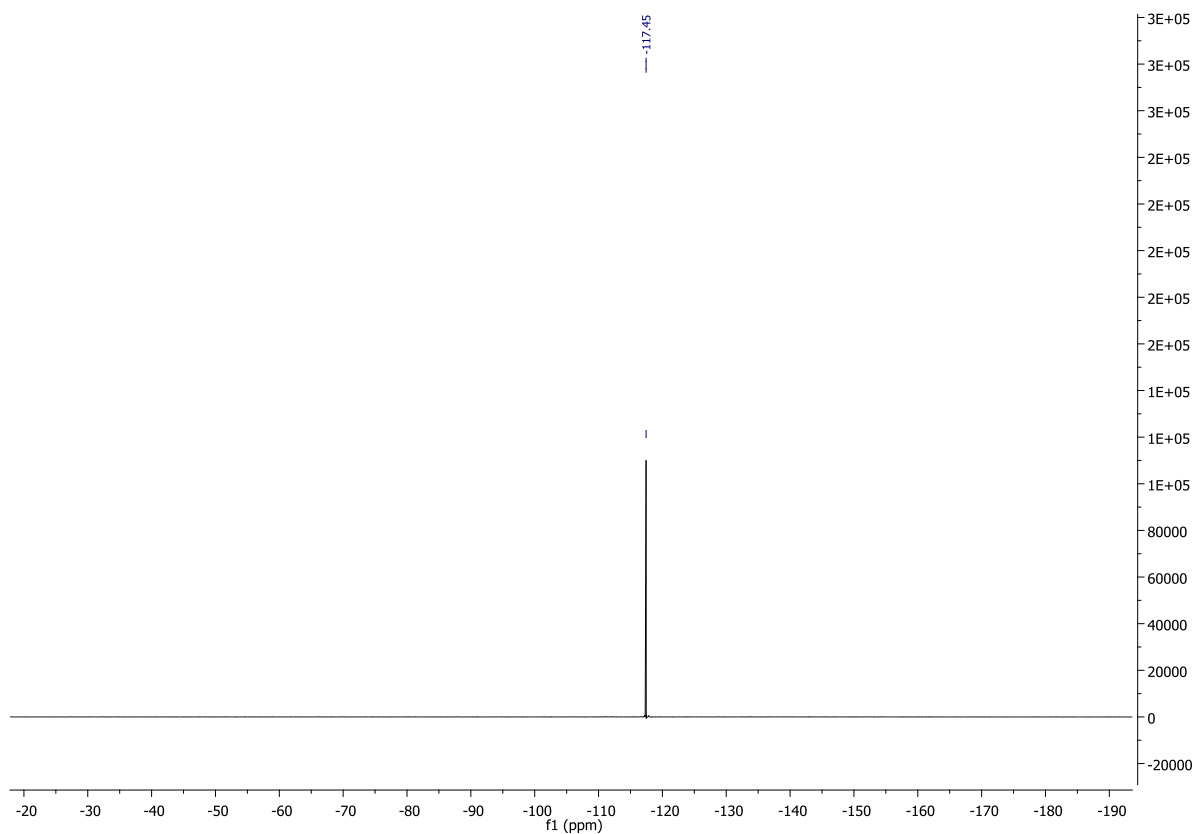
¹H NMR of 7i



¹³C NMR of 7i



¹⁹F NMR of 7i

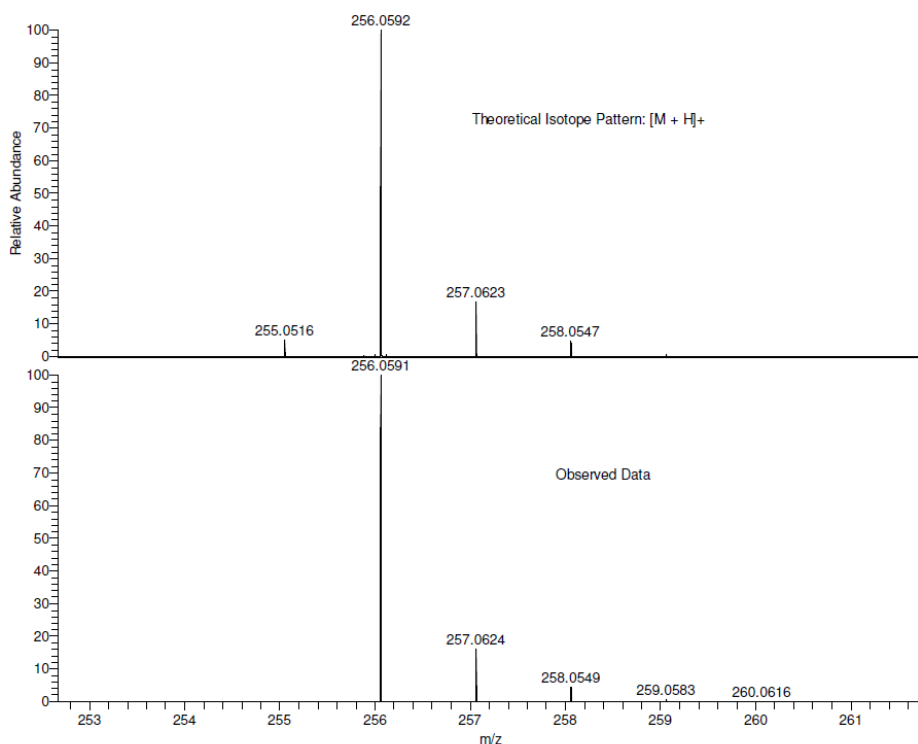


HRMS of 7i

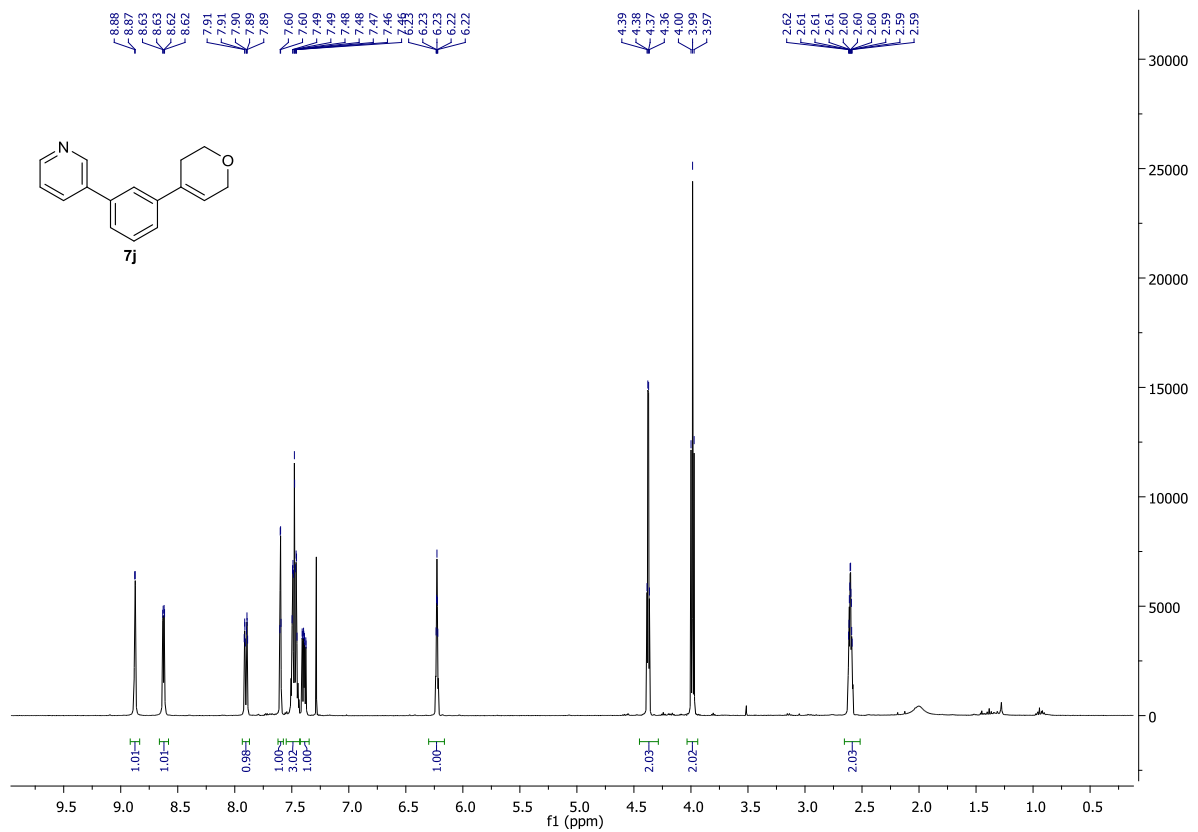
CS101 MW=255?
ASAP(SOLID)

EPSRC National Centre Swansea
LTQ Orbitrap XL

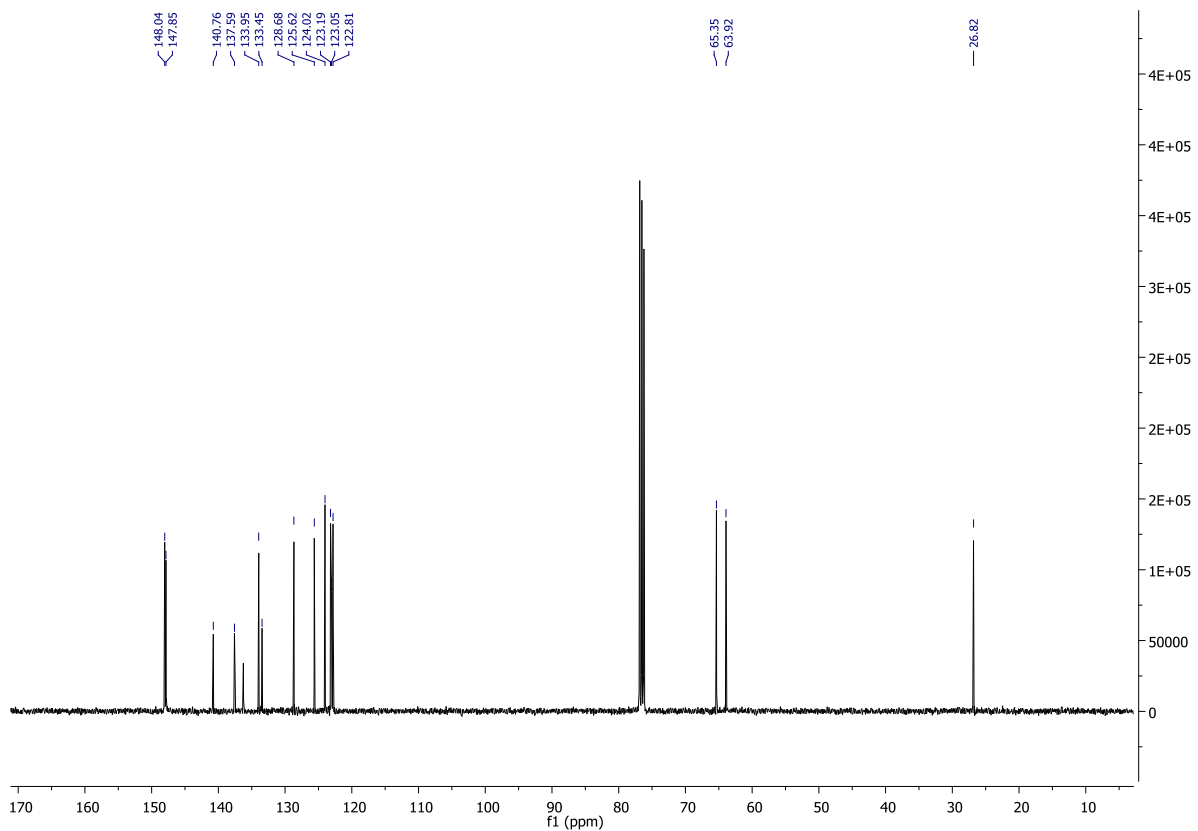
Ciaran
05/11/2014 15:21:47



¹H NMR of 7j



¹³C NMR of 7j

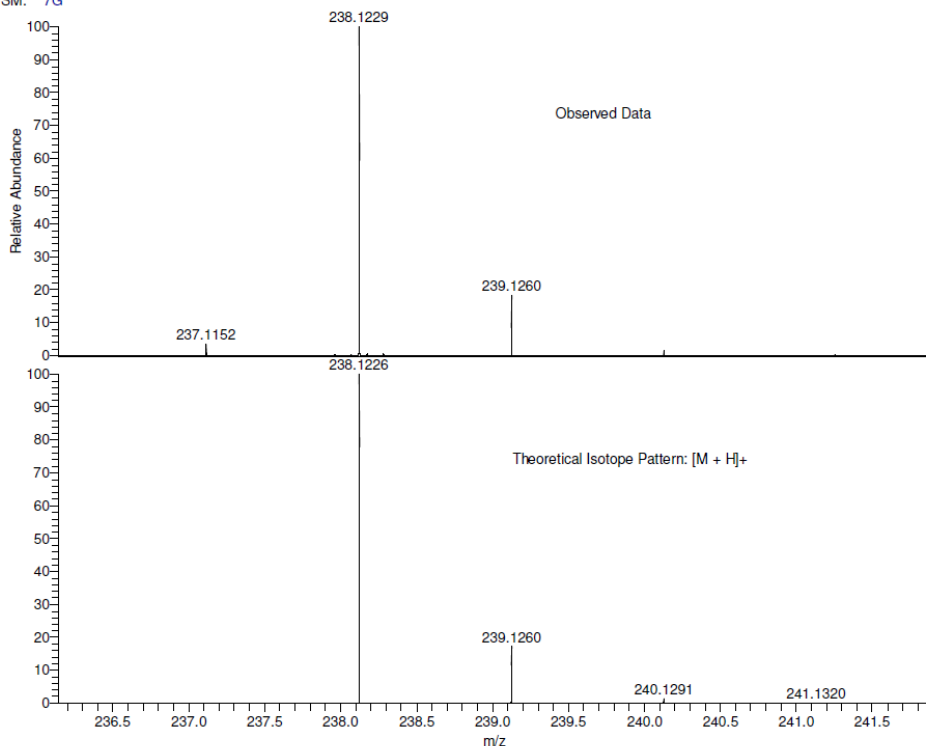


HRMS of 7j

CS81 MW-237?
ASAP(SOLID)
SM: 7G

EPSRC National Centre Swansea
LTQ Orbitrap XL

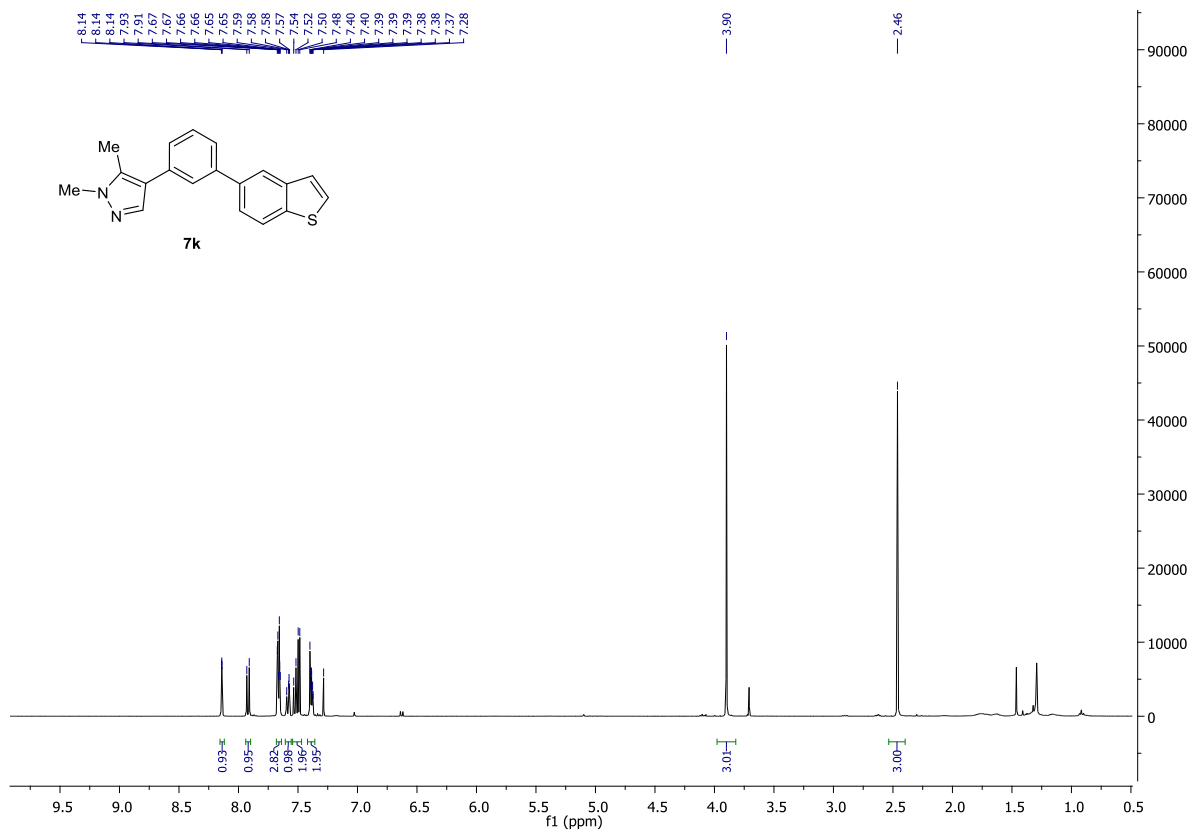
Ciaran
05/11/2014 15:40:49



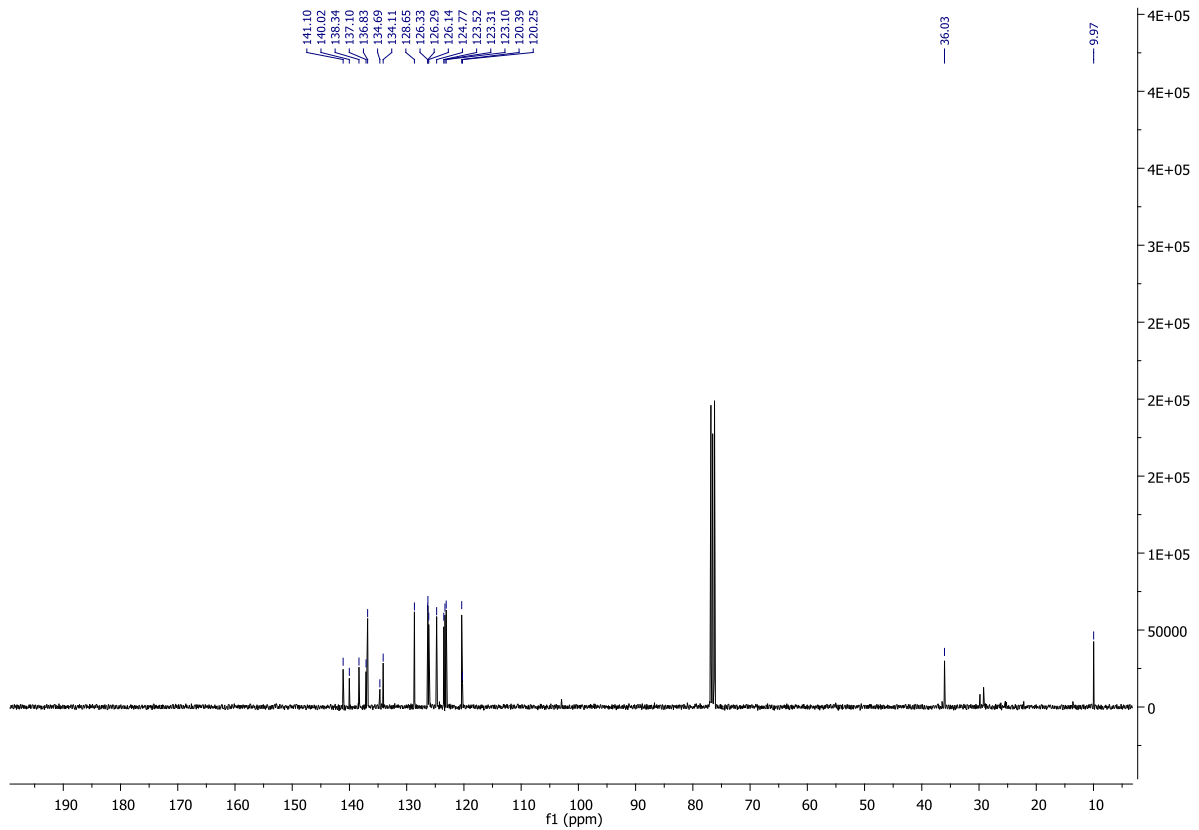
NL:
3.77E7
STRWAT363-PG-HASP#10-16
RT: 0.54-0.88 AV: 7 T: FTMS
+ p APCI corona Full ms
[100.00-800.00]

NL:
1.96E4
C₁₆H₁₅NOH:
C₁₆H₁₆N₁O₁
p (gss, s/p:40) Chrg 1
R: 100000 Res .Pwr .@FWHM

¹H NMR of 7k



¹³C NMR of 7k

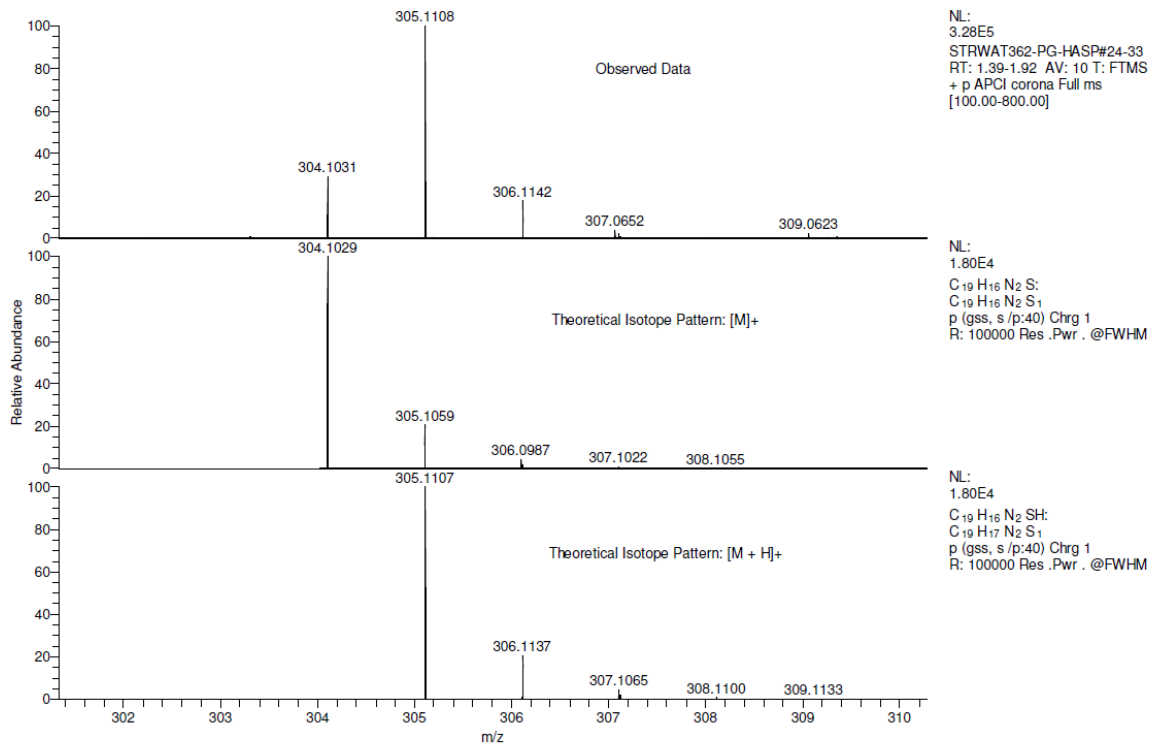


HRMS of 7k

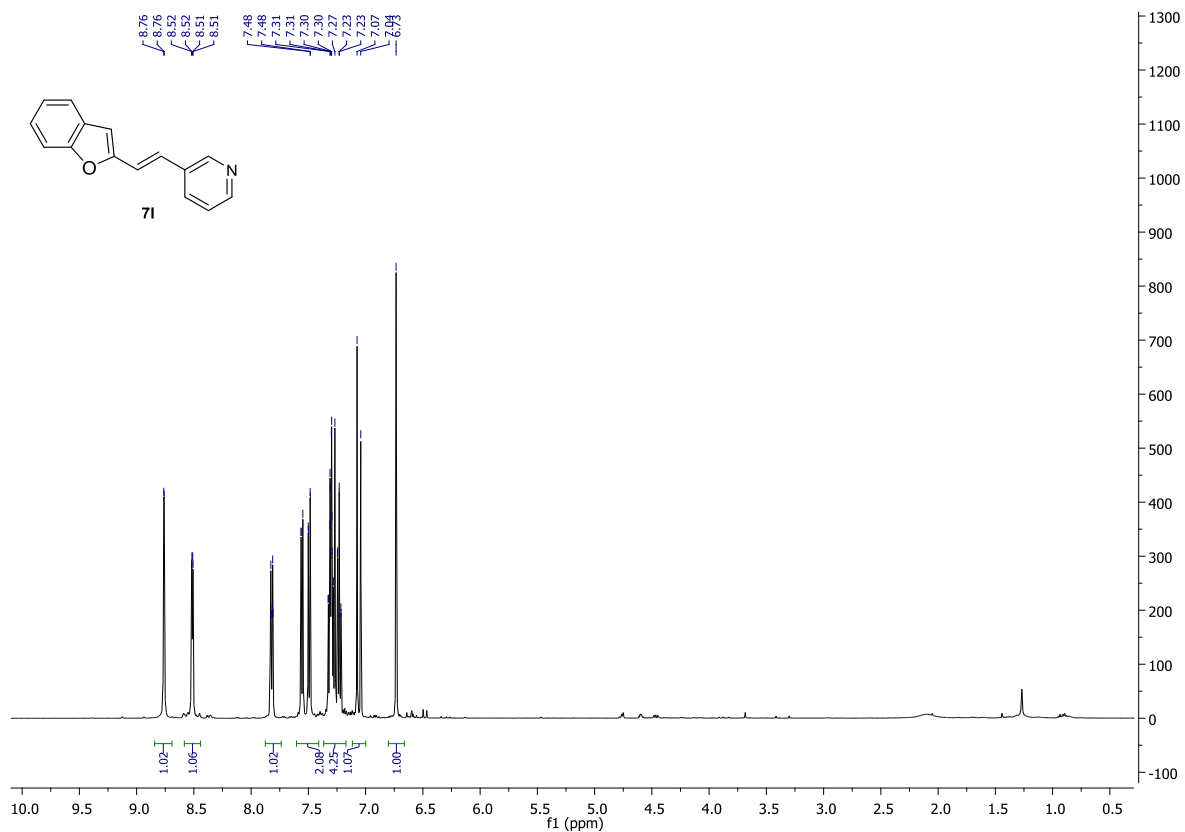
CS100 MW=304?
ASAP(SOLID)

EPSRC National Centre Swansea
LTQ Orbitrap XL

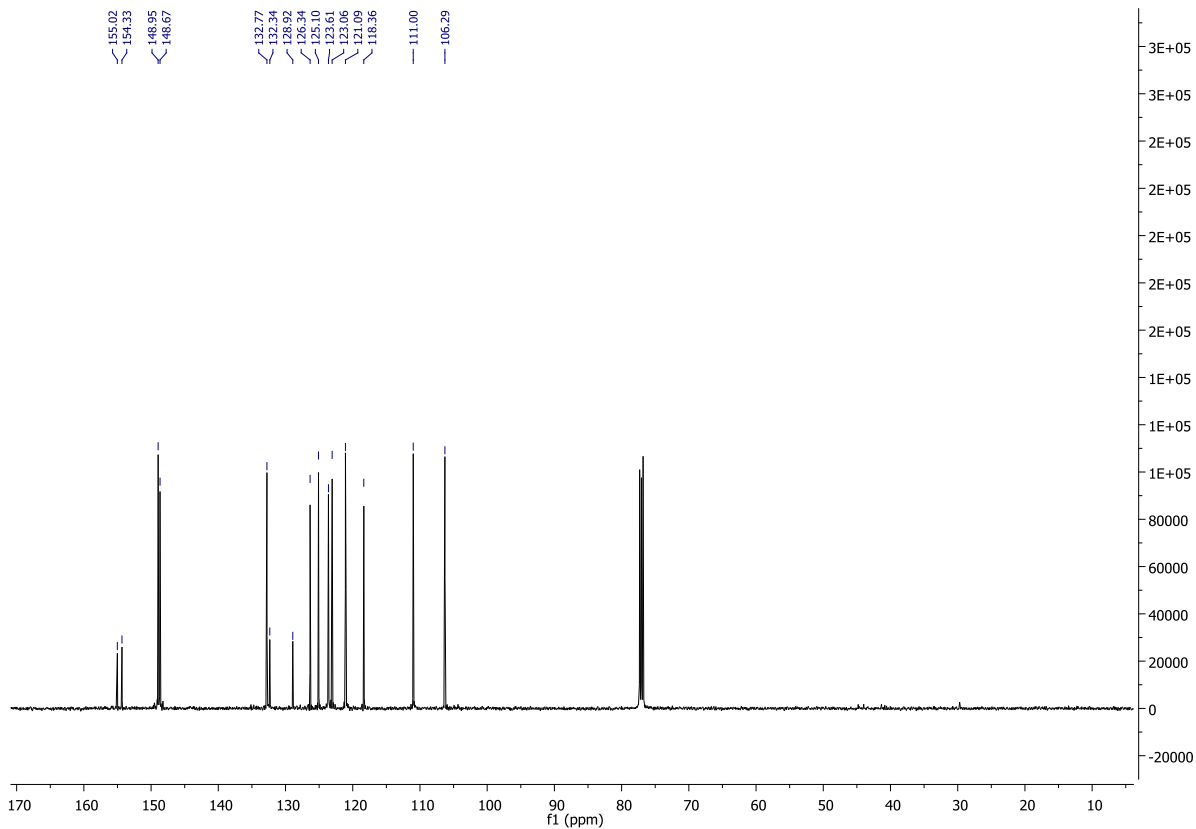
Ciaran
05/11/2014 15:35:24



¹H NMR of 71



¹³C NMR of 71

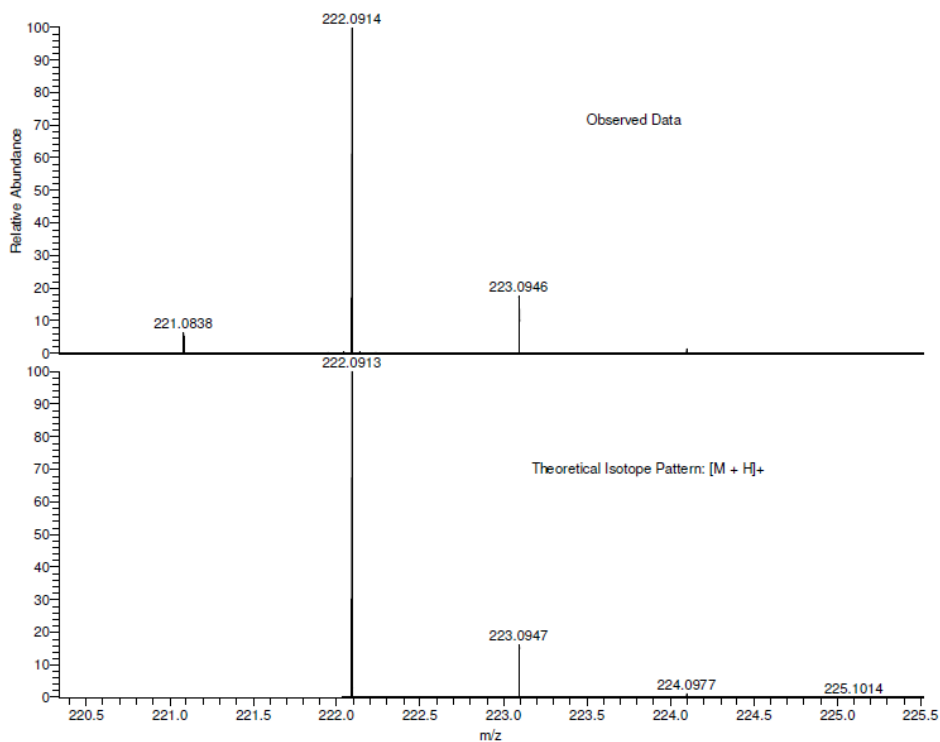


HRMS of 7l

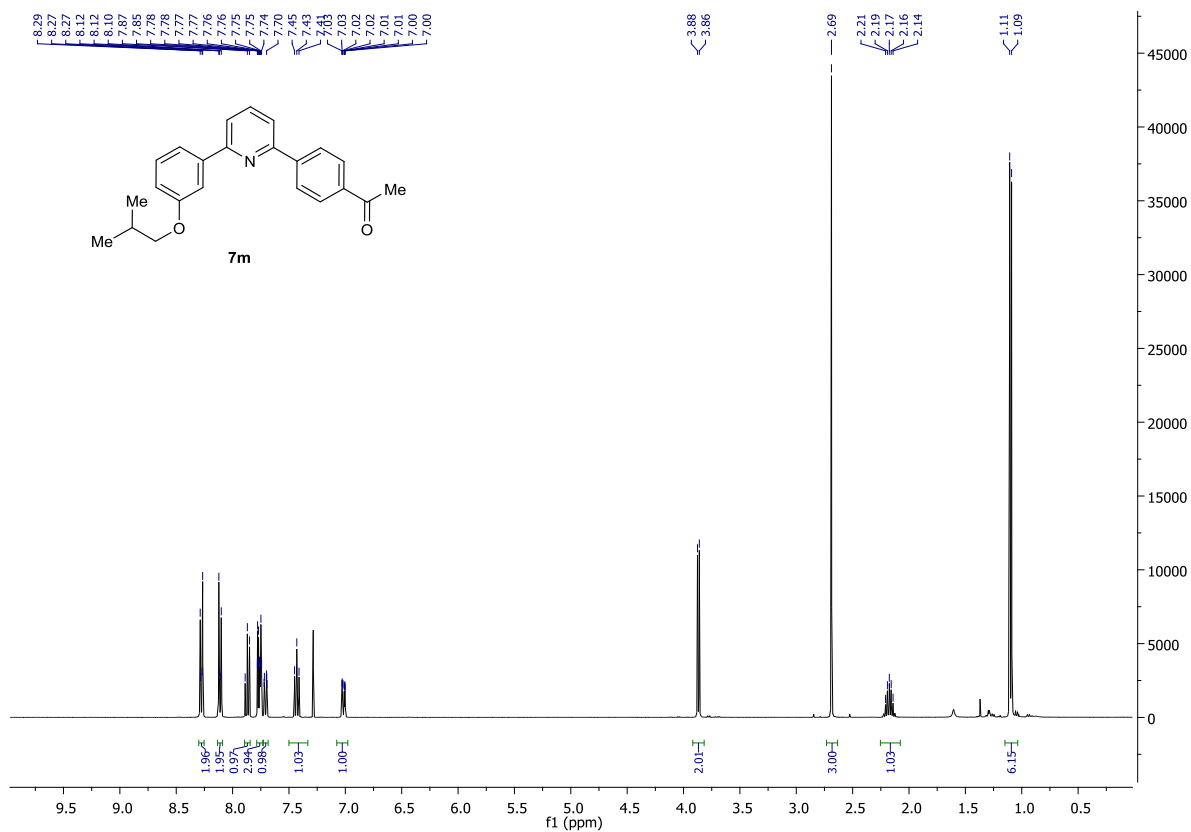
CS98 MW=221?
ASAP(SOLID)

EPSRC National Centre Swansea
LTQ Orbitrap XL

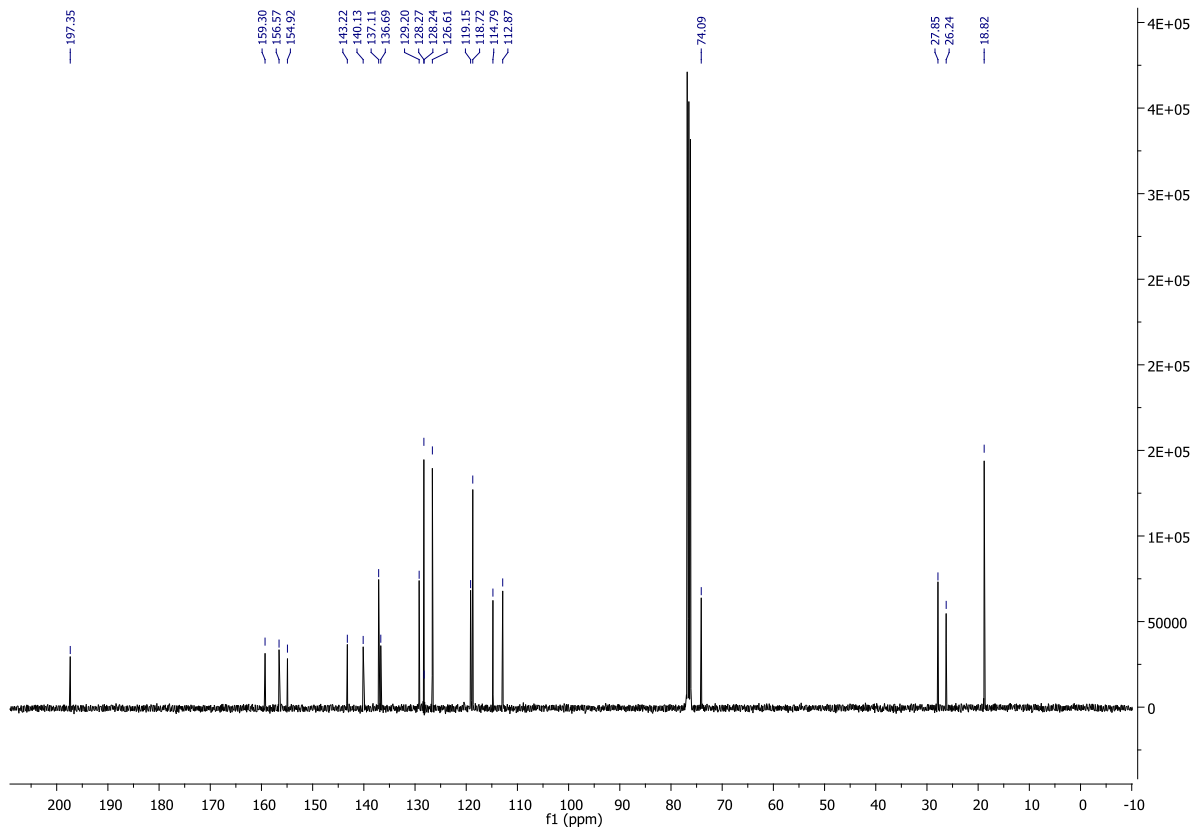
Ciaran
05/11/2014 15:31:44



¹H NMR of 7m



¹³C NMR of 7m

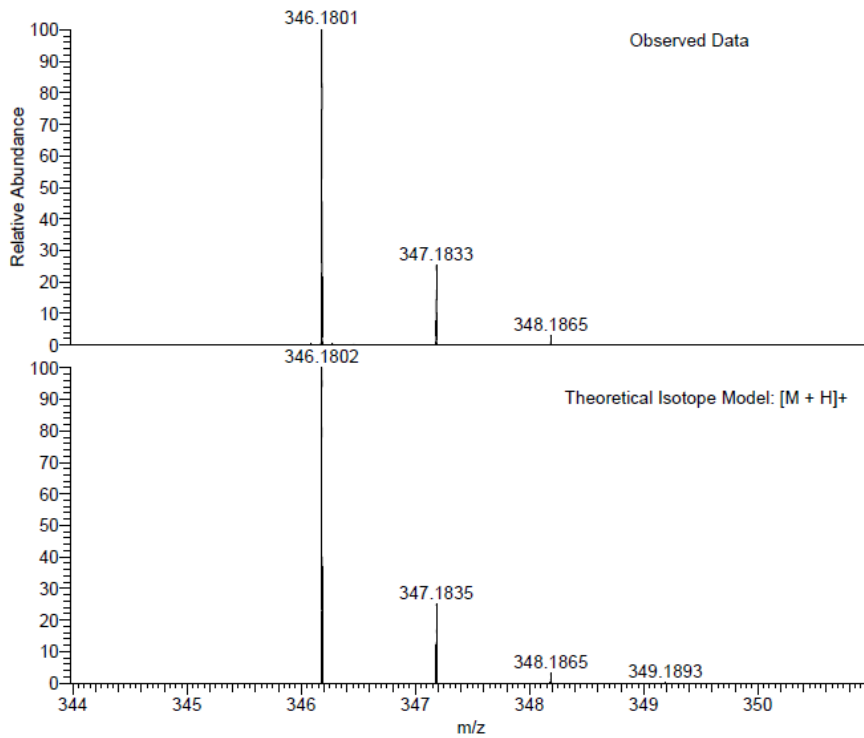


HRMS of 7m

CS190-A1 MW=345?
(DCM)/MeOH + NH4OAc

EPSRC National Facility Swansea
LTQ Orbitrap XL

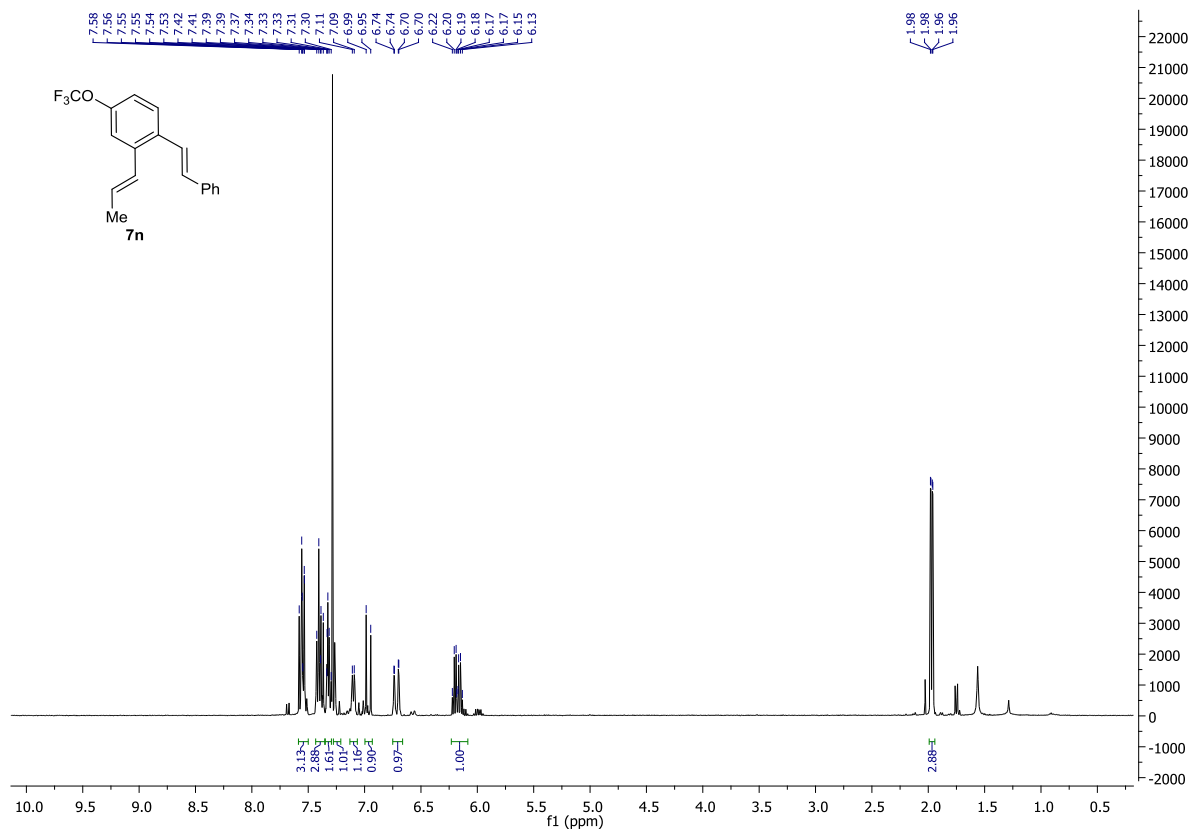
Ciaran Seath
06/03/2015 16:09:14



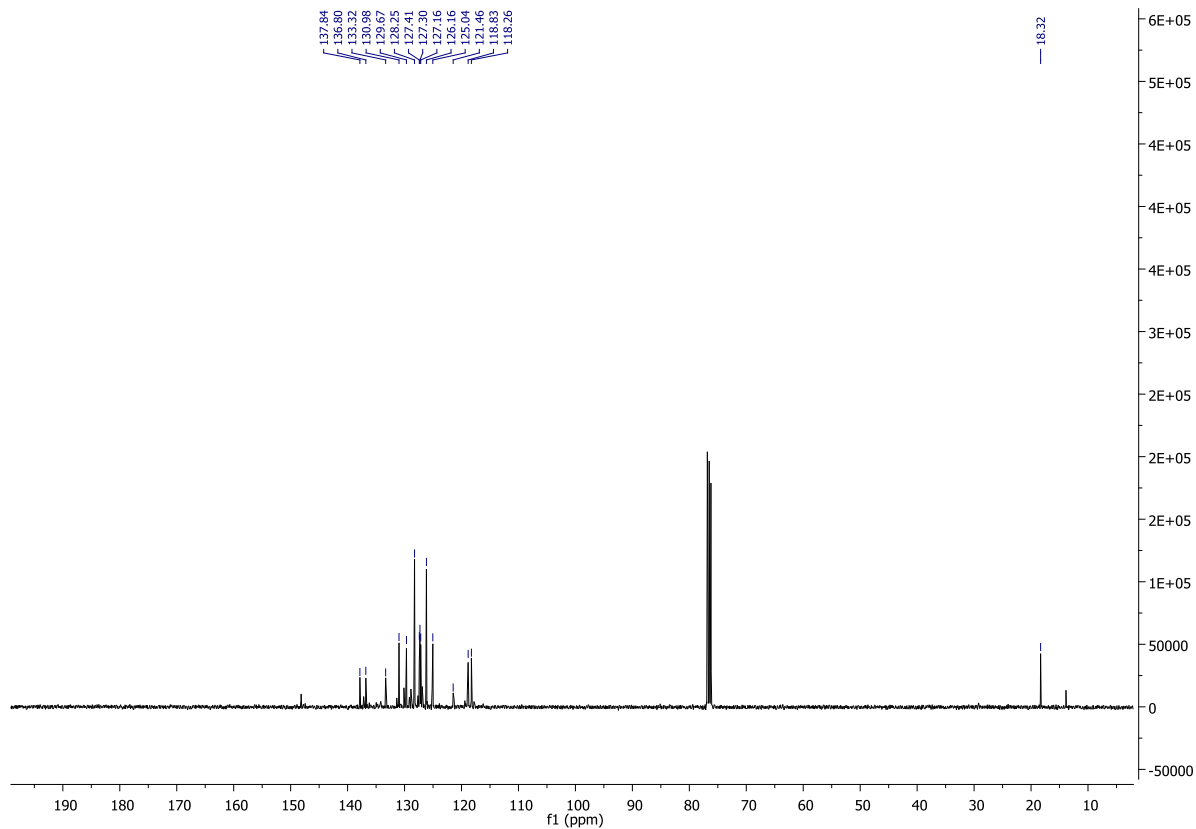
NL:
1.87E8
STRWAT445-OE-HNESP#14-
26 RT: 0.29-0.54 AV: 10 T:
FTMS + p NSI Full ms
[140.00-1935.00]

NL:
1.81E4
C₂₃H₂₃NO₂H:
C₂₃H₂₄N₁O₂
p (gss, s /p:40) Chrg 1
R: 100000 Res .Pwr .@FWHM

¹H NMR of 7n



¹³C NMR of 7n

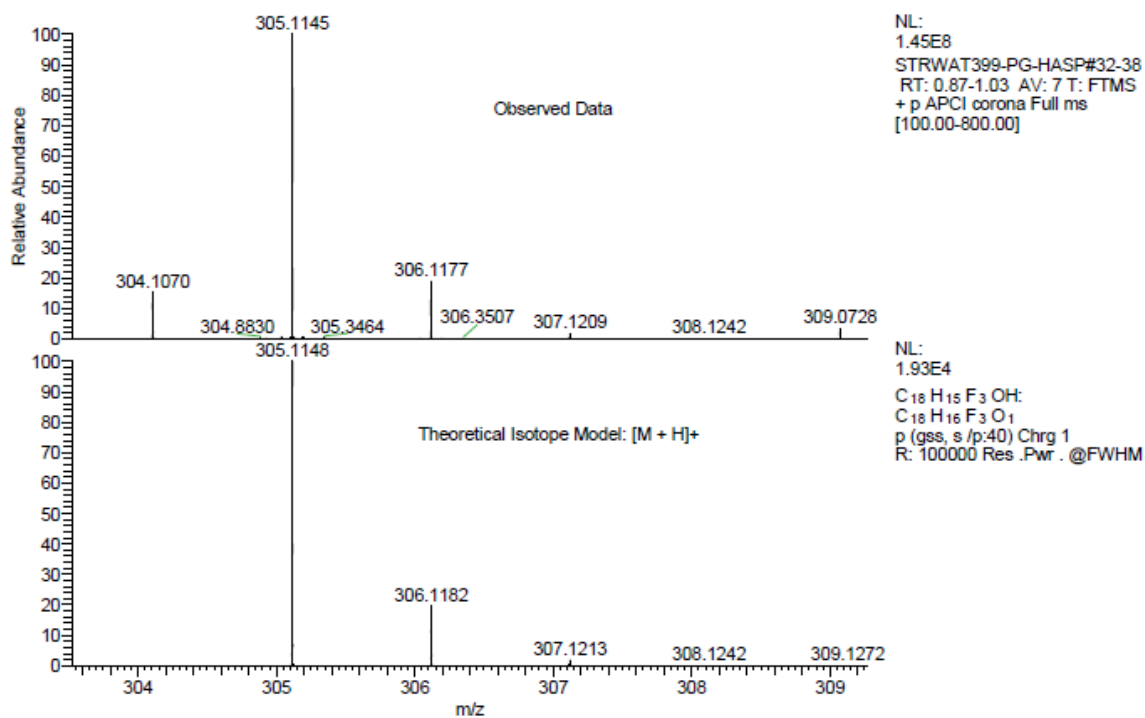


HRMS of 7n

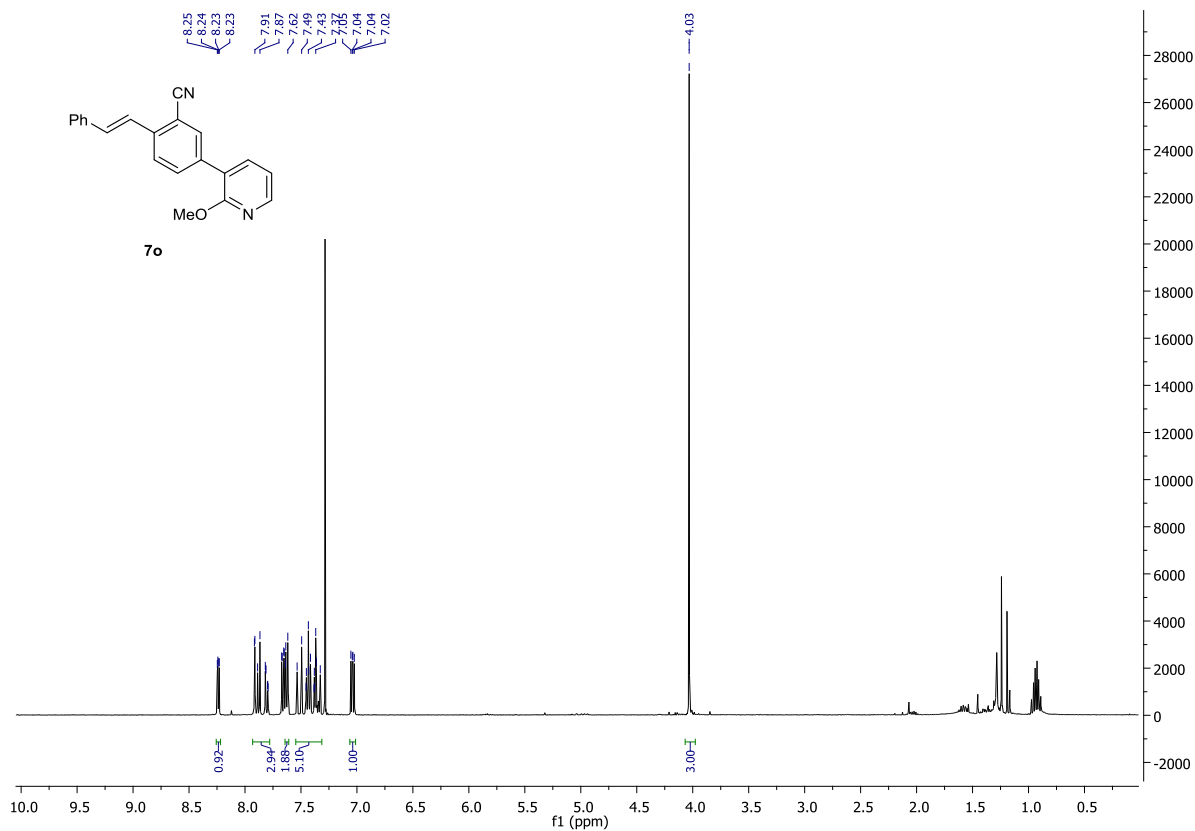
CS171-A1 MW=304?
ASAP (SOLID)

EPSRC National Facility Swansea
LTQ Orbitrap XL

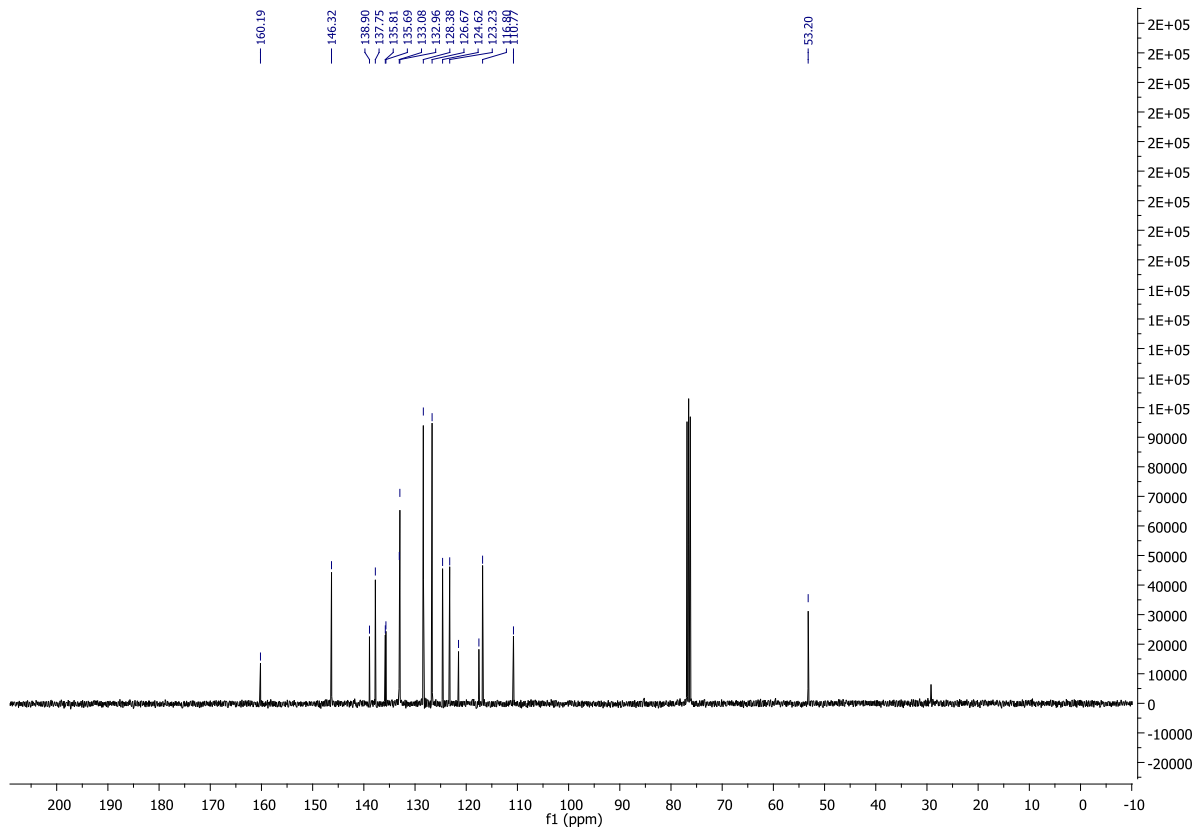
Ciaran Seath
27/01/2015 03:16:57 PM



¹H NMR of 7o



¹³C NMR of 7o

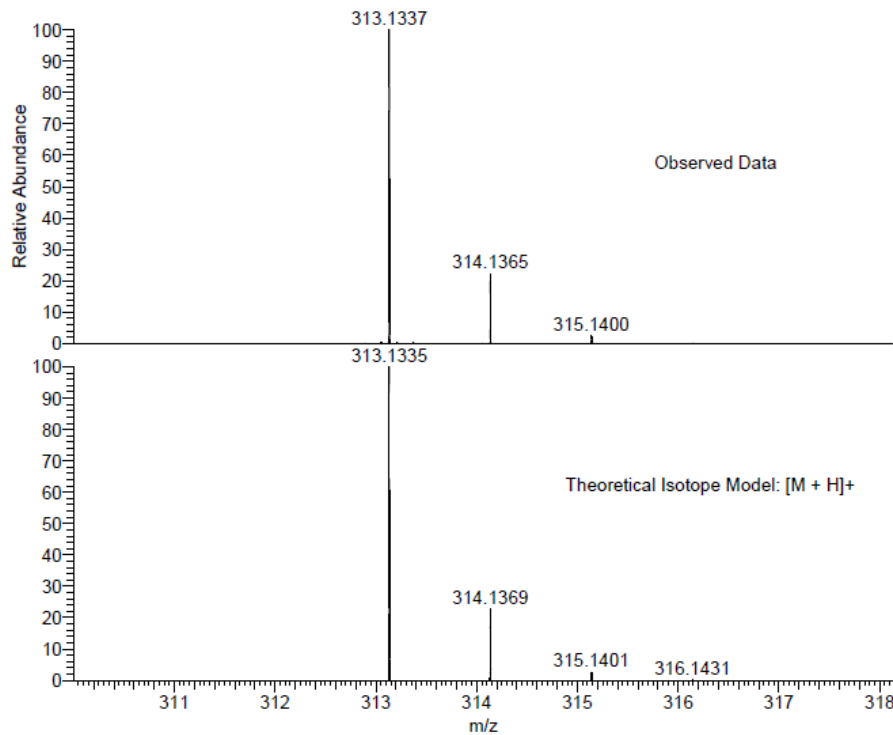


HRMS of 7o

CS165-A1 MW=312?
(DCM)/MeOH + NH4OAc
C21H16N2O

EPSRC National Facility Swansea
LTQ Orbitrap XL

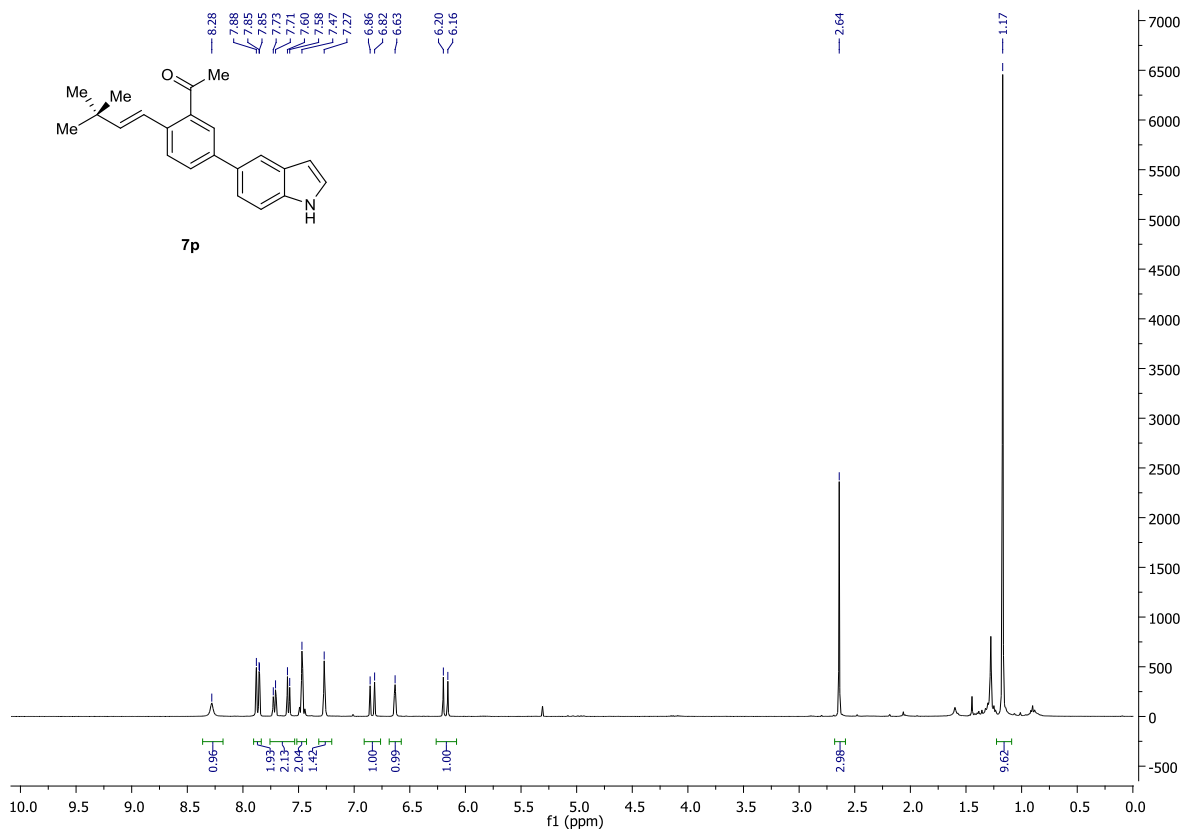
Ciaran Seath
23/01/2015 12:33:58



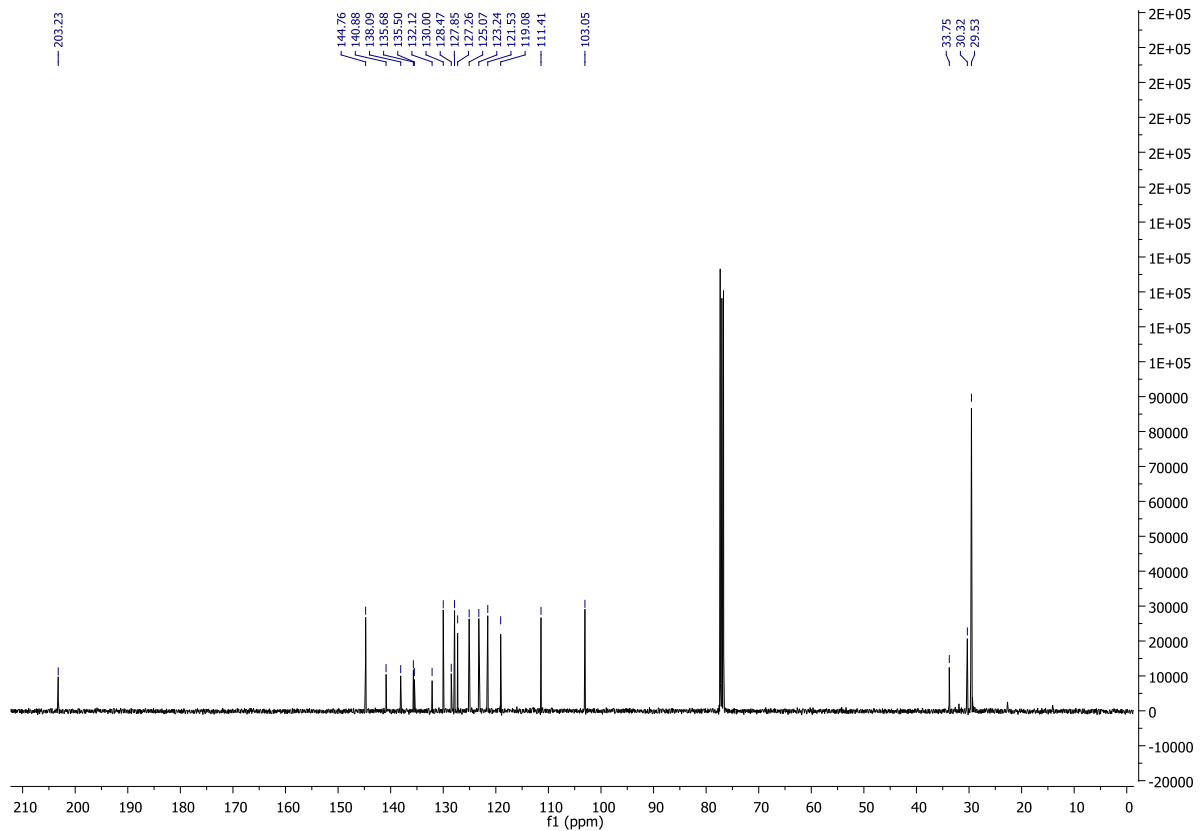
NL:
5.07E6
STRWAT403-OE-HNESP#27-
40 RT: 0.65-1.03 AV: 14 T:
FTMS + p NSI Full ms
[140.00-1935.00]

NL:
1.85E4
C₂₁H₁₆N₂OH:
C₂₁H₁₇N₂O₁
p (gss, s/p:40) Chrg 1
R: 100000 Res .Pwr . @FWHM

¹H NMR of 7p



¹³C NMR of 7p

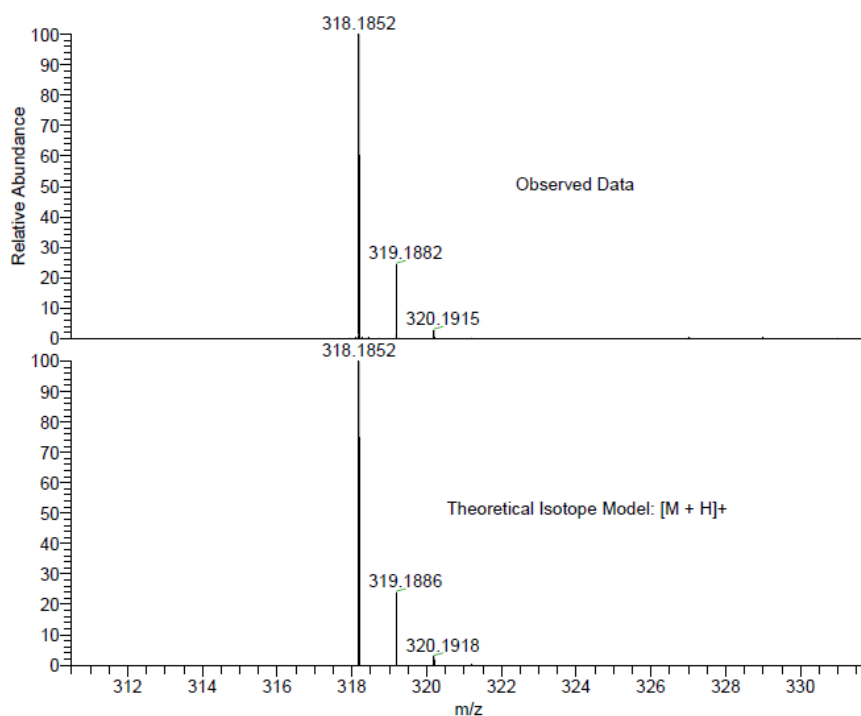


HRMS of 7p

CS167-A1 MW=317?
(DCM)/MeOH + NH4OAc
C22H23NO

EPSRC National Facility Swansea
LTQ Orbitrap XL

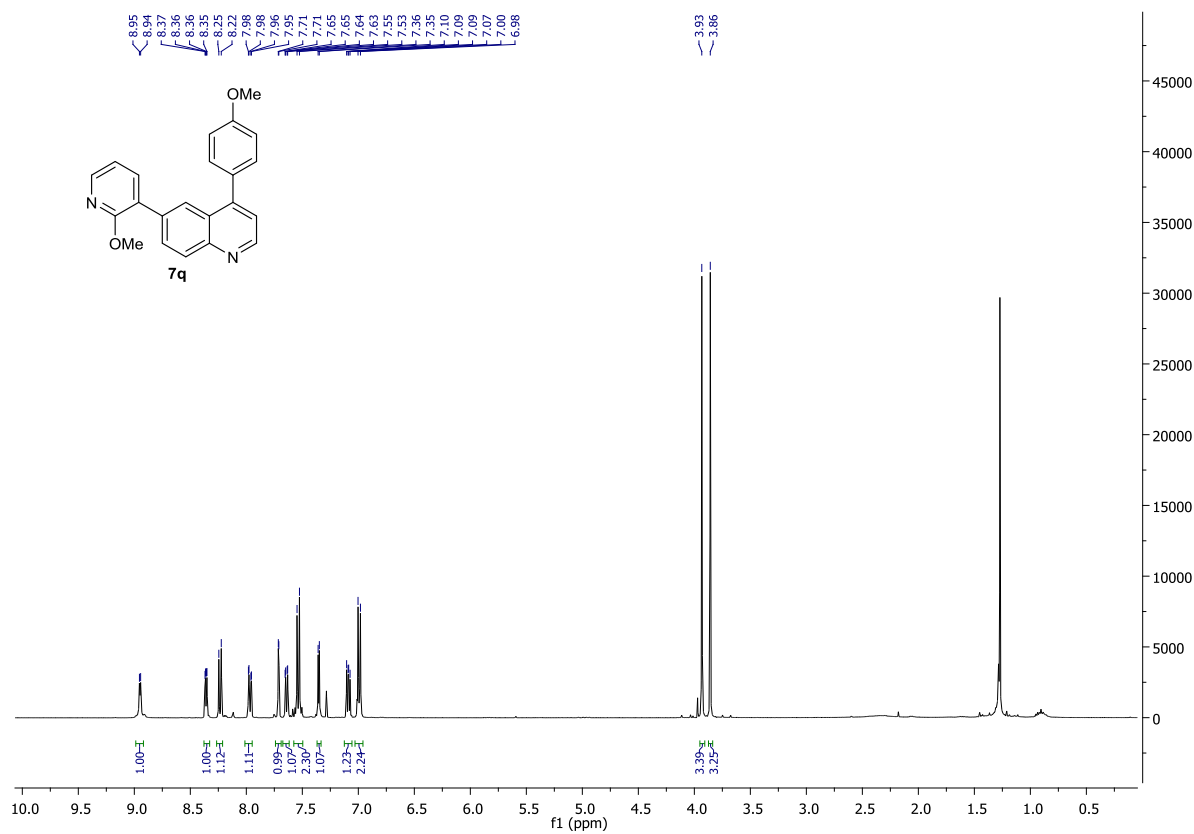
Ciaran Seath
23/01/2015 12:31:09



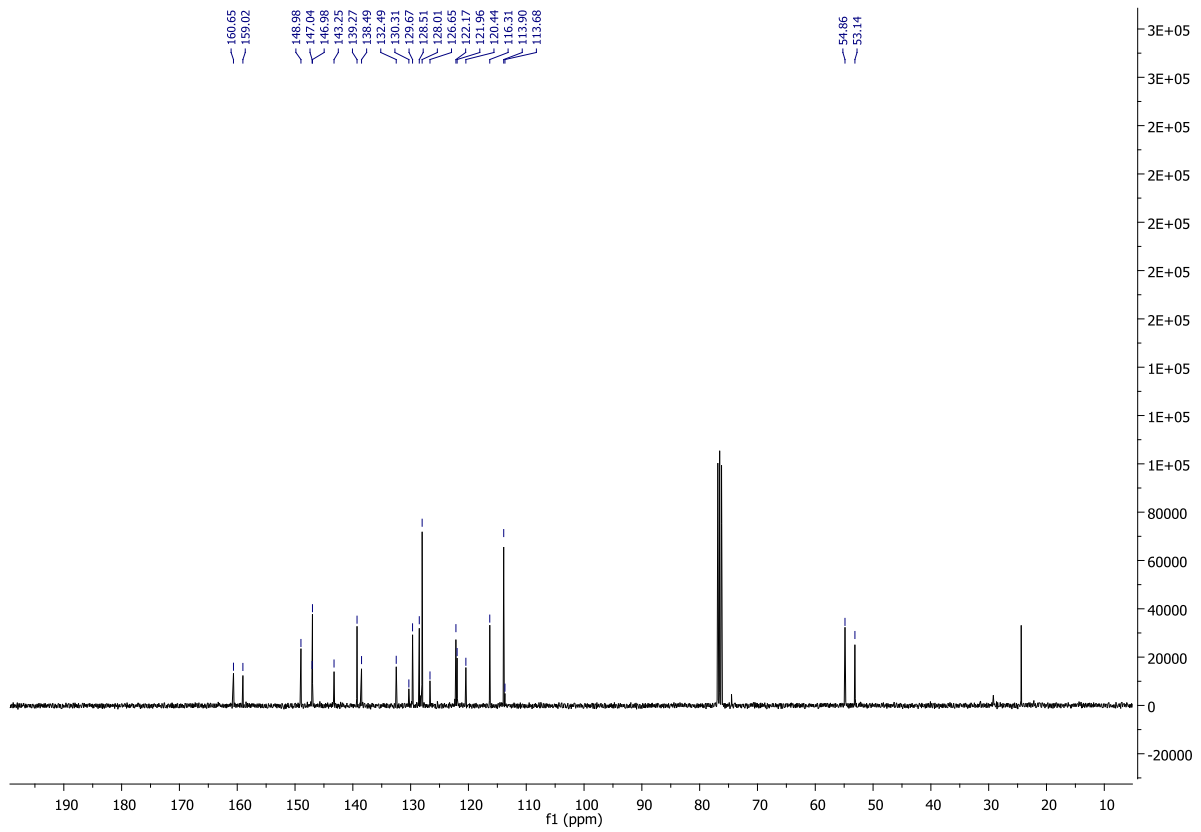
NL:
1.49E7
STRWAT402-OE-HNESP#9-22
RT: 0.15-0.53 AV: 14 T:
FTMS + p NSI Full ms
[140.00-1935.00]

NL:
1.84E4
C₂₂H₂₃NOH:
C₂₂H₂₄N₁O₁
p (gss, s /p:40) Chrg 1
R: 100000 Res .Pwr . @FWHM

¹H NMR of 7q



¹³C NMR of 7q

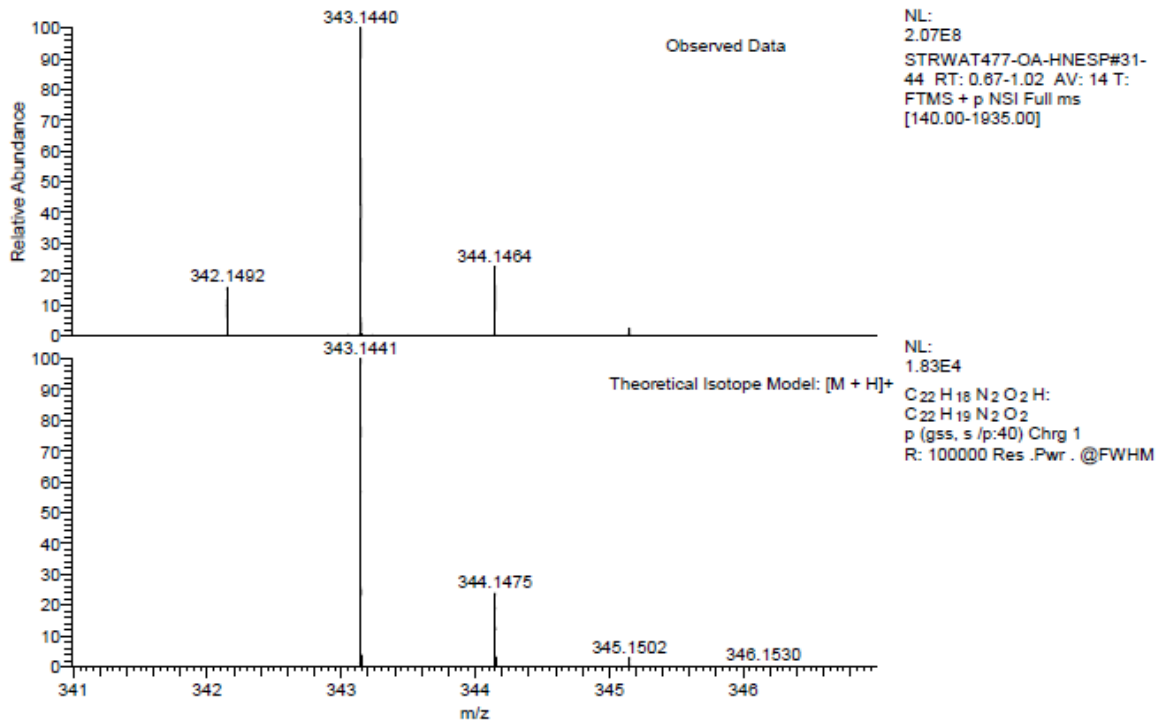


HRMS of 7q

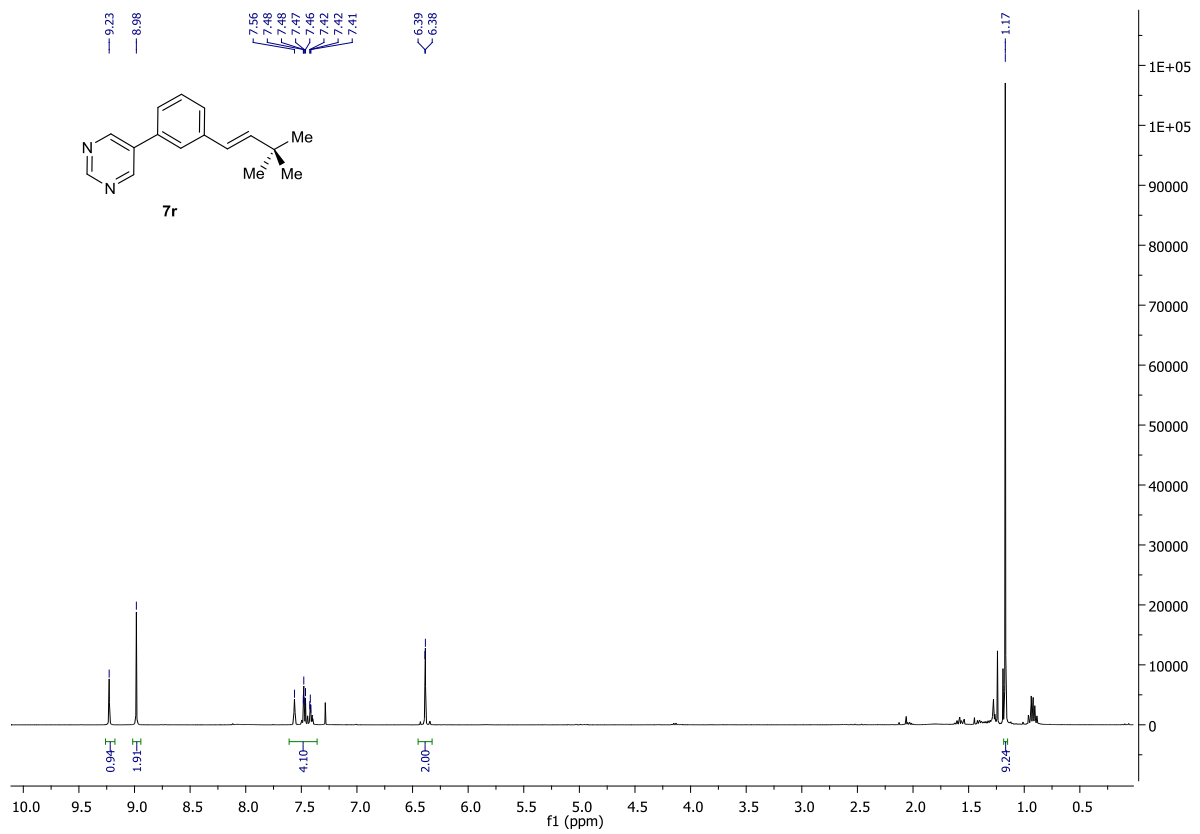
CS210-A1 MW=342?
C22H18N2O2
(DCM)/MeOH + NH4OAc

EPSRC National Facility Swansea
LTQ Orbitrap XL

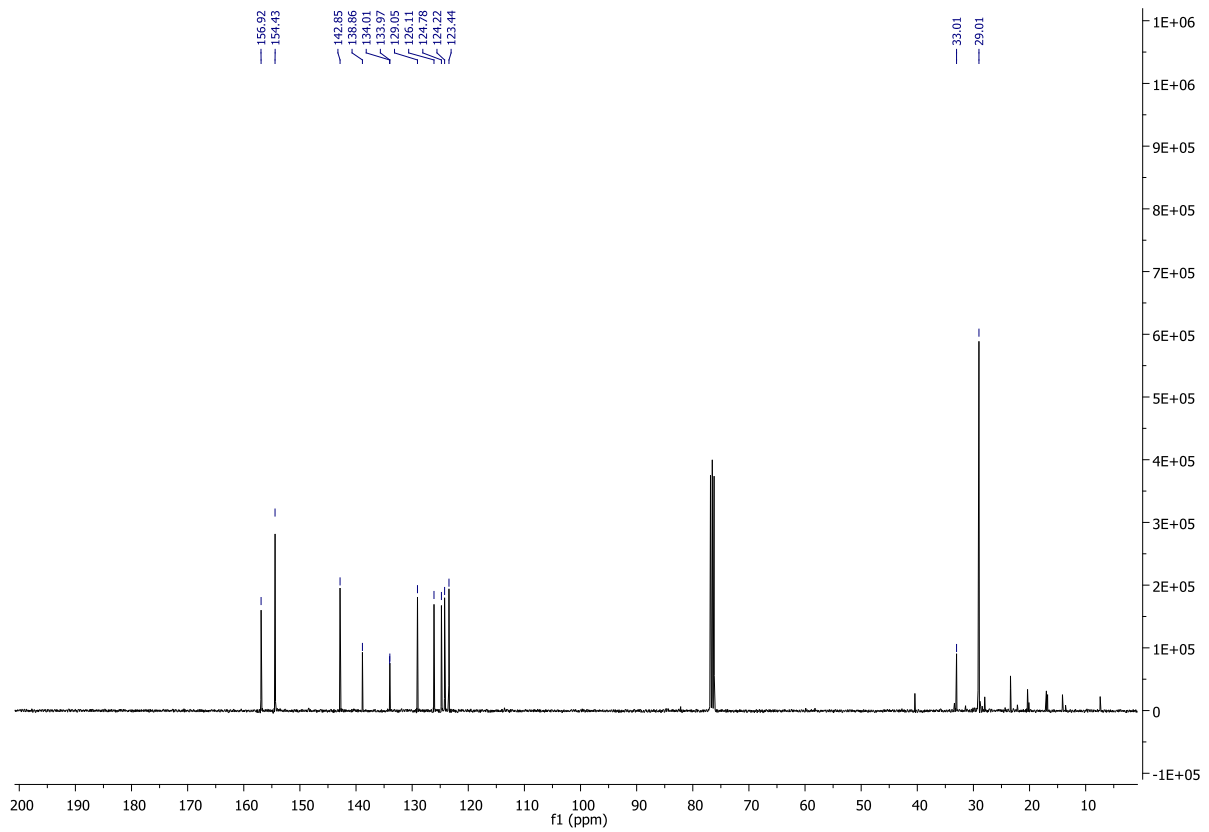
Ciaran Seath
16/04/2015 07:29:24



¹H NMR of 7r



¹³C NMR of 7r

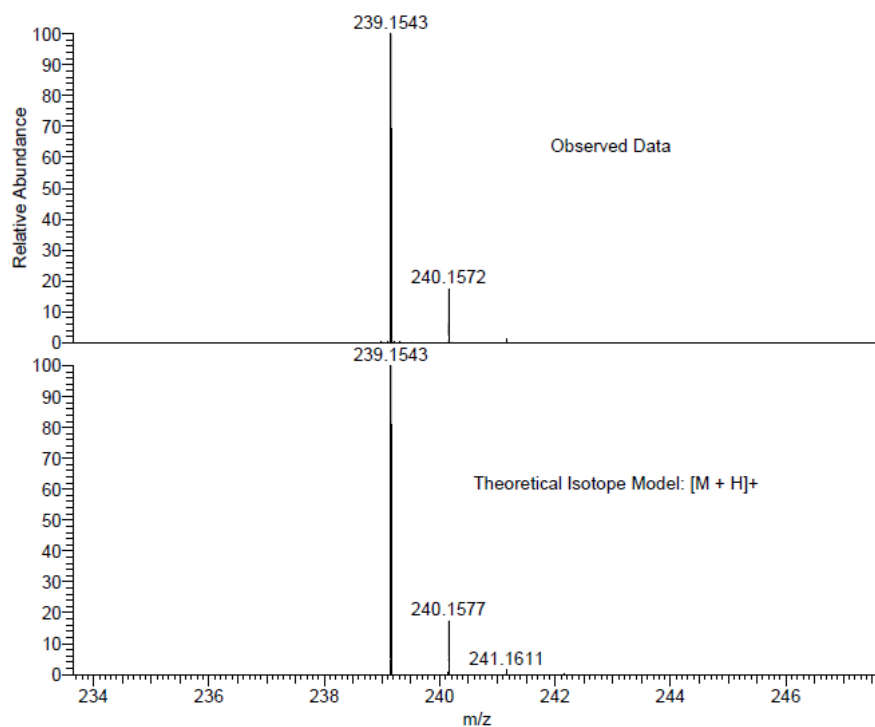


HRMS of 7r

CS172-A1 MW=238?
(DCM)/MeOH + NH4OAc
C16H18N2

EPSRC National Facility Swansea
LTQ Orbitrap XL

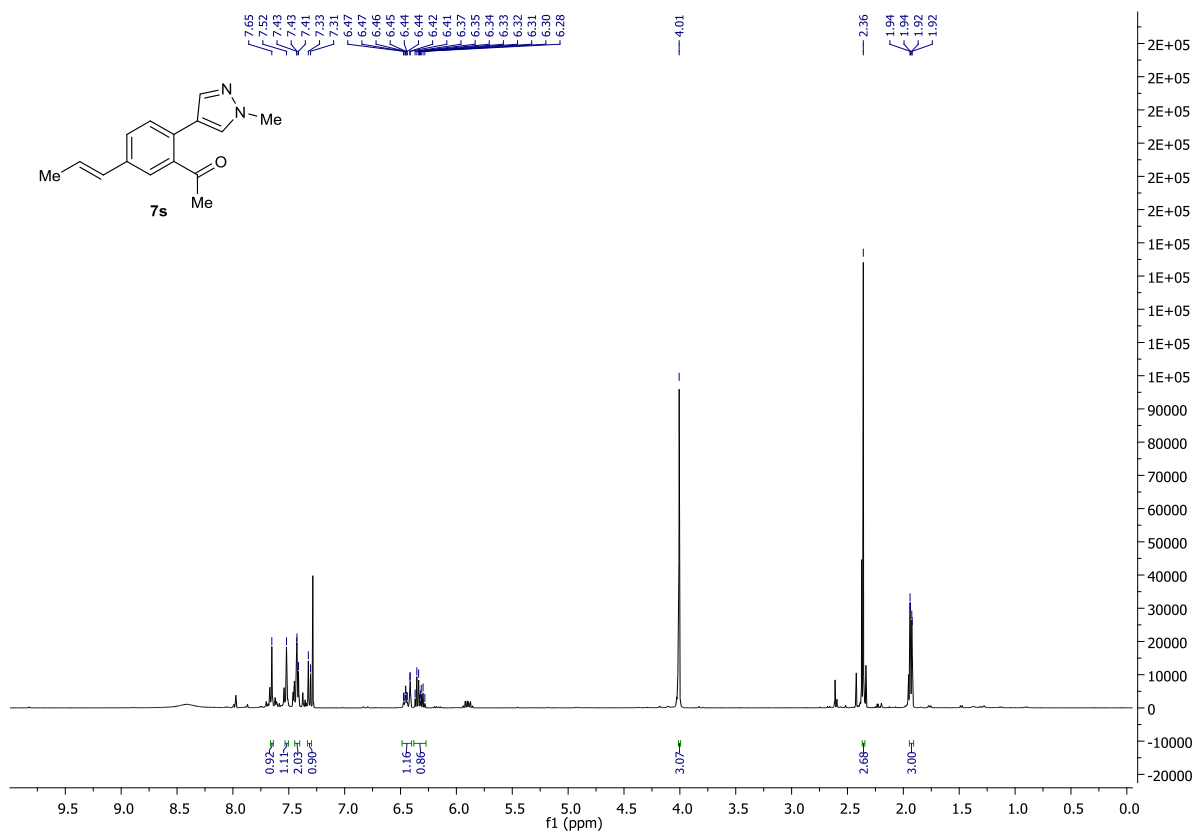
Ciaran Seath
23/01/2015 12:25:31



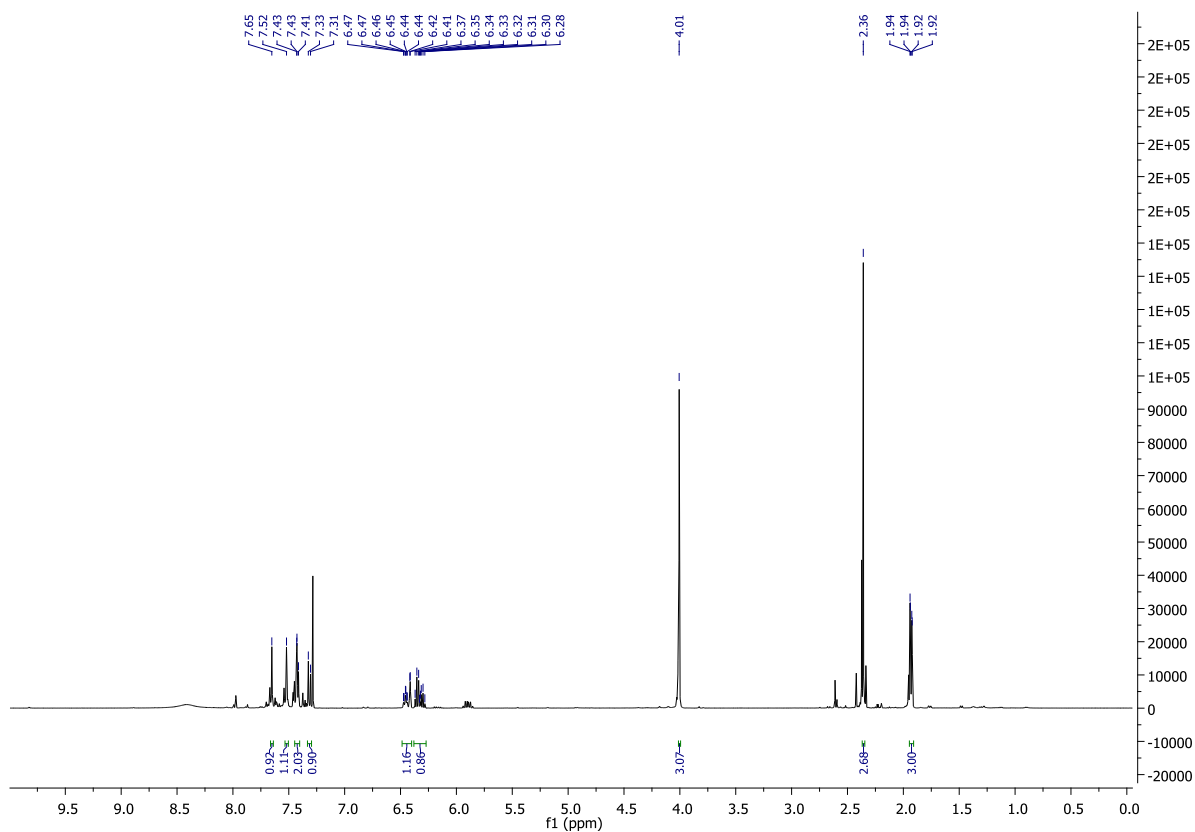
NL:
4.09E7
STRWAT400-OE-HNESP#29-
43 RT: 0.66-1.03 AV: 15 T:
FTMS + p NSI Full ms
[140.00-1935.00]

NL:
1.96E4
C₁₆H₁₈N₂H:
C₁₆H₁₈N₂
p (gss, s /p:40) Chrg 1
R: 100000 Res .Pwr .@FWHM

¹H NMR of 7s



¹³C NMR of 7s



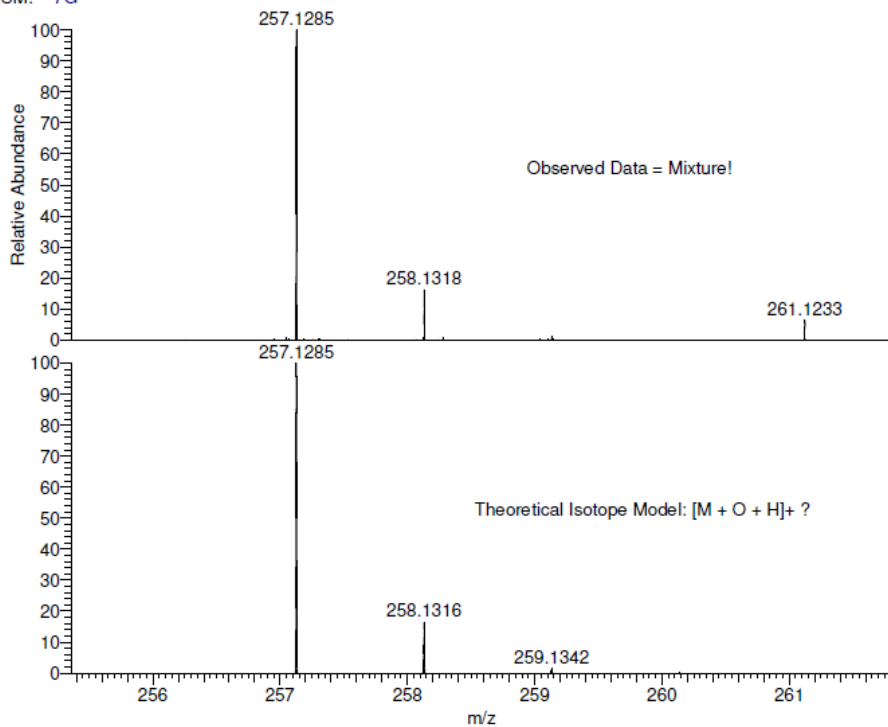
HRMS of 7s

CS176-A1 MW=240?
C₁₅H₁₆N₂O
(DCM)/MeOH + NH₄OAc

EPSRC National Facility Swansea
LTQ Orbitrap XL

Ciaran Seath
06/03/2015 16:26:22

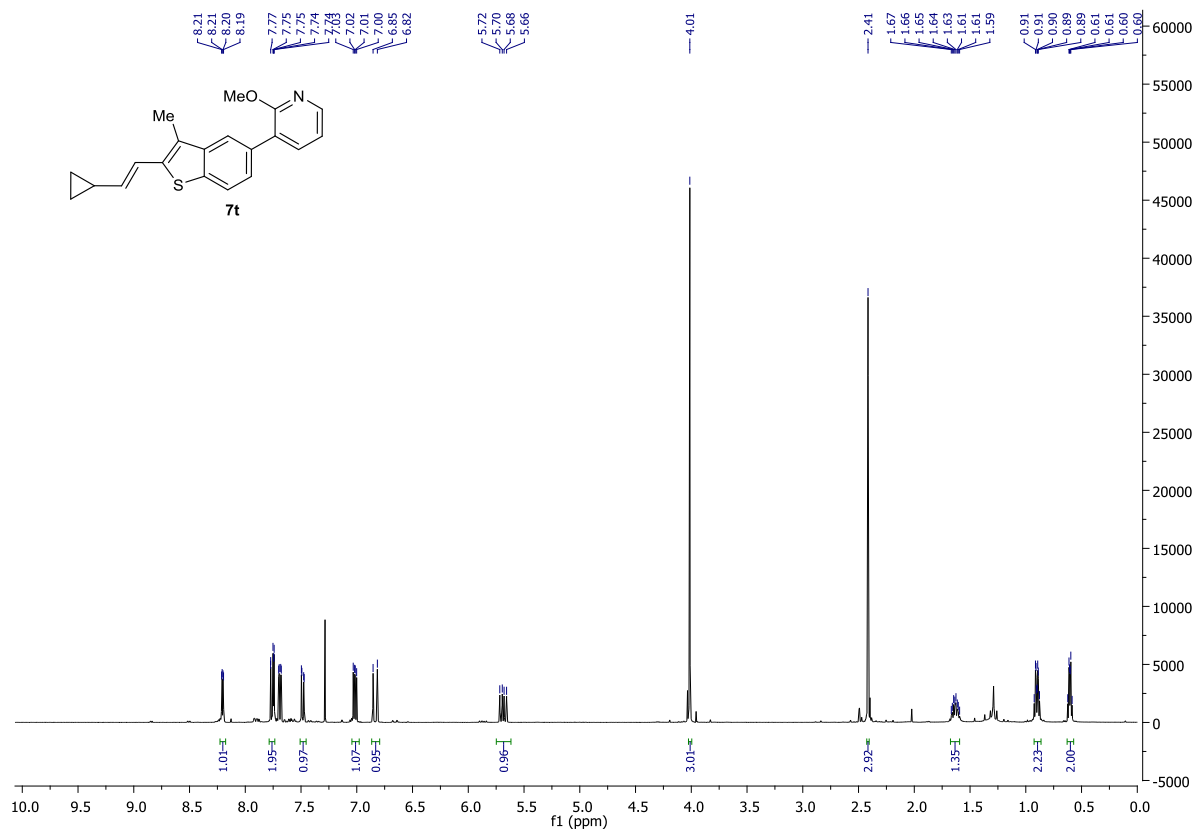
SM: 7G



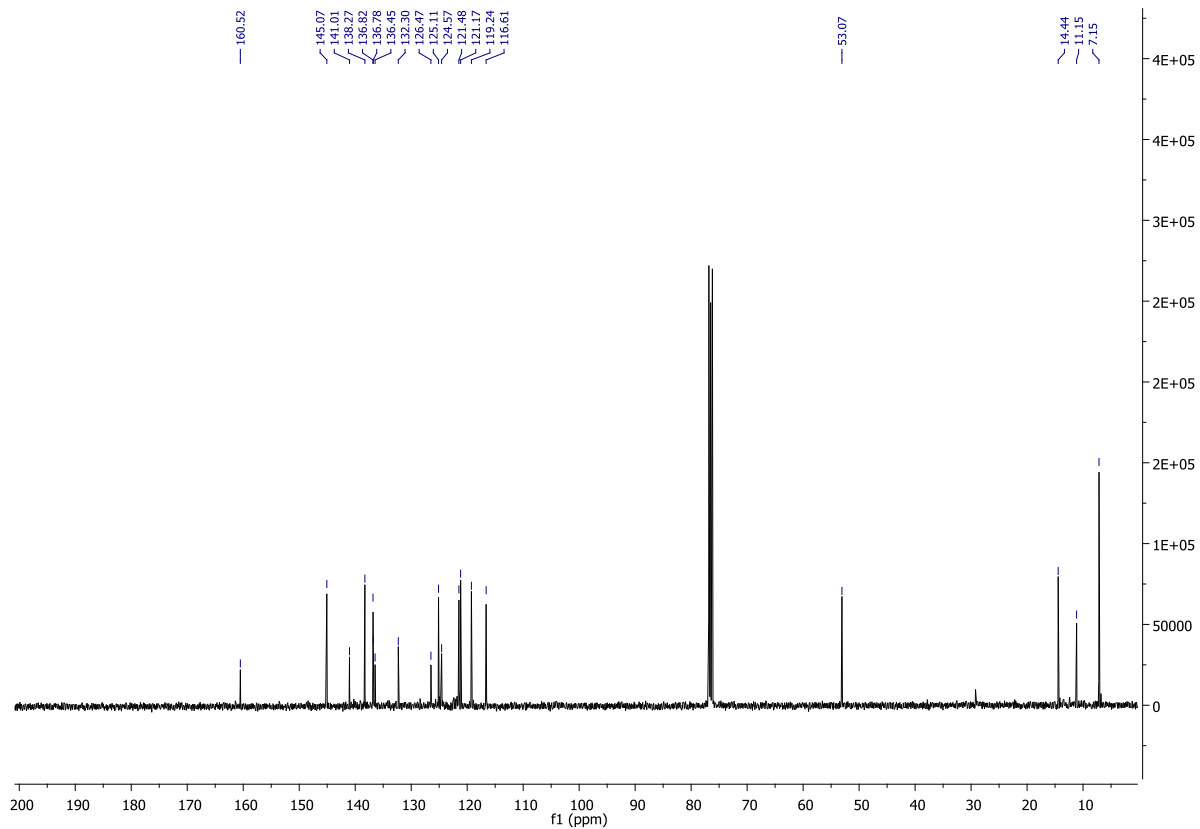
NL:
4.16E7
STRWAT451-OE-HNESP#29-
46 RT: 0.66-1.04 AV: 16 T:
FTMS + p NSI Full ms
[140.00-1935.00]

NL:
9.84E4
C₁₅H₁₆N₂OOH:
C₁₅H₁₇N₂O₂
p (gss, s/p:8) Chrg 1
R: 50000 Res .Pwr . @FWHM

¹H NMR of 7t



¹³C NMR of 7t

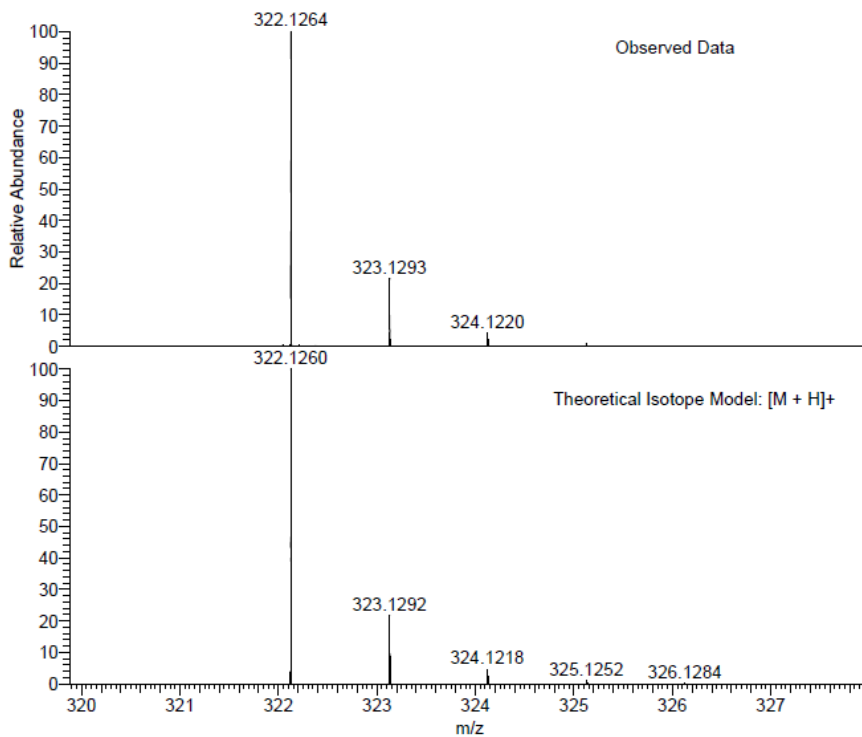


HRMS of 7t

CS180-A1 MW=317
(DCM)/MeOH + NH4OAc

EPSRC National Facility Swansea
LTQ Orbitrap XL

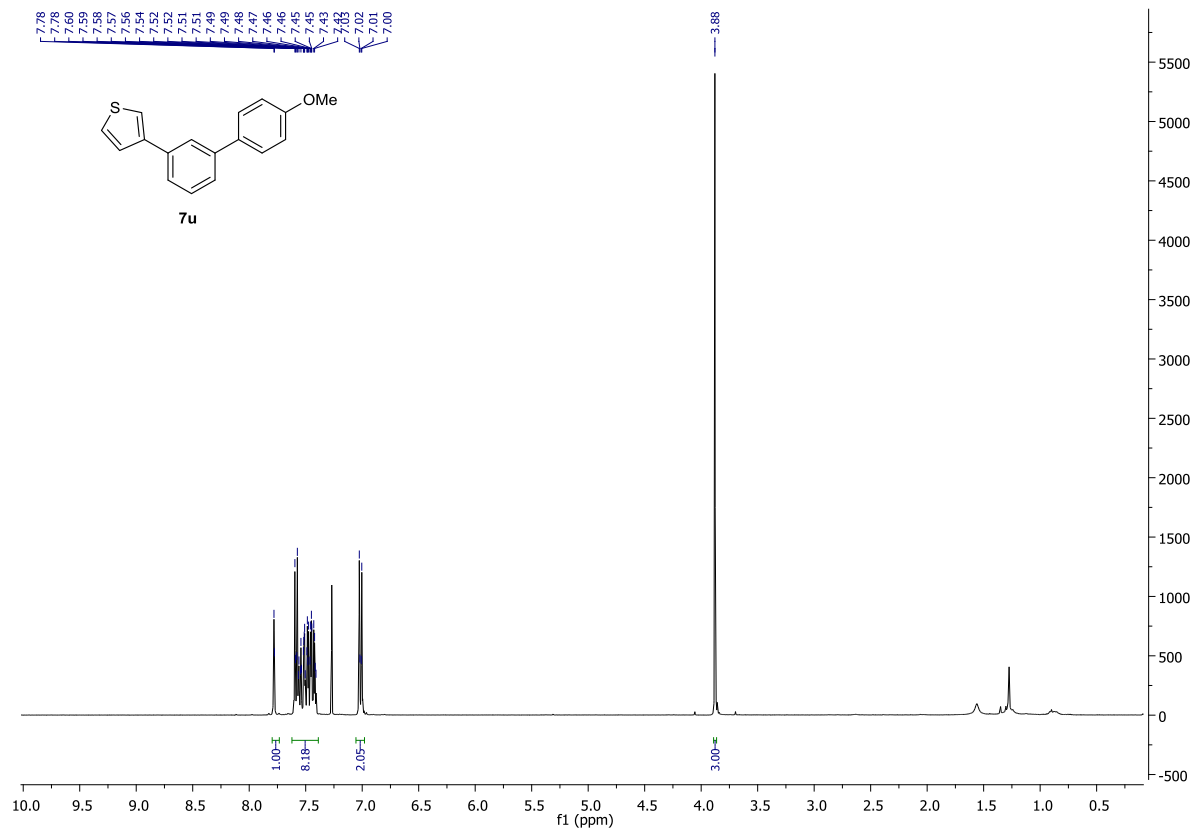
Ciaran Seath
06/03/2015 16:29:13



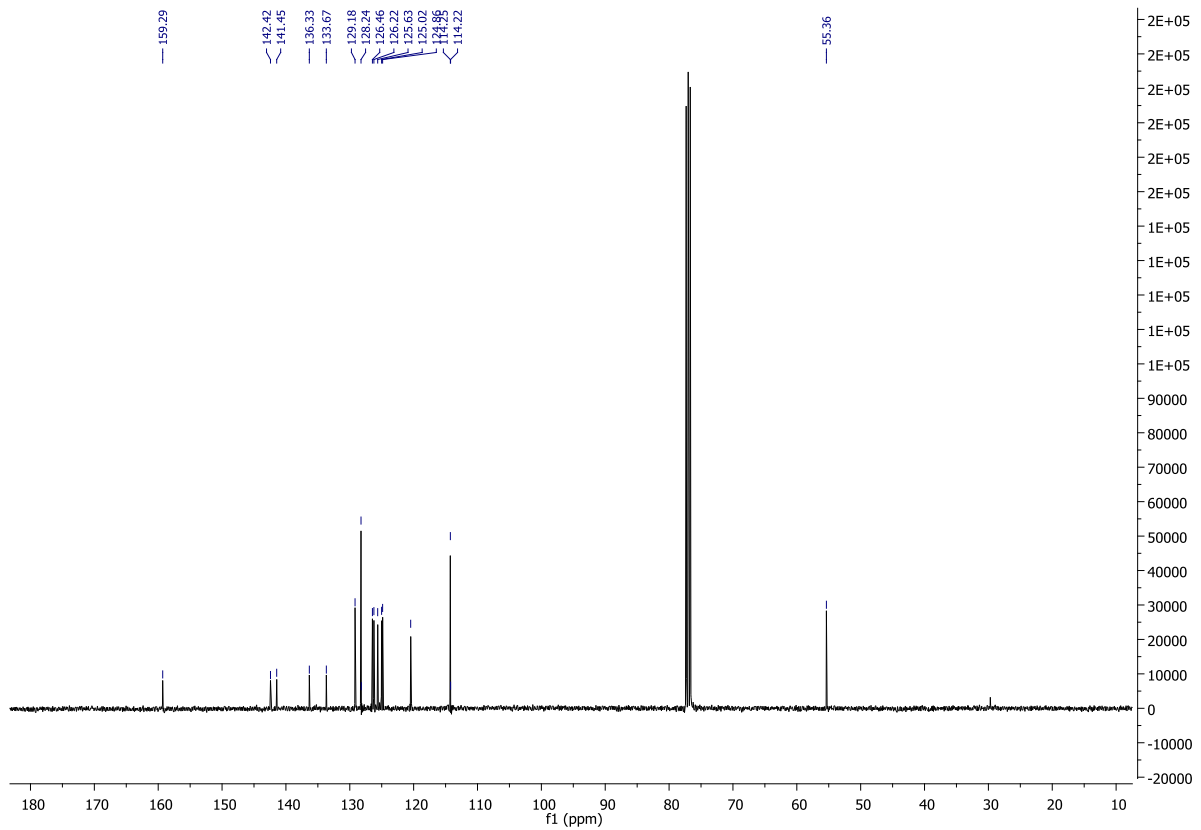
NL:
9.35E7
STRWAT452-OE-HNESP#14-
26 RT: 0.29-0.54 AV: 10 T:
FTMS + p NSI Full ms
[140.00-1935.00]

NL:
1.78E4
C₂₀H₁₉NOSH:
C₂₀H₂₀N₁O₁S₁
p (gss, s /p:40) Chrg 1
R: 100000 Res .Pwr . @FWHM

¹H NMR of 7u



¹³C NMR of 7u

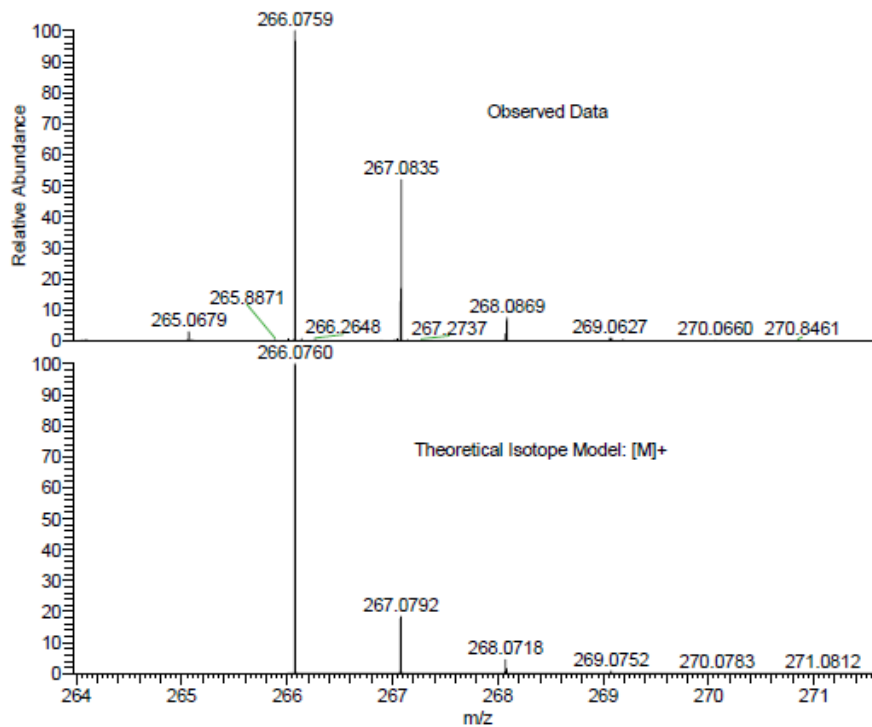


HRMS of 7u

CS158-A1 MW=286?
ASAP (CH3CN)

EPSRC National Facility Swansea
LTQ Orbitrap XL

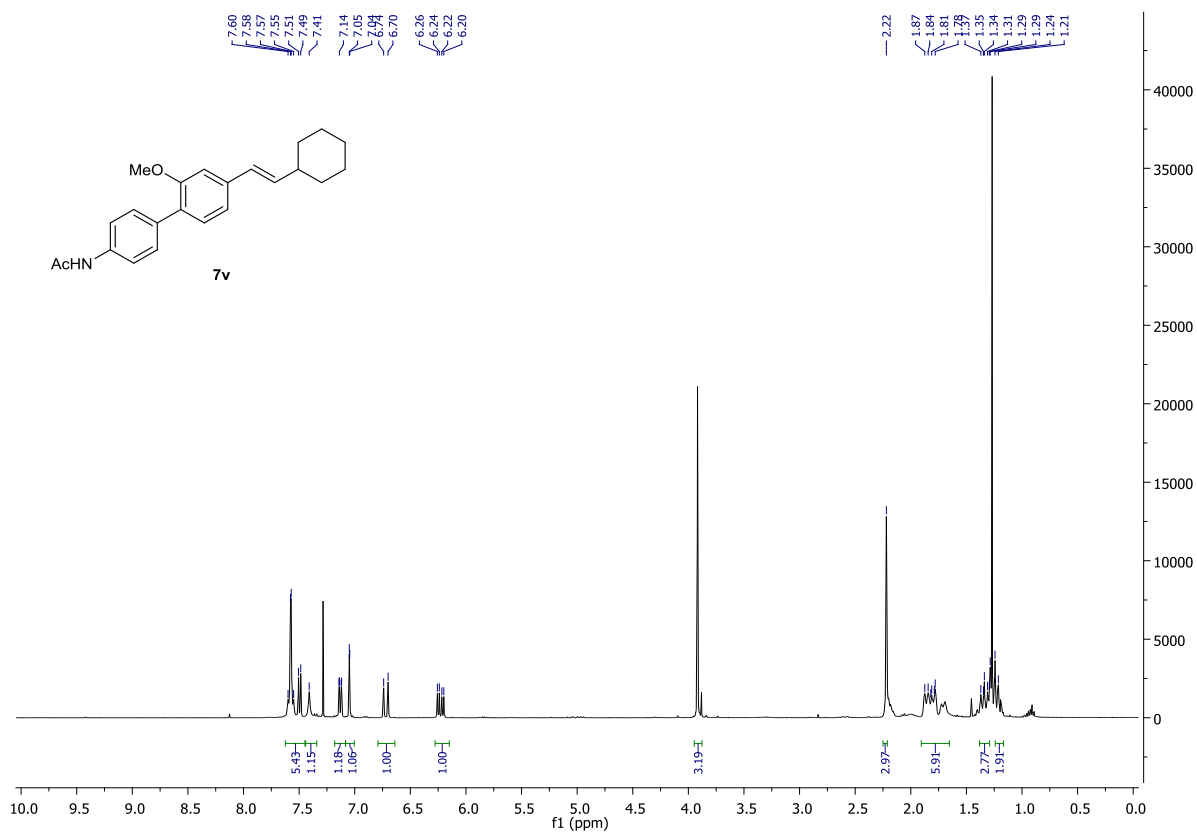
Ciaran
10/02/2015 03:25:06 PM



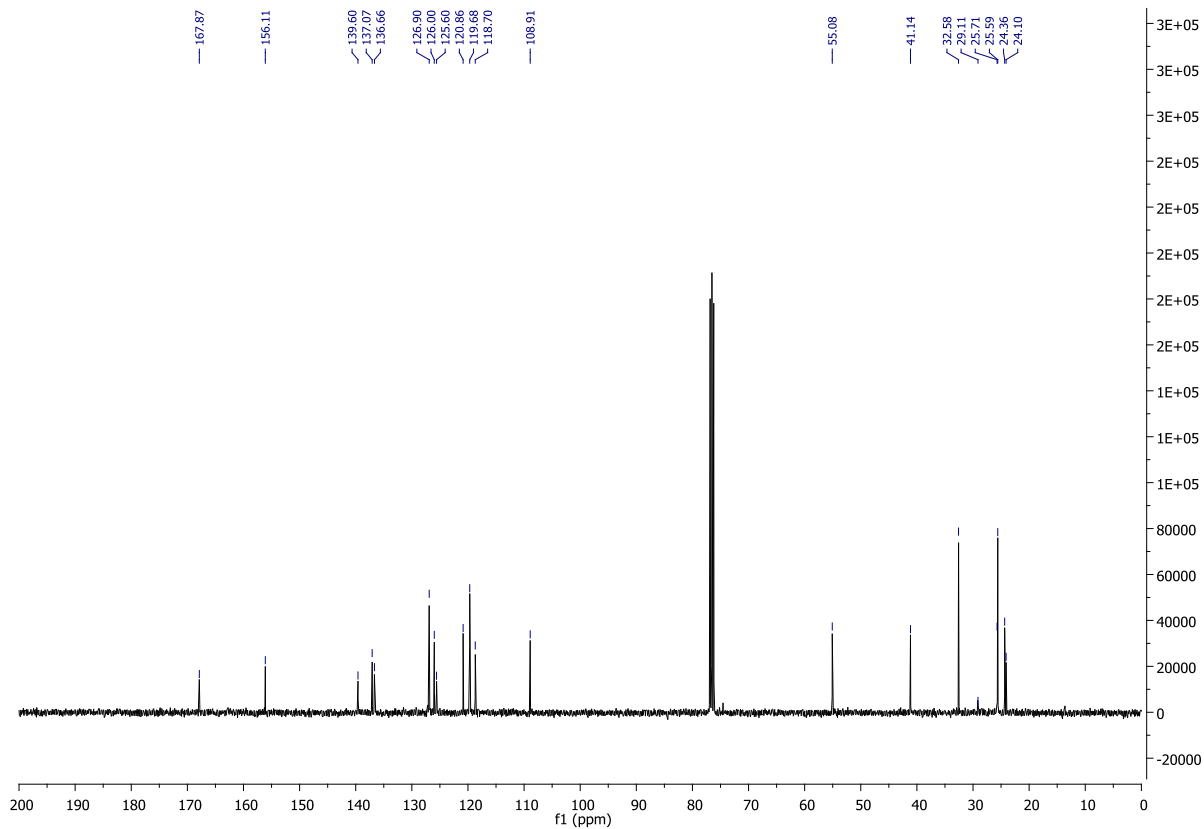
NL:
1.30E6
STRWAT406-PG-HASP#134-
146 RT: 4.30-4.63 AV: 13 T:
FTMS + p APCI corona Full ms
[100.00-800.00]

NL:
1.85E4
C₁₇H₁₄OS:
C₁₇H₁₄O₁S₁
p (gss, s /p:40) Chrg 1
R: 100000 Res .Pwr . @FWHM

¹H NMR of 7v



¹³C NMR of 7v

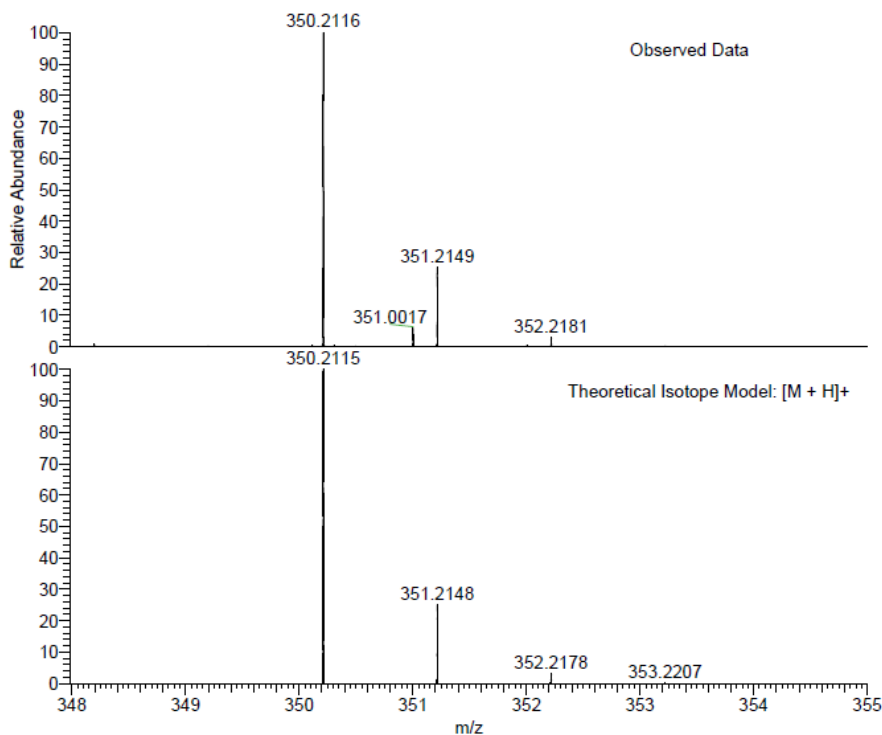


HRMS of 7v

CS178-A1 MW=349?
(DCM)/MeOH + NH4OAc

EPSRC National Facility Swansea
LTQ Orbitrap XL

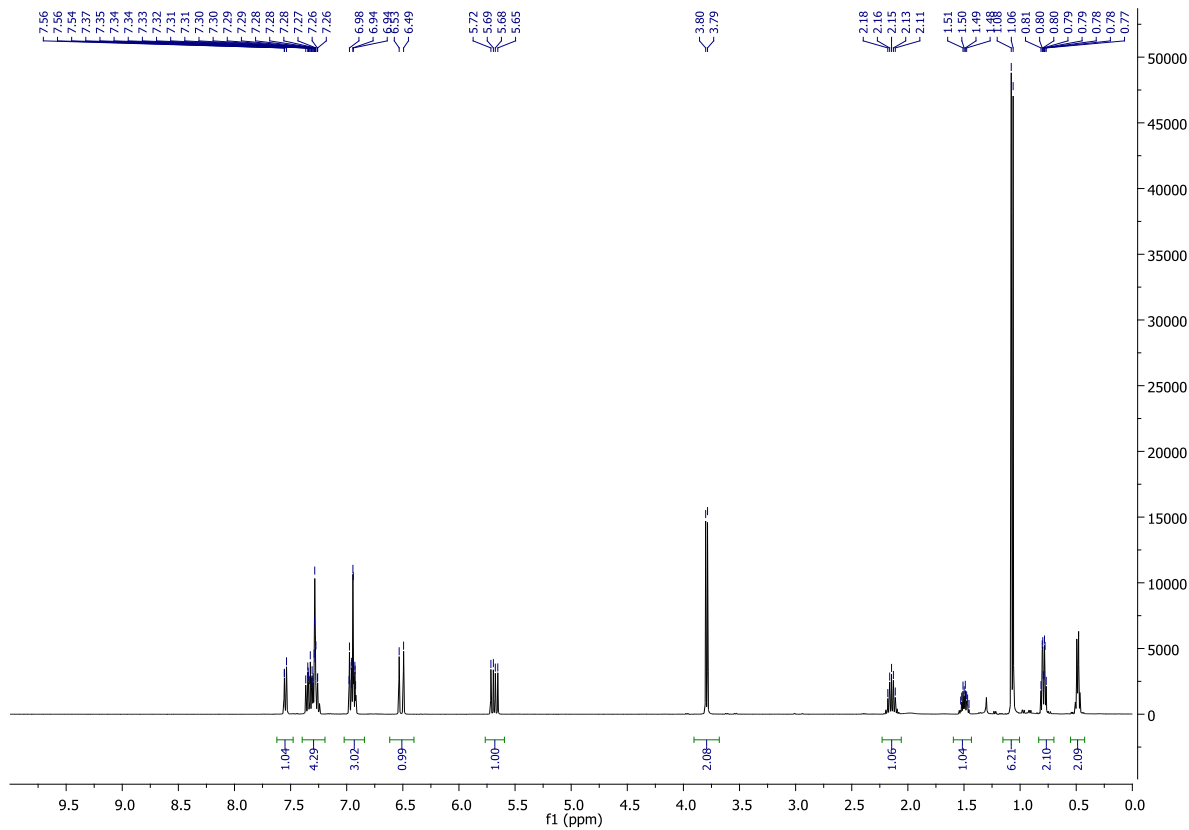
Ciaran Seath
06/03/2015 16:32:04



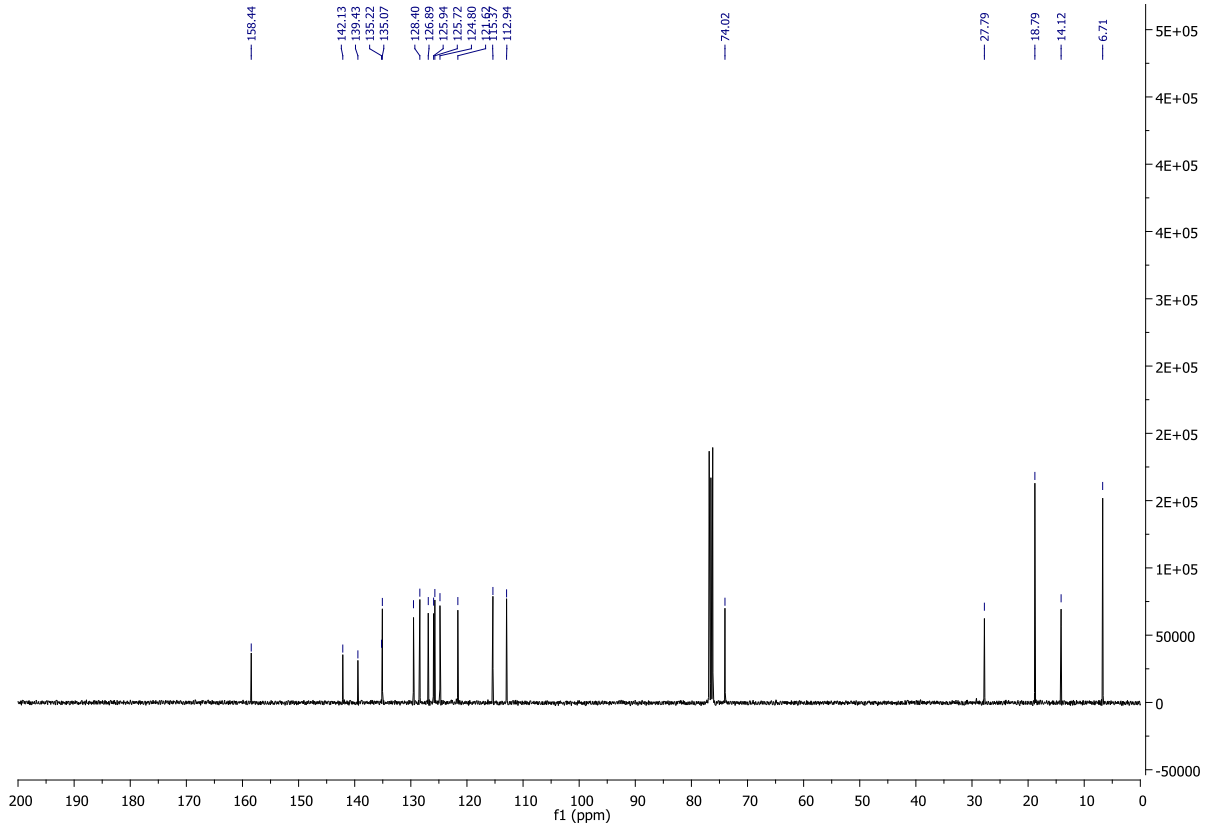
NL:
2.49E7
STRWAT453-OE-HNESP#14-
26 RT: 0.29-0.54 AV: 10 T:
FTMS + p NSI Full ms
[140.00-1935.00]

NL:
1.81E4
C₂₃ H₂₇ NO₂ H:
C₂₃ H₂₈ N₁ O₂
p (gss, s /p:40) Chrg 1
R: 100000 Res .Pwr . @FWHM

¹H NMR of 7w



¹³C NMR of 7w

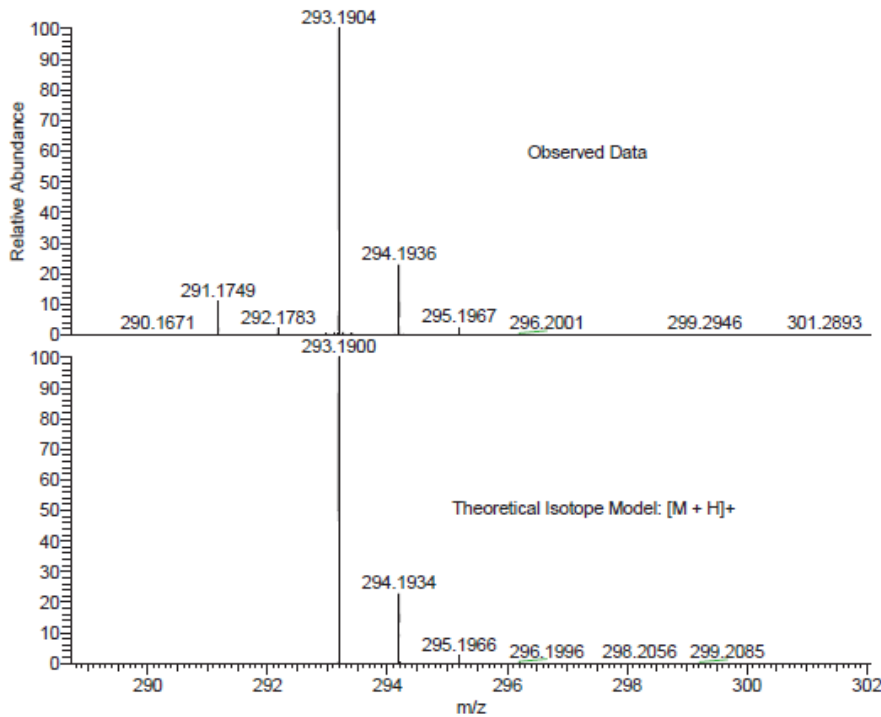


HRMS of 7w

CS188-A1 MW=282?
ASAP (DCM)

EPSRC National Facility Swansea
LTQ Orbitrap XL

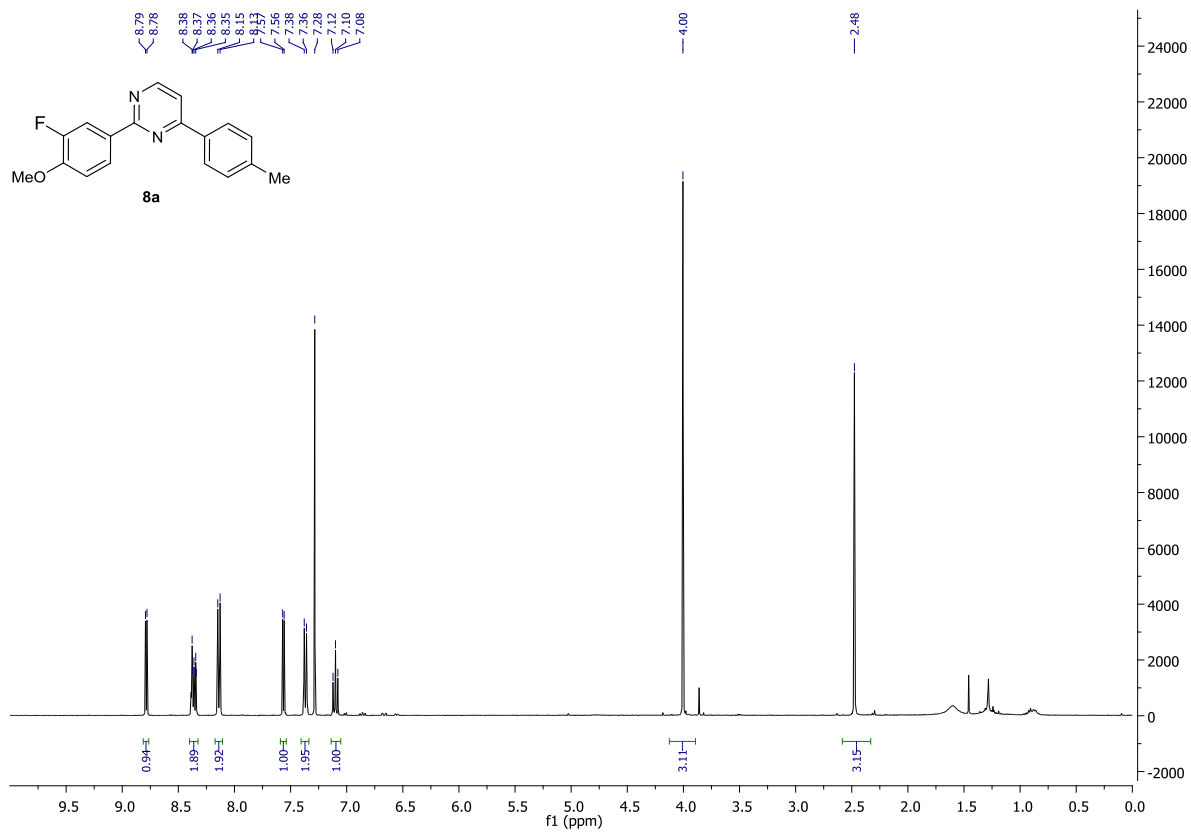
Ciaran Seath
27/01/2015 12:52:55 PM



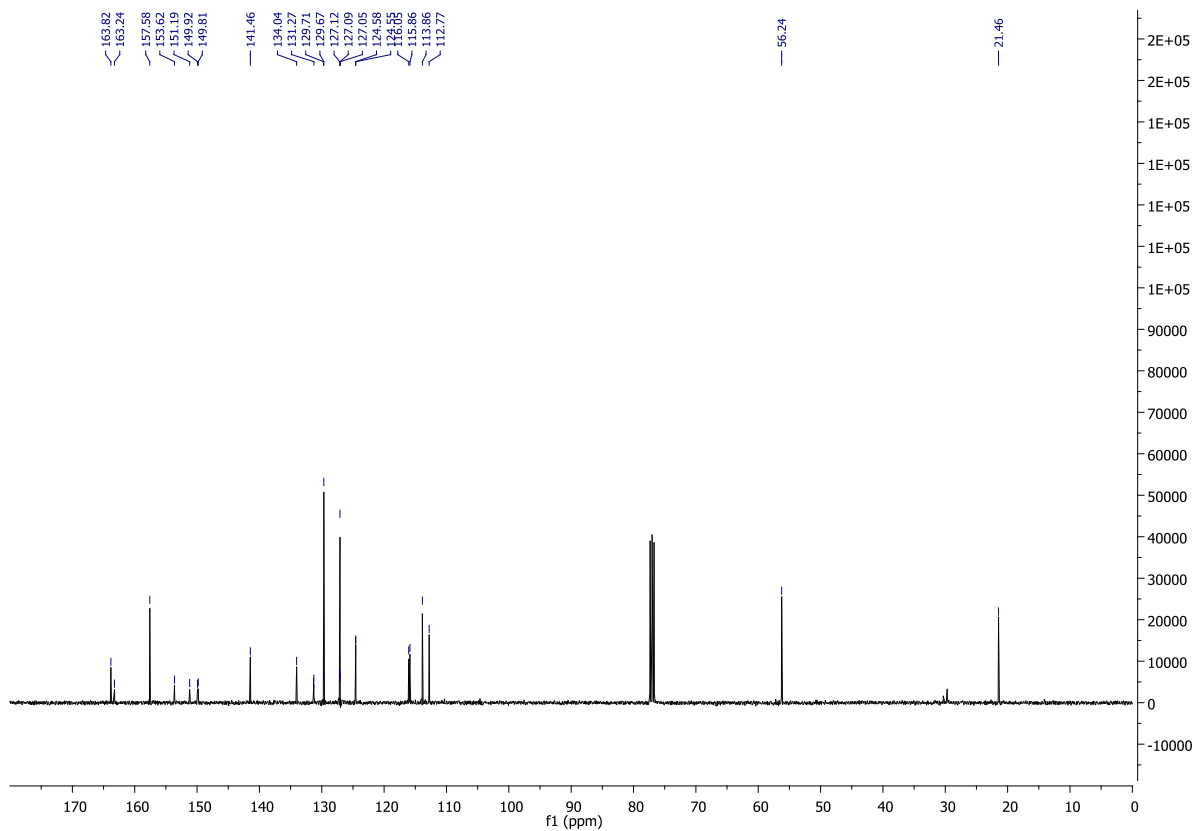
NL:
2.42E7
STRWAT401-PE-HASP#21-42
RT: 0.57-1.15 AV: 22 T: FTMS
+ p APCI corona Full ms
[100.00-800.00]

NL:
1.86E4
C₂₁H₂₄OH:
C₂₁H₂₅O₁
p (gss, s /p:40) Chrg 1
R: 100000 Res .Pwr . @FWHM

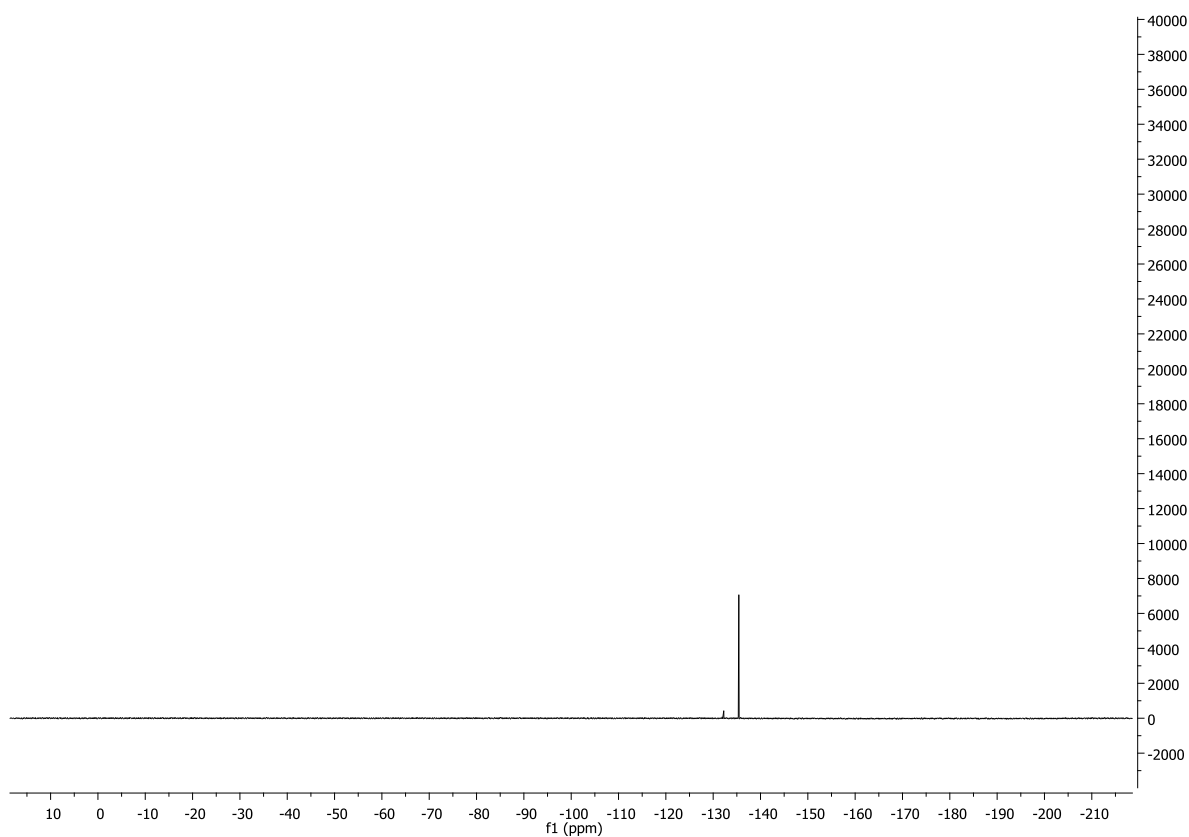
¹H NMR of 8a



¹³C NMR of 8a



¹⁹F NMR of 8a

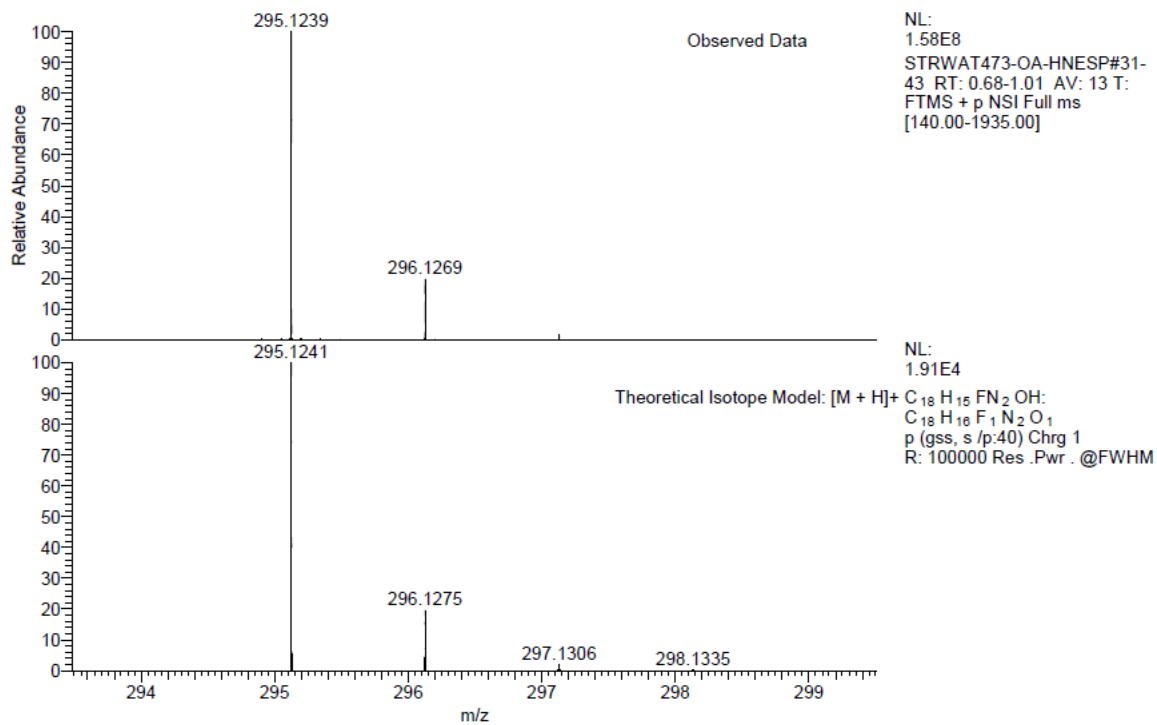


HRMS of 8a

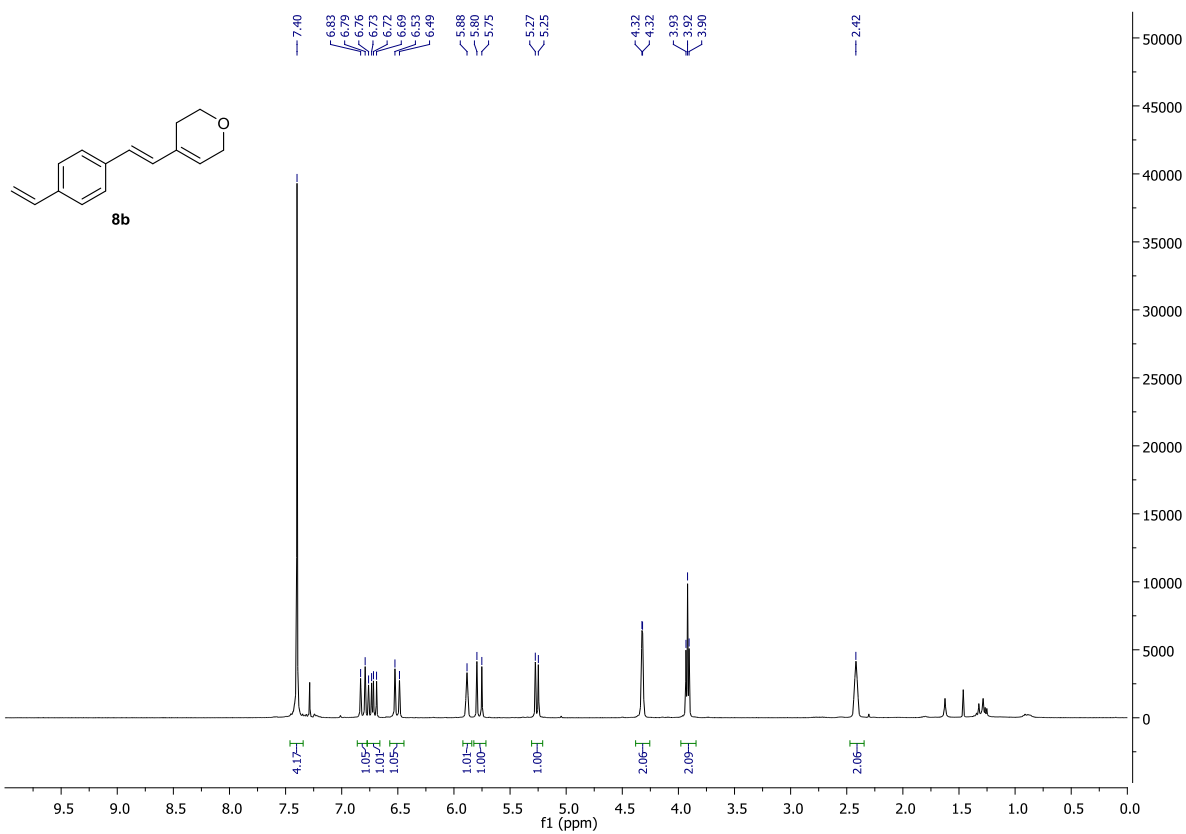
JF372 MW=294?
C₁₈H₁₅FN₂O
(DCM)/MeOH + NH₄OAc

EPSRC National Facility Swansea
LTQ Orbitrap XL

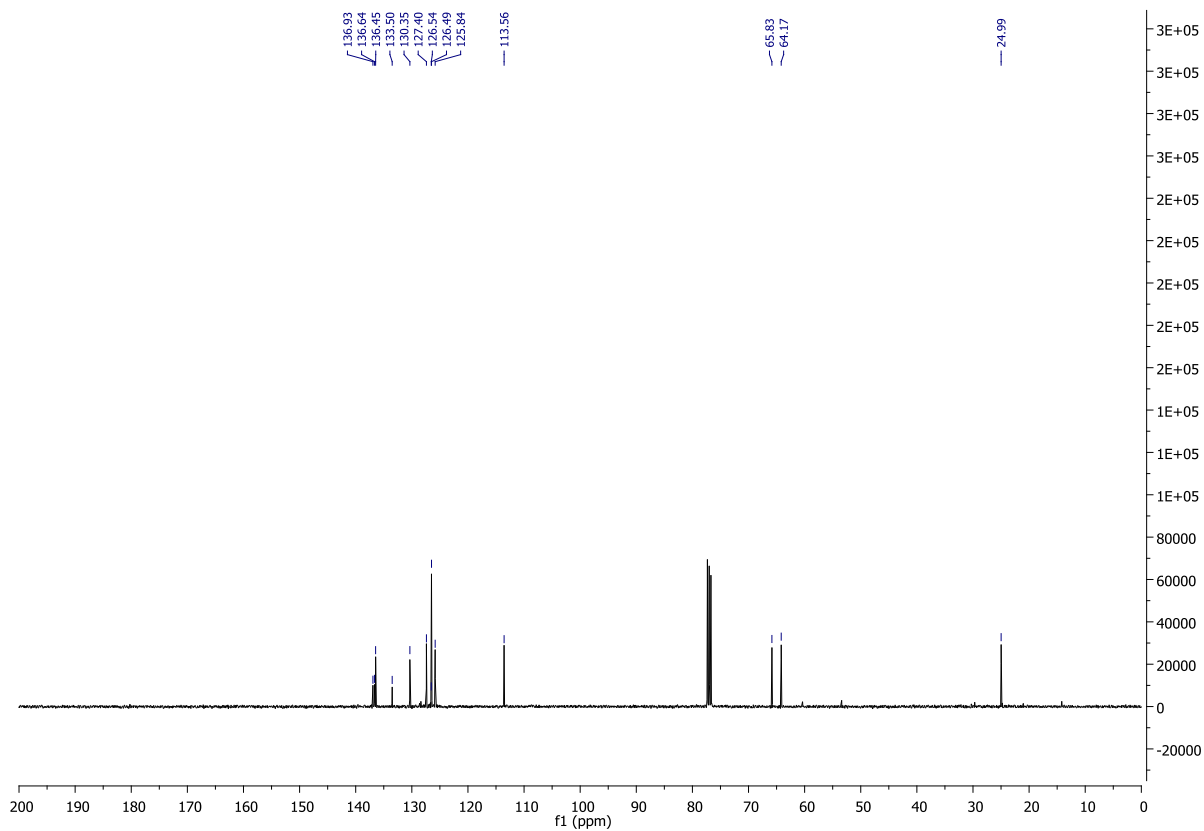
James Fyfe
16/04/2015 07:20:51



¹H NMR of 8b



¹³C NMR of 8b

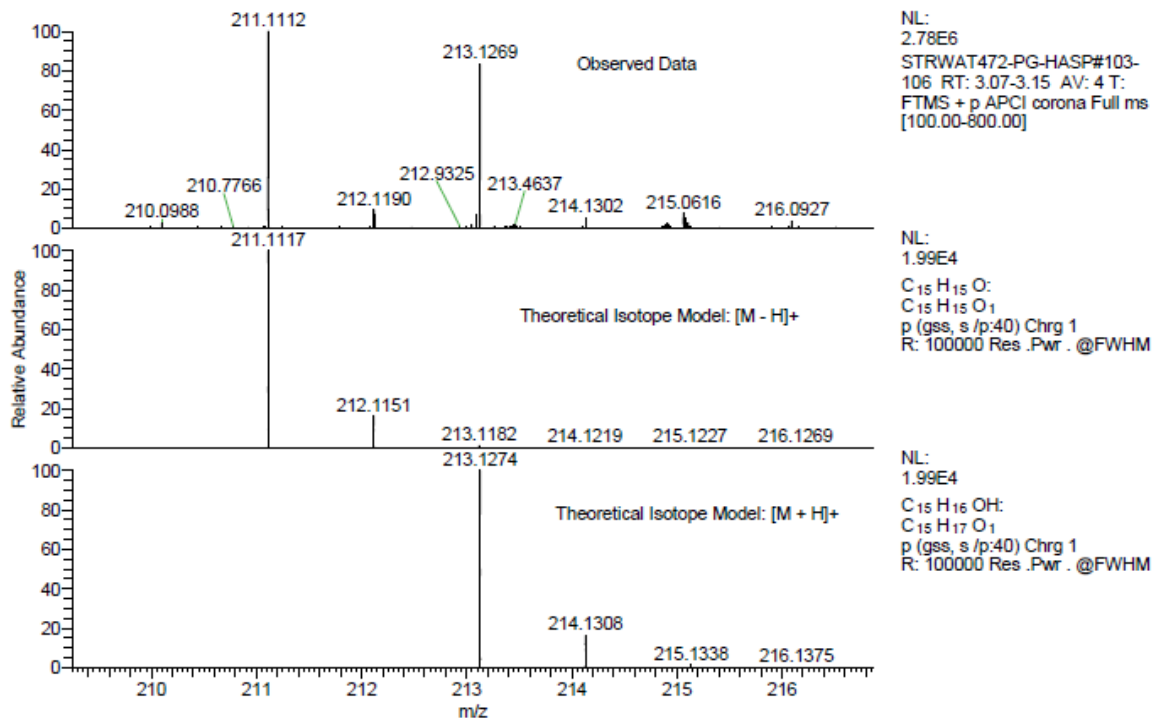


HRMS of 8b

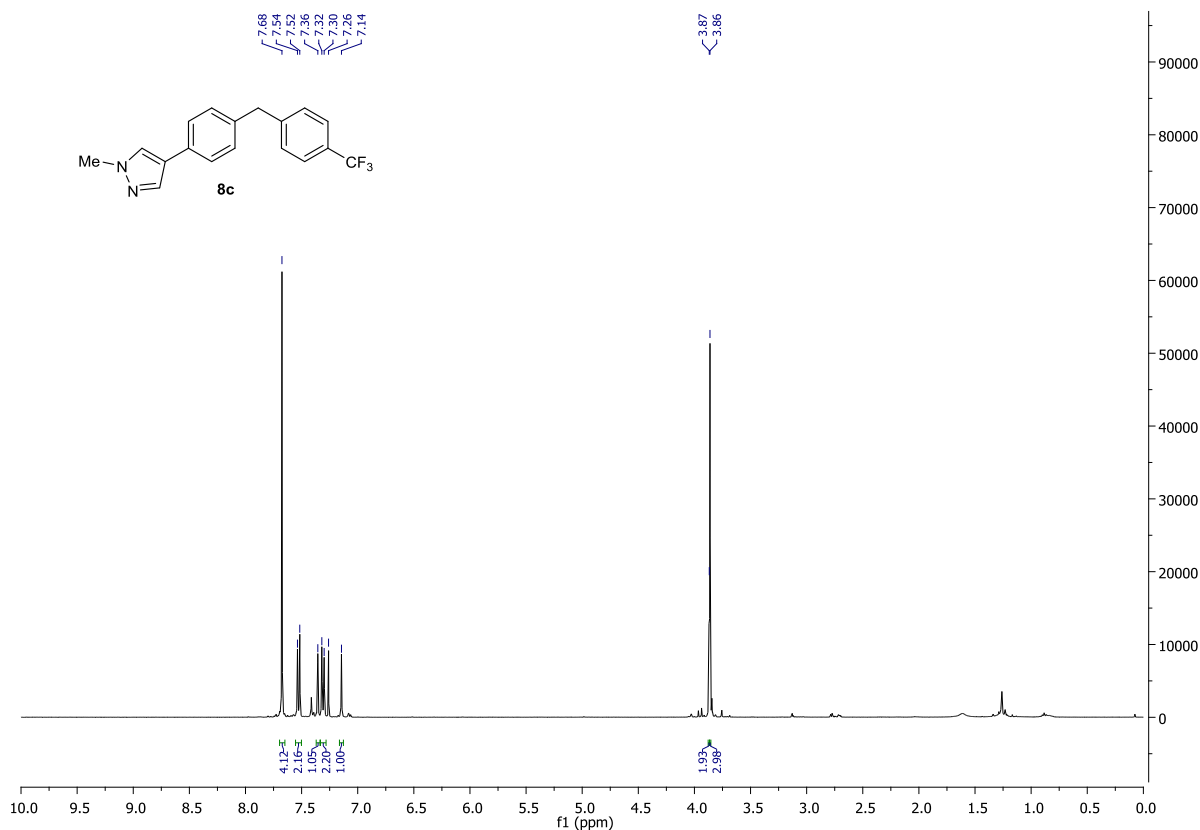
JF381 MW=212?
ASAP (SOLID)

EPSRC National Facility Swansea
LTQ Orbitrap XL

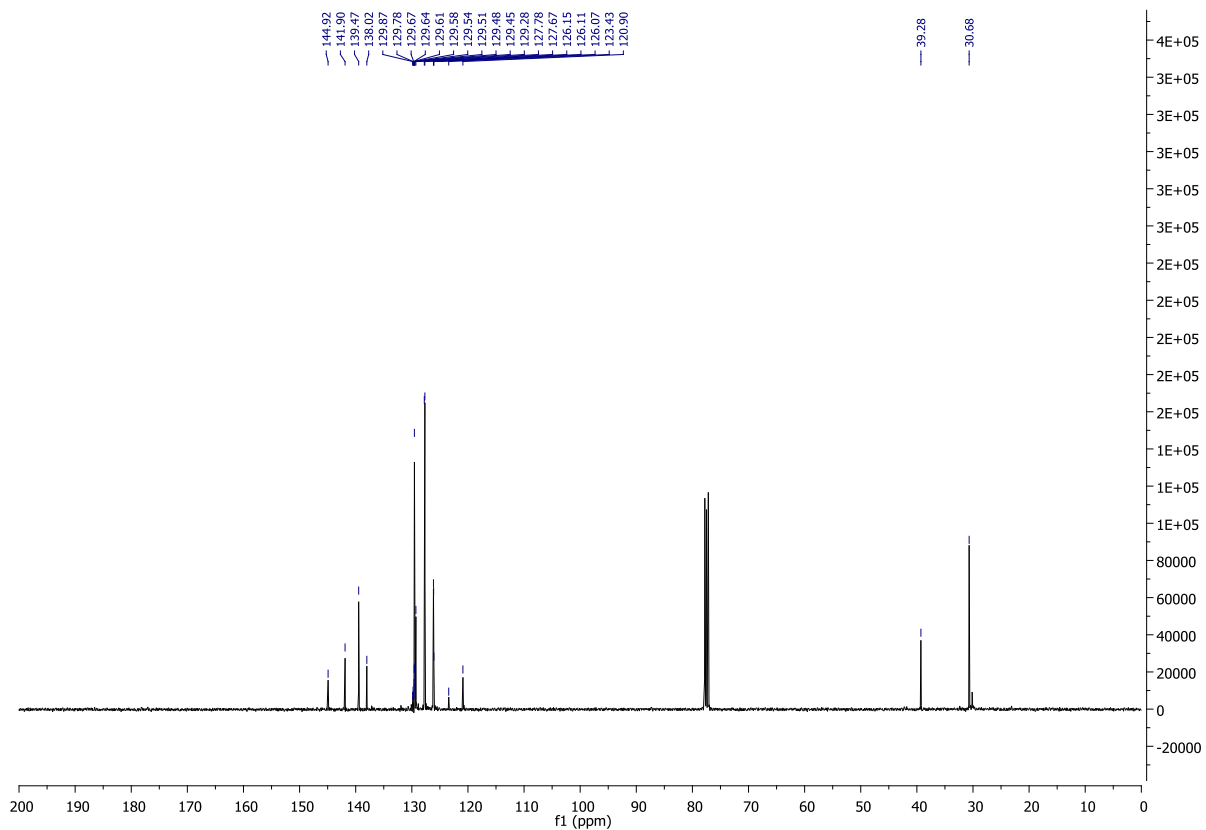
James
21/04/2015 12:35:31 PM



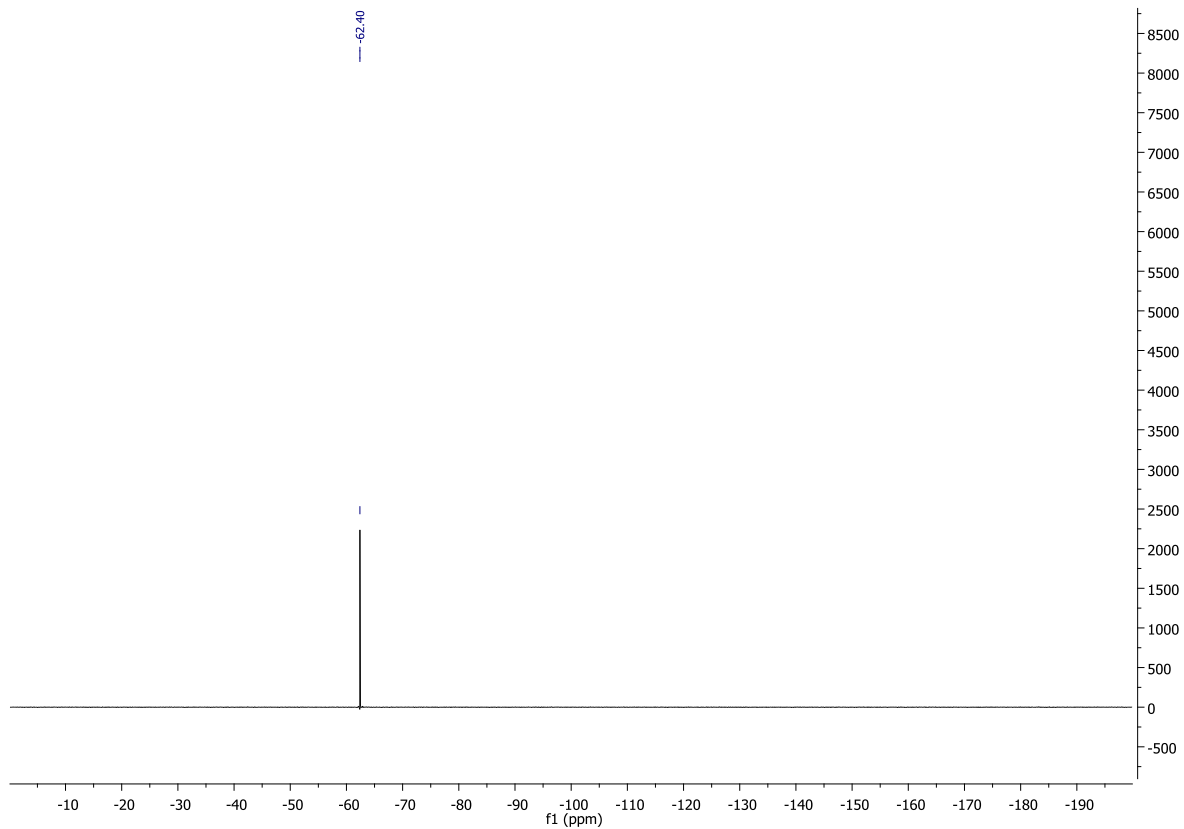
¹H NMR of 8c



¹³C NMR of 8c



¹⁹F NMR of 8c

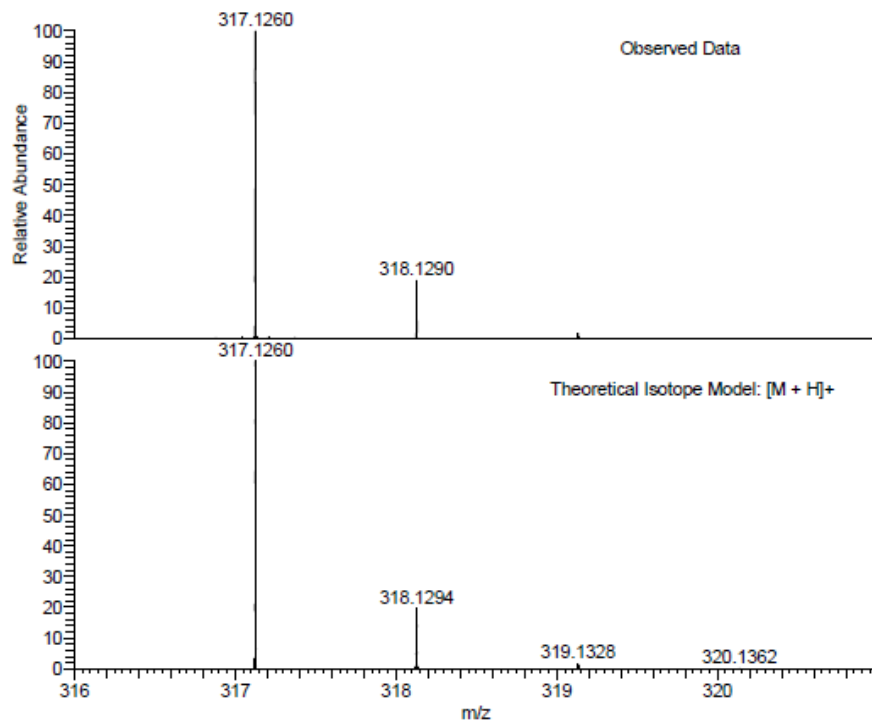


HRMS of 8c

JF383 MW=316?
C₁₈H₁₅F₃N₂
(DCM)/MeOH + NH₄OAc

EPSRC National Facility Swansea
LTQ Orbitrap XL

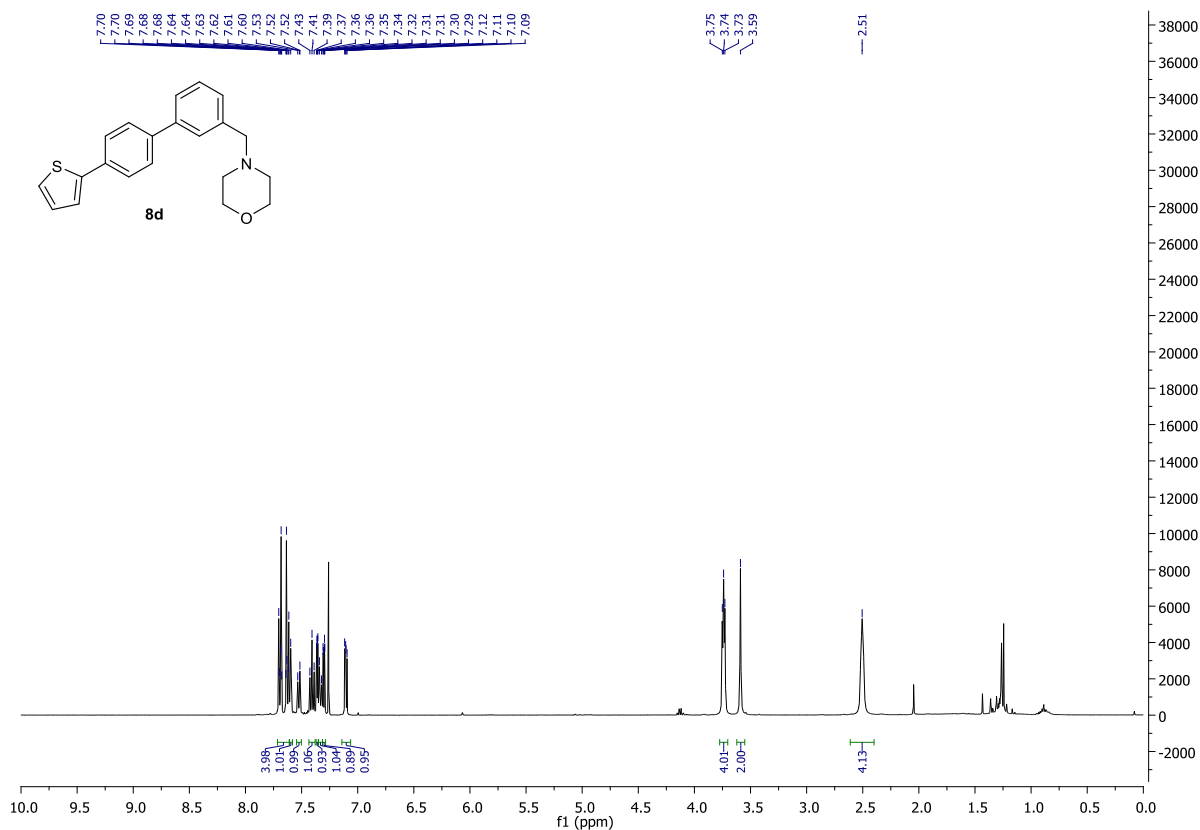
James Fyfe
20/04/2015 12:08:15 PM



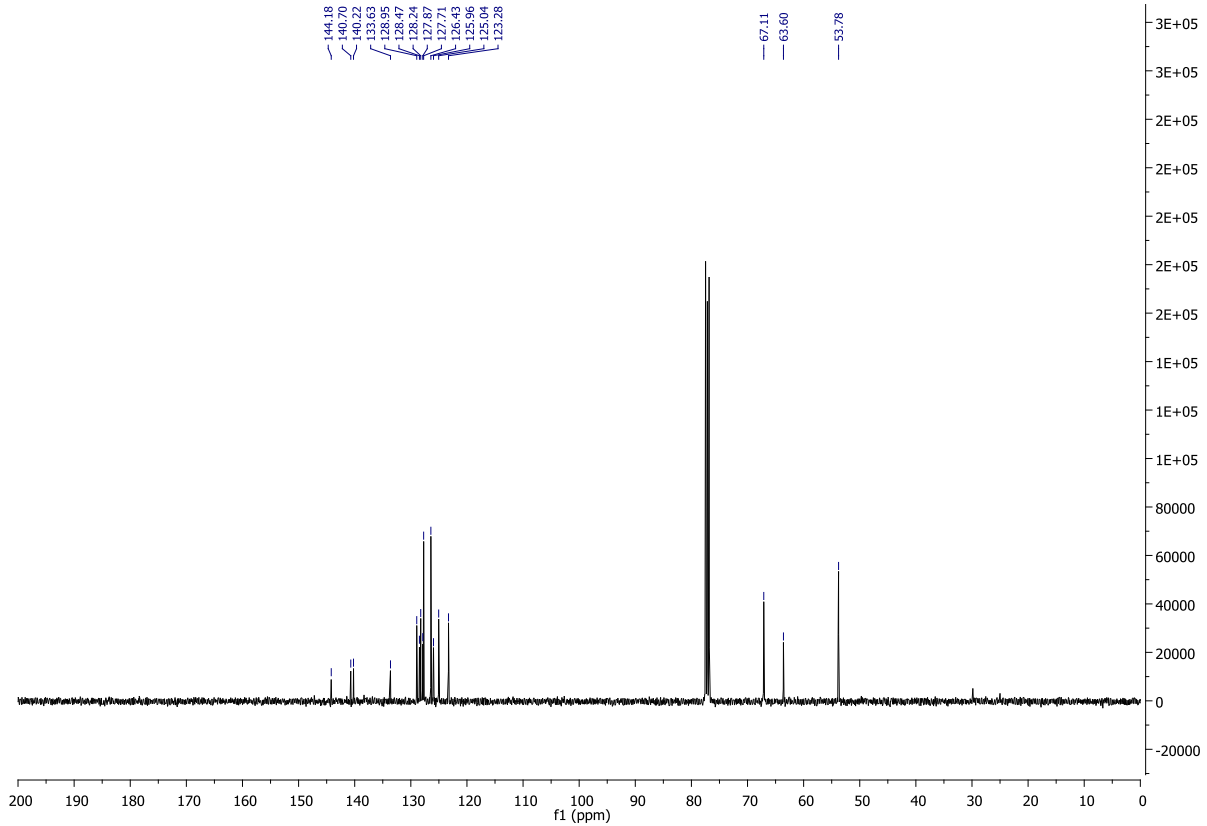
NL:
1.22E8
STRWAT478-OR-HNESP#7-
19 RT: 0.11-0.43 AV: 13 T:
FTMS + p NSI Full ms
[140.00-1935.00]

NL:
1.92E4
C₁₈ H₁₅ F₃ N₂ H:
C₁₈ H₁₆ F₃ N₂
p (gss, s /p:40) Chrg 1
R: 100000 Res .Pwr . @FWHM

¹H NMR of 8d



¹³C NMR of 8d

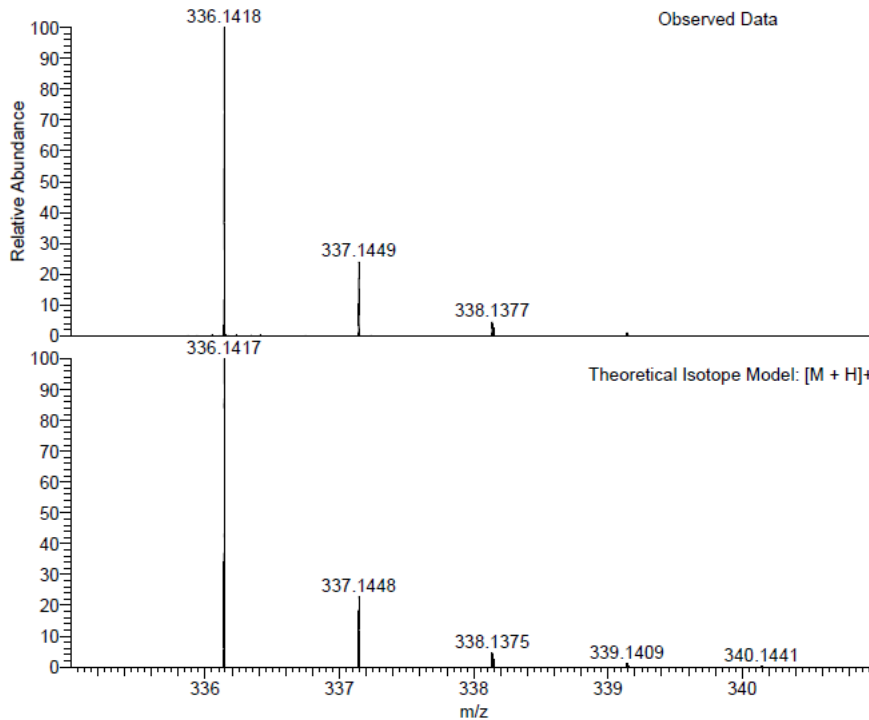


HRMS of 8d

JF368 MW=335?
C₂₁H₂₁NOS
(DCM)/MeOH + NH₄OAc

EPSRC National Facility Swansea
LTQ Orbitrap XL

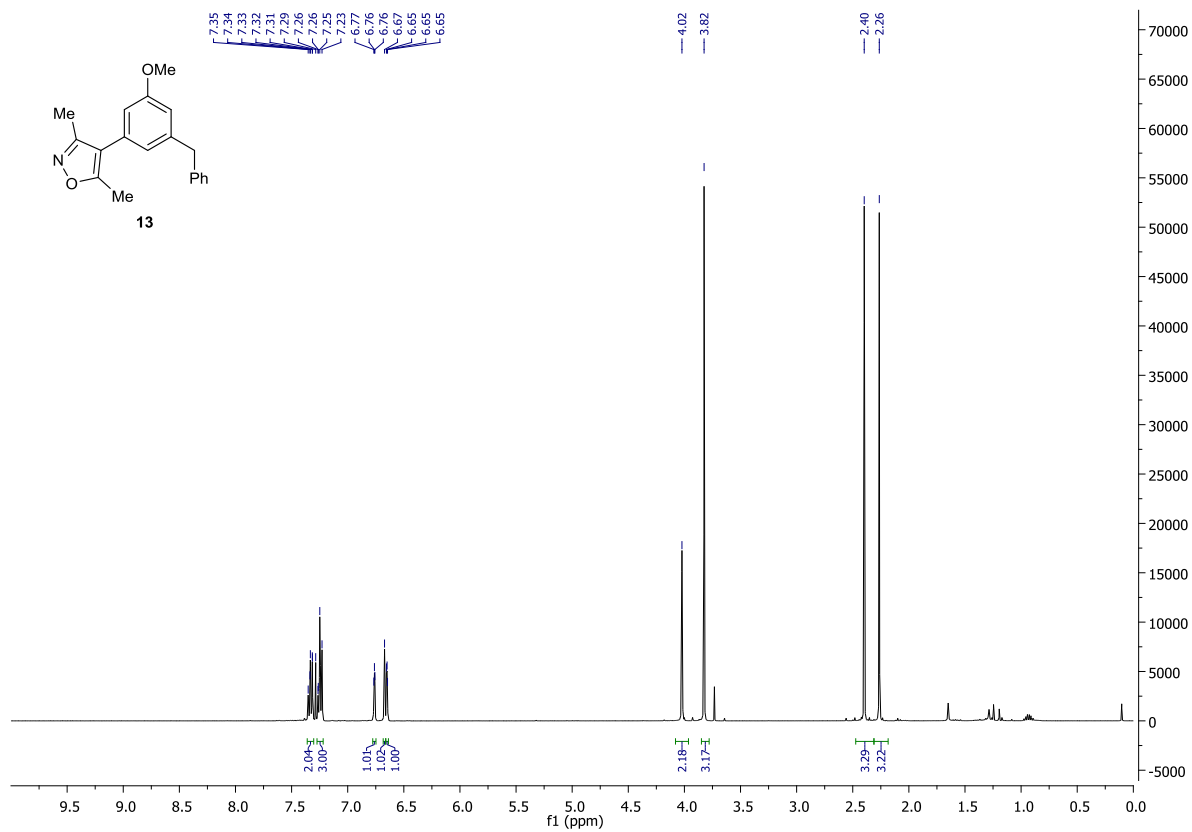
James Fyfe
16/04/2015 07:26:33



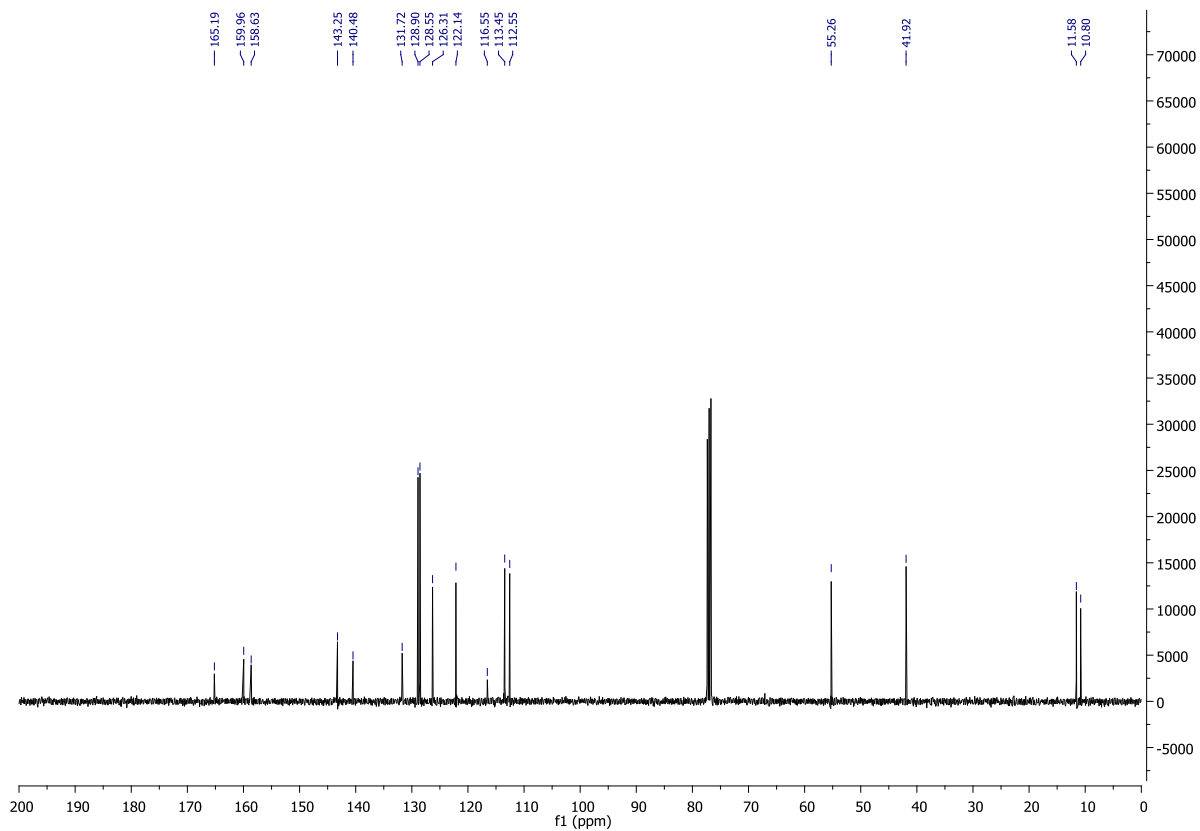
NL:
1.09E8
STRWAT476-OA-HNESP#31-
44 RT: 0.67-1.02 AV: 14 T:
FTMS + p NSI Full ms
[140.00-1935.00]

NL:
1.76E4
C₂₁H₂₁NOSH:
C₂₁H₂₂N₁O₁S₁
p (gss, s /p:40) Chrg 1
R: 100000 Res .Pwr . @FWHM

¹H NMR of 13



¹³C NMR of 13

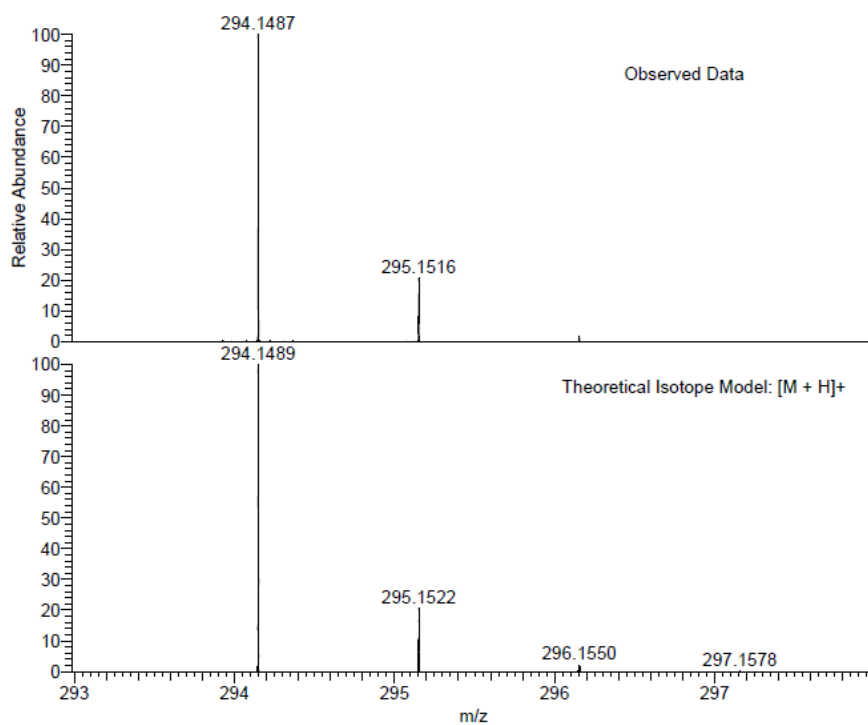


HRMS of 13

CS233-A1 MW=293?
C19H19NO2
(DCM)/MeOH + NH4OAc

EPSRC National Facility Swansea
LTQ Orbitrap XL

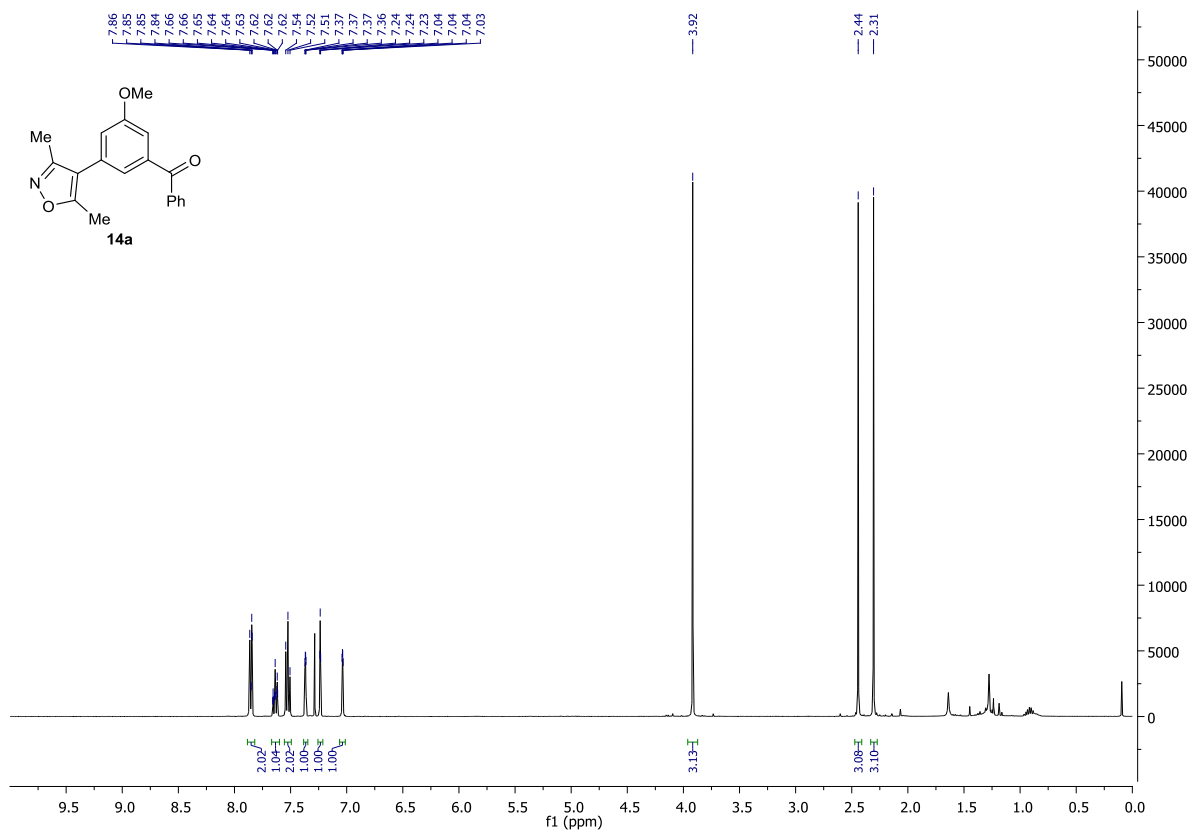
Ciaran Seath
16/04/2015 07:23:42



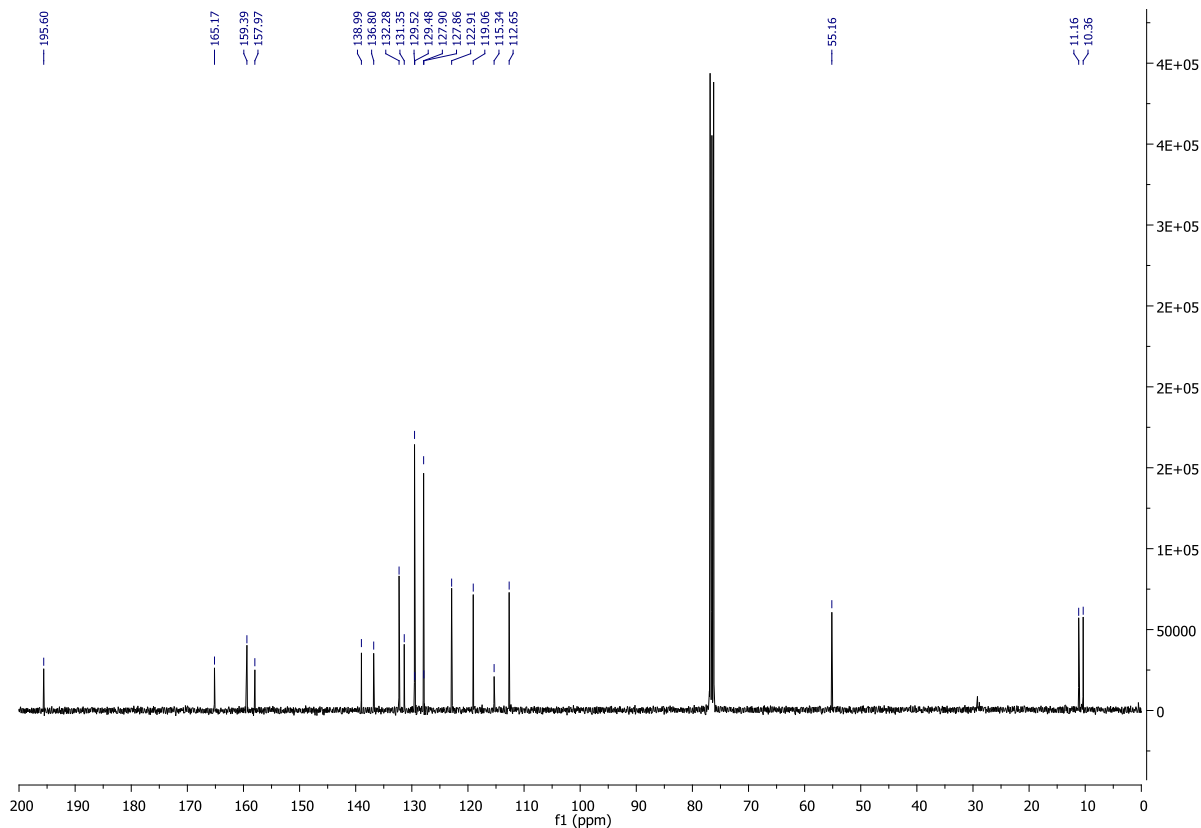
NL:
4.00E8
STRWAT474-OA-HNESP#31-
44 RT: 0.67-1.02 AV: 14 T:
FTMS + p NSI Full ms
[140.00-1935.00]

NL:
1.89E4
C₁₉ H₁₉ NO₂ H:
C₁₉ H₂₀ N₁ O₂
p (gss, s /p:40) Chrg 1
R: 100000 Res .Pwr . @FWHM

¹H NMR of 14a



¹³C NMR of 14a

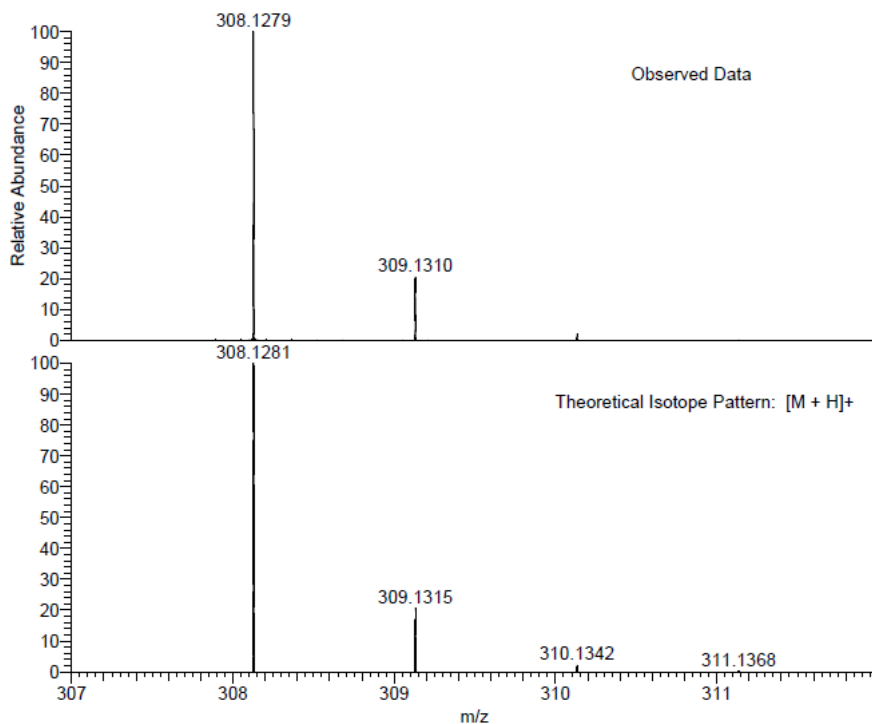


HRMS of 14a

CS262 MW=307?
C₁₉H₁₇NO₃
(DCM)/MeOH + NH₄OAc

EPSRC National Facility Swansea
LTQ Orbitrap XL

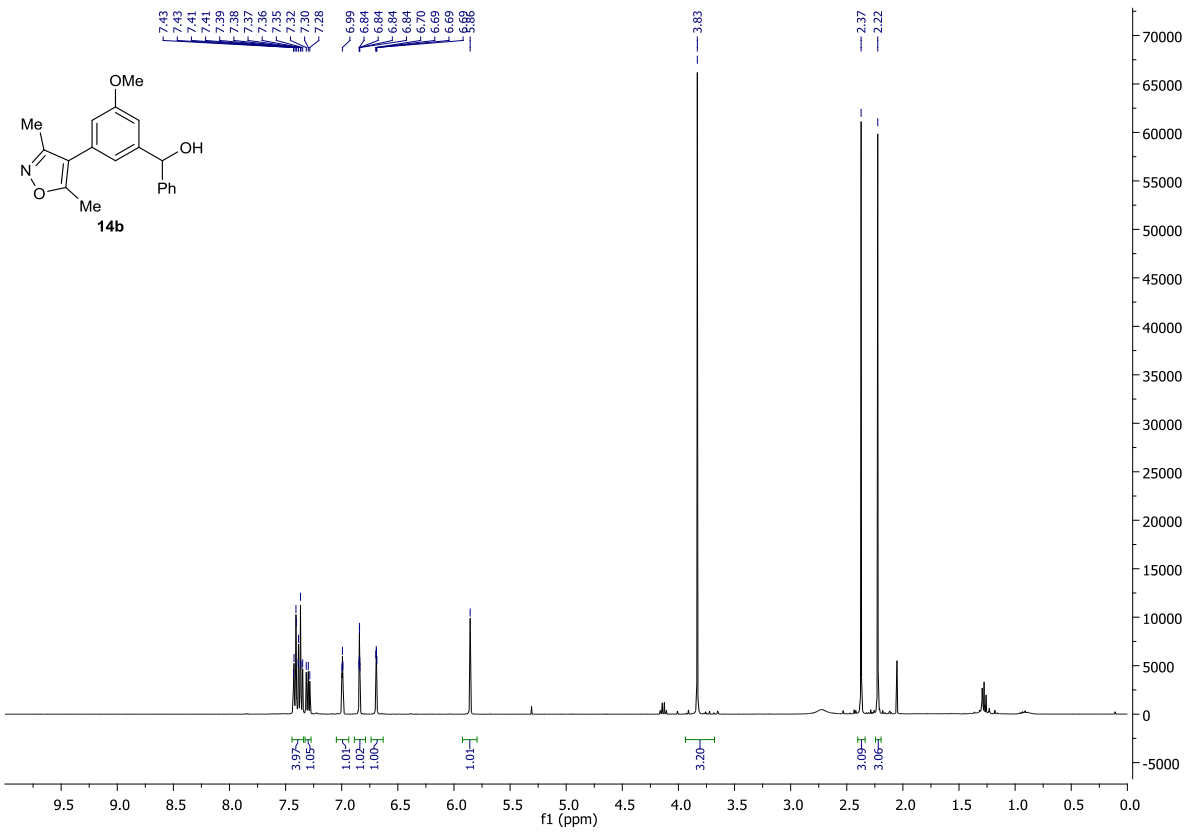
Ciaran Seath
01/05/2015 12:30:48



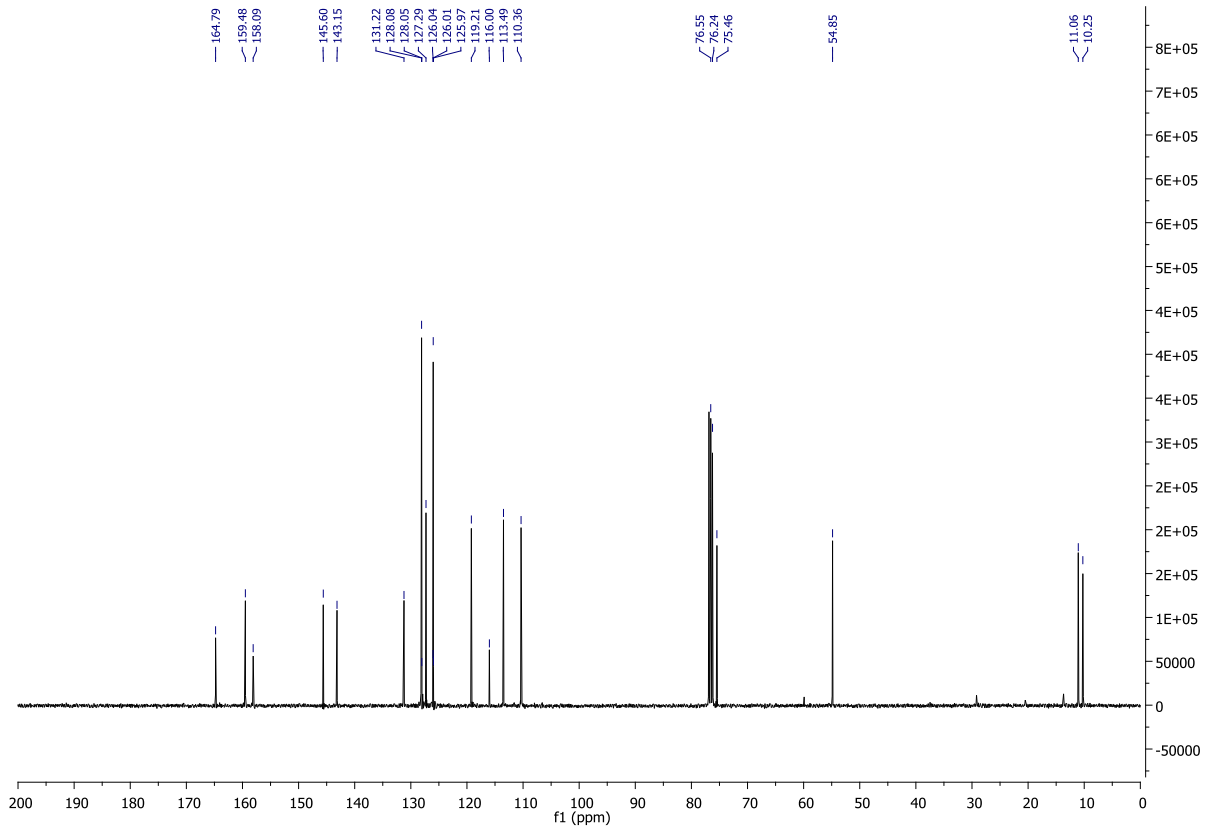
NL:
2.50E7
STRWAT492-OR-HNESP#27-
43 RT: 0.67-1.04 AV: 14 T:
FTMS + p NSI Full ms
[140.00-1935.00]

NL:
1.89E4
C₁₉H₁₇NO₃H:
C₁₉H₁₈N₁O₃
p (gss, s /p:40) Chrg 1
R: 100000 Res .Pwr . @FWHM

¹H NMR of 14b



¹³C NMR of 14b

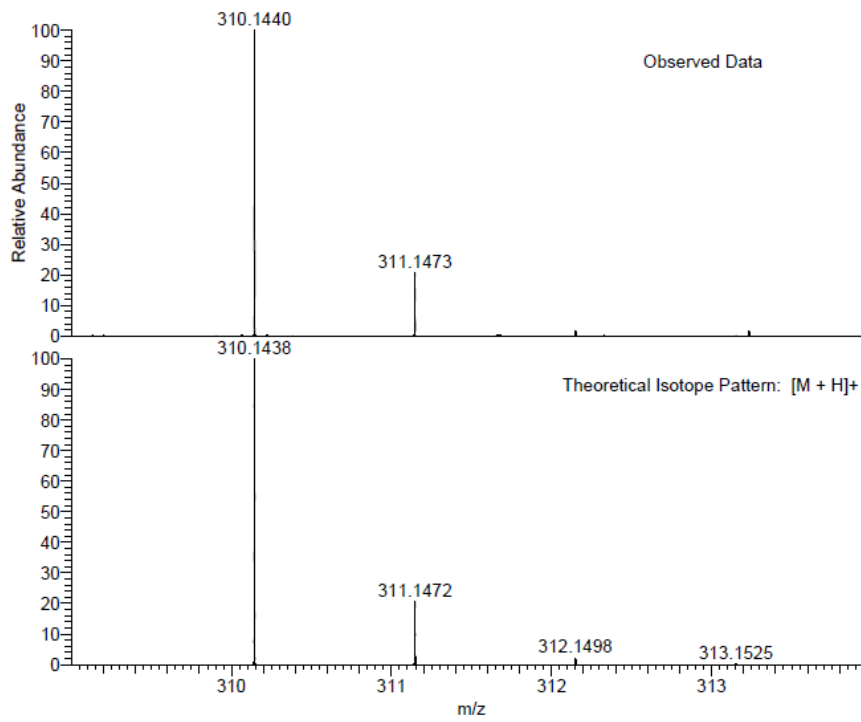


HRMS of 14b

CS263 MW=309?
C₁₉H₁₉NO₃
(DCM)/MeOH + NH₄OAc

EPSRC National Facility Swansea
LTQ Orbitrap XL

Ciaran Seath
01/05/2015 12:27:57



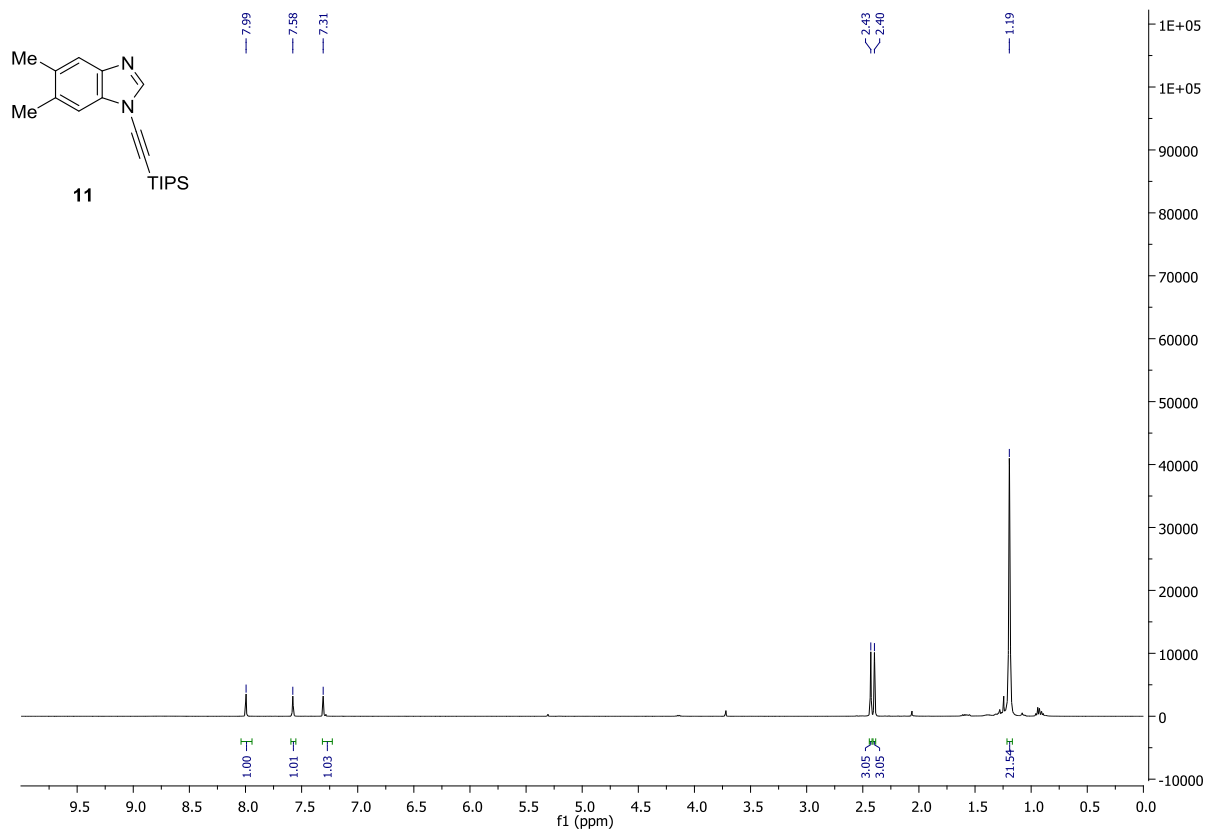
NL:
9.36E5
STRWAT491-OR-HNESP#24-
45 RT: 0.66-1.04 AV: 14 T:
FTMS + p NSI Full ms
[140.00-1935.00]

NL:
1.89E4
C₁₉H₁₉NO₃ H:
C₁₉H₂₀N₁O₃
p (gss, s /p:40) Chrg 1
R: 100000 Res. Pwr. . @FWHM

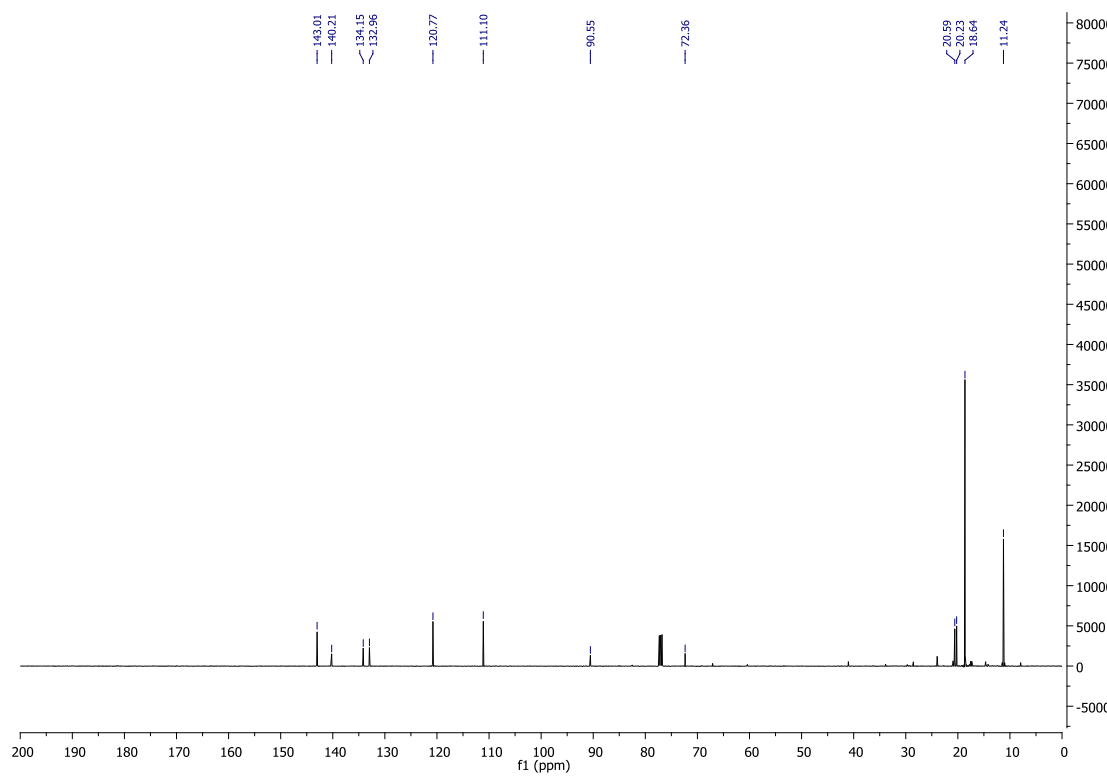
Chapter 2

9. ^1H and ^{13}C NMR Spectra

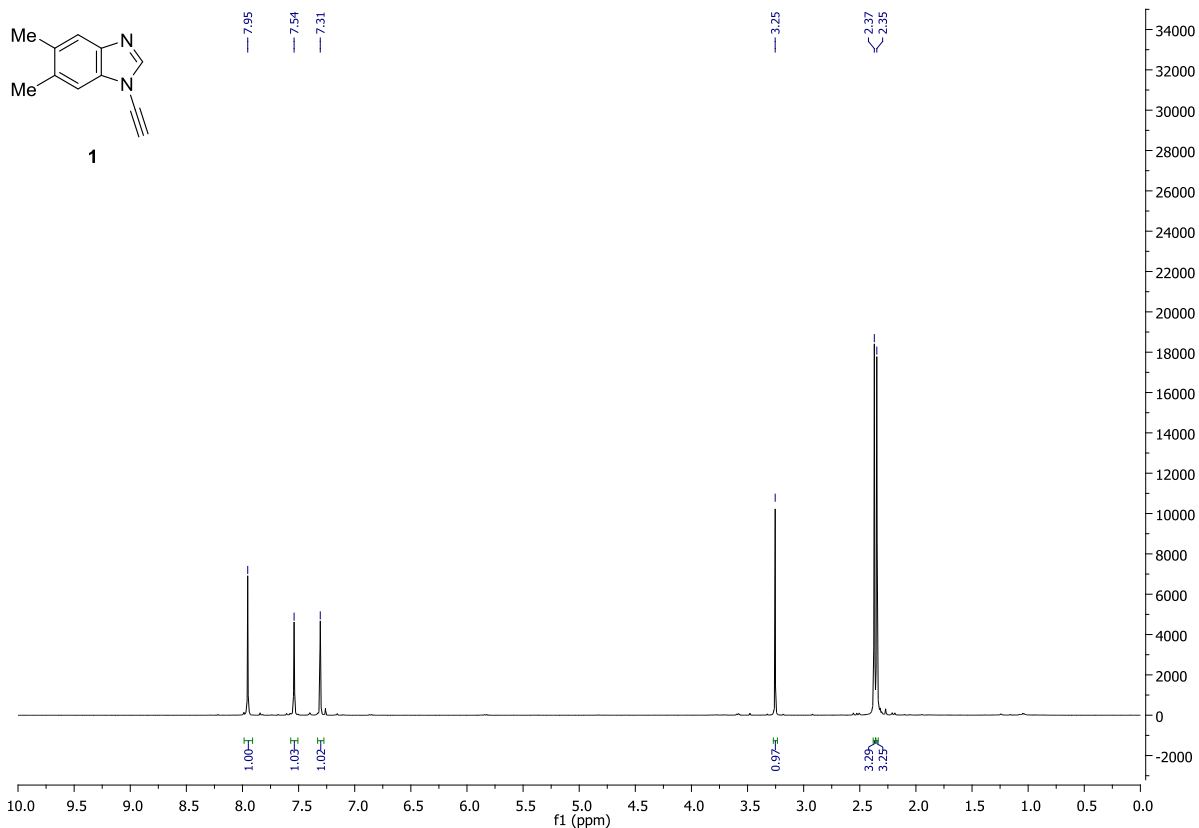
^1H NMR of 11



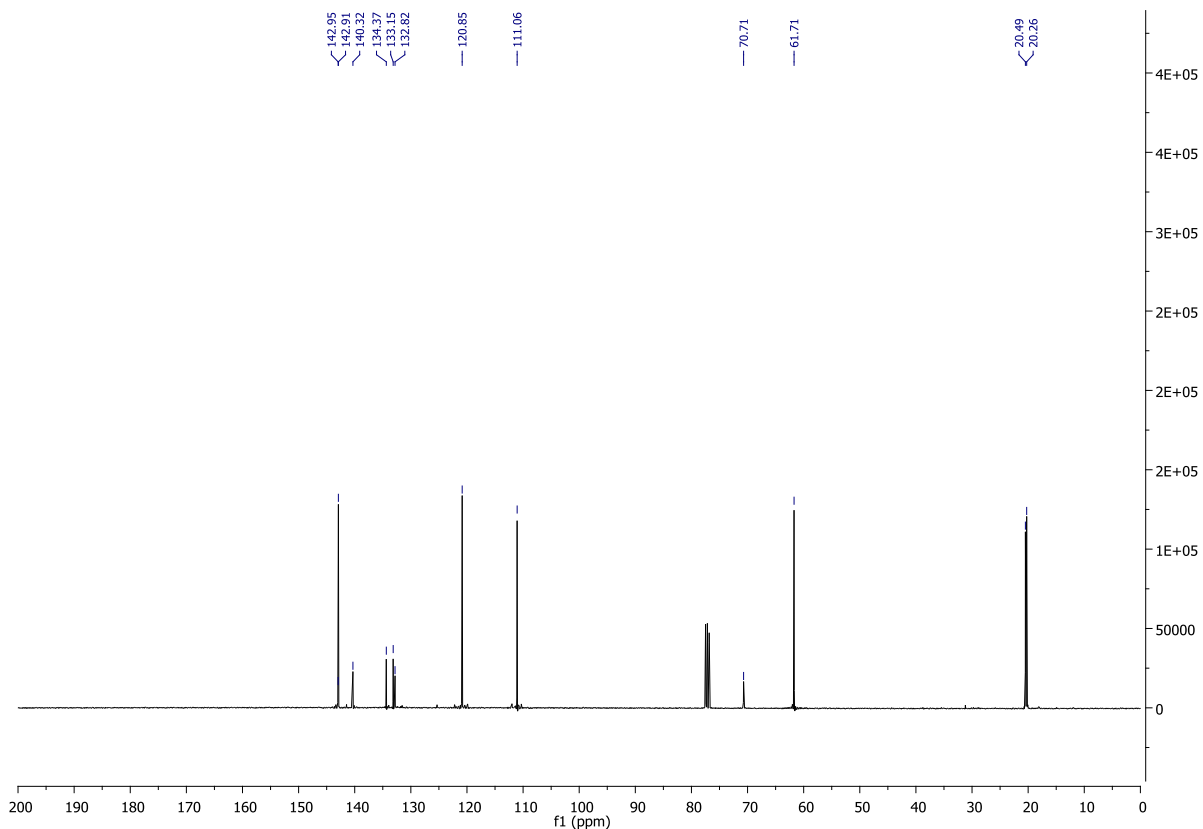
^{13}C NMR of 11



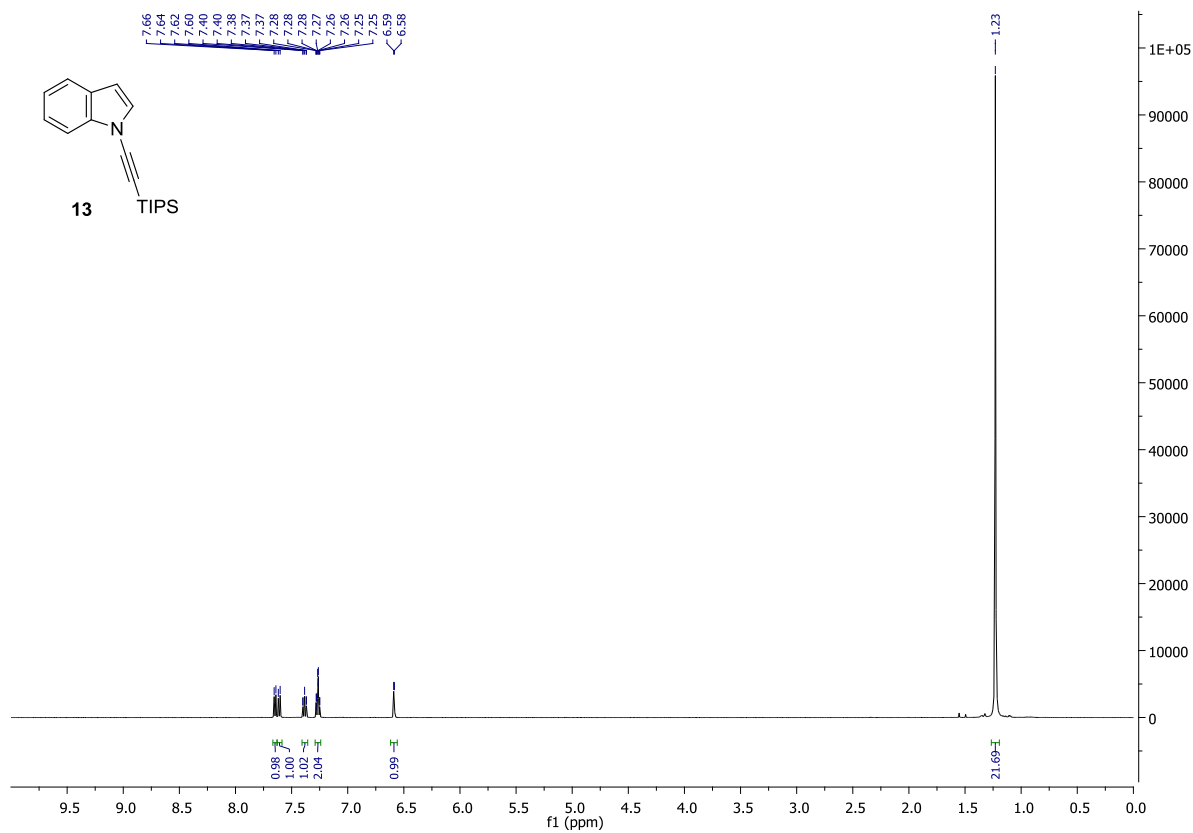
¹H NMR of 1



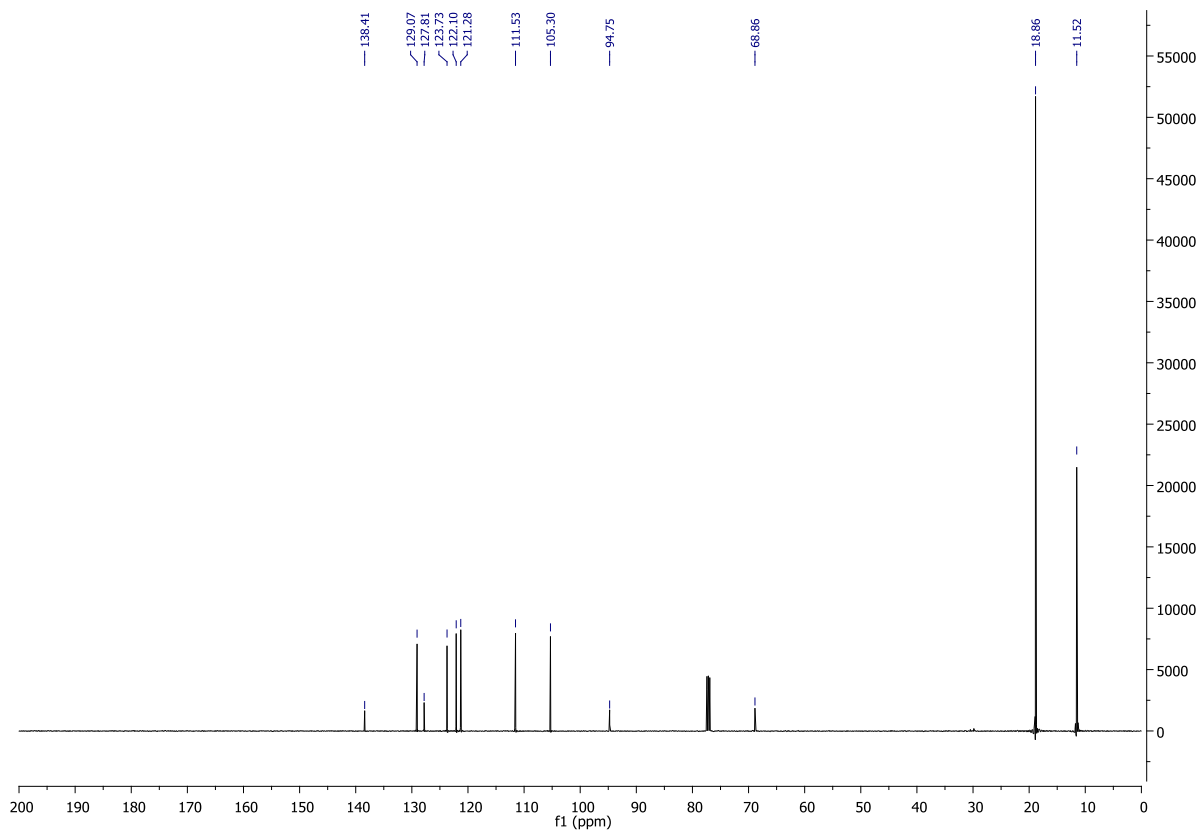
¹³C NMR of 1



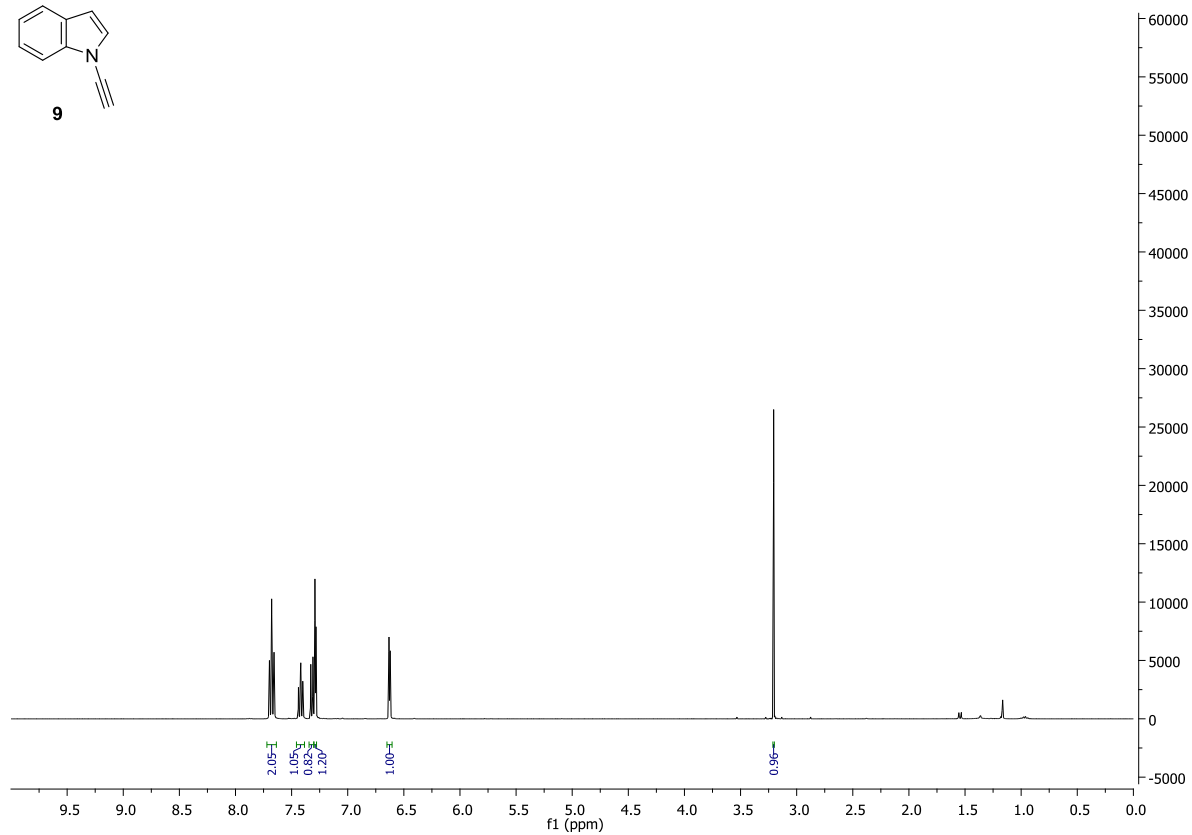
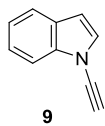
¹H NMR of 13



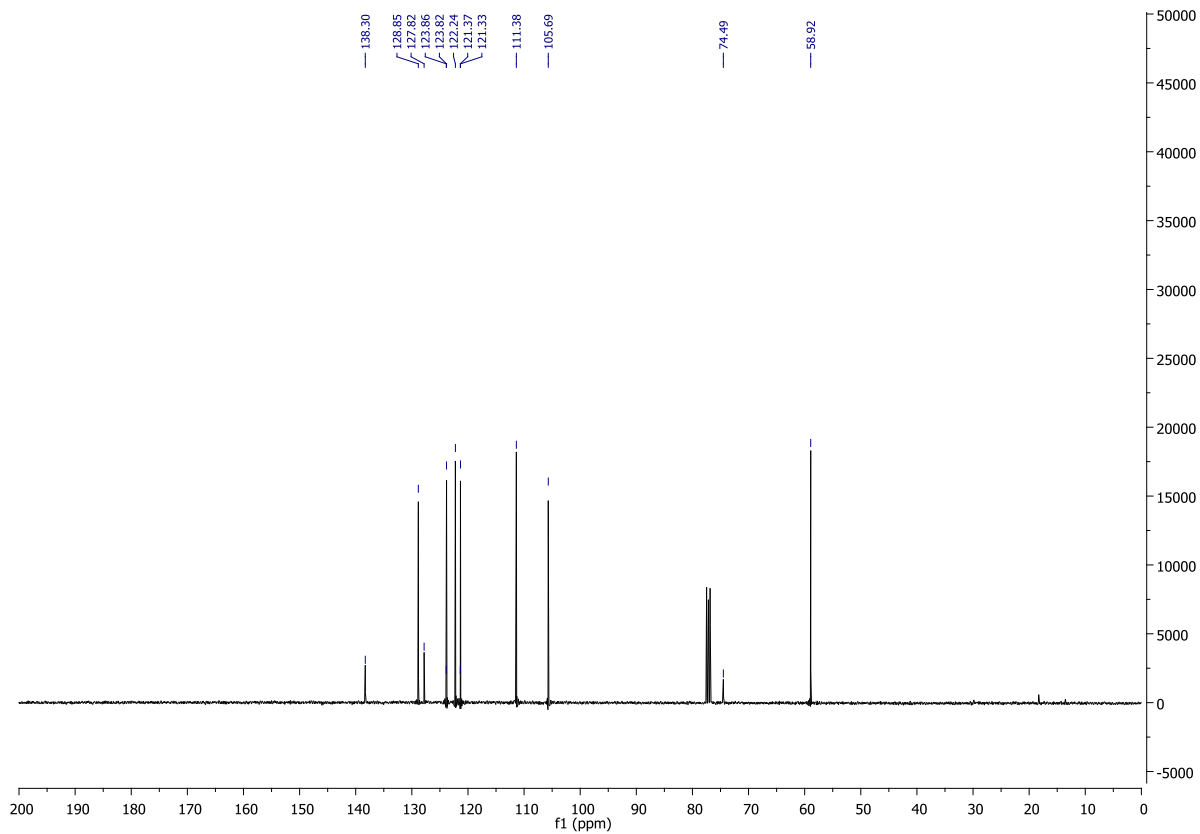
¹³C NMR of 13



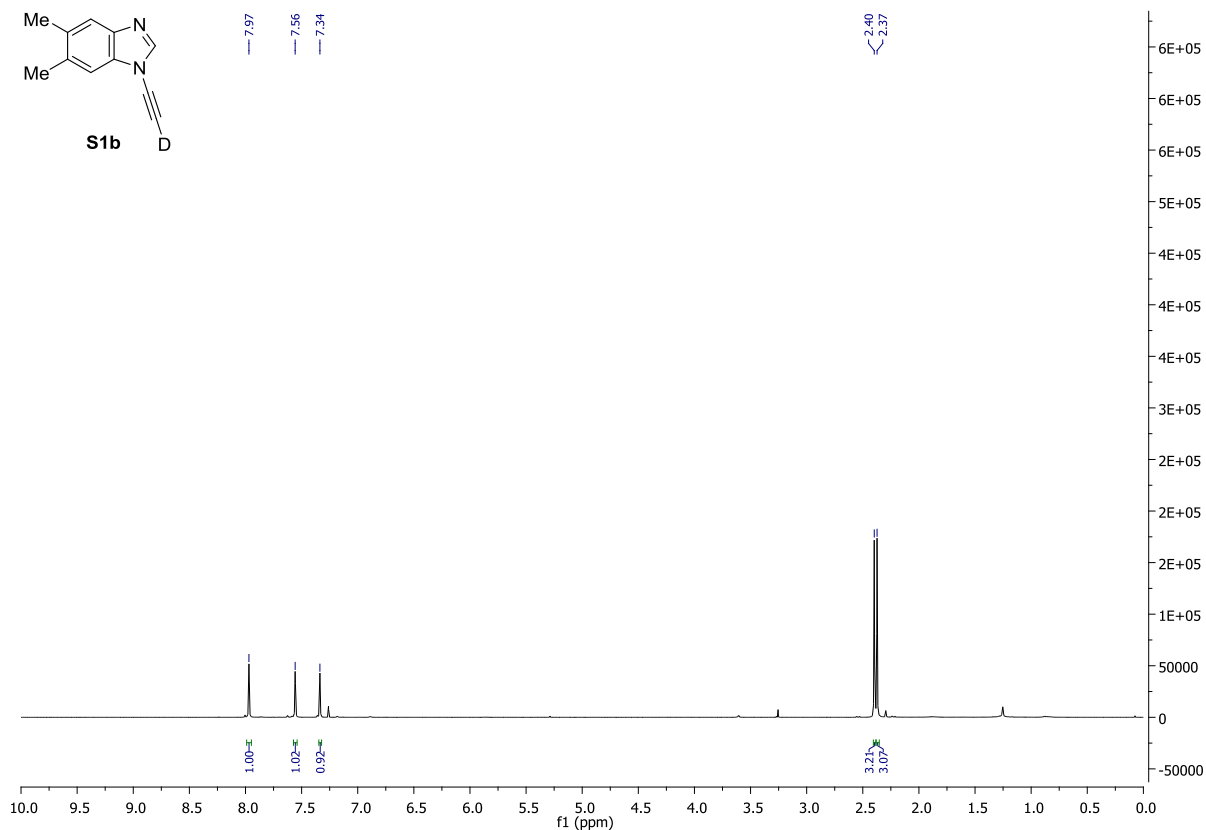
¹H NMR of 9



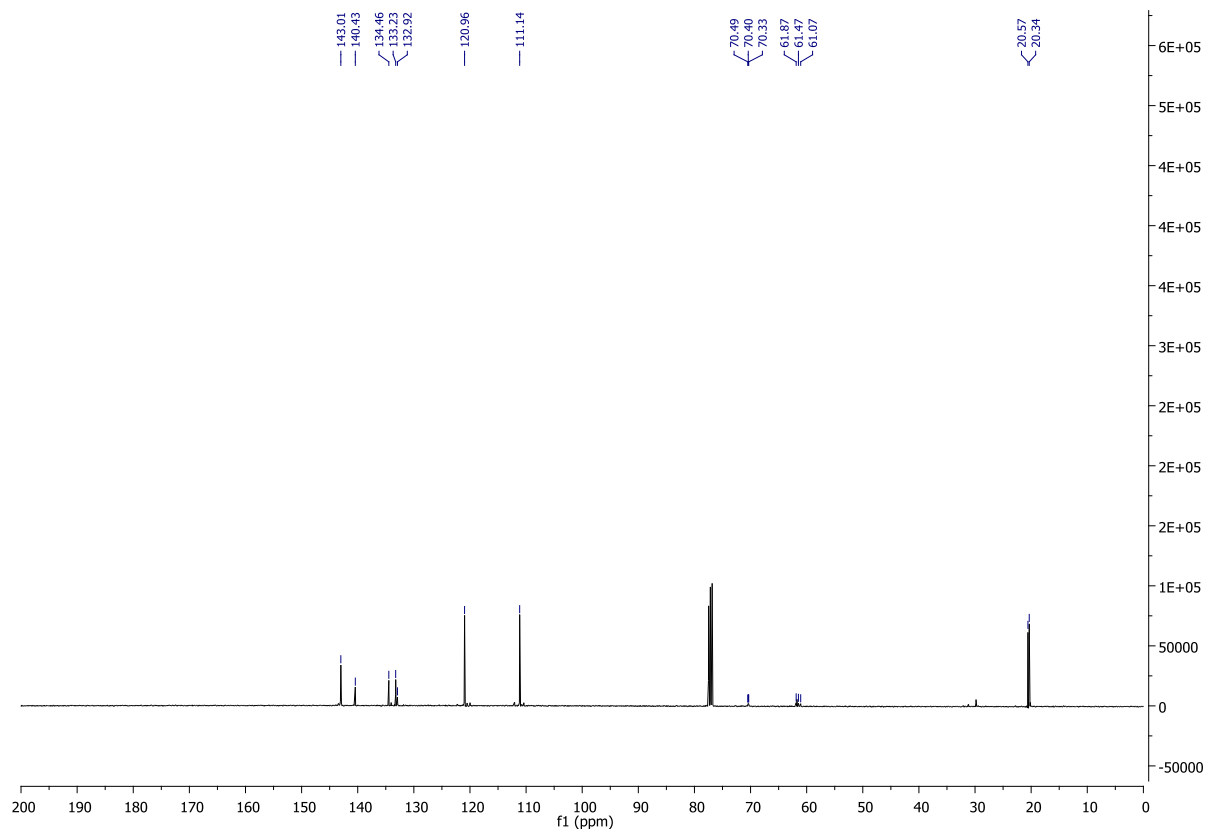
¹³C NMR of 9



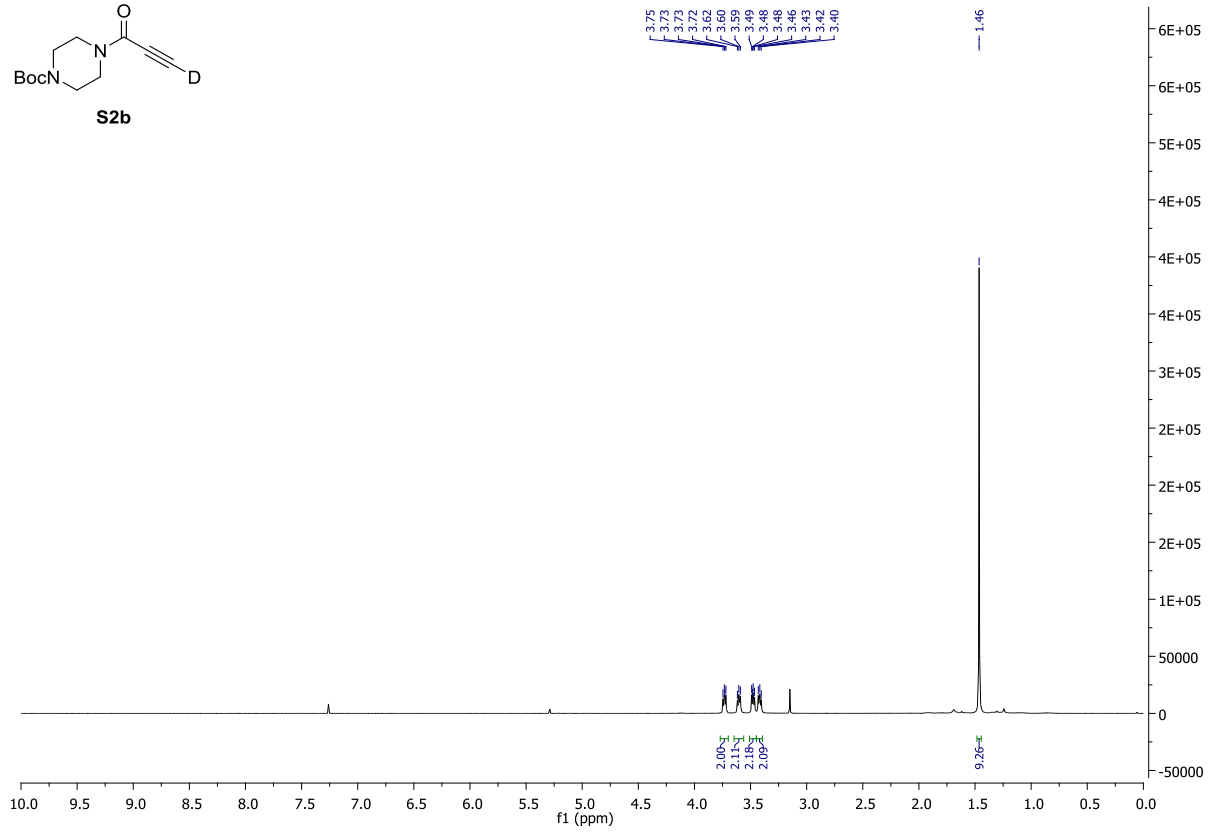
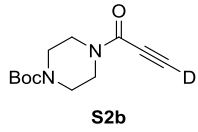
¹H NMR of S1b



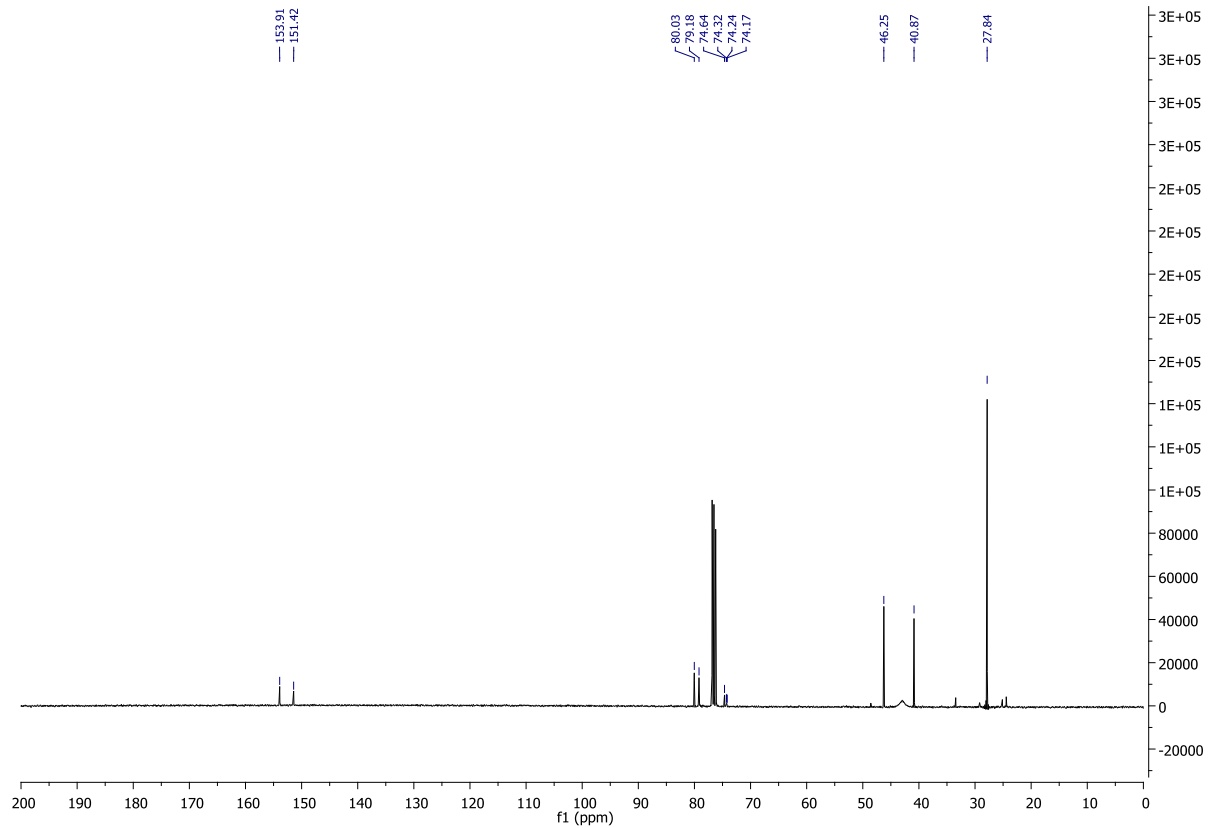
¹³C NMR of S1b



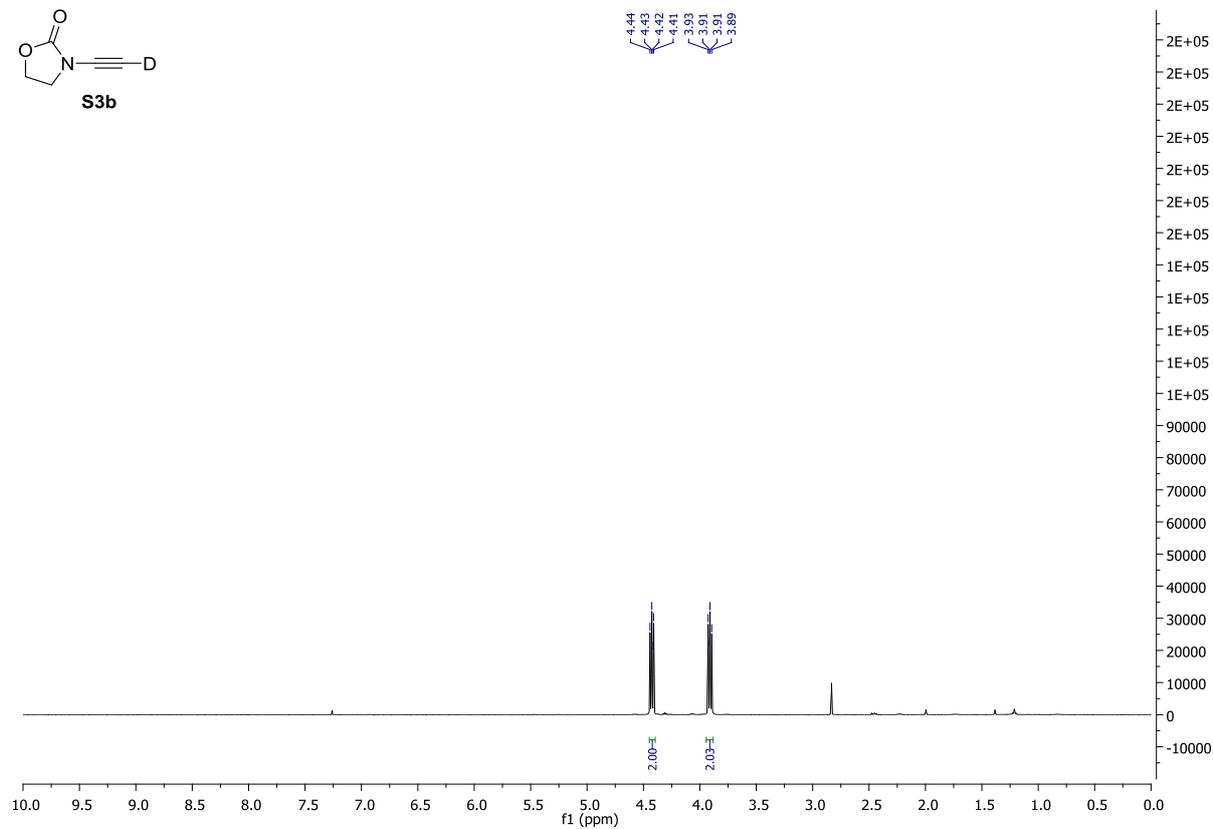
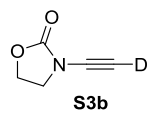
¹H NMR of S2b



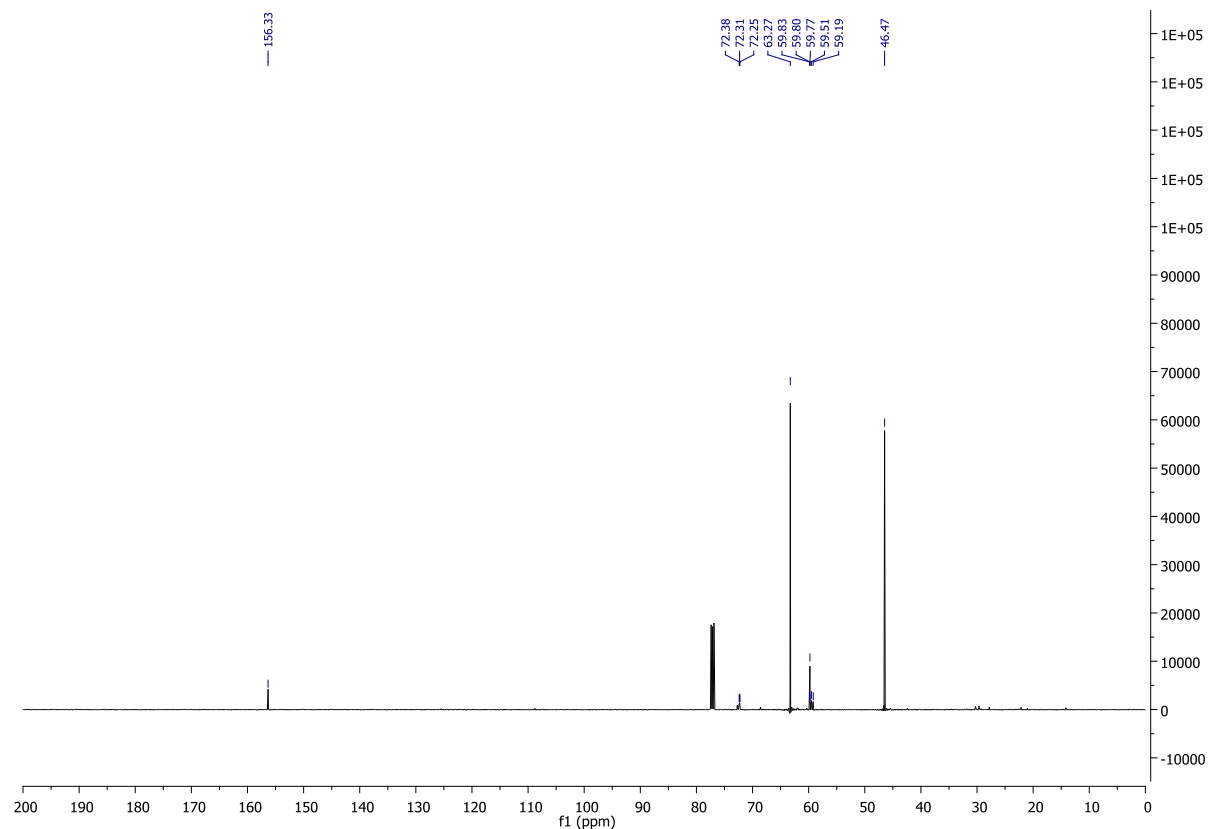
¹³C NMR of S2b



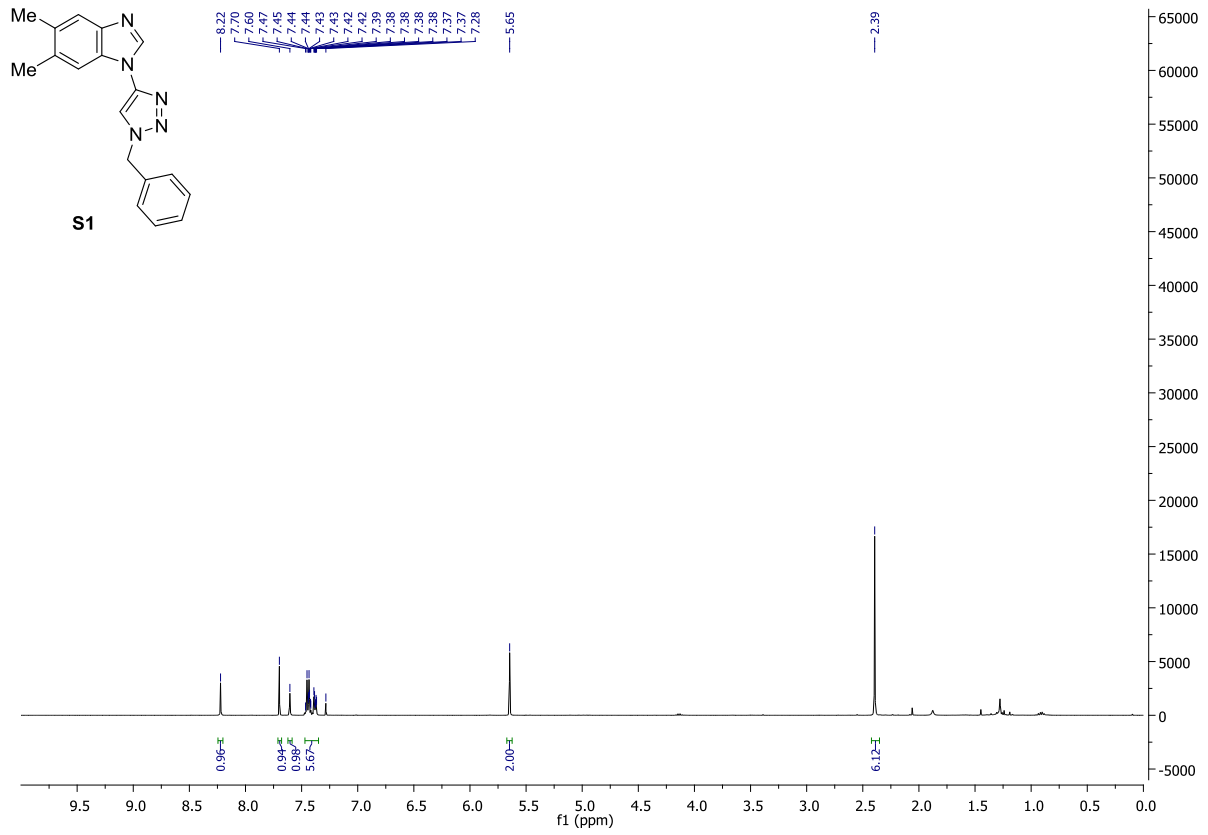
¹H NMR of S3b



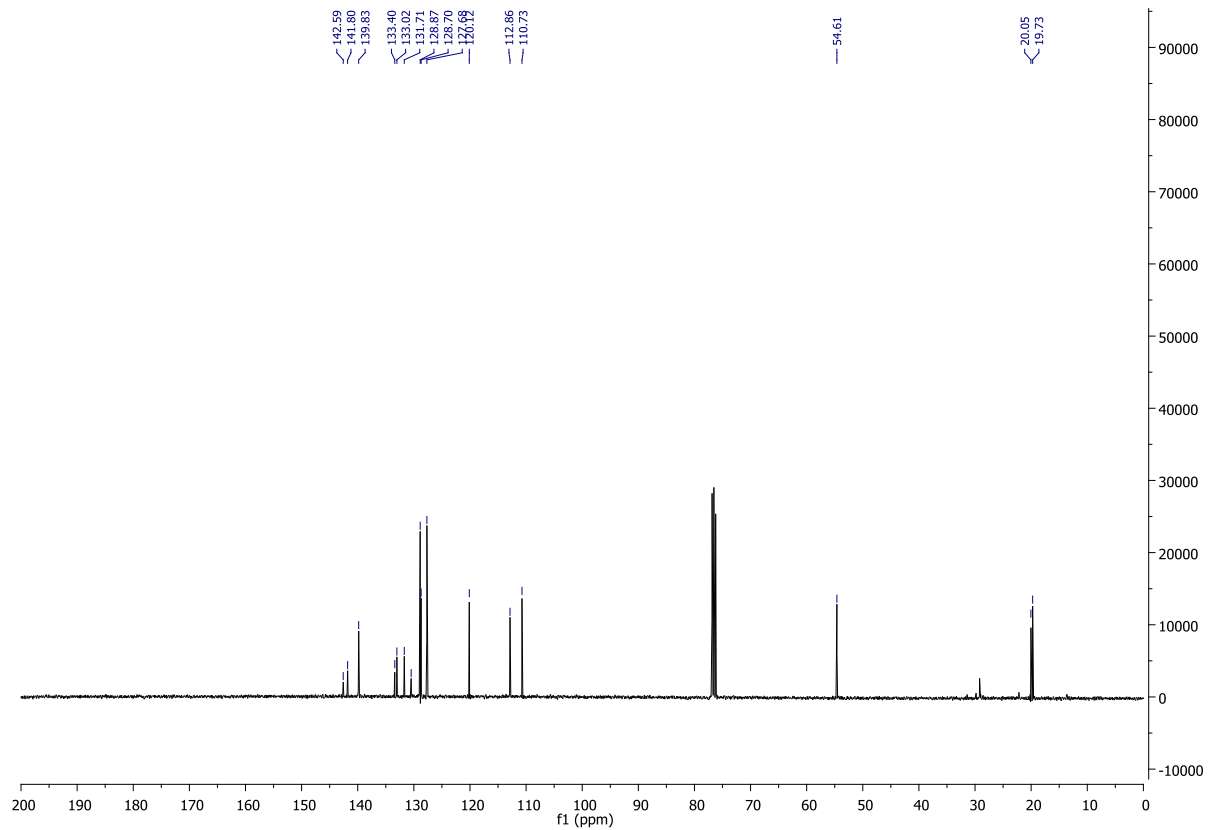
¹³C NMR of S3b



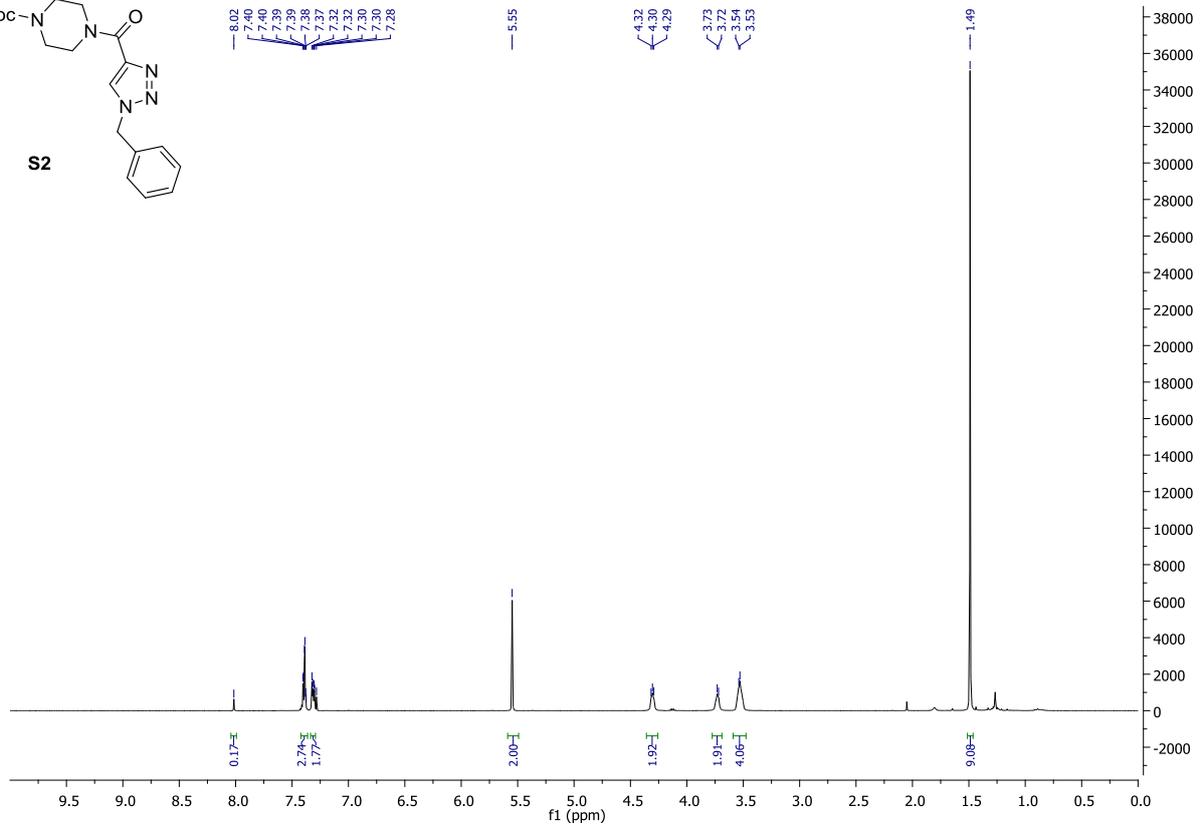
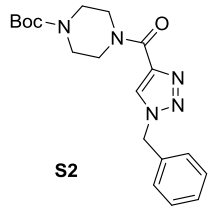
¹H NMR of S1



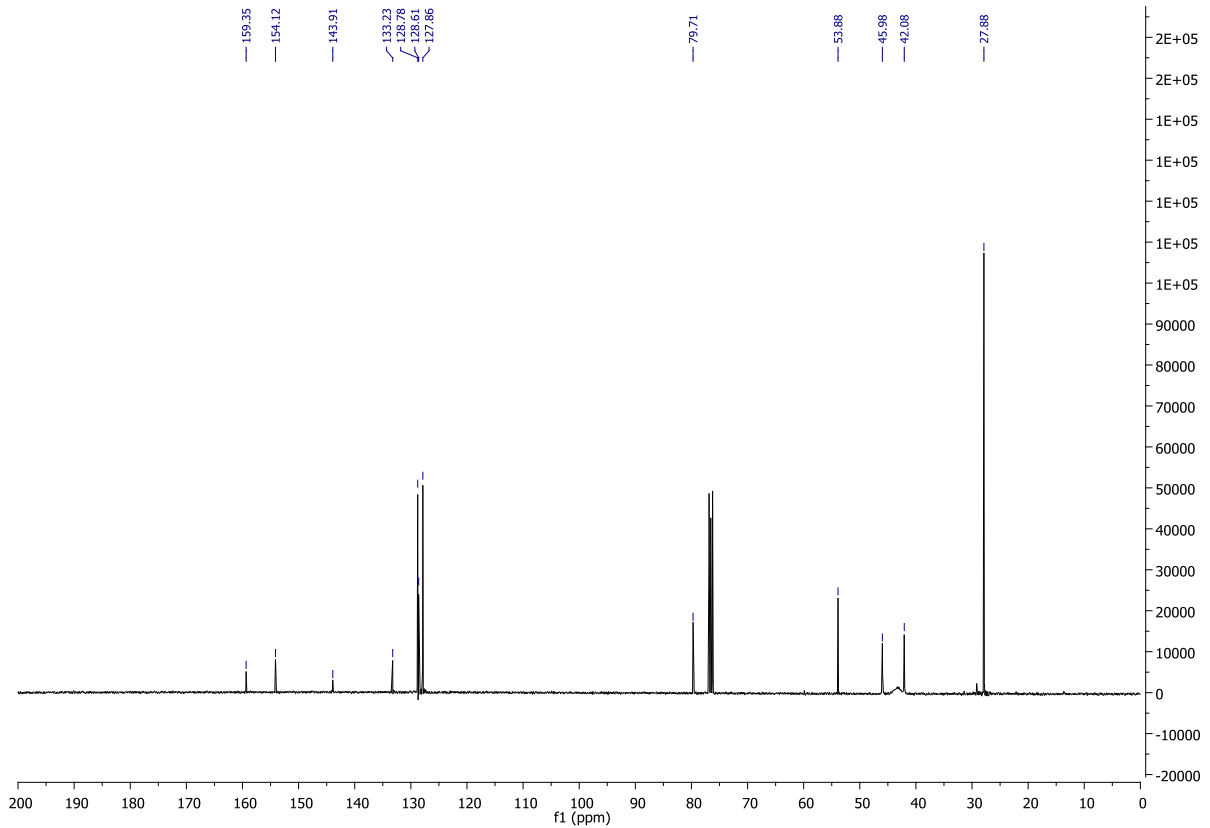
¹³C NMR of S1



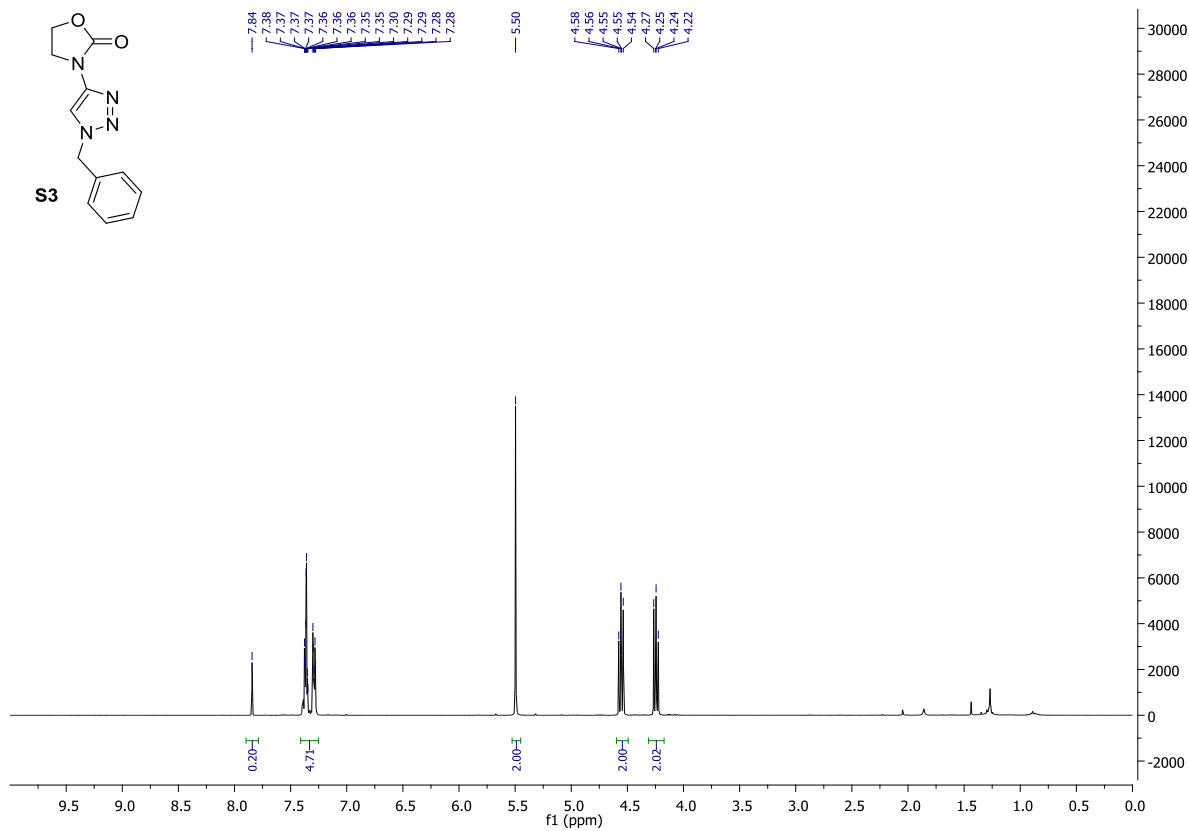
¹H NMR of S2



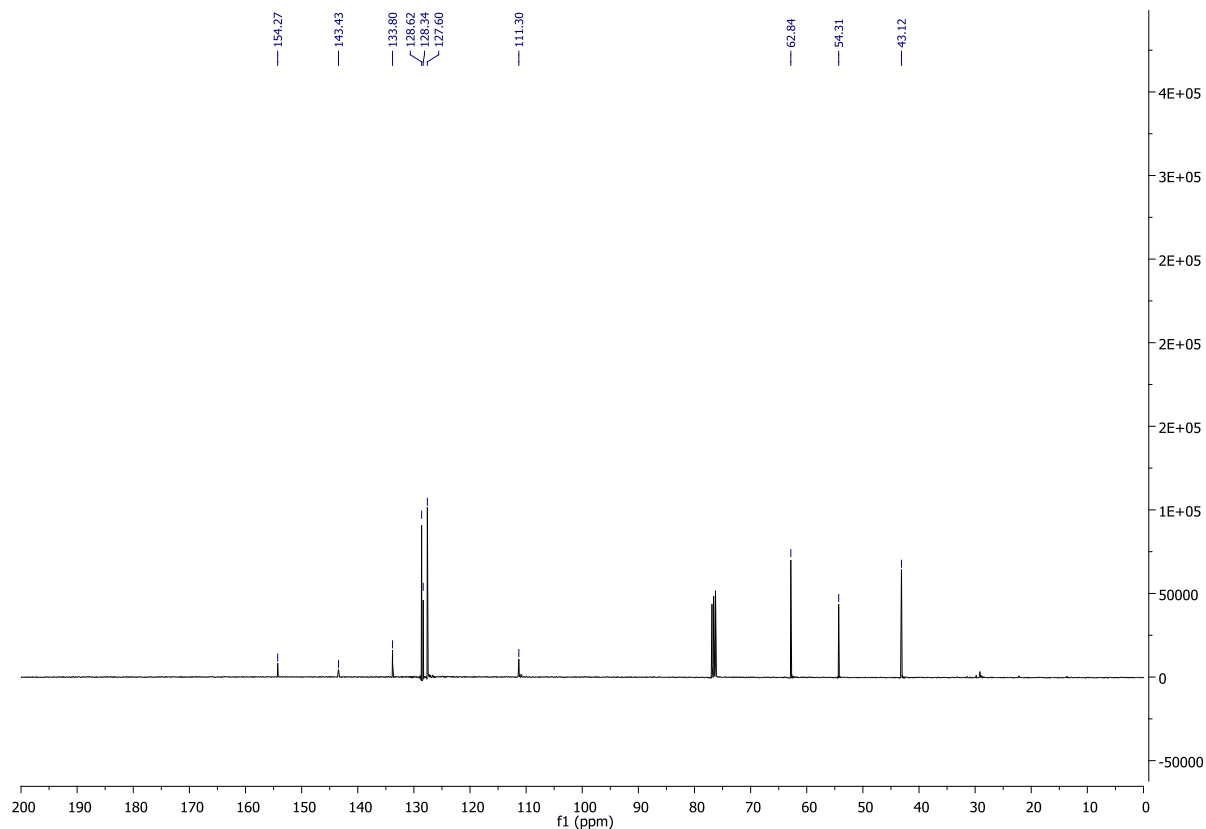
¹³C NMR of S2



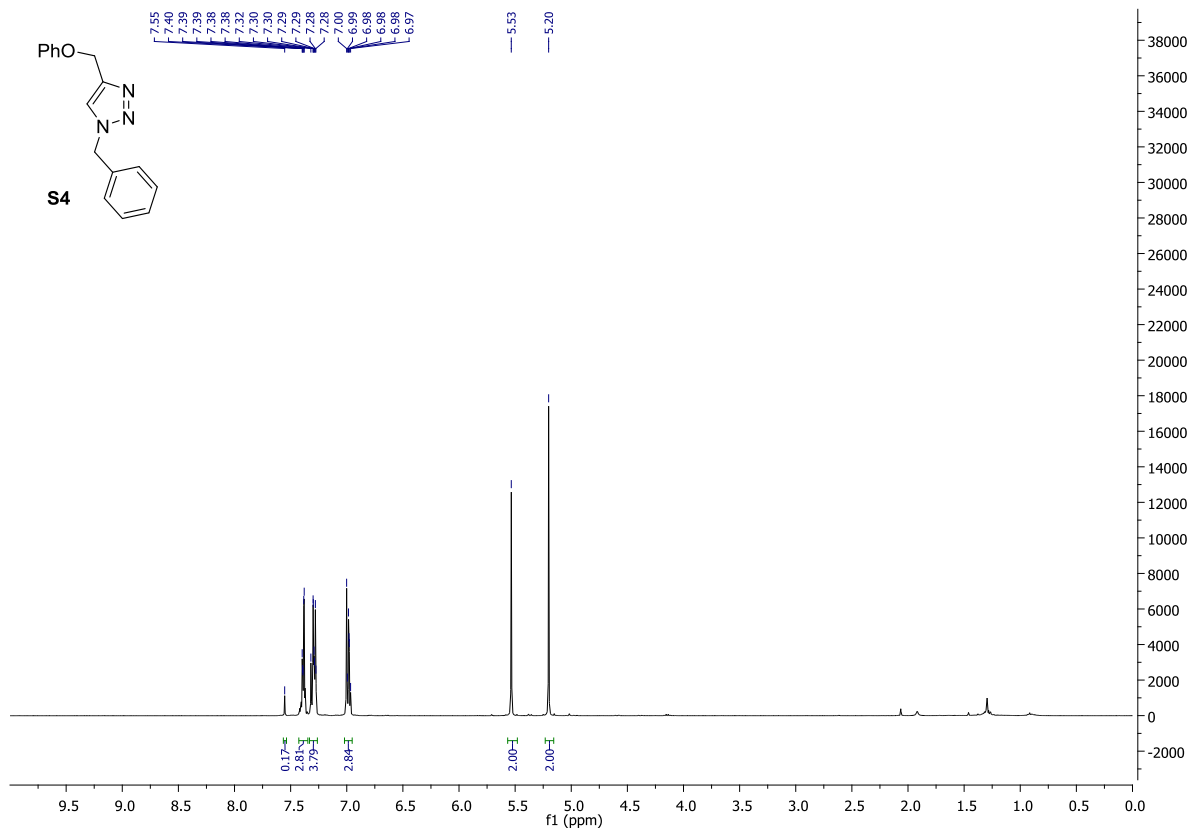
¹H NMR of S3



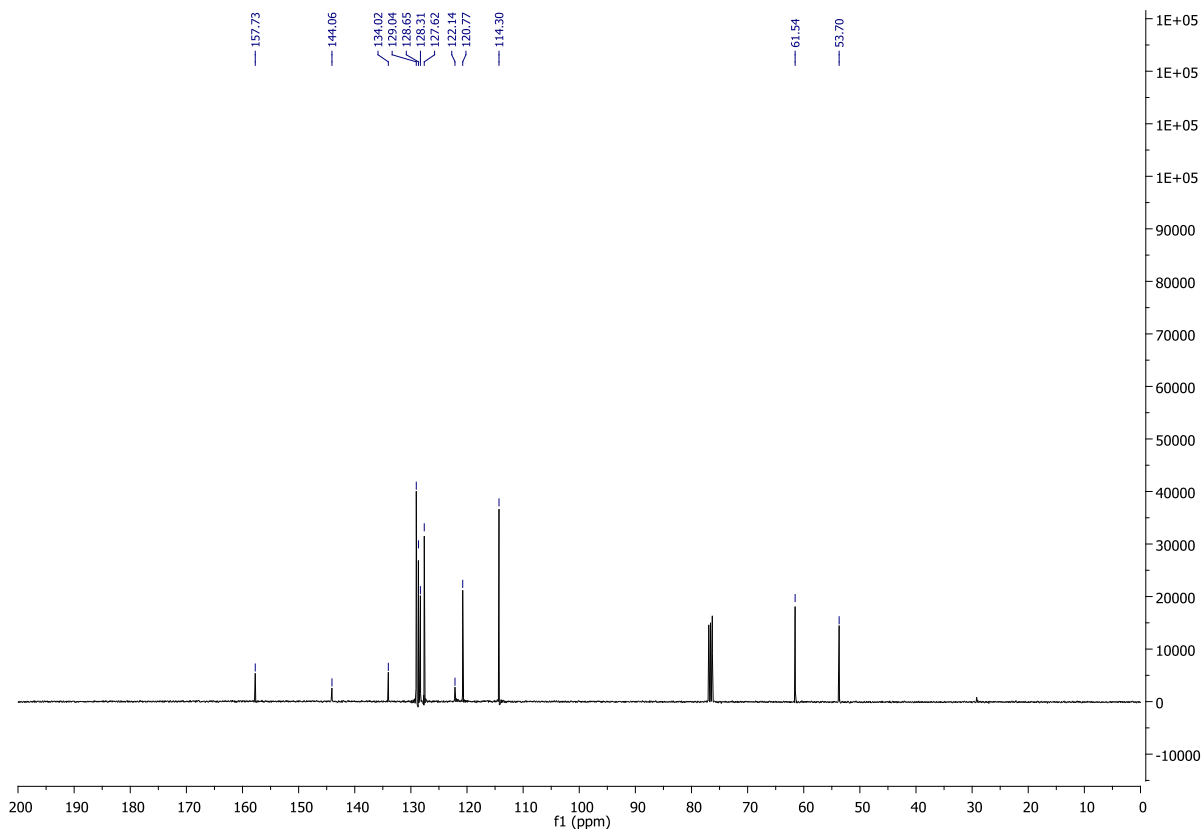
¹³C NMR of S3



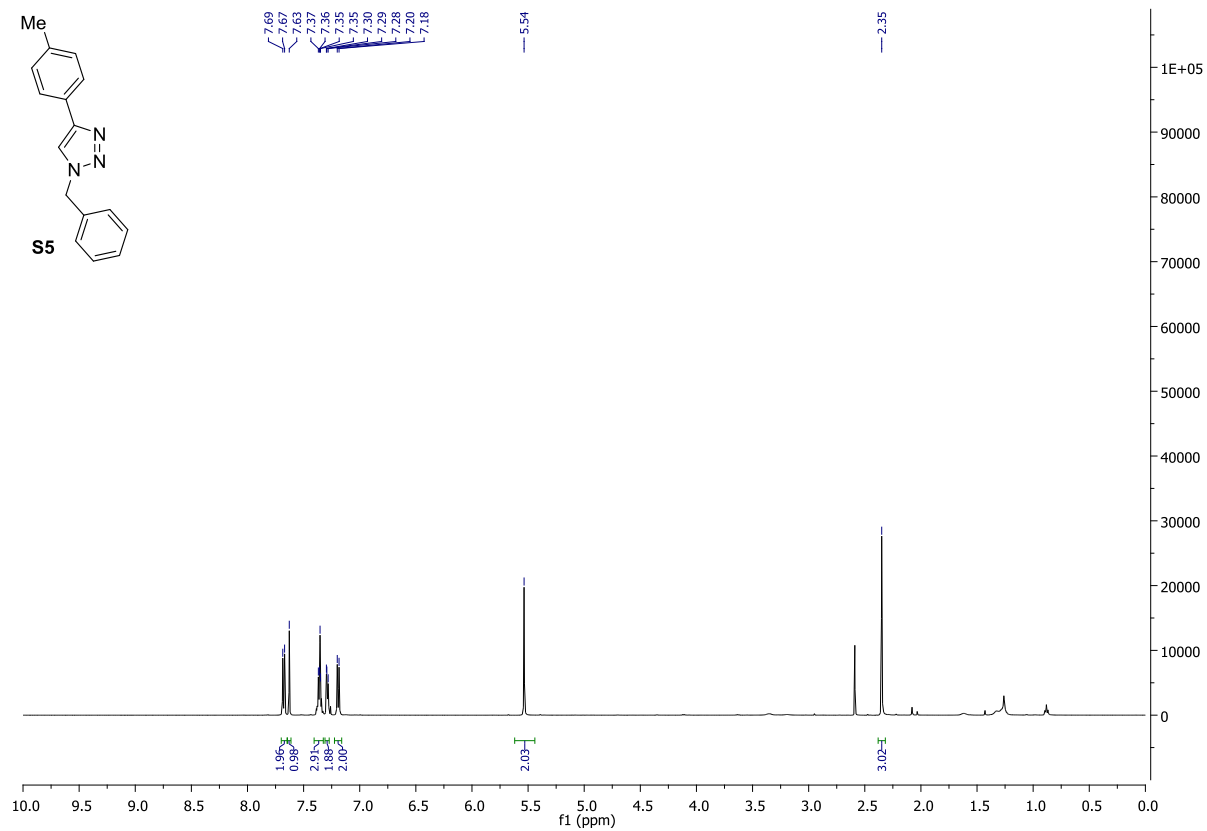
¹H NMR of S4



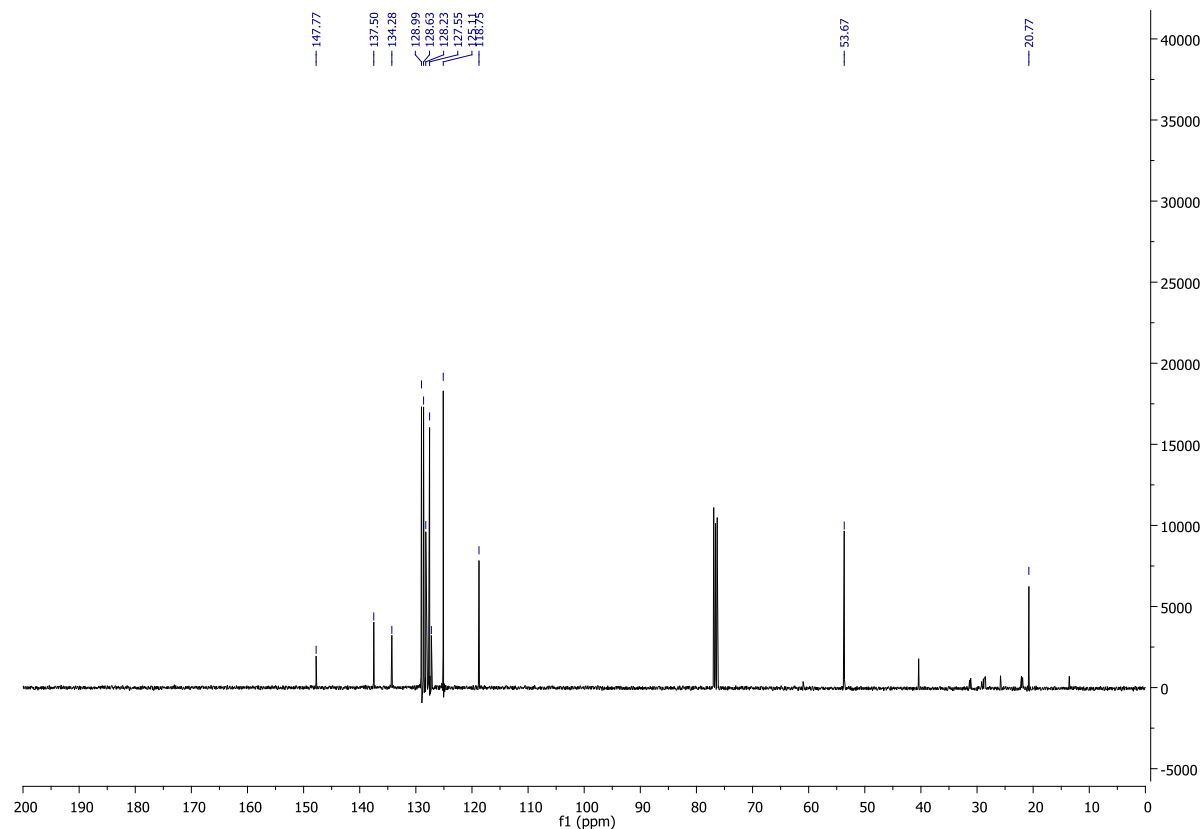
¹³C NMR of S4



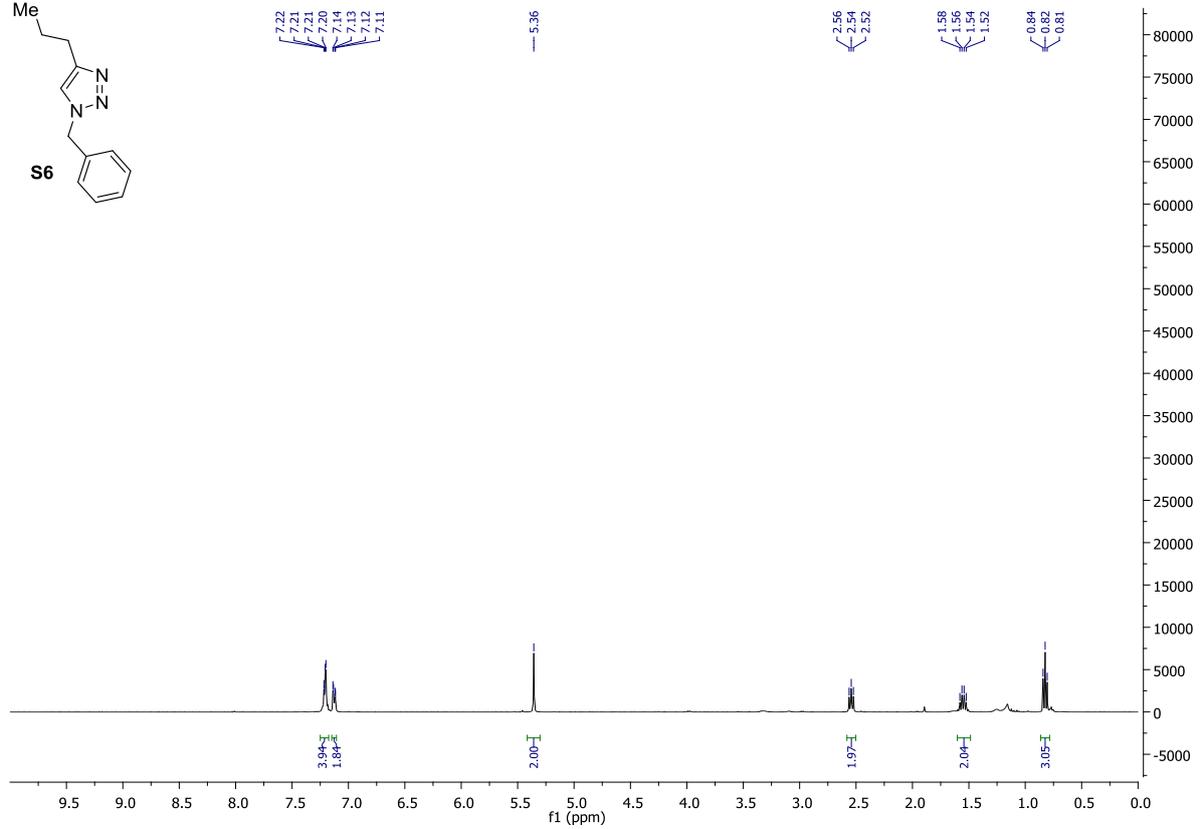
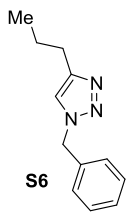
¹H NMR of S5



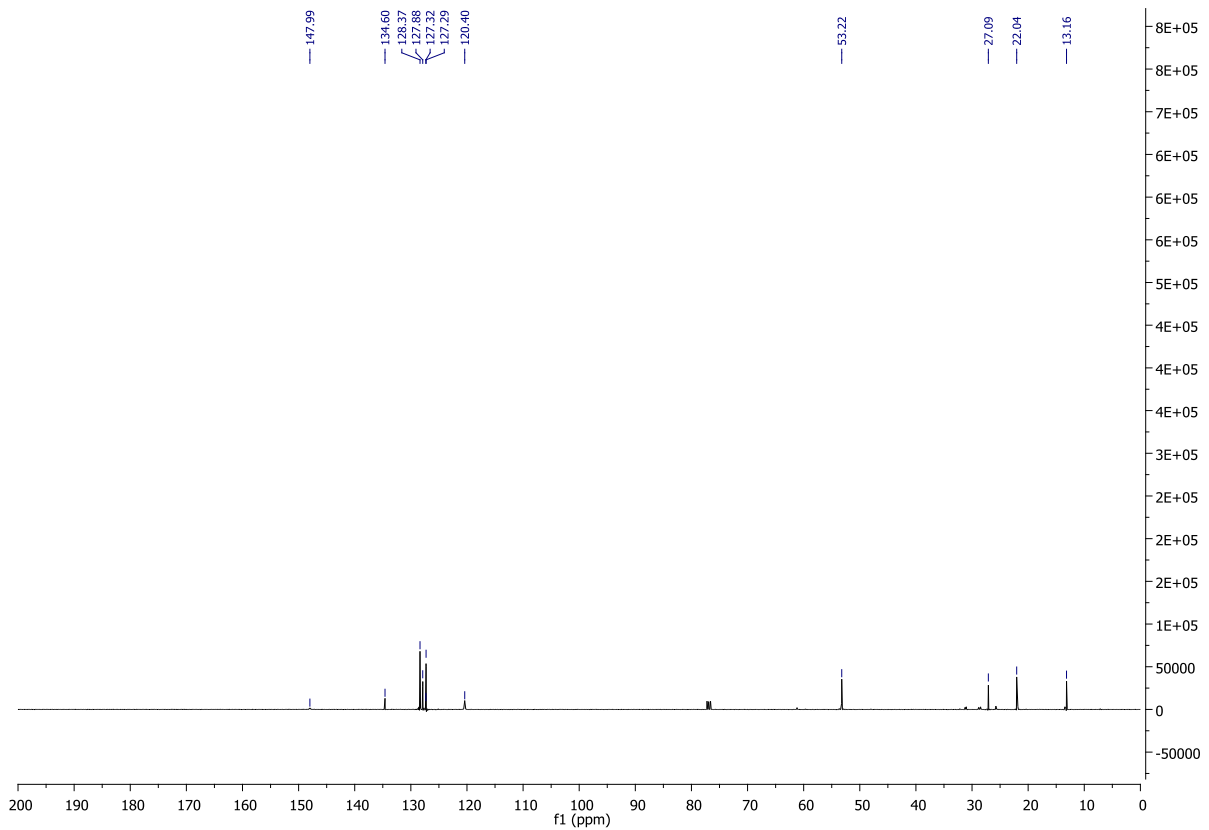
¹³C NMR of S5



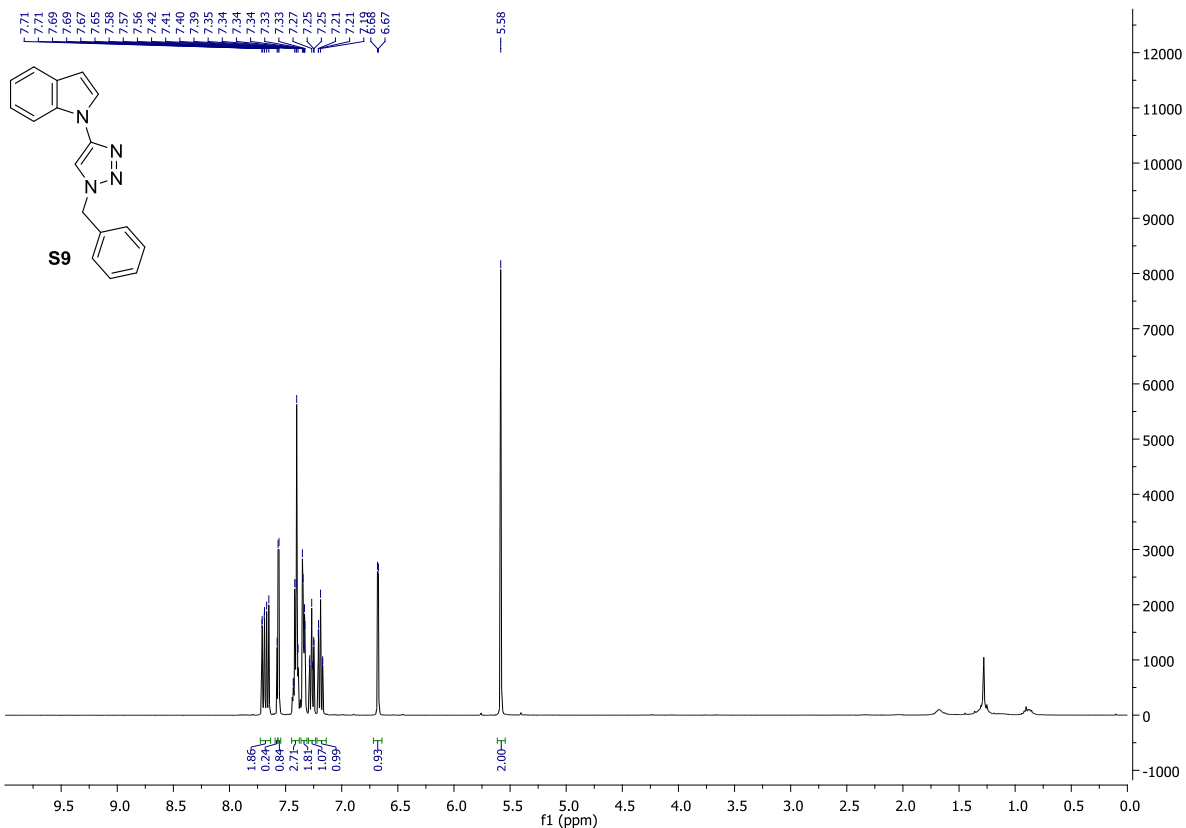
¹H NMR of S6



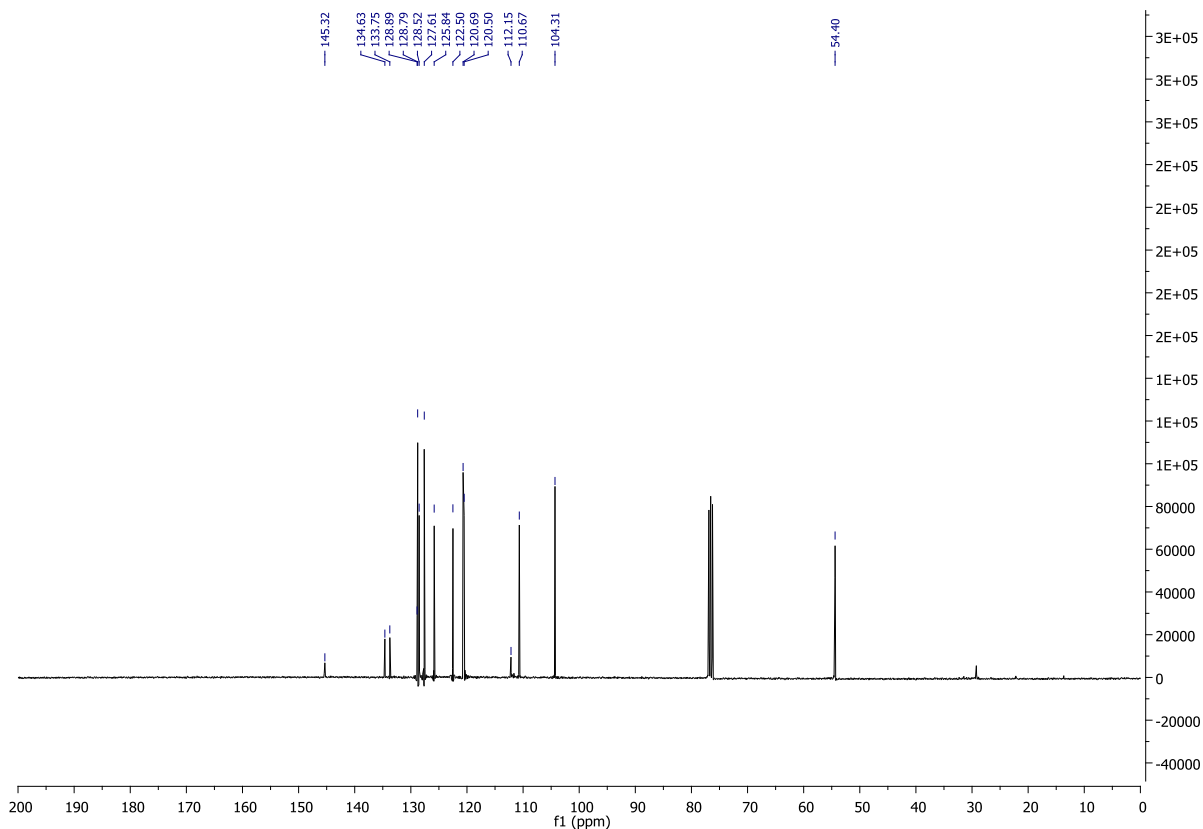
¹³C NMR of S6



¹H NMR of S9

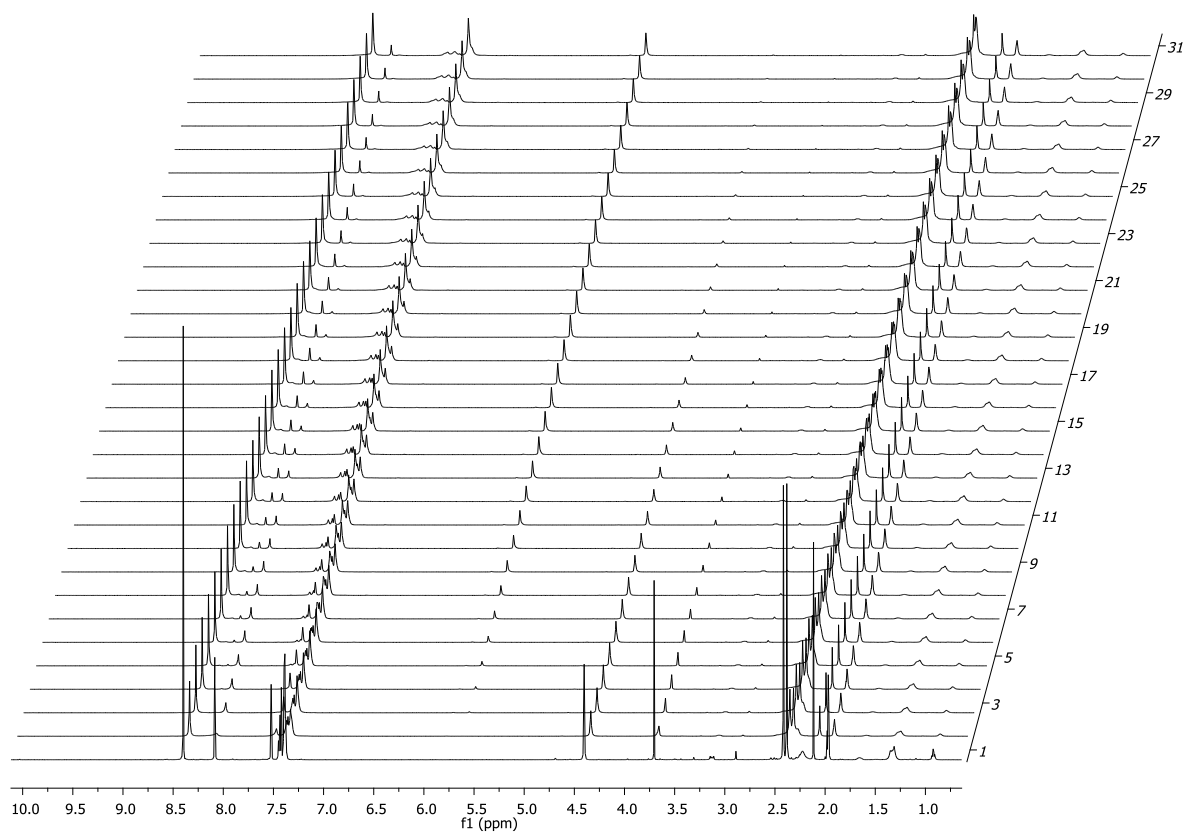


¹³C NMR of S9

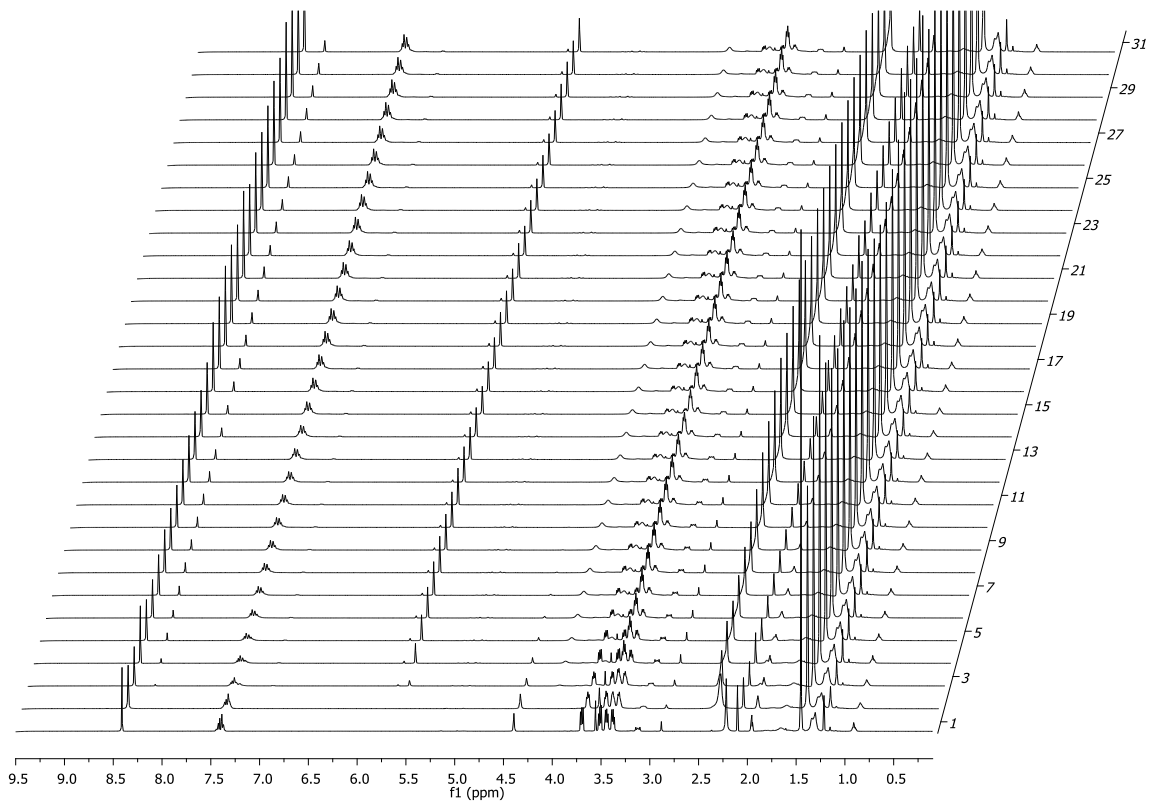


10. ^1H NMR spectra from kinetic experiments

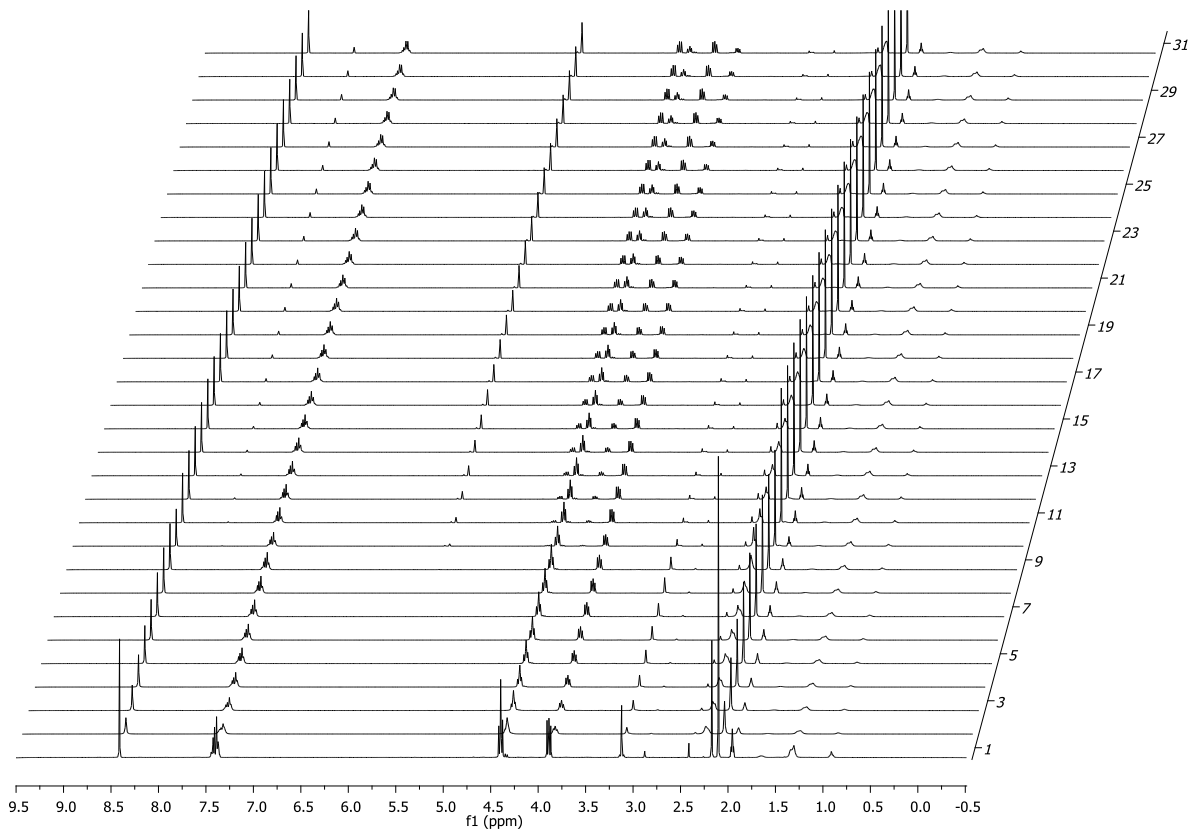
Rate of 1



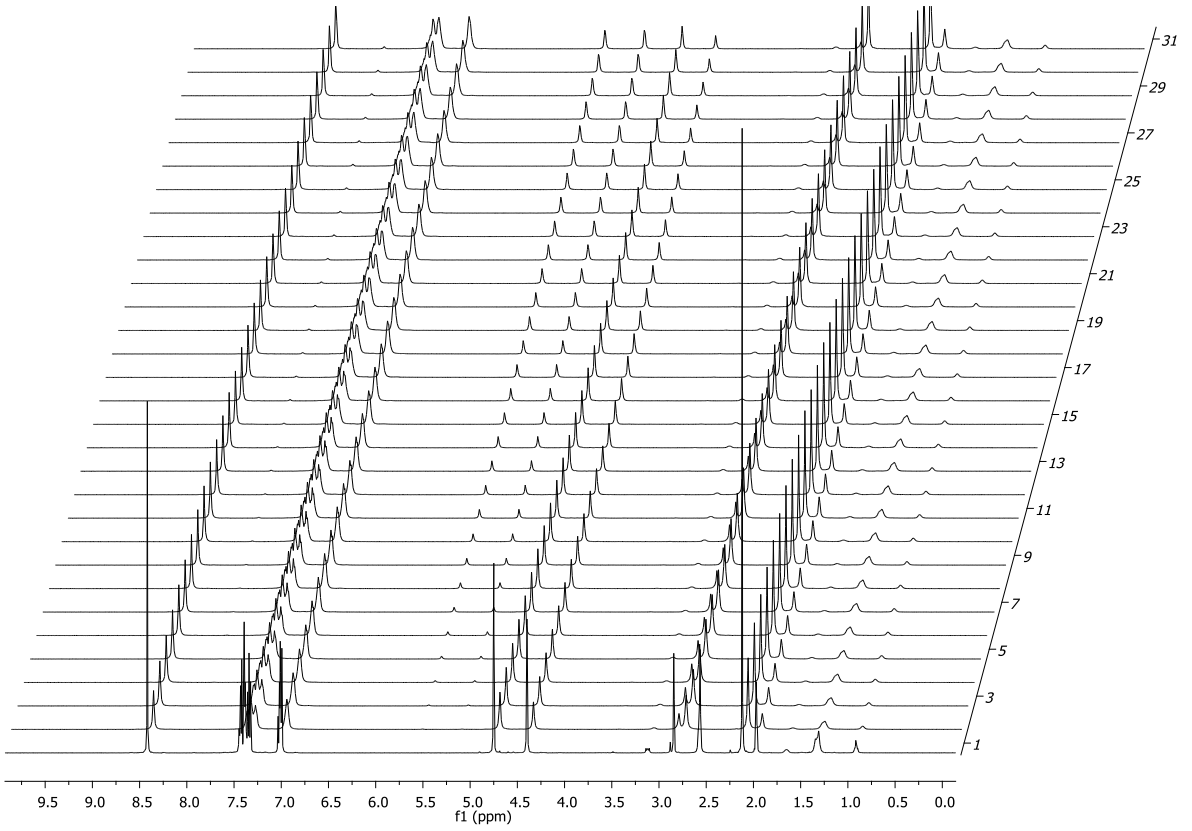
Rate of 2



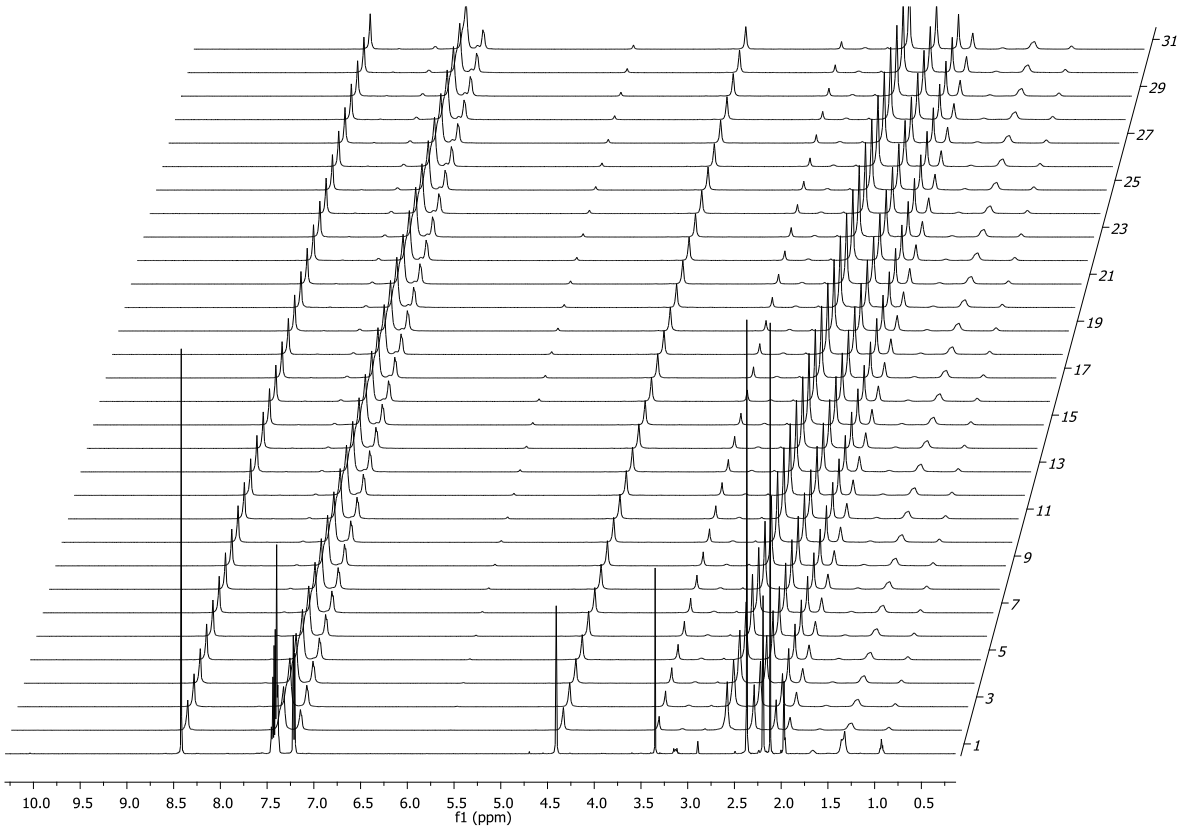
Rate of 3



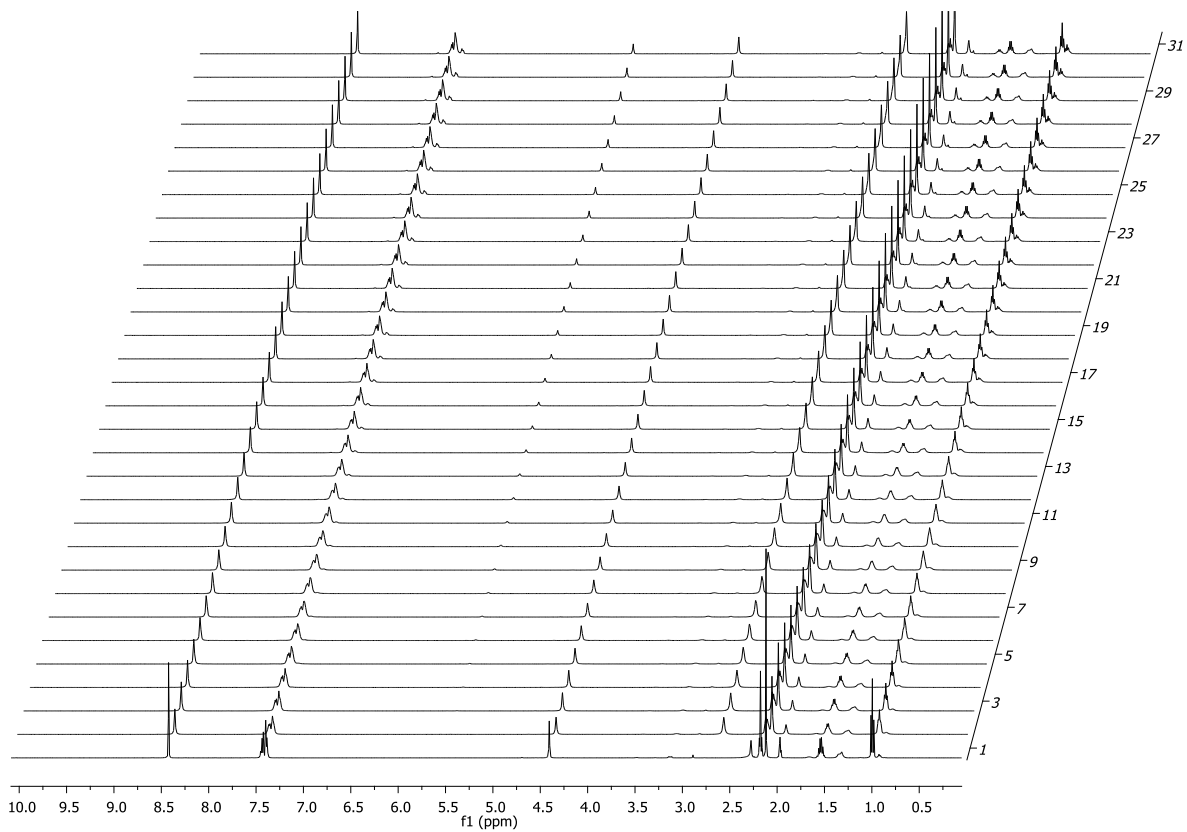
Rate of 4



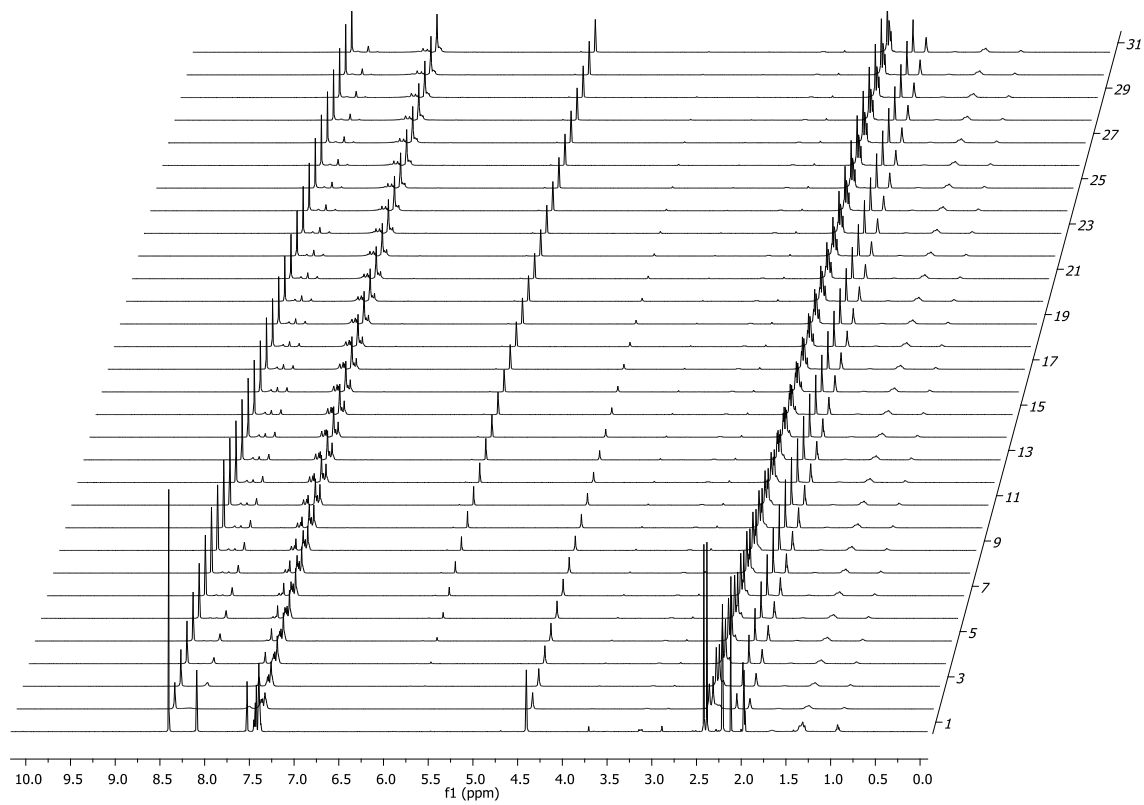
Rate of 5



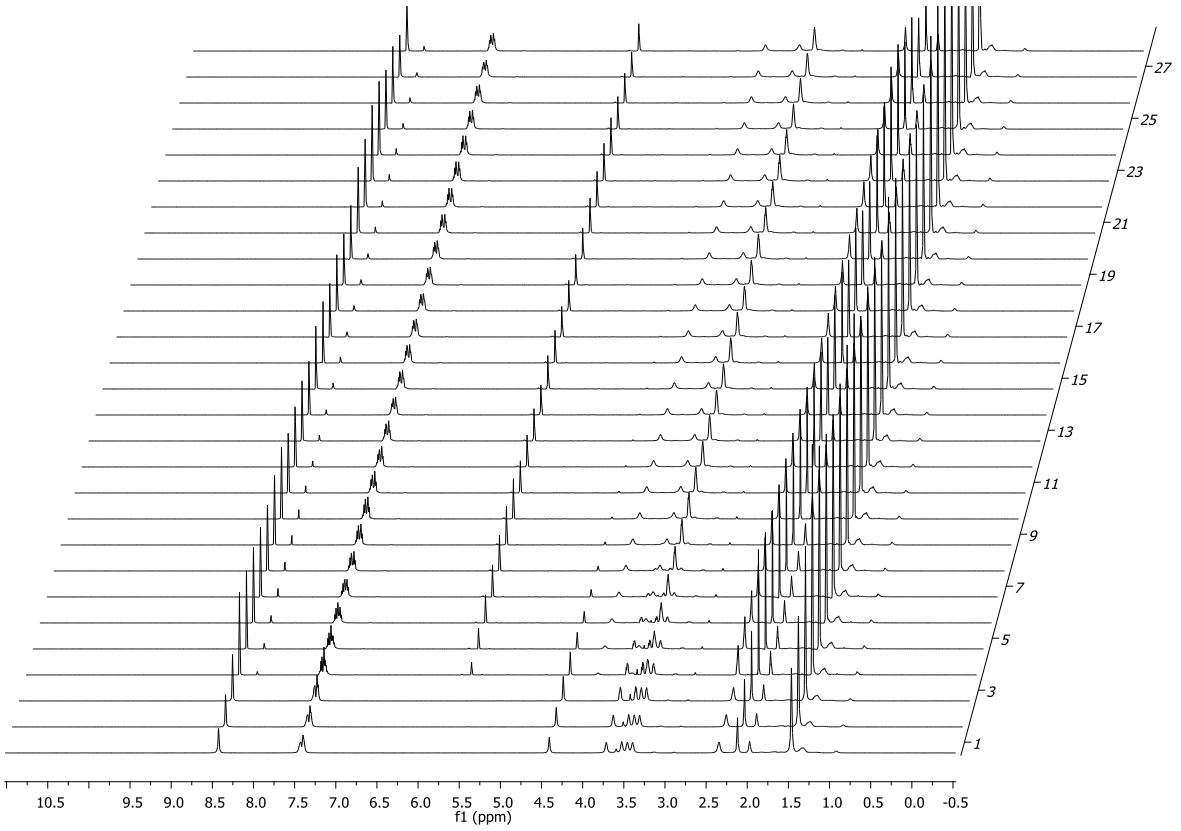
Rate of 6



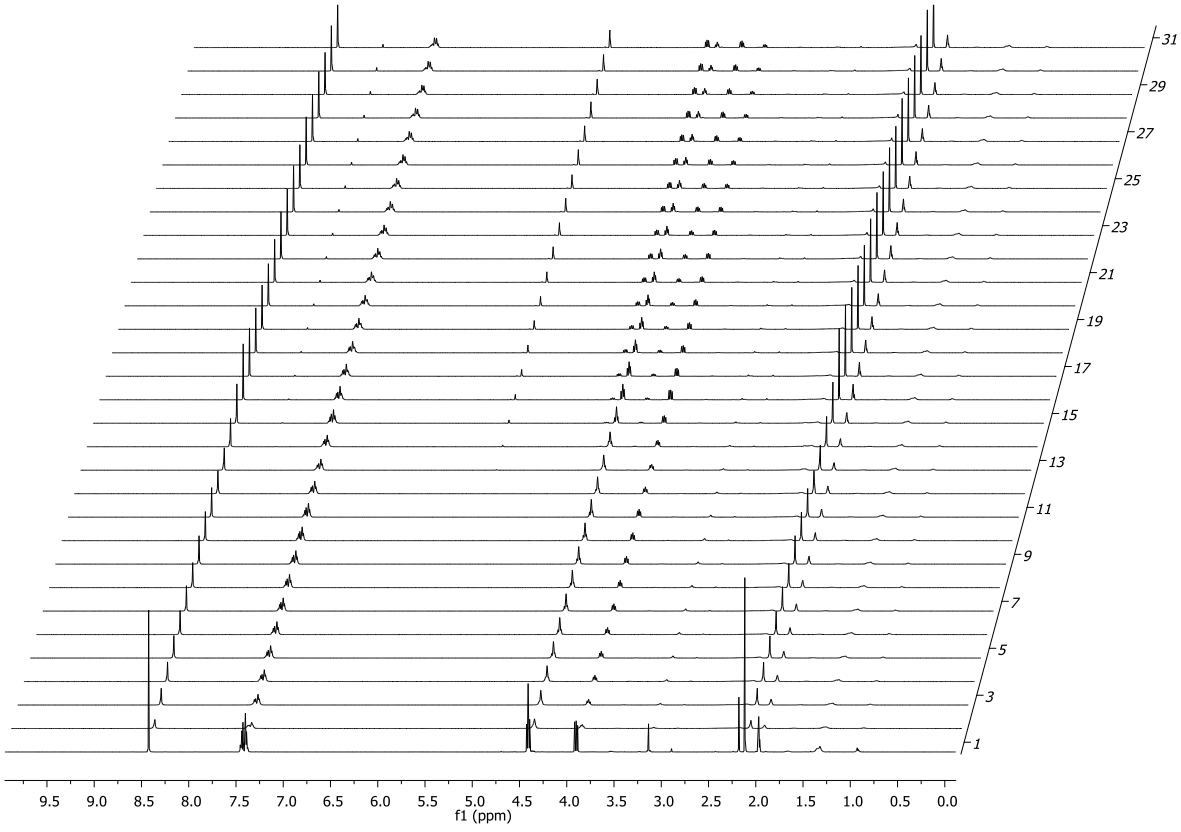
Rate of S1b



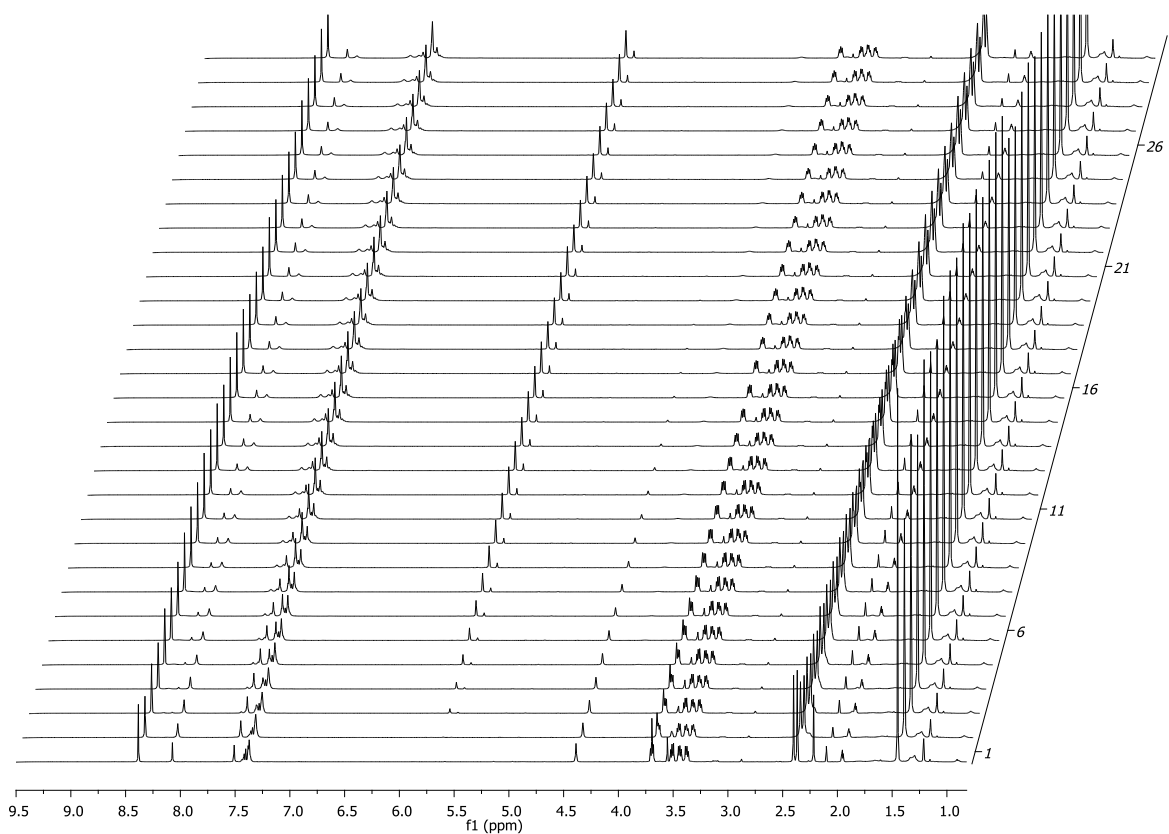
Rate of S2b



Rate of S3b

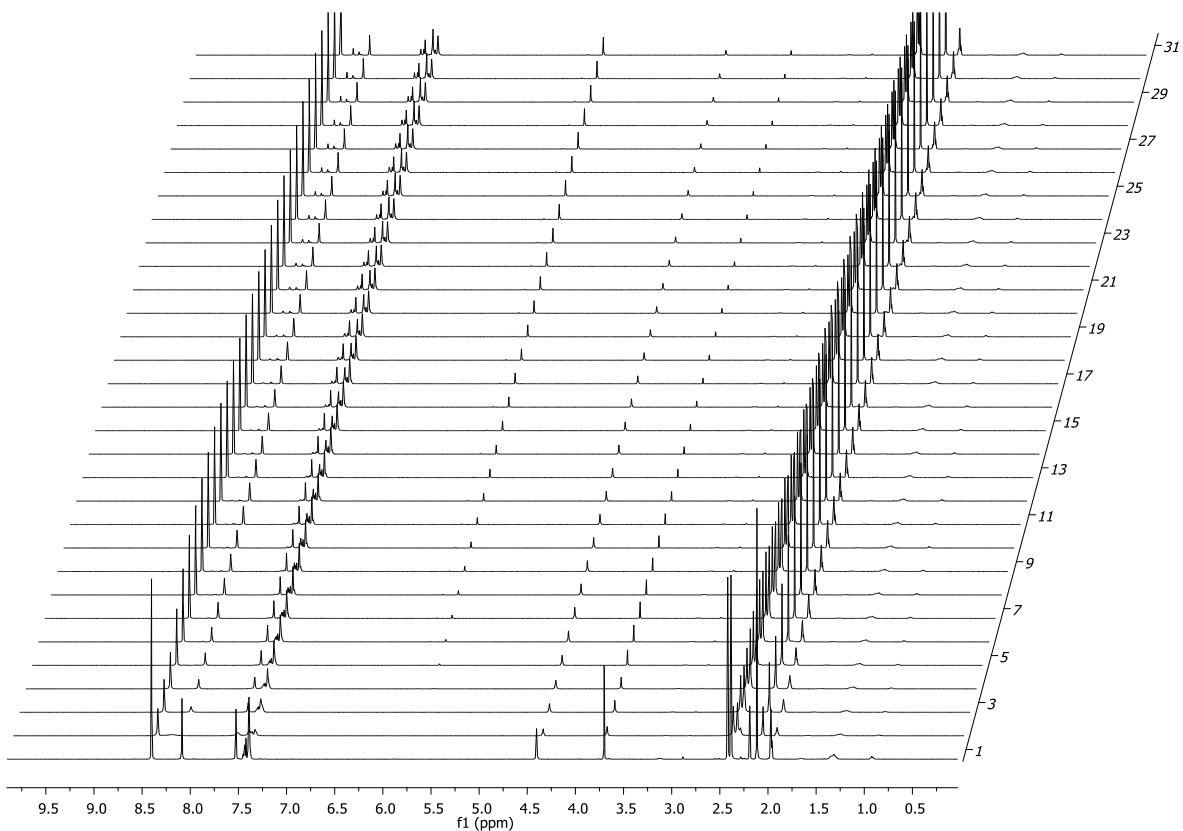


Competition experiment between 1 and 2

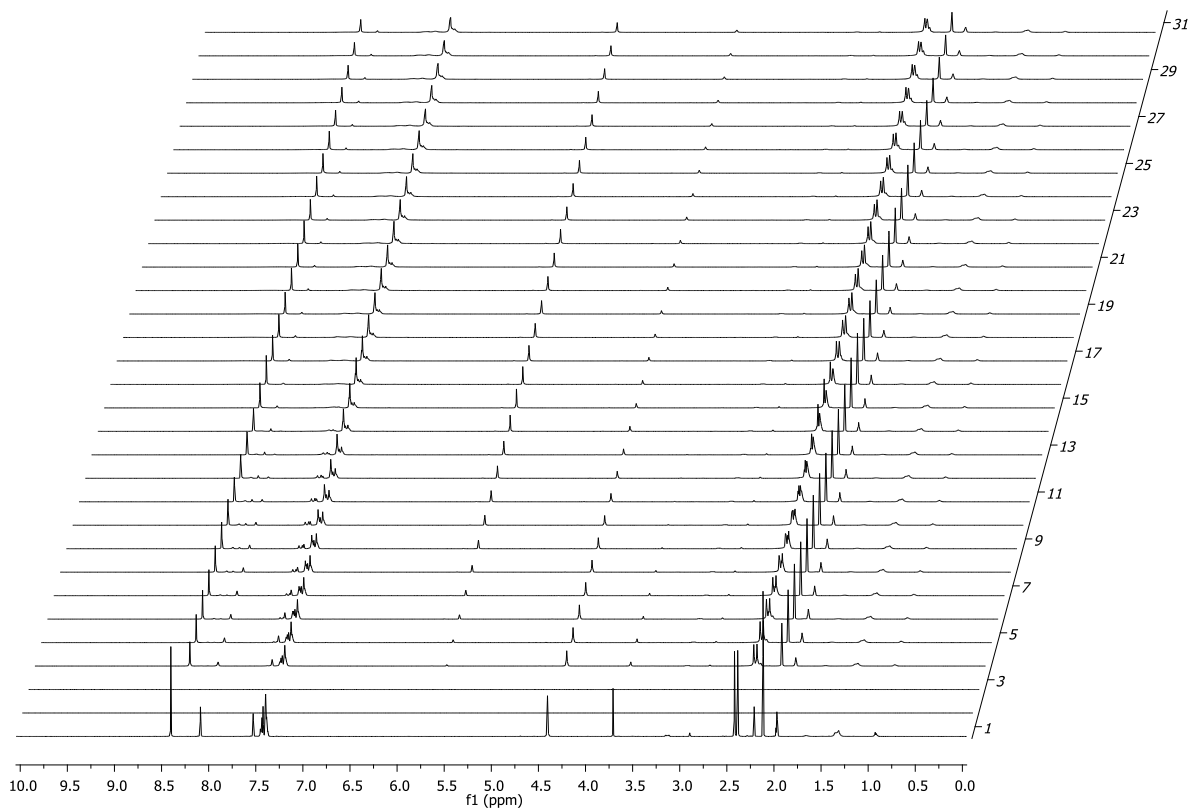


[Azide] variation with 1

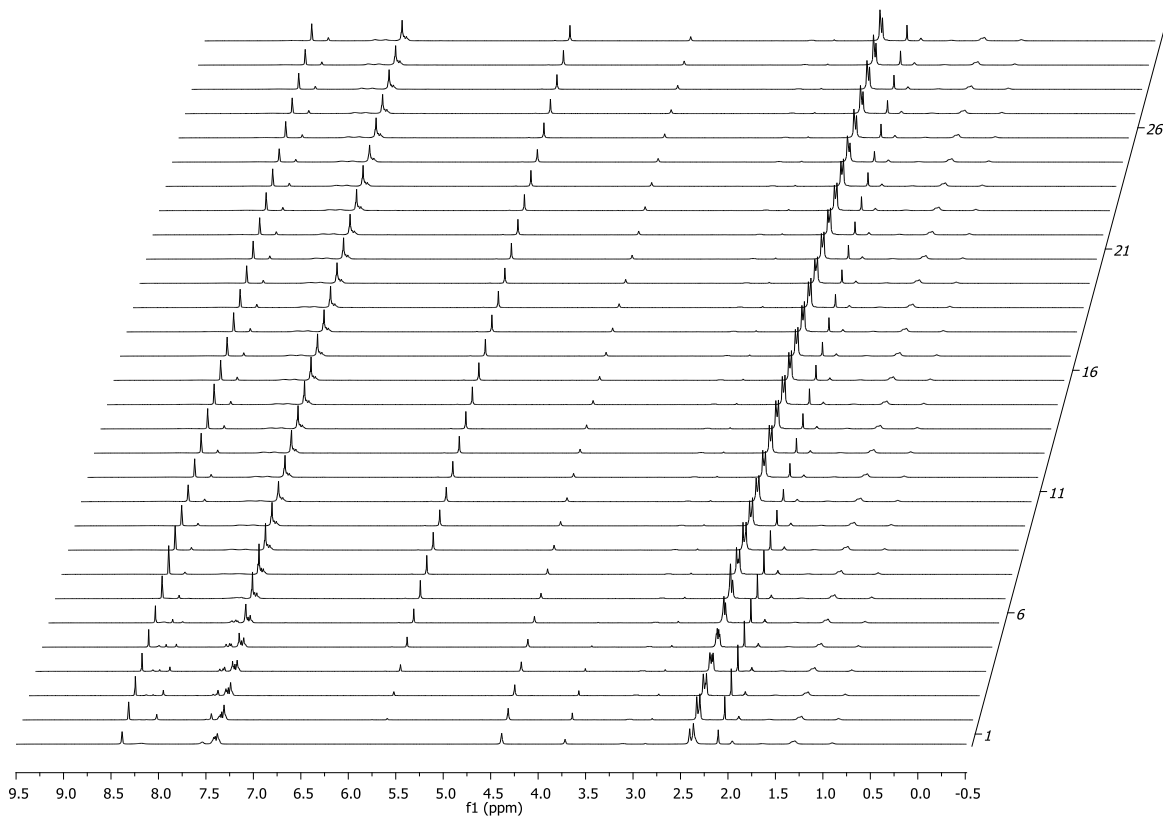
0.4 equiv azide



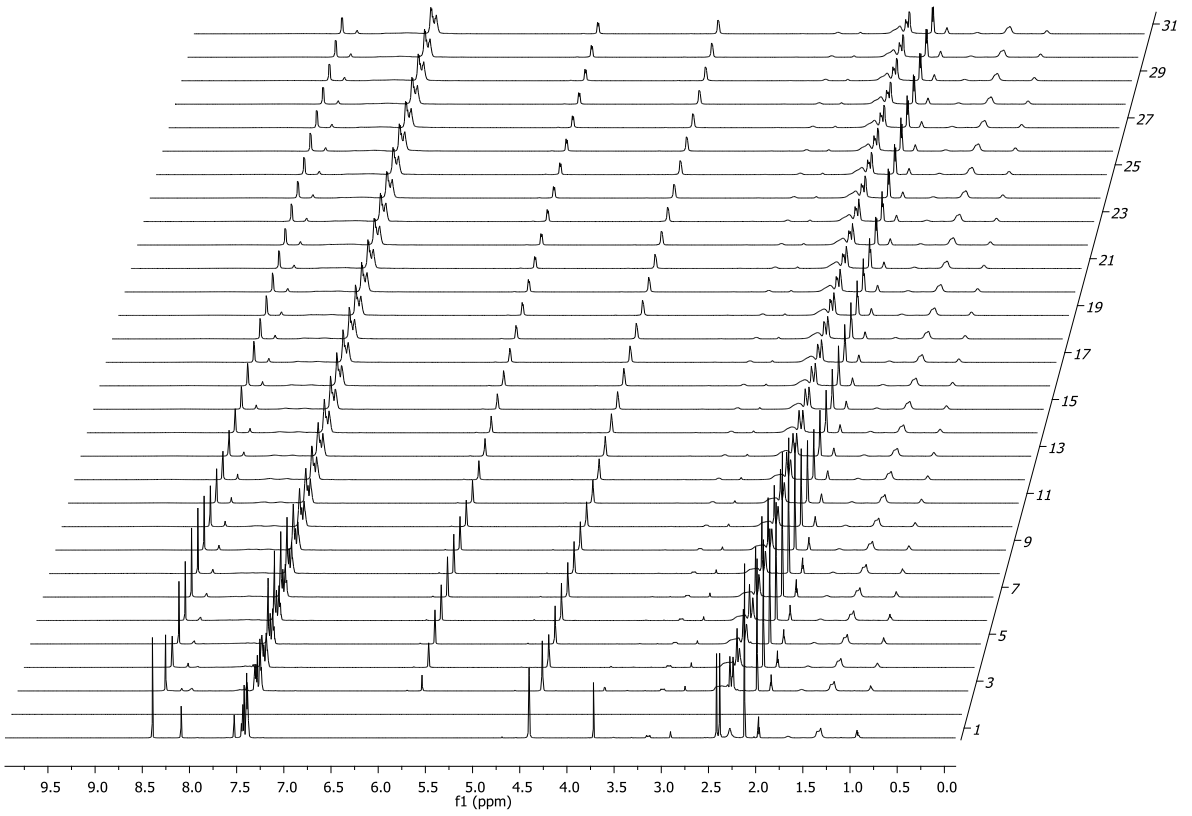
1.25 equiv azide



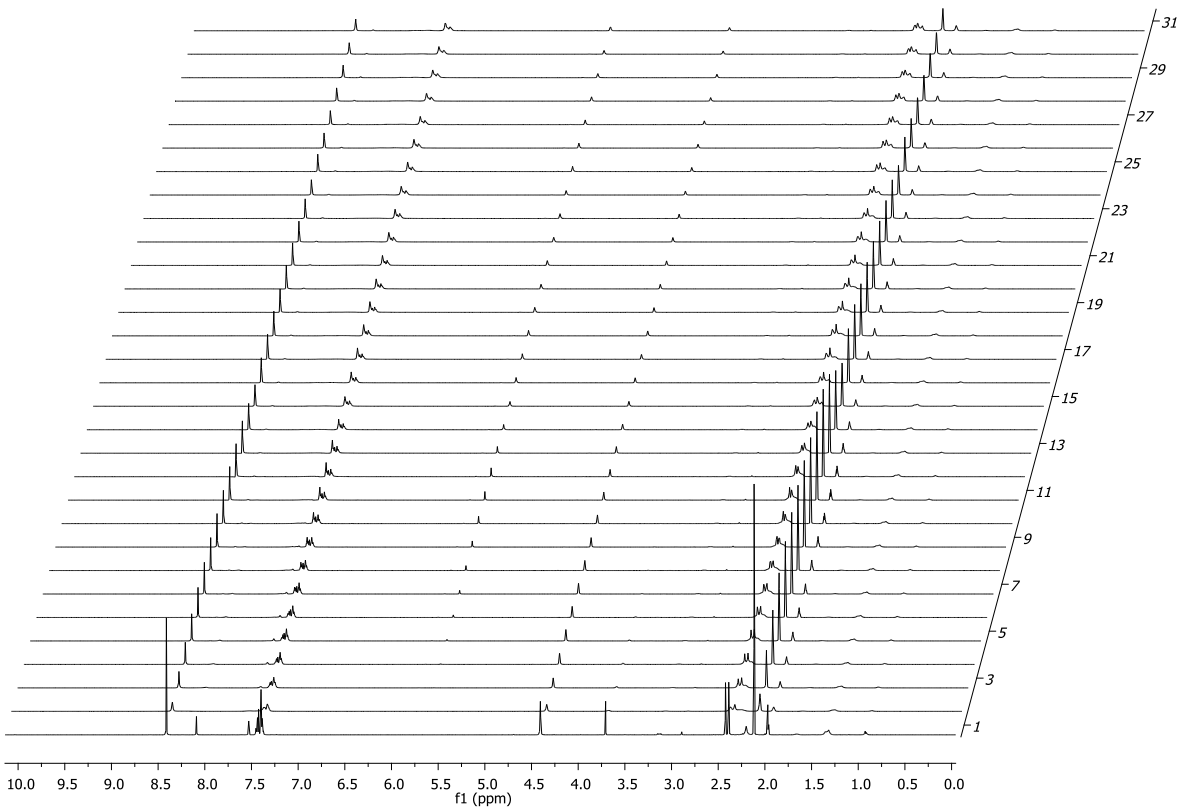
2 equiv azide



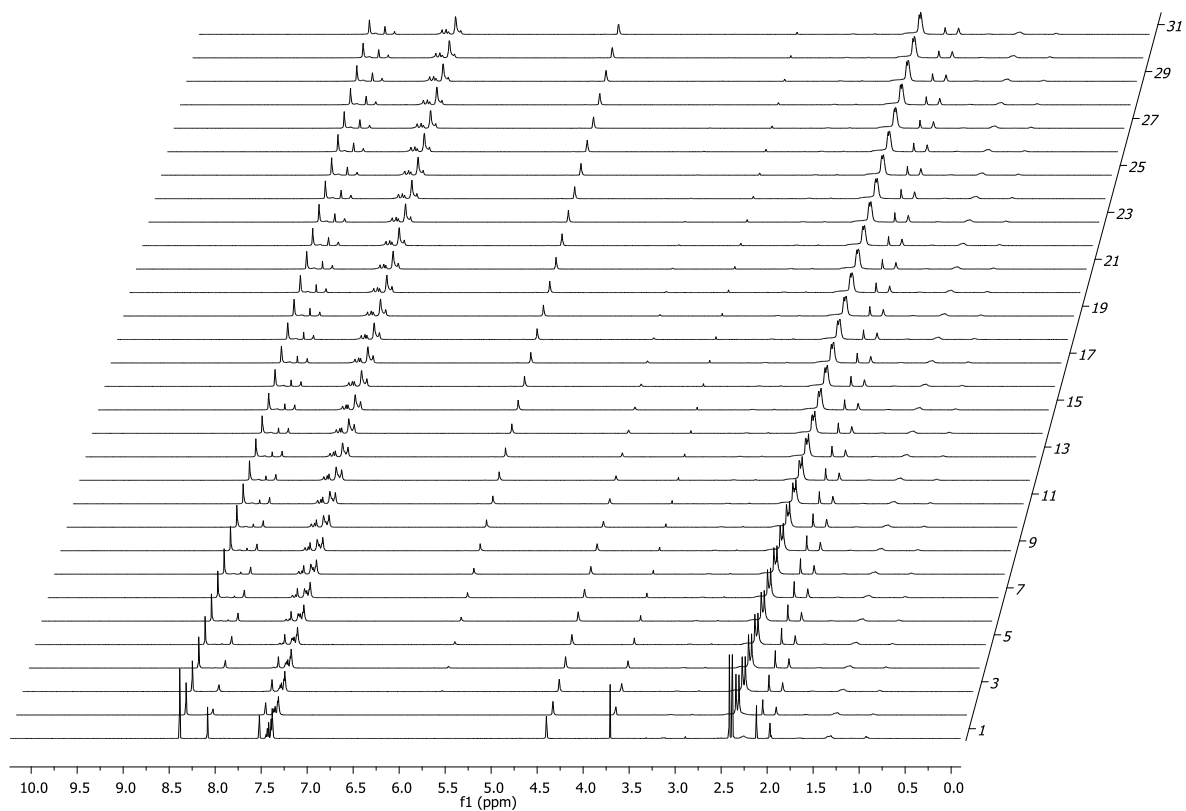
2.2 equiv azide



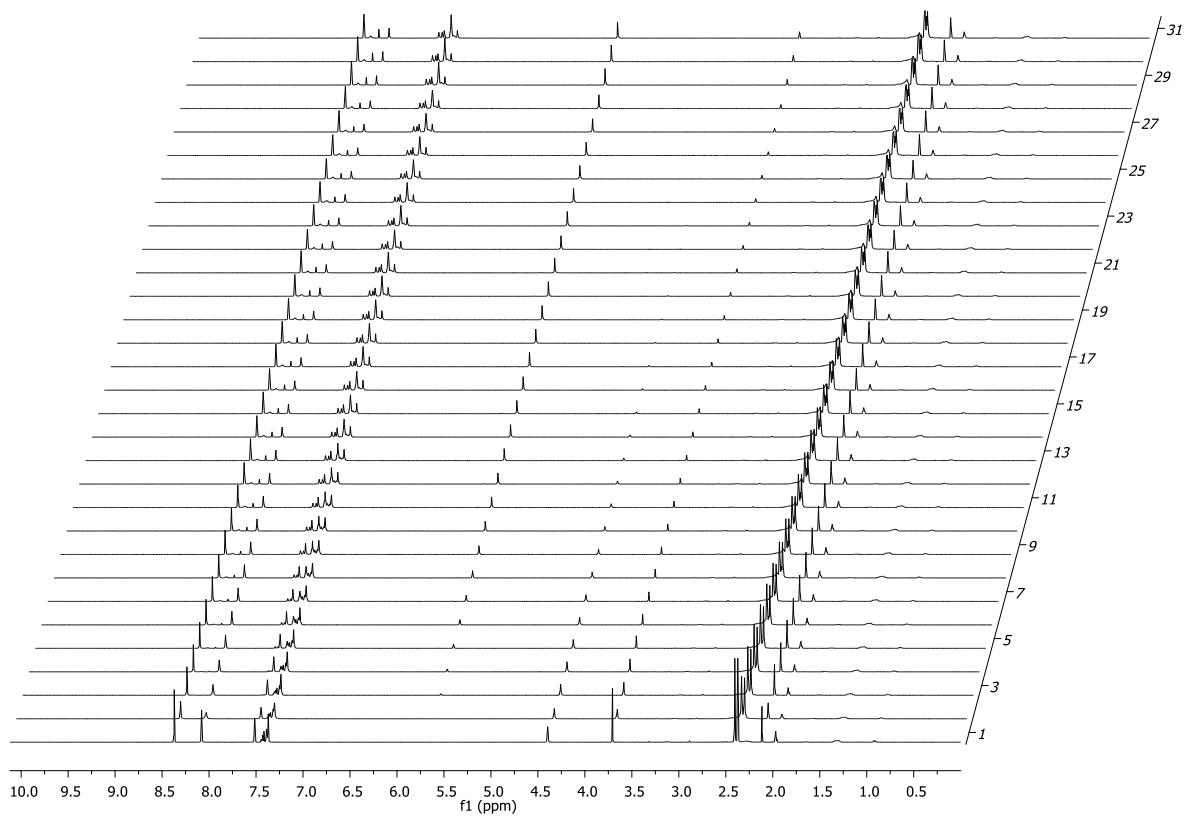
[1] variation
0.5 equiv



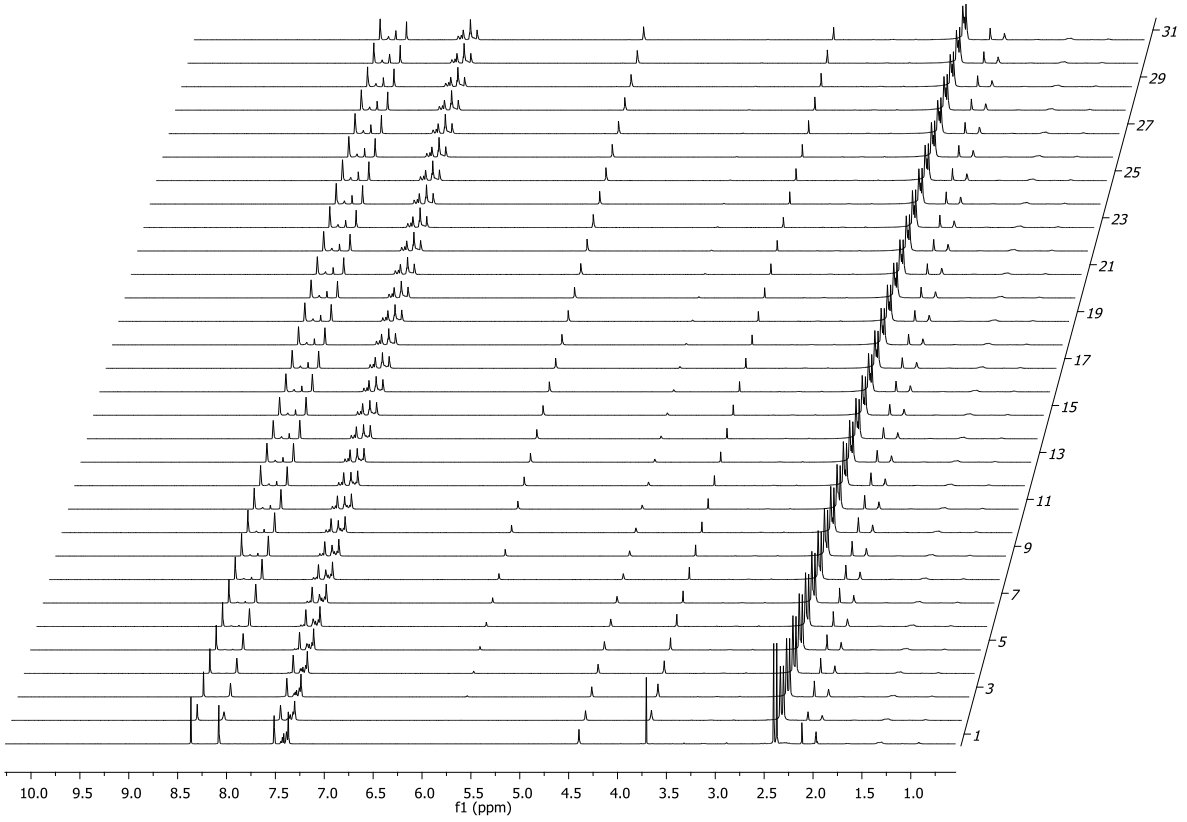
1.5 equiv



2 equiv

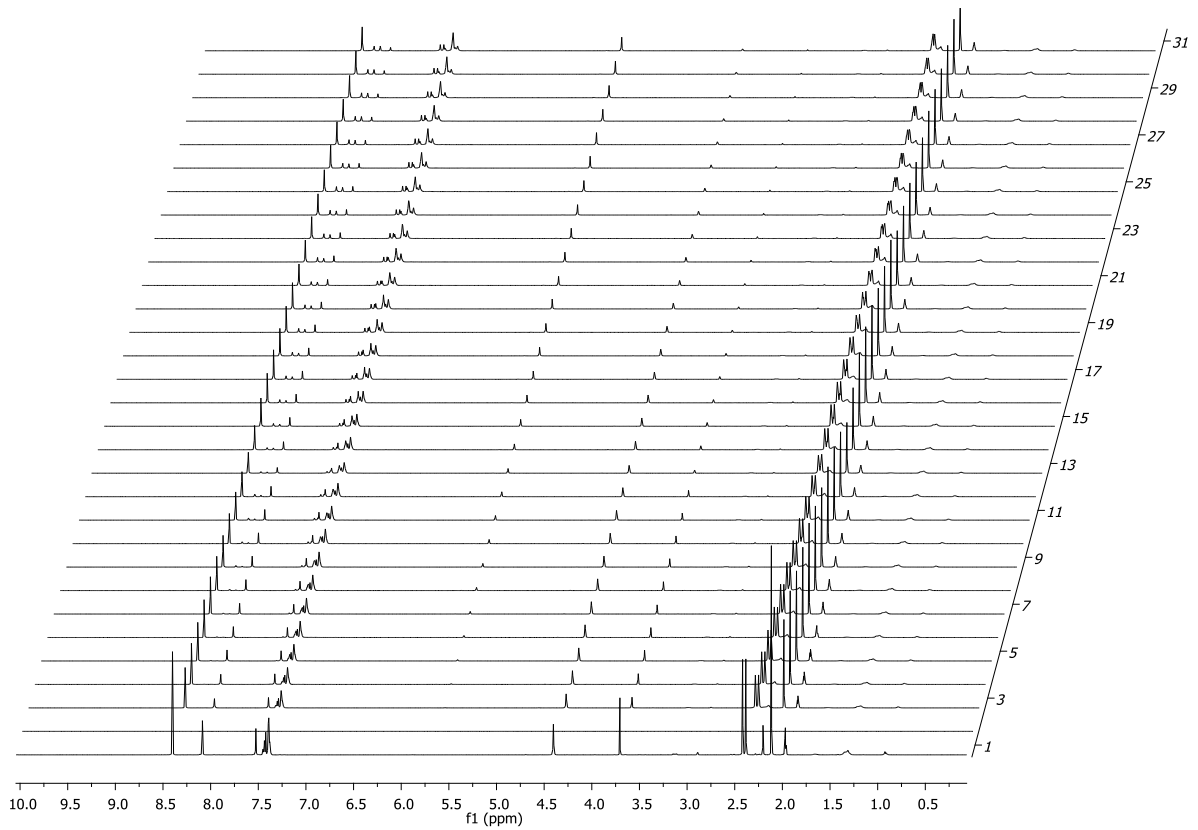


2.5 equiv

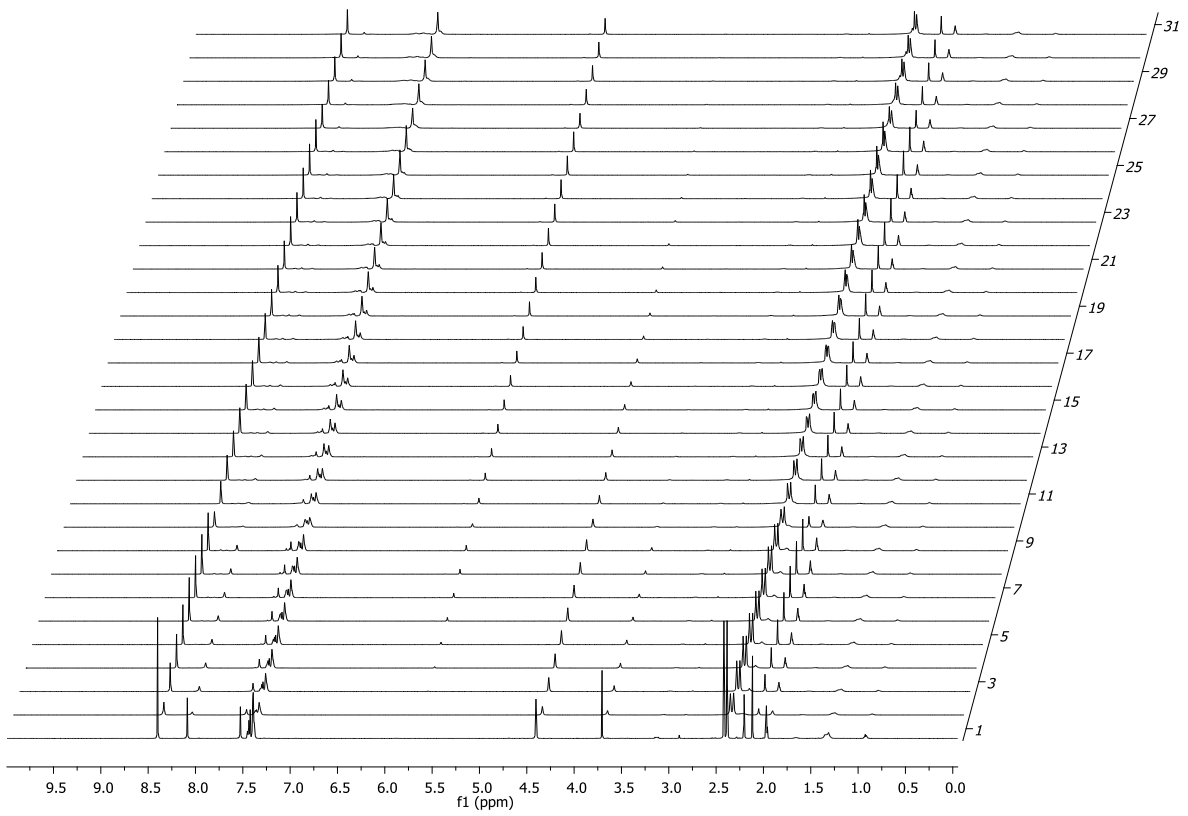


[Cu(OAc)₂] variation

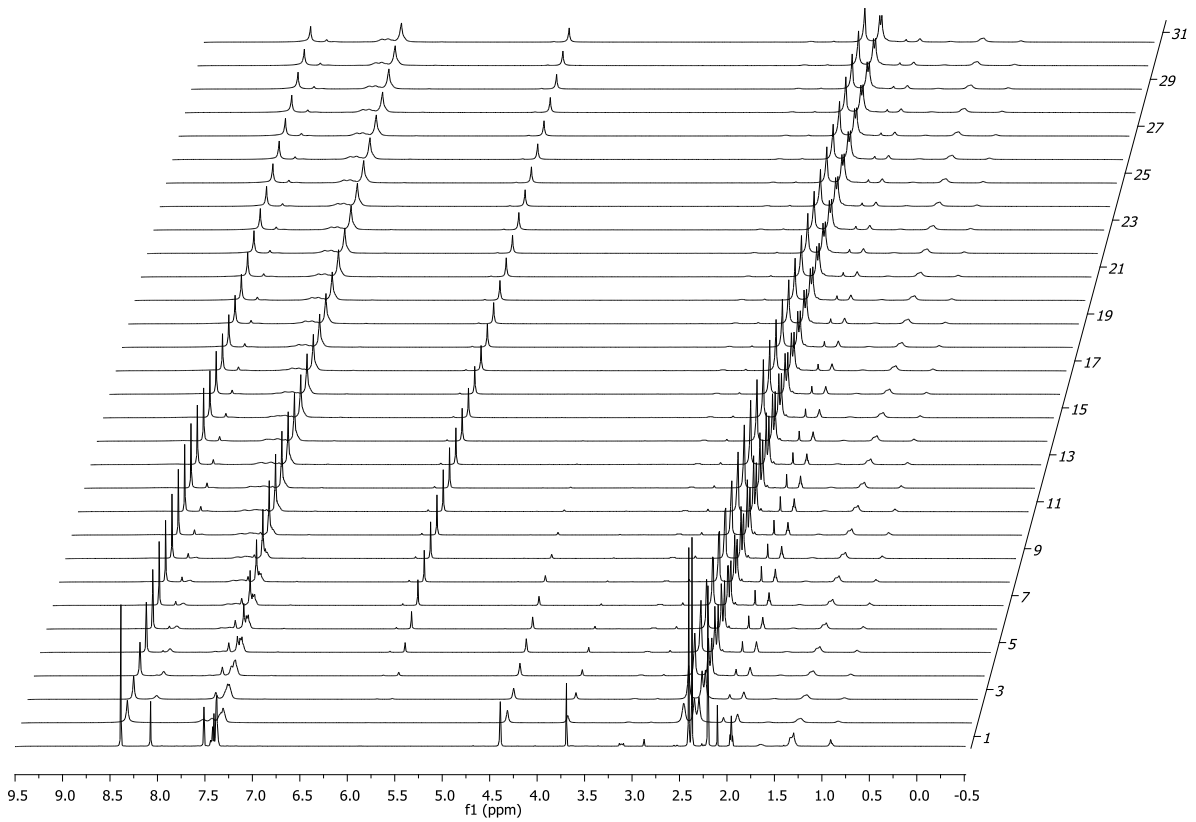
2.5 mol%



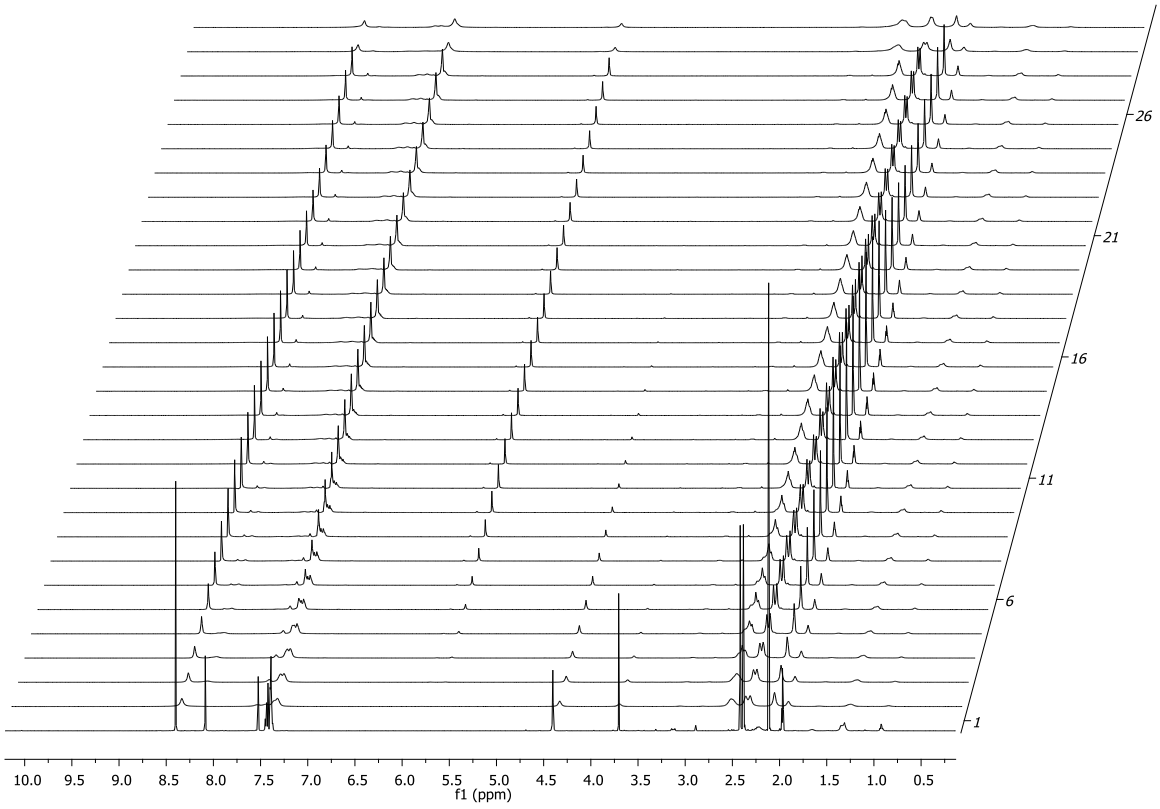
7.5 mol%



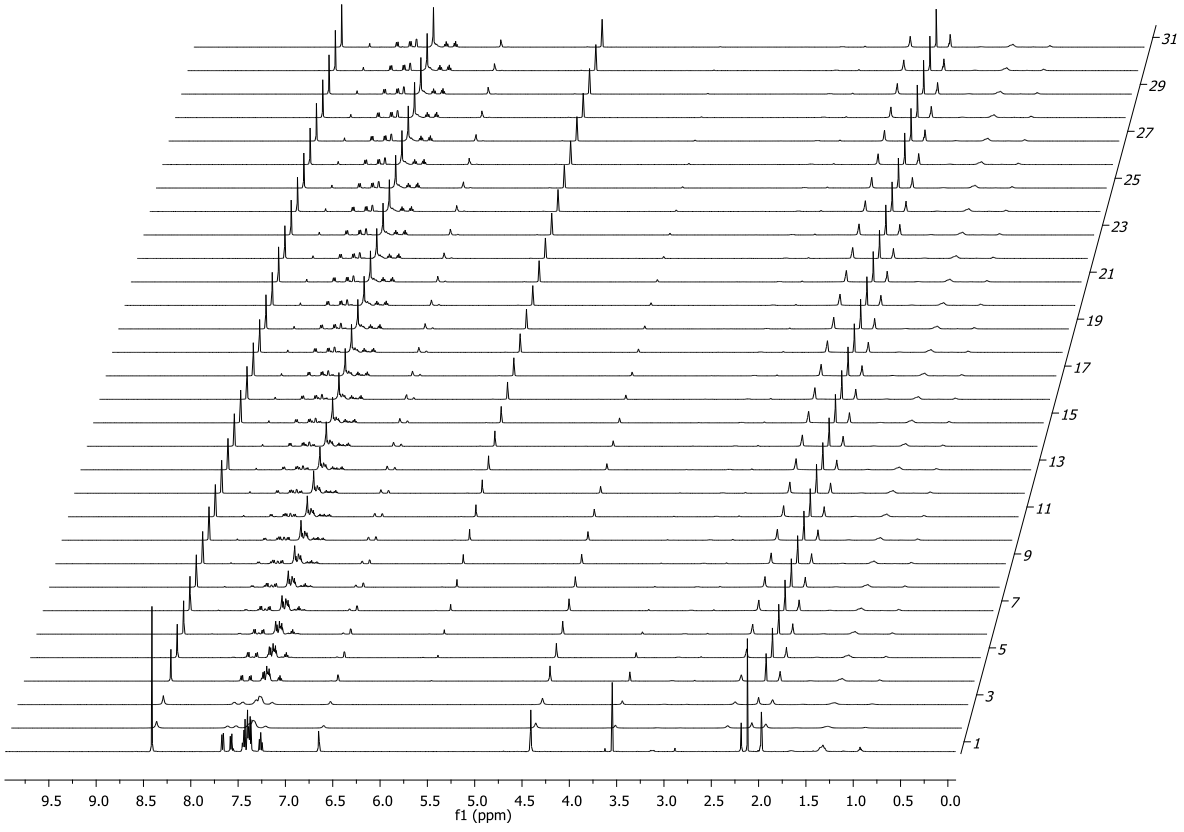
10 mol%



20 mol%

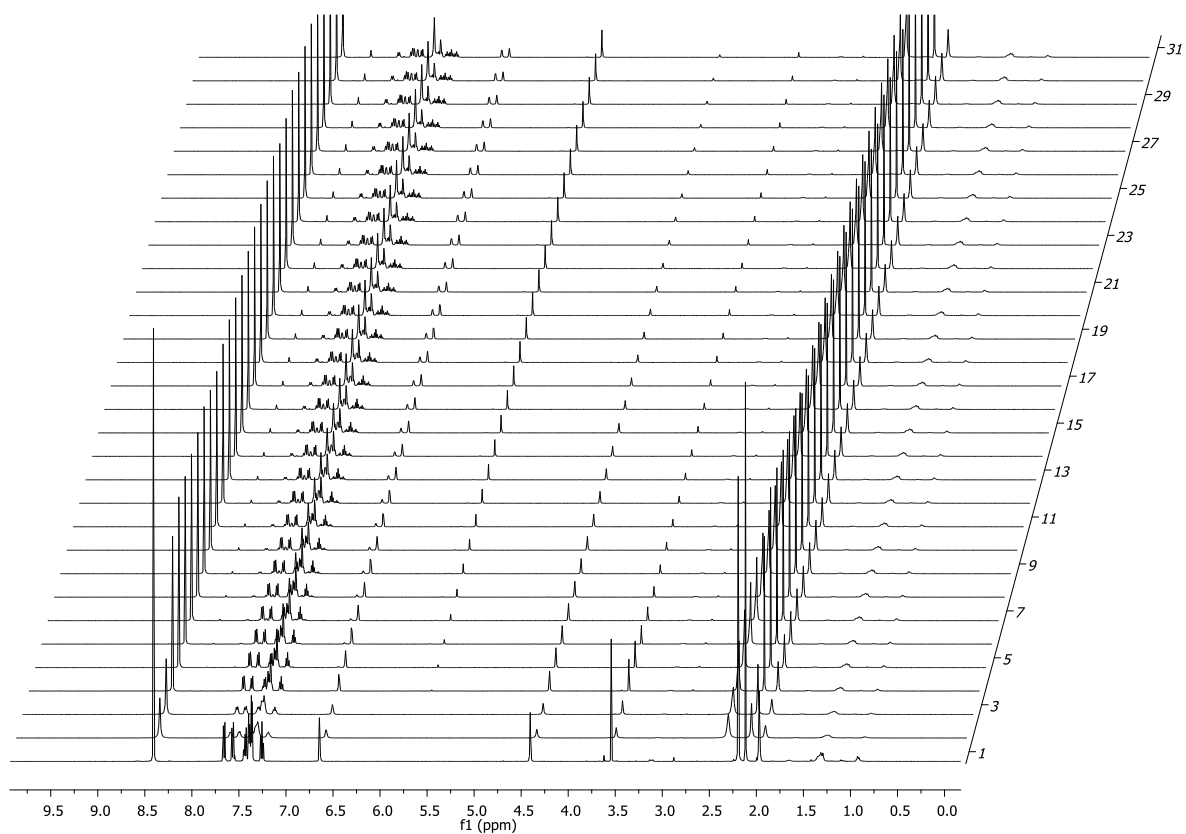


Rate of 9

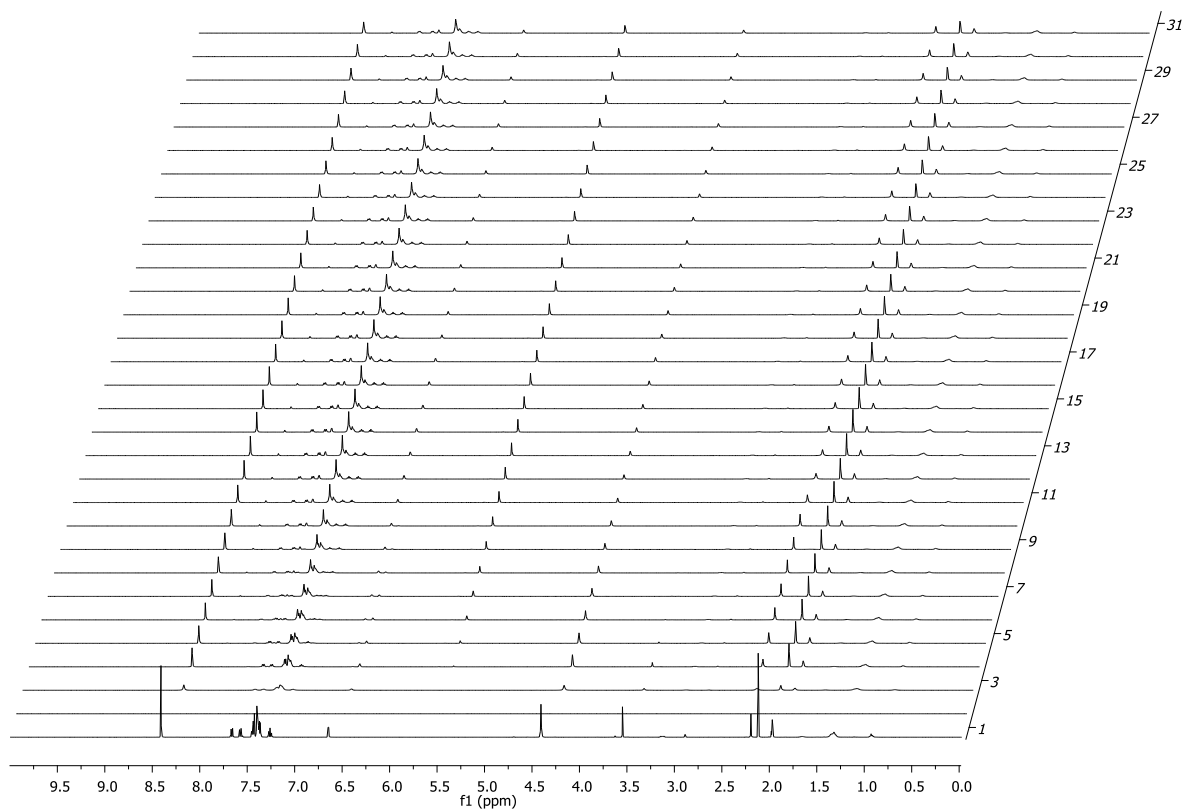


[Azide] variation with 9

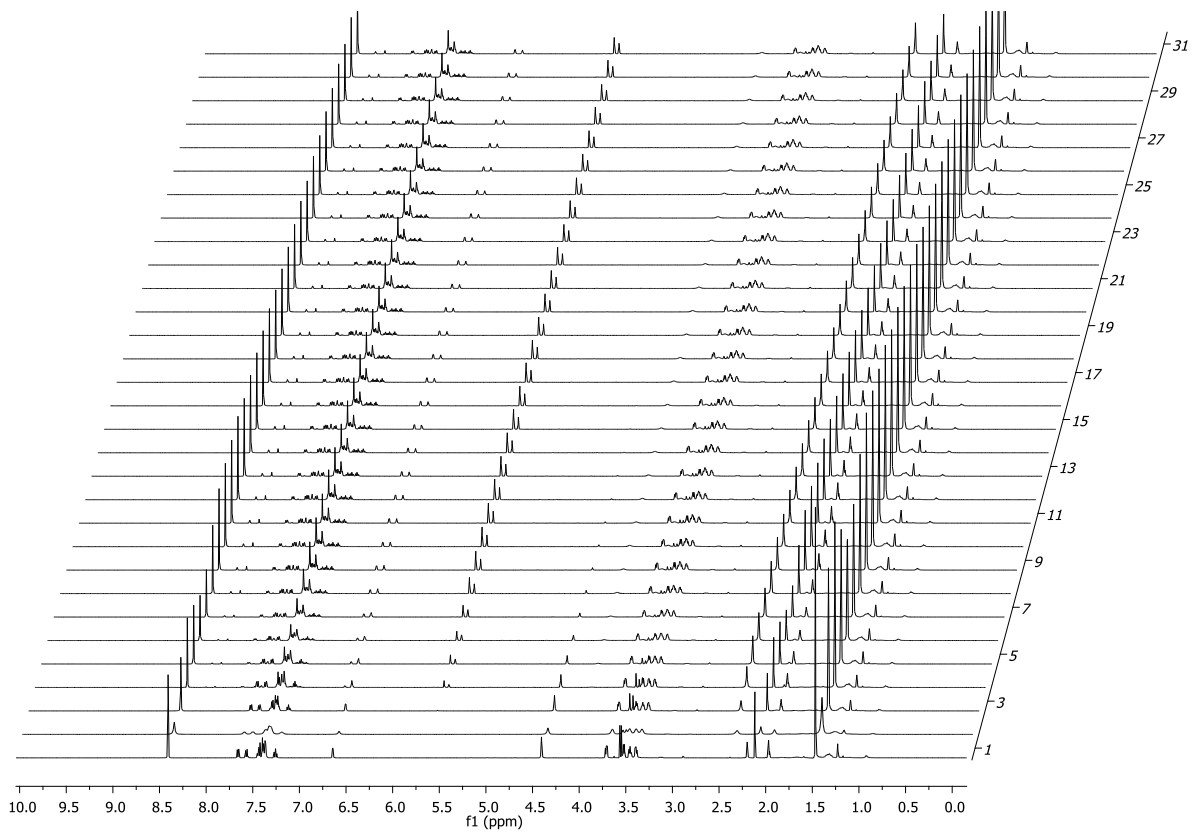
0.5 equiv



1.5 equiv



Competition experiment between 9 and 2



1 ¹H NMR and ¹³C NMR

